The formation of vanadium deposits in the Archean Rivière Bell Complex, Quebec: Insights from Fe-Ti oxide chemistry.

Matthew Polivchuk

A thesis submitted to the Faculty of Graduate and Postdoctoral Studies
in partial fulfillment of the requirements for the degree
Master of Science in Earth Sciences

Department of Earth and Environmental Sciences
Faculty of Science
University of Ottawa

ABSTRACT

Cryptic trends in the trace element chemistry of Fe-Ti oxide minerals have been used to elucidate the magmatic processes responsible for the formation of Fe-Ti-V deposits in the Rivière Bell Complex layered mafic-ultramafic intrusion near Matagami, Quebec, Canada. Although metamorphism at greenschist-amphibolite facies conditions has modified the primary igneous compositions of magnetite and ilmenite, their Cr and V contents appear to have been unaffected. Chemostratigraphic variations of these elements in Fe-Ti oxides therefore remain valid tracers of magmatic differentiation, even in metamorphosed settings. Injections of compositionally evolved, Fe-Ti oxide-laden magma into a more primitive ferrogabbroic host are presumably responsible for sharp decreases in the Cr and V concentrations of Fe-Ti oxides that coincide with lithostratigraphic changes from predominantly disseminated gabbros to ultramafic sequences closely interlayered with massive oxides. These injections highlight the multistage magmatic history of the layered series of the Rivière Bell Complex and its vanadium ore horizons.

RÉSUMÉ

Les variations cryptiques de la chimie des éléments traces des minéraux d'oxyde de Fe-Ti ont été utilisées pour élucider les processus magmatiques responsables de la formation de dépôts de Fe-Ti-V dans l'intrusion mafique et ultramafique du complexe de la Rivière Bell à Matagami, Québec, Canada. Bien que le métamorphisme au faciès schiste vert - amphibolite ait modifié les compositions ignées primaires de la magnétite et de l'ilménite, leurs teneurs en Cr et V semble ne pas avoir été affectées. Les variations chimico-stratigraphiques de ces éléments dans les oxydes de Fe-Ti restent donc des traceurs valables de la différenciation magmatique, même dans des contextes métamorphisés. Les injections de magma différentié, chargés d'oxyde de Fe-Ti, dans un encaissant ferrogabbroïque plus primitif sont possiblement responsables pour une diminution importante des concentrations en Cr et V des oxydes de Fe-Ti qui coïncident avec les modifications lithostratigraphiques, des gabbros disséminés aux séquences ultramafiques interlitées avec les oxydes massifs. Ces injections de magma mettent en évidence l'histoire magmatique polyphasée des séquences litées du Complexe de la Rivière Bell et de ses horizons de minerai de vanadium.

Acknowledgments

First, thank you to Dr. Sarah Dare for supervising this project, and we acknowledge that this project was funded in part by her NSERC Discovery Grant (RGPIN-2015-05924) and University of Ottawa start-up funds. We thank VanadiumCorp Resources Inc. for permitting us access to their drill cores and outcrops for sampling purposes, and thank Réjean Girard and his staff at IOS Services Géoscientifique in Chicoutimi, Quebec for their hospitality and allowing us the use of their facilities and equipment during sampling sessions. I also need to thank Glenn Poirer for his enthusiastic assistance with the electron microprobe at the University of Ottawa, and thank Zhaoping Yang, Simon Jackson (Geologic Survey of Canada, Ottawa) and Samuel Morfin (UOttawa) for their help with LA-ICP-MS analyses, and for their insightful discussions. Thanks also to Alain Mauviel and George Mrazek at the University of Ottawa for preparing thin sections. Thanks to Dr. Keiko Hattori and Dr. Richard Ernst for serving as examiners of this thesis and for their helpful comments. Finally, I have to thank my family for their unwavering support of all of my pursuits, academic or otherwise.

Table of Contents

List of Figures

List of Tables

1 INTRODUCTION

Vanadium deposits in mafic igneous intrusions generally occur as stratiform, Fe-Ti oxide-rich layers, in which V is primarily concentrated in titaniferous magnetite (Taner et al., 1998). While layered mafic intrusions (LMI) are a relatively common feature on Earth (Scoates and Wall, 2015), not all contain economically significant concentrations of V-rich magnetite, and among those that do, the geologic processes responsible for their formation remain enigmatic. Most petrogenetic models for the formation of V ores fall into one of two broad categories: those involving progressive fractional crystallization of a common parental magma in a closed system (e.g. Upper Zone of the Bushveld Complex, South Africa; Reynolds, 1985b), or those in which a magma chamber behaves as an open system, and Fe-Ti-V oxide ore horizons form through multiple injections of magma (e.g. Panzhihua intrusion, China; Pang et al., 2009). Which model a LMI falls into is often inferred by examining cryptic trends, i.e. variations in mineral chemical compositions (e.g. Mg# of pyroxenes, An-content of plagioclase) across its igneous stratigraphy, since sharp changes in cryptic trends are generally thought to reflect changes in magma composition that arise from processes supplementary to progressive differentiation, such as magma injections (Barnes et al., 2004; Ashwal et al., 2005; Tegner et al., 2006; Namur et al., 2010). In Fe-Ti oxides, the concentrations of trace elements such as Cr and V have traditionally been used for these purposes, since both are highly compatible in magnetite and ilmenite during fractional crystallization, and therefore their abundances in these minerals should be sensitive indicators of changes in magma composition (McCarthy and Cawthorn, 1983; Jang et al., 2001; Tegner et al., 2006; Charlier et al., 2007; Namur et al., 2010).

Advancements in analytical techniques such as laser ablation inductively coupled plasma mass spectrometry (LA-ICP-MS) have led to the characterization of a broader suite of trace

elements in Fe-Ti oxides in a variety of geologic settings (Klemme et al., 2006; Méric et al., 2012; Dare et al., 2012, 2014; Liu et al., 2015), which may allow for the use of additional elements as tracers of magmatic processes. This has application in determining the petrogenesis of layered intrusions and associated ore deposits, particularly in metamorphic environments where the igneous silicate mineralogy is not well preserved. However, although the partitioning behaviour of many trace elements during fractionation is understood, very little is known about their behaviour during post-magmatic processes such as metamorphism. In this study, we attempt to use the trace element compositions of magnetite and ilmenite to model the formation of vanadium deposits in the Rivière Bell Complex (RBC), a Neoarchean LMI near Matagami, Quebec, Canada that has been metamorphosed to greenschist-amphibolite facies. The geochemistry and petrogenesis of the RBC have been previously studied by several authors (Maier et al., 1996, Taner et al., 1998; Goutier, 2005; Munoz, 2010; Roudaut, 2013), who have analyzed whole-rock compositions and some mineral compositions (by electron microprobe) of rocks throughout the intrusion. However, only a few studies have focused on its vanadium mineralization (Taner et al., 1998; Roudaut, 2013), none of which have examined chemostratigraphic variations across its Fe-Ti oxide-rich layered series. Nor have they considered the potential effects of metamorphism on the chemical compositions of Fe-Ti oxides. We present in this study the first LA-ICP-MS data from Fe-Ti oxides in the RBC, and combined with detailed petrographic observations attempt to determine which trace elements are present in concentrations that reflect the primary magmatic compositions of these minerals, and which may be susceptible to modification during post-magmatic processes. Cryptic trends of trace elements deemed representative of igneous processes are then considered alongside lithostratigraphic and field observations to determine whether the vanadium ore deposits formed in a magma chamber that was open or closed to recurrent magma injections.

2 GEOLOGY OF THE RIVIÈRE BELL COMPLEX

2.1 Regional Geology

The RBC, which is also commonly referred to as the Bell River Complex, is a mafic-ultramafic intrusion located near the town of Matagami, Quebec on the northern margin of the Abitibi Greenstone Belt in the Superior Province of Canada (Fig. 1a, b). The regional geology of the Matagami area has been previously described in detail by several authors (e.g. Freeman, 1939; Jenney, 1961; Piché et al., 1993; Maier et al., 1996; Goutier, 2005; Ross et al., 2014), from which the following is summarized. The RBC intrudes the volcanic rocks of the Watson Lake and overlying Wabassee groups (Fig. 1c). The Watson Lake group is approximately 2 km thick and predominantly felsic in nature, composed of basal massive and lobate dacites overlain by effusive rhyolites that are identifiable across a distance of at least 19 km on the southwestern margin of the RBC (Ross et al., 2014). Above the Watson Lake group are the mafic-to-intermediate volcanic rocks of the Wabassee Group, which itself is subdivided into basal andesitic basalts of the Allard River unit and overlying pillowed basalts of the Bell River unit (Piché et al., 1993). Separating the Watson Lake and Wabassee groups is the so-called Key Tuffite, a 0.3-12 m thick volcanoclastic-exhalative unit comprised of andesitic tuff (Genna et al., 2014). The Key Tuffite has long been recognized as marker horizon for numerous Zn-rich volcanogenic massive sulfide (VMS) deposits in the Matagami Mining Camp (Fig. 1c) (Jenney, 1961; Genna et al., 2014; Ross et al. 2014).

Similar U-Pb ages of zircons in the Watson Lake rhyolite (2725.9 ± 0.8 Ma, Ross et al., 2014) and granophyric rocks from the top of the RBC (2724.6 ± 2.5 Ma, Mortenson, 1993) suggest that the RBC is a Neoarchean-aged synvolcanic intrusion. In the model of Maier et al. (1996), the felsic volcanics of the Watson Lake group were subaqueously erupted from

differentiates of the RBC following its initial intrusion into the upper crust. Heat from the emplacement of the intrusion also likely drove hydrothermal circulation responsible for the formation of the various VMS deposits in the subsequently deposited Key Tuffite (Carr et al., 2008). These were then overlain by the mafic volcanics of the Wabassee Group, following which the RBC underwent one final stage of emplacement by intruding the overlying volcanic sequence. Such a model is supported by the continuous nature of rare-earth element (REE) differentiation trends between the intrusive rocks of the RBC and the volcanic rocks of the Wabassee and Watson Lake groups (Maier et al., 1996).

The RBC occupies the core of two prominent anticlines in the region: the northwest-southeast trending, northwest plunging Galinée anticline, and the east-west trending Pouchot anticline (Fig. 2) (Beaudry and Gaucher, 1986; Goutier, 2005). The geologic relationships between the RBC and its country rocks are best observed on the southwestern flank of the Galinée anticline, where they are relatively undeformed and dip at approximately 56° southwest (Maier et al., 1996). Most of the remainder of the southern and southeastern flanks are in fault contact with the Wabassee group and younger siliciclastic sedimentary rocks of the Taibi Group (Fig. 2a) (Goutier, 2005). Rocks dip sub-vertically on the northern flank of the Galinée anticline, and the volcanic stratigraphy is complicated by fault-related repetition of several structural blocks in what is referred to as the Lac Garon high-strain zone. However, the stratigraphy broadly correlates with that observed in the southwest (Piché et al., 1993). The RBC and its country rocks have also been variably metamorphosed at greenschist to amphibolite facies conditions (Goutier, 2005). This is likely related to a combination of regional deformation associated with N-S shortening, and local contact metamorphism resulting from the emplacement

of various felsic intrusions in the region, most notably the Lac Olga pluton along the northern margin of the RBC at 2693 ± 3 Ma (Jolly, 1978; Mortenson, 1993).

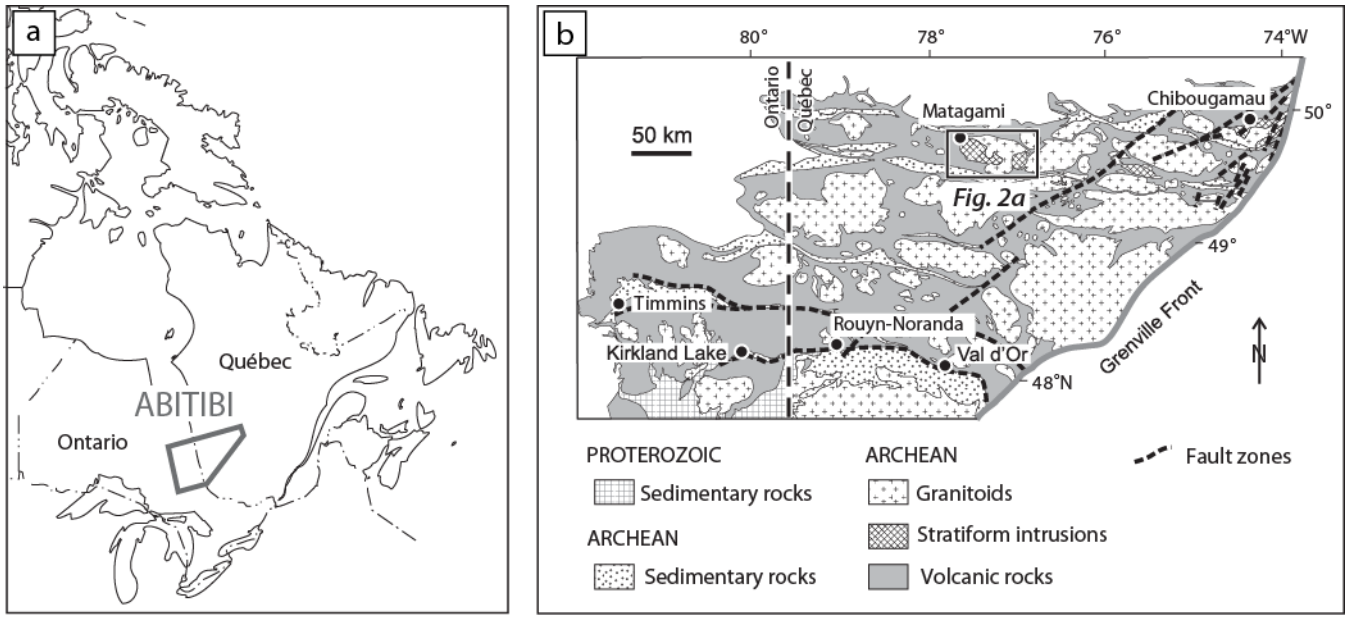

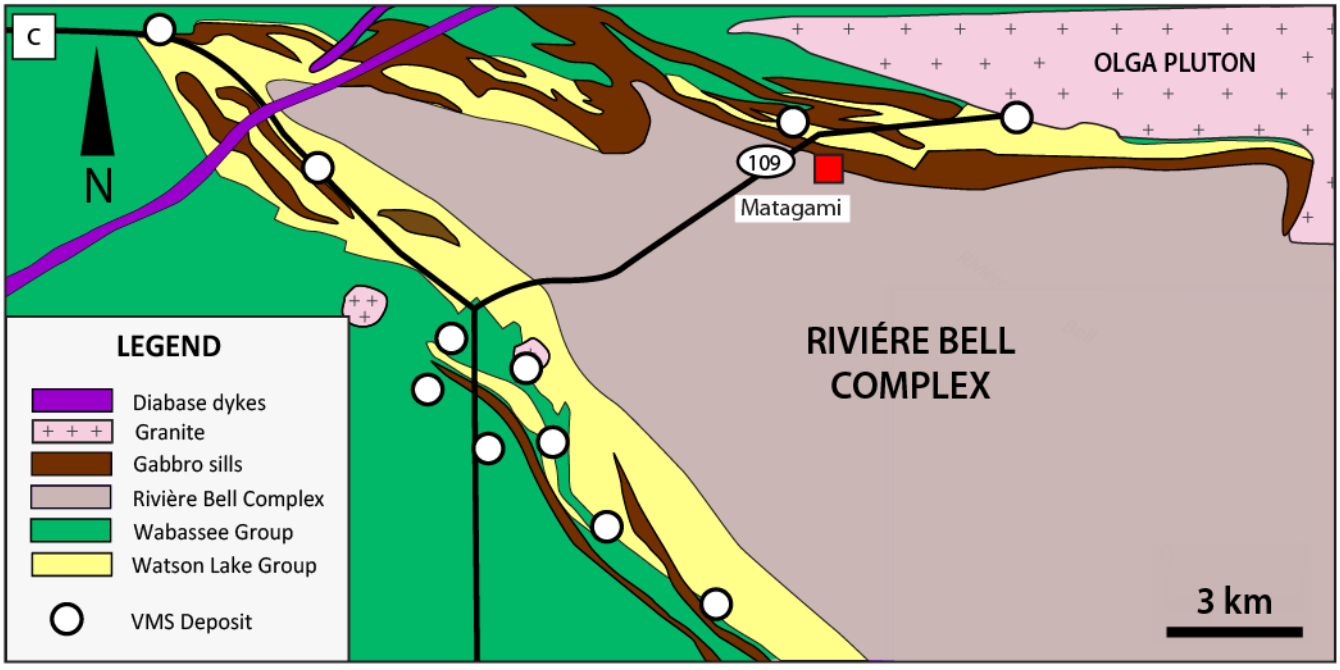

Fig. 1. Regional geology of the Abitibi Greenstone Belt and Matagami region. **a.** Location of the Abitibi Greenstone Belt in Canada; **b.** Simplified geology of the Abitibi Greenstone Belt, showing the location of the Rivière Bell Complex near Matagami; **c.** Simplified geology of the Matagami region, showing the geological relationships between the Rivière Bell Complex and the felsic and volcanic country rocks of the Watson Lake and Wabassee Groups, respectively, and the locations of historically significant VMS deposits. **a** and **b** modified from Ross et al. (2014) after Daigneault et al. (2002) ; **c** modified from Genna et al. (2014).

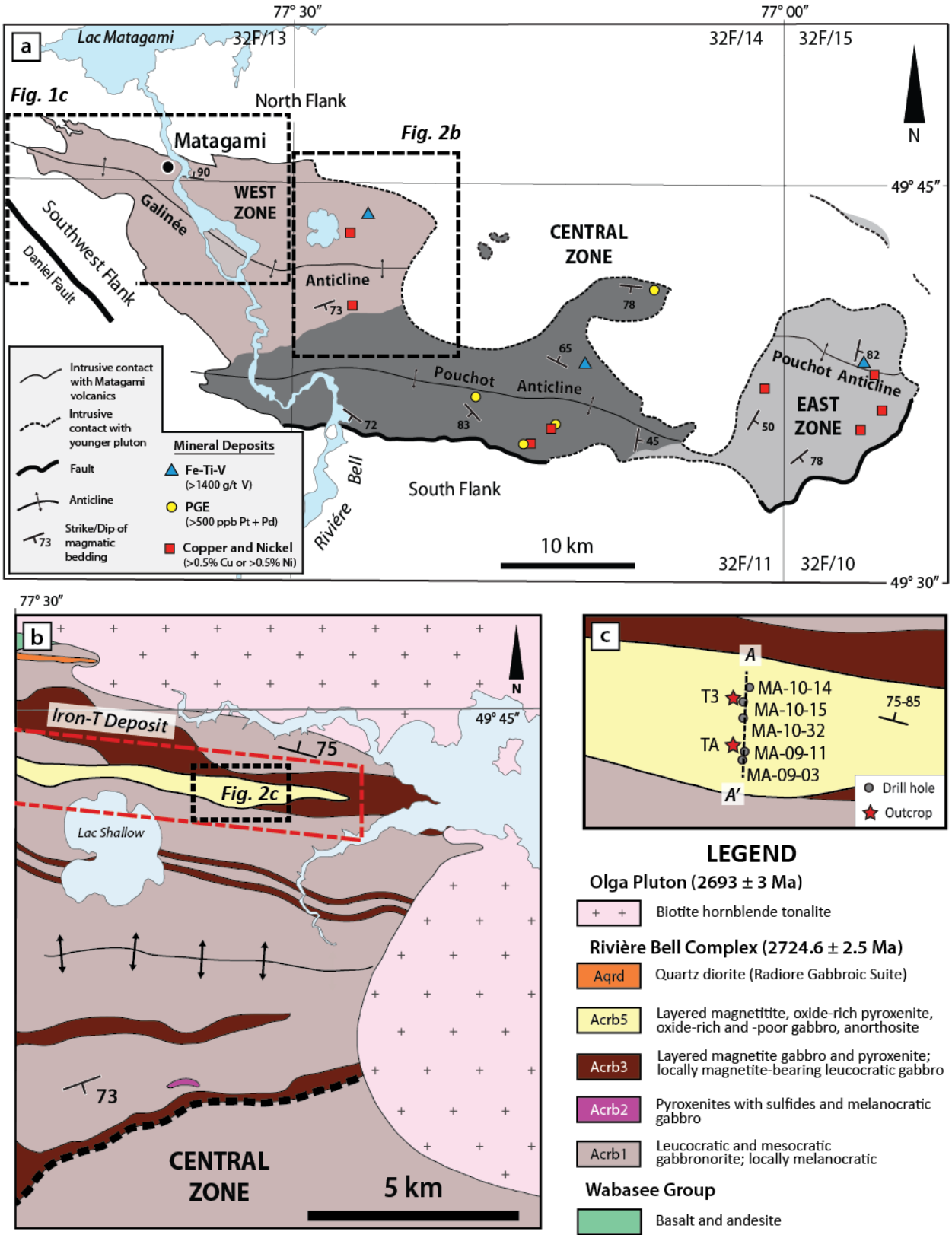

Fig. 2. Geology of the Rivière Bell Complex. **a.** Regional subdivisions of the Rivière Bell Complex as defined by Goutier (2005) and locations of various prospective magmatic mineral deposits; **b.** Geology of the West Zone of the Rivière Bell Complex in the region of the Iron T property. Red box marks the location and regional extent of the Iron-T property; **c.** Surface locations of the outcrops and diamond drill holes from which samples were collected for this study. A-A' indicates the profile along which the cross-section in Fig. 3 is constructed. After Goutier (2005).

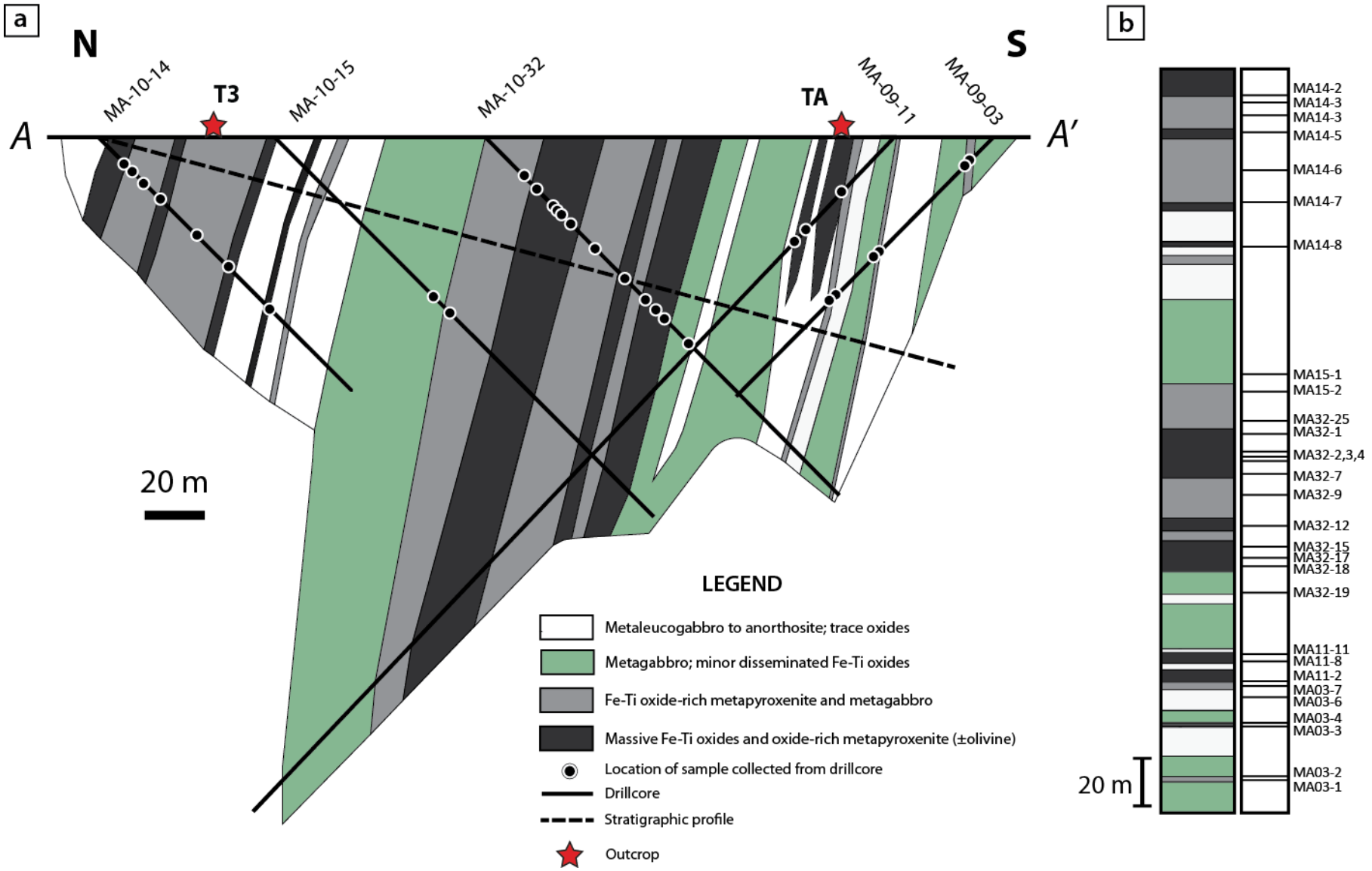

Fig. 3. Stratigraphy of the Iron-T deposit with drill core sample locations. **a.** Schematic cross-section of the RBC at the Iron-T deposit (from A-A' in Fig. 2c) with positions of hand samples from which thin sections were made plotted along their respective drill holes (modified from Roudaut, 2013); **b.** Generalized stratigraphic column (left) and projected depths of hand samples in this study (right) corresponding to the stratigraphic profile in **a** (dashed line). Note that the lithologies shown in the stratigraphic column of **b** are those of the samples that have been projected onto the schematic stratigraphic profile, and not necessarily those that are intersected by the profile line as shown in **a.**

2.2 Geology of Fe-Ti-V deposits in the Rivière Bell Complex

The intrusive rocks of the RBC cover an area of about 25 km by 65 km, and it has been interpreted to represent a subvolcanic sill which, prior to deformation, had a maximum thickness of about 6.5 km (Maier et al., 1996; Goutier, 2005; Carr et al., 2008). It hosts several prospective magmatic mineral deposits (Fig. 2), including Fe-Ti-V, Ni-Cu, and potential reef-style Pt-Pd deposits (Goutier, 2005; Munoz, 2010), and previous studies have consequently compared it to other world-class layered intrusions such as the Stillwater Complex, USA (Freeman 1939) and the Bushveld Complex, South Africa (Maier et al. 1996; Taner et al. 1998). Goutier (2005) subdivided the intrusion into three zones based on lithological characteristics, and which are interpreted to represent different stages of its evolution (Fig. 2a). The Central Zone is believed to represent the oldest and deepest portion of the RBC, and is composed predominantly of layered gabbros and minor pyroxenites that are host to the majority of its PGE mineralization (Goutier 2005). The Western Zone is the youngest, uppermost portion, which has been stratigraphically subdivided by previous studies into an upper border/granophyre zone; a layered zone, consisting of variably magnetite- and ilmenite-rich gabbros, pyroxenites, and anorthosites that are cumulatively 500-1000 m thick; and a 5 km thick basal Main zone that is composed of massive gabbros (Sharpe, 1968; Maier et al., 1996). The Eastern Zone of the RBC is of intermediate age, and consists primarily of leucogabbros and anorthosites (Goutier, 2005).

Fe-Ti-V deposits associated with the 'Iron-T' property in the RBC are located in the eastern portion of the West Zone, approximately 1.8 km N-NE of Lac Shallow (Fig. 2b). Inferred mineral resource estimates for the Iron-T property, which is currently owned by VanadiumCorp Resources, total 14.38 Mt at 0.77% V_2O_5Eq (Dupéré, 2011). They are hosted by the magnetite- and ilmenite-rich metapyroxenites and metagabbros of an WNW-ESE trending unit within the

layered zone of the RBC (unit Acrb5, Fig. 2b) (Goutier 2005). This unit is approximately 500 m thick, and aeromagnetic data suggests it has a total lateral extent of about 10 km across the northern limb of the Galinee Anticline, 7.8 km of which are contained within the Iron-T property (Dupéré, 2011). It consists of several banded, Fe-Ti oxide-rich melanocratic horizons, which cumulatively may be meters to tens-of-meters thick, that are interlayered with more massive leucocratic horizons made up of oxide-poor gabbros, leucogabbros, and anorthosites (Fig. 3) (Goutier, 2005; Roudaut, 2013). Layering in the region of the deposit strikes at approximately 285 degrees and dips subvertically between 75 and 85 degrees (Dupéré, 2011; Roudaut, 2013), and contacts between the banded melanocratic and leucocratic horizons are generally well-defined (Taner et al., 1998).

Igneous layering in the oxide-rich melanocratic portions of the RBC may be both compositional or textural, and apart from regional-scale deformation the rocks presumably retain their macroscale igneous textures, despite being metamorphosed. Compositional layering is characterized by changes in mineralogy (Figs. 4, 5). Oxide-rich layers are typically centimeters to decimeters thick, consisting of semi-massive or massive oxides and magnetite- and ilmenite-pyroxenites, gabbros, and rare dunites, with alteration mineralogies representative of amphibolite facies. Metamorphosed pyroxenites generally appear dark grey-green due to the alteration of pyroxene to actinolite (e.g. Fig. 5a), whereas gabbros appear as variably blotchy mixtures of white and green from the alteration of pyroxenes and plagioclase to calcic amphiboles, chlorite, and epidote (Fig. 5b). These melanocratic lithologies occur interlayered with each other, and with oxide-poor metagabbros or metaleucogabbros of similarly variable thickness.

Textural layering occurs in the form of modally graded layers, where Fe-Ti oxides and/or mafic minerals within individual layers exhibit normal grading (e.g. Fig. 5c.). In cumulates of

gabbroic protoliths, this effectively produces semi-rhythmically layered sequences where Fe-Ti oxides and plagioclase are internally concentrated at the base and top of individual layers, respectively (Fig. 4a, b, d). Contacts between the oxide-rich bases of layers and plagioclase-rich portions of underlying layers are typically sharp. However, not all layers exhibit mineral grading, and it is quite common for magnetite-rich bands to have relatively homogenous mineral proportions. In such cases, both upper and lower contacts between successive layers are sharp and well-defined (Figs. 4c, 5a-b, 6).

Lateral continuity of layering in the region of the Iron-T deposit is variable. Correlation of drill cores suggests that melanocratic, oxide-rich horizons are not necessarily continuous down-dip over scales of tens-of-meters (Fig. 3) (Roudaut, 2013), and analogous cases of individual layers pinching out along strike are common in outcrop (Figs. 4a-c, 6, 7e). Consequently, layers may bifurcate or merge together to form thicker layers. Potential evidence of dynamic processes occurring during the development of layering is also observed, including features such as apparent cross-stratification and fault-bend fold-like layering (Fig. 7a, c). These have been interpreted in the RBC and other layered intrusions as having formed due to gravitational instabilities producing currents of magma and/or crystal slurries in a partially-crystalline magma chamber (Roudaut, 2013; Maier et al., 2013; Namur et al., 2015). Other features of interest include an abrupt lateral contact between two rhythmically layered magnetite gabbro sequences at oblique angles to each other (Fig. 7b), and the presence of several leucogabbronorite enclaves that are up to 2 meters in width, around which thin magnetite bands are deflected (Fig. 7d, e). Such enclaves are interpreted by Roudaut (2013) to be autoliths ripped up from the underlying massive gabbros, implying that the gabbros were at least partially crystallized prior to the formation of the melanocratic layered rocks above it.

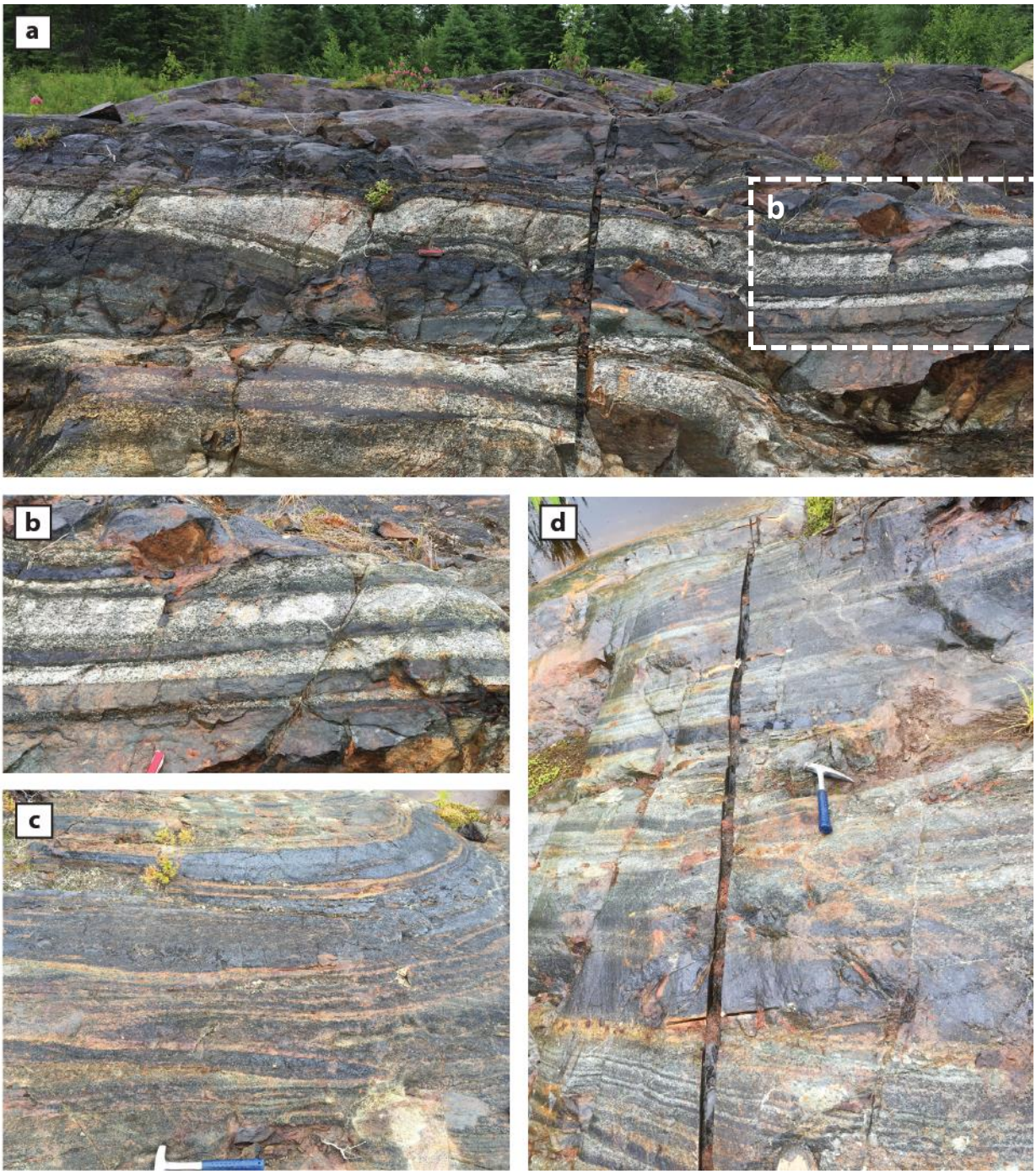

Fig. 4. Igneous layering textures of the RBC within the Iron-T property at outcrop T3. **a.** Interlayered centimeter-to-decimeters thick, variably oxide-rich metaleucogabbro (speckled white layers) and metapyroxenite (dark green-grey layers). Swiss army knife for scale; **b.** Close-up of a sequence of several centimeters-thick oxide-rich pyroxenites and leucogabbros. Melanocratic bands exhibit both sharp and modally graded upper contacts with overlying leucogabbros. Note the tapering lowermost leucocratic band; **c.** Discontinuous ribbon-like banded massive oxides and gabbros. Massive oxides exhibit sharp upper and lower contacts; **d.** Cyclically layered magnetite gabbro. Some layers exhibit internal normal grading of oxides and mafic minerals.

Fig. 5. Photos of representative oxide-rich lithologies and layering textures observed in drill cores. **a**. Homogeneous magnetite-rich olivine pyroxenite layer with sharp upper and lower contacts with adjacent leucogabbros, MA-09-11, ~40.7 m drill core depth; **b**. Magnetite-rich metagabbro layer with sharp upper and lower contacts with neighbouring leucogabbros, MA-10-32, ~76.6 m drill core depth; **c.** Massive oxide layer with normally graded Fe-Ti oxides. Note the sharp basal contact with underlying leucogabbro with alteration rim of amphiboles, MA-10-32, ~78.2 m drill core depth.

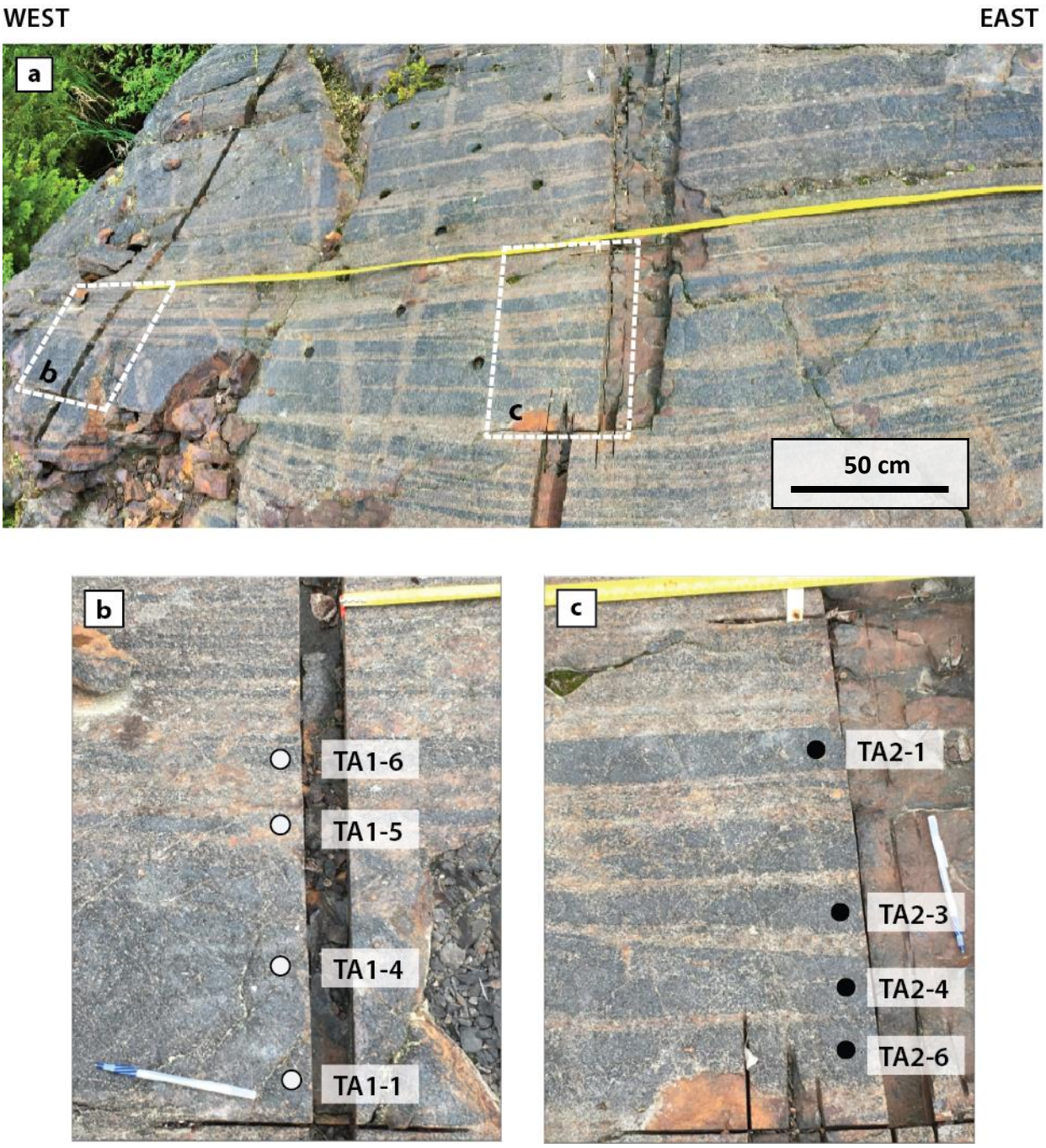

Fig. 6. Layering relationships within the Iron-T property at outcrop TA. **a.** Interlayered massive oxides and pyroxenites. Several oxide bands bifurcate (see **b** and **c**) or display lateral variations in thickness. Note that the panorama-style of the photo results in a slight apparent curvature of the lowermost layering, which is actually straight; **b.** profile TA1; **c.** profile TA2. White and black circles in **b** and **c**, respectively, indicate locations from which Fe-Ti oxides were analyzed. The single thick massive oxide layer at the base of TA1 laterally thins and bifurcates to form the two lowermost bands in TA2. The oxide bands corresponding to samples TA1-6 and TA1-5 are laterally correlative with those of TA2-1 and TA2-3, respectively. The oxide band separating TA2-1 and TA2-3 in **c** pinches out prior to profile TA1 (see **a**). Way up is towards the north.

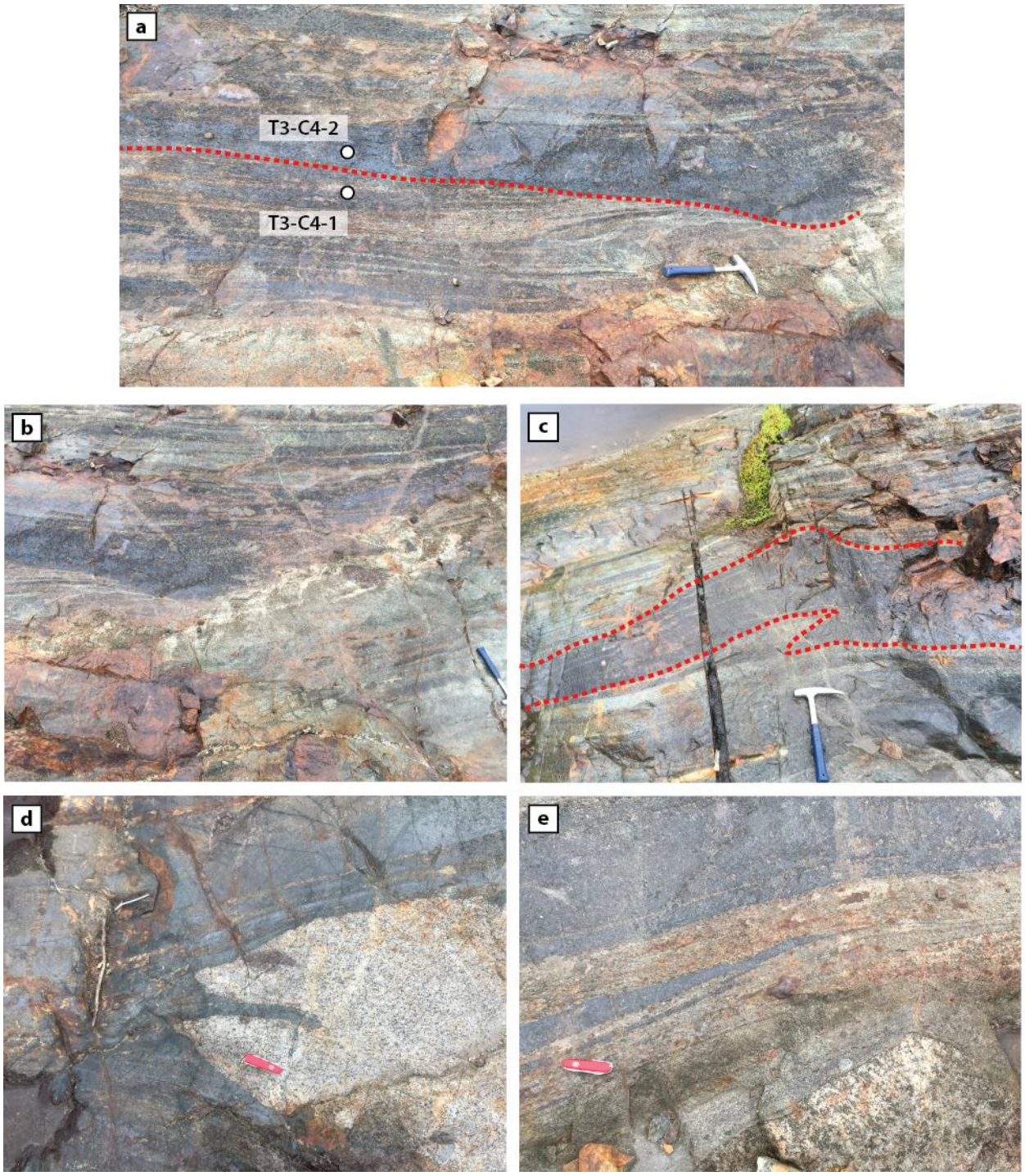

Fig. 7. Irregular layering features in outcrops of the RBC within the Iron-T property; **a.** Cross-stratified oxide-rich layers in outcrop T3. The 10-20 cm thick massive oxides above the inferred cross-stratification plane (dashed line) truncates several thin oxide and gabbro bands below it. White circles represent sampling locations; **b.** Contact between two rhythmically layered magnetite gabbro sequences in outcrop T3. Layering in the bottom right of the photo is oriented approximately 20° off of that in the upper left, which are separated by an amorphous leucocratic zone; **c.** Apparent thrust fault-bend folding of a sequence of several closely spaced massive oxide bands in outcrop T3. Dashed lines indicate the upper and lower contacts of the bent oxide band; **d.** Centimeters-thick massive oxide bands deflecting around a leucogabbronorite enclave in outcrop TA; **e.** Banded Fe-Ti oxides and pyroxenites gently bending around a leucogabbronorite enclave in outcrop TA. Note how several pyroxenite bands merge together as a magnetite band pinches out laterally. All photos are oriented stratigraphic way-up.

3 SAMPLING METHODS

3.1 Drill core sampling

Sampling was conducted from five drill cores which cumulatively intersect approximately 300 m of igneous stratigraphy in the Fe-Ti oxide-rich layered unit host to the Iron-T deposit (Acrb5) (Figs. 2c, 3). The cores in question were made available by VanadiumCorp Resources Inc., and sampling was performed at IOS Services Géoscientifiques Inc. in Chicoutimi, Quebec, where the cores are stored. The geographic details of the drill holes from which they were collected are listed in Table 1. Correlation of these drill cores was performed previously by Roudaut (2013) and updated in this study based on personal observations.

A total of 41 polished thin sections (Table 2) were prepared from 30 oriented hand samples - each about 10-50 cm in length - that were collected from the drill cores. The depth of each sample along its respective drill core was recorded, and their approximate positions within the stratigraphy are shown in Fig. 3. The majority of thin sections were prepared from the bases of oxide-rich layers, although a few were selected to cross the contact between two successive layers (or in the case of sample MA32-18, across both the upper and lower contact of a 1 cm thick oxide-rich olivine gabbro that is over- and underlain by oxide-poor leucogabbros) in order to examine if mineral compositions vary across adjacent layers at a thin section scale.

The stratigraphic depth of each thin section (Table 2) was determined by projecting its drill core depth onto a single linear profile plunging orthogonal to layering, originating at the intersection point of drill core MA-10-14 and the surface (Fig. 3). Although the dip of layering is observed to vary between 75-85 degrees in the region of these drill cores (Dupéré 2011; Roudaut, 2013), for the purposes of this study it is assumed that layering has a constant dip of 75

degrees to the north. The stratigraphic depths of the samples along this profile were calculated for the three south-plunging drill holes (MA-10-14, MA-10-5, and MA-10-32) with the formula

$$Stratigraphic\ Depth = \Delta X * cos\ 15 - (Drillcore\ Depth) * sin(75 - \theta) - \Delta E * sin15$$

and for the two north-plunging drill holes (MA-09-11 and MA-09-03) with the formula

$$Stratigraphic\ Depth = (Drillcore\ Depth) * cos(\theta - 15) + \Delta X * cos15 - \Delta E * sin15$$

where θ is the angle at which the drill hole in question plunges into the surface, ΔE is the elevation difference between where it and MA-10-14 each intersect the surface, and ΔX is the horizontal N-S distance from the top of the drill hole to that of MA-10-14 (Table 1).

Table 1. Geographic details of drill cores that were sampled in this study.

Drill hole ID	UTM East[1]	UTM North[1]	ΔX (m) [2]	Elevation (E) (m)	ΔE (m) [3]	Plunge	
						Angle (°)	Direction
MA-10-14	324998.31	5511873.14	0	289.63	0	45	S
MA-10-15	324965.22	5511814.21	58.93	292.88	3.25	45	S
MA-10-32	324964.51	5511743.44	129.7	291.22	1.59	46	S
MA-09-11	324968.93	5511605.74	267.4	294.20	4.57	45.5	N
MA-09-03	324959.67	5511573.67	299.47	292.55	2.92	45	N

[1] Datum is NAD83, UTM Zone 18

[2] ΔX is the geographic N-S distance between the point of intersection of the drill core with the surface and that of the northernmost drill core (MA-10-14).

[3] ΔE is the elevation difference between the points where the drill hole in question and MA-10-14 intersect the surface.

It is important to note that this composite stratigraphic profile is assumed to lie in a single N-S plane, despite the geographic positions of the drill holes spanning an E-S distance of approximately 40 m (Table 1). Since the primary objective of this study is to examine vertical chemostratigraphic trends across the Iron-T deposit as a means of studying magmatic processes, it is assumed that there are no geochemical variations either along strike or down-dip within the igneous stratigraphy. As such, this E-W offset between drill holes is disregarded. Additionally, in cases such as the southern portion of Fig. 3a, where the correlation of drill cores MA-09-03, MA-09-11, and MA-10-32 suggests that several massive oxide layers pinch out down-dip, these layers have been extrapolated down-dip onto the schematic stratigraphic profile (Fig. 3b).

Table 2. Projected stratigraphic depths of thin sections prepared from drill core samples. Hand sample ID refers to the drill core sample from which the thin section was made (Fig. 3). Reported thin section depths are to the center of the thin section in question. Projected depth calculated using the formulas outlined in section 3.1.

Thin Section ID	Drill core	Hand Sample ID	Drill core Depth (m)	Projected Stratigraphic Depth (m)
MA14-2A	MA-10-14	MA14-2	10.64	9.21
MA14-2D	MA-10-14	MA14-2	11.06	9.58
MA14-3A	MA-10-14	MA14-3	15.75	13.64
MA14-3B-T	MA-10-14	MA14-3	15.91	13.78
MA14-3B-B	MA-10-14	MA14-3	16.10	13.94
MA14-4	MA-10-14	MA14-4	20.43	17.69
MA14-5A	MA-10-14	MA14-5	28.50	24.68
MA14-5C	MA-10-14	MA14-5	28.75	24.90
MA14-6A-T	MA-10-14	MA14-6	46.73	40.47
MA14-6B	MA-10-14	MA14-6	47.04	40.74
MA14-7A	MA-10-14	MA14-7	59.83	51.81
MA14-7B	MA-10-14	MA14-7	59.95	51.92
MA14-8A	MA-10-14	MA14-8	80.22	69.47
MA14-8B	MA-10-14	MA14-8	80.38	69.61
MA15-1	MA-10-15	MA15-1	73.50	119.73
MA15-2	MA-10-15	MA15-2	81.82	126.94
MA32-25	MA-10-32	MA32-25	17.02	139.46
MA32-1A	MA-10-32	MA32-1	24.13	145.55
MA32-1C	MA-10-32	MA32-1	24.39	145.78
MA32-2A-T	MA-10-32	MA32-2	32.25	152.51
MA32-2A-B	MA-10-32	MA32-2	32.40	152.64
MA32-2B	MA-10-32	MA32-2	32.63	152.84
MA32-3	MA-10-32	MA32-3	34.53	154.47
MA32-4	MA-10-32	MA32-4	35.85	155.60
MA32-7	MA-10-32	MA32-7	41.32	160.29
MA32-9	MA-10-32	MA32-9	52.35	169.74
MA32-12	MA-10-32	MA32-12	62.89	178.78
MA32-15	MA-10-32	MA32-15	74.25	188.51
MA32-17	MA-10-32	MA32-17	78.60	192.24
MA32-18	MA-10-32	MA32-18	83.88	196.77
MA32-19	MA-10-32	MA32-19	94.57	205.93
MA11-11	MA-09-11	MA11-11	46.62	234.15
MA11-8	MA-09-11	MA11-8	41.48	236.68
MA11-2	MA-09-11	MA11-2	25.15	244.72
MA03-7	MA-09-03	MA03-7	77.25	249.89
MA03-6	MA-09-03	MA03-6	74.89	251.07
MA03-4	MA-09-03	MA03-4	55.32	260.85
MA03-3	MA-09-03	MA03-3	54.25	261.39
MA03-2	MA-09-03	MA03-2	14.28	281.37
MA03-1B	MA-09-03	MA03-1	12.10	282.46
MA03-1A	MA-09-03	MA03-1	11.96	282.53

3.2 Outcrop Sampling

In addition to sampling from drill cores, Fe-Ti oxide-rich samples were collected from two outcrops of the RBC (identified as TA and T3 following Dupéré, 2011) that lie near the plane formed by the five drill cores of interest in this study (Table 3). Outcrop TA is located approximately 50 m WNW from the surface location of drill hole MA-10-15 (Fig. 2c), and is correlative with the uppermost, oxide-rich 50 m of the schematic stratigraphic profile (Fig. 3). Outcrop T3 is roughly 60 m NNW from MA-09-11, and is presumably correlative with the lowermost massive oxide band intersected by MA-09-11. Sampling was performed with the intention of investigating variations in Fe-Ti oxide chemistry on a smaller scale (< 1 m) and their implications for the formation of geologic features that are suggestive of dynamic magma chamber processes (see section 2.2). Note that while the approximate geographic relationships between these outcrops and the locations of the sampled drill holes are known, the stratigraphic depths of these samples relative to those collected from drill cores cannot be accurately determined. For this reason, the Fe-Ti oxide chemistry of samples collected from outcrop are not included with data from drill core samples when considering deposit-scale chemostratigraphic variations below.

From outcrop T3, two samples (T3-C4-1 and T3-C4-2) were collected from a channel cut across the cross-stratified oxide layers shown in Fig. 7a. T3-C4-2 is taken from massive oxides located 5 cm above the trace of the cross-stratification plane, while T3-C4-1 is 5 cm below. From outcrop TA, two channels were cut perpendicular across a sequence of several centimeters-thick massive oxide bands that are interlayered with relatively oxide-poor pyroxenites (Fig. 6). The two channels, TA1 (Fig. 6b) and TA2 (Fig. 6c), are separated along strike by approximately 2 m. Four samples were taken from each channel, corresponding to four oxide layers that are laterally

correlative across the sequence. The lowermost two samples from each channel represent a single massive band (~20 cm outcrop thickness) at TA1 which has thinned and laterally bifurcated into two separate bands, approximately 5 cm thick each, at TA2 (note that these two samples are also more closely spaced at TA2 than they are at TA1). The uppermost two samples from each channel are from two oxide layers that are laterally continuous across the sequence, although they do slightly thin out towards TA1.

Table 3. Details of thin sections prepared from outcrop samples. Refer to Figs. 4 and 6.

Outcrop	GPS Coordinates of Outcrop	Thin Section ID	Details
T3	N 49° 44' 00.4" W 77° 25' 44.9"	T3-C4-1	Oxide-rich band 5 cm above cross-stratification horizon
		T3-C4-2	Oxide-rich band 5 cm below cross-stratification horizon
TA	N 49° 43' 53.7" W 77° 25' 44.7"	TA1-1	Laterally correlative with TA2-6
		TA1-4	Laterally correlative with TA2-4
		TA1-5	Laterally correlative with TA2-3
		TA1-6	Laterally correlative with TA2-1
		TA2-6	Laterally correlative with TA1-1
		TA2-4	Laterally correlative with TA2-4
		TA2-3	Laterally correlative with TA2-3
		TA2-1	Laterally correlative with TA1-6

4 PETROGRAPHY

Thin sections were analyzed optically by petrographic microscope and with backscatter electron (BSE) imagery using an electron microprobe analyzer (EMPA) at the University of Ottawa. Mineralogy, modal Fe-Ti oxide proportions, and oxide microtextures (i.e. exsolutions and alteration textures) were documented (Table 4). If a thin section crossed a distinct contact between adjacent layers, defined as either 1) a sharp change in cumulate or alteration mineralogy, or 2) similar mineralogy, but with a sharp change in relative modal proportions, the above characteristics were documented separately for each sub-lithology.

4.1 Lithological descriptions

Host rocks from which mineral compositions were analyzed in this study are predominantly massive Fe-Ti oxides (*n*=3) and oxide-rich melanocratic lithologies such as pyroxenites (*n*=15) and olivine pyroxenites (*n*=15), gabbros (*n*=10), olivine gabbros and gabbronorites (*n*=4), and dunite (*n*=1). Oxide-poor lithologies (<5% Fe-Ti oxides) include leucogabbros (*n*=11). In most cases the primary cumulate mineral assemblages of the samples are not preserved (Table 4). Instead, they are overprinted by mineral assemblages and textures typical of metamorphism at amphibolite facies conditions. Consequently, in most cases the prefix “meta” should be affixed to the above-listed lithologies. However, for clarity it will be excluded during the following discussion.

Other than those samples classified as massive oxides (>90 percent Fe-Ti oxides), olivine-bearing pyroxenites are typically the most oxide-rich lithologies collected in this study. They consistently contain greater than 45 percent medium-to-coarse grained Fe-Ti oxides with high ratios of magnetite to ilmenite (Mgt/Ilm = 3-9) (Fig. 8). Their cumulate silicate minerals

show variable degrees of alteration. Relatively fresh, subhedral clinopyroxene up to 4 mm long is occasionally present (Fig. 9a), although in most cases it is only preserved as patchy high-relief cores, potentially with relict cleavages traces (Fig. 9b). Aggregates of fine, pale-green chlorite are often observed around the margins of, or completely replacing, clinopyroxene in these cases. This style of chlorite alteration is also typical of interstitial silicate patches in massive oxide samples (Fig. 11a). Coarse, anhedral olivine is observed in several samples, along with a potential second generation of equigranular, fine-grained olivine that occur in clusters or as rims around cores of serpentine (Fig. 9a), or associated with clinopyroxene. The highly polygonal grain boundaries of this finer variety of olivine, if igneous in nature, would indicate greater amounts of subsolidus interface adjustment (Reynolds, 1985a; Vernon, 2004), such as has been documented in peridotites from other layered igneous complexes such the Rum Layered Suite, Scotland (Emeleus et al., 1996). However, its resemblance to olivine typically found in metamorphic rocks (Vernon, 2004) and tendency to form rims between Fe-Ti oxides and altered interstitial silicates suggests they may be coronas of metamorphic origin. Both varieties of olivine in these rocks may be pseudomorphically altered to serpentine or saponite (Fig.9b).

Pyroxenites examined in this study most often exhibit pervasive pseudomorphic alteration of medium-grained pyroxenes to fine-grained masses of actinolite (Fig. 9c), although distinct high-relief cores of clinopyroxene are preserved in some samples (Fig. 9d). The only other cumulate minerals are disseminated to semi-massive (20-60%) magnetite and ilmenite, which coexist in highly variable proportions across the samples analyzed, although magnetite is always present in greater amounts than ilmenite (Fig. 8). Other alteration minerals include chlorite, minor hornblende that occasionally forms dark blue-green rims around the margins of magnetite (Fig. 9d), and rarely colourless monoclinic amphiboles that presumably belong to the

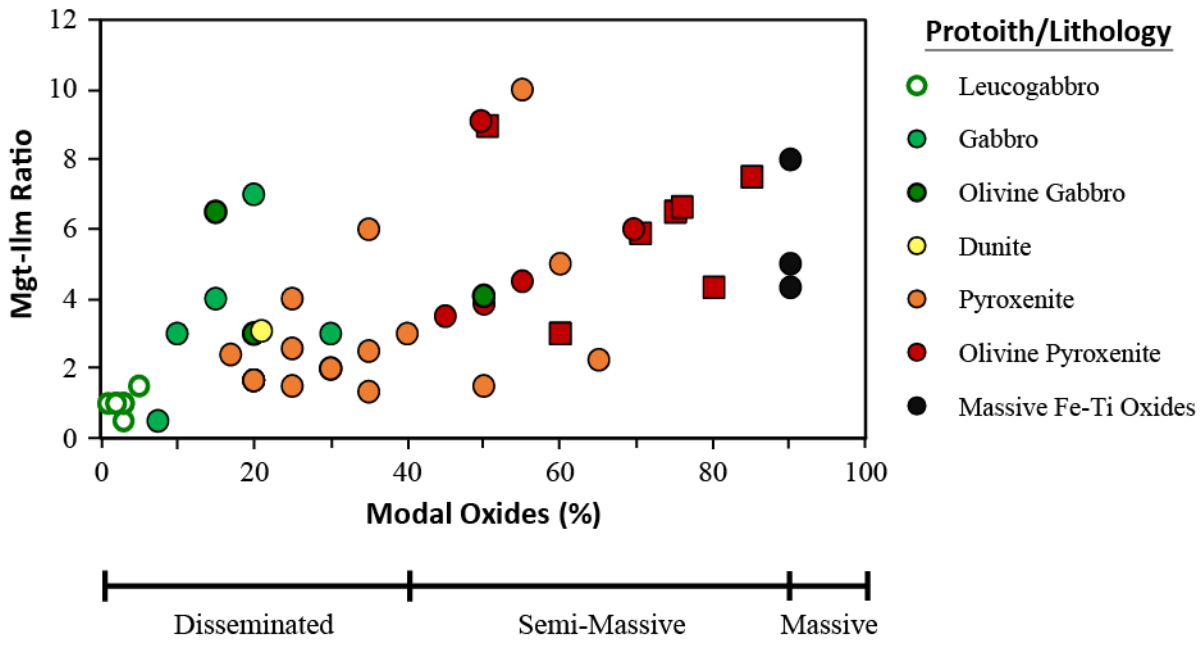

Fig. 8. Ratio between primary magnetite (mgt) and ilmenite (ilm) versus the total amount primary Fe-Ti oxides (mgt + ilm) within a sample. Circles indicate drill core samples; squares indicate outcrop samples. Samples are broadly classified as either disseminated, semi-massive, or massive oxides as indicated, based on the total amount of Fe-Ti oxides that they contain.

cummingtonite-grunerite series. Parallel, sublinear ilmenite lamellae may also be found mixed in with altered silicate assemblages, likely as an exsolution product from original Ti-rich pyroxene (Fig. 9c). Two samples (MA32-1A, MA32-1C) also show evidence of hydrothermal alteration and shearing, and contain abundant chlorite and serpentine.

Olivine-bearing gabbros and the lone dunite sampled in this study are relatively unaltered, and their primary cumulate mineralogy and textures are easily distinguished. Anhedral Fe-Ti oxides in olivine gabbros occur disseminated between rounded olivine, subhedral clinopyroxene and plagioclase, and minor anhedral orthopyroxene. Grain sizes of all minerals typically range between 0.5-2 mm (Fig. 9e). Brown Ti-rich hornblende forms rims around magnetite in samples MA03-1A and -1B, and incipient alteration of pyroxenes to Ca-amphiboles and chlorite, and of olivine to serpentine and iddingsite, is observed in MA14-2D. Magnetite and

ilmenite typically make up 15-30% of these samples, again with magnetite in higher proportions, although a 1 cm thick band of olivine gabbro in sample MA32-18 (sub-lithology *b*) is approximately 50 percent oxides (Table 4).

Most gabbros and leucogabbros contain few, if any, relict igneous ferromagnesian silicates. Instead they are dominantly composed of varying proportions of hornblende, actinolite, chlorite, epidote, Fe-Ti oxides, and variably sausseritized plagioclase, although the two leucogabbro sub-lithologies of MA32-18 exhibit comparatively little alteration, and contain fresh clinopyroxene. A few gabbros display a weak igneous foliation defined by the horizontal alignment of medium-to-coarse grained plagioclase lathes, but may also exhibit a secondary foliation defined by the alignment of fine hornblende (Fig. 9f). As metamorphism makes the determination of the modal proportions of primary igneous minerals difficult, for the purposes of this study no distinction was made between gabbros and melagabbros, while leucogabbros are those in which plagioclase makes up greater than 65 percent of the modal mineralogy in thin section. In gabbros, disseminated oxides make up 10-35% of the modal mineralogy (with the exception of MA32-25, a strongly deformed sample that contains <10% oxides) and magnetite is consistently present in greater amounts than coarse-grained ilmenite (Mgt/Ilm ≈ 1.5-7.5). Leucogabbros characteristically contain only minor-to-trace amounts of Fe-Ti oxides (<5%) which in most cases is entirely ilmenite, as any primary magnetite appears to have been preferentially replaced during metamorphism (see section 4.3). However, the inferred primary magnetite contents, based on the presence of relict skeletal ilmenite exsolutions, suggest that magnetite and ilmenite had originally crystallized in approximately equal amounts (Fig. 8).

Apatite is uncommonly present as an accessory phase in these rocks. It is most notable in low proportions (<5%) within four consecutive samples in the upper 25 m of the composite

stratigraphic profile (Table 4), in which it may be up to 2 mm in length and is subhedrally associated with Fe-Ti oxides in gabbros or pyroxenites (Fig. 11i). It is only observed in one other sample, a massive oxide layer at around 190 m depth (MA32-15), in which it is euhedral and up to 500 μm in length, situated within an interstitial silicate patch altered to chlorite.

Fine sulfides are present in small amounts (<2%) in all of the rocks examined, and consist mostly of pyrrhotite and chalcopyrite with lesser amounts of pyrite and pentlandite (the latter of which is variably altered to violarite). This is a typical magmatic sulfide assemblage in rocks metamorphosed to greenschist-amphibolite facies (Duran et al., 2015), and the various phases predominantly occur disseminated as anhedral, multiphase grains, or on the margins of coarser-grained Fe-Ti oxides. They also may form rounded inclusions within magnetite or ilmenite. However, in samples exhibiting greater degrees of Fe-Ti oxide alteration, patchy sulfides may occur along ilmenite lamellae within altered magnetite, potentially due to remobilization during metamorphism (Fig. 11j).

4.2 Fe-Ti oxide microtextures

Fe-Ti oxide textures observed in this study are similar to those described in previous studies of the Rivière Bell Complex (Taner et al., 1998; Roudaut, 2013) and other titaniferous magnetite-rich intrusions (e.g. Buddington and Lindsley, 1964; Reynolds, 1985a; Von Gruenewaldt et al., 1985; Pang et al., 2008b*;* Tan et al., 2016*).* These include both primary igneous textures and those formed at subsolidus conditions or during metamorphism. Since the objective of this study relies on the analyses of primary Fe-Ti oxides as a means of elucidating igneous processes, it is important to distinguish the textural varieties of these minerals that are representative of primary processes from those that are secondary.

4.2.1 Primary magnetite microtextures

Textures in primary, titaniferous magnetite are quite variable in the RBC. In disseminated rocks magnetite is typically medium-grained and anhedral, and commonly intergrown with medium-grained, granular ilmenite interstitial to igneous or metamorphic silicate minerals, whereas in massive or semi-massive samples it forms coarse, interconnected matrices with coexisting ilmenite. However, primary igneous textures are generally not well preserved due to varying degrees of replacement by silicates as a result of metamorphism (section 4.3). Additionally, intergrown oxides in semi-massive and massive samples have seemingly undergone extensive subsolidus deformation or re-adjustment, because grain boundaries between neighbouring magnetite grains, when identifiable, are highly irregular. They may also be may be exaggerated by fractures or concentrations of fine ilmenite granules. 120-degree triple junctions between adjacent oxides are typically not observed. Magnetite is exsolution-rich in all samples, the most common product of which being ilmenite, either as granules or coarse and/or fine lamellae. Exsolutions of aluminous spinel are commonly observed as well.

4.2.1.1 Ilmenite exsolutions

Most, if not all, of the ilmenite exsolutions in magnetite are presumably not exsolutions in the strictest sense, as the solubility of ilmenite in magnetite is too low to account for the large amounts of ilmenite that are commonly found hosted in magnetite in igneous settings (Buddington and Lindsley, 1964; Von Gruenewaldt et al., 1985). Magnetite (Fe_3O_4) crystallizes from magma at high temperatures in solid solution with ülvospinel (Fe_2TiO_4), but between which an immiscibility gap exists below approximately 600°C (Vincent et al., 1957; Lindsley, 1991). Therefore, it has long been recognized that ‘exsolutions’ of ilmenite ($FeTiO_3$) are likely the

product of oxidation of the ülvospinel component to ilmenite, followed by its segregation within the host magnetite either prior to, or following physical exsolution of the ülvospinel itself (Buddington and Lindsley, 1964). The various morphologies of ilmenite that are found within magnetite can thus be described in terms of having formed either above or below the magnetite-ülvospinel solvus.

Ilmenite exsolutions observed in this study that were likely formed by oxidation-exsolution (oxy-exsolution) above the magnetite-ülvospinel solvus include subrounded granules and relatively coarse lamellae that are aligned along the {111} planes of magnetite (Fig. 10a-b). These ilmenite varieties are present in most of the samples examined, although their size and prevalence varies considerably from sample-to-sample, and often within a thin section as well. Lamellae are typically less than 50 μm wide, though they can be greater than 100 μm, and commonly exhibit changes in thickness along their lengths. They are often discontinuous, and may or may not terminate before intersecting lamellae in opposing orientations (Fig. 10a). However, "sandwich"-style lamellae (Haggerty, 1991) which span the entire length of their host magnetite grain are also occasionally observed.

Granule-style ilmenite oxy-exsolutions are most often observed concentrated along either fractures in magnetite, or along its margins with adjacent magnetite or silicates, in which cases they are referred to as external granules (e.g. Fig. 10b) (Haggarty, 1991). Their tendency to concentrate along grain margins is presumably due to greater amounts of diffusion of the oxidized ülvospinel component at elevated temperatures through the magnetite host (Von Gruenewaldt et al., 1985). These granules typically exhibit polygonal, subrounded habits and range in diameter from 20-200 μm, although most are less than 100 μm wide. They are observed in most of the magnetite-bearing samples in this study, although they are present in significantly

higher abundances in extensively metamorphosed gabbros relative to more oxide-rich lithologies or less altered olivine-bearing gabbros. In extreme cases such as MA32-25, a gabbro which contains partially-replaced magnetite and a pervasive metamorphic foliation, many of these ilmenite granules have seemingly amalgamated into coarse, often foliated aggregates. These polycrystalline aggregates may be similar in size to coarse, primary ilmenite, but are distinguished due to the discretely bireflectant nature of each of the individual granules that are at different crystallographic orientations (Fig. 10c).

Ilmenite exsolutions that formed below the ülvospinel-magnetite solvus exist in most cases as very fine lamellae aligned parallel to the {111} planes of magnetite (Fig. 10d-e), and are likely pseudomorphs of original ülvospinel exsolutions that were subsequently oxidized to ilmenite, referred to by Willemse (1969) as "protoilmenite". These trellis-style lamellae are typically only several microns wide but may be hundreds of microns long, and form densely packed "cloth-texture" networks (Vincent and Phillips, 1954; Von Gruenewaldt et al., 1985). As previously noted by Taner et al. (1998), magnetite grains cut parallel to {111} show these lamellae intersecting in equilateral triangles (Fig. 10d), whereas sections cut parallel to {100} planes show lamellae intersecting at 90 degrees. The densely-packed nature and opposing bireflectant orientations of this cloth-textured ilmenite produces a patchy anisotropy of magnetite when examined under reflected light (Fig. 10e).

In some samples, very fine ilmenite hosted within magnetite consists of abundant blotchy, almost vermicular internal granules (e.g. Fig. 10b). However, a weak alignment of some of the more elongate granules parallel to that of coexisting protoilmenite lamellae suggests that they are coarsened, and perhaps slightly deformed variants of the protoilmenite. This texture is similar to the composite exsolution lamellae described in magnetite in other igneous settings

(Von Gruenewaldt et al., 1985; Haggarty, 1991). While protoilmenite or composite lamellae are usually quite pervasive within their host magnetite grains, their abundance is often noticeably lower - or they are absent entirely - in the vicinity of coarser ilmenite lamellae, or along the margins of primary ilmenite intergrown with magnetite. The brighter nature of these exsolution-free zones in BSE images also indicates that this magnetite is more Fe-rich (Fig. 10d,f). This suggests that the Ti component of the magnetite-ülvospinel solid solution may have diffused into the coarse ilmenite.

4.2.1.2 Hercynitic spinel exsolutions

Exsolutions of aluminous spinel are observed within magnetite in approximately half of the samples examined in this study. They are most abundant in semi-massive and massive lithologies, but are also observed in some gabbroic samples, albeit less pervasively. Energy dispersive spectrometry (EDS) analyses of these exsolutions indicate that they are an intermediate solid-solution between hercynite ($FeAl_2O_4$) and spinel *senso stricto* ($MgAl_2O_4$) with minor amounts of zinc, commonly referred to as pleonaste in the literature. They are most commonly present as blebs and lamellae parallel to the {100} planes of magnetite, and display a maximum thickness of approximately 10 μm (Fig.10d), although they are finer (<5 μm) when present in gabbros. In some Fe-Ti oxide-rich samples - most notably those from outcrops TA and T3, which consistently contain greater than 50 percent magnetite – a variety of these exsolutions is observed wherein three or four circular spinel blebs have connected (or nearly so) at 90 degree angles about a central axis (Fig. 10e). These “clover-like” exsolutions are typically 30-50 μm in diameter, and may have formed via migration of individual lamellae through magnetite along their respective {100} planes at elevated temperatures until they met along a common axis. In all

cases, when spinel exsolutions coexist with fine protoilmenite lamellae, textural evidence suggests that the spinel exsolved from the magnetite host first, as they always crosscut the ilmenite lamellae. This is supported by experimental studies which show that Mg-Al spinel exsolves from magnetite above the ülvospinel-magnetite solvus (Price, 1981).

It should be noted that while all of the above exsolutions have been described in terms of subsolidus processes occurring during the initial cooling of the RBC, elevated temperatures associated with potentially multiple episodes of metamorphism may have modified pre-existing exsolutions, or even produced new generations. However, if multiple generations do exist it is impossible to distinguish between them based simply on textural analysis, and therefore no further attempt is made in this study.

4.2.2 Primary ilmenite microtextures

Along with the magnetite-hosted oxy-exsolution products, medium-to-coarse grained ilmenite is present in all of the samples analyzed. This variety of ilmenite typically ranges in size from 0.4-2 mm, is anhedral, and may occur either as discrete disseminated grains or intergrown with magnetite. Unlike magnetite, ilmenite almost always exhibits sharp, relatively smooth grain boundaries with both cumulate and alteration silicate minerals (Fig. 11d). It also exhibits well-defined, though irregular and subangular contacts with magnetite when the two are intergrown, though very fine phyllosilicate alteration minerals may concentrate between the margins of the two minerals. As noted by other authors (e.g. Von Gruenewaldt et al., 1985), its coarse grain size and textural relationships with cumulate silicates suggest that this variety of ilmenite is a primary phase that crystallized from the parental magma concurrently with titaniferous magnetite. However, it also commonly contains very fine (<10 μm wide) exsolution lamellae oriented

parallel to its (0001) planes (Fig. 10f), and which may be slightly curved in more deformed samples. Routine EDS analyses indicates that these exsolutions are essentially pure Fe-oxide, and therefore may be either magnetite or hematite, as their ultrafine nature makes it impossible to determine optically. However, they are morphologically very similar to ilmenite-hosted magnetite exsolutions that are observed in the Xinjie mafic intrusion in China (Tan et al., 2016), and are therefore considered as such in this study. Additionally, aluminous spinel occasionally either line the outer margins of these lamellae or occur as partitions within them, either concentrated at the tip or in between plates of magnetite.

4.2.3 Secondary magnetite

Optically homogenous magnetite occasionally occurs as fracture fillings or associated with veins in oxide-rich lithologies. This variety of magnetite may occur as very fine disseminated grains within a vein, but is most commonly present as irregular overgrowths up to 100 μm thick on the external margins of fractured primary magnetite (Fig. 10g). The two varieties of magnetite are easily distinguished under reflected light due to the exsolution-free character of the overgrowths that contrasts with the exsolution-rich host magnetite. Due to its association with veins, this fracture filling magnetite is considered to be of hydrothermal origin and to have formed at lower temperatures than coarse titaniferous magnetite.

4.3 Alteration textures

Magnetite from most of the analyzed samples exhibits some degree of replacement to silicates, the extent of which is broadly correlated with the lithology of the host rock. In massive oxides or oxide-rich pyroxenites, incipient replacement of magnetite along its margins by chlorite is

commonly observed where magnetite is in contact with interstitial silicates. (Fig. 11a-b). Similar, but more pervasive alteration textures are observed in disseminated magnetite in some metagabbros (Fig. 11c-d). In contrast, ilmenite remains relatively unaltered in all cases, and therefore retains its smooth, rounded margins, whereas magnetite exhibits irregular, jagged margins reflecting the subhedral habit of the replacing chlorite. However, this selective replacement of magnetite is most prevalent in oxide-poor leucogabbros, wherein disseminated magnetite is often completely replaced (or nearly so) by chlorite and/or dark green hornblende, and occasionally minor actinolite, epidote and biotite. While small amounts of relict, patchy magnetite may be preserved in some instances (e.g. Fig. 11e-f), generally the only indication that it was originally present are relict lamellar or composite ilmenite exsolutions that preserve their {111} orientations. In undeformed samples these lamellae may even be geometrically contained by pseudo grain boundaries that presumably represent the previous margins of the now-replaced magnetite (Fig. 11g-j).

The importance of lithology on the degree of magnetite replacement is exemplified at the base of the lowermost massive oxide layer encountered in drillcore (sample MA11-2, approximately 245 m stratigraphic depth). Magnetite at the very base of this layer exhibits a textural gradient at the contact between the massive oxides and underlying oxide-barren leucogabbro, such that it becomes increasingly replaced towards the leucogabbro (Fig. 11k-l). The transition from unaltered magnetite to it being almost completely replaced occurs over about 2-3 mm. The exact minerals replacing the magnetite in this specific case are unknown, as it still appears opaque in transmitted light, but the metamorphic minerals at the alteration front include hornblende, chlorite, and acicular actinolite that radiates from the oxides. Just as in the disseminated samples, coarse granular ilmenite and exsolution lamellae remain unaltered.

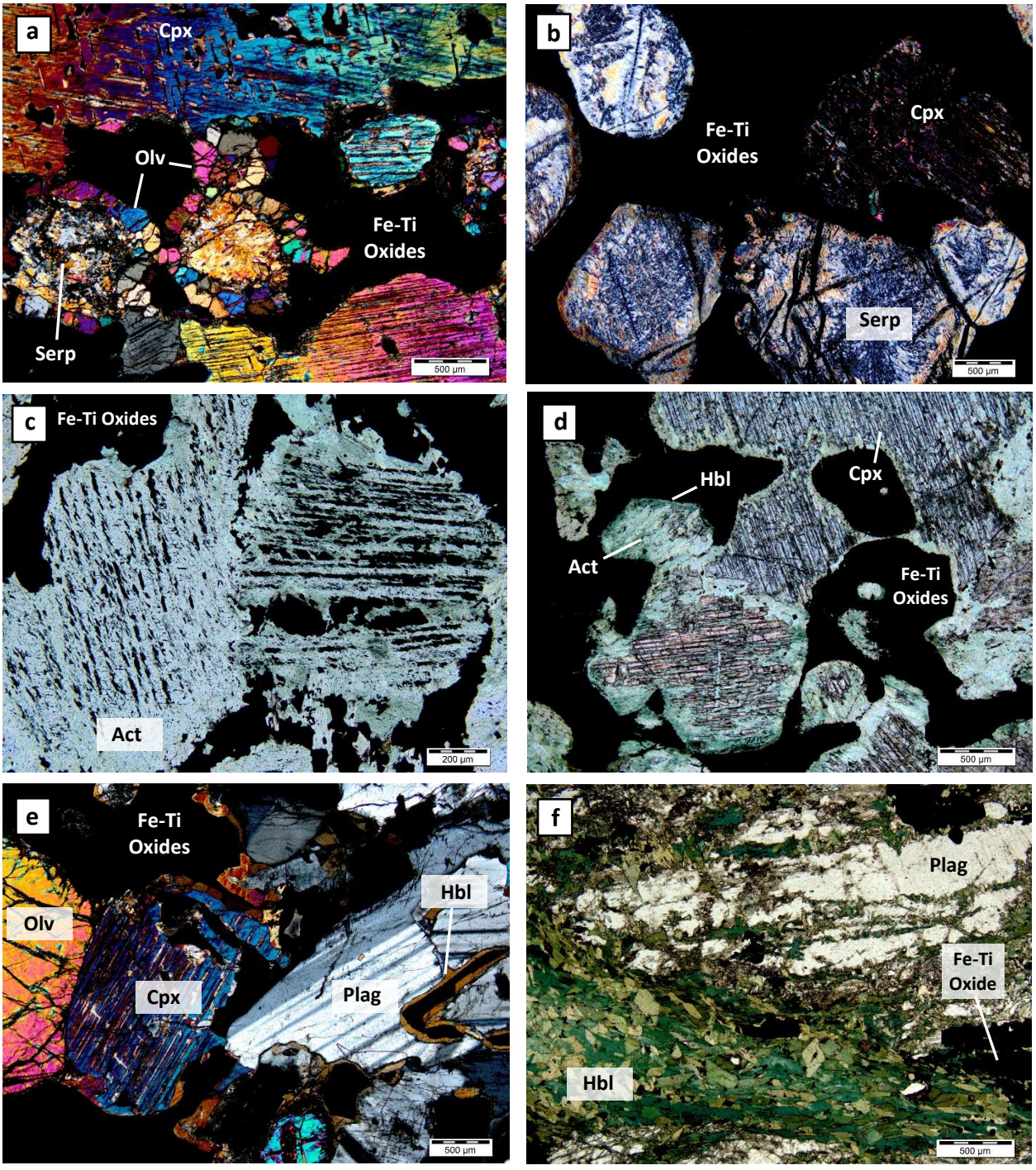

Fig. 9. Representative photomicrographs of Fe-Ti oxide-rich lithologies. **a.** Oxide-rich olivine pyroxenite, with coarse cumulate clinopyroxene and fine granular olivine coronas around serpentinized cores, TA2-6, XPL; **b.** Oxide-rich olivine pyroxenite. Primary cumulus olivine has been completely altered to serpentine, MA11-11, XPL; **c.** Fe-Ti oxide-rich metapyroxenite in which primary pyroxene has been completely altered to actinolite. Parallel linear opaques in the pyroxene pseudomorphs are ilmenite that was likely exsolved from Ti-rich pyroxene, MA14-7A, PPL; **d.** Oxide-rich pyroxenite with primary clinopyroxene exhibiting marginal alteration to actinolite, as well as dark green hornblende on the margins of some Fe-Ti oxides, MA14-8A, PPL; **e.** Unaltered olivine gabbro with disseminated Fe-Ti oxides. Note brown hornblende rims around opaque oxides, MA03-1A, XPL; **f.** Metagabbro with foliated hornblende and partially sausseritized plagioclase, MA14-4, PPL; Olv=olivine; Cpx=clinopyroxene; Act=actinolite; Hbl=hornblende; Serp=serpentine; Plag=plagioclase.

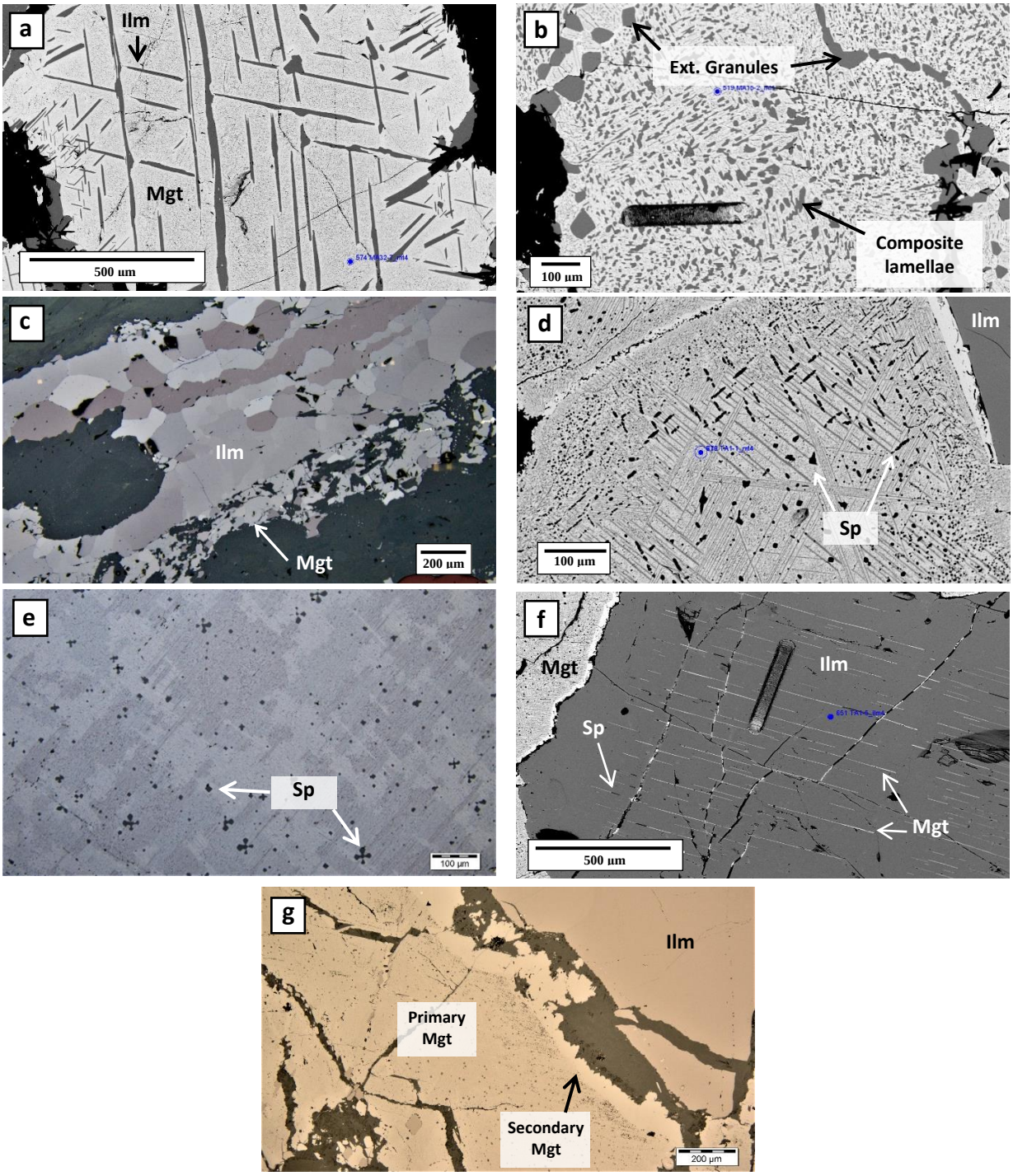

Fig. 10. BSE images (**a, b, d, f)** and photomicrographs **(c, e, g)** of Fe-Ti oxide microtextures. **a.** Coarse networks of ilmenite lamellae and internal/external granules in magnetite. Note that the spotty texture of magnetite in between ilmenite lamellae is due to the presence of a second generation of protoilmenite and spinel exsolutions – MA32-7; **b.** Composite-style ilmenite exsolutions in magnetite, with polygonal external granules concentrated on grain margins and fractures – MA15-2; **c.** Coarse agglomerate of fine ilmenite granules with partially replaced magnetite in a foliated metagabbro. Individual granules were presumably exsolution products from now-altered magnetite – MA32-25, RL; **d.** Coexisting networks of fine hercynitic spinel lamellae (black dashes) along the {100} planes of magnetite, and very fine protoilmenite (dark grey) along the {111} planes. Note the bright, exsolution-free magnetite along the margin of the coarse ilmenite in the top right corner – TA1-4; **e.** "Clover" shaped hercynitic spinel and patchy anisotropy of host magnetite due to the "cloth texture" produced by multiple orientations of protoilmenite lamellae – TA1-4, RL. **f.** Very fine magnetite exsolution lamellae (with occasional black spinel segments) in coarse ilmenite – MA11-11; **g.** Fracture-filling secondary magnetite overgrowths on primary titaniferous magnetite – TA2-4. RL. Mgt=magnetite; Ilm=ilmenite; Sp=hercynitic spinel. Laser ablation tracks in **b** and **f** are 52x300 µm. Blue dots in **a, b, d,** and **f** show location and diameter (20 µm) of EMPA spot analyses.

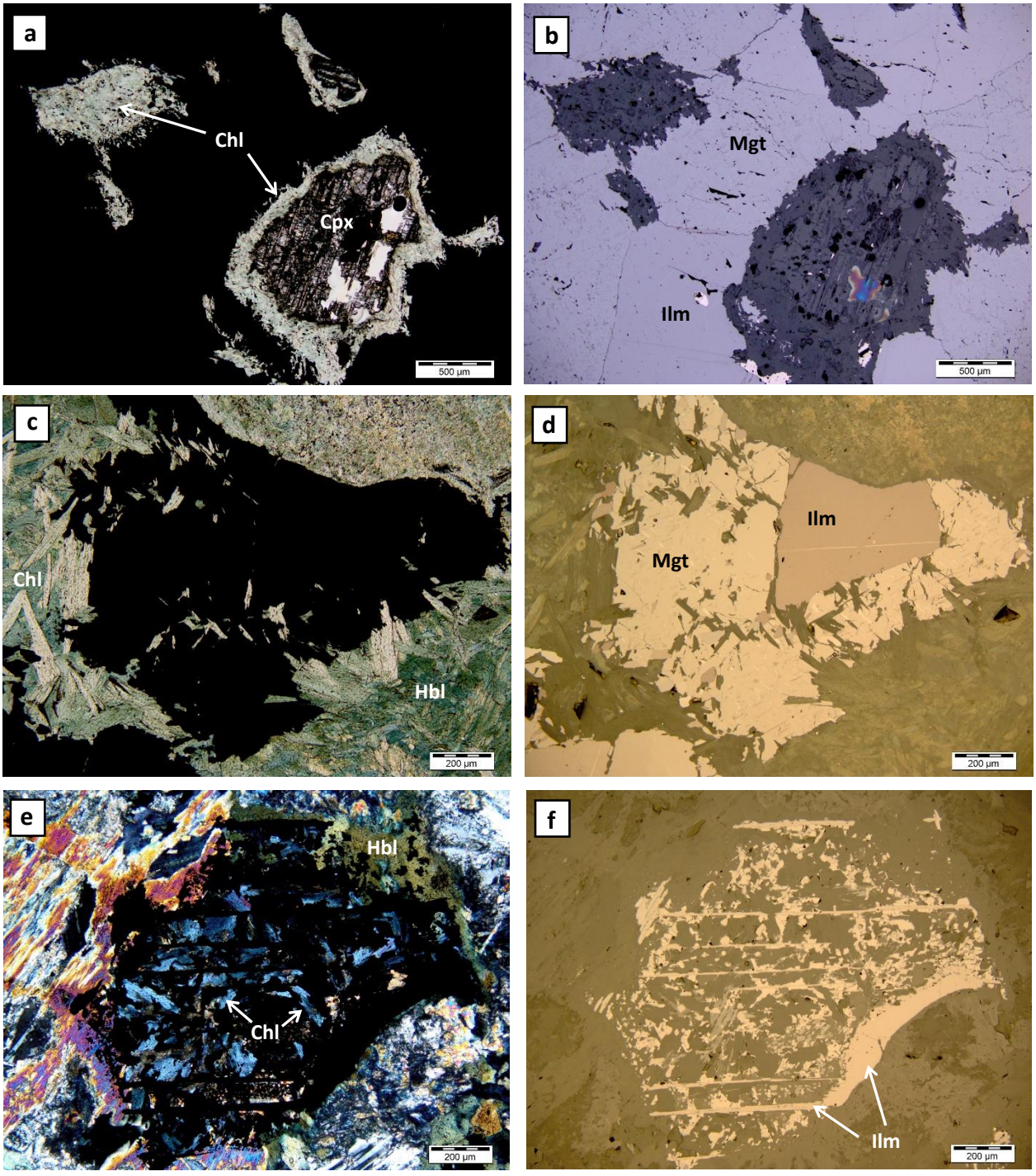
a
Chl
Cpx
500 µm
b
Mgt
Ilm
500 µm
c
Chl
Hbl
200 µm
d
Ilm
Mgt
200 µm
e
Hbl
Chl
200 µm
f
Ilm
200 µm

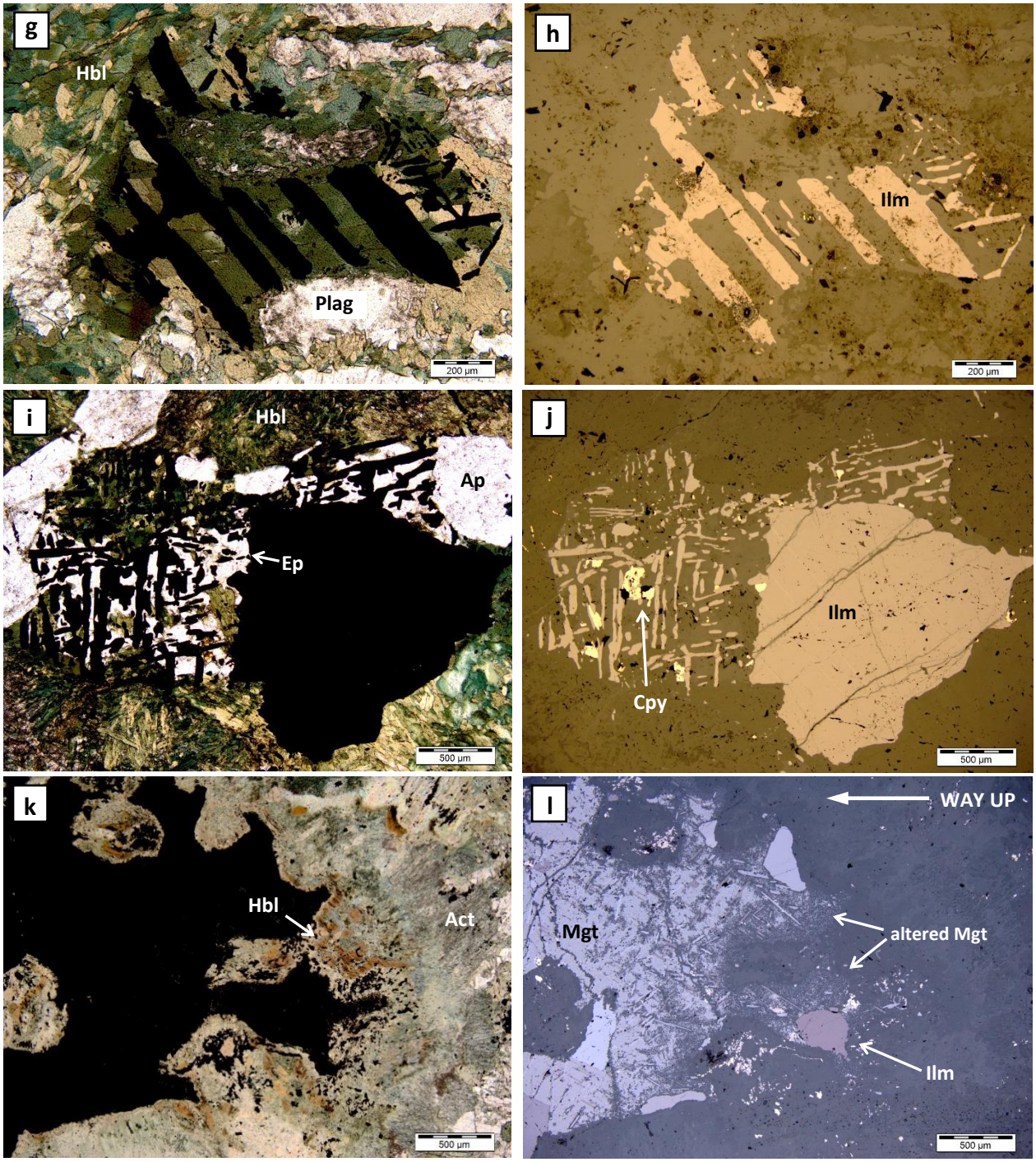

Fig.11. Photomicrographs in polarized (PPL - **a, c, g, i, k**; XPL – **e)** and reflected light (**b, d, f, h, j, l**) showing alteration textures of Fe-Ti oxides. **a-b.** Marginal replacement of magnetite by chlorite, with relict interstitial clinopyroxene in massive Fe-Ti oxides – MA32-17; **c-d.** Chlorite partially replacing disseminated magnetite in metagabbro – MA03-7; **e-f.** Extensive replacement of disseminated magnetite by chlorite in metaleucogabbro. Very fine patches of magnetite remain along the edges of relict horizontal ilmenite lamellae – MA03-3; **g-h.** Relict trellis and "sandwich" ilmenite lamellae from magnetite that has been completely replaced by hornblende in a metaleucogabbro – MA14-3B-B; **i-j:** Coarse primary ilmenite and relict ilmenite exsolution lamellae from previously intergrown magnetite, now replaced by hornblende and epidote. Note coarse subhedral apatite, and fine anhedral chalcopyrite among lamellar ilmenite **–** MA14-3B-B; **k-l.** Gradationally replaced magnetite at the base of a massive oxide layer. Fe-Ti oxides overlying the grains in this photo (i.e. to the left) are massive and unaltered; underlying it is an oxide-barren leucogabbro. Magnetite in this photo is increasingly replaced towards the leucogabbro. Granular and lamellar ilmenite are unaltered – MA11-2. Mgt=magnetite; Ilm=ilmenite; Hbl=hornblende; Act=actinolite; Ep=epidote; Plag=plagioclase; Ap=apatite; Cpy=chalcopyrite.

Table 4. Mineralogical characteristics of thin sections analyzed from drill core and outcrop samples from the Rivière Bell Complex. "X" indicates that the mineral in question is present in the given sample. Note that the protoliths as listed are based on the silicate mineralogy of the sample, and that prefixes describing the Fe-Ti oxide rich nature of these rocks have been omitted. The prefix "meta" should also be affixed in most cases, but is excluded for clarity. Massive oxides are those samples that contain greater than 90% Fe-Ti oxides. Mineral abbreviations are as follows: Act=actinolite; Ap=apatite; Bt=biotite; Chl=Chlorite; Cpx=clinopyroxene; Ep=epidote; Hbl=hornblende; Idd=iddingsite; Ilm=ilmenite; Mgt=magnetite; Musc=muscovite; Olv=olivine; Opx=orthopyroxene; Plag=plagioclase; Serp=serpentine; Ti-Hbl=titanium-rich hornblende; Trem=tremolite.

Stratigraphic Depth (m)	Thin Section ID	Sub-lithology	Relict Primary Minerals				Alteration Mineralogy					Accessory Minerals	Modal Fe-Ti Oxides* (%)	Mgt/Ilm Ratio*	Protolith (based on silicate mineralogy co-existing with Fe-Ti oxides)
			Plag	Olv	Cpx	Opx	Act	Hbl	Ep	Serp	Chl				
9.21	**MA14-2A**			X						X			20	3	Dunite
9.58	**MA14-2D**		X	X	X		X	X		X	X	Idd	15	6.5	Olivine Gabbro
13.64	**MA14-3A**		X		X		X	X			X		20	7	Gabbro
13.78	**MA14-3B-T**		X				X	X	X		X	Musc	30	3	Gabbro
13.94	**MA14-3B-B**		X				X	X	X		X	Ap	3	1	Leucogabbro
17.69	**MA14-4**	*a*	X					X	X			Ap	20	1.67	Gabbro
17.69	**MA14-4**	*b*	X				X	X	X		X	Ap	3	0.5	Leucogabbro
24.68	**MA14-5A**						X	X				Ap	30	2	Pyroxenite
24.90	**MA14-5C**	*a*	X				X	X	X		X		30	2	Gabbro
24.90	**MA14-5C**	*b*	X					X	X		X		2	1	Leucogabbro
40.47	**MA14-6A-T**		X				X	X	X		X	Bt	20	1.67	Gabbro
40.74	**MA14-6B**	*a*					X	X			X		25	1.5	Pyroxenite
40.74	**MA14-6B**	*b*	X					X	X		X		2	1	Leucogabbro
51.81	**MA14-7A**	*a*	X					X	X		X		2	1	Leucogabbro
51.81	**MA14-7A**	*b*					X				X		35	1.33	Pyroxenite
51.92	**MA14-7B**		X				X	X	X		X		35	1.33	Gabbro
69.47	**MA14-8A**	*a*	X				X	X	X		X		1	1	Leucogabbro
69.47	**MA14-8A**	*b*			X		X	X					20	1.67	Pyroxenite
69.61	**MA14-8B**						X	X			X		35	2.5	Pyroxenite
119.73	**MA15-1**		X				X	X	X			Musc	20	1.67	Gabbro
126.94	**MA15-2**			X			X			X	X		50	4	Olivine Pyroxenite
139.46	**MA32-25**		X					X	X		X	Musc	7.5	0.5	Gabbro
145.55	**MA32-1A**						X			X	X		35	6	Pyroxenite
145.78	**MA32-1C**						X			X	X		55	10	Pyroxenite
152.51	**MA32-2A-T**				X		X				X		25	2.5	Pyroxenite
152.64	**MA32-2A-B**	*a*			X		X						65	2.25	Pyroxenite
152.64	**MA32-2A-B**	*b*			X		X						15	2.5	Pyroxenite
152.84	**MA32-2B**				X		X						50	1.5	Pyroxenite
154.47	**MA32-3**				X		X	X					25	4	Pyroxenite
155.60	**MA32-4-b**						X		X				40	3	Pyroxenite

Table 4 (cont'd).

Stratigraphic Depth (m)	Thin Section ID	Sub-lithology	Relict Primary Minerals				Alteration Mineralogy					Accessory Minerals	Modal Fe-Ti Oxides* (%)	Mgt/Ilm Ratio*	Protolith (based on silicate mineralogy co-existing with Fe-Ti oxides)
			Plag	Olv	Cpx	Opx	Act	Hbl	Ep	Serp	Chl				
160.29	**MA32-7**							X		X	X		45	3.5	Olivine Pyroxenite
169.74	**MA32-9**				X		X						60	5	Pyroxenite
178.78	**MA32-12**			X	X		X			X			70	6	Olivine Pyroxenite
188.51	**MA32-15**									X		Ap	90	8	Massive Oxides
192.24	**MA32-17**				X					X			90	5	Massive Oxides
196.77	**MA32-18**	*a*	X		X						X		3	1	Leucogabbro
196.77	**MA32-18**	*b*	X	X	X								50	4	Olivine Gabbro
196.77	**MA32-18**	*c*	X		X						X		3	1	Leucogabbro
205.93	**MA32-19**		X		X		X	X	X			Musc	15	4	Gabbro
234.15	**MA11-11**			X	X					X	X		55	4.5	Olivine Pyroxenite
236.68	**MA11-8**			X	X		X			X	X		50	9	Olivine Pyroxenite
244.72	**MA11-2**			X	X		X				X		90	4.5	Massive Oxides
249.89	**MA03-7**						X	X			X		10	3	Gabbro
251.07	**MA03-6**		X				X	X			X	Bt, Musc	2	1	Leucogabbro
260.85	**MA03-4**		X				X	X			X	Musc	20	3	Gabbro
261.39	**MA03-3**		X				X	X			X	Bt	7	1.5	Leucogabbro
281.37	**MA03-2**		X				X	X			X	Bt, Musc	5	1.5	Leucogabbro
282.46	**MA03-1B**		X	X	X	X						Ti-Hbl	20	3	Olivine Gabbronorite
282.53	**MA03-1A**		X	X	X	X						Ti-Hbl	30	2	Olivine Gabbronorite
Outcrop	**T3-C4-1**			X	X		X			X	X		65	5.5	Olivine Pyroxenite
Outcrop	**T3-C4-2**				X		X			X	X	Trem	70	6	Olivine Pyroxenite
Outcrop	**TA1-6**			X	X					X	X		75	6.5	Olivine Pyroxenite
Outcrop	**TA1-5**			X	X					X			80	4.3	Olivine Pyroxenite
Outcrop	**TA1-4**			X	X					X			85	7.5	Olivine Pyroxenite
Outcrop	**TA1-1**			X	X		X			X			60	3	Olivine Pyroxenite
Outcrop	**TA2-1**			X	X					X	X		75	6.5	Olivine Pyroxenite
Outcrop	**TA2-3**			X	X								75	6.5	Olivine Pyroxenite
Outcrop	**TA2-4**			X	X		X			X	X		60	3	Olivine Pyroxenite
Outcrop	**TA2-6**				X		X			X	X		50	9	Olivine Pyroxenite

***** Modal Fe-Ti Oxides and Mgt/Ilm ratios were determined using only modal proportions of primary magnetite and ilmenite (i.e. magnetite-hosted ilmenite exsolutions and secondary magnetite of hydrothermal origin were not included). Where magnetite has been partially or completely replaced by silicates, particularly in leucogabbros, these values include magnetite that is inferred to have originally been part of the magmatic assemblage based on the presence relict ilmenite exsolution lamellae.

5 ANALYTICAL METHODS

5.1 Fe-Ti oxides

5.1.1 LA-ICP-MS analyses

The concentrations of 25 trace elements (Mg, Al, Si, P, Ca, Sc, Ti, V, Cr, Mn, Co, Ni, Cu, Zn, Ga, Ge, Y, Zr, Nb, Mo, Sn, Hf, Ta, W, Pb) in coarse-grained (i.e. primary) magnetite (n = 262) and ilmenite (n = 271) were analyzed in-situ using LA-ICP-MS on polished thin sections of the samples listed in Table 4. Note that in sample MA11-2, Fe-Ti oxides from the altered base of the massive layer (Fig. 11k-l) were analyzed in addition to unaltered grains within the massive layer itself. Analyses were performed at the University of Ottawa and the Geologic Survey of Canada, Ottawa, following the protocol of Dare et al. (2014). Analytical conditions used at both labs were similar and are summarized in Tables 5 and 6. Both LA-ICP-MS systems are comprised of a Photon Machines Analyte (193 nm) Excimer laser system and a 7700 Agilent quadropole ICP-MS. Calibration was performed using USGS certified reference material GSE-1g, a synthetic glass containing 10% Fe that is doped with approximately 500 ppm of each trace element (Jochum et al., 2005), using ^{57}Fe as the internal standard (Table 7).

All grains were analyzed using single-line rasters approximately 300 μm long (60 s acquisition time; 5 μm/s scan speed) with a 30 s gas blank prior to acquisition. 52 μm diameter ablation beams were used for all analyses except for samples MA03-3, MA03-6, and the altered oxides of MA11-2, where Fe-Ti oxides were finer grained, and therefore a 30 μm beam was used. Consideration was made to incorporate representative amounts of exsolution products in the analyses of the oxides (ilmenite and/or spinel in magnetite; magnetite in ilmenite) in order to better represent their primary compositions before subsolidus oxy-exsolution processes took

place. In most cases, between 3-7 grains each of magnetite and ilmenite were analyzed from each thin section, and an average composition was then taken as representative of the sample. If a distinct contact between adjacent Fe-Ti oxide-bearing sub-lithologies was exhibited within a thin section (as defined in section 4), grains were analyzed and averaged from each sub-lithology separately.

Unknowns were analyzed in batches of 10-12, with each batch followed by analyses of certified references materials GSE-1g, GSD-1g (USGS Fe-rich basaltic glass doped with 40-50 ppm of each trace element, Jochum et al., 2005), GOR-128g (natural komatiitic glass, Jochum et al., 2006) and in-house standard BC28, a Ti-rich magnetite from the Bushveld Complex (Dare et al., 2014) to monitor accuracy and precision, and to ensure that results were consistent between the two laboratories (Tables 7 and 8). Results of GSD-1g analyses are generally accurate, with most elements within 5 percent relative difference (% rel. diff.) of certified values on both machines. Relative standard deviations (RSD) of the cumulative analyses are also below 10% for all elements. Analyses of GOR-128g produce accurate and precise results on both machines for all elements with mass numbers less than ^{74}Ge. Heavier elements that are present in sub-ppm amounts in GOR-128g tend to produce less consistent results (e.g. Nb, Mo, Sn, Ta), although Ge, Hf, W, and Pb, all of which are also at sub-ppm levels, produce accurate results on both machines. Results of BC28 magnetite analyses also compare well between the two labs (<12% rel. diff.) for all elements except those present in low abundances (Mo, Sn, Pb) or which are heterogeneously distributed (Cu).

All data obtained via LA-ICP-MS were reduced using the software Iolite (Paton et al., 2011). Si, P, S, Ca, and Cu signals were examined in Iolite to monitor for inclusions of silicate, phosphate, or sulfide phases, which, if present, were removed from the integration in question. If

doing so split an analysis into two portions of unequal acquisition times (denoted *a* and *b* in equation 1, below), which Iolite integrates as separate analyses, a single composition for the grain of interest was obtained by calculating a weighted average of the two portions as follows:

$$C(x) = C_a(x) * \left[\frac{t_a}{t_a + t_b}\right] + C_b(x) * \left[\frac{t_b}{t_a + t_b}\right] \quad (1)$$

where $C(x)$ is the weighted concentration of element *x* in the grain of interest; $C_a(x)$ and $C_b(x)$ are the concentrations of element *x* in portions *a* and *b* of the analysis, respectively; and t_a and t_b are the acquisitions times for portions *a* and *b* of the analysis, respectively. The first 5-10 s of signal following the 30 s gas blank was also excluded from each integration to account for signal stabilization.

Table 5. Analytical details of LA-ICP-MS analyses

		Geologic Survey of Canada, Ottawa	University of Ottawa
Laser Ablation System		Photon-Machines Analyte 193 nm Excimer	
ICP-MS		Agilent 7700x	
Laser Frequency		10 Hz	15 Hz
Pulse Energy		5 mJ/pulse	5 mJ/pulse
Stage Speed		5 µm/s	
Beam Diameter		30-52 µm	
Dwell Time		10 ms for all elements	See Table 6
Analysis Procedure		30 s of gas blank; 60 s of signal	
Carrier Gas Flow*	MFC1: MFC2:	Helium (0.6 L /min) Helium (0.4 L/min)	Helium (1 L/min) n/a
Ar Flow Rate		1.07 L/min	0.7 L/min
Internal Standard		Fe (data from EMPA)	
Reference Material for Calibration		GSE-1g (USGS-synthetic glass)	
Reference Materials for Monitoring		GSD-1g (USGS-synthetic glass) GOR-128g (Komatiitic natural glass)	
In-house Moniter		BC28 (Magnetite from Bushveld Complex)	
Monitor Signal for Inclusions		Si, S, P Ca, Cu	

***** MFC = mass flow controller

Table 6. Isotopic dwell times used during LA-ICP-MS analyses at the University of Ottawa.

Isotope		Dwell Time (ms)
24	Mg	5
27	Al	5
29	Si	5
31	P	5
34	S	5
44	Ca	5
45	Sc	10
47	Ti	5
51	V	10
52	Cr	10
55	Mn	10
59	Co	10
60	Ni	10
63	Cu	20
66	Zn	10
69	Ga	10
74	Ge	20
89	Y	20
90	Zr	10
93	Nb	10
95	Mo	20
118	Sn	15
178	Hf	10
181	Ta	10
182	W	10
208	Pb	10

5.1.2 EMPA analyses

To assist with the standardization of LA-ICP-MS analyses, the concentrations of Al, Ca, Cr, Fe, Mn, Mg, Ni, Si, Ti, V, and Zn were directly measured in magnetite and ilmenite by EMPA, using a JOEL JXA-8230 SuperProbe at the University of Ottawa. Grains were analyzed by wavelength dispersive spectrometry (WDS) using a beam current of 40 nA and accelerating potential of 20 kV. Analytical parameters, including the standards used in calibration and correction of interferences of Ti on V and V on Cr, follow the protocol presented in Duparc et al. (2016). A 20 μm spot size was used to include fine exsolutions, when present, in the analyses of the host oxide phase. An average total Fe value (Fe^{2+} + Fe^{3+}) of both magnetite and ilmenite for each thin section (or sub-lithology) of interest was then calculated from up to 7 grains of each mineral. Analyses with weight percent oxide (wt.% oxide) totals less than 98.5%, or greater than 101.5% were excluded from the calculation of these averages. In-house standard BC28 was also analyzed to ensure accuracy and precision were maintained during each analytical session (Table 8).

Table 7. Results of LA-ICP-MS analyses of reference materials. All element concentrations given in ppm. uOttawa refers to analyses that were performed at the University of Ottawa. GSC refers to analyses that were performed at the Geologic Survey of Canada.

`				**CALIBRATION** GSE-1g		**MONITOR** GSD-1g						**MONITOR** GOR-128g					
	Detection Limits			**Certificate Value**		**Certificate Value**		**uOttawa (this study)**		**GSC (this study)**		**Working Value**		**uOttawa (this study)**		**GSC (this study)**	
Isotope	uOttawa[1] (52-30 um)	GSC (52 um)	EMPA (20 µm)	avg	std	avg	std	avg (n=48)	std	avg (n=26)	Std	Avg	std	avg (n=48)	Std	avg (n=27)	Std
24Mg	0.11-0.38	0.15	89	21106	181	21709	241	21670	252	22142	409	156826	1810	150645	2074	154180	9317
27Al	0.23-0.84	0.31	62	68804	2117	70922	1588	70837	1548	74498	2125	52446	900	47541	1568	48958	2148
29Si	42.6-98.8	40.77	55	250994	7011	248657	3739	250786	6310	253158	6026	215553	1870	210955	7144	216609	8964
31P	1.19-2.22	5.18	-	-	-	860	160	1280	395	2310	113	N.A.	N.A.	140	35	210	14
44Ca	15.6-38.16	7.43	65	52858	2143	51429	714	52685	1115	54331	1227	44571	857	42360	1434	42828	1741
45Sc	0.03-0.09	0.03	-	530	20	52	2	54	3	57	3	32	1	30	2	31	2
47Ti	0.07-0.39	0.07	198	450	42	7432	360	7852	290	8110	250	1727	72	1561	69	1621	71
51V	0.01-0.05	0.02	90	440	20	44	2	48	4	46	1	189	13	190	4	191	4
52Cr	0.11-0.43	0.62	170	400	80	42	3	46	1	47	1	2272	171	2317	52	2299	61
55Mn	0.06-0.17	0.16	106	590	20	220	20	221	3	229	3	1363	70	1354	16	1402	34
59Co	0.01-0.04	0.02	-	380	20	40	2	40	1	40	1	92	6	86	1	90	4
60Ni	0.83-1.90	0.17	116	440	30	58	4	59	4	60	1	1074	61	1044	20	1107	91
63Cu	0.03-0.09	0.14	-	380	40	42	2	41	1	44	2	64	13	61	1	62	3
66Zn	0.10-0.36	0.08	525	460	10	54	2	55	1	55	2	75	7	71	1	78	4
69Ga	0.02-0.04	0.013	-	490	70	54	7	53	1	55	1	8.7	1.10	7.9	0.20	8.4	0.33
74Ge	0.05-0.09	0.164	-	320	80	32	8	33	1	33	1	0.96		1.1	0.11	1.0	0.1
89Y	0.001-0.002	0.005	-	410	30	42	2	41	2	45	3	12	0.50	10	0.71	11	0.76
90Zr	0.01-0.03	0.008	-	410	30	42	2	43	3	47	3	10	0.50	7.66	1.56	10	0.62
93Nb	0.002-0.01	0.005	-	420	40	42	3	42	1	43	1	0.10	0.01	0.13	0.10	0.08	0.01
95Mo	0.01-0.04	0.02	-	390	30	39	3	41	1	41	1	0.71	0.26	0.53	0.04	0.59	0.07
118Sn	0.29-0.58	0.013	-	280	50	29	6	32	1	29	1	0.22	0.09	3.61	0.99	0.22	0.04
178Hf	0.003-0.01	0.006	-	395	7	39	2	40	2	44	3	0.35	0.02	0.31	0.04	0.32	0.03
181Ta	0-0.002	0.005	-	390	40	40	4	39	1	42	2	0.02	0.00	0.70	4.60	0.02	0.00
182W	0.006-0.02	0.02	-	430	50	43	4	44	1	44	1	16	2.40	16.0	2.35	16	0.44
208Pb	0.01-0.03	0.01	-	378	12	50	2	51	1	51	1	0.35	0.04	0.34	0.11	0.31	0.04

[57]Fe was used as the internal standard for all analyses using the following values: 9.8 wt.% (GSE-1g), 10.3 wt.% (GSD-1g), and 7.6 wt.% (GOR-128g). Certificate and working values taken from Dare et al. (2014). P is not calibrated by GSE-1g, and is only used to monitor signals for inclusions.

[1]Ranges in detection limits for LA-ICP-MS analyses at uOttawa correspond to the different beam diameters used during laser ablation of Fe-Ti oxides (noted in brackets).

Table 8. Results of LA-ICP-MS and EMPA analyses of in-house reference material BC28. All element concentrations given in ppm. uOttawa refers to analyses that were performed at the University of Ottawa. GSC refers to analyses that were performed at the Geologic Survey of Canada.

	IN-HOUSE MONITOR										
	BC-28										
	Detection Limits									EMPA	
Isotope	uOttawa[1] (52-30 um)	GSC (52 um)	EMPA (20 um)	Working Value	uOttawa (this study) avg (n=51)	std	GSC (this study) avg (n=27)	std		avg (n=35)	std
24Mg	0.11-0.38	0.15	89	11618	10948	1546	12112	919		12983	795
27Al	0.23-0.84	0.31	62	20787	18191	1870	20295	2110		20477	1358
29Si	42.6-98.8	40.77	55	220	930	479	302	91		185	43
31P	1.19-2.22	5.18	-	N.A.	31	13	3	3		-	-
44Ca	15.6-38.16	7.43	65	24	16	24	N/A	N/A		27	37
45Sc	0.03-0.09	0.03	-	31.0	27.2	1.5	28.6	2.6		-	-
47Ti	0.07-0.39	0.07	198	87615	76666	4251	76809	4608		76976	1598
51V	0.01-0.05	0.02	90	9603	9351	406	9079	255		8548	245
52Cr	0.11-0.43	0.62	170	1172	1376	62	1342	40		1049	391
55Mn	0.06-0.17	0.16	106	2125	1920	138	2018	131		2105	189
59Co	0.01-0.04	0.02	-	241	282	28	300	10		-	-
60Ni	0.83-1.90	0.17	116	573	589	30	591	20		558	66
63Cu	0.03-0.09	0.14	-	33.0	19.5	27.7	3.9	8.9		-	-
66Zn	0.10-0.36	0.08	525	588	459	158	406	57		479	671
69Ga	0.02-0.04	0.013	-	41.1	47.0	1.9	46.4	2.6		-	-
74Ge	0.05-0.09	0.164	-	0.86	0.76	0.06	0.73	0.09		-	-
89Y	0.001-0.002	0.005	-	0.08	0.03	0.06	0.03	0.02		-	-
90Zr	0.01-0.03	0.008	-	27.5	21.9	2.1	23.5	4.4		-	-
93Nb	0.002-0.01	0.005	-	1.72	1.52	0.10	1.49	0.14		-	-
95Mo	0.01-0.04	0.02	-	0.76	0.46	0.07	0.57	0.09		-	-
118Sn	0.29-0.58	0.013	-	2.20	4.15	0.88	1.18	0.07		-	-
178Hf	0.003-0.01	0.006	-	0.58	0.85	0.07	0.94	0.13		-	-
181Ta	0-0.002	0.005	-	0.07	0.13	0.01	0.13	0.03		-	-
182W	0.006-0.02	0.02	-	0.51	0.02	0.01	0.02	0.02		-	-
208Pb	0.01-0.03	0.01	-	1.98	0.58	0.29	0.07	0.03		-	-

[57]Fe was used as the internal standard using a value of 57.2 wt.%. Working values (whole-rock) taken from Dare et al. (2014). P was only used to monitor signals for inclusions.

[1]Ranges in detection limits for LA-ICP-MS analyses at uOttawa correspond to the different beam diameters used during ablation of Fe-Ti oxides (noted in brackets).

5.1.3 Correction of Fe concentration of magnetite

^{57}Fe is used as the internal standard for LA-ICP-MS analyses of magnetite. However, since magnetite often contains coarse ilmenite exsolutions that could not be accurately incorporated in a 20 μm EMPA beam, its Fe concentrations as determined by EMPA will presumably be higher than would be expected from the primary grains prior to subsolidus oxy-exsolution processes. Additionally, as noted in section 5.1.1, these exsolutions are purposely included in the ablation beam during LA-ICP-MS analyses. It is therefore necessary to correct the Fe concentration of magnetite for this discrepancy in the amount of the ilmenite component that was incorporated during analyses of magnetite by the two analytical methods. The corrected concentration of Fe in the primary magnetite of a given sample (Fe_{Mgt}^{Corr}) to be used as the internal standard for corresponding LA-ICP-MS analyses was thus calculated by mass balance as follows:

$$Fe_{Mgt}^{Corr} = (Fe_{Mgt}^{EMPA})(1 - X_{exsolution}) + (Fe_{Ilm}^{EMPA})(X_{exsolution}) \quad (2)$$

where Fe_{Mgt}^{EMPA} is the average concentration of Fe in magnetite from the sample as determined by EMPA; Fe_{Ilm}^{EMPA} is the average of concentration of Fe in coexisting primary ilmenite as determined by EMPA; and $X_{exsolution}$ is the fraction of ilmenite exsolutions within magnetite from the sample in question that were too coarse to include during EMPA analyses, but which were incorporated during LA-ICP-MS analyses.

The value of $X_{exsolution}$ used for each sample was calculated by assuming that the Ti content of magnetite as determined by LA-ICP-MS (which proportionally reflects the incorporation of exsolutions within each analysis line), following normalization to the corrected internal standard Fe value ($Ti_{Mgt\ Laser}^{Fe^{Corr}}$), should equal the mass balance-corrected Ti content of magnetite as determined by EMPA (Ti_{Mgt}^{Corr}). This assumption is supported by the agreement in Ti

concentrations of BC28 (which is exsolution-free) between LA-ICP-MS and EMPA (Table 8). Therefore, if

$$Ti_{Mgt\ Laser}^{Fe^{Corr}} = (Fe_{Mgt}^{Corr})(Ti_{Mgt\ Laser}^{Fe=1}) \quad (3)$$

where $Ti_{Mgt\ Laser}^{Fe=1}$ is the Ti content of magnetite as determined through LA-ICP-MS normalized to an internal standard Fe value of 1 wt.% (default output from Iolite), and

$$Ti_{Mgt}^{Corr} = \left(Ti_{Mgt}^{EMPA}\right)(1 - X_{exsolution}) + (Ti_{Ilm}^{EMPA})(X_{exsolution}) \quad (4)$$

where Ti_{Mgt}^{EMPA} and Ti_{Ilm}^{EMPA} are the average concentrations of Ti, as determined by EMPA, in magnetite and coexisting primary ilmenite from the sample in question, respectively, then setting equations (3) and (4) equal, substituting equation (2) for Fe_{Mgt}^{Corr}, and solving for $X_{exsolution}$ gives

$$X_{exsolution} = \frac{(Ti_{Mgt\ Laser}^{Fe=1})\left(Fe_{Mgt}^{EMPA}\right) - Ti_{Mgt}^{EMPA}}{\left(Ti_{Ilm}^{EMPA} - Ti_{Mgt}^{EMPA}\right) - (Ti_{Mgt\ Laser}^{Fe=1})(Fe_{Ilm}^{EMPA} - Fe_{Mgt}^{EMPA})} \quad (5)$$

Table 13 lists the values of $X_{exsolution}$ and the variables used in equation (5) for the average magnetite of each sample analyzed, along with the resultant Fe_{Mgt}^{Corr} values. Note that in the few instances where the numerator of equation (5) is negative, thus producing a negative $X_{exsolution}$ value, a value of zero was used for $X_{exsolution}$. Negative values arise in cases where ilmenite exsolutions are only present in small amounts, and the host magnetite is still relatively Ti-rich. Therefore, the Ti concentrations in magnetite as determined by EMPA may have been marginally greater than those determined by LA-ICP-MS.

It is important to note that equations 2-5 use the Fe and Ti concentrations of primary ilmenite rather of those of the exsolutions themselves, under the assumption that the major element chemistry of the two textural varieties does not greatly differ. To ensure this assumption

is valid, the compositions of coarse ilmenite exsolution lamellae from four samples were analyzed by EMPA and compared to those of coexisting primary ilmenite (Table 14). The relative differences in both the Fe and Ti content between the two varieties of ilmenite are less than 5% for all four samples. Therefore, we conclude that using the Fe and Ti values of primary ilmenite in the place of exsolutions is valid for the purposes of this study. It should also be noted that although these more accurate exsolution compositions are known for the four samples from which they were analyzed, for consistency's sake, the Fe and Ti concentrations of corresponding primary ilmenite were still used in correcting the Fe content of their magnetite.

5.2 Silicates

Plagioclase (n = 28), clinopyroxene (n = 27), and olivine (n = 21) compositions from select samples in which these phases are preserved were analyzed by EMPA using the JOEL JXA-8230 SuperProbe at the University of Ottawa. A beam current of 20 nA, accelerating voltage of 20 kV, and 10 μm spot size were used for all analyses. Up to five grains of each phase were analyzed per sample, from which a representative average was calculated. Since many of the grains in these samples display some degree of alteration to hydrous phases including Ca-amphiboles and chlorite (see section 5.1), attempts were made to avoid altered portions of the primary mineral of interest. Resultant analyses with wt.% oxide totals less than 98.5% or greater than 101.5% were excluded from the calculation of this average.

6 RESULTS

6.1 Fe-Ti oxide chemical compositions

6.1.1 EMPA results

Average magnetite and ilmenite compositions from drill core and outcrop samples as determined by EMPA are listed in Tables 9-12. Full results of EMPA analyses of Fe-Ti oxides are provided in Appendix 1. The average total Fe-content of magnetite from each sample (Fe_{Mgt}^{EMPA}) was proportionally re-calculated for the presence of ilmenite exsolutions that were incorporated in LA-ICP-MS analyses but not during EMPA (Fe_{Mgt}^{Corr}), as outlined in section 5.1.3. These corrected Fe values are listed in Table 13, along with the calculated average proportion of ilmenite exsolutions ($X_{exsolution}$) for each sample that were used in their determination. Fe_{Mgt}^{EMPA} ranges from 60-75 wt.% and is broadly correlated with $X_{exsolution}$ (which ranges from 0-30%) such that the most exsolution-rich samples are also those in which the host magnetite is most enriched in Fe (Fig. 12a). Correcting Fe_{Mgt}^{EMPA} for these exsolutions translates to a reduction in the Fe value by up to 17% in the most exsolution-rich magnetite, and Fe_{Mgt}^{Corr} resultantly ranges between 57-70 wt.% (Fig. 12b). In general, magnetite from disseminated gabbros and pyroxenites is more Fe-rich (typically between 65-70 wt.%) than that from semi-massive and massive oxides (60-65 wt.%) (Fig. 13a).

The Fe content of primary ilmenite exhibits a similar relationship with host lithology and Fe-Ti oxide fraction. (Fig. 13b). Average Fe-values range between 31-36 wt.%, and just as with magnetite (following the recalculation of its Fe content), ilmenite from disseminated gabbros and pyroxenites is consistently more Fe-rich (33-36 wt.%) than is ilmenite from massive Fe-Ti oxides and olivine-bearing pyroxenites and gabbros (31-33 wt.%). The compositions of

magnetite-hosted ilmenite exsolutions are also similar to those of primary ilmenite from within the same sample (Table 14), with the relative differences in Fe-content between the two varieties being less than 5% for all four samples analyzed.

6.1.2 LA-ICP-MS results

Elements that are consistently above detection limits of both LA-ICP-MS machines (Table 7) in magnetite and ilmenite include Mg, Al, Sc, Ti, V, Cr, Mn, Co, Ni, Zn, Zr, and Ga, in addition to Hf and Nb in ilmenite only. The average concentrations for the above-listed elements in magnetite and ilmenite from drill core and outcrop samples are listed in Tables 15-18. However, as discussed in section 5.1.1, uncertainties regarding the accuracy of Zr and Nb data are presumably larger than for other elements, particularly at very low (i.e. sub-ppm) concentrations. Si, Ca, and Cu results were highly variable, presumably due to silicate or sulfide inclusions that were not obvious during data reduction, while Ge, Y, Mo, Sn, Ta, W, and Pb were all intermittently detected, but are too low in abundance to ensure accuracy and precision. Re, platinum group elements (PGE), and rare-earth elements (REE) were consistently not detected. Full results from LA-ICP-MS analyses of Fe-Ti oxides are provided in Appendix 2.

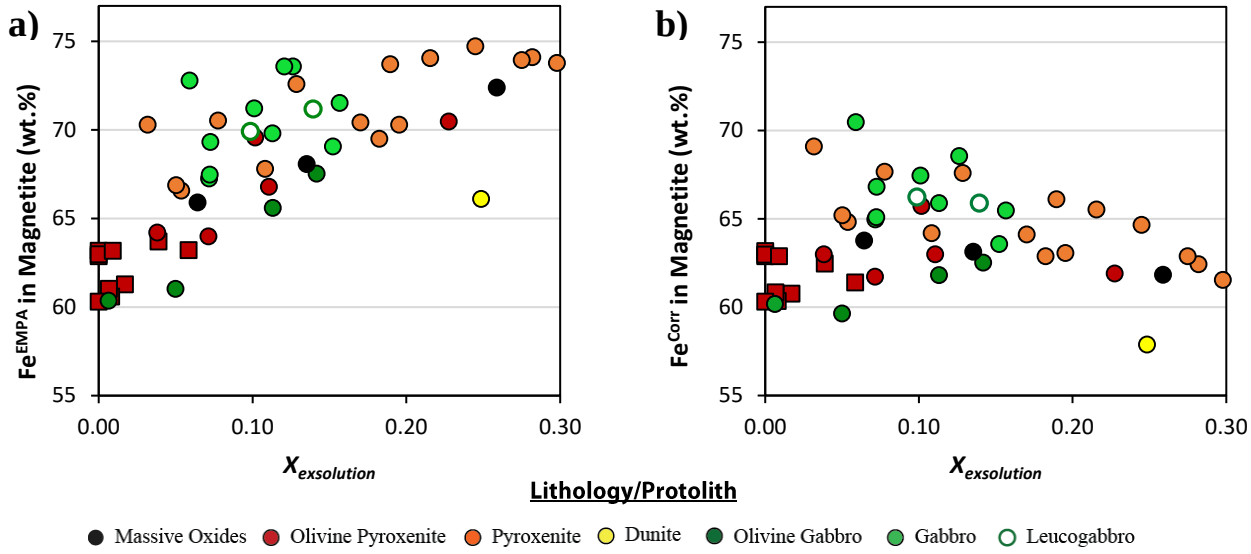

Fig. 12. Fe content of magnetite versus the calculated proportion of ilmenite exsolutions ($X_{exsolution}$) determined to be present in magnetite. **a.** The raw Fe content of magnetite, as determined by EMPA (Fe_{Mgt}^{EMPA}); **b.** the corrected Fe content of magnetite, recalculated to account for the presence of ilmenite exsolutions (Fe_{Mgt}^{Corr}). Circles represent drill core samples; squares represent outcrop samples.

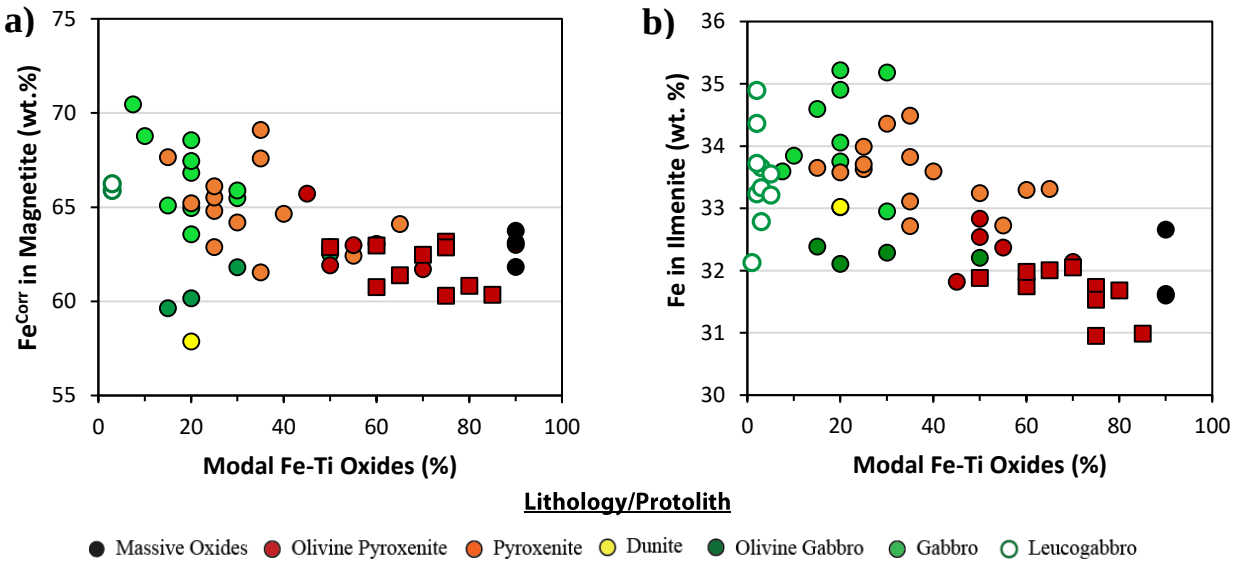

Fig. 13. Fe content of Fe-Ti oxides (determined by EMPA) versus total amount of oxides in a sample. **a.** Magnetite, following the correction of Fe for the presence of ilmenite exsolutions (Fe_{Mgt}^{Corr}); **b.** Ilmenite. Circles represent drill core samples; squares represent outcrop samples.

Table 9. Results of EMPA analyses of primary magnetite from drill core samples. Listed compositions are the averages of *n* grains analyzed per sample. Fe_2O_3 values were calculated by charge balance. All values are in wt.%.

Detection Limits:			*0.011*	*0.026*	*0.016*	*0.066*	*0.024*		*0.044*	*0.017*	*0.016*	*0.017*	*0.018*	*0.016*			
Stratigraphic Depth (m)	**Sample**	***n***	**CaO**	**Cr_2O_3**	**Al_2O_3**	**ZnO**	**FeO**	**Fe_2O_3**	**TiO_2**	**NiO**	**MnO**	**V_2O_3**	**MgO**	**SiO_2**	**Total**	**Total Fe[a] avg**	**std**
9.21	MA12-2A	5	0.00	0.09	3.70	0.06	36.28	52.39	5.84	0.03	0.13	1.41	0.56	0.04	100.52	**66.10**	*(2.26)*
9.58	MA14-2D	6	0.00	0.11	3.99	0.10	40.90	41.70	11.13	0.03	0.23	1.22	0.58	0.03	100.00	**61.02**	*(1.96)*
13.64	MA14-3A	5	0.00	0.16	0.91	0.02	35.50	56.90	4.87	0.02	0.16	1.27	0.06	0.05	99.93	**69.06**	*(3.03)*
13.78	MA14-3B-T	5	0.00	0.18	1.77	0.08	32.55	62.72	1.43	0.02	0.06	1.37	0.08	0.02	100.29	**71.52**	*(0.75)*
17.69	MA14-4	5	0.00	0.03	0.61	0.05	31.51	66.31	0.41	0.00	0.03	1.09	0.01	0.03	100.08	**73.58**	*(0.42)*
24.68	MA14-5A	5	0.00	0.07	0.82	0.12	36.55	54.35	6.30	0.02	0.21	1.13	0.05	0.02	99.64	**67.81**	*(3.19)*
24.90	MA14-5C	5	0.00	0.09	0.26	0.17	35.00	58.31	4.52	0.01	0.12	1.37	0.00	0.02	99.88	**69.81**	*(2.97)*
40.47	MA14-6A-T	5	0.00	0.12	0.87	0.06	35.53	57.21	4.86	0.01	0.12	1.24	0.06	0.04	100.13	**69.32**	*(0.73)*
40.74	MA14-6B	5	0.00	0.07	0.56	0.18	38.12	51.34	8.10	0.01	0.25	1.00	0.03	0.01	99.64	**66.56**	*(2.64)*
51.81	MA14-7A	5	0.00	0.09	0.08	0.02	31.54	66.89	0.50	0.03	0.03	1.01	0.00	0.01	100.19	**74.05**	*(0.36)*
51.92	MA14-7B	5	0.00	0.09	0.15	0.06	32.96	63.72	2.11	0.01	0.07	1.06	0.01	0.00	100.24	**72.58**	*(2.45)*
69.47	MA14-8A	6	0.00	0.19	0.66	0.18	37.67	52.15	7.58	0.03	0.33	1.05	0.02	0.03	99.89	**66.88**	*(2.78)*
69.61	MA14-8B	5	0.00	0.19	0.17	0.09	34.74	59.16	4.21	0.03	0.19	1.28	0.01	0.02	100.10	**70.28**	*(1.78)*
119.73	MA15-1	6	0.01	0.48	0.32	0.07	38.11	52.24	7.59	0.03	0.18	1.48	0.01	0.03	100.54	**67.26**	*(3.26)*
126.94	MA15-2	2	0.01	0.02	2.63	0.03	33.60	60.43	2.78	0.04	0.10	0.98	0.51	0.07	101.18	**70.47**	*(0.27)*
139.46	MA32-25	4	0.01	0.49	0.13	0.01	32.26	64.60	1.03	0.03	0.03	2.15	0.01	0.04	100.77	**72.78**	*(1.35)*
145.55	MA32-1A	4	0.00	0.09	0.45	0.13	32.00	66.11	0.89	0.03	0.06	0.97	0.03	0.04	100.78	**73.77**	*(0.34)*
145.78	MA32-1C	6	0.00	0.05	0.33	0.10	31.75	66.76	0.58	0.03	0.02	1.08	0.02	0.03	100.72	**74.10**	*(0.40)*
152.51	MA32-2A-T	5	0.00	0.08	0.68	0.04	31.75	66.26	0.60	0.02	0.04	0.91	0.03	0.03	100.44	**73.71**	*(0.63)*
152.64	MA32-2A-B-a	4	0.00	0.09	1.95	0.07	33.70	60.27	2.89	0.04	0.12	1.01	0.19	0.02	100.33	**70.42**	*(0.71)*
152.64	MA32-2A-B-b	4	0.00	0.09	2.40	0.10	33.74	60.36	2.75	0.03	0.13	0.76	0.15	0.02	100.52	**70.52**	*(0.79)*
152.84	MA32-2B	5	0.00	0.05	2.62	0.15	34.13	58.70	3.48	0.03	0.13	0.92	0.34	0.03	100.58	**69.50**	*(0.67)*
154.47	MA32-3	5	0.00	0.07	0.47	0.12	31.45	66.83	0.38	0.02	0.03	0.99	0.02	0.02	100.40	**73.94**	*(0.33)*
155.60	MA32-4	3	0.00	0.04	0.25	0.02	31.86	67.47	0.51	0.02	0.02	0.88	0.01	0.01	101.10	**74.72**	*(0.36)*
160.29	MA32-7	6	0.00	0.06	1.87	0.22	33.42	59.43	3.26	0.05	0.12	1.03	0.43	0.04	99.93	**69.57**	*(2.34)*
169.74	MA32-9	6	0.00	0.00	2.54	0.04	32.44	61.24	1.96	0.02	0.06	1.00	0.49	0.04	99.82	**70.29**	*(2.03)*
178.78	MA32-12	3	0.01	0.01	3.59	0.02	37.79	48.33	7.88	0.03	0.21	0.95	0.53	0.04	99.38	**63.99**	*(1.51)*
188.51	MA32-15	5	0.00	0.01	1.02	0.05	31.90	64.42	1.28	0.04	0.04	1.13	0.37	0.05	100.30	**72.38**	*(0.52)*
192.24	MA32-17	5	0.00	0.00	2.31	0.09	34.07	56.91	4.39	0.04	0.11	1.23	0.86	0.05	100.06	**68.07**	*(1.63)*
196.77	MA32-18-a	4	0.01	0.16	2.12	0.04	32.31	62.49	1.30	0.03	0.04	1.17	0.17	0.06	99.88	**71.17**	*(1.27)*
196.77	MA32-18-b	3	0.01	0.21	3.44	0.06	34.90	55.47	4.44	0.03	0.12	1.13	0.57	0.05	100.42	**67.53**	*(2.86)*
196.77	MA32-18-c	2	0.00	0.14	2.23	0.02	33.99	59.35	3.16	0.03	0.08	1.03	0.30	0.05	100.36	**69.91**	*(1.92)*
205.93	MA32-19	5	0.02	0.55	0.88	0.04	35.52	54.84	4.96	0.03	0.10	1.43	0.03	0.25	98.65	**67.47**	*(2.26)*
234.15	MA11-11	5	0.00	0.19	3.32	0.02	36.43	49.81	7.15	0.05	0.23	1.25	0.94	0.04	99.45	**64.20**	*(0.96)*
236.68	MA11-8	5	0.00	0.03	2.80	0.07	36.12	53.42	5.86	0.04	0.20	0.93	0.54	0.16	100.19	**66.79**	*(0.97)*
244.72	MA11-2	4	0.00	0.01	3.93	0.05	36.48	51.96	6.28	0.04	0.16	1.09	0.82	0.08	100.90	**65.90**	*(0.43)*
244.72	MA11-2 (Altered)	4	0.01	0.01	3.92	0.17	36.11	51.95	5.62	0.02	0.14	1.00	0.17	0.08	99.12	**65.63**	*(2.54)*
249.89	MA03-7	7	0.00	0.39	0.07	0.02	31.11	66.67	0.23	0.03	0.02	1.11	0.00	0.11	99.64	**73.58**	*(0.41)*
260.85	MA03-4	6	0.00	0.38	0.66	0.02	33.65	61.33	2.78	0.05	0.07	1.21	0.02	0.04	100.17	**71.21**	*(2.53)*
282.46	MA03-1B	5	0.00	1.43	4.77	0.03	38.53	42.97	9.09	0.06	0.22	1.22	0.94	0.08	99.35	**60.35**	*(0.61)*
282.53	MA03-1A	6	0.01	0.42	3.61	0.03	35.08	52.82	5.04	0.06	0.13	1.33	0.64	0.09	99.26	**65.59**	*(2.89)*

[a] Total Fe calculated as the sum of elemental Fe^{2+} and Fe^{3+}.

Table 10. Results of EMPA analyses of primary magnetite from outcrop samples. Listed compositions are the averages of *n* grains analyzed per sample. Fe_2O_3 values were calculated by charge balance. All values are in wt.%.

Detection Limits:		*0.011*	*0.026*	*0.016*	*0.066*	*0.024*		*0.044*	*0.017*	*0.016*	*0.017*	*0.018*	*0.016*			
Sample	***n***	**CaO**	**Cr_2O_3**	**Al_2O_3**	**ZnO**	**FeO**	**Fe_2O_3**	**TiO_2**	**NiO**	**MnO**	**V_2O_3**	**MgO**	**SiO_2**	**Total**	**Total Fe[a]** avg	std
T3-C4-1	5	0.00	0.00	3.68	0.10	38.29	46.88	8.55	0.03	0.23	1.02	0.63	0.09	99.50	**63.22**	*(0.85)*
T3-C4-2	5	0.00	0.01	3.68	0.07	38.19	47.59	8.29	0.02	0.21	1.02	0.63	0.08	99.79	**63.70**	*(0.78)*
TA1-1	5	0.00	0.02	3.57	0.03	39.86	42.97	10.65	0.02	0.25	0.89	0.74	0.02	99.04	**61.28**	*(0.58)*
TA1-4	5	0.00	0.01	3.74	0.05	40.12	41.84	11.29	0.03	0.27	0.86	1.01	0.03	99.25	**60.58**	*(0.45)*
TA1-5	5	0.01	0.04	4.11	0.05	40.08	42.45	10.74	0.03	0.24	0.93	0.82	0.04	99.54	**61.03**	*(0.44)*
TA1-6	5	0.00	0.01	3.89	0.04	40.28	41.35	11.32	0.03	0.28	0.94	0.95	0.06	99.16	**60.31**	*(1.06)*
TA2-1	5	0.00	0.01	3.71	0.05	39.04	46.13	9.24	0.03	0.30	1.01	0.74	0.11	100.38	**63.17**	*(0.48)*
TA2-3	5	0.01	0.01	3.66	0.02	39.44	45.40	9.72	0.04	0.32	0.90	0.77	0.11	100.41	**62.87**	*(0.65)*
TA2-4	5	0.00	0.02	3.81	0.03	39.47	45.49	9.66	0.03	0.37	0.87	0.68	0.07	100.49	**62.97**	*(0.59)*
TA2-6	6	0.00	0.00	3.84	0.02	39.04	46.15	9.25	0.04	0.32	0.89	0.71	0.06	100.31	**63.17**	*(0.96)*

[a] Total Fe calculated as the sum of elemental Fe^{2+} and Fe^{3+}.

Table 11. Results of EMPA analyses of primary ilmenite from drill core samples. Listed compositions are the averages of *n* grains analyzed per sample. Fe_2O_3 values were calculated by charge balance to account for magnetite exsolutions that were included in the analyses beam. All values are in wt.%.

Detection Limits:			*0.011*	*0.026*	*0.016*	*0.066*	*0.024*		*0.044*	*0.017*	*0.016*	*0.017*	*0.018*	*0.016*			
Stratigraphic Depth (m)	Sample	***n***	**CaO**	**Cr_2O_3**	**Al_2O_3**	**ZnO**	**FeO**	**Fe_2O_3**	**TiO_2**	**NiO**	**MnO**	**V_2O_3**	**MgO**	**SiO_2**	**Total**	**Total Fe[a]** avg	std
9.21	MA14-2A	5	0.00	0.01	0.06	0.01	47.22		50.93	0.00	0.78	0.01	0.60	0.00	99.62	**33.02**	*(0.16)*
9.58	MA14-2D	5	0.00	0.01	0.03	0.01	46.31		51.46	0.00	0.77	0.00	0.73	0.01	99.33	**32.39**	*(0.42)*
10.18	MA14-3A	5	0.00	0.00	0.05	0.01	47.21		50.33	0.00	1.51	0.00	0.12	0.00	99.24	**33.02**	*(0.33)*
13.78	MA14-3B-T	5	0.00	0.01	0.03	0.06	47.11		50.73	0.00	1.29	0.03	0.08	0.00	99.36	**32.95**	*(0.37)*
13.94	MA14-3B-B	5	0.00	0.04	0.00	0.02	48.12		50.91	0.00	1.10	0.13	0.04	0.06	100.44	**33.66**	*(0.21)*
17.69	MA14-4-a	3	0.00	0.01	0.00	0.02	48.26		49.38	0.00	1.08	0.03	0.05	0.00	98.83	**33.75**	*(0.73)*
17.69	MA14-4-b	2	0.01	0.01	0.04	0.00	47.63		49.51	0.01	1.13	0.14	0.03	0.01	98.50	**33.31**	*(0.08)*
24.68	MA14-5A	5	0.00	0.01	0.04	0.12	49.13		48.58	0.00	1.49	0.10	0.14	0.00	99.62	**34.36**	*(0.70)*
24.90	MA14-5C-a	4	0.00	0.01	0.04	0.09	50.30		47.29	0.00	1.17	0.16	0.06	0.01	99.12	**35.18**	*(0.74)*
24.90	MA14-5C-b	2	0.00	0.04	0.00	0.00	49.89		47.12	0.01	1.49	0.32	0.03	0.01	98.89	**34.89**	*(0.14)*
40.47	MA14-6A-T	4	0.01	0.01	0.05	0.10	49.91		48.40	0.01	0.99	0.10	0.18	0.01	99.75	**34.90**	*(0.13)*
40.74	MA14-6B-a	4	0.00	0.01	0.05	0.13	48.60		48.54	0.00	1.33	0.08	0.08	0.00	98.81	**33.99**	*(0.51)*
40.74	MA14-6B-b	3	0.00	0.04	0.05	0.07	47.51		49.14	0.00	1.54	0.41	0.11	0.01	98.89	**33.23**	*(0.17)*
51.81	MA14-7A-a	4	0.00	0.01	0.03	0.09	49.14		48.11	0.00	1.43	0.09	0.08	0.01	98.99	**34.37**	*(0.20)*
51.81	MA14-7A-b	3	0.00	0.01	0.04	0.07	49.31		47.53	0.00	1.46	0.18	0.06	0.00	98.66	**34.49**	*(0.07)*
69.47	MA14-8A-a	4	0.00	0.09	0.04	0.14	45.94		50.73	0.00	2.40	0.63	0.08	0.01	100.04	**32.13**	*(0.29)*
69.47	MA14-8A-b	4	0.00	0.02	0.02	0.03	48.01		49.34	0.00	1.90	0.05	0.04	0.00	99.41	**33.58**	*(0.26)*
69.61	MA14-8B	5	0.00	0.01	0.01	0.04	47.34		49.60	0.00	1.90	0.05	0.07	0.00	99.01	**33.11**	*(0.26)*
119.73	MA15-1	6	0.01	0.04	0.01	0.04	43.20	6.44	49.38	0.01	1.07	0.20	0.05	0.01	100.43	**35.22**	*(0.37)*
126.94	MA15-2	5	0.00	0.01	0.03	0.01	43.80	2.83	51.78	0.01	1.44	0.00	0.74	0.03	100.68	**32.83**	*(0.19)*
139.46	MA32-25	4	0.01	0.02	0.01	0.02	45.44	2.33	51.60	0.00	0.88	0.07	0.04	0.00	100.40	**33.59**	*(0.50)*
145.55	MA32-1A	5	0.00	0.00	0.03	0.04	46.77		50.65	0.00	1.66	0.00	0.23	0.00	99.38	**32.71**	*(0.23)*
145.78	MA32-1C	5	0.01	0.00	0.04	0.03	46.79		50.51	0.00	1.51	0.00	0.24	0.00	99.13	**32.72**	*(0.13)*
152.51	MA32-2A-T	4	0.01	0.00	0.02	0.08	48.08		49.11	0.00	1.68	0.02	0.10	0.00	99.11	**33.63**	*(0.20)*
152.64	MA32-2A-B-a	4	0.00	0.00	0.08	0.07	47.63		49.36	0.01	1.81	0.00	0.05	0.00	99.02	**33.31**	*(0.12)*
152.64	MA32-2A-B-a	4	0.00	0.01	0.03	0.02	48.11		49.51	0.00	1.68	0.00	0.08	0.00	99.46	**33.65**	*(0.29)*
152.84	MA32-2B	5	0.00	0.01	0.03	0.08	47.53		49.94	0.00	1.58	0.00	0.16	0.00	99.33	**33.24**	*(0.37)*
154.47	MA32-3	5	0.00	0.01	0.04	0.06	48.19		49.52	0.00	1.75	0.02	0.15	0.00	99.75	**33.71**	*(1.07)*
155.60	MA32-4	5	0.00	0.02	0.06	0.07	48.03		49.40	0.00	1.36	0.07	0.14	0.00	99.17	**33.59**	*(0.62)*
160.29	MA32-7	5	0.00	0.00	0.01	0.00	44.09	1.27	51.90	0.01	1.28	0.00	0.72	0.00	99.28	**31.82**	*(0.28)*
169.74	MA32-9	6	0.00	0.00	0.05	0.01	44.22	3.05	50.78	0.00	1.12	0.00	0.17	0.00	99.39	**33.29**	*(1.18)*
178.78	MA32-12	5	0.00	0.00	0.03	0.00	44.10	1.67	51.68	0.01	1.05	0.00	0.75	0.00	99.29	**32.14**	*(0.55)*
188.51	MA32-15	5	0.01	0.01	0.02	0.01	45.21		51.51	0.01	0.93	0.01	2.11	0.00	99.85	**31.62**	*(0.46)*
192.24	MA32-17	5	0.00	0.00	0.03	0.01	45.18		51.12	0.01	0.94	0.00	1.89	0.00	99.20	**31.60**	*(0.13)*
196.77	MA32-18-a	5	0.01	0.01	0.02	0.02	44.21	3.10	50.88	0.00	0.77	0.00	0.43	0.00	99.45	**33.33**	*(0.28)*
196.77	MA32-18-b	4	0.01	0.02	0.04	0.00	42.47	3.22	51.25	0.01	0.59	0.00	1.70	0.00	99.33	**32.20**	*(0.14)*
196.77	MA32-18-c	3	0.00	0.00	0.03	0.03	43.81	2.76	51.08	0.00	0.76	0.00	0.76	0.00	99.24	**32.79**	*(0.11)*
205.93	MA32-19	5	0.00	0.04	0.02	0.01	43.47	5.39	49.38	0.00	0.90	0.07	0.02	0.00	99.32	**34.59**	*(0.16)*

[a] Total Fe calculated as the sum of elemental Fe^{2+} and Fe^{3+}.

Table 11. (cont'd)

Detection Limits:			0.011	0.026	0.016	0.066	0.024		0.044	0.017	0.016	0.017	0.018	0.016			
Stratigraphic Depth (m)	**Sample**	***n***	**CaO**	**Cr_2O_3**	**Al_2O_3**	**ZnO**	**FeO**	**Fe_2O_3**	**TiO_2**	**NiO**	**MnO**	**V_2O_3**	**MgO**	**SiO_2**	**Total**	**Total Fe[a]** avg	std
234.15	MA11-11	5	0.00	0.01	0.03	0.01	43.19	2.78	51.50	0.00	1.32	0.00	1.01	0.00	99.89	**32.37**	*(0.37)*
236.68	MA11-8	5	0.00	0.01	0.06	0.01	46.52		50.83	0.01	1.36	0.00	0.83	0.00	99.72	**32.54**	*(0.16)*
244.72	MA11-2	5	0.00	0.00	0.03	0.01	46.69		51.53	0.01	0.90	0.00	1.03	0.00	100.25	**32.66**	*(0.14)*
244.72	MA11-2 (Altered)	5	0.00	0.01	0.00	0.01	46.88		51.67	0.00	1.06	0.00	0.04	0.00	99.72	**32.79**	*(0.13)*
249.89	MA03-7	5	0.00	0.03	0.01	0.01	48.39		50.18	0.01	1.69	0.07	0.03	0.05	100.48	**33.84**	*(0.05)*
251.07	MA03-6	5	0.01	0.09	0.01	0.03	48.21		50.05	0.00	1.41	0.31	0.07	0.09	100.29	**33.72**	*(0.49)*
260.85	MA03-4	5	0.00	0.01	0.01	0.02	48.69		50.73	0.01	1.16	0.06	0.05	0.02	100.76	**34.06**	*(0.12)*
281.37	MA03-2	5	0.00	0.01	0.01	0.04	47.97		49.83	0.00	1.08	0.28	0.02	0.04	99.28	**33.55**	*(0.25)*
282.46	MA03-1B	5	0.00	0.05	0.06	0.02	43.96	1.75	52.23	0.01	0.74	0.00	1.29	0.04	100.16	**32.11**	*(0.17)*
282.53	MA03-1A	5	0.00	0.01	0.05	0.00	46.16		51.82	0.01	0.84	0.00	1.13	0.05	100.07	**32.29**	*(0.06)*

[a] Total Fe calculated as the sum of elemental Fe^{2+} and Fe^{3+}.

Table 12. Results of EMPA analyses of primary ilmenite from outcrop samples. Listed compositions are the averages of *n* grains analyzed per sample. Fe_2O_3 values were calculated by charge balance to account for magnetite exsolutions that were included in the analyses beam. All values are in wt.%.

Detection Limits:		0.011	0.026	0.016	0.066	0.024		0.044	0.017	0.016	0.017	0.018	0.016			
Sample	***n***	**CaO**	**Cr_2O_3**	**Al_2O_3**	**ZnO**	**FeO**	**Fe_2O_3**	**TiO_2**	**NiO**	**MnO**	**V_2O_3**	**MgO**	**SiO_2**	**Total**	**Total Fe[a]** avg	std
T3-C4-1	5	0.00	0.01	0.05	0.02	45.76		51.33	0.00	0.69	0.00	1.43	0.04	99.34	**32.00**	*(0.09)*
T3-C4-2	5	0.00	0.01	0.04	0.01	45.83		51.45	0.01	0.66	0.00	1.56	0.03	99.60	**32.05**	*(0.24)*
TA1-6	3	0.00	0.00	0.03	0.01	44.26		51.33	0.01	0.67	0.00	2.14	0.02	98.47	**30.95**	*(0.16)*
TA1-5	5	0.00	0.01	0.03	0.01	43.95	1.21	52.58	0.01	0.69	0.00	1.47	0.00	99.97	**31.68**	*(0.32)*
TA1-4	5	0.01	0.01	0.03	0.01	42.78	1.37	52.82	0.00	0.63	0.00	2.29	0.01	99.96	**30.99**	*(0.06)*
TA1-1	5	0.00	0.01	0.04	0.01	43.71	1.51	52.40	0.01	0.72	0.00	1.50	0.01	99.91	**31.75**	*(0.43)*
TA2-1	5	0.00	0.00	0.04	0.01	45.38		52.27	0.01	0.70	0.00	1.82	0.07	100.29	**31.74**	*(0.19)*
TA2-3	5	0.00	0.00	0.03	0.04	45.08		52.61	0.01	0.63	0.00	2.07	0.07	100.55	**31.53**	*(0.22)*
TA2-4	4	0.00	0.00	0.03	0.00	45.72		52.13	0.01	0.66	0.00	1.80	0.04	100.38	**31.98**	*(0.21)*
TA2-6	5	0.00	0.00	0.03	0.00	45.58		51.82	0.01	0.65	0.00	1.72	0.01	99.84	**31.88**	*(0.17)*

[a] Total Fe calculated as the sum of elemental Fe^{2+} and Fe^{3+}

Table 13. Average Fe contents of magnetite proportionally corrected for the presence of ilmenite exsolutions (Fe_{Mgt}^{Corr}), and the variables used in its calculation. Rel. Diff. is the relative difference between Fe_{Mgt}^{Corr} and the uncorrected Fe value (Fe_{Mgt}^{EMPA}). All other values are in wt.% except $X_{exsolution}$, which is the weight fraction of ilmenite exsolutions. Variables are as defined in section 5.1.3.

Sample	Ti_{Mgt}^{EMPA}	Ti_{Ilm}^{EMPA}	$Ti_{Mgt\ Laser}^{Fe=1}$	Fe_{Mgt}^{EMPA}	Fe_{Ilm}^{EMPA}	$X_{exsolution}$	Fe_{Mgt}^{Corr}	Rel. Diff. (%)
	A	B	C	D	E	$\frac{(CD-A)}{(B-A)-C(E-D)}$		
MA12-2A	3.50	30.52	0.18	66.10	33.02	0.25	**57.88**	12.44
MA14-2D	6.67	30.84	0.13	61.02	33.29	0.05	**59.63**	2.27
MA14-3A	2.92	30.16	0.11	69.06	33.02	0.15	**63.57**	7.95
MA14-3B-T	0.86	30.40	0.08	71.52	32.95	0.16	**65.48**	8.45
MA14-4	0.25	29.60	0.06	73.58	33.75	0.13	**68.55**	6.83
MA14-5A	3.77	29.12	0.10	67.81	34.36	0.11	**64.19**	5.34
MA14-5C	2.71	28.34	0.09	69.81	35.18	0.11	**65.89**	5.61
MA14-6A-T	2.91	29.00	0.07	69.32	34.90	0.07	**66.82**	3.60
MA14-6B	4.85	29.09	0.09	66.56	33.99	0.05	**64.81**	2.63
MA14-7A	0.30	28.48	0.10	74.05	34.49	0.22	**65.52**	11.52
MA14-7B	1.26	29.41	0.07	72.58	33.82	0.13	**67.60**	6.87
MA14-8A	4.54	29.57	0.09	66.88	33.58	0.05	**65.21**	2.51
MA14-8B	2.53	29.72	0.05	70.28	33.11	0.03	**69.10**	1.68
MA15-1	4.55	29.59	0.10	67.26	35.22	0.07	**64.96**	3.42
MA15-2	1.67	31.03	0.13	70.47	32.83	0.23	**61.91**	12.15
MA32-25	0.62	30.92	0.03	72.78	33.59	0.06	**70.46**	3.18
MA32-1A	0.53	30.35	0.15	73.77	32.71	0.30	**61.54**	16.58
MA32-1C	0.35	30.27	0.14	74.10	32.72	0.28	**62.43**	15.74
MA32-2A-T	0.36	29.43	0.09	73.71	33.63	0.19	**66.11**	10.31
MA32-2A-B-a	1.73	29.58	0.10	70.42	33.31	0.17	**64.11**	8.96
MA32-2A-B-b	1.65	29.67	0.06	70.52	33.65	0.08	**67.65**	4.06
MA32-2B	2.08	29.93	0.11	69.50	33.24	0.18	**62.89**	9.52
MA32-3	0.23	29.68	0.13	73.94	33.71	0.27	**62.88**	14.96
MA32-4	0.31	29.61	0.12	74.72	33.59	0.24	**64.65**	13.48
MA32-7	1.95	31.10	0.07	69.57	31.82	0.10	**65.73**	5.52
MA32-9	1.17	30.43	0.11	70.29	33.29	0.20	**63.06**	10.28
MA32-12	4.72	30.97	0.11	63.99	32.14	0.07	**61.72**	3.55
MA32-15	0.77	30.87	0.14	72.38	31.62	0.26	**61.84**	14.57
MA32-17	2.63	30.64	0.10	68.07	31.60	0.14	**63.13**	7.25
MA32-18-a	0.78	30.49	0.07	71.17	33.33	0.14	**65.90**	7.41
MA32-18-b	2.66	30.71	0.11	67.53	32.20	0.14	**62.52**	7.41
MA32-18-c	1.89	30.61	0.07	69.91	32.79	0.10	**66.24**	5.24
MA32-19	2.97	29.59	0.08	67.47	34.59	0.07	**65.10**	3.52
MA11-11	4.29	30.87	0.08	64.20	32.37	0.04	**62.99**	1.89
MA11-8	3.51	30.46	0.10	66.79	32.54	0.11	**63.00**	5.67
MA11-2	3.77	30.88	0.09	65.90	32.66	0.06	**63.76**	3.25
MA11-2 (Altered)	3.37	30.96	0.07	65.63	32.79	0.04	**64.31**	2.01
MA03-7	0.14	30.08	0.05	73.58	33.84	0.12	**68.78**	6.52
MA03-4	1.67	30.40	0.07	71.21	34.06	0.10	**67.45**	5.27
MA03-1B	5.45	31.30	0.09	60.35	32.11	0.01	**60.17**	0.30
MA03-1A	3.02	31.06	0.10	65.59	32.29	0.11	**61.82**	5.74

Table 13. (cont'd)

Sample	Ti_{Mgt}^{EMPA}	Ti_{Ilm}^{EMPA}	$Ti_{Mgt\ Laser}^{Fe=1}$	Fe_{Mgt}^{EMPA}	Fe_{Ilm}^{EMPA}	$X_{exsolution}$	Fe_{Mgt}^{Corr}	Rel. Diff. (%)
	A	B	C	D	E	$\frac{(CD-A)}{(B-A)-C(E-D)}$		
T3-C4-1	5.13	30.76	0.11	63.22	32.00	0.06	**61.39**	2.89
T3-C4-2	4.97	30.83	0.10	63.70	32.05	0.04	**62.47**	1.93
TA1-1	6.38	30.76	0.11	61.28	30.95	0.02	**60.76**	0.85
TA1-4	6.77	31.51	0.12	60.58	31.68	0.01	**60.35**	0.39
TA1-5	6.44	31.66	0.11	61.03	30.99	0.01	**60.83**	0.33
TA1-6	6.79	31.40	0.10	60.31	31.75	0.00*	**60.31**	0.00
TA2-1	5.54	31.32	0.08	63.17	31.74	0.00*	**63.17**	0.00
TA2-3	5.83	31.53	0.09	62.87	31.53	0.00*	**62.87**	0.00
TA2-4	5.79	31.24	0.08	62.97	31.98	0.00*	**62.97**	0.00
TA2-6	5.54	31.06	0.09	63.17	31.88	0.01	**62.89**	0.45

*$X_{exsolution}$ values manually input to zero. See section 5.1.3 for details.

Table 14. Comparison of the compositions of coexisting primary ilmenite (Ilm) and magnetite-hosted ilmenite exsolutions from select samples (determined by EMPA). Averages (avg) and standard deviations (std) calculated from *n* analyses per sample.

	MA-14-3A				**MA-14-5A**				**MA-32-1C**				**MA-32-3B**			
	Primary Ilm		**Exsolutions**		**Primary Ilm**		**Exsolutions**		**Primary Ilm**		**Exsolutions**		**Primary Ilm**		**Exsolutions**	
	avg (n=5)	std	avg (n=5)	std	avg (n=5)	std	avg (n=6)	std	avg (n=5)	std	avg (n=7)	std	avg (n=5)	std	avg (n=8)	std
Wt.% oxide																
CaO	**0.00**	0.00	**0.00**	0.00	**0.00**	0.00	**0.00**	0.00	**0.01**	0.00	**0.00**	0.00	**0.00**	0.00	**0.00**	0.01
Cr_2O_3	**0.00**	0.00	**0.02**	0.02	**0.01**	0.00	**0.01**	0.01	**0.00**	0.00	**0.01**	0.01	**0.01**	0.01	**0.00**	0.00
Al_2O_3	**0.05**	0.02	**0.16**	0.18	**0.04**	0.02	**0.06**	0.12	**0.04**	0.05	**0.00**	0.00	**0.03**	0.04	**0.05**	0.08
ZnO	**0.01**	0.02	**0.02**	0.03	**0.12**	0.07	**0.02**	0.02	**0.03**	0.05	**0.02**	0.03	**0.08**	0.09	**0.04**	0.03
TiO_2	**50.3**	0.59	**50.7**	0.32	**48.6**	0.89	**49.5**	0.71	**50.5**	0.23	**51.3**	0.58	**49.9**	0.52	**51.2**	0.47
FeO	**47.2**	0.47	**46.8**	0.45	**49.1**	1.00	**47.5**	0.55	**46.8**	0.19	**46.3**	0.37	**47.5**	0.53	**46.1**	0.56
NiO	**0.00**	0.00	**0.01**	0.01	**0.00**	0.00	**0.00**	0.00	**0.00**	0.01	**0.00**	0.00	**0.00**	0.00	**0.00**	0.01
MnO	**1.51**	0.03	**1.38**	0.07	**1.49**	0.03	**1.46**	0.04	**1.51**	0.03	**1.65**	0.07	**1.58**	0.03	**1.54**	0.04
V_2O_3	**0.00**	0.00	**0.05**	0.04	**0.10**	0.03	**0.24**	0.09	**0.00**	0.00	**0.06**	0.02	**0.00**	0.00	**0.02**	0.02
MgO	**0.12**	0.05	**0.03**	0.06	**0.14**	0.02	**0.03**	0.01	**0.24**	0.04	**0.06**	0.03	**0.16**	0.03	**0.19**	0.19
SiO_2	**0.00**	0.00	**0.01**	0.01	**0.00**	0.00	**0.01**	0.01	**0.00**	0.00	**0.00**	0.00	**0.00**	0.00	**0.01**	0.00
TOTAL	**99.2**	0.20	**99.2**	0.31	**99.6**	0.35	**98.8**	0.14	**99.1**	0.30	**99.4**	0.46	**99.3**	0.29	**99.2**	0.28
Element (ppm)																
Ca	**0.0**	0.0	**0.0**	0.0	**14.3**	28.6	**0.0**	0.0	**42.9**	35.0	**0.0**	0.0	**0.0**	0.0	**14.5**	36.4
Cr	**27.4**	33.5	**153.8**	139.6	**41.1**	33.5	**75.7**	77.9	**27.4**	33.5	**67.2**	95.1	**68.4**	61.2	**8.2**	21.7
Al	**275**	131	**824**	974	**191**	109	**344**	618	**191**	287	**25**	20	**159**	227	**265**	405
Zn	**80**	124	**126**	219	**964**	577	**165**	136	**225**	411	**170**	213	**611**	743	**297**	269
Ti	**301604**	3526	**303725**	1895	**291152**	5346	**296604**	4272	**302706**	1356	**307381**	3496	**299314**	3118	**306782**	2840
Fe	**330173**	3271	**327445**	3151	**343587**	6998	**331982**	3833	**327235**	1317	**323572**	2566	**332411**	3677	**322677**	3932
Ni	**0.0**	0.0	**71.2**	58.7	**15.7**	31.4	**31.7**	36.3	**31.4**	62.9	**15.5**	37.9	**15.7**	31.4	**34.8**	53.6
Mn	**11695**	230	**10684**	551	**11571**	217	**11334**	309	**11695**	230	**12746**	535	**12222**	232	**11937**	275
V	**27**	33	**363**	246	**707**	234	**1613**	625	**14**	27	**404**	132	**0**	0	**116**	165
Mg	**724**	278	**173**	355	**856**	140	**211**	53	**1447**	219	**373**	156	**965**	153	**1135**	1163
Si	**18.7**	22.9	**32.0**	29.2	**9.3**	18.7	**38.9**	25.5	**18.7**	22.9	**14.5**	15.9	**9.3**	18.7	**59.7**	17.3

Table 15. Results of LA-ICP-MS analyses of magnetite from drill core samples. Average trace element concentrations (avg) and standard deviations (std) are calculated from *n* analyses per sample.

Stratigraphic Depth (m)	Sample	*n*	Mg (ppm)		Al (ppm)		Sc (ppm)		Ti (ppm)	
			avg	std	avg	std	avg	std	avg	std
9.21	MA14-2A	5	**3297.54**	*(1007.08)*	**13491.33**	*(2783.94)*	**20.74**	*(12.08)*	**102161.34**	*(60795.88)*
9.58	MA14-2D	6	**3188.36**	*(638.00)*	**21772.87**	*(1610.00)*	**20.36**	*(5.41)*	**78744.89**	*(13100.00)*
13.64	MA14-3A	5	**763.20**	*(219.83)*	**5933.45**	*(2056.09)*	**7.98**	*(4.28)*	**70687.82**	*(11494.42)*
13.78	MA14-3B-T	5	**577.11**	*(195.10)*	**12109.33**	*(3253.37)*	**4.71**	*(0.87)*	**54869.77**	*(17990.82)*
17.69	MA14-4	5	**353.33**	*(164.00)*	**9386.36**	*(3390.00)*	**4.92**	*(1.53)*	**39500.61**	*(12900.00)*
24.68	MA14-5A	5	**498.08**	*(110.57)*	**3518.67**	*(275.13)*	**5.29**	*(1.41)*	**65161.56**	*(14079.15)*
24.90	MA14-5C	4	**241.91**	*(222.66)*	**2243.16**	*(387.98)*	**2.21**	*(0.86)*	**56066.50**	*(10828.73)*
40.47	MA14-6A-T	4	**572.92**	*(28.75)*	**5581.34**	*(720.26)*	**3.06**	*(0.42)*	**48029.78**	*(4036.07)*
40.74	MA14-6B	6	**362.10**	*(103.23)*	**5101.31**	*(955.61)*	**5.86**	*(1.04)*	**61542.41**	*(4046.65)*
51.81	MA14-7A	4	**165.07**	*(66.83)*	**1346.08**	*(720.69)*	**10.89**	*(11.84)*	**63776.77**	*(56215.82)*
51.92	MA14-7B	5	**250.15**	*(39.08)*	**3650.51**	*(746.77)*	**6.04**	*(1.05)*	**48825.13**	*(3905.68)*
69.47	MA14-8A	6	**374.49**	*(93.84)*	**6555.05**	*(698.72)*	**5.94**	*(1.44)*	**58034.58**	*(6394.33)*
69.61	MA14-8B	5	**156.94**	*(68.27)*	**3361.11**	*(1543.62)*	**3.67**	*(1.95)*	**33901.30**	*(15331.46)*
119.73	MA15-1	5	**186.08**	*(89.09)*	**3719.80**	*(1774.11)*	**3.20**	*(1.05)*	**63453.55**	*(12011.71)*
126.94	MA15-2	5	**3398.80**	*(186.55)*	**10310.30**	*(323.37)*	**25.63**	*(7.62)*	**83465.52**	*(16892.99)*
139.46	MA32-25	5	**171.49**	*(153.79)*	**1538.32**	*(755.57)*	**0.55**	*(0.33)*	**24078.49**	*(13503.76)*
145.55	MA32-1A	5	**724.14**	*(112.74)*	**1765.57**	*(730.37)*	**15.41**	*(1.88)*	**94156.13**	*(12164.29)*
145.78	MA32-1C	5	**737.81**	*(150.69)*	**2254.94**	*(858.08)*	**26.09**	*(8.80)*	**87833.54**	*(22148.88)*
152.51	MA32-2A-T	5	**797.54**	*(338.62)*	**7475.59**	*(992.52)*	**7.31**	*(4.29)*	**58707.34**	*(42481.67)*
152.64	MA32-2A-B-a	5	**1535.29**	*(722.09)*	**12806.55**	*(650.13)*	**10.48**	*(1.44)*	**64668.62**	*(7503.49)*
152.64	MA32-2A-B-b	4	**995.88**	*(394.83)*	**11959.66**	*(1804.43)*	**5.65**	*(1.69)*	**38209.70**	*(16686.88)*
152.84	MA32-2B	5	**1574.50**	*(473.94)*	**12287.04**	*(361.03)*	**13.26**	*(1.90)*	**71653.63**	*(11177.03)*
154.47	MA32-3	5	**584.40**	*(453.24)*	**2726.71**	*(571.14)*	**9.03**	*(7.49)*	**83265.16**	*(62892.27)*
155.60	MA32-4B	5	**416.28**	*(80.80)*	**2757.96**	*(344.13)*	**7.71**	*(1.36)*	**74815.83**	*(13791.90)*
160.29	MA32-7	6	**2014.79**	*(848.75)*	**5010.70**	*(1323.47)*	**15.74**	*(4.68)*	**49175.80**	*(16703.11)*
169.74	MA32-9	6	**2991.35**	*(871.21)*	**12016.30**	*(1839.52)*	**11.96**	*(2.22)*	**68882.10**	*(5544.03)*
178.78	MA32-12	5	**3093.46**	*(662.46)*	**19169.32**	*(747.23)*	**17.99**	*(1.59)*	**65942.77**	*(3577.39)*
188.51	MA32-15	5	**7247.31**	*(1296.66)*	**12503.47**	*(3099.39)*	**26.37**	*(5.60)*	**85582.61**	*(24308.37)*
192.24	MA32-17	5	**6183.10**	*(718.38)*	**12731.10**	*(419.04)*	**20.40**	*(4.14)*	**64179.51**	*(12284.47)*
196.77	MA32-18-a	5	**1438.24**	*(306.57)*	**20401.29**	*(2508.40)*	**5.07**	*(1.42)*	**49224.05**	*(10720.72)*
196.77	MA32-18-b	5	**4200.22**	*(354.30)*	**20125.82**	*(999.91)*	**12.59**	*(3.02)*	**66386.06**	*(13909.04)*
196.77	MA32-18-c	4	**2002.71**	*(871.90)*	**23010.63**	*(1360.70)*	**4.36**	*(0.29)*	**47288.75**	*(2244.85)*
205.93	MA32-19	6	**333.32**	*(165.00)*	**6879.84**	*(1637.21)*	**2.77**	*(0.73)*	**48997.95**	*(9150.41)*
234.15	MA11-11	5	**5009.26**	*(381.61)*	**16999.34**	*(737.14)*	**15.68**	*(2.74)*	**53025.86**	*(10534.45)*
236.68	MA11-8	5	**2971.90**	*(1185.22)*	**12204.18**	*(628.05)*	**12.28**	*(4.16)*	**64950.34**	*(10867.86)*
244.72	MA11-2	6	**4445.14**	*(406.14)*	**17856.02**	*(660.82)*	**11.23**	*(1.18)*	**55099.37**	*(5292.69)*
244.72	MA11-2 (Altered)	5	**980.87**	*(318.69)*	**15640.40**	*(1952.93)*	**6.43**	*(2.74)*	**44786.07**	*(12670.68)*
249.89	MA03-7	7	**128.35**	*(113.96)*	**419.76**	*(362.13)*	**0.71**	*(0.22)*	**37524.56**	*(12776.90)*
260.85	MA03-4	6	**539.38**	*(251.48)*	**11899.32**	*(1132.06)*	**2.46**	*(1.18)*	**45708.69**	*(12774.68)*
282.46	MA03-1B	5	**4945.84**	*(630.39)*	**23551.10**	*(1423.07)*	**11.08**	*(0.52)*	**56149.12**	*(1396.56)*
282.53	MA03-1A	6	**4788.90**	*(298.24)*	**21992.07**	*(973.15)*	**12.57**	*(3.12)*	**61942.53**	*(14400.75)*

Table 15. (cont'd)

Stratigraphic Depth (m)	Sample	*n*	V (ppm)		Cr (ppm)		Mn (ppm)		Co (ppm)	
			avg	std	**avg**	std	**avg**	std	**avg**	std
9.21	MA14-2A	5	**7451.19**	*(978.93)*	**526.06**	*(53.56)*	**2996.68**	*(2100.34)*	**166.14**	*(11.01)*
9.58	MA14-2D	6	**7751.25**	*(526.00)*	**807.62**	*(49.80)*	**1961.52**	*(454.00)*	**206.97**	*(21.60)*
13.64	MA14-3A	5	**7823.97**	*(341.06)*	**1027.13**	*(56.18)*	**2791.91**	*(575.11)*	**80.54**	*(31.50)*
13.78	MA14-3B-T	5	**8261.89**	*(810.15)*	**1046.06**	*(39.90)*	**2100.50**	*(658.34)*	**133.13**	*(16.46)*
17.69	MA14-4	5	**6952.85**	*(593.00)*	**306.75**	*(20.20)*	**1116.05**	*(363.00)*	**29.65**	*(6.05)*
24.68	MA14-5A	5	**7437.87**	*(269.44)*	**489.40**	*(32.93)*	**2761.28**	*(539.55)*	**127.56**	*(13.57)*
24.90	MA14-5C	4	**9261.36**	*(597.83)*	**777.77**	*(44.02)*	**1826.20**	*(355.04)*	**49.59**	*(6.76)*
40.47	MA14-6A-T	4	**8579.63**	*(389.91)*	**731.85**	*(79.84)*	**1540.11**	*(125.13)*	**128.44**	*(11.19)*
40.74	MA14-6B	6	**6940.95**	*(240.50)*	**537.60**	*(54.36)*	**2298.79**	*(168.57)*	**115.90**	*(12.42)*
51.81	MA14-7A	4	**6275.96**	*(534.34)*	**563.66**	*(82.95)*	**2581.38**	*(2152.90)*	**96.00**	*(14.41)*
51.92	MA14-7B	5	**6983.10**	*(359.44)*	**642.81**	*(45.30)*	**2000.37**	*(170.86)*	**97.21**	*(6.45)*
69.47	MA14-8A	6	**7461.02**	*(935.82)*	**1336.58**	*(139.80)*	**3179.51**	*(376.92)*	**88.92**	*(19.92)*
69.61	MA14-8B	5	**9209.88**	*(1540.81)*	**1517.06**	*(149.97)*	**1852.20**	*(782.20)*	**48.14**	*(19.53)*
119.73	MA15-1	5	**11001.19**	*(2027.00)*	**3642.41**	*(662.82)*	**2197.00**	*(409.80)*	**86.25**	*(16.81)*
126.94	MA15-2	5	**6267.65**	*(477.76)*	**248.16**	*(6.68)*	**3501.56**	*(569.78)*	**198.84**	*(7.60)*
139.46	MA32-25	5	**16343.40**	*(2057.84)*	**4274.36**	*(1761.41)*	**698.67**	*(355.90)*	**52.36**	*(5.92)*
145.55	MA32-1A	5	**5373.51**	*(297.87)*	**517.35**	*(88.47)*	**4269.81**	*(512.16)*	**85.86**	*(5.71)*
145.78	MA32-1C	5	**5890.99**	*(411.79)*	**286.06**	*(5.69)*	**3741.33**	*(925.87)*	**64.39**	*(5.01)*
152.51	MA32-2A-T	5	**5628.38**	*(474.96)*	**555.68**	*(55.31)*	**2805.00**	*(1835.83)*	**101.91**	*(10.69)*
152.64	MA32-2A-B-a	5	**6185.11**	*(100.93)*	**542.93**	*(66.14)*	**2982.25**	*(262.05)*	**134.04**	*(3.87)*
152.64	MA32-2A-B-b	4	**5094.06**	*(481.70)*	**595.87**	*(75.14)*	**2035.22**	*(756.00)*	**127.22**	*(14.69)*
152.84	MA32-2B	5	**5777.37**	*(206.10)*	**391.07**	*(11.01)*	**3028.45**	*(424.00)*	**160.44**	*(6.14)*
154.47	MA32-3	5	**5583.71**	*(793.30)*	**481.78**	*(56.83)*	**3874.64**	*(2815.25)*	**91.62**	*(22.83)*
155.60	MA32-4B	5	**5373.27**	*(164.58)*	**253.44**	*(21.77)*	**2915.86**	*(469.34)*	**128.84**	*(11.64)*
160.29	MA32-7	6	**7612.44**	*(383.90)*	**508.19**	*(43.19)*	**2024.43**	*(469.45)*	**226.68**	*(11.16)*
169.74	MA32-9	6	**6477.53**	*(374.61)*	**77.13**	*(3.90)*	**2380.09**	*(248.13)*	**140.69**	*(26.06)*
178.78	MA32-12	5	**6832.52**	*(99.60)*	**108.74**	*(2.23)*	**2196.53**	*(75.81)*	**150.59**	*(14.52)*
188.51	MA32-15	5	**6558.45**	*(220.92)*	**144.33**	*(9.74)*	**2443.80**	*(388.40)*	**130.29**	*(29.23)*
192.24	MA32-17	5	**7991.19**	*(273.62)*	**260.23**	*(8.10)*	**2013.90**	*(274.77)*	**178.08**	*(15.50)*
196.77	MA32-18-a	5	**8570.39**	*(570.41)*	**1530.10**	*(136.20)*	**1323.32**	*(313.59)*	**120.14**	*(55.96)*
196.77	MA32-18-b	5	**7768.60**	*(276.35)*	**1555.83**	*(71.40)*	**2186.42**	*(358.30)*	**173.17**	*(18.02)*
196.77	MA32-18-c	4	**7854.76**	*(202.08)*	**1416.37**	*(21.13)*	**1433.03**	*(84.32)*	**160.70**	*(46.71)*
205.93	MA32-19	6	**10527.49**	*(585.37)*	**4675.24**	*(857.69)*	**1412.34**	*(250.01)*	**51.82**	*(10.42)*
234.15	MA11-11	5	**9418.62**	*(168.13)*	**1445.09**	*(72.63)*	**2174.73**	*(528.36)*	**198.92**	*(9.11)*
236.68	MA11-8	5	**6603.70**	*(220.00)*	**955.36**	*(56.31)*	**2833.31**	*(405.00)*	**182.72**	*(20.84)*
244.72	MA11-2	6	**7677.78**	*(291.22)*	**310.27**	*(9.40)*	**1885.17**	*(214.02)*	**205.81**	*(7.03)*
244.72	MA11-2 (Altered)	5	**7897.37**	*(455.40)*	**334.54**	*(28.25)*	**1423.71**	*(359.37)*	**80.23**	*(15.02)*
249.89	MA03-7	7	**8263.46**	*(1085.45)*	**7470.52**	*(705.07)*	**1988.73**	*(667.66)*	**37.47**	*(15.53)*
260.85	MA03-4	6	**8986.60**	*(1005.58)*	**7254.26**	*(713.66)*	**1808.34**	*(476.64)*	**218.86**	*(54.26)*
282.46	MA03-1B	5	**9176.88**	*(211.30)*	**11009.61**	*(549.97)*	**1803.25**	*(84.87)*	**233.69**	*(5.52)*
282.53	MA03-1A	6	**8997.74**	*(195.44)*	**9983.75**	*(764.33)*	**2014.06**	*(447.43)*	**209.31**	*(6.97)*

Table 15. (cont'd).

Stratigraphic Depth (m)	Sample	n	Ni (ppm)		Zn (ppm)		Ga (ppm)		Zr (ppm)	
			avg	std	avg	std	avg	std	avg	std
9.21	MA14-2A	*5*	**255.31**	*(24.95)*	**488.03**	*(105.37)*	**51.30**	*(8.00)*	**14.92**	*(12.10)*
9.58	MA14-2D	*6*	**301.74**	*(18.60)*	**537.59**	*(48.10)*	**51.65**	*(4.51)*	**16.30**	*(3.94)*
13.64	MA14-3A	*5*	**169.14**	*(26.68)*	**848.25**	*(242.22)*	**39.35**	*(5.11)*	**12.14**	*(3.79)*
13.78	MA14-3B-T	*5*	**223.72**	*(9.35)*	**956.62**	*(271.67)*	**58.14**	*(4.96)*	**6.29**	*(2.78)*
17.69	MA14-4	*5*	**60.26**	*(6.53)*	**1986.96**	*(804.00)*	**78.14**	*(4.52)*	**1.24**	*(0.65)*
24.68	MA14-5A	*5*	**209.17**	*(3.10)*	**1738.03**	*(220.74)*	**43.13**	*(0.94)*	**3.17**	*(0.72)*
24.90	MA14-5C	*4*	**139.23**	*(8.91)*	**1568.02**	*(827.53)*	**30.33**	*(1.54)*	**1.69**	*(0.60)*
40.47	MA14-6A-T	*4*	**180.02**	*(4.33)*	**1093.93**	*(234.90)*	**51.88**	*(4.17)*	**1.91**	*(0.28)*
40.74	MA14-6B	*6*	**177.40**	*(18.81)*	**1292.00**	*(335.96)*	**46.28**	*(3.72)*	**3.25**	*(0.68)*
51.81	MA14-7A	*4*	**210.32**	*(20.22)*	**1077.29**	*(743.82)*	**31.21**	*(4.33)*	**1.58**	*(1.41)*
51.92	MA14-7B	*5*	**203.18**	*(2.36)*	**2589.97**	*(403.75)*	**40.77**	*(5.45)*	**1.98**	*(0.23)*
69.47	MA14-8A	*6*	**290.10**	*(20.37)*	**2587.34**	*(269.81)*	**41.75**	*(2.99)*	**5.21**	*(0.76)*
69.61	MA14-8B	*5*	**288.28**	*(38.23)*	**2234.75**	*(1106.46)*	**44.14**	*(5.49)*	**2.44**	*(1.21)*
119.73	MA15-1	*5*	**226.25**	*(17.64)*	**1965.37**	*(988.80)*	**51.14**	*(9.13)*	**2.89**	*(1.14)*
126.94	MA15-2	*5*	**226.90**	*(10.62)*	**426.18**	*(16.46)*	**41.31**	*(1.91)*	**13.23**	*(2.96)*
139.46	MA32-25	*5*	**256.06**	*(17.79)*	**940.21**	*(674.12)*	**56.60**	*(7.37)*	**1.25**	*(0.54)*
145.55	MA32-1A	*5*	**191.11**	*(19.83)*	**983.23**	*(600.77)*	**19.30**	*(3.24)*	**9.63**	*(2.62)*
145.78	MA32-1C	*5*	**204.99**	*(24.09)*	**1443.67**	*(656.12)*	**29.47**	*(3.96)*	**13.75**	*(6.14)*
152.51	MA32-2A-T	*5*	**213.49**	*(17.42)*	**991.77**	*(321.97)*	**39.49**	*(5.69)*	**5.63**	*(4.40)*
152.64	MA32-2A-B-a	*5*	**258.06**	*(5.71)*	**683.55**	*(179.46)*	**40.83**	*(1.25)*	**6.65**	*(0.65)*
152.64	MA32-2A-B-b	*4*	**197.87**	*(24.32)*	**642.21**	*(186.64)*	**39.85**	*(1.89)*	**2.21**	*(1.43)*
152.84	MA32-2B	*5*	**223.60**	*(6.28)*	**558.87**	*(100.20)*	**38.44**	*(1.20)*	**9.13**	*(2.26)*
154.47	MA32-3	*5*	**150.70**	*(25.35)*	**589.56**	*(257.13)*	**35.14**	*(3.36)*	**5.07**	*(4.49)*
155.60	MA32-4B	*5*	**199.39**	*(6.83)*	**1057.77**	*(243.49)*	**36.99**	*(1.94)*	**4.60**	*(1.01)*
160.29	MA32-7	*6*	**305.82**	*(12.05)*	**936.19**	*(218.24)*	**47.88**	*(1.74)*	**4.84**	*(2.15)*
169.74	MA32-9	*6*	**171.54**	*(17.93)*	**463.86**	*(55.41)*	**46.20**	*(2.09)*	**6.72**	*(0.92)*
178.78	MA32-12	*5*	**202.07**	*(8.49)*	**371.81**	*(22.37)*	**43.83**	*(0.33)*	**4.38**	*(0.41)*
188.51	MA32-15	*5*	**236.59**	*(19.22)*	**193.04**	*(75.09)*	**38.56**	*(1.88)*	**8.90**	*(1.51)*
192.24	MA32-17	*5*	**240.78**	*(17.60)*	**283.97**	*(30.32)*	**44.58**	*(1.03)*	**6.81**	*(1.75)*
196.77	MA32-18-a	*5*	**201.80**	*(34.41)*	**529.14**	*(151.12)*	**61.31**	*(2.73)*	**6.47**	*(2.94)*
196.77	MA32-18-b	*5*	**213.39**	*(27.76)*	**434.55**	*(52.72)*	**50.69**	*(1.31)*	**8.24**	*(3.33)*
196.77	MA32-18-c	*4*	**260.34**	*(19.87)*	**594.57**	*(72.24)*	**58.53**	*(2.01)*	**2.59**	*(0.24)*
205.93	MA32-19	*6*	**261.65**	*(41.78)*	**639.97**	*(140.04)*	**53.43**	*(3.75)*	**1.94**	*(0.74)*
234.15	MA11-11	*5*	**468.34**	*(6.35)*	**291.62**	*(33.48)*	**48.38**	*(1.23)*	**5.01**	*(2.31)*
236.68	MA11-8	*5*	**293.73**	*(9.24)*	**425.08**	*(20.86)*	**42.18**	*(1.60)*	**6.86**	*(1.83)*
244.72	MA11-2	*6*	**296.10**	*(16.22)*	**330.70**	*(38.56)*	**45.72**	*(2.41)*	**4.72**	*(0.74)*
244.72	MA11-2 (Altered)	*5*	**140.07**	*(27.46)*	**1373.42**	*(305.96)*	**51.38**	*(3.38)*	**3.63**	*(1.18)*
249.89	MA03-7	*7*	**217.16**	*(26.03)*	**70.27**	*(126.19)*	**28.65**	*(3.18)*	**0.50**	*(0.20)*
260.85	MA03-4	*6*	**423.02**	*(36.73)*	**795.91**	*(213.22)*	**60.73**	*(9.32)*	**2.33**	*(0.66)*
282.46	MA03-1B	*5*	**509.39**	*(3.94)*	**468.35**	*(75.96)*	**50.69**	*(0.93)*	**4.40**	*(0.29)*
282.53	MA03-1A	*6*	**440.56**	*(21.47)*	**426.14**	*(73.11)*	**50.36**	*(1.19)*	**6.37**	*(3.85)*

Table 16. Results of LA-ICP-MS analyses of primary ilmenite from drill core samples. Average trace element concentrations (avg) and standard deviations (std) are calculated from *n* analyses per sample.

Stratigraphic Depth (m)	Sample	*n*	Mg (ppm)		Al (ppm)		Sc (ppm)		Ti (ppm)	
			avg	std	**avg**	std	**avg**	std	**avg**	std
9.21	MA14-2A	5	**3508.90**	*(718.0)*	**183.59**	*(20.3)*	**57.59**	*(7.24)*	**278754.84**	*(2811.6)*
9.58	MA14-2D	3	**3606.09**	*(870.7)*	**308.82**	*(161.6)*	**74.03**	*(2.64)*	**271212.27**	*(1192.5)*
13.64	MA14-3A	5	**816.06**	*(237.0)*	**80.38**	*(41.4)*	**41.73**	*(8.38)*	**273134.84**	*(2354.0)*
13.78	MA14-3B-T	5	**526.91**	*(205.1)*	**139.18**	*(81.3)*	**20.49**	*(2.60)*	**269471.69**	*(9596.2)*
13.94	MA14-3B-B	5	**335.95**	*(39.8)*	**18.91**	*(8.9)*	**6.72**	*(2.00)*	**250192.22**	*(9813.8)*
17.69	MA14-4-a	4	**290.32**	*(70.7)*	**215.24**	*(55.2)*	**31.80**	*(1.91)*	**264296.25**	*(2914.2)*
17.69	MA14-4-b	4	**236.50**	*(39.9)*	**53.69**	*(24.9)*	**13.00**	*(2.10)*	**252173.36**	*(2367.6)*
24.68	MA14-5A	5	**793.07**	*(89.8)*	**56.05**	*(16.0)*	**24.53**	*(2.46)*	**252454.16**	*(2290.6)*
24.90	MA14-5C-a	3	**511.42**	*(134.7)*	**190.12**	*(178.9)*	**17.79**	*(4.11)*	**262090.96**	*(4536.0)*
24.90	MA14-5C-b	1	**345.44**		**170.98**		**6.44**		**264733.69**	
40.47	MA14-6A-T	3	**974.27**	*(403.3)*	**295.98**	*(180.1)*	**19.13**	*(4.10)*	**271119.20**	*(565.9)*
40.74	MA14-6B-a	5	**547.56**	*(93.9)*	**95.33**	*(63.1)*	**27.19**	*(3.58)*	**268133.15**	*(6311.0)*
40.74	MA14-6B-b	4	**923.34**	*(236.8)*	**173.85**	*(143.8)*	**12.20**	*(1.92)*	**285710.79**	*(4111.5)*
51.81	MA14-7A-a	2	**416.16**	*(27.1)*	**20.38**	*(2.6)*	**10.39**	*(2.23)*	**256706.69**	*(1958.8)*
51.81	MA14-7A-b	5	**551.28**	*(119.1)*	**64.18**	*(71.9)*	**43.91**	*(10.39)*	**263238.43**	*(4171.6)*
69.47	MA14-8A-a	4	**607.68**	*(190.7)*	**70.20**	*(38.3)*	**9.22**	*(3.81)*	**274653.20**	*(9133.5)*
69.47	MA14-8A-b	4	**506.50**	*(238.5)*	**231.49**	*(299.2)*	**35.32**	*(6.27)*	**261852.91**	*(3689.5)*
69.61	MA14-8B	4	**450.60**	*(65.0)*	**27.16**	*(17.2)*	**29.38**	*(3.84)*	**266148.52**	*(2110.0)*
119.73	MA15-1	6	**397.43**	*(61.0)*	**47.79**	*(15.6)*	**11.57**	*(4.30)*	**245053.72**	*(10958.8)*
126.94	MA15-2	5	**4402.97**	*(222.6)*	**140.20**	*(11.0)*	**70.13**	*(13.52)*	**272320.87**	*(10979.8)*
139.46	MA32-25	4	**257.05**	*(61.5)*	**16.34**	*(4.3)*	**5.68**	*(0.96)*	**230597.35**	*(8350.0)*
145.55	MA32-1A	5	**1292.13**	*(165.0)*	**12.03**	*(4.7)*	**50.52**	*(7.52)*	**278786.45**	*(6132.6)*
145.78	MA32-1C	5	**1314.26**	*(162.0)*	**16.76**	*(5.5)*	**84.14**	*(6.84)*	**274202.80**	*(3649.2)*
152.51	MA32-2A-T	5	**607.85**	*(46.2)*	**91.30**	*(94.7)*	**37.79**	*(5.17)*	**270314.53**	*(4775.7)*
152.64	MA32-2A-B-a	4	**420.71**	*(33.5)*	**90.47**	*(47.3)*	**26.48**	*(3.51)*	**274715.90**	*(4125.2)*
152.64	MA32-2A-B-b	4	**441.23**	*(104.2)*	**170.86**	*(85.4)*	**36.84**	*(8.10)*	**272841.66**	*(5687.9)*
152.84	MA32-2B	5	**1041.07**	*(186.2)*	**125.20**	*(54.7)*	**45.78**	*(2.96)*	**276677.62**	*(2258.7)*
154.47	MA32-3	5	**788.37**	*(94.7)*	**46.23**	*(21.5)*	**30.86**	*(3.42)*	**249150.94**	*(3933.0)*
155.60	MA32-4	5	**996.81**	*(174.2)*	**121.07**	*(180.1)*	**31.72**	*(4.21)*	**262247.45**	*(5093.2)*
160.29	MA32-7	5	**3881.77**	*(1417.1)*	**41.96**	*(32.1)*	**59.03**	*(10.73)*	**235960.88**	*(17097.4)*
169.74	MA32-9	6	**944.42**	*(446.8)*	**137.07**	*(94.7)*	**29.70**	*(11.37)*	**245037.81**	*(15710.0)*
178.78	MA32-12	5	**4232.48**	*(3055.0)*	**528.34**	*(233.9)*	**48.28**	*(3.59)*	**248292.62**	*(15605.5)*
188.51	MA32-15	5	**11656.12**	*(1140.3)*	**135.60**	*(33.5)*	**63.56**	*(5.70)*	**249882.35**	*(5943.0)*
192.24	MA32-17	5	**10451.99**	*(859.6)*	**156.08**	*(19.2)*	**67.91**	*(6.56)*	**266355.08**	*(8721.9)*
196.77	MA32-18-a	5	**2284.79**	*(937.8)*	**236.33**	*(112.3)*	**25.79**	*(4.39)*	**279951.16**	*(3538.2)*
196.77	MA32-18-b	4	**9009.15**	*(457.5)*	**264.96**	*(199.5)*	**34.18**	*(4.24)*	**239438.87**	*(13970.5)*
196.77	MA32-18-c	3	**4257.78**	*(711.2)*	**300.76**	*(183.9)*	**22.51**	*(0.80)*	**262177.13**	*(9577.6)*
205.93	MA32-19	5	**323.37**	*(171.3)*	**487.41**	*(719.1)*	**15.08**	*(1.26)*	**255640.21**	*(16575.7)*
234.15	MA11-11	5	**6021.80**	*(2050.8)*	**184.63**	*(31.9)*	**59.44**	*(3.75)*	**262895.26**	*(9788.0)*
236.68	MA11-8	5	**4637.04**	*(1551.7)*	**171.47**	*(43.3)*	**42.54**	*(8.29)*	**268162.44**	*(8529.2)*
244.72	MA11-2	5	**5852.68**	*(281.0)*	**193.39**	*(66.4)*	**40.99**	*(6.23)*	**252368.54**	*(5329.6)*
244.72	MA11-2 (Altered)	5	**476.56**	*(52.1)*	**142.63**	*(77.0)*	**61.07**	*(22.60)*	**263625.74**	*(6120.6)*
249.89	MA03-7	4	**284.95**	*(12.7)*	**16.32**	*(8.2)*	**6.70**	*(1.80)*	**245358.61**	*(24144.7)*
251.07	MA03-6	5	**480.89**	*(88.5)*	**55.37**	*(32.0)*	**7.75**	*(4.03)*	**267182.02**	*(12172.6)*
260.85	MA03-4	5	**455.47**	*(76.5)*	**199.09**	*(156.0)*	**11.94**	*(3.21)*	**238327.97**	*(14904.2)*
281.37	MA03-2	5	**256.25**	*(73.2)*	**26.48**	*(17.6)*	**6.82**	*(2.64)*	**247724.48**	*(6310.4)*
282.46	MA03-1B	5	**7325.59**	*(865.4)*	**229.59**	*(107.5)*	**45.91**	*(4.56)*	**256052.87**	*(4464.7)*
282.53	MA03-1A	5	**6070.40**	*(614.0)*	**155.08**	*(8.5)*	**47.72**	*(4.14)*	**258007.73**	*(4896.4)*

Table 16. (cont'd)

Stratigraphic Depth (m)	Sample	*n*	V (ppm)		Cr (ppm)		Mn (ppm)		Co (ppm)		Ni (ppm)	
			avg	std	**avg**	std	**avg**	std	**avg**	std	**avg**	std
9.21	MA14-2A	5	**552.95**	*(14.9)*	**20.10**	*(2.4)*	**5445.20**	*(276.1)*	**96.65**	*(5.2)*	**39.89**	*(3.3)*
9.58	MA14-2D	3	**409.63**	*(51.7)*	**32.76**	*(12.8)*	**5397.25**	*(243.2)*	**78.85**	*(12.5)*	**35.42**	*(4.0)*
13.64	MA14-3A	5	**609.75**	*(81.8)*	**51.23**	*(8.1)*	**10322.71**	*(384.3)*	**54.60**	*(12.4)*	**21.85**	*(6.1)*
13.78	MA14-3B-T	5	**700.19**	*(112.6)*	**59.71**	*(14.8)*	**8885.30**	*(526.3)*	**58.62**	*(13.7)*	**22.91**	*(2.4)*
13.94	MA14-3B-B	5	**1395.48**	*(501.7)*	**486.25**	*(175.7)*	**8049.63**	*(254.0)*	**29.00**	*(5.2)*	**8.80**	*(3.7)*
17.69	MA14-4-a	4	**668.00**	*(73.4)*	**19.25**	*(2.4)*	**7103.53**	*(284.1)*	**14.95**	*(2.6)*	**4.81**	*(0.7)*
17.69	MA14-4-b	4	**1557.41**	*(245.0)*	**67.65**	*(13.6)*	**6899.33**	*(63.5)*	**15.09**	*(4.6)*	**4.36**	*(0.8)*
24.68	MA14-5A	5	**1122.02**	*(94.5)*	**32.36**	*(4.0)*	**9839.65**	*(129.0)*	**90.66**	*(7.9)*	**35.06**	*(6.0)*
24.90	MA14-5C-a	3	**1416.18**	*(168.5)*	**62.83**	*(1.4)*	**7866.60**	*(321.5)*	**49.97**	*(10.0)*	**19.75**	*(3.1)*
24.90	MA14-5C-b	1	**2065.67**		**247.39**		**11423.99**		**45.64**		**12.28**	
40.47	MA14-6A-T	3	**1045.71**	*(40.6)*	**60.56**	*(3.4)*	**7048.42**	*(206.7)*	**70.03**	*(5.0)*	**24.22**	*(2.1)*
40.74	MA14-6B-a	5	**892.28**	*(93.3)*	**46.96**	*(15.8)*	**9768.46**	*(1538.4)*	**71.60**	*(5.5)*	**24.83**	*(9.6)*
40.74	MA14-6B-b	4	**2905.61**	*(524.2)*	**233.41**	*(63.8)*	**10669.56**	*(592.9)*	**40.05**	*(10.3)*	**14.56**	*(2.3)*
51.81	MA14-7A-a	2	**1062.57**	*(42.6)*	**62.24**	*(22.4)*	**9754.51**	*(73.9)*	**70.33**	*(0.3)*	**10.15**	*(0.6)*
51.81	MA14-7A-b	5	**1087.73**	*(90.6)*	**37.13**	*(1.0)*	**9721.34**	*(126.5)*	**106.44**	*(11.5)*	**34.18**	*(4.1)*
69.47	MA14-8A-a	4	**4576.48**	*(1266.2)*	**572.18**	*(38.2)*	**16318.88**	*(1757.1)*	**57.64**	*(7.4)*	**25.61**	*(14.7)*
69.47	MA14-8A-b	4	**796.13**	*(85.5)*	**76.86**	*(10.5)*	**12897.79**	*(367.1)*	**67.06**	*(9.6)*	**37.78**	*(4.5)*
69.61	MA14-8B	4	**918.92**	*(50.3)*	**68.07**	*(5.8)*	**11925.57**	*(391.3)*	**64.59**	*(9.7)*	**46.37**	*(4.7)*
119.73	MA15-1	6	**1710.97**	*(361.3)*	**258.67**	*(57.4)*	**8100.57**	*(95.7)*	**74.50**	*(8.5)*	**38.05**	*(3.5)*
126.94	MA15-2	5	**413.11**	*(17.6)*	**8.38**	*(2.0)*	**10908.60**	*(546.5)*	**118.33**	*(22.0)*	**33.26**	*(7.3)*
139.46	MA32-25	4	**1012.08**	*(223.8)*	**144.52**	*(35.6)*	**6793.64**	*(327.0)*	**58.00**	*(2.3)*	**30.73**	*(2.4)*
145.55	MA32-1A	5	**340.48**	*(63.9)*	**12.41**	*(4.7)*	**11865.27**	*(1058.5)*	**74.88**	*(6.8)*	**18.31**	*(4.0)*
145.78	MA32-1C	5	**413.55**	*(65.8)*	**13.35**	*(3.3)*	**10560.35**	*(379.4)*	**56.13**	*(4.5)*	**17.94**	*(1.6)*
152.51	MA32-2A-T	5	**520.09**	*(88.2)*	**23.84**	*(8.2)*	**11338.37**	*(177.1)*	**62.60**	*(4.7)*	**16.44**	*(2.4)*
152.64	MA32-2A-B-a	4	**452.43**	*(46.0)*	**23.16**	*(7.5)*	**12270.57**	*(323.5)*	**51.49**	*(3.2)*	**14.80**	*(1.9)*
152.64	MA32-2A-B-b	4	**511.56**	*(39.2)*	**18.92**	*(2.7)*	**11667.26**	*(120.3)*	**61.69**	*(3.6)*	**14.37**	*(0.7)*
152.84	MA32-2B	5	**480.44**	*(30.9)*	**13.11**	*(1.3)*	**10928.30**	*(228.5)*	**75.94**	*(1.9)*	**18.85**	*(2.4)*
154.47	MA32-3	5	**814.53**	*(76.9)*	**35.40**	*(6.3)*	**11085.06**	*(163.8)*	**88.13**	*(5.7)*	**25.45**	*(3.3)*
155.60	MA32-4	5	**834.90**	*(42.1)*	**14.91**	*(1.7)*	**9503.23**	*(307.7)*	**102.08**	*(5.3)*	**22.61**	*(2.1)*
160.29	MA32-7	5	**429.54**	*(46.0)*	**23.31**	*(4.8)*	**9515.43**	*(1561.7)*	**133.89**	*(33.7)*	**37.90**	*(16.6)*
169.74	MA32-9	6	**440.30**	*(28.7)*	**3.99**	*(1.0)*	**8068.60**	*(243.6)*	**50.36**	*(14.7)*	**12.27**	*(4.9)*
178.78	MA32-12	5	**380.57**	*(23.3)*	**5.58**	*(0.8)*	**7375.51**	*(763.8)*	**69.54**	*(9.5)*	**27.92**	*(3.3)*
188.51	MA32-15	5	**563.01**	*(50.4)*	**7.24**	*(0.5)*	**6643.29**	*(229.7)*	**80.16**	*(14.0)*	**29.21**	*(11.6)*
192.24	MA32-17	5	**542.82**	*(25.2)*	**12.35**	*(1.6)*	**6695.21**	*(335.1)*	**110.92**	*(11.3)*	**36.36**	*(6.6)*
196.77	MA32-18-a	5	**478.64**	*(27.3)*	**51.34**	*(6.4)*	**5755.97**	*(604.1)*	**43.05**	*(25.0)*	**22.64**	*(8.2)*
196.77	MA32-18-b	4	**531.85**	*(64.1)*	**78.92**	*(19.6)*	**4436.14**	*(304.4)*	**107.56**	*(14.0)*	**51.63**	*(5.2)*
196.77	MA32-18-c	3	**427.42**	*(44.8)*	**55.52**	*(10.5)*	**5607.47**	*(834.4)*	**90.74**	*(3.0)*	**41.02**	*(5.6)*
205.93	MA32-19	5	**1150.55**	*(79.7)*	**233.15**	*(29.6)*	**6627.97**	*(531.3)*	**69.17**	*(5.3)*	**43.34**	*(3.7)*
234.15	MA11-11	5	**559.91**	*(27.4)*	**53.09**	*(4.8)*	**9353.79**	*(1222.7)*	**85.53**	*(15.4)*	**53.23**	*(9.1)*
236.68	MA11-8	5	**423.88**	*(51.7)*	**33.13**	*(6.7)*	**9907.24**	*(455.7)*	**109.30**	*(13.8)*	**47.20**	*(10.1)*
244.72	MA11-2	5	**481.88**	*(40.9)*	**13.40**	*(2.8)*	**6584.83**	*(551.3)*	**93.08**	*(9.2)*	**25.08**	*(13.2)*
244.72	MA11-2 (Altered)	5	**641.62**	*(211.0)*	**13.90**	*(3.4)*	**7571.70**	*(142.1)*	**27.06**	*(1.9)*	**9.47**	*(4.3)*
249.89	MA03-7	4	**921.36**	*(170.7)*	**364.06**	*(75.4)*	**12327.16**	*(267.0)*	**42.07**	*(4.5)*	**23.79**	*(3.2)*
251.07	MA03-6	5	**2880.20**	*(427.1)*	**1683.88**	*(282.9)*	**10319.08**	*(2425.2)*	**42.73**	*(12.7)*	**14.20**	*(6.4)*
260.85	MA03-4	5	**978.31**	*(106.4)*	**299.83**	*(30.1)*	**8476.00**	*(561.4)*	**107.01**	*(8.8)*	**55.19**	*(5.5)*
281.37	MA03-2	5	**1854.58**	*(1148.5)*	**175.19**	*(137.1)*	**7251.91**	*(427.3)*	**23.77**	*(3.1)*	**14.29**	*(12.0)*
282.46	MA03-1B	5	**485.77**	*(44.9)*	**259.42**	*(68.7)*	**5169.92**	*(533.9)*	**101.30**	*(5.5)*	**74.35**	*(7.6)*
282.53	MA03-1A	5	**463.27**	*(20.9)*	**232.00**	*(7.2)*	**6087.21**	*(494.9)*	**89.56**	*(13.7)*	**58.42**	*(7.7)*

Table 16. (cont'd)

Stratigraphic Depth (m)	Sample	*n*	Zn (ppm)		Ga (ppm)		Zr (ppm)		Nb (ppm)		Hf (ppm)	
			avg	std	**avg**	std	**avg**	std	**avg**	std	**avg**	std
9.21	MA14-2A	5	**29.30**	*(6.87)*	**0.54**	*(0.12)*	**71.73**	*(6.04)*	**34.27**	*(1.85)*	**3.50**	*(0.38)*
9.58	MA14-2D	3	**15.68**	*(5.61)*	**0.73**	*(0.38)*	**136.77**	*(1.27)*	**22.31**	*(0.68)*	**3.75**	*(0.10)*
13.64	MA14-3A	5	**34.76**	*(6.32)*	**1.02**	*(0.15)*	**75.54**	*(3.46)*	**19.86**	*(4.97)*	**2.41**	*(0.32)*
13.78	MA14-3B-T	5	**31.74**	*(4.06)*	**1.40**	*(0.20)*	**34.29**	*(6.88)*	**19.58**	*(3.91)*	**1.65**	*(0.52)*
13.94	MA14-3B-B	5	**52.23**	*(9.31)*	**0.22**	*(0.09)*	**6.49**	*(1.53)*	**38.88**	*(10.17)*	**0.39**	*(0.12)*
17.69	MA14-4-a	4	**38.58**	*(5.20)*	**2.74**	*(0.05)*	**14.05**	*(2.08)*	**57.32**	*(6.04)*	**1.32**	*(0.28)*
17.69	MA14-4-b	4	**35.99**	*(2.86)*	**1.09**	*(0.24)*	**7.99**	*(1.14)*	**52.35**	*(0.87)*	**0.68**	*(0.10)*
24.68	MA14-5A	5	**54.69**	*(10.89)*	**3.31**	*(0.20)*	**10.71**	*(1.14)*	**14.11**	*(1.71)*	**0.49**	*(0.06)*
24.90	MA14-5C-a	3	**72.38**	*(15.95)*	**1.61**	*(0.42)*	**6.57**	*(3.07)*	**21.80**	*(3.11)*	**0.35**	*(0.06)*
24.90	MA14-5C-b	1	**65.60**		**0.38**		**1.62**		**46.09**		**0.16**	
40.47	MA14-6A-T	3	**45.83**	*(4.00)*	**2.44**	*(0.35)*	**12.48**	*(2.62)*	**15.73**	*(7.05)*	**0.50**	*(0.05)*
40.74	MA14-6B-a	5	**42.91**	*(19.64)*	**2.23**	*(0.51)*	**15.66**	*(3.43)*	**12.26**	*(2.68)*	**0.69**	*(0.19)*
40.74	MA14-6B-b	4	**47.52**	*(6.21)*	**0.26**	*(0.07)*	**10.18**	*(6.97)*	**20.37**	*(7.10)*	**0.27**	*(0.10)*
51.81	MA14-7A-a	2	**87.80**	*(7.39)*	**0.25**	*(0.02)*	**2.19**	*(0.82)*	**13.04**	*(1.37)*	**0.18**	*(0.05)*
51.81	MA14-7A-b	5	**84.87**	*(3.46)*	**0.80**	*(0.27)*	**6.82**	*(2.78)*	**11.70**	*(1.62)*	**0.44**	*(0.11)*
69.47	MA14-8A-a	4	**70.61**	*(8.53)*	**0.09**	*(0.04)*	**2.32**	*(0.85)*	**7.48**	*(1.36)*	**0.13**	*(0.06)*
69.47	MA14-8A-b	4	**65.66**	*(3.06)*	**0.88**	*(0.41)*	**30.62**	*(22.92)*	**14.18**	*(4.07)*	**0.99**	*(0.45)*
69.61	MA14-8B	4	**79.67**	*(5.71)*	**1.57**	*(0.11)*	**25.43**	*(1.99)*	**11.00**	*(1.89)*	**0.99**	*(0.06)*
119.73	MA15-1	6	**56.39**	*(7.74)*	**2.37**	*(0.50)*	**6.96**	*(1.52)*	**11.56**	*(2.03)*	**0.26**	*(0.05)*
126.94	MA15-2	5	**35.09**	*(6.61)*	**0.67**	*(0.10)*	**54.01**	*(6.51)*	**11.31**	*(0.60)*	**1.42**	*(0.17)*
139.46	MA32-25	4	**46.10**	*(3.25)*	**1.00**	*(0.07)*	**15.31**	*(2.79)*	**7.66**	*(2.11)*	**0.51**	*(0.15)*
145.55	MA32-1A	5	**41.07**	*(6.62)*	**0.39**	*(0.16)*	**43.61**	*(1.06)*	**13.21**	*(1.08)*	**1.46**	*(0.15)*
145.78	MA32-1C	5	**53.96**	*(20.77)*	**0.70**	*(0.10)*	**59.37**	*(6.65)*	**12.25**	*(1.74)*	**2.10**	*(0.08)*
152.51	MA32-2A-T	5	**41.70**	*(8.53)*	**1.26**	*(0.15)*	**45.07**	*(5.34)*	**9.98**	*(2.12)*	**1.25**	*(0.08)*
152.64	MA32-2A-B-a	4	**45.13**	*(27.24)*	**1.24**	*(0.14)*	**48.38**	*(12.95)*	**8.33**	*(1.75)*	**0.96**	*(0.30)*
152.64	MA32-2A-B-b	4	**65.93**	*(18.77)*	**1.38**	*(0.11)*	**52.75**	*(3.20)*	**8.85**	*(2.62)*	**1.62**	*(0.15)*
152.84	MA32-2B	5	**47.89**	*(12.61)*	**1.36**	*(0.09)*	**53.96**	*(5.96)*	**9.65**	*(0.70)*	**1.57**	*(0.11)*
154.47	MA32-3	5	**45.17**	*(10.49)*	**2.40**	*(0.38)*	**17.81**	*(7.52)*	**13.31**	*(2.93)*	**0.67**	*(0.21)*
155.60	MA32-4	5	**38.21**	*(3.80)*	**2.13**	*(0.41)*	**25.11**	*(5.09)*	**9.57**	*(1.51)*	**0.75**	*(0.11)*
160.29	MA32-7	5	**71.33**	*(30.01)*	**0.43**	*(0.24)*	**37.65**	*(6.91)*	**8.16**	*(3.85)*	**1.24**	*(0.08)*
169.74	MA32-9	6	**59.53**	*(10.03)*	**1.26**	*(0.16)*	**27.00**	*(5.99)*	**7.56**	*(1.09)*	**0.89**	*(0.23)*
178.78	MA32-12	5	**34.78**	*(10.59)*	**0.92**	*(0.22)*	**34.31**	*(2.45)*	**9.25**	*(0.34)*	**1.23**	*(0.10)*
188.51	MA32-15	5	**62.73**	*(7.29)*	**1.22**	*(0.26)*	**33.23**	*(4.67)*	**10.70**	*(0.64)*	**1.20**	*(0.20)*
192.24	MA32-17	5	**42.71**	*(16.64)*	**1.11**	*(0.16)*	**42.10**	*(5.93)*	**10.77**	*(1.24)*	**1.46**	*(0.22)*
196.77	MA32-18-a	5	**43.80**	*(10.10)*	**0.77**	*(0.22)*	**66.27**	*(7.13)*	**12.76**	*(4.35)*	**1.66**	*(0.20)*
196.77	MA32-18-b	4	**44.47**	*(19.04)*	**0.56**	*(0.53)*	**48.35**	*(4.65)*	**10.93**	*(4.91)*	**1.34**	*(0.19)*
196.77	MA32-18-c	3	**37.82**	*(7.26)*	**0.43**	*(0.17)*	**53.67**	*(5.56)*	**13.23**	*(4.52)*	**1.19**	*(0.14)*
205.93	MA32-19	5	**44.79**	*(5.71)*	**2.21**	*(0.37)*	**10.89**	*(0.63)*	**11.10**	*(1.57)*	**0.53**	*(0.03)*
234.15	MA11-11	5	**48.93**	*(5.86)*	**0.81**	*(0.23)*	**45.64**	*(3.46)*	**14.94**	*(1.94)*	**1.54**	*(0.14)*
236.68	MA11-8	5	**26.61**	*(5.03)*	**0.78**	*(0.21)*	**46.60**	*(2.08)*	**10.44**	*(2.41)*	**1.37**	*(0.27)*
244.72	MA11-2	5	**36.14**	*(8.67)*	**0.39**	*(0.10)*	**43.84**	*(1.69)*	**10.85**	*(0.44)*	**1.50**	*(0.11)*
244.72	MA11-2 (Altered)	5	**26.74**	*(8.71)*	**0.54**	*(0.23)*	**30.14**	*(1.46)*	**2.36**	*(0.61)*	**0.61**	*(0.08)*
249.89	MA03-7	4	**64.43**	*(2.45)*	**0.30**	*(0.07)*	**6.84**	*(1.01)*	**12.06**	*(1.59)*	**0.25**	*(0.08)*
251.07	MA03-6	5	**56.21**	*(24.86)*	**0.82**	*(0.34)*	**4.80**	*(1.84)*	**14.53**	*(3.82)*	**0.11**	*(0.04)*
260.85	MA03-4	5	**29.95**	*(5.89)*	**1.09**	*(0.10)*	**13.73**	*(2.72)*	**9.41**	*(1.06)*	**0.37**	*(0.12)*
281.37	MA03-2	5	**48.09**	*(3.36)*	**1.10**	*(0.66)*	**3.63**	*(1.49)*	**31.05**	*(8.04)*	**0.27**	*(0.11)*
282.46	MA03-1B	5	**16.78**	*(5.55)*	**0.53**	*(0.19)*	**57.75**	*(4.45)*	**14.40**	*(4.05)*	**1.65**	*(0.25)*
282.53	MA03-1A	5	**13.97**	*(1.71)*	**0.46**	*(0.12)*	**52.95**	*(7.00)*	**13.85**	*(2.32)*	**1.65**	*(0.22)*

Table 17. Results of LA-ICP-MS analyses of magnetite from outcrop samples. Average trace element concentrations (avg) and standard deviations (std) are calculated from *n* analyses per sample.

Sample	*n*	Mg (ppm)		Al (ppm)		Sc (ppm)		Ti (ppm)		V (ppm)		Cr (ppm)	
		avg	std	avg	std	avg	std	avg	std	avg	std	avg	std
T3-C4-1	5	**3383.77**	*(189.18)*	**16452.30**	*(564.46)*	**15.05**	*(1.23)*	**66275.75**	*(3217.11)*	**6991.00**	*(226.66)*	**134.05**	*(4.42)*
T3-C4-2	5	**3556.02**	*(262.26)*	**16185.76**	*(646.42)*	**13.87**	*(2.60)*	**59750.14**	*(6171.44)*	**7386.93**	*(209.34)*	**116.94**	*(6.93)*
TA1-1	5	**4390.27**	*(539.85)*	**19777.49**	*(1021.80)*	**21.26**	*(1.30)*	**67986.65**	*(2837.80)*	**7035.62**	*(85.92)*	**291.29**	*(7.13)*
TA1-4	5	**5537.41**	*(174.97)*	**18694.20**	*(279.15)*	**23.31**	*(0.69)*	**69724.57**	*(948.50)*	**6740.73**	*(68.59)*	**232.23**	*(7.33)*
TA1-5	5	**4266.56**	*(283.25)*	**19802.03**	*(397.12)*	**19.73**	*(0.76)*	**66066.44**	*(1327.19)*	**7113.34**	*(38.61)*	**336.19**	*(21.82)*
TA1-6	5	**4811.17**	*(326.17)*	**18734.18**	*(910.69)*	**19.52**	*(1.31)*	**60347.22**	*(1561.95)*	**7527.10**	*(202.08)*	**284.10**	*(5.65)*
TA2-1	5	**4361.07**	*(264.12)*	**18245.25**	*(955.08)*	**16.00**	*(0.91)*	**53287.96**	*(824.33)*	**8151.11**	*(320.84)*	**312.80**	*(16.04)*
TA2-3	5	**4383.57**	*(204.82)*	**19133.79**	*(711.68)*	**20.05**	*(0.85)*	**53958.39**	*(2094.94)*	**7014.21**	*(76.44)*	**466.47**	*(25.27)*
TA2-4	5	**3940.53**	*(152.26)*	**20118.21**	*(1118.84)*	**18.65**	*(1.25)*	**50714.27**	*(789.74)*	**6848.38**	*(159.83)*	**361.81**	*(19.83)*
TA2-6	6	**4120.35**	*(367.45)*	**20872.18**	*(643.55)*	**17.22**	*(2.15)*	**57764.57**	*(1076.69)*	**6849.78**	*(164.79)*	**293.85**	*(7.30)*

Table 17. (cont'd)

Sample	*n*	Mn (ppm)		Co (ppm)		Ni (ppm)		Zn (ppm)		Ga (ppm)		Zr (ppm)	
		avg	std	avg	std	avg	std	avg	std	avg	std	av	std
T3-C4-1	5	**2244.39**	*(162.80)*	**150.71**	*(16.71)*	**184.49**	*(9.53)*	**466.80**	*(19.44)*	**46.03**	*(1.05)*	**5.46**	*(0.49)*
T3-C4-2	5	**2038.40**	*(168.55)*	**179.78**	*(16.91)*	**223.24**	*(18.78)*	**441.69**	*(20.81)*	**47.71**	*(0.48)*	**4.70**	*(1.16)*
TA1-1	5	**2164.27**	*(249.37)*	**159.81**	*(17.87)*	**252.81**	*(10.93)*	**297.10**	*(25.64)*	**45.48**	*(1.43)*	**5.56**	*(0.65)*
TA1-4	5	**2152.20**	*(98.82)*	**186.28**	*(9.06)*	**272.12**	*(5.73)*	**288.10**	*(14.01)*	**44.43**	*(0.68)*	**6.19**	*(0.21)*
TA1-5	5	**1937.38**	*(140.43)*	**175.47**	*(7.40)*	**269.16**	*(9.59)*	**334.63**	*(36.10)*	**45.84**	*(0.68)*	**5.18**	*(0.26)*
TA1-6	5	**2305.01**	*(176.32)*	**183.21**	*(16.41)*	**279.63**	*(18.20)*	**295.23**	*(40.76)*	**44.61**	*(1.37)*	**5.28**	*(0.39)*
TA2-1	5	**2318.24**	*(191.96)*	**196.41**	*(11.17)*	**299.54**	*(8.42)*	**253.74**	*(39.51)*	**46.62**	*(2.13)*	**4.18**	*(0.19)*
TA2-3	5	**2411.47**	*(471.82)*	**200.04**	*(11.83)*	**281.60**	*(7.99)*	**257.20**	*(27.79)*	**46.33**	*(0.54)*	**4.94**	*(0.18)*
TA2-4	5	**2755.97**	*(336.41)*	**204.39**	*(6.94)*	**279.83**	*(13.97)*	**278.82**	*(20.10)*	**47.40**	*(1.37)*	**4.64**	*(0.27)*
TA2-6	6	**2369.18**	*(397.83)*	**188.71**	*(16.07)*	**273.25**	*(16.25)*	**358.52**	*(87.51)*	**47.23**	*(0.81)*	**4.37**	*(0.43)*

Table 18. Results of LA-ICP-MS analyses of primary ilmenite from outcrop samples. Average trace element concentrations (avg) and standard deviations (std) are calculated from *n* analyses per sample.

Sample	*n*	Mg (ppm)		Al (ppm)		Sc (ppm)		Ti (ppm)		V (ppm)		Cr (ppm)		Mn (ppm)	
		avg	std.	avg	std.	avg	std.	avg	std.	avg	std.	avg	std.	avg	std.
T3-C4-1	5	**8047.86**	*(394.00)*	**351.86**	*(201.15)*	**43.47**	*(2.91)*	**257956.62**	*(9467.07)*	**427.71**	*(28.32)*	**4.03**	*(0.84)*	**4976.07**	*(281.72)*
T3-C4-2	5	**8513.04**	*(225.05)*	**389.43**	*(162.60)*	**54.67**	*(5.53)*	**258852.79**	*(7613.98)*	**470.08**	*(70.27)*	**5.10**	*(1.33)*	**4671.27**	*(46.87)*
TA1-1	5	**8211.19**	*(2150.01)*	**335.34**	*(90.64)*	**60.76**	*(4.46)*	**262128.00**	*(10983.80)*	**410.34**	*(31.79)*	**13.17**	*(2.80)*	**5278.12**	*(376.41)*
TA1-4	5	**11528.28**	*(1873.75)*	**277.11**	*(98.58)*	**58.23**	*(6.52)*	**252258.60**	*(21500.20)*	**377.95**	*(51.34)*	**9.20**	*(1.79)*	**4717.92**	*(344.95)*
TA1-5	5	**8464.90**	*(1753.34)*	**314.27**	*(132.43)*	**60.83**	*(5.03)*	**268202.88**	*(9732.71)*	**394.48**	*(23.79)*	**13.42**	*(3.04)*	**4942.71**	*(489.27)*
TA1-6	5	**11173.91**	*(935.26)*	**300.74**	*(138.29)*	**52.04**	*(8.15)*	**224035.25**	*(11960.70)*	**460.82**	*(70.23)*	**14.91**	*(3.27)*	**4434.28**	*(305.79)*
TA2-1	5	**9870.76**	*(1120.79)*	**168.28**	*(47.83)*	**57.62**	*(5.66)*	**235247.78**	*(13566.98)*	**446.56**	*(9.75)*	**11.14**	*(2.60)*	**4974.10**	*(216.61)*
TA2-3	5	**10960.44**	*(447.37)*	**405.50**	*(112.41)*	**55.86**	*(4.52)*	**233524.14**	*(11738.11)*	**478.65**	*(54.42)*	**35.38**	*(8.86)*	**4361.47**	*(143.66)*
TA2-4	5	**9846.22**	*(1037.31)*	**377.13**	*(249.64)*	**62.72**	*(10.30)*	**232021.98**	*(12023.36)*	**407.64**	*(45.25)*	**15.30**	*(4.45)*	**4602.07**	*(202.42)*
TA2-6	5	**9442.46**	*(1009.45)*	**325.99**	*(237.78)*	**70.11**	*(10.81)*	**269374.61**	*(3320.59)*	**416.27**	*(49.92)*	**14.60**	*(6.24)*	**4658.11**	*(264.58)*

Table 18. (cont'd)

Sample	*n*	Co (ppm)		Ni (ppm)		Zn (ppm)		Ga (ppm)		Zr (ppm)		Nb (ppm)		Hf (ppm)	
		avg	std.	avg	std.	avg	std.	avg	std.	avg	std.	avg	std.	avg	std.
T3-C4-1	*5*	**82.78**	*(7.06)*	**31.60**	*(2.84)*	**53.49**	*(24.95)*	**0.76**	*(0.53)*	**39.56**	*(3.29)*	**8.76**	*(0.73)*	**1.38**	*(0.15)*
T3-C4-2	*5*	**93.34**	*(1.73)*	**37.42**	*(2.97)*	**57.39**	*(16.54)*	**0.92**	*(0.53)*	**40.07**	*(3.86)*	**8.88**	*(0.95)*	**1.41**	*(0.13)*
TA1-1	*5*	**71.19**	*(10.28)*	**37.90**	*(5.21)*	**28.16**	*(2.90)*	**0.85**	*(0.31)*	**45.85**	*(4.12)*	**9.98**	*(0.99)*	**1.55**	*(0.13)*
TA1-4	*5*	**93.34**	*(10.66)*	**45.05**	*(5.11)*	**28.52**	*(5.87)*	**0.72**	*(0.26)*	**43.28**	*(4.45)*	**9.33**	*(1.57)*	**1.42**	*(0.15)*
TA1-5	*5*	**81.89**	*(11.09)*	**43.20**	*(5.60)*	**28.45**	*(8.09)*	**0.75**	*(0.32)*	**45.49**	*(1.99)*	**10.93**	*(1.42)*	**1.51**	*(0.11)*
TA1-6	*5*	**94.90**	*(5.05)*	**47.74**	*(4.49)*	**35.52**	*(9.39)*	**0.81**	*(0.40)*	**45.27**	*(4.80)*	**10.33**	*(1.94)*	**1.45**	*(0.15)*
TA2-1	*5*	**96.42**	*(15.94)*	**48.25**	*(4.62)*	**28.55**	*(4.36)*	**0.44**	*(0.18)*	**43.44**	*(1.61)*	**9.81**	*(1.06)*	**1.49**	*(0.11)*
TA2-3	*5*	**101.02**	*(4.13)*	**51.40**	*(3.38)*	**39.79**	*(6.32)*	**1.16**	*(0.29)*	**41.41**	*(5.85)*	**10.15**	*(1.33)*	**1.55**	*(0.23)*
TA2-4	*5*	**93.68**	*(8.44)*	**44.10**	*(3.39)*	**32.68**	*(10.99)*	**0.69**	*(0.49)*	**49.47**	*(6.20)*	**10.47**	*(1.93)*	**1.67**	*(0.18)*
TA2-6	*5*	**92.87**	*(11.53)*	**44.92**	*(5.32)*	**26.88**	*(11.88)*	**0.66**	*(0.59)*	**52.37**	*(5.44)*	**10.31**	*(1.35)*	**1.73**	*(0.08)*

6.1.3 Comparison between EMPA and LA-ICP-MS results

Fig. 14 shows how the results of EMPA and LA-ICP-MS analyses of magnetite compare prior to and following the correction of the raw EMPA data by mass balance for ilmenite exsolutions and application of Fe_{Mgt}^{Corr} as the internal standard for LA-ICP-MS data. Note that following these recalculations, Ti necessarily plots 1:1 between the two methods as a consequence of the procedure used to calculate Fe_{Mgt}^{Corr} (see section 5.1.3). Fig. 15 shows how the trace element compositions of ilmenite compare between the two analytical techniques.

Following the re-calculation of the EMPA data, the concentrations of Mn in magnetite agree between the two techniques much better than they do when Fe_{Mgt}^{EMPA} is used as the internal standard for LA-ICP-MS data (Fig. 14). The corrected Mg concentrations of magnetite also agree slightly better between the two techniques than do the uncorrected values, albeit still not as closely as they do for ilmenite. This scatter in Mg, along with the tendency for the Al and Zn concentrations of magnetite as determined by LA-ICP-MS to be greater than by EMPA likely reflects better incorporation of pleonaste exsolutions in the analysis beam of the former. In ilmenite, Cr and Ni are generally below EMPA detections limits and thus poorly agree with the LA-ICP-MS results (Fig 15), whereas they tend to agree better in magnetite where their concentrations are greater. Note that for magnetite with low Cr levels (i.e. below EMPA detection limits) the LA-ICP-MS results seem to generally be above the detections limits of the EMPA. This presumably reflects a combination of 1) the actual Cr concentrations being close to the detection limits of EMPA, and 2) its heterogeneous distribution within magnetite of a given sample. EMPA analyses of grains in which Cr is below detection limits output a value of zero, which when averaged with analyses at or above detection limits results in a mean value for the thin section that is below the actual detection limits of the EMPA, as seen in Fig. 14. LA-ICP-

MS data, on the other hand, presumably reflects the true Cr concentration of magnetite. This could in part explain a similar trend that is observed at low V concentrations in ilmenite (Fig. 15). However, the disagreement between EMPA and LA-ICP-MS in V begins at levels about 10 times the detection limits of the EMPA. This may instead suggest that there are unidentified interferences with V that are inflating its results at low abundances during LA-ICP-MS analyses.

Other inconsistencies in ilmenite data between EMPA and LA-ICP-MS include strong disagreements in Al contents, even at levels that are well above the detection limits of both techniques; Zn levels being much higher in EMPA data; and LA-ICP-MS resulting in consistently lower Ti contents than are detected by EMPA. The variations in Al may be related to exsolutions of pleonaste. Aluminous spinel plates have been documented in ilmenite from other gabbroic intrusion (e.g. McEnroe et al., 2000) and may be present at the tips of magnetite exsolution lamellae in ilmenite from the RBC (Fig. 10f). As in magnetite, discrepancies in the amounts of these exsolutions that are included in the areas analyzed between the two analytical techniques could produce the large amounts of scatter that are observed. However, it is unlikely that this can also explain such a pronounced and consistent increase in Zn when ilmenite is analyzed by EMPA. The values plotted in Fig. 15 are the average compositions for each sample; however, intra-sample standard deviations in the Zn content of ilmenite from EMPA results are often quite large relative to its average concentration in a sample (Appendix 1). This signifies that Zn is heterogeneously distributed within ilmenite of most samples. Intra-sample variations from LA-ICP-MS analyses, however, are noticeably lower than those from EMPA (Appendix 2), which suggests that there may be compositional zonation of Zn within ilmenite as well. The consistently higher EMPA results are therefore likely due to one or two analyses per sample of highly enriched portions of grains that have inflated the sample averages.

The incorporation of magnetite exsolutions during LA-ICP-MS analyses of ilmenite could partially explain its consistently lower Ti results compared to those of EMPA. These exsolutions account for up to 10 percent of primary ilmenite, and thus their incorporation in the laser ablation line would presumably lower the overall Ti content of the area analyzed by several percent, especially if the magnetite is Ti-poor. However, it is not feasible with the current dataset to correct the ilmenite data in the same manner as was performed for primary magnetite in this study (i.e. re-calculating the internal standard Fe value). The correction of magnetite required a practical estimate of the Fe and Ti contents of its ilmenite exsolutions, for which the compositions of coexisting primary ilmenite are deemed sufficient (Table 14). The direct equivalent, i.e. using the compositions of coexisting primary magnetite as representative of the exsolutions in ilmenite, is not applicable, since EDS analysis of the exsolutions indicates that they are pure Fe-oxide in composition. Their Fe-content is therefore likely several weight percent higher than that of primary titaniferous magnetite, presuming that they are even magnetite at all. The interpretation that these exsolutions are magnetite is primarily made on textural grounds (see section 4.2.2), but hematite would produce a similar EDS signature. If they were in fact hematite, this would considerably change the Fe content needed to correct the ilmenite data. Additionally, it is uncertain how pronounced the effect of using GSE-1g (which only contains 450 ppm Ti) as the calibrating standard for LA-ICP-MS has on accurately reproducing the high Ti contents of ilmenite. The disagreement in Ti values seen in Fig. 15 may therefore just be a reflection of the inaccuracies that result from using a reference material with such low concentrations of Ti to analyze for its abundance in a mineral as enriched as ilmenite. This argument is supported by the results of Mg and Mn, as their EMPA and LA-ICP-MS results agree well at concentrations below 1 wt.%, but at higher concentrations also skew towards higher EMPA values.

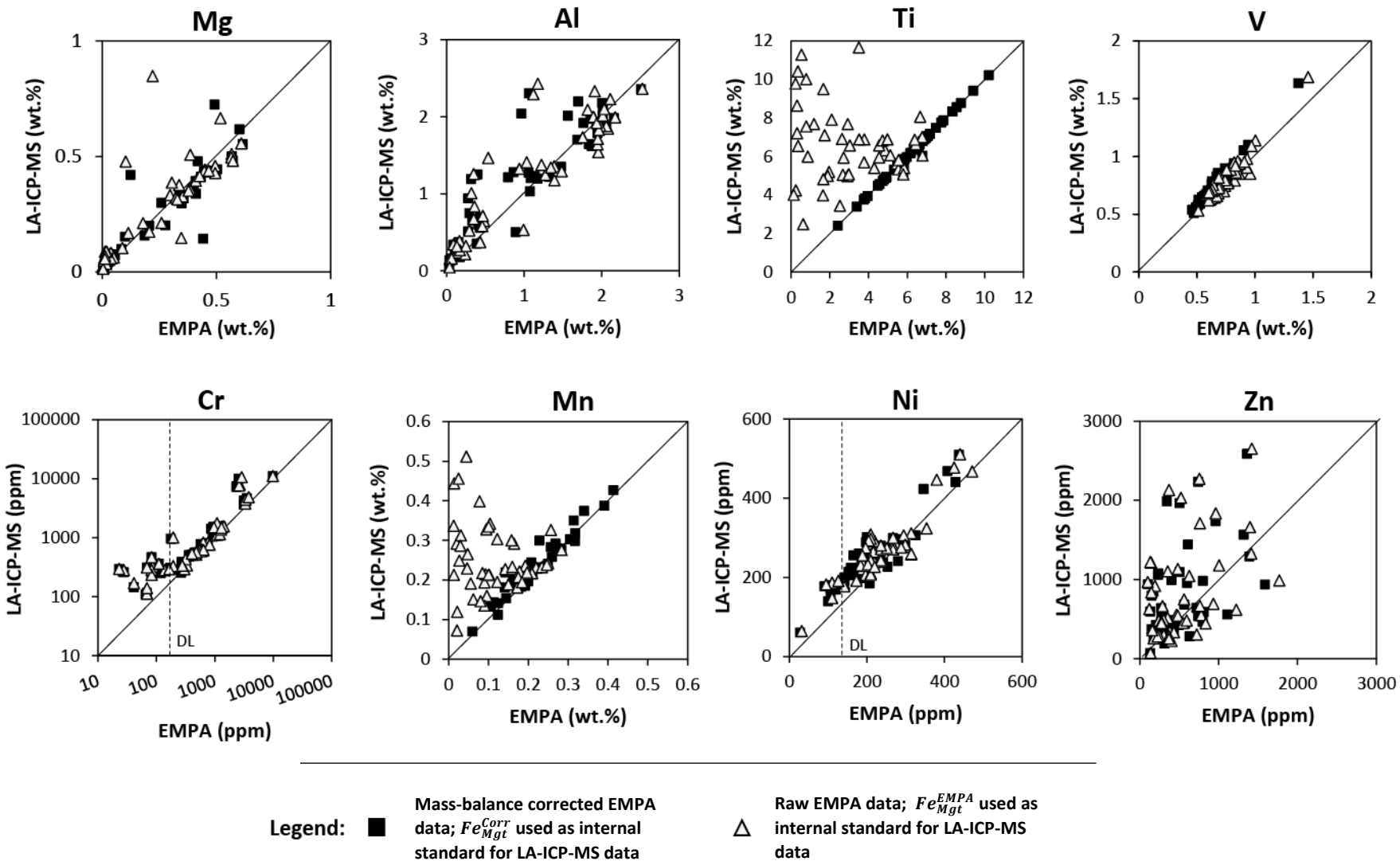

Fig. 14. Comparison of average magnetite compositions as determined by LA-ICP-MS and EMPA for elements that were analyzed for by both techniques. Open triangles represent the raw EMPA data plotted against LA-ICP-MS results that use the raw total Fe contents of magnetite (determined by EMPA) as the internal standard. Closed squares show EMPA data that has been re-calculated by mass-balance to account for coarse ilmenite exsolutions that were incorporated during LA-ICP-MS analyses but not EMPA, plotted against the LA-ICP-MS data that use the re-calculated Fe contents of magnetite as the internal standard. Solid line is the 1:1 line. Vertical dashed lines show the detection limits (DL) of EMPA for select elements.

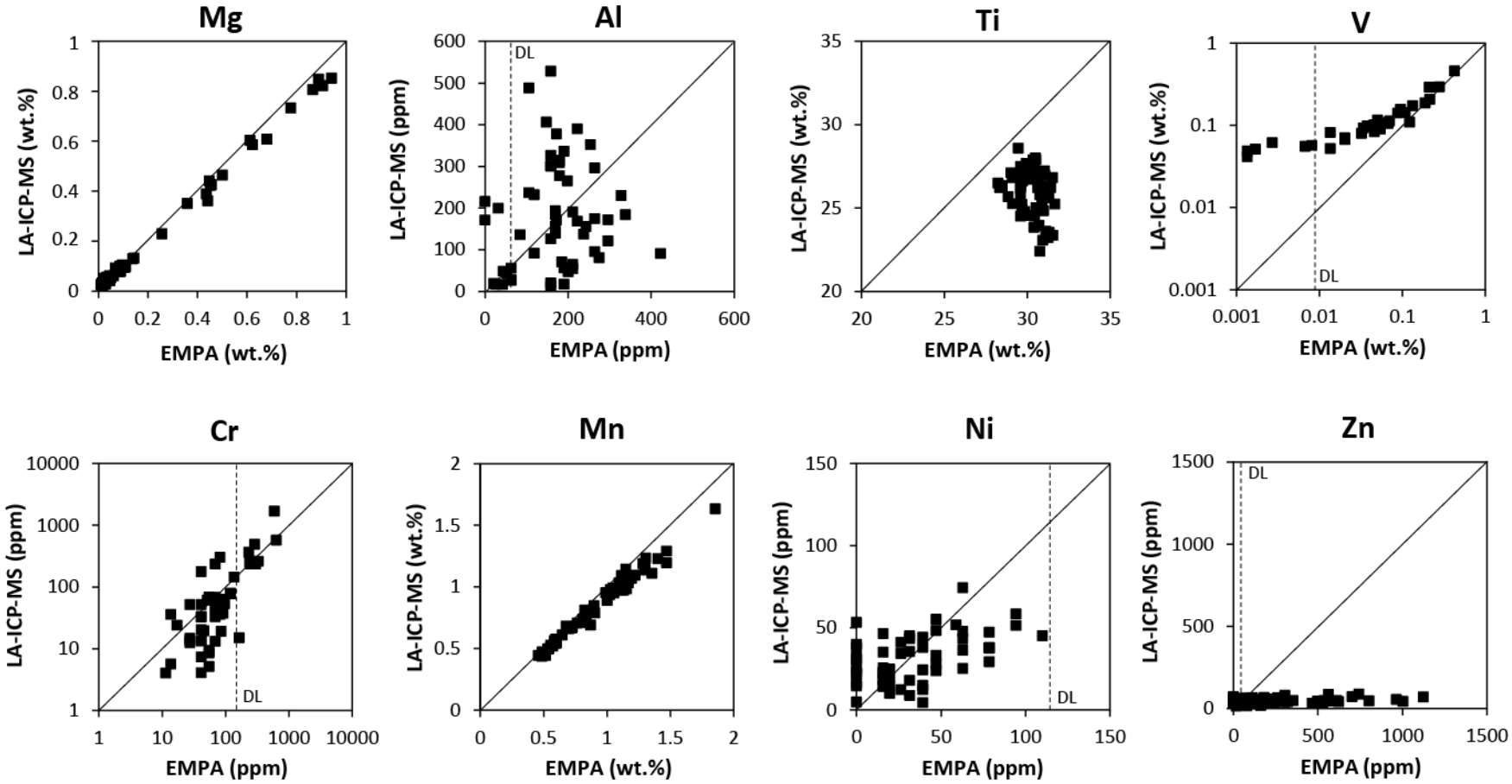

Fig. 15. Comparison of average ilmenite compositions as determined by LA-ICP-MS and EMPA for elements that were analyzed by both techniques. Note that unlike in magnetite, no corrections were made to account for potential exsolution lamellae included in the analyses. Solid line is the 1:1 line. Vertical dashed lines show the detection limits (DL) of EMPA for select elements.

6.1.4 Comparison of magnetite and ilmenite trace element compositions

The V content of magnetite, the principle ore mineral in the Iron-T deposit (Taner et al., 1998), is between 0.5-1.1 wt.% for most samples, although in one sample (MA32-25) it reaches 1.5 wt.%. (Table 15). Ilmenite is comparatively less-enriched in V, with concentrations ranging between 0.03-0.3 wt.% (Table 16). Al, Cr, Zn, Ni, Co, and Ga are also consistently present in higher concentrations in magnetite than they are in ilmenite, whereas ilmenite is more enriched in Ti, Mn, Mg, Sc, Zr, Nb, and Hf (Fig. 16). These findings generally agree with several previous studies examining the trace element chemistry of Fe-Ti oxides in magmatic settings (e.g. Méric et al., 2012; Dare et al., 2012, 2014).

Several elements are also more consistently enriched in Fe-Ti oxides hosted by certain lithologies. Both magnetite and ilmenite from massive oxide samples, semi-massive olivine pyroxenites, and relatively unaltered olivine gabbros are consistently more enriched in Mg, Sc, Mn, Co, Zr, and Ni than are grains hosted by altered pyroxenites and gabbros (Fig. 16). Conversely, Fe-Ti oxides are notably more enriched in Cr and V in most gabbros than all other lithologies. Ilmenite from gabbros and pyroxenites is also typically most enriched in Mn, while their magnetite is more enriched in Zn.

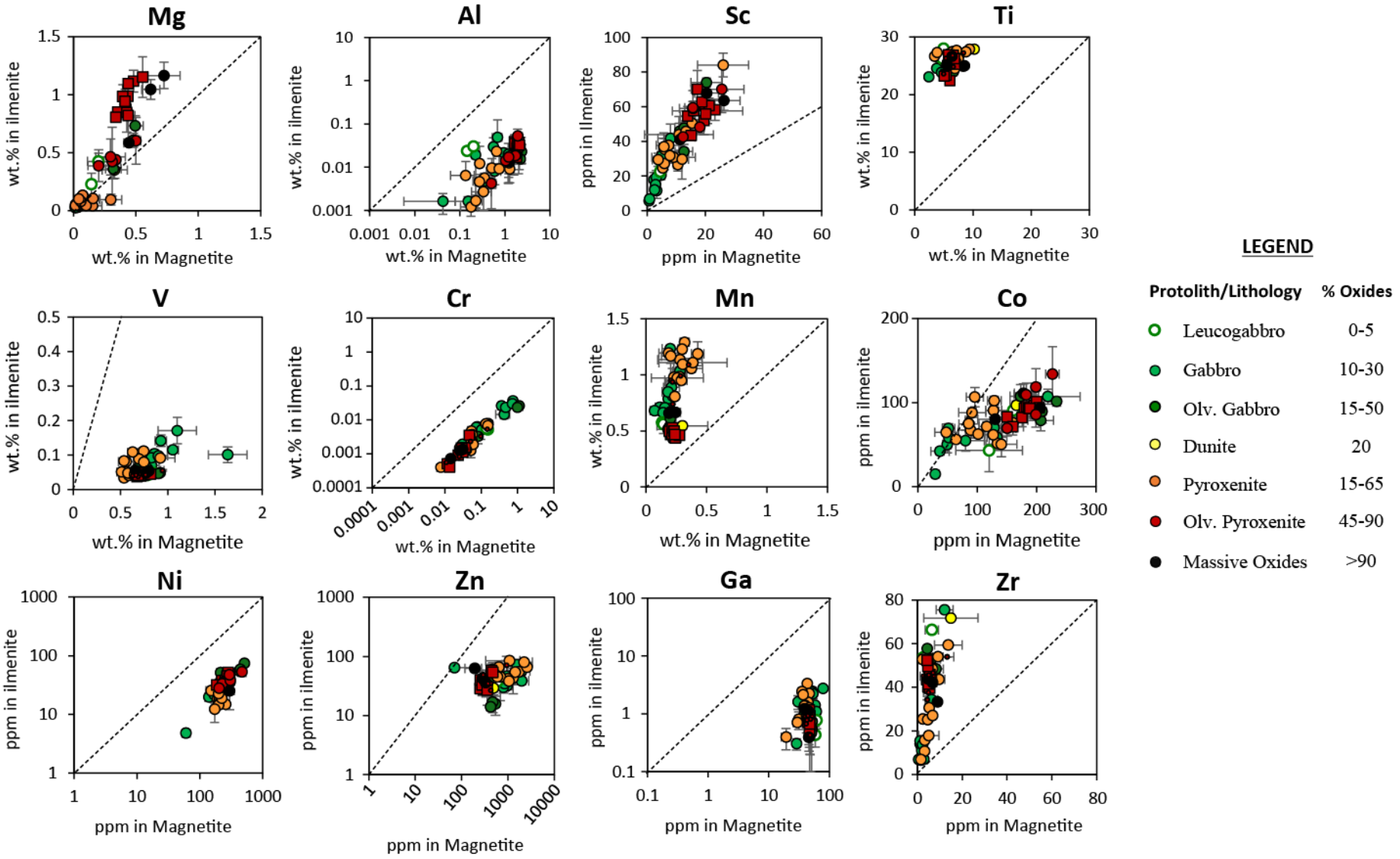

Fig. 16. Binary diagrams comparing the concentrations of select trace elements in magnetite with their concentrations in ilmenite from the same sample. Circles represent drill core samples; square represent outcrop samples. Data points represent the average composition of a sample. Error bars are calculated as one standard deviation on either side of the mean, and represent the natural variation in Fe-Ti oxide compositions within a thin section. Dashed lines are the 1:1 lines.

6.1.5 Deposit-scale Fe-Ti oxide chemostratigraphic variations

Fig. 17 shows the average concentrations of Mg, Al, Sc, Ti, V, Cr, Mn, Co, Ni, Zn, Ga, and Zr in both magnetite and ilmenite, as well as the Nb and Hf contents of ilmenite, plotted against stratigraphic depth for all drill core samples. Note that for sample MA11-2 (~245 m depth), from which altered oxides at the base of the massive oxide layer were analyzed in addition to unaltered grains from within the layer itself, only the data from the unaltered Fe-Ti oxides are included in the profiles of Fig. 17. A comparison of the chemistries from the two textural varieties in this variably altered sample is discussed in section 6.1.7. Error bars in Fig. 17 represent the natural variation in Fe-Ti oxide compositions within a thin section or sub-lithology, and are calculated as one standard deviation on either side of the mean. Intra-sample variation of most elements is generally small (RSD <20%) and in most cases is insignificant relative to chemostratigraphic variations that are observed at a deposit-scale, with a few exceptions. Magnetite from several samples show large variations in Ti (up to 90% RSD), and the samples where these are greatest also exhibit highly variable Mn contents. As can be seen in Fig. 14, Ti and Mn are the elements whose concentrations are most sensitive to the incorporation of ilmenite during the analysis of magnetite. Therefore, these large variations presumably represent significant differences in the proportions of ilmenite exsolutions that were incorporated during each individual analysis of magnetite, which were then used in the calculation of the sample average. However, Zn concentrations in both oxides are also highly variable in many samples (up to 70% RSD), and generally do not correspond with variations in either Ti or Mn. Additionally, ilmenite that was analyzed from oxide-poor leucogabbros consistently displays greater intrasample variations in several elements (e.g. Cr, V) than do oxides from other lithologies.

Each trace element exhibits unique chemostratigraphic behaviour in Fe-Ti oxides, the nature of which are discussed are in detail below. Systematic chemostratigraphic variations in the compositions of magnetite and ilmenite are typically only apparent when examined over scales of tens-to-hundreds of meters. Furthermore, much of the variation that is observed is seemingly due to the tendency for Fe-Ti oxides hosted by particular lithologies to be preferentially depleted or enriched in certain elements. For instance, oxides hosted by gabbros, and particularly oxide-poor leucogabbros, tend to be noticeably and consistently depleted in Ni, Co, Mg, Sc, Zr, and Hf, but enriched in Cr and V, relative to samples of other lithologies that are at similar stratigraphic depths (i.e. within 10-20 m). However, even with this apparent lithological influence on Fe-Ti oxide chemistry, several elements do exhibit broadly similar chemostratigraphic trends. For example, Cr and V exhibit broadly similar local cryptic depletion-and-reversal cycles. Cr, however, also exhibits an overall deposit-scale depletion trend in both magnetite and ilmenite - at least for all lithologies other than leucogabbros – that is not observed in V. Ni, Co, Mg, and Al also all become progressively, albeit erratically depleted across the lower 150 m of stratigraphy, but they all exhibit different trends in the upper 70 m. In contrast, Mn and Zn show stretches of up-section enrichment that approximately correspond to depletion cycles in Cr, V, and Ni. Although the ratio of the concentration of each element in magnetite-to-ilmenite may vary from sample to sample, they do not systematically increase or decrease with depth (Fig. 18).

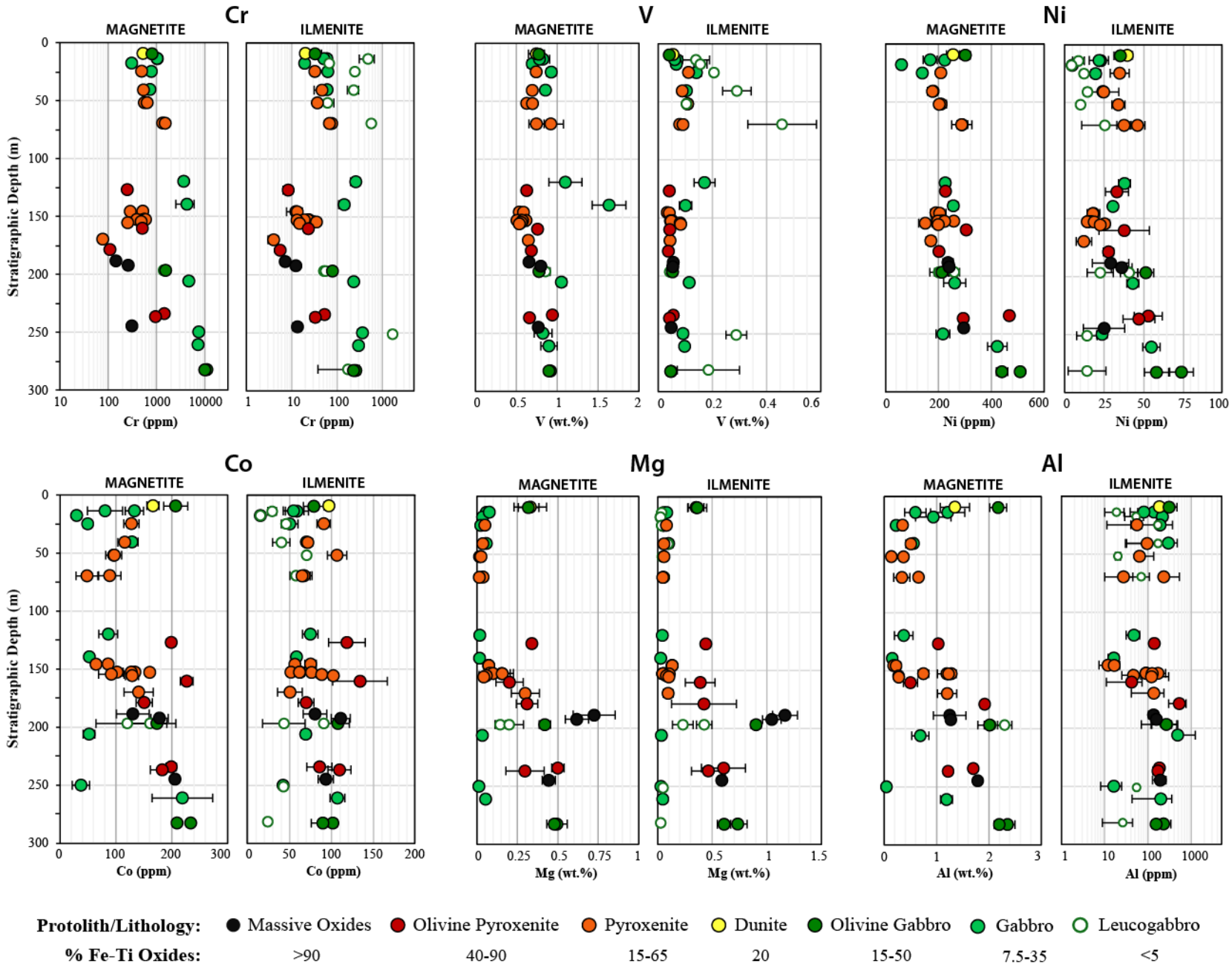

Fig. 17. Chemostratigraphic profiles showing deposit-scale variations in the trace element compositions of primary Fe-Ti oxides from drill core samples. Data points represent the average concentrations of the given element in the Fe-Ti oxide from the sample. Error bars, calculated as one standard deviation on either side of the mean, represent natural variations in the composition of the oxide within a sample.

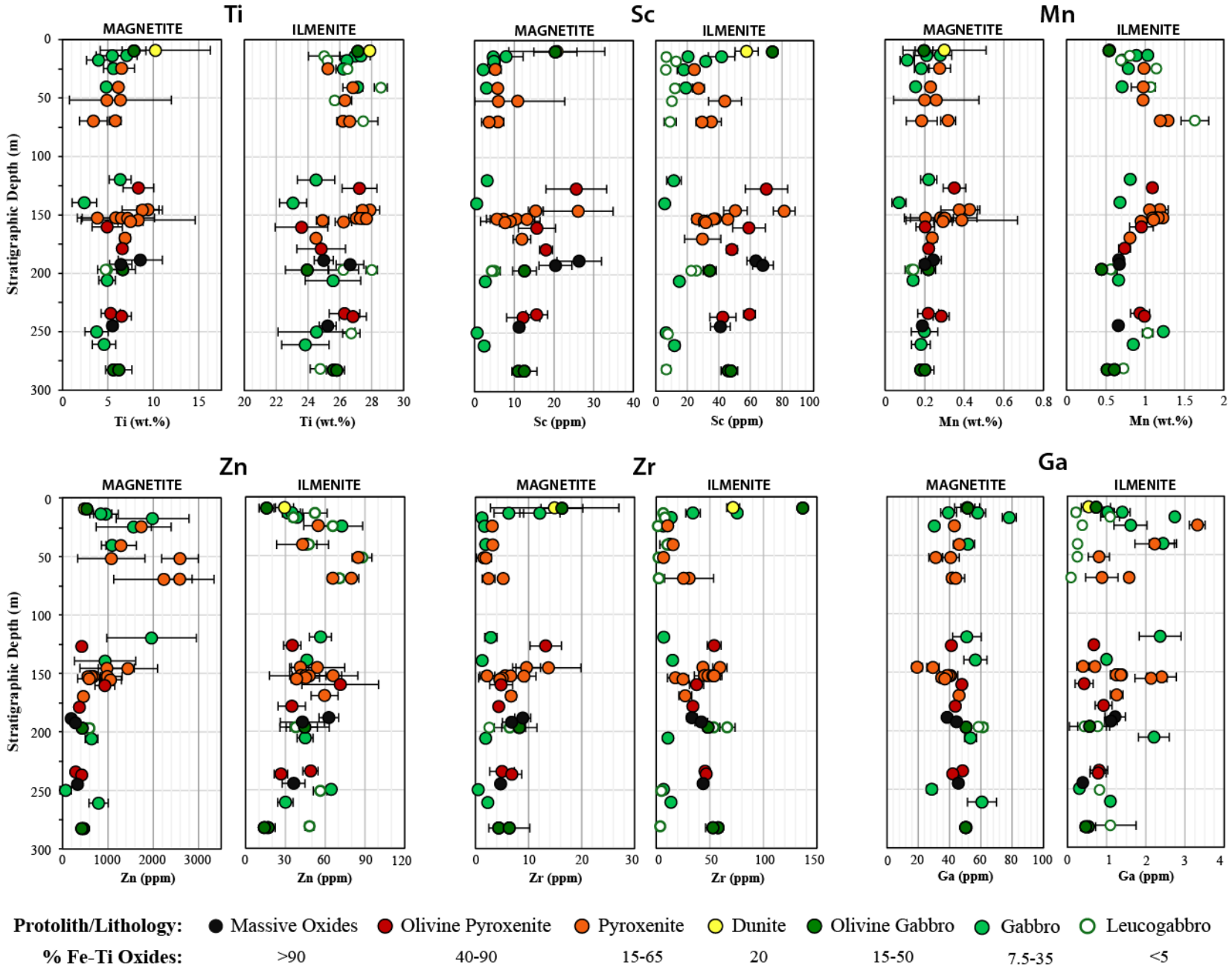

Fig. 17 (cont'd). Chemostratigraphic profiles showing deposit-scale variations in trace compositions of magnetite and primary Fe-Ti oxides from drill core samples. Data points represent the average concentrations of the given element in the Fe-Ti oxide from the sample. Error bars, calculated as one standard deviation on either side of the mean, represent natural variations in the composition of the oxide within a sample.

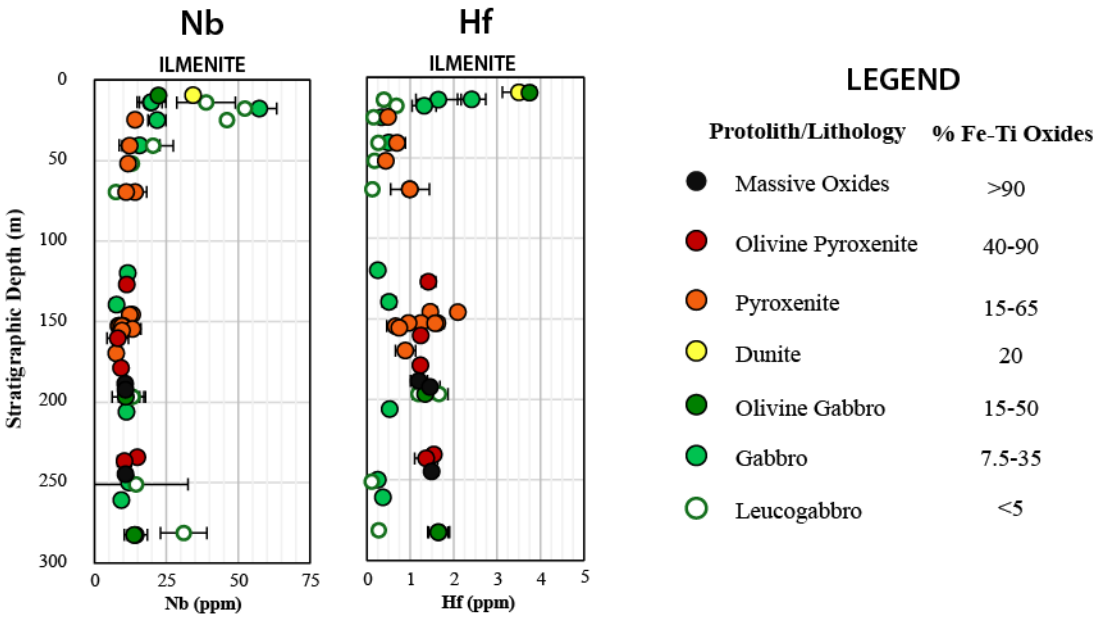

Fig. 17 (cont'd). Chemostratigraphic profiles showing deposit-scale variations in the trace element compositions of primary Fe-Ti oxides from drill core samples. Data points represent the average concentrations of the given element in the Fe-Ti oxide from the sample. Error bars, calculated as one standard deviation on either side of the mean, represent natural variations in the composition of the mineral within a sample.

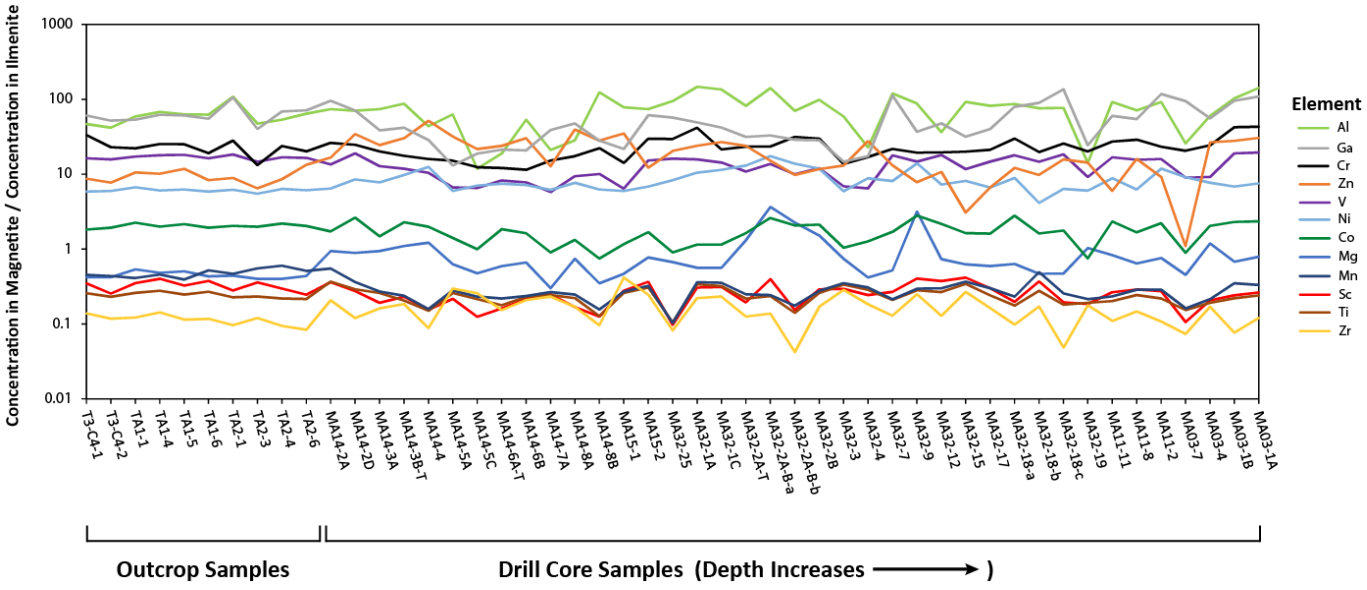

Fig. 18. Variations in the ratios of the concentrations of trace elements between coexisting magnetite and ilmenite. Note the logarithmic scale used on the vertical axis.

6.1.5.1 Deposit-scale variations in magnetite compositions

Trace elements such as Cr and V, which are strongly compatible in magnetite in silicate melts and thus behave compatibly during fractionation (e.g. Barnes et al., 2004; Namur et al., 2010; Dare et al., 2014), are commonly used to trace the geochemical evolution of LMIs. The data obtained in this study allows us to compare their chemostratigraphic behaviour with those of other trace elements which are usually present in Fe-Ti oxides in lower concentrations, and therefore less studied, and determine if they may be useful in deciphering the petrogenesis of the Iron-T deposit. However, magnetite compositions fluctuate significantly - and at a variety of scales - across the layered rocks of the Iron-T deposit (Fig. 17). In some cases these fluctuations occur somewhat systematically with depth, either across the entirety of the deposit or at localized levels within it, while in other instances they are more erratic in nature. Furthermore, there are notable differences between the cryptic trends of Cr and V and those of other elements that are compatible in Fe-Ti oxides such as Ni, Co, and Mg, all of which would typically be expected to behave similarly to Cr and V during fractionation of a magma crystallizing the mafic and ultramafic rocks represented in this study (Dare et al., 2014). Since Cr is the most strongly compatible trace element in magnetite in magmatic systems, and its concentration in magnetite in this study spans more than two orders of magnitude, its chemostratigraphic behaviour will be described below first. Cryptic trends of other trace elements will then be compared to those of Cr.

The highest Cr concentrations in magnetite (Cr_{Mgt}) occur in the olivine gabbros at the base of the composite stratigraphic profile, where they exceed 1 wt.% (Fig. 17). Its concentrations slightly decrease upwards over the next 30 m before sharply decreasing by more than an order of magnitude (to 310 ppm) upon the first appearance of massive oxides at ~250 m

depth. A gradual enrichment over the next 10 m in the overlying olivine pyroxenites is then punctuated by a local maximum (Cr_{Mgt} ~ 0.4 wt.%) in gabbros situated at approximately 200 m. Another sharp decrease coincides with another sequence of massive oxides and pyroxenites, reaching the absolute minimum Cr concentration observed in the profile (~80 ppm) at 170 m. A sharp cryptic reversal up to 500 ppm is then followed by a sequence of pyroxenites wherein Cr_{Mgt} fluctuates between 200-600 ppm. In the 20 m immediately overlying this pyroxenite sequence, Cr_{Mgt} differs by an order of magnitude between two enriched gabbroic samples (Cr_{Mgt} >3000 ppm) and a depleted olivine pyroxenite layer situated midway between them (Cr_{Mgt} ~250 ppm). A 50 m oxide-barren gap in the stratigraphy is then followed by a relatively steady upwards-depletion trend in Cr across interlayered pyroxenite- and gabbro-hosted magnetites over the next 50 m or so, although magnetite from gabbros is typically enriched in Cr by several hundred ppm. A minor reversal in the uppermost 20 m to a local maximum of 1000 ppm roughly coincides with the re-occurrence of olivine gabbros and a dunite layer. Notably, this depletion trend in the upper 70 m of the stratigraphy roughly aligns with the slope of the depletion trend defined by enriched gabbros in the lower 200 m. Cumulatively, these seemingly produce an intermittent deposit-scale depletion trend, upon which sharply-depleted oxide-rich ultramafic horizons are superimposed.

Of the other elements that are compatible into magnetite, V displays the most similar depletion trends with respect to Cr, with cryptic reversals occurring at similar stratigraphic levels. It also appears to be similarly enriched in magnetite hosted by gabbros relative to other lithologies. However, V does not exhibit the same broad, deposit-scale depletion trend that is seen in the Cr profile. V_{Mgt} remains relatively consistent between about 0.5-1 wt.% throughout the profile, with the notable exception of MA32-25 at 140 m, in which it reaches an absolute

maximum of 1.5 wt.%. Other differences include the fact that the relative magnitudes of its cryptic reversals are not as great as they are for Cr, and similarly, decreases in V coinciding with the occurrence of massive oxide layers are not nearly as pronounced. For example, magnetite from the massive oxide layer at 245 m contains only about 7% less V than grains from the gabbros only 5 m below, compared to 95% less Cr.

Ni, like Cr, is highest in magnetite at the base of the profile (~500 ppm), and exhibits a broad depletion trend across the length of the profile. It also mirrors several localized cryptic patterns that are observed in both Cr and V, including the upwards-enrichment in olivine pyroxenites around 235 m and the cryptic reversal associated with the olivine pyroxenite (MA32-7) at 160 m. However, magnetite from gabbros is notably not as enriched in Ni as it is in Cr and V relative to other lithologies at similar depths. Consequently, the samples that define cryptic reversals and local maxima in Cr_{Mgt} and V_{Mgt} – several of which are gabbros (e.g. MA32-19, 205 m) - do not necessarily coincide with samples exhibiting local maxima in Ni_{Mgt}. This is highlighted by the fact that the absolute minimum Ni_{Mgt} value (60 ppm) occurs over 100 m above those of Cr and V, in a gabbro at 17 m depth that immediately precedes the cryptic reversal associated with olivine gabbros and dunites.

Co and Al exhibit similar, weakly-defined depletion trends in magnetite, particularly across the lower 200 m of the profile, with Co broadly decreasing from ~220 ppm at the base to less than 100 ppm at 150 m, and Al decreasing from almost 2.5 wt.% to less than 0.5 wt.%. However, their values at any given stratigraphic level are much more erratic than the trends shown by Cr, V, and Ni, largely due to the noticeably depleted nature of magnetite in several gabbros relative to other host lithologies. Magnetite is also strongly depleted in Mg (typically containing less than 0.1 wt.%) in all disseminated gabbros and pyroxenites. In contrast, massive

and semi-massive samples consistently contain greater than 0.25 wt.% Mg, as do all the relatively unaltered olivine gabbro samples. In the upper 70 m, however, Co, Mg, and Al all display different trends. Co_{Mgt} appears to consistently increase in pyroxenite from 70-25 m (from ~50-130 ppm), where it sharply drops in gabbros before increasing again in the upper 10 m. In contrast, Mg and Al appear to neither increase nor consistently decrease in magnetite over most of the upper 75 m, remaining lower than 0.1 wt.% and 0.8 wt.%, respectively. Both become more enriched in the upper 10-20 m, however, with Mg_{Mgt} increasing in the uppermost olivine gabbro and dunite samples, while the cryptic reversal in Al begins about 10 m below in several of the underlying gabbros.

No other elements that are present in magnetite show clear cryptic trends well-correlated with stratigraphic depth. However, Sc and Zr are both consistently depleted in magnetite from gabbroic host rocks in a similar manner to Mg, Al, and Co. Ti_{Mgt} and Mn_{Mgt} are similarly low in the highly-altered gabbro (MA32-25) at 140 m (both are the minimum values observed across their respective profiles – 2.4 wt.% Ti and 700 ppm Mn) but this is the only sample displaying such an obvious depletion in these two elements, and as is discussed in section 7.1.3, there is reason to doubt that its data are in fact representative of its primary magnetite compositions. The chemostratigraphic profiles of Ti_{Mgt} and Mn_{Mgt} otherwise mirror each other quite strongly. Both remain relatively consistent between 4-6 wt.% and 0.1-0.3 wt.%, respectively, save for a zone of up-section enrichment between 200-150 m (Mn_{Mgt} increases to >0.4 wt.% while Ti_{Mgt} increases to nearly 10 wt.%). Zn concentrations also increase upwards from approximately 200 ppm to greater than 1000 ppm between 200-150 m. Unlike Ti and Mn, however, they do not drop off again at 70 m. Instead, magnetite becomes even more enriched in Zn (up to a maximum of greater than 2500 ppm) - albeit with large intrasample variations - before returning to 500 ppm in

the uppermost 10 m. Ga_{Mgt}, for the most part, also remains relatively constant (typically between 40-60 ppm) throughout much of the profile, although a sharp upwards depletion coincides with the pyroxenite sequence between 160-145 m where Ti, Mn, and Zr increase, before dropping again to 20 ppm. Like several other elements its concentrations in rocks from the upper 20 m are quite variable, ranging between 30-80 ppm across the gabbros and dunite at this level.

6.1.5.2 Deposit-scale variations in primary ilmenite compositions

For all lithologies other than oxide-poor leucogabbros, chemostratigraphic trends for most trace elements present in ilmenite are similar to those of corresponding magnetite (Fig. 17). Most notably, sharp depletions in Cr are coincident with the occurrences of massive oxides and olivine pyroxenites in the lower 200 m of the stratigraphy, while interlayered pyroxenite-gabbros also define a similar depletion trend in the upper 70 m. Ilmenite from gabbros is also relatively enriched in Cr and V, but depleted in Sc, Zr, and Hf relative to more oxide-rich or unaltered lithologies (i.e. olivine gabbros) at similar stratigraphic levels. Just as seen in Fig. 14, Mg is clearly depleted in all gabbro- and pyroxenite-hosted ilmenite relative to other lithologies at similar stratigraphic levels. Mn notably displays a clearer correlation with stratigraphy in ilmenite than it does in magnetite, particularly in the massive oxide-to-ultramafic sequence between 200-150 m, where Mn_{Ilm} steadily increases from 0.5 wt.% to 1.25 wt.%. However, gabbros overlying this sequence are noticeably depleted relative to the underlying and interlayered ultramafic rocks. This up-section enrichment trend is also not continued across the shallower gabbro-pyroxenite sequence, where Mn_{Ilm} decreases back to 0.5 wt.%, with pyroxenites typically being slightly more enriched than interlayered gabbros. Except for the depleted nature of Hf in gabbros, Nb and Hf remain relatively constant across most of the

stratigraphy (between 5-20 ppm and 0.5-2 ppm, respectively), but spike in the interlayered gabbro, leucogabbro, and dunite sequence in the upper 20m (up to >50 ppm Nb and ~4 ppm Hf).

One of the most conspicuous features in the profiles of Fig. 17, however, is the manner in which trace ilmenite grains that are hosted by leucogabbros are often strongly enriched in Cr and V. Cr concentrations may be up to an order of magnitude higher in ilmenite when hosted by leucogabbros relative to more oxide-rich rocks at similar stratigraphic levels, while V concentrations are up to five times higher. There is also considerably more intrasample variation in the compositions of ilmenite in these rocks, as evidenced by the comparatively large standard deviations in Cr_{Ilm} and V_{Ilm} relative to other samples. However, it should be noted that this enrichment and increased variability is not systematic across all the rocks classified as leucogabbros in this study. Ilmenite from the two leucogabbro sub-lithologies of sample MA32-18, which are relatively unaltered compared to most other gabbros or leucogabbros in this study, both contain similar concentrations of Cr and V as the interlayered olivine gabbro, as does coexisting magnetite in this sample. Additionally, ilmenite from the leucogabbro sub-lithology of MA14-7A, which unlike MA32-18 has been clearly metamorphosed, also exhibits no strong enrichment in either Cr or V.

While Cr and V are consistently enriched in leucogabbro-hosted ilmenite, it is often depleted in others elements. These includes all those elements that are similarly depleted in disseminated gabbro hosts (Mg, Ni, Co, Sc, Zr, and Hf), as well as Ga in the upper 70 m of the profile. And unlike the non-ubiquitous nature of their enrichment in Cr and V, the depletion of these elements in ilmenite is observed in all leucogabbros that have been pervasively altered – i.e. all those except the two sub-lithologies of MA32-18. However, even ilmenite from these

leucogabbros of MA32-18 are strongly depleted in Mg relative to the olivine gabbro band that separates them.

6.1.6 Outcrop-scale variations in Fe-Ti oxide compositions

Fig. 19 shows how magnetite and ilmenite compositions vary across the bifurcating and thinning Fe-Ti oxide-rich bands from the two channels cut from outcrop TA (Fig. 6), and the apparent cross-stratified oxide layers in outcrop T3 (Fig. 7a). These samples were analyzed to determine if outcrop-scale geochemical variations can provide insight into how such features form in layered intrusions. Variations in magnetite and ilmenite compositions were generally small for most elements in these samples (Tables 17, 18). Therefore, only Cr, V, and Ni are shown in Fig. 19, as these are the most strongly compatible elements in magnetite during fractionation (Dare et al., 2014) and should best reflect compositional changes of the magma at these small scales.

6.1.6.1 TA outcrop results

Compared to the cyclic up-section depletion and reversal trends that occur in Cr, V, and Ni at a deposit-scale, and the wide compositional ranges that are associated with them, Fe-Ti oxide compositions vary relatively little over the 40-50 cm profiles of TA1 and TA2 (Fig. 19a). The concentrations of most elements in Fe-Ti oxides within the eight samples from the two profiles are similar to those of sample MA11-2, the massive oxide band at 245 m of the composite stratigraphic profile (Fig. 17). This supports the geographic interpretation that this outcrop and the massive oxide layer intersected in drill core are approximately laterally correlative (Fig. 3). There are, however, distinct differences in Fe-Ti oxide compositions across the four bands from

which samples were analyzed in from outcrop TA (labelled 1-4 from the base up in Fig. 19a). In the easternmost channel (TA2), Cr in magnetite increases upwards from 300-500 ppm across bands 1-3 (an outcrop distance of approximately 20 cm), but drops to only ~300 ppm in the uppermost band approximately 20 cm up. A similar trend is present in coexisting ilmenite, with Cr concentrations ranging from 10-35 ppm. However, the concentrations of V (~0.7-0.8 wt.% in magnetite; 400-500 ppm in ilmenite) and Ni (270-300 ppm in magnetite; 40-50 ppm in ilmenite) remain more or less constant across the four bands.

In terms of lateral variations, Fe-Ti oxide compositions from bands 1 and 4 from the TA2 profile are essentially identical to their correlative samples in the TA1 profile, 2 m to the west. However, those of band 2, which has thickened and merged with band 1 at TA1, and band 3, which thins towards the west, are slightly different at TA1 than they are at TA2, most notably in their Cr content. Magnetite from both bands at TA1 contain approximately 30 percent less Cr relative to their correlative counterparts at TA2. Ilmenite in band 2 is only marginally depleted at TA1 relative to TA2 (taking intrasample variations into account); however, in band 3 it contains up to 60 percent less Cr.

6.1.6.2 T3 outcrop results

As with the TA outcrop samples, cryptic variations in the two samples collected on either side of the apparent cross-stratification plane between successive oxide layers in outcrop T3 are minor (Fig. 19b). Although Cr_{Mgt} appears to decrease from 134 ppm below the cross-stratification plane (sample T3-C4-1) to 117 ppm above (T3-C4-2), this decrease is not mirrored by Cr_{Ilm} (which is less than 10 ppm in both samples) nor by most other trace elements. In fact, V and Ni

concentrations are slightly higher in both magnetite and ilmenite above the cross-stratification plane than they are below – with V_{Mgt} and Ni_{Mgt} increasing on average from 0.70-0.74 wt.% and 185-223 ppm, and V_{Ilm} and Ni_{Ilm} increasing from 427-470 ppm 32-37 ppm, respectively. Compared to cryptic variations observed at a deposit scale, these differences in mineral compositions are presumably insignificant. However, it is noteworthy that although the geographic location of outcrop T3 suggests that these samples are correlative with the uppermost oxide-rich zone of the composite stratigraphic profile (Fig. 3), their oxide compositions do not closely agree with those of any drill core samples at or around this level. While the concentrations of V, Ni, and several other trace elements in magnetite from T3-C4-1 and T3-C4-2 are similar in magnitude to those of the pyroxenites located at about 40-50 m in Fig. 17 (drill core samples MA14-6B, -7A, -7B), Cr is significantly depleted in both oxide phases in the T3 samples. Cr_{Mgt} values are four to five times lower than those of the presumably correlative drill core samples, and its ilmenite contains the lowest amounts of Cr (4-5 ppm).of all the samples collected in this study.

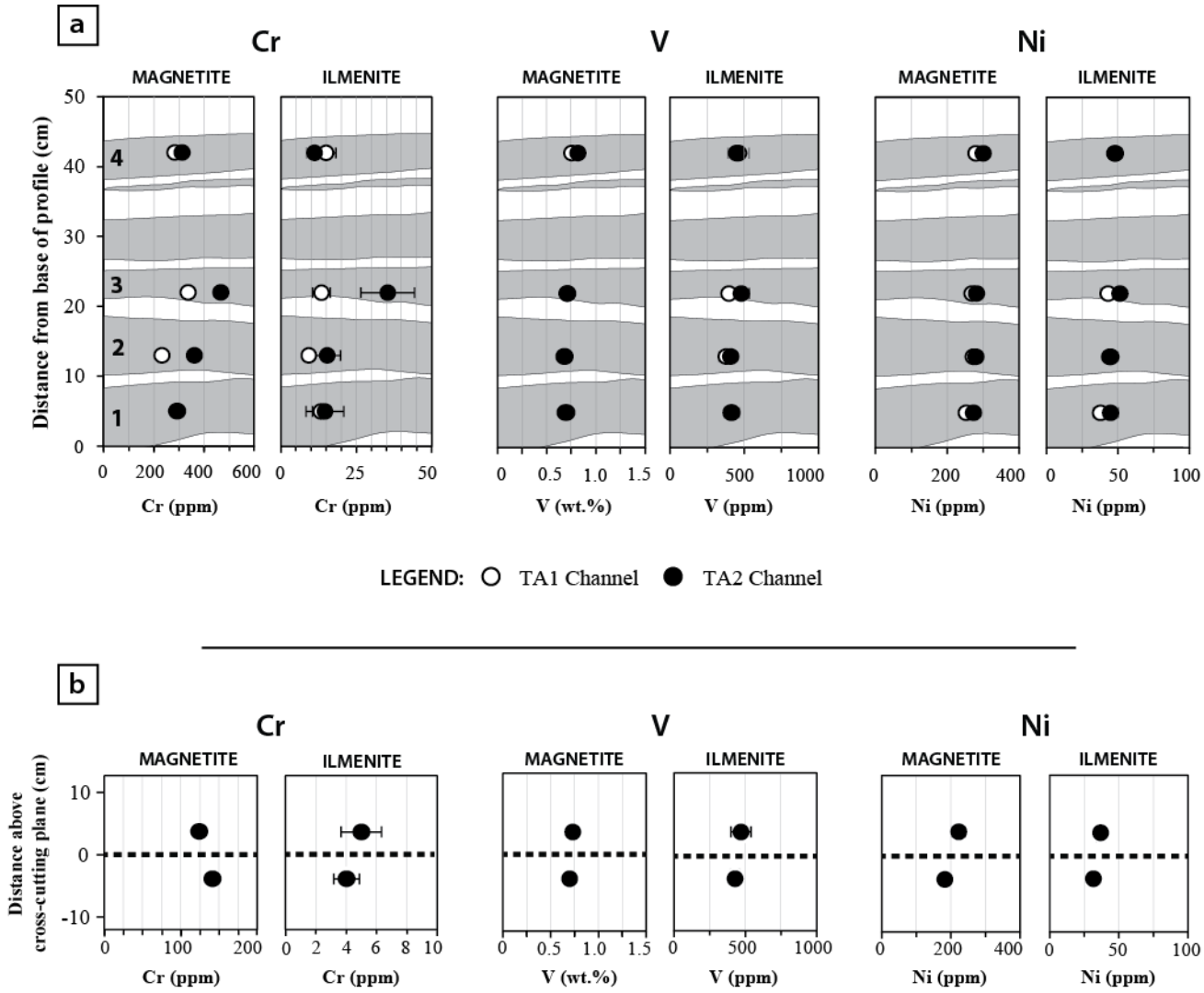

Fig. 19. Variations in Fe-Ti oxide chemistry across irregular layering features of interest observed in outcrops. **a.** Vertical and lateral variations in the Cr, V, and Ni concentrations of magnetite and ilmenite across the sequence of closely spaced, laterally bifurcating oxide-rich layers seen in outcrop TA. Shaded horizontal bands schematically depict the oxide-rich layers as intersected by channel TA2. Note that bands 1 and 2 merge and thicken towards channel TA1, 2 meters to the west, while band 3 thins and bends upwards following the upper margin of band 2 (see Fig. 6). Data points correspond to the samples shown in Fig. 6. Note that the actual y-axis positions of each pair of correlative TA1 and TA2 samples are not necessarily the same due to the vertical displacement of the oxide layers along the length of the outcrop – however, in each case both samples are plotted at the positions of those taken from channel TA2 to highlight the fact that both were taken from the same laterally correlative oxide layer. **b.** Variations in the Cr, V, and Ni concentrations of Fe-Ti oxides on either side of the apparent cross-stratification horizon observed between successive oxide layers in outcrop T3 (dashed line in Fig. 7a). Data points in both **a.** and **b.** indicate the average oxide composition of the sample. Error bars, calculated as one standard deviation on either side of the mean, represent natural variability in the composition of the mineral within a thin section.

6.1.7 Comparison of altered and unaltered Fe-Ti oxide compositions in MA11-2

To assess whether the alteration of magnetite that is observed to varying degrees in the RBC (Fig. 11) is accompanied by compositional changes in either it or ilmenite, Fe-Ti oxide compositions from the gradationally altered base of the massive oxide layer represented by MA11-2 (Fig. 11k-l) were compared to those of overlying unaltered grains from within the same massive band (situated at 245 m depth on Fig. 17). The unaltered oxide grains that were analyzed are all contained within the same thin section as the altered ones and are all within 3 cm of the base of the massive layer, which has an otherwise sharp contact with the underlying oxide-barren leucogabbro. Fig. 20 and Fig. 21 show the results of these analyses for magnetite and ilmenite, respectively. Trace element concentrations are plotted against Ti to distinguish compositional variations that are potentially due to alteration from those that could arise as a result of different amounts of exsolution phases being incorporated in each analysis.

Altered magnetite is strongly depleted in Mg relative to unaltered grains (approximately 80% rel. diff), and Co and Ni are both depleted in the former by about 50% (Fig. 20). In contrast, Zn is three-to-five times more enriched in altered magnetite. Sc, Mn, and Zr are positively correlated with Ti regardless of whether or not magnetite is altered, suggesting the abundances of these elements are strongly influenced by the inclusion of ilmenite exsolutions during LA-ICP-MS analyses. Al, V, and Cr appear to be neither depleted nor enriched in altered magnetite, although V and Cr do show a weak negative correlation with Ti. This may indicate that they become enriched in the host magnetite during the oxy-exsolution of ilmenite. Several altered magnetite grains are also slightly enriched in Ga relative to other grains, although it, too, may be negatively correlated with Ti.

Ilmenite from the altered zone is also notably depleted in Mg and Co relative to unaltered grains, in addition to Zr, Nb, and Hf (Fig. 21). There is no clear difference in the Al, Cr, and Mn concentrations of altered ilmenite relative to the unaltered grains. The remaining elements are more ambiguous, as the concentration of an element may be correlated with Ti in one of either altered or unaltered ilmenite, but not the other. For example, V and Sc both unmistakeably increase with Ti in altered ilmenite grains, whereas Ga and Zn decrease, albeit with anomalously enriched outliers in V and Ga. However, unaltered grains show no such relationship. In contrast, Ni is positively correlated with Ti in unaltered ilmenite, but not in the altered grains. However, despite these irregularities there is no unambiguous enrichment or depletion in Sc, V, Ni, Ga, or Zn in either textural variety, as there is always some compositional overlap between them.

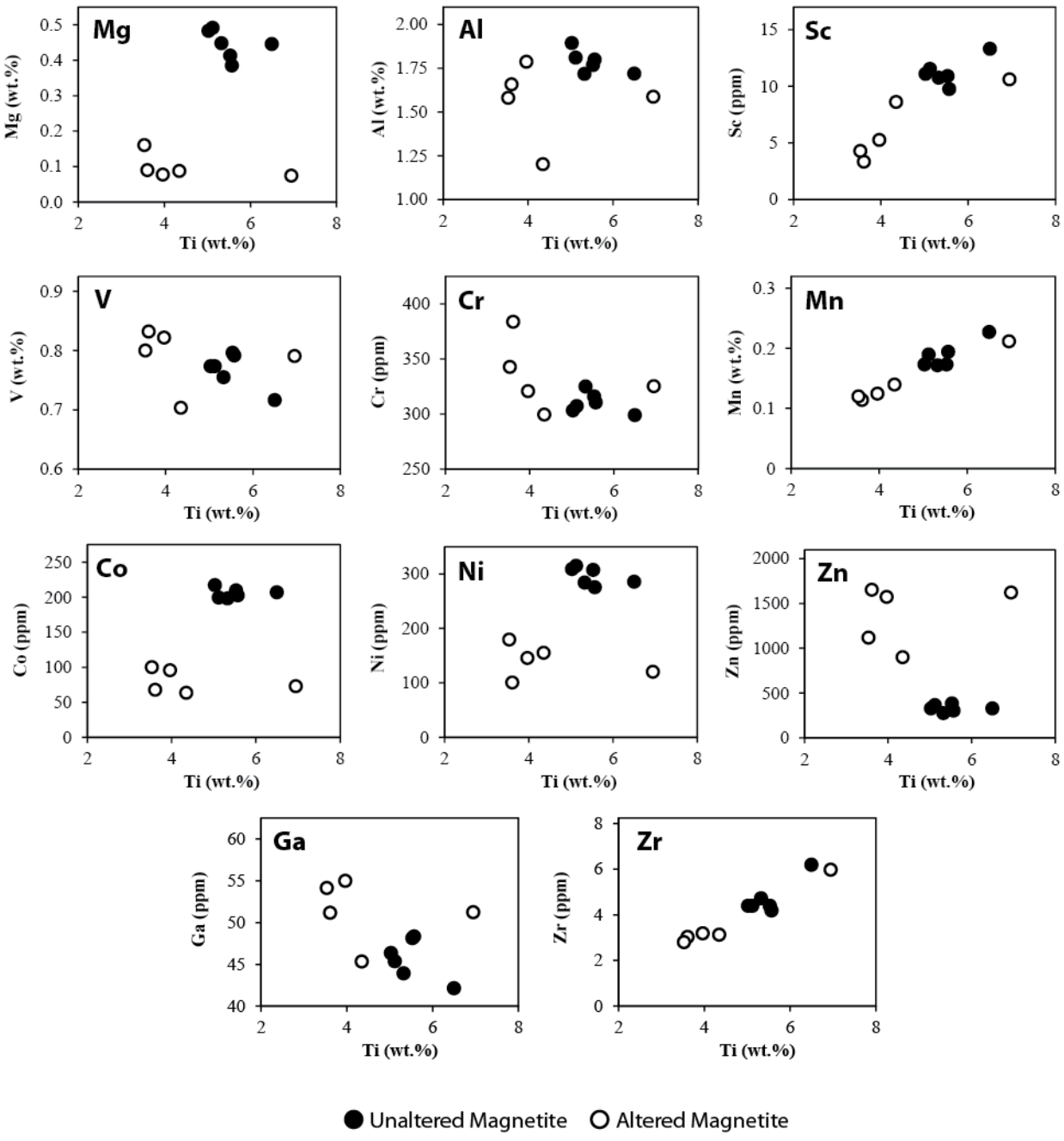

Fig. 20. Comparison of altered and unaltered magnetite compositions from sample MA11-2. Altered magnetite refers to relict grains that were analyzed from the 2-3 mm thick gradational zone at the base of the massive oxide layer at this stratigraphic level (approx. 245 m depth) where magnetite near the contact with the underlying leucogabbro is increasingly replaced by silicates towards the leucogabbro (Fig. 11k-l). Unaltered magnetite refers to grains that were analyzed from the massive oxide layer (within 3 cm of the basal contact) where Fe-Ti oxides exhibit little textural alteration.

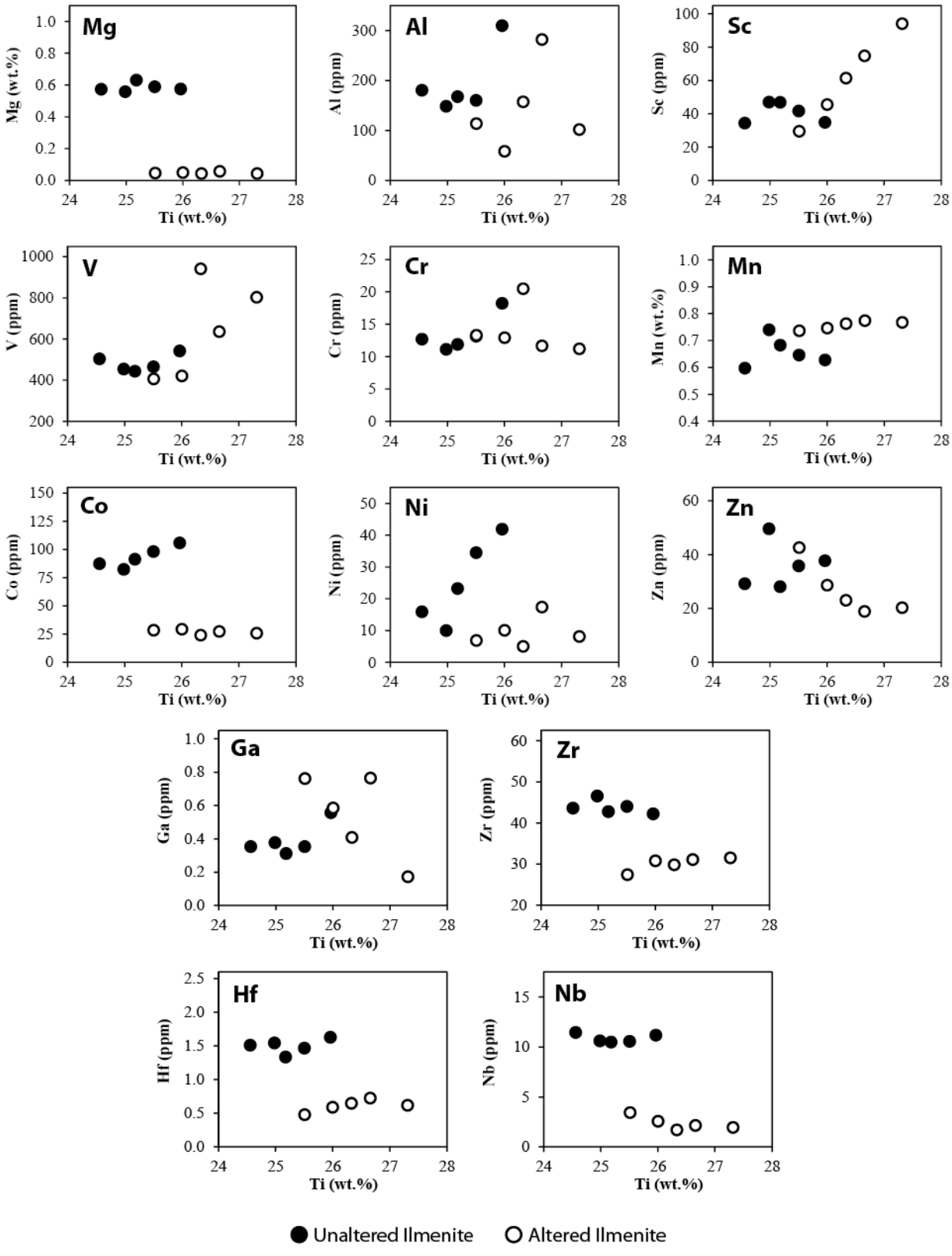

Fig. 21. Comparison of altered and unaltered ilmenite compositions from sample MA11-2. "Altered" ilmenite refers to grains that were analyzed from the 2-3 mm thick gradational zone at the base of the massive oxide layer at this stratigraphic level (approx. 245 m depth) where magnetite in contact with the underlying leucogabbro is increasingly replaced by silicates towards the leucogabbro – note that ilmenite displays little textural alteration itself, however (Fig. 11k-l). "Unaltered" ilmenite refers to grains that were analyzed from the massive oxide layer (within 3 cm of the basal contact) where Fe-Ti oxides exhibit little textural alteration.

6.2 Silicate mineral chemical compositions

The average compositions of relict clinopyroxene, olivine, and plagioclase from select drill core samples are given in Tables 19-21, and full results are provided in Appendix 3. Fig. 22 shows how the Mg-number (Mg# = 100*Mg/[Mg+Fe]) of clinopyroxene, the anorthite content (%An = 100*Ca/[Ca+Na+K]) of plagioclase, and the forsterite content (%Fo = 100*Mg/[Mg+Fe]) of olivine vary with depth across the Iron-T deposit. Note that since not all thin sections from which silicates were analyzed contain either unaltered or suitably-sized relict cores of these minerals, the number of thin sections from which they were analyzed is not the same for each.

6.2.1 Clinopyroxene

Clinopyroxene was analyzed from nine samples: three disseminated pyroxenites (MA14-5A, -8A, MA32-3) in which it is present as relict cores within grains that are partially altered to amphiboles (e.g. Fig. 9d); three massive oxide samples (MA32-15, -17, MA11-2) in which partially altered, high-relief relict grains occur interstitially in frameworks of magnetite and ilmenite (Fig. 9b); and three from olivine gabbros (MA14-2D, MA03-1A, -1B) where clinopyroxene is relatively fresh apart from incipient marginal alteration (Fig. 9e). It should be noted that in several cases the number of analyses used in calculation of the sample average is low (n = 1-2) (Table 19). This is because several grains returned wt.% oxide totals below 98.5%, presumably due to the unintentional incorporation of very fine hydrous alteration phases during the analyses, and were thus not considered when calculating the average.

In general, clinopyroxene is more Fe-rich in the three samples from the upper 70 m of the profile (Mg# ~70) than are those at the very base of the profile (Mg# ~72-73), while grains from

the massive oxide band at 245 m are slightly more Mg-rich (Mg# =74.5) than are the basal samples (Fig. 22a). However, the most noticeable feature is the anomalously Mg-rich nature of clinopyroxene from the two massive oxide samples at around 190 m (Mg# ~78-82), although intrasample variations between grains are also large (Table 19). It should be noted that these two samples (MA32-15, -17) also contain the most Mg-rich magnetite and ilmenite observed in this study (Fig. 17).

6.2.2 Olivine

Medium- to coarse-grained, anhedral olivine (i.e. clearly primary) was analyzed from three olivine gabbros (MA14-2D, MA03-1A, -1B) and one olivine pyroxenite (MA11-8), while the fine-grained, polygonal variety of olivine (e.g. Fig. 9a) was analyzed from MA11-2. Although data only exists for samples from the base and very top of the composite stratigraphic profile, the average composition of olivine at the top (%Fo ~ 47) is noticeably less Mg-rich than in all the samples in the lower half of the profile (Fig. 22b). The average compositions of olivine near the base (%Fo ~53-54) are otherwise similar, though the polygonal variety of MA11-2 is slightly more Mg-rich (%Fo ~55).

6.2.3 Plagioclase

Plagioclase was analyzed from three olivine gabbro samples (MA14-2D, MA03-1B, MA03-1A) and five leucogabbro samples (MA03-2, -3, -6, MA11-2, MA14-8A-a), as these lithologies are typically those in which coarse igneous plagioclase is best preserved with minimal saussuritization. Note that the plagioclase analyzed from MA11-2 is from the oxide-barren

leucogabbro directly below the lower contact of the massive oxide band from which Fe-Ti oxides in this sample were analyzed. Plagioclase from all of the samples is labradorite, with average compositions ranging between 59-66 %An, although An content may vary by several percent within any given thin section (Table 21). Although, like olivine, the spatial resolution of plagioclase data for this section of the RBC being studied is low, its compositions do not appear to systematically change across the 300 m stratigraphic profile (Fig. 22c).

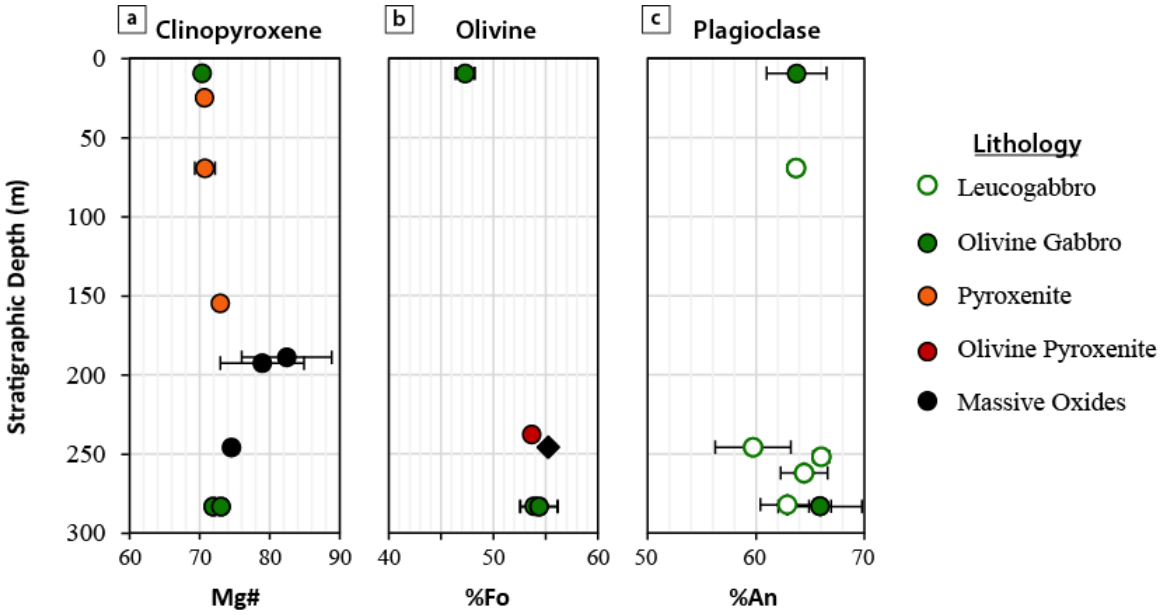

Fig. 22. Chemostratigraphic profiles showing deposit-scale variations in silicate compositions. **a**. Clinopyroxene; **b.** Olivine. Circles indicate that the analyzed olivine was coarse and anhedral (i.e. cumulate), while the diamond indicates that it was fine-grained and polygonal (i.e. potentially recrystallized). **c.** Plagioclase. Data points represent the average compositions of the mineral in the thin section. Error bars are calculated as one standard deviation on either side of the mean.

Table 19. Results of EMPA analyses of clinopyroxene from select drill core samples. Listed compositions are the average of *n* analyses per sample. All values are in wt.% except for Mg# = 100*Mg/(Mg+Fe).

Stratigraphic Depth (m)	Sample	*n*	K_2O	CaO	Al_2O_3	FeO	MgO	MnO	TiO_2	Cr_2O_3	V_2O_3	ZnO	Na_2O	SiO_2	Total	Mg# avg	Mg# std
9.58	MA14-2D	3	0.02	21.68	1.72	9.86	13.12	0.25	0.37	0.02	0.05	0.01	0.25	51.38	98.73	**70.34**	*(0.71)*
24.86	MA14-5A	1	0.01	22.64	1.59	9.31	12.61	0.30	0.17	0.02	0.09	0.06	0.23	51.57	98.60	**70.70**	*(0.00)*
69.47	MA14-8A-b	4	0.02	21.66	1.81	9.73	13.19	0.33	0.33	0.01	0.04	0.01	0.21	51.36	98.69	**70.75**	*(1.44)*
154.47	MA32-3	2	0.01	22.34	1.76	8.62	13.04	0.32	0.34	0.02	0.05	0.02	0.41	51.63	98.56	**72.96**	*(0.45)*
188.51	MA32-15	4	0.00	23.80	1.47	5.79	15.12	0.13	0.30	0.00	0.02	0.00	0.14	52.46	99.23	**82.45**	*(6.43)*
192.24	MA32-17	3	0.00	23.10	1.39	6.98	14.59	0.18	0.27	0.01	0.03	0.02	0.16	52.08	98.81	**78.95**	*(5.98)*
244.72	MA11-2	2	0.00	22.01	2.11	8.60	14.13	0.23	0.41	0.00	0.01	0.02	0.22	51.63	99.39	**74.54**	*(0.51)*
282.46	MA03-1B	3	0.00	21.44	2.34	9.32	13.49	0.24	0.50	0.03	0.07	0.03	0.32	50.99	98.76	**72.08**	*(0.51)*
282.53	MA03-1A	5	0.00	21.64	2.18	9.12	13.89	0.23	0.44	0.03	0.08	0.00	0.30	51.05	98.96	**73.08**	*(0.70)*

Table 20. Results of EMPA analyses of olivine from select drill core samples. Listed compositions are the average of *n* analyses per sample. All values are in wt.% except for %Fo = 100*Mg/(Mg+Fe).

Stratigraphic Depth (m)	Sample	*n*	K_2O	CaO	Al_2O_3	FeO	MgO	MnO	TiO_2	Cr_2O_3	V_2O_3	ZnO	Na_2O	NiO	SiO2	Total	% Fo avg	% Fo std
9.58	MA14-2D*	5	0.01	0.03	0.00	43.03	21.66	0.56	0.01	0.00	0.00	0.01	0.01	0.03	35.00	100.36	**47.29**	*(0.90)*
236.68	MA11-8*	4	0.00	0.04	0.00	38.58	25.05	0.73	0.00	0.01	0.00	0.00	0.00	0.03	34.97	99.41	**53.65**	*(0.42)*
244.72	MA11-2**	4	0.00	0.02	0.01	37.55	25.98	0.60	0.00	0.01	0.00	0.00	0.00	0.02	35.37	99.58	**55.23**	*(0.41)*
282.46	MA03-1B*	3	0.00	0.04	0.00	38.82	25.47	0.53	0.00	0.00	0.00	0.00	0.01	0.02	35.13	100.02	**53.91**	*(0.35)*
282.53	MA03-1A*	5	0.00	0.04	0.00	38.36	25.61	0.52	0.00	0.01	0.00	0.00	0.00	0.03	35.01	99.60	**54.35**	*(1.80)*

*Olivine is medium- to coarse-grained, rounded, and anhedral.
**Olivine is fine-grained, equigranular, and polygonal.

Table 21. Results of EMPA analyses of plagioclase from select drill core samples. Listed compositions are the average of *n* analyses per sample. All values are in wt.% except for %An = 100*Ca/(Ca+Na+K).

Stratigraphic Depth (m)	Sample	*n*	K_2O	CaO	Al_2O_3	FeO	MgO	MnO	TiO_2	Cr_2O_3	Na_2O	SiO_2	Total	% An avg	% An std
9.58	MA14-2D	4	0.06	13.22	31.05	0.10	0.00	0.01	0.01	0.00	4.11	51.43	100.01	**63.75**	*(2.76)*
69.47	MA14-8A-a	3	0.04	13.17	30.87	0.10	0.00	0.01	0.01	0.00	4.13	51.53	99.87	**63.67**	*(0.54)*
244.72	MA11-2	3	0.03	12.30	30.12	0.10	0.00	0.00	0.00	0.01	4.57	52.60	99.73	**59.72**	*(3.49)*
251.07	MA03-6	4	0.02	13.64	31.41	0.10	0.00	0.00	0.04	0.01	3.86	50.83	99.91	**66.02**	*(0.74)*
261.39	MA03-3	4	0.03	13.22	31.02	0.05	0.00	0.01	0.00	0.00	4.02	51.27	99.61	**64.43**	*(2.16)*
281.37	MA03-2	4	0.04	12.96	30.77	0.03	0.00	0.00	0.00	0.00	4.21	51.75	99.76	**62.87**	*(2.48)*
282.46	MA03-1B	3	0.02	13.50	31.10	0.22	0.04	0.01	0.00	0.01	3.84	51.04	99.78	**65.91**	*(1.02)*
282.53	MA03-1A	3	0.02	13.55	31.08	0.18	0.02	0.00	0.01	0.01	3.86	51.03	99.75	**65.91**	*(3.85)*

7 DISCUSSION

The primary concentration of any trace element in a mineral in igneous rocks is dependent on (1) the partition coefficient of the element into the mineral in question ($D^{mineral/melt}$); (2) its concentration in the parental magma, which will evolve with differentiation according to its bulk partition coefficient (K_D) into the crystallizing mineral assemblages; and (3) co-crystallizing minerals and the paragenetic sequence in which they saturate from the melt, which itself is dependent on physical conditions such as temperature, pressure, oxygen fugacity (fO_2), and H_2O content of the melt (Snyder et al., 1993; Toplis and Carroll, 1995; Toplis and Corgne, 2002; Botcharnikov et al., 2008; Dare et al., 2012). Systematic cryptic trends in layered intrusions, including those of Fe-Ti oxides, are therefore generally considered to be the result of fractional crystallization and differentiation of the parental magma. In a magma chamber behaving as a closed system (i.e. one that does not experience successive inputs of magma), elements that are highly compatible into Fe-Ti oxides such as Cr ($D_{Cr}^{Mgt} =$ 50-600, $D_{Cr}^{Ilm} =$ 11-40; Leeman et al., 1978; Jensen et al., 1993; Klemme et al., 2006) and V ($D_{V}^{Mgt} =$ 7-34, $D_{V}^{Ilm} =$ 1.4-22; Toplis and Corgne, 2002; Klemme et al., 2006) would be expected to behave compatibly during fractionation of a magma from which these minerals are cumulate phases (i.e. K_D >1). As a result, Cr and V should be most strongly enriched in the most primitive magnetite and ilmenite, and any subsequently crystallizing Fe-Ti oxides will be continuously less-enriched in these elements due to their progressive removal from the residual magma. In a layered intrusion crystallizing from the base upwards, the concentrations of these compatible elements might then be expected to progressively decrease with height. In unmetamorphosed intrusions, sharp changes in cryptic depletion trends are often attributed to injections of more primitive magma that mix with and re-enrich the resident magma in depleted components (Namur et al., 2010;

Song et al., 2013). Alternatively, the development of compositional and thermal gradients within a magma due to fractional crystallization could result in the development of double-diffusive layering (Huppert and Sparks, 1984). In some LMIs, periodic reversals in cryptic depletion trends have been attributed to the differentiation of such layers as essentially chemically independent systems (Tegner et al., 2006).

Most trace elements do not exhibit systematic cryptic trends in Fe-Ti oxides across the Iron-T deposit. This includes both Cr and V, which are broadly characterized by several intervals of up-section depletion, each punctuated by cryptic reversals to more primitive compositions (Fig. 17). However, there also appears to be a distinct lithological control on the compositions of Fe-Ti oxides. For example, Cr and V are consistently enriched in magnetite and ilmenite in disseminated gabbros – and especially in the trace amounts of ilmenite present in several leucogabbros – relative to massive oxides and ultramafic rocks (Figs. 16, 17). Yet, elements such as Ni, Co, and Mg, which are also compatible into magnetite in silicate magmas ($D_{Ni}^{Mgt} =$ 20-80; $D_{Co}^{Mgt} =$ 5-20; $D_{Mg}^{Mgt} =$ 1-3.5; Toplis and Corgne, 2002) and would thus be expected to behave in a similar manner to Cr and V, are comparatively depleted in most disseminated gabbros. This is reflected in their chemostratigraphic trends, which notably differ from those of Cr and V, and from each other (Fig. 17). These deviations from expected trends suggest that the chemical compositions of Fe-Ti oxides in the RBC may have been modified from their primary igneous compositions. Fe-Ti oxides are known to be susceptible to sub-solidus intergranular re-equilibration during the initial cooling of the intrusion, particularly with ferromagnesian silicates (Frost, 1991). However, the rocks of the RBC have also been metamorphosed, and magnetite consequently exhibits some degree of alteration or replacement in many of the samples analyzed in this study (Fig. 11). It is therefore possible that the chemical compositions of Fe-Ti oxides

have been modified by either sub-solidus re-equilibration or metamorphic reactions, or both. Any attempt to use the chemistries of magnetite and ilmenite to study the petrogenesis of V deposits in the RBC necessarily requires knowledge of their primary igneous compositions. Therefore, in the following discussion we first examine which trace elements are reliable tracers of magmatic processes, and which may have had their primary concentrations in Fe-Ti oxides modified by secondary processes.

7.1 Modification of primary Fe-Ti oxide compositions

7.1.1 Post-cumulus modification of Fe-Ti oxide compositions

Alteration of a mineral's primary chemical composition can occur through several modes of 'diffusive modification', a term used by Tanner et al. (2014) to describe the diffusive interchange occurring either between compositional zones within a mineral, or between a mineral and the adjacent media (i.e. melts, minerals, or volatile-rich fluids) as they attempt to attain equilibrium. Even in unmetamorphosed layered intrusions, it is becoming increasingly recognized that the effects of such processes must be understood before cryptic trends can be used to trace differentiation histories of a magma. In the Bushveld Complex, for example, both the 'trapped liquid shift', i.e. the reaction of cumulate minerals with an evolved intercumulate liquid, and subsolidus intercrystal re-equilibration during prolonged cooling of the intrusion have been identified as important modifiers of the trace element chemistries of cumulate minerals (Cawthorn, 2007; Tanner et al., 2014). While these studies on the Bushveld have primarily focused on the importance of diffusive modification in silicate minerals, recent studies have shown that they may also affect cumulate apatite compositions (Cawthorn, 2013). Thus, there is

no reason to think that similar processes could not have also modified the compositions of Fe-Ti oxides in the RBC.

Unlike the Bushveld Complex, however, the geology of the RBC is complicated by its history of metamorphism at greenschist-amphibolite facies conditions. It is therefore reasonable to expect that diffusive modification of cumulate Fe-Ti oxides could also take place during periods of elevated temperatures associated with such events. One of the characteristics of mafic rocks metamorphosed up to amphibolite facies are the continuous changes in mineral compositions that are associated with prograde reactions between coexisting phases such as plagioclase, epidote, chlorite, and the calcic-amphiboles, actinolite and hornblende (Liou et al., 1974; Apted and Liou, 1983; Maruyama et al., 1983). However, most experiments that have studied phase equilibria of metabasites begin with starting materials of basaltic glass, and ilmenite or Ti-poor magnetite are typically only minor constituents of the resulting mineral parageneses. Therefore, the effects of prograde metamorphism on the chemistries of primary Fe-Ti oxides, and particularly on their trace element compositions, are relatively unknown. All of the samples from the RBC analyzed in this study have, to the best of our knowledge, experienced the same metamorphic histories, and therefore it is not possible to comment on the systematics of any potential prograde compositional changes. However, the replacement of magnetite to varying degrees by Fe-Mg-Al silicates in many of these rocks (Fig. 11) is strong evidence that it is unstable during metamorphism. It is therefore important to consider whether this textural alteration that is associated with metamorphic reactions is accompanied by chemical modification of the Fe-Ti oxides.

One challenge in determining whether diffusive modification of Fe-Ti oxides occurs during metamorphism, however, is distinguishing such modifications from those which may

have taken place during the initial cooling of the intrusion, prior to metamorphism. It is widely accepted that Fe-Ti oxides are susceptible to subsolidus re-equilibration with Fe-Mg silicates such as olivine and pyroxenes in igneous cumulates (Frost, 1991). This predominantly involves the exchange of Mg and Fe^{2+} between magnetite or ilmenite and the silicate phase, which for an ideal scenario involving re-equilibration with olivine proceeds as follows:

$$2MgFe_2O_4 \textit{ (in magnetite)} + Fe_2SiO_4 \textit{ (in olivine)} = 2Fe_3O_4 + Mg_2SiO_4 \textit{ (in olivine)}$$

$$2MgTiO_3 \textit{ (in ilmenite)} + Fe_2SiO_4 \textit{ (in olivine)} = 2FeTiO_3 + Mg_2SiO_4 \textit{ (in olivine)}$$

The reactions above proceed to the right as temperatures decrease, thus pushing magnetite and ilmenite towards their end-member compositions while olivine becomes increasingly Mg-rich (Frost, 1991). Equivalent reactions between Fe-Ti oxides and pyroxenes would also result in an increase in the Mg# of the pyroxene. These reactions will also be more strongly promoted with increasing silicate-oxide ratios. Consequently, Fe-Ti oxides from disseminated layers in LMIs such as the Bushveld Complex and the Panzhihua intrusion, China - both of which have no pronounced history of metamorphism - are generally less Mg-rich than are those from massive oxide layers in these same intrusions (Klemm et al., 1985; Von Gruenewaldt et al., 1985; Pang et al., 2008a)

In the RBC, it is also true that Fe-Ti oxides from semi-massive and massive oxides are generally more Mg-rich than are those from disseminated samples (Fig. 16). However, among the various disseminated lithologies examined in this study, magnetite and ilmenite hosted by most gabbros, leucogabbros, and pyroxenites (i.e. the most strongly altered lithologies) contain unmistakably lower Mg-concentrations ($Mg_{Mgt,\ Ilm}$ <0.25 wt.%) than do the less-altered olivine-bearing gabbros (Mg_{Mgt} = 0.3-0.5 wt.%; Mg_{Ilm} = 0.3-1 wt.%). Additionally, of all the samples

classified as leucogabbros in this study, the only two in which ilmenite contains Mg concentrations above 0.1 wt.% are the two sub-lithologies in MA32-18 (sub-lithologies *a* and *c*), both of which are only weakly altered compared to all other leucogabbros. They are also the only two leucogabbros that contain relict magnetite that was coarse enough to be analyzed by LA-ICP-MS. These results suggest that while disseminated samples may have generally experienced more extensive pre-metamorphic subsolidus re-equilibration between Fe-Ti oxides and silicates than did massive or semi-massive oxides, metamorphism further modified the chemistry of oxides hosted by gabbros and pyroxenites

This interpretation is strongly supported by sample MA11-2 and the compositional differences that exist between unaltered Fe-Ti oxides within the massive oxide layer at 245 m, and grains from its texturally altered basal contact (Figs. 20, 21). The strongly Mg-depleted nature of the altered grains relative to unaltered ones less than 3 cm above is unlikely to be the result of pre-metamorphic re-equilibration with cumulate Fe-Mg silicates in the underlying leucogabbro. This is because although the basal contact of the massive layer is now lined with metamorphic minerals (principally acicular actinolite), the now-altered oxides appear to have been predominantly in contact with plagioclase (Fig. 11k). No prior studies have identified that any substantial re-equilibration of Mg occurs between Fe-Ti oxides and plagioclase. Butcher and Merkle (1987) found that in the Bushveld Complex, the margins of magnetite grains that are in contact with plagioclase are occasionally depleted in Mg and Al relative to their cores; however, they attributed this to either the reaction of magnetite with intercumulus liquid or the migration of aluminous exsolutions (i.e. pleonaste, corundum) to grain boundaries, rather than re-equilibration with plagioclase. Furthermore, it is likely that any diffusive exchange of Mg would proceed against the primary concentration gradient between plagioclase and Fe-Ti oxides, further

enriching the latter. This is because Mg is more compatible in magnetite (D_{Mg}^{Mgt} = 1-3.5; Toplis and Corgne, 2002) and ilmenite (D_{Mg}^{Ilm} = 1.3-1.5; Charlier et al., 2007) than in plagioclase (D_{Mg}^{Plag} = 0.04; Aigner-Torres et al., 2007), and elemental diffusion is partially dependent on the relative compatibility of an element between two minerals (Meurer and Boudreau, 1996; Nex et al., 2002; Tanner et al., 2014).

The differences in the chemistries of the two textural varieties of Fe-Ti oxides in MA11-2 are also unlikely to reflect their primary compositions. While the chemical compositions of magnetite and ilmenite could presumably vary with depth within a massive oxide layer, such a large discrepancy in the Mg-contents of the two zones (altered oxides are depleted in Mg by approximately 80 percent relative to unaltered grains) over less than 3 cm cannot be realistically attributed to differentiation. Moreover, the concentrations of elements compatible in Fe-Ti oxides would be expected to decrease upwards within a massive band, as McCarthy and Cawthorn (1983) observed in the Cr contents of magnetite across the Main Magnetite Layer of the Bushveld Complex. However, in MA11-2, Mg is strongly enriched in the upper of the two domains within the sample. Additionally, Cr concentrations of both magnetite and ilmenite in this sample are essentially identical between the altered and unaltered grains (Figs. 20, 21).

Metamorphic alteration of magnetite in silicate-rich host rocks therefore appears to promote the removal of Mg from Fe-Ti oxides, presumably related to the formation of metamorphic Fe-Mg-Al silicates such as chlorite and Ca-amphiboles. If all of the compositional differences between the altered and unaltered oxides in MA11-2 can then be attributed to re-equilibration during metamorphism, then this Mg-loss during alteration of magnetite is accompanied by the removal of other divalent cations such as Ni and Co, albeit less

pronouncedly (Fig. 20). These elements are also expelled from primary ilmenite, along with high field strength elements (HFSE) such as Zr, Hf, and Nb, even though ilmenite is otherwise texturally unaltered in these rocks (Fig. 21). Additionally, magnetite appears to become further enriched in Zn. On the other hand, Cr, V, Mn, Ga, Sc, and Al all appear to have undergone no substantial oxide-silicate re-equilibration in the altered oxides of MA11-2 during metamorphism. We also note that re-equilibration between Fe-Ti oxides and sulfides (predominantly chalcopyrite and pyrrhotite, with minor pentlandite and violarite) in these rocks is presumably inconsequential, due to the small amounts of sulfides (typically <2%) that are present in all of the analyzed samples.

Invoking compositional modification of Fe-Ti oxides due to metamorphism helps explain much of the erratic chemostratigraphic behaviour that many elements exhibit across the Iron-T deposit (Fig. 17). Variable degrees of modification between grains could also explain why intra-sample compositional variations are occasionally quite large. The effects of diffusive modification on cryptic trends are most apparent for Ni, Co, Mg, Zr, and Hf in gabbros and leucogabbros, which, in conjunction with the depleted nature of altered oxides in contact with the leucogabbro in MA11-2, suggests that such metamorphic re-equilibration processes are ubiquitous in plagioclase-rich protoliths. However, it is unclear by examining chemostratigraphic trends alone whether these elements have similarly re-equilibrated in lithologies where plagioclase is not present. For example, although Mg is also consistently depleted in both magnetite and ilmenite in disseminated pyroxenites, Ni, Co, Zr, and Hf all show no obvious evidence of depletion, relative to other samples at similar depths, in any lithologies other than gabbros (Fig. 17). There are three potential reasons why this may be: 1) certain trace elements are susceptible to diffusion in altered gabbros but not pyroxenites, and their concentrations in Fe-

Ti oxides of the latter accurately reflect their primary abundances; 2) their primary concentrations in pyroxenites were slightly greater than they are currently, and were modified by re-equilibration but to a lesser degree than occurred in gabbros; or 3) their primary concentrations in pyroxenites were initially much greater than in gabbros, and similar magnitudes of re-equilibration have affected both lithologies.

One means of testing which of these reasons explains the cryptic behaviour of Fe-Ti oxides in the RBC is to compare the concentrations of trace elements that partition similarly into magnetite or ilmenite (e.g. elements which both have $D^{mineral/melt} >> 1$), but which seemingly behave differently during oxide-silicate re-equilibration. In a system in which no rocks have experienced re-equilibration between Fe-Ti oxides and silicates, the concentrations of these elements in magnetite should be well-correlated, regardless of rock type, since inter-sample variations would presumably solely reflect the differentiation of the parent magma. However, if one of the elements is susceptible to diffusive modification during cooling and/or metamorphism but the other is not, then the former's concentrations in altered disseminated lithologies should deviate from the differentiation trend of massive/semi-massive oxides, where re-equilibration would be less pronounced due to the lower proportion of silicates-to-oxides, and unaltered rocks. Additionally, if the diffusion of an element is favoured in one disseminated lithology over another (e.g. gabbros versus pyroxenites), the magnitude of this deviation will be different in each case.

To test this, we plotted a series of binary diagrams comparing the V, Ni, Co, and Zn contents of magnetite with their corresponding Cr concentrations, according to lithology and oxide content (Fig. 23). All of these elements are strongly compatible into magnetite (Dare et al., 2014) and should therefore exhibit positively-correlated differentiation trends with Cr if the

rocks were unmodified, with the slope of the trend varying according to their respective partition coefficients. Comparing Cr and V (Fig. 23a), neither of which appear to be susceptible to silicate-oxide diffusion (Fig. 20), there are no consistent deviations from the depletion trend that are suggestive of any processes other than magmatic differentiation. However, both Ni and Co (Fig. 23b-c) in gabbros are negatively offset from their 'unmodified' trends, which are defined by massive/semi-massive samples and unaltered olivine gabbros, as is expected. In contrast, Zn, which apparently becomes enriched in magnetite during metamorphism (Fig. 20), is positively offset (Fig. 23d). Pyroxenites, however, are more ambiguous. Their Ni-Cr values tend to plot intermediately between the unmodified trend and those of gabbros, whereas they are depleted in Co, and enriched in Zn, to similar degrees as gabbros.

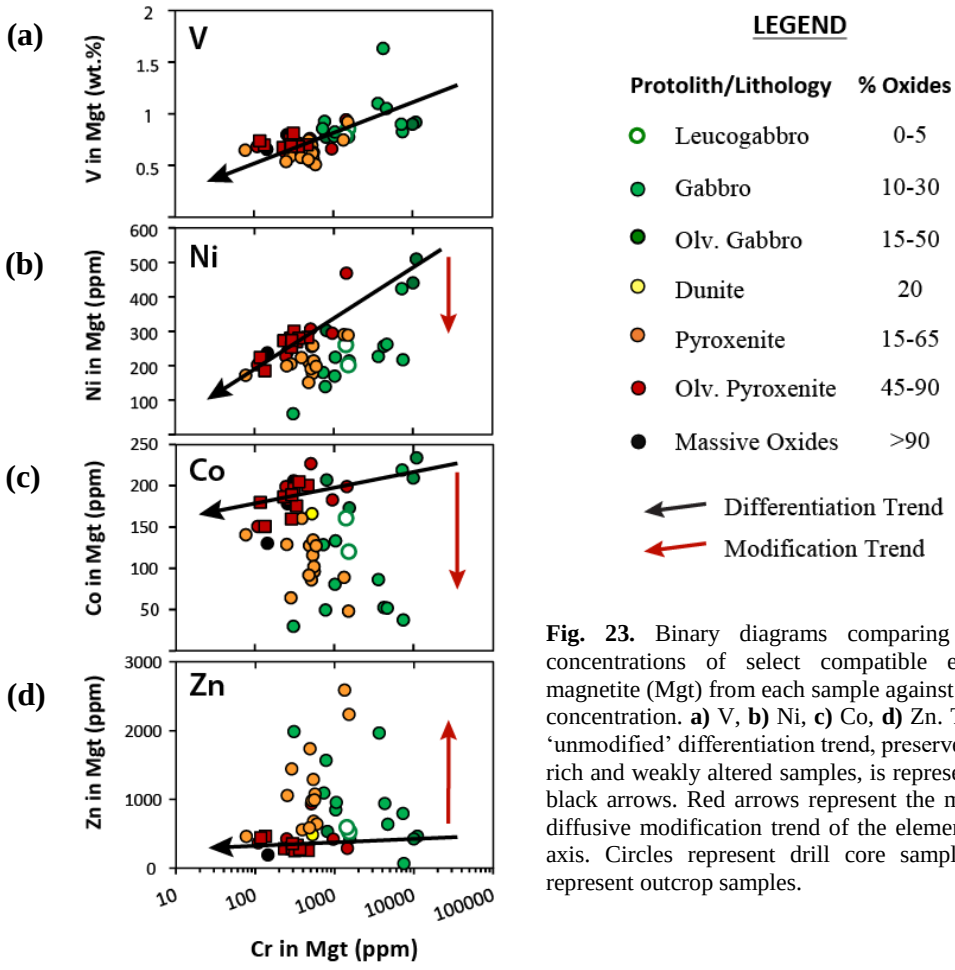

Fig. 23. Binary diagrams comparing the mean concentrations of select compatible elements in magnetite (Mgt) from each sample against its mean Cr concentration. **a)** V, **b)** Ni, **c)** Co, **d)** Zn. The primary 'unmodified' differentiation trend, preserved by oxide-rich and weakly altered samples, is represented by the black arrows. Red arrows represent the metamorphic diffusive modification trend of the element on the y-axis. Circles represent drill core samples; squares represent outcrop samples.

The different magnitudes of the deviations from the unmodified Ni-Cr trend exhibited by gabbros and pyroxenites in Fig. 23 suggests that diffusive modification of certain trace elements in Fe-Ti oxides during metamorphism may do so to varying degrees depending on the lithology of the protolith. This is potentially a consequence of the different metamorphic mineral assemblages characteristic of gabbros and pyroxenites in this study with which Fe-Ti oxides may re-equilibrate, and which themselves are inherently dependent on bulk composition. Gabbros and leucogabbros are generally comprised of the transitional greenschist-amphibolite facies silicate assemblage of plagioclase + hornblende ± actinolite ± chlorite ± epidote (Table 4). In contrast, the dominant amphibole in pyroxenites is actinolite, presumably due to the lack of Al in the bulk-rock composition to facilitate the widespread conversion to aluminous hornblende. As noted above, diffusion is partially dependent on the natural affinity of an element between co-existing minerals (i.e. its partitioning behaviour during fractionation). Diffusive modification of trace elements between Fe-Ti oxides and amphiboles during metamorphism may therefore be more strongly promoted by the presence of hornblende over actinolite.

As discussed above, the trivalent cations Cr, V, Sc, Ga, and Al, along with the divalent Mn, are the only elements that were seemingly unsusceptible to diffusive modification in the now altered oxides of MA11-2 during metamorphism. However, it is noteworthy that the dominant amphibole associated with the contact between the massive oxide layer and underlying leucogabbro in MA11-2 is actinolite (Fig. 11k), whereas most other altered gabbros and leucogabbros contain abundant hornblende (e.g. Figs. 9f, 11g). The prograde conversion of the intrinsically Al-poor actinolite to hornblende necessarily requires an influx of Al via several coupled substitutions, typically achieved in metabasites during reactions with plagioclase (Spear, 1981; Schumacher, 2007). However, in many pyroxenites in this study, small amounts of dark

green hornblende are observed on the margins of pseudomorphs of actinolite after clinopyroxene where they are in contact with Fe-Ti oxides (Fig. 9d). These textures suggest that reactions between actinolite and Fe-Ti oxides are facilitating the exchange of Al and the conversion of actinolite to hornblende. Consequently, there may be reason to doubt that the Al contents of Fe-Ti oxides as determined in this study are entirely representative of their primary concentrations. This may explain some of the scatter in Al results that are observed in Figs. 16 and 17, particularly in gabbros. Additionally, Sc and Ga readily substitute for octahedrally-coordinated Al in the amphibole crystal structure, as evidenced by the synthesis of Sc- and Ga-rich end-members of pargasite by Raudsepp et al. (1991). It is therefore possible that these elements also re-equilibrate between Fe-Ti oxides and amphiboles during hornblende-forming reactions, potentially explaining why they also commonly appear depleted in oxides hosted by hornblende-rich gabbros and leucogabbros (Fig. 17), despite not appearing to have had their concentrations modified in oxides from the texturally altered portion of sample MA11-2.

It should be noted that the reasons for why some elements re-equilibrate during metamorphism and others do not, or likewise why certain elements may diffuse more readily in certain protoliths than others, are largely speculation at this point. Data on diffusion behaviour in magnetite exist for only a few cations (Fe, Ti, Cr, Co, Ni, Mn, and Al; Van Orman and Crispin, 2010), and virtually none exists for ilmenite. Furthermore, elements diffuse at different rates in different minerals, and these rates are complicated functions of several variables, including the diffusion coefficient of the element for the given mineral, temperature, oxygen fugacity, crystallographic diffusion pathways, the compositions of the two minerals and the concentration gradient between them, and their respective partition coefficients (Chakraborty, 2008). Most of these variables are unknown with the present dataset. However, cations with lower charges and

smaller atomic radii are generally more susceptible to diffusion than larger cations with higher charge (Brady and Cherniak, 2010), which may partially explain why divalent cations like Mg, Ni, and Co appear to more readily re-equilibrate in Fe-Ti oxides than do trivalent cations like Cr and V. Notably, the consistently lower Zr and Hf concentrations of ilmenite in altered gabbros would seem to contradict this generalization, as both are tetravalent. However, zircon and baddeleyite coronas around ilmenite have been documented in several other mafic intrusions, attributed to the exsolution and reaction of Zr with surrounding silicates during cooling (Charlier et al., 2007; Morriset and Scoates, 2008). It is therefore possible that Zr and other HFSE that substitute for Ti^{4+} in the octahedral site of ilmenite (Pearce, 1990) were similarly exsolved from ilmenite in the RBC at elevated temperatures during cooling or metamorphism. No zircon or baddeleyite was explicitly observed in our samples, although bright, exsolution-free rims on the margins of magnetite are often observed along shared grained boundaries with primary ilmenite in BSE images (e.g. Fig. 10f). Routine EDS analyses of several of these rims indicates that at least some are Ti-poor magnetite, from which we interpret that Ti had diffused from the original titaniferous magnetite into ilmenite during subsolidus re-equilibration. However, only a small number of these rims were analyzed by EDS, and it is therefore possible that some zircon rims were present in our samples that were not documented. Further study of trace element diffusion and the metamorphic phase relations of Fe-Ti oxide-rich mafic rocks is needed before more definitive interpretations can be made from these results.

7.1.2 Trapped liquid shift

Based on the above discussion, Cr and V are among the only trace elements that we can say with reasonable confidence have not had their concentrations in Fe-Ti oxides modified by sub-solidus

re-equilibration during metamorphism. However, in addition to modification by intergranular re-equilibration, the compositions of cumulate minerals can also be modified by reaction with a depleted intercumulus liquid, referred to as the trapped liquid shift (TLS) (Barnes et al., 1986). Significantly, a recent study of the Tellness Fe-Ti deposit in Norway identified that the TLS can reduce the Cr content of primary cumulate ilmenite by up to 20 percent (Charlier et al., 2007). It is therefore necessary to consider whether such processes have affected the compositions of Fe-Ti oxides in the Iron-T deposit.

Calculating the magnitude of the TLS in any sample typically requires knowledge of its bulk-rock composition, which were not analyzed in this study, and the proportions of intercumulus minerals, which are undeterminable due to the highly-altered nature of most of the rocks in the RBC. Therefore, with the available data it is not possible to quantify any potential TLS in our samples. However, we argue that compared to cryptic variations that are observed at a deposit-scale across the Iron-T deposit, the effects of any TLS would presumably have little influence on any interpretations of magmatic processes. In the Tellness deposit it was determined that the TLS occurred to the greatest degree in the most primitive cumulates, i.e. those in which the Cr contents of ilmenite were greatest, where a trapped liquid fraction of 54 percent resulted in a 20 percent reduction in the Cr content of primary ilmenite (Charlier et al., 2007). The relative magnitude of the TLS then progressively decreased in more evolved cumulates. If we suppose that a similar 20 percent decrease in Cr occurred in the most primitive magnetite of the Iron-T deposit (MA03-1A and -1B, each with ~1 wt.% Cr), then the initial cumulate magnetite could have contained up to 1.2 wt.% Cr. Since this magnetite occurs at the very base of our composite stratigraphic profile, if we also assume that the TLS would be less pronounced at all shallower depths (i.e. in theoretically more evolved cumulates), then there will be very little

change in the overall cryptic trends of magnetite, since Cr_{Mgt} spans more than two orders of magnitude in our study (Fig. 17). Additionally, since Cr is the most compatible element in Fe-Ti oxides, the difference in its concentration between cumulate oxides and a depleted trapped liquid would be greater than for all other trace elements. The trapped liquid shift will therefore modify the concentrations of elements like V less than it will Cr, meaning the stratigraphic trends of V in Fig. 17 would also probably not change much. Any modification of Fe-Ti oxide chemistry by the TLS is thus presumed to be insignificant for the purposes of this study, since tracing the differentiation history of a magma chamber relies more heavily on broad chemostratigraphic trends than on absolute trace element concentrations in any given sample.

7.1.3 Effect of exsolutions on the trace element chemistry of magnetite

It is also important to consider the presence of exsolutions within Fe-Ti oxides and the effect they may have on the distribution of trace elements within the grain when analyzing and interpreting mineral chemistry data. The development of exsolutions may lead to the local concentration of certain trace elements in either the host or the exsolved phase, essentially through intra-oxide re-equilibration (Frost, 1991). For instance, Fig. 14 clearly indicates that in magnetite, the sequestration of Ti in ilmenite oxy-exsolutions is strongly accompanied by Mn, while Fig. 20 suggests that Sc and Zr also behave similarly. In contrast, V and Cr become concentrated in the host magnetite (Cawthorn et al., 1983; Taner et al., 1998). Care was taken to include representative amounts of lamellar or composite-style exsolutions during LA-ICP-MS analyses of magnetite and ilmenite to account for these discrepancies, and the internal standard Fe value of magnetite was corrected accordingly, as outlined in section 5. However, it is important to note that granule-style ilmenite exsolutions (section 4.2.1.1) were difficult to

proportionally incorporate during analyses of magnetite, and were generally avoided in most samples. Granule exsolutions are present in most samples in this study, but are most prevalent in strongly altered disseminated gabbros. It is therefore possible that the calculated proportions of ilmenite exsolutions in magnetite from these samples ($X_{exsolution}$) are underestimated, meaning their corrected Fe values (Fe_{Mgt}^{Corr}) are overestimated (Table 13). This may partially explain why magnetite in disseminated gabbros is consistently more Fe-rich than other lithologies (Fig. 13a). Furthermore, since Fe was used as the internal standard for LA-ICP-MS data, if its value is artificially high then this would produce inflated trace element concentrations.

However, granule exsolutions generally make up less than 10 percent of the volume of magnetite in most of the samples examined. Since ilmenite contains approximately half the total Fe as magnetite, an increase in the calculated $X_{exsolution}$ value of magnetite of 10 percent will only result in a relative decrease in our calculated Fe_{Mgt}^{Corr} values – and, by extension, the corresponding sample's trace element concentrations – of about 5 percent. Given the large range in concentrations that Cr and V display in this study, especially at stratigraphic levels associated with sharp depletions or enrichments, a 5 percent change in their concentrations in any given sample will not influence chemostratigraphic trends to any significant extent. Furthermore, ilmenite is also most Fe-rich in disseminated gabbros (Fig. 13b), which suggests that Fe-Ti oxides are inherently more Fe-rich in these lithologies.

The only sample where the omission of exsolutions may have significantly influenced the resultant compositions of magnetite are MA32-25 (approx. 140 m depth, Fig. 17), where metamorphism and deformation has apparently resulted in the sequestration of abundant ilmenite granules into coarse, foliated agglomerations (Fig. 10c). Note that this sample also represents the outlier in V_{Mgt} in Figs. 16 and 23. In MA32-25 the calculated amount of exsolutions ($X_{exsolution}$ =

6%, Table 13) is likely very low, and accordingly the corrected Fe value is the highest of any magnetite in this study (Fe_{Mgt}^{Corr} = 70.5 wt.%). Since magnetite in this sample is also partially replaced, determining the actual amount of exsolutions that the amalgamated ilmenite granules represent is difficult. However, if we assume that they represent a similar amount of exsolutions as the maximum calculated value from the other samples ($X_{exsolution}$ = 30%), then this would result in a significant relative decrease in Fe_{Mgt}^{Corr} of about 13 percent. It is therefore unlikely that the composition of magnetite in MA32-25, as determined in this study, accurately represents its primary chemistry, and should be considered with caution when interpreting cryptic trends.

7.2 Interpretation of Fe-Ti oxide cryptic trends

Despite the compositional modifications of magnetite and ilmenite that have evidently occurred in the RBC, our results suggest that their Cr and V concentrations are representative of their primary igneous compositions, and therefore remain valid tracers of magma differentiation. This is beneficial for our objective of determining the petrogenetic processes responsible for the formation of the Iron-T deposit, since these elements are highly compatible in Fe-Ti oxides and have been used to trace the magma evolution of other notable LMIs (e.g. Cawthorn and McCarthy, 1980; Klemm et al., 1985; Jang and Naslund, 2003; Tegner et al., 2006; Charlier et al., 2007; Namur et al., 2010). Based on our results, any petrogenetic model must account for several key observations. Most importantly, it must account for the aperiodic, local up-section cryptic depletions and reversals exhibited by both Cr and V in rocks containing >5% Fe-Ti oxides (Fig. 17). Notably, the stratigraphic levels at which these local depletion trends occur ubiquitously coincide with lithostratigraphic changes from Cr-V enriched disseminated gabbros to relatively depleted massive oxides and/or semi-massive oxides in ultramafic hosts. For Cr,

these depleted oxide-rich ultramafic horizons also appear to occur within a broader, deposit-scale depletion trend that is defined by the enriched gabbroic samples in the lower 200 m of the composite stratigraphic profile, and which continues through interlayered disseminated gabbros and pyroxenites in the upper 70 m. Additionally, the model must account for the strongly Cr-V enriched nature of trace ilmenite grains in many leucogabbros.

Fe-Ti oxide mineralization in the upper portions of mafic intrusions is generally attributed to progressive Fe-enrichment of a tholeiitic parental magma (Wager and Brown, 1968). Following sufficient fractional crystallization of silicate-rich rocks, the residual magma becomes saturated in Fe and Ti, at which point magnetite and/or ilmenite become cumulate phases. Classic examples of this include the Skaergaard intrusion in Greenland (McBirney and Noyes, 1979) and the Bushveld Complex in South Africa (Reynolds, 1985). Although deeper levels of the Bushveld were presumably subject to frequent magma injections, the entirety of its 2 km thick, magnetite-rich Upper Zone (UZ) - which is also host to one of the world's most important V deposits in its Main Magnetite Layer – is widely considered to have progressively crystallized in a closed system from a common parent magma (Reynolds et al., 1985b). This conclusion is in part supported by cryptic trends of several cumulus minerals, namely silicates (Ashwal et al., 2005; Tanner et al., 2014), but also magnetite, which becomes progressively depleted in V with height across the UZ (Klemm et al., 1985; Barnes et al., 2004).

More recently, Tegner et al. (2006) identified several cryptic depletion-and-reversal cycles within the kilometers-scale depletion trend of the UZ that range in thickness from 100-500m (Fig. 24). Each of these cycles is in part characterized by more pronounced up-section decreases in the V contents of magnetite, punctuated by abrupt cryptic reversals to more enriched compositions at the base of the overlying cycle (Fig. 24d). Similar compositional cycles have

been documented in other layered intrusions such as the Sept Iles Intrusive Suite in Canada (Fig. 25), where cryptic reversals in the Cr content of magnetite have been attributed to periodic injections of primitive magma (Namur et al., 2010). Tegner et al. (2006), however, concluded that following the crystallization of gabbronorites in the Bushveld's Main Zone, which would have produced a dense residual liquid that would pond at the base of the magma column and create a stable density profile, the UZ magma became stratified as a result of double-diffusive convection instigated by the slower diffusion of major elements relative to heat. Each of these magma layers would then compositionally evolve independently, except for mixing that might occur at layer boundaries as the density of the basal magma equalized with that of the overlying layer due to magnetite crystallization in the former. Magma injections are therefore not necessarily required to produce compositional reversals in layered intrusions.

Previous studies of the RBC have compared its evolution to that of the Bushveld Complex, as they both contain an Fe-Ti oxide-rich layered sequence overlying several kilometers of massive gabbros (Fig. 27) (Maier et al., 1996; Taner et al., 1998). Maier et al. (1996) inferred the tholeiitic nature of the RBC based on compositional similarities in REE patterns to the overlying tholeiitic volcanic rocks of the Wabasee and Watson Lake groups, with which the intrusion is believed to be cogenetic. They also found that the compositions of silicate minerals in layered rocks near the town of Matagami, approximately 15 km west of the Iron-T deposit, were more evolved than those of massive gabbronorites in the underlying Main zone (Table 22), supporting a model of continuous magma differentiation. The cryptic trends in Fe-Ti oxides identified across the Iron-T deposit in this study also show some broad similarities to those of the Bushveld Complex. The manner in which Cr displays intermittent intervals of considerable depletion within a more gradual, deposit-scale depletion trend, at least in all rocks containing

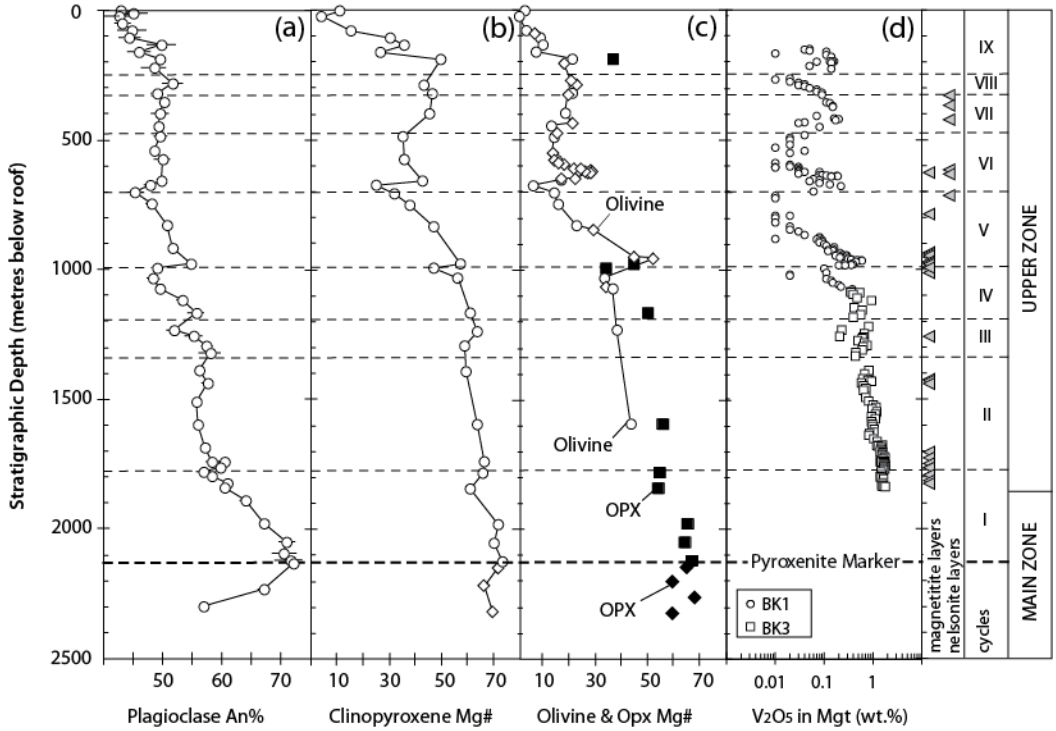

Fig. 24. Compositional stratigraphic variations in the Bierkraal drill cores (BK1 and BK3) from the western limb of the Bushveld Complex. (a) An% of plagioclase; (b) Mg# of clinopyroxene; (c) Fo% of olivine and Mg# of orthopyroxene; and (d) V_2O_5 content of magnetite. Circles and squares indicate data of Tegner et al. (2006); diamonds indicate data of Cawthorn et al. (1991). I-IX represent double-diffusive convection cycles. Dashed lines indicate the boundaries between cycles. Triangles indicate levels at which magnetitite and nelsonite layers occur. Modified from Tegner et al. (2006).

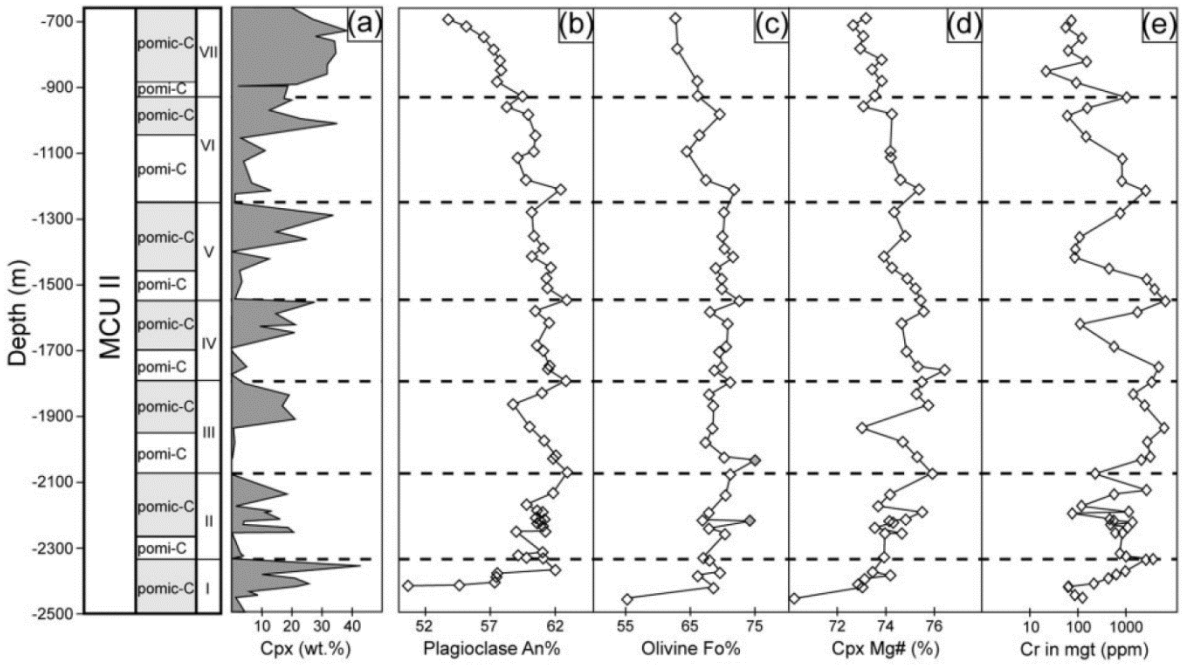

Fig. 25. Modal and compositional stratigraphic variations in the Main Cyclic Unit II (MCU II) of the Sept Iles layered intrusion. (a) Mineral mode of clinopyroxene (cpx); (b) An content of plagioclase; (c) Fo content of olivine; (d) Mg# of clinopyroxene; (e) Cr content of magnetite. I-VII represent the seven cyclic units of the MCU II that are interpreted to be the result of inputs of primitive magma. pomi-C and pomic-C represent cumulate mineral assemblages of plagioclase-olivine-magnetite-ilmenite and plagioclase-olivine-magnetite-ilmenite-clinopyroxene, respectively, following the terminology of Irvine (1982). From Namur et al. (2010).

>5% Fe-Ti oxides (Fig.17), is particularly reminiscent of the V trend observed in the UZ of the Bushveld (Fig. 24d). Although V exhibits no such deposit-scale depletion trend in the RBC, the thickness of the composite profile studied (~300 m) is less than one-quarter the thickness of the UZ, and there are several similarly-thick sections of the Bushveld where V also exhibits comparatively little stratigraphic variation, particularly at deeper levels within the UZ (Barnes et al., 2004; Tegner et al., 2006).

There are, however, several key differences between the RBC and UZ of the Bushveld Complex that strongly suggest they are the products of different petrogenetic processes. The cyclic cryptic trends of the Bushveld identified by Tegner et al. (2006) show no dependence on host rock type, and its monomineralic magnetite layers show no consistent association with any sharp decreases in the V content of magnetite (Fig. 24). In fact, several of its magnetitite layers occur at the V-enriched bases of a cycle. Additionally, Klemm et al. (1985) found that throughout the UZ, the Cr content of Bushveld magnetite is, on average, greater in massive layers than it is in disseminated grains in mafic host rocks. This strongly contrasts with our findings in the RBC, in which Fe-Ti oxides from massive oxide layers are among the most depleted in Cr. Our results therefore argue against a Bushveld-like model invoking double-diffusive convection as the mechanism responsible for the irregular cryptic trends of Fe-Ti oxides in the RBC.

The RBC is also distinguished from the Bushveld on a lithological basis, due to the presence of oxide-rich ultramafic rocks in its upper layered zone. Ultramafic rocks are common in layered intrusions, however in large intrusions they typically occur at lower structural levels, since progressive differentiation produces compositionally evolved residual magmas that ultimately crystallize mafic rocks in the upper levels. Accordingly, apart from its more than

twenty magnetitite layers, the UZ of the Bushveld Complex is comprised of olivine- and non-olivine bearing gabbronorites, diorites, and anorthosites with disseminated magnetite (Cawthorn et al., 2015). As discussed above, Maier et al. (1996) proposed a similar model of closed system differentiation to describe the evolution of the RBC. They also extended this model to suggest that the massive gabbros of the Main zone were themselves underlain by a hidden ultramafic sequence (Fig. 27) – possibly represented by Central Zone of the RBC mapped by Goutier (2005) (Fig. 2a). The layered rocks sampled by Maier et al. (1996), however, were notably collected from outcrops located approximately 15 km west of the region of the RBC sampled in this study, and consisted of no massive oxides or rocks containing ultramafic silicate mineralogies. Thus, the presence of abundant Fe-Ti oxide-rich pyroxenites, olivine pyroxenites, and rare dunites in this more-eastern portion of the RBC's layered series must be taken into account when considering its formation. Determining the mode of origin of these ultramafic-massive oxide sequences may be key in interpreting the observed cryptic trends.

7.2.1 Models for the formation of Fe-Ti oxide layers

The mechanisms involved in the development of layering in igneous intrusions are highly debated. The formation of predominantly Fe-Ti oxide layers is no exception, as this intrinsically requires either in-situ crystallization of large amounts of magnetite and/or ilmenite, or their physical separation from co-crystallizing minerals. In-situ crystallization of abundant Fe-Ti oxides could be attributed to changes in intensive parameters of the magma (e.g. oxygen fugacity, temperature, pressure, composition), potentially as a result of magma additions, such that phase stability fields shift and oxide-crystallization is promoted (Namur et al., 2015 and references therein). However, many of the layering textures observed in the RBC are broadly

similar to those observed in other LMIs that have been attributed to dynamic processes, examples of which include crystal settling, the physical separation of an immiscible Fe-rich liquid, or sorting of cumulate minerals in a flowing crystal slurry (see reviews by Reynolds, 1985b; Maier et al., 2013). It is therefore of interest to examine whether any of these models are applicable to the oxide-rich ultramafic horizons found in the RBC.

7.2.1.1 Crystal settling

The crystallization of rocks containing Fe-Ti oxides alongside primarily olivine and pyroxenes may occur due to crystal fractionation and sorting. In dry ferrobasaltic magma, the sequence in which minerals crystallize with decreasing temperature is generally olivine + plagioclase, followed by clinopyroxene, and finally magnetite and/or ilmenite. The order in which the Fe-Ti oxide minerals crystallize strongly depends on oxygen fugacity, with magnetite crystallizing before ilmenite, and in greater cotectic proportions, at fO_2 conditions at or above the quartz-fayalite-magnetite (QFM) redox buffer (Toplis and Carroll, 1995). Segregation of cumulate minerals within the magma via density sorting could then result in the accumulation of oxides, olivine, and clinopyroxene at the chamber floor, while the less dense plagioclase floats to the top of the fluid column (Namur et al., 2015).

Density-driven segregation of Fe-Ti oxides and ferromagnesian minerals could also be theoretically enhanced if the magma is sufficiently water-rich. The presence of water in ferrobasaltic magma systematically depresses the temperature at which plagioclase crystallizes, whereas it has almost no effect on the temperatures at which Fe-Ti oxides crystallize. As a result, a magma with sufficiently high water content (typically above 3 wt.% H_2O) at optimal fO_2

conditions can crystallize assemblages of olivine + clinopyroxene + magnetite (Botcharnikov et al., 2008; Howarth and Prevac, 2013). If this were the case in the RBC, it could potentially explain the presence of such prominent ultramafic horizons, when they are seldom observed in the upper levels of other large mafic intrusions. However, suggesting that the RBC crystallized from a wet parental magma contradicts the prevalence of Fe-Ti oxides in the upper portions of the intrusion. Magmatic H_2O leads to early crystallization of spinel minerals (such as magnetite) in basaltic magma, thus promoting calc-alkaline differentiation trends without Fe-enrichment (Sisson and Grove, 1993). We would therefore not expect the residual magma that formed the upper layered series of the RBC to be sufficiently enriched in Fe as is required to crystallize Fe-Ti oxides.

In the RBC, there is field evidence of crystal settling in the form of cyclic phase layering in outcrop T3 (Fig. 4). Massive oxide layers intersected by drill cores also occasionally display diffuse upper contacts due to normal modal grading of Fe-Ti oxides (Fig. 5c). However, layers of various lithologies also frequently exhibit well-defined upper contacts, with no internal grading (Fig. 5a, b). Particularly in outcrop TA, almost all of the closely spaced, centimeters-thick oxide bands have quite sharp upper contacts with interlayered pyroxenite (Fig. 6). Crystal fractionation and density sorting has been regarded by other authors as an implausible mechanism of forming such sharply defined oxide layers, due to the high yield strength of basaltic magma which prevents the segregation of small magnetite crystals (McBirney and Noyes, 1979; Maier et al., 2013). It has been proposed that a magma could be abruptly pushed into the Fe-Ti oxide stability field by sudden changes in oxygen fugacity (Ulmer, 1969) or pressure (Cawthorn and Ashwal, 2009), thus requiring relatively small degrees of settling. However, Toplis and Carroll (1996) determined that the maximum cotectic proportion of magnetite in dry ferrobasaltic magma is

only about 45 percent in systems open to oxygen, and even less in systems closed to it. Therefore, appreciable crystal sorting would still presumably be required to segregate the amounts of Fe-Ti oxides necessary to form the semi-massive and massive layers in the RBC. Furthermore, simple crystal fractionation and vertical settling cannot adequately account for the variable thicknesses and lateral continuity of many layers. We therefore conclude that a mechanism supplementary to gravitationally-driven crystal settling is necessary to completely model the formation of oxide-layering in the Iron-T deposit.

7.2.1.2 Liquid immiscibility

Liquid immiscibility is a commonly proposed model for the development of layering in igneous intrusions. Immiscible silicate and Fe-oxide liquids have been produced in several studies (e.g. Philpotts, 1967; Roedder, 1987; Tollari et al., 2006), and early interpretations of the Panzhihua intrusion were that its Fe-Ti-V orebodies crystallized from an immiscible Fe-oxide liquid (Zhou et al., 2005). However, there is great deal of experimental evidence that does not support large-scale immiscibility in mafic intrusions. The aforementioned studies that experimentally produced immiscible Fe-oxide liquids did so using starting liquid compositions very different to those typically observed in nature, whereas in natural basaltic systems, magnetite and ilmenite generally crystallize before the magma becomes saturated in an Fe-oxide liquid (Toplis and Carroll, 1995, 1996; Tollari et al., 2006). Cawthorn and Ashwal (2009) also argued that if such an Fe-oxide liquid were to form, it would percolate into interstitial spaces in the underlying cumulates, rather than form planar layers with sharp basal contacts, such as those observed in the RBC. Alternatively, immiscibility between Fe-rich and Fe-poor silicate liquids has been identified in the Skaergaard and Sept Iles intrusions, based on the presence of contrasting Fe-rich

and Si-rich melt inclusions in apatite and olivine in the upper portions of their stratigraphy (Jakobsen et al., 2005; Charlier et al., 2011; Namur et al., 2012). However, no such melt inclusions were observed in rocks from the RBC in this study. Therefore, based on the above arguments and lack of any textural evidence of liquid immiscibility in our samples, we conclude that the layered oxide-rich rocks of the RBC did not crystallize from an immiscible Fe-rich liquid.

7.2.1.3 Flowing crystal slurries

Crystal slurries are becoming increasingly recognized to have played important roles in the development of layering in other mafic intrusions (Irvine et al., 1998; Maier et al., 2013). In the Bushveld Complex, subsidence-driven slumping of partially crystalline magma has been cited as a means of promoting increased sorting of cumulate minerals along the base of the magma chamber (Maier et al., 2013; Forien et al., 2015). This effectively led to interlayered oxide- (magnetite or chromite) and silicate-dominated rocks that thicken and become increasingly mineralogically distinct in the down-dip direction. Successive flows may also erode the unconsolidated top layer of footwall cumulates, resulting in sharp boundaries between layers. Invoking flow-driven cumulate sorting of crystal slurries in the RBC could explain why we frequently observe such sharply defined, mineralogically sorted layering in outcrops. Down-flow thickening of accumulated Fe-Ti oxide layers (Maier et al., 2013) may also account for why countless massive and semi-massive oxide bands of varying thicknesses are observed in the two outcrops of the RBC that were visited (Figs. 4, 6), but were only rarely encountered in drill cores, despite that fact that MA-10-14 and MA-09-11 are stratigraphically correlative with the outcrops (Fig. 3). Additionally, the manner in which oxide bands deflect around leucocratic

enclaves in outcrop TA (Fig. 7d-e), which Roudaut (2013) interpreted to be autoliths from footwall gabbronorites that were ripped up by magma currents, is very similar to features observed in the Skaergaard intrusion that Irvine et al. (1998) attributed to density-driven flow of partially crystalline magma around the autoliths at the floor of the magma chamber.

Layering textures in the RBC therefore appear to strongly support a genetic model wherein dynamic flow of crystal slurries played a significant role in the development of its oxide-rich layered series. However, if this is the case then two considerations need to be made. First, what caused these flowing slurries to develop within the intrusion? And second, can this interpretation account for the observed geochemical trends of Fe-Ti oxides? Crystal slurries in the Skaergaard intrusion are believed to have initially formed through fractional crystallization along the ceiling and walls of the magma chamber (Irvine et al., 1998). Crystal-liquid mixtures then flowed downwards due to gravity, spreading out along the base of the magma chamber and forming modally sorted layers that are now part of intrusion's Layered Series. Cross-stratified layering also developed due to alternating episodes of deposition and differential erosion of semi-consolidated cumulates (Irvine et al., 1998). In the Bushveld Complex, central subsidence of its enormous magma chamber due to crustal loading during magma emplacement may have triggered downslope slumping of semi-consolidated cumulates, in the process producing its massive magnetite seams and interlayered silicate-rich rocks (Maier et al., 2013). A key factor in both of these models, though, is neither intrusion appears to have necessarily required magma injections as the driving force behind the flow of crystal slurries. In both cases, currents were driven by gravitational instabilities along the walls or dipping floor of the partially crystalline magma chamber. This is supported geochemically for the UZ of the Bushveld as discussed above, and throughout the Skaergaard there are no significant changes in either cumulate

mineralogy or the trace element chemistry of ilmenite that are suggestive of magma replenishment (Jang and Naslund, 2003).

In many other layered intrusions, however, abrupt changes in chemostratigraphic trends are attributed to injections of magma from an external reservoir that mix with the resident magma. Both the Sept Iles (Namur et al. 2010) and Panzhihua (Pang et al., 2009; Song et al., 2013) intrusions are believed to have been subject to frequent magma injections. The Panzhihua intrusion is particularly notable since the intruding magma may have been magnetite-laden. Howarth et al. (2013) proposed that Ti-magnetite primarily crystallized in a deeper-seated staging chamber from an H_2O-rich magma, which then intruded as a magnetite-rich slurry into the resident Panzhihua magma chamber. The dense Fe-Ti oxides then settled to the chamber floor to form its Fe-Ti-V ore bodies. Additionally, although the UZ of the Bushveld Complex is regarded as having crystallized from a common parental magma in a closed system, numerous lithologic and compositional reversals across its Lower and Critical Zones are widely attributed to major replenishments of primitive magma (Maier et al., 2013). Cumulate sorting and ductile deformation of some chromitite layers in the Bushveld has also been attributed to the lateral flow of crystal slurries prompted by these episodic magma replenishments (Maier and Barnes, 2008).

In the RBC, the sharp, aperiodic changes in Fe-Ti oxide chemistry to more evolved compositions that are coincident with lithostratigraphic changes from gabbroic rocks to dominantly ultramafic horizons seem then to be best explained by injections of evolved, relatively Cr- and V-depleted magma. This injecting magma was also likely to have been partially crystalline, with Fe-Ti oxides and ferromagnesian silicates perhaps having crystallized in a deeper-seated staging chamber, and which were then carried as a crystal slurry into the RBC magma chamber. Lateral flow of these slurries during their emplacement would have promoted

density sorting of its cumulate minerals, thus allowing for the separation of large amounts of Fe-Ti oxides and silicate minerals into discrete layers. Frequent successive currents could have partially eroded semi-consolidated footwall cumulates, resulting in the sharp contacts that are frequently observed between closely-spaced layers, as well as being a means of creating the cross-stratified oxide layers that are observed in outcrop T3 (Figs. 7a). This could also explain why plagioclase is not typically associated with the most oxide-rich layers in these ultramafic horizons of the stratigraphy. If it had originally been part of the injected crystal slurries, it would have presumably floated upwards during the sorting of each sequence, and therefore be most susceptible to erosion.

Injections of Fe-Ti oxide-rich crystal slurries also potentially explain the irregular chemostratigraphy across oxide layers sampled from outcrops of the RBC (Fig. 19). Although compositional variations observed at an outcrop-scale are relatively minor, neither the lateral differences nor the up-section increases in Cr that are observed in the closely-spaced oxide layers in outcrop TA would be expected from a system where basal crystallization or gravitational settling were the dominant layer-forming processes (Maier et al., 2013). However, turbulent lateral flow and crystal sorting would presumably not sort minerals by composition, and therefore can account for both of these observations.

7.2.2 Origin of deposit-scale Cr-depletion trend in layered pyroxenite-gabbros

In contrast to the Cr- and V-depleted nature of oxide-rich ultramafic sequences in the lower 200 m of the stratigraphic profile through the Iron-T deposit, disseminated pyroxenite samples in the upper 70 m are typically only slightly depleted relative to interlayered gabbros (Fig. 17). It is

therefore unlikely that these shallower pyroxenites are the product of magma injections. This section of the profile is approximately correlative with outcrop T3 (Fig. 3), which is partially characterized by cyclically-layered sequences with intra-layer phase grading (Fig. 4d). The more-or-less continuous depletion trends in disseminated rocks over the upper 70 m, particularly in Cr, may then be the product of cyclic crystal fractionation and gravitational settling from a ferrogabbroic magma in a locally closed-system. The slightly more Cr- and V-rich nature of disseminated gabbros at these levels are potentially just the result of minor geochemical discrepancies between layers.

Interestingly, however, the slope of the Cr depletion trend over the upper 70 m is also intermittently continuous with that defined by enriched gabbros at deeper stratigraphic levels. This could indicate that all of these samples are genetically related. Although V does not exhibit a similar deposit-scale depletion trend, this may be a consequence of the strong influence of fO_2 on its partitioning behaviour in Fe-Ti oxides. Toplis and Corgne (2002) showed that the magnetite-melt partition coefficient of V is highly sensitive to changes in oxygen fugacity at and above the QFM buffer. This is because V^{3+}, V^{4+}, and V^{5+} exist simultaneously in most magmas, but it is V^{3+} that is preferentially incorporated in magnetite. However, increased oxidation will increase the amounts of V^{4+} and V^{5+} in the melt at the expense of V^{3+}, lowering the effective bulk partition coefficient of V. The high proportion of magnetite to ilmenite in most of our samples (Fig. 8) indicates that the prevailing fO_2 conditions in the RBC were consistently above the QFM buffer (Toplis and Carroll, 1995). However, local fluctuations in fO_2 could occur if magnetite was crystallizing in a system closed to oxygen, as this lowers the Fe^{3+}/Fe^{2+} ratio of the residual melt (Toplis and Carroll, 1996). As a result, internally fluctuating fO_2 may result in V not necessarily exhibiting a consistent depletion trend in Fe-Ti oxides with fractional crystallization due to its

changing compatibility. In contrast, although the partition coefficient of Cr - which in nature predominantly exists in the 2+, 3+, and 6+ oxidation states - is also generally a function of oxygen fugacity, above the QFM buffer it remains relatively consistent for most minerals (Mallmann and O'Neill, 2009). Therefore, with its lower dependence on fO_2, the depletion trend of Cr in Fe-Ti oxides might be expected to better reflect differentiation. If we exclude the possibility that this intermittent deposit-scale Cr trend is simply coincidence, it could then be interpreted that all of the disseminated rocks that constitute the trend are genetically related to a common parent magma.

Such an interpretation, however, raises the question of the timing of the injections that produced the Cr-V depleted oxide-rich ultramafic horizons with respect to the formation of this background trend. For this, we consider two possibilities. First, although the resident RBC magma must have been sufficiently Fe-rich as to crystallize cumulate Fe-Ti oxides, the potentially Fe-Ti oxide-laden injecting magma may have been even more dense. Consequently, the secondary, crystal-laden magmas could have flowed along the temporary floor of the magma chamber and displaced the less dense resident magma upwards, rather than mix with it. This is similar to the model proposed by Cawthorn (2007) to explain drastic changes in the Cr content of orthopyroxene in the Bushveld Complex at the Critical Zone-Main Zone boundary. Minimal magma mixing would then mean that the displaced resident magma would retain most of its original trace element budget, and subsequent cyclic crystallization of layered Fe-Ti oxide-bearing gabbro-pyroxenites would continue the differentiation trend of those beneath the injected horizons. Alternatively, the deposit-scale depletion trend of Cr could be interpreted as having developed prior to the injection of the oxide-rich slurries. This would effectively mean that the Cr-depleted, oxide-rich horizons represent sills into an already crystalline, dominantly

ferrogabbroic column that had progressively crystallized from a common parent magma in an otherwise closed system.

7.2.3 Origin of Cr-V enriched ilmenite in leucogabbros

In stark contrast to the Cr-V depleted, Fe-Ti oxide-rich ultramafic horizons, it seems unlikely that the highly-enriched nature of ilmenite in several leucogabbros is the product of a separate generation of more primitive magma injections, as they are frequently closely interlayered with more disseminated gabbros and pyroxenites (Fig. 17). Rather, we propose that Fe-Ti oxides in these rocks, which are present in very low amounts (Fig. 8), are late-crystallizing intercumulus phases. Both Cr and V are highly incompatible into plagioclase during fractionation (Aigner-Torres et al., 2007; Laubier et al., 2014), and therefore fractional crystallization of abundant cumulus plagioclase in these leucocratic layers would serve to enrich a trapped residual liquid in Cr and V (Fig. 26). Fe-Ti oxides that crystallize from this intercumulus liquid would then reflect its enriched nature, the effects of which being amplified by the highly compatible nature of Cr and V into Fe-Ti oxides over other potentially crystallizing silicate phases. This interpretation is similar to that made by Duparc et al. (2016) to explain unusually Cr- and Ni-rich magnetite from felsic plutons in the La Grande region of the Superior Province, which should have crystallized from evolved magmas with very low overall Cr and Ni contents. Therefore, like other authors (e.g. Cawthorn, 2007), we caution against including the chemistries of intercumulus minerals when examining cryptic trends to model magma evolution.

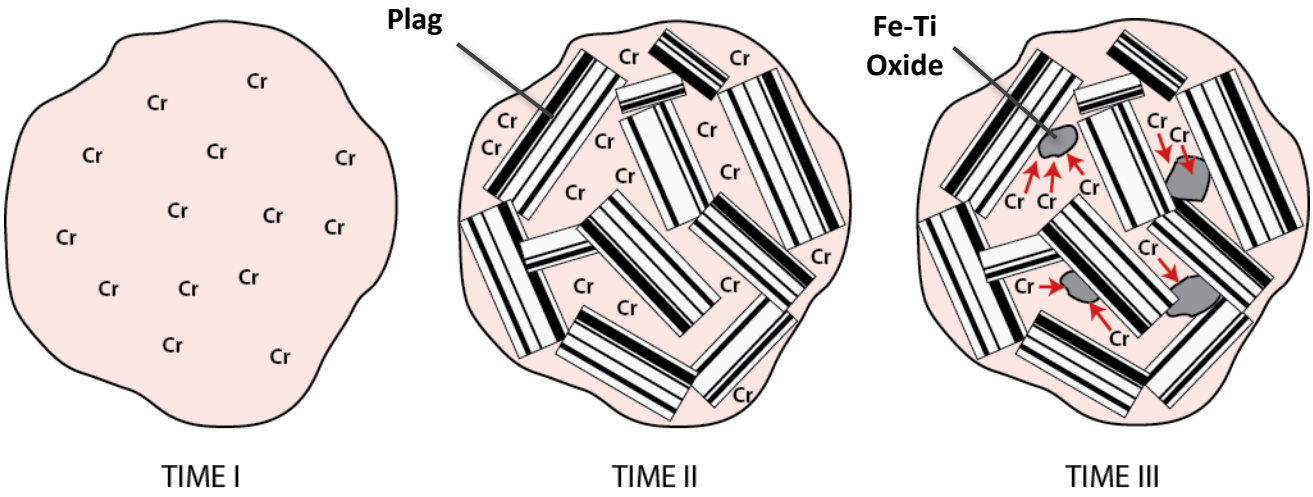

Fig. 26. Schematic illustration depicting the formation of highly Cr-enriched intercumulus Fe-Ti oxides during the crystallization of plagioclase-rich rocks (e.g. leucogabbros). ***Time I*:** Differentiation drives a parental magma to a composition that contains an initial concentration of Cr, $\mathbf{C}^{Cr}_{Parent}$; ***Time II:*** Local fractional crystallization of large amounts of cumulate plagioclase (for which $\boldsymbol{D}_{Cr} << 1$) results in the residual magma becoming increasingly enriched in Cr (i.e. $\mathbf{C}^{Cr}_{Residual} > \mathbf{C}^{Cr}_{Parent}$). This residual magma may then get trapped as an intercumulus liquid between the plagioclase grains; ***Time III:*** Fe-Ti oxides crystallize late as intercumulus phases from the trapped liquid. The compositions of these minerals consequently reflect the composition of the relatively Cr-rich intercumulus liquid, and not that of the original parent magma. Note that V, which is also highly compatible into Fe-Ti oxides but incompatible into plagioclase, would theoretically behave similarly to Cr in this scenario.

7.2.4 Comparison with previous petrogenetic models for the RBC

Invoking injections of crystal slurries as the mechanism responsible for the formation of magnetite-rich horizons in the RBC obviously contrasts with the closed-system differentiation model previously proposed by Maier et al. (1996). However, we argue that the rocks from the layered series that they used to construct their model may not have been representative of those that host the Iron-T deposit. As noted above, the relatively oxide-poor rocks of the layered zone analyzed by Maier et al. (1996) were collected approximately 15 km west of our study area, and clinopyroxene and plagioclase compositions in their samples are consistently more evolved than those analyzed in this study (Table 22). This roughly agrees with the silicate compositions obtained by Roudaut (2013), who analyzed rocks from a similar region of the Iron-T deposit as

this study. We acknowledge that the Mg# values of clinopyroxene in this study may be exaggerated from their primary magmatic compositions as a result of re-equilibration with Fe-Ti oxides (see section 7.1.1). This may even partially explain the anomalously high Mg-contents of interstitial clinopyroxene in several of the massive oxides samples in this study (Fig. 22). However, the An-content of plagioclase is generally considered to be resistant to re-equilibration due to sluggish cation diffusion rates (Morse, 1984). All of the plagioclase analyzed in this study are from gabbroic samples that would have crystallized from what we interpret to be the resident magma into which the oxide-rich crystal slurries were injected. This is significant, because it means that the resident magma in our study area was more primitive than that which formed the layered rocks studied by Maier et al. (1996).

Based on this discrepancy in silicate compositions, Roudaut (2013) interpreted that the layered zone of the RBC at the Iron-T deposit had formed through partial mixing of an evolved, Fe-Ti enriched residual liquid, i.e. the differentiated product of the underlying Main zone gabbronorites, and an injected primitive liquid, similar in composition to the parental magma of the Main zone described by Maier et al. (1996). We also note, however, that regional mapping by Goutier (2005) delineates two distinct layered units in the West Zone of the RBC: Acrb5, which hosts the Iron-T deposit and from which the samples of this study and Roudaut (2013) are taken, and Acrb3, another Fe-Ti oxide bearing unit which appears to be cross-cut by Acrb5 (Fig. 2b). Such a cross-cutting relationship may imply that Acrb5 represents an intrusion into the RBC, potentially a sill from an entirely different generation of magmatic activity (Fig. 27). Alternatively, in the context of the magma-mixing model of Roudaut (2013), it may have been an injection of primitive magma which only locally mixed with the more evolved resident magma, and around which the latter continued to crystallize. In either case, the different layered

units in the West Zone of the RBC may have formed through different magmatic histories. The layered rocks studied by Maier et al. (1996) are potentially from Acrb3, and could be representative of the evolved product of the initial RBC magma. In contrast, the more primitive rocks of Acrb5 analyzed in this study and by Roudaut (2013) formed from magma injections that had limited spatial extents within the complex. This more primitive unit must have then experienced a subsequent influx of Cr- and V-depleted (i.e. more evolved) magma in order to deposit the oxide-rich crystal slurries responsible for the irregular cryptic trends of Fe-Ti oxides.

The proposed multi-stage magmatic history of the West Zone of the RBC can thus be summarized as follows:

1) Initial emplacement of a tholeiitic basaltic magma, from which the massive gabbronorites of the Main zone were formed via fractional crystallization. Differentiation progressively drove the residual magma to more evolved, Fe-Ti-V rich compositions.
2) Crystallization of the Fe-Ti oxide-bearing upper layered zone (unit Acrb3) begins from the residual ferrobasaltic magma. The compositions of silicate minerals in these rocks (i.e. those of Maier et al., 1996) reflect the evolved nature of the differentiated parental magma.
3) More primitive magma is injected into the RBC chamber in the vicinity of what is now the Iron-T deposit, either partially mixing with the evolved resident magma, or as a sill into a solidified Acrb3. This primitive sill or hybrid magma forms the basis of the layered pyroxenite-gabbro-leucogabbro rocks of Acrb5.
4) Frequent injections of more evolved, Fe-Ti oxide-rich crystal slurries are then emplaced into the locally more primitive hybrid magma or solidified Acrb5. However, the timing of this second generation of relatively Cr-V depleted injections is unknown based on the

available data. If the injected slurries were sufficiently dense, they may have been emplaced intermittently in sequence with the fractionally crystallizing primitive host magma, flowing along the temporary floor of the magma chamber and displacing the host magma upwards as to preserve the latter's Cr depletion trend in Fe-Ti oxides. Alternatively, they may have intruded as late-stage sills into an already solidified column that had fractionally crystallized in a locally closed system.

Note that this model is partially based on the igneous cross-cutting relationships mapped by Goutier (2005) and the E-W variations in mineral chemistry that are observed across the layered zone on the northern limb of the Galinée anticline. To test this hypothesis, future work should sample from units Acrb3 and Acrb5 along a N-S transect where they intersect near the Iron-T deposit (Fig. 2b), and analyze their mineral and bulk-rock compositions to determine their genetic relationship.

Table 22. Comparison of silicate mineral chemical compositions as determined in this study with those of prior studies of the Rivière Bell Complex.

	Maier et al. (1996)		This study	Roudaut (2013)
Stratigraphic Zone **Unit (Goutier, 2005)**	Main Zone (Acrb1)	Layered Zone (Acrb3?)	Layered Zone (Acrb5)	Layered Zone (Acrb5)
An% of Plagioclase	66-74	51-55	59-66	76
Mg# of Cpx	66-75	56-64	70-82	68

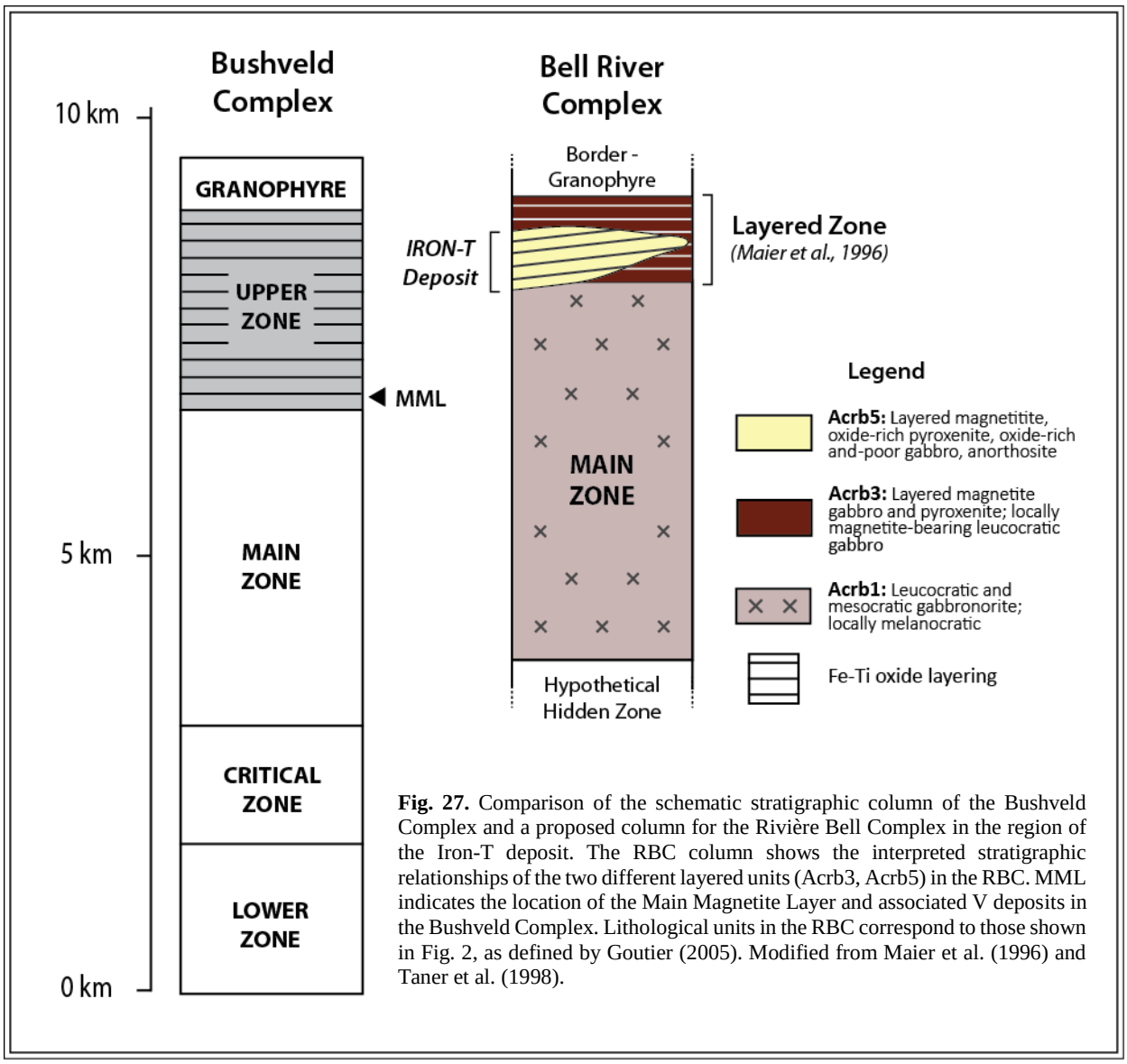

Fig. 27. Comparison of the schematic stratigraphic column of the Bushveld Complex and a proposed column for the Rivière Bell Complex in the region of the Iron-T deposit. The RBC column shows the interpreted stratigraphic relationships of the two different layered units (Acrb3, Acrb5) in the RBC. MML indicates the location of the Main Magnetite Layer and associated V deposits in the Bushveld Complex. Lithological units in the RBC correspond to those shown in Fig. 2, as defined by Goutier (2005). Modified from Maier et al. (1996) and Taner et al. (1998).

8 CONCLUSIONS

Despite their history of metamorphism, the trace element compositions of Fe-Ti oxide minerals in the upper layered series of the Rivière Bell Complex record a complex history of multistage magmatism that is directly related to the formation of Fe-Ti-V ore horizons. The Cr, V, and Mn contents of cumulate titaniferous magnetite and ilmenite appear to have been unmodified by secondary processes such as metamorphism and subsolidus silicate-oxide re-equilibration. The common practice of using Cr and V as tracers of magmatic differentiation in mafic intrusions therefore remains applicable even in metamorphosed settings. Most other trace elements, however, are seemingly susceptible to intergranular diffusive modification during metamorphism, and particularly so when Fe-Ti oxides are disseminated in mafic host rocks. The abundances of these elements in cumulate magnetite or ilmenite in metamorphic settings therefore may not be representative of their primary compositions, unless the host-rock is sufficiently oxide-rich as to ensure that minimal re-equilibration with magmatic or metamorphic silicate minerals is possible.

The close relationship between variations in the chemostratigraphy of Fe-Ti oxides and lithostratigraphy across the layered rocks host to the Fe-Ti-V deposits of the Iron-T property in the RBC are strongly suggestive of open system magmatic processes. Frequent injections of relatively Cr- and V-depleted magma into a primitive ferrogabbroic host are presumably responsible for several sharp changes in the cryptic trends of Fe-Ti oxides over the 300 m section of igneous stratigraphy examined in this study. These depleted horizons also display layering textures indicative of laterally flowing crystal slurries, which promoted the sorting of cumulate Fe-Ti oxides into well-defined massive and semi-massive layers of variable thickness and lateral extent. The timing of these injections relative to the crystallization of the more primitive host

body is, however, undetermined. A consistent deposit-scale Cr depletion trend defined by the primitive disseminated host rocks could have formed either prior to, or in sequence with the injection of the Cr-V depleted, Fe-Ti oxide-rich slurries. In the former case, the most economic, Fe-Ti oxide-rich portions of the Iron-T deposit would then essentially represent sills into the RBC. In either scenario, regional geologic relationships and lateral variations in silicate mineral compositions across the northern layered series of the RBC suggest that the primitive ferrogabbroic host unit of the Iron-T deposit also represents an intermediate-stage magma injection into the evolved upper portion of the complex.

REFERENCES

Aigner-Torres, M., Blundy, J., Ulmer, P., Pettke, T. (2007) Laser ablation ICPMS study of trace element partitioning between plagioclase and basaltic melts: an experimental approach. *Contributions to Mineralogy and Petrology.* 153: 647-667.

Apted, M.J. and Liou, J.G. (1983) Phase relations among greenschist, epidote-amphibolite, and amphibolite in a basaltic system. *American Journal of Science.* 283-A: 328-354.

Ashwal, L.D., Webb, S.J., Knoper, M.W. (2005) Magmatic stratigraphy in the Bushveld northern lobe: continuous geophysical and mineralogical data from the 2950 m Bellevue drillcore. *South African Journal of Geology.* 108: 199-232.

Barnes, S.J. (1986) The effect of trapped liquid crystallization on cumulus mineral compositions in layered intrusions. *Contributions to Mineralogy and Petrology.* 93: 524–531.

Barnes, S.-J., Maier, W.D., Ashwal, L.D. (2004) Platinum-group element distribution in the Main Zone and Upper Zone of the Bushveld Complex, South Africa. *Chemical Geology.* 208: 293-317.

Beaudry, C.T. and Gaucher, E. (1986) Cartographie géologique de la region de Matagami. Ministère de l'Énergie et des Resources du Québec, report MB 86-32.

Botcharnikov, R.E., Almeev, R.R., Koepke, J., Holtz, F. (2008) Phase relations and liquid lines of descent in hydrous ferrobasalt – implications for the Skaergaard intrusion and Columbia River basalts. *Journal of Petrology.* 49(9): 1687-1727.

Brady, J. B. and Cherniak, D. J. (2010). Diffusion in minerals: An overview of published experimental diffusion data. In: Zhang, Y. and Cherniak, D. J. (eds). *Diffusion in Minerals and Melts.* Mineralogical Society of America and Geochemical Society, Reviews in Mineralogy and Geochemistry 72: 899-920.

Buddington, A.F. and Lindsley, D.H. (1964) Iron-titanium oxide minerals and synthetic equivalents. *Journal of Petrology.* 5: 310-357.

Butcher, A.R. and Merkle, R.K.W. (1987) Postcumulus modification of magnetite grains in the upper zone of the Bushveld Complex, South Africa. *Lithos.* 20: 247-260.

Carr, P.M., Cathles III, L.M., Barrie, C.T. (2008) On the size and spacing of volcanogenic massive sulfide deposits within a district with application to the Matagami district, Quebec. *Economic Geology.* 103: 1395-1409.

Cawthorn, R.G. (2007) Cr and Sr: keys to parental magmas and processes in the Bushveld Complex, South Africa. *Lithos.* 95: 381-398.

Cawthorn, R.G. (2013) Rare earth element abundances in apatite in the Bushveld Complex – a consequence of the trapped liquid shift effect. *Geology.* 41 (5): 603-606.

Cawthorn, R.G. (2015). The Bushveld Complex, South Africa. In: Charlier, B., Namur, O., Latypov, R., Tegner, C. (Eds.), *Layered Intrusions*. Springer Netherlands, Dordrecht. p. 517-588.

Cawthorn, R.G. and Ashwal, L.D. (2009) Origin of anorthosite and magnetitite layers in the Bushveld Complex, constrained by major element compositions of plagioclase. *Journal of Petrology.* 50(9): 1607-1637.

Cawthorn, R.G. and McCarthy, T.S. (1980) Variations in Cr content of magnetite from the Upper Zone of the Bushveld Complex – evidence for heterogeneity and convection currents in magma chambers. *Earth and Planetary Science Letters.* 46: 335-343.

Cawthorn, R.G., McCarthy, T.S., Davies, G. (1983) Vertical chemical gradients in a single grain of magnetite from the Bushveld Complex, South Africa. *Mineralogical Magazine.* 47: 27-34.

Cawthorn, R.G, Meyer, P.S., Kruger, F.J. (1991) Major addition of magma at the Pyroxenite Marker in the western Bushveld Complex, South Africa. *Journal of Petrology.* 32: 739-763.

Chakraborty, S. (2008) Diffusion in solid silicates: a tool to track timescales of processes comes of age. *Annual Review of Earth and Planetary Sciences.* 36: 153-190.

Charlier, B., Skår, Ø., Korneliussen, A., Duchesne, J.-C., Vander Auwera, J. (2007) Ilmenite composition in the Tellnes Fe–Ti deposit, SW Norway: fractional crystallization, postcumulus evolution and ilmenite–zircon relation. *Contributions to Mineralogy and Petrology.* 154: 119-134.

Charlier, B., Namur, O., Toplis, M.J., Schiano, P., Cluzel, N., Higgins, M.D., Vander Auwera, J. (2011) Large-scale silicate liquid immiscibility during differentiation of tholeiitic basalt to granite and the origin of the Daly gap. *Geology.* 39: 907-910.

Daigneault, R., Mueller, W., Chown, E.H. (2002) Oblique Archean subduction: accretion and exhumation of an oceanic arc during dextral transpression, Southern Volcanic Zone, Abitibi Subprovince Canada. *Precambrian Research.* 115: 261-290.

Dare, S.A.S., Barnes S.-J., Beaudoin, G. (2012) Variation in trace element content of magnetite crystallized from fractionating sulfide liquid, Sudbury, Canada: implications for provenance discrimination. *Geochimica et Cosmochimica Acta.* 88: 27-50.

Dare, S.A.S., Barnes, S.-J., Beaudoin, G., Méric, J., Boutroy, E., Potvin-Doucet, C. (2014) Trace elements in magnetite as petrogenetic indicators. *Mineralium Deposita.* 49: 785-796.

Duparc, Q., Dare, S.A.S., Cousineau, P.A., Goutier, J. (2016) Magnetite chemistry as a provenance indicator in Archean metamorphosed sedimentary rocks. *Journal of Sedimentary Research.* 86: 542-563.

Dupéré, M. (2011) Technical report, vanadium-titanium-iron resource estimation of the Iron-T property, Matagami area, Quebec, Canada. SGS Canada Inc. 89 p.

Duran, C.J., Barnes, S.-J., Corkery, J.T. (2015) Chalcophile and platinum-group element distribution in pyrites from the sulfide-rich pods of the Lac des Iles Pd deposits, Western Ontario, Canada: Implications for post-cumulus re-equilibration of the ore and the use of pyrite compositions in exploration. *Journal of Geochemical Exploration.* 158: 223-242.

Emeleus, C.H., Cheadle, M.J., Hunter, R.H., Upton, B.G.J., Wadsworth, W.J. (1996) The Rum Layered Suite. *Developments in Petrology.* 15: 403-439.

Forien, M., Tremblay, J., Barnes, S.-J., Burgisser, A., Pagé, P. (2015) The role of viscous particle segregation in forming chromite layers from slumped crystal slurries: insights from analogue experiments. *Journal of Petrology.* 56(12): 2425-2444.

Freeman, B.C. (1939) The Rivière Bell Complex, northwestern Quebec. *Journal of Geology.* 47(1): 27-46.

Frost, B.R. (1991). Magnetic petrology: factors that control the occurrence of magnetite in crustal rocks. In: Lindsley, D.H. (ed.), *Oxide Minerals: Petrologic and Magnetic Significance*. Mineralogical Society of America Reviews in Mineralogy 25: 489-509.

Genna, D., Gaboury, D., Roy, G. (2014) The Key Tuffite, Matagami camp, Abitibi Greenstone Belt, Canada: petrogenesis and implications for VMS formation and exploration. *Mineralium Deposita.* 49: 489-512.

Goutier, J. (2005) Géologie de la région de la baie Ramsay 32F/10 et de la rivière Opaoca 32F/11. Ministère des resources naturelles et de la faune. RG 2005-01: 58 p.

Haggerty, S.E. (1991) Oxide-textures; a mini-atlas. In: Lindsley, D.H. (ed.), *Oxide Minerals: Petrologic and Magnetic Significance*. Mineralogical Society of America Reviews in Mineralogy 25. p. 129-219.

Howarth, G.H. and Prevac, S.A. (2013) Hydration vs. oxidation: modelling implications for Fe-Ti oxide crystallization in mafic intrusions, with specific reference to the Panzhihua intrusion, SW China. *Geoscience Frontiers.* 4: 555-569.

Howarth, G.H., Prevec, S.A., Zhou M.-F. (2013) Timing of Ti-magnetite crystallization and silicate disequilibrium in the Panzhihua mafic layered intrusion: implications for ore-forming processes. *Lithos.* 170-171: 73-89.

Huppert, H.E. and Sparks, R.S.J. (1984) Double-diffusive convection due to crystallization in magmas. *Annual Review of Earth and Planetary Science.* 12: 11-37.

Irvine, T.N. (1982) Terminology for layered intrusions. *Journal of Petrology.* 23: 127-162.

Irvine, T.N., Anderson, J.C.O., Brooks, C.K. (1998) Included blocks (and blocks within blocks) in the Skaergaard intrusion: geological relations and the origins of rhythmic modally graded layers. *Geological Society of American Bulletin.* 110: 1398-1447.

Jang, Y.D. and Naslund, H.R. (2003) Major and trace element variation in ilmenite in the Skaergaard intrusion: petrologic implications. *Chemical Geology.* 193:109-125.

Jakobsen, J.K., Veksler, I.V., Tegner, C., Brooks, C.K. (2005) Immiscible iron- and silica-rich melts in basalt petrogenesis documented in the Skaergaard intrusion. *Geology*. 33: 885-888.

Jochum K.P., Willbold, M., Raczek, I., Stoll, B., Herwig, K. (2005) Chemical characterisation of the USGS reference glasses GSA-1G, GSC-1G, GSD-1G, GSE-1G, BCR-2G, BHVO-2G and BIR-1G using EPMA, ID-TIMS, ID-ICP-MS and LA-ICP-MS. *Geostandards and Geoanalytical Research.* 29(3): 285-302.

Jochum, K.P., Stoll, B., Herwig, K., Willbold, M., Hofmann, A.W., Amini, M., Aarburg, S., Abouchami, W., Hellebrand, E., Mocek, B. and Raczek, I. (2006) MPI-DING reference glasses for in situ microanalysis: New reference values for element concentrations and isotope ratios. *Geochemistry, Geophysics, Geosystems*. 7(2): 1-44.

Jenney, C.P. (1961) Geology and ore deposits of the Mattagami area, Quebec. *Economic Geology.* 56: 740-757.

Jensen, J.C., Nielsen, F.M., Duchesne, J.C., Demaiffe, D., Wilson, J.R. (1993) Magma influx and mixing in the Bjerkreim-Sokndal layered intrusion, South Norway: evidence from the boundary between two megacyclic units at Storeknuten. Lithos. 29: 311–325.

Jolly, W.T. (1978) Metamorphic history of the Archean Abitibi belt. In: Fraser, J.A., Heywood W.W. (eds) *Metamorphism of the Canadian Shield.* Geological Survey of Canada, Paper 78-10, pp. 63-78.

Klemm, D.D., Henckel, J., Dehm, R., Von Gruenewaldt, G. (1985) The geochemistry of titanomagnetite in magnetite layers and their host rocks in the eastern Bushveld Complex. *Economic Geology.* 89: 1075-1088.

Klemme, S., Günther, D., Hametner, K., Prowatke, S., Zack, T. (2006) The partitioning of trace elements between ilmenite, ulvospinel, armalcolite and silicate melts with implications for the early differentiation of the moon. *Chemical Geology.* 234: 251-263.

Laubier, M., Grove, T.L., Langmuir C.H. (2014). Trace element mineral/melt partitioning for basaltic and basaltic andesitic melts: an experimental and laser ICP-MS study with application to the oxidation state of mantle source regions. *Earth and Planetary Science Letters.* 392: 265-278.

Leeman, W.P, Ma, M.-S., Murali, R., Schmitt, R.A. (1978) Empirical estimation of magnetite/liquid distribution coefficients for some transition elements. *Contributions to Mineralogy and Petrology*. 65(3): 269-272.

Lindsley, D.H. (1991) Experimental studies of oxide minerals. In: Lindsley, D.H. (ed.), *Oxide Minerals: Petrologic and Magnetic Significance*. Mineralogical Society of America Reviews in Mineralogy 25. p. 69-106.

Liou, J.G., Kuniyoshi, S., Ito, K. (1974) Experimental studies of the phase relations between greenschist and amphibolite in a basaltic system. *American Journal of Science.* 274: 613-632.

Maier, W.D., and Barnes, S.-J. (2008) Platinum-group elements in the UG1 and UG2 chromitites and the Bastard reef at Impala platinum mine, western Bushveld Complex. *South African Journal of Geology.* 111: 159-176.

Maier, W.D., Barnes, S-J., Pellet, T. (1996) The economic significance of the Rivière Bell Complex, Abitibi subprovince, Quebec. *Canadian Journal of Earth Science.* 33: 967-980.

Maier, W.D., Barnes, S.-J., Groves, D.I. (2013) The Bushveld Complex, South Africa: formation of platinum–palladium, chrome- and vanadium-rich layers via hydrodynamic sorting of a mobilized cumulate slurry in a large, relatively slowly cooling, subsiding magma chamber. *Mineralium Deposita.* 48: 1-56.

Mallmann, G. and O'Neill, H.S.C. (2009) The crystal/melt partitioning of V during mantle melting as a function of oxygen fugacity compared with some other elements (Al, P, Ca, Sc, Ti, Cr, Fe, Ga, Y, Zr and Nb). *Journal of Petrology.* 50(9): 1765-1794.

Maruyama, S., Suzuki, K., Liou, J.G. (1983) Greenschist-amphibolite transition equilibria at low pressures. *Journal of Petrology.* 24(4): 583-604.

McBirney, A.R. and Noyes, R.M. (1979). Crystallization and layering of the Skaergaard intrusion. *Journal of Petrology.* 20(3): 487-554.

McCarthy, T.S. and Cawthorn, R.G. (1983) The geochemistry of vanadiferous magnetite in the Bushveld Complex: implications for crystallization mechanisms in layered complexes. *Mineralium Deposita.* 18: 505-518.

McEnroe, S.A., Robinson, P., Panish, P.T. (2000) Chemical and petrographic characterization of ilmenite in oxide-rich cumulates of the Sokndal Region, Rogaland, Norway. *Norges Geologiske Undersokelse.* 436: 49-56.

Méric, J., Dare, S.A.S., Barnes, S.-J., Beaudoin, G. (2012) The use of trace elements in Fe-oxides in deducing the fractionation history of a silicate magma. *Mineralogical Magazine.* 76(6): 2101.

Meurer, W.P. and Boudreau, A.E. (1996) Petrology and mineral compositions of the middle banded series of the Stillwater Complex, Montana. *Journal of Petrology.* 37(3): 583-607.

Mortenson, J.K. (1993) U-Pb geochronology of the eastern Abitibi subprovince. Part 1: Chibougamau-Matagami-Joutel region. *Canadian Journal of Earth Science.* 30: 11-28.

Morriset, C.-E. and Scoates, J.S. (2008) Origin of zircon rims around ilmenite in mafic plutonic rocks of Proterozoic anorthosite suites. *The Canadian Mineralogist.* 46 (2): 289-304.

Morse, S.A. (1984) Cation diffusion in plagioclase feldspar. *Science.* 225(4661): 504-505.

Munoz, C.M.T. (2010) Distribution of platinum-group elements in the Ebay claim, central part of the Rivière Bell Complex, Matagami, Quebec. Université du Québec à Chicoutimi. Unpublished Masters thesis.

Namur, O., Charlier, B., Toplis, M.J., Higgins, M.D., Liégeois, J.-P., Vander Auwera, J. (2010) Crystallization sequence and magma chamber processes in the ferrobasaltic Sept Iles layered intrusion, Canada. *Journal of Petrology.* 51(6): 1203-1236.

Namur, O., Abily, B., Boudreau, A.E., Blanchette, F., Bush, J.W.M, Ceuleneer, G., Charlier, B., Donaldson, C.H., Duchesne, J.-C., Higgins, M.D., Morata, D., Nielsen, T.F.D., O'Driscoll, B., Pang, K.N., Peacock, T., Spandler, C.J., Toramaru, A., Veksler, I.V. (2015) Igneous layering in basaltic magma chambers. In: Charlier, B., Namur, O., Latypov, R., Tegner, C. (eds.), *Layered Intrusions*. Springer Netherlands, Dordrecht, p. 75-152.

Namur, O., Charlier, B., Holness, M.B. (2012) Dual origin of Fe-Ti-P gabbros by immiscibility and fractional crystallization of evolved tholeiitic basalts in the Sept Iles layered intrusion. *Lithos.* 154: 100-114.

Nex, P.A.M., Cawthorn, R.G., Kinnaird, J.A. (2002). Geochemical effects of magma addition: compositional reversals and decoupling of trends in the Main Zone of the Western Bushveld Complex. *Mineralogical Magazine*. 66: 833-856.

Pang, K.-N., Li, C., Zhou, M.-F., Ripley, E. (2008a) Abundant Fe-Ti oxide inclusions in olivine from the Panzhihua and Hongge layered intrusions, SW China: evidence for early saturation of Fe-Ti oxides in ferrobasaltic magma. *Contributions to Mineralogy and Petrology*. 156: 307-321.

Pang, K.-N., Zhou, M.-F., Lindsley, D., Zhao, D., Malpas, J. (2008b) Origin of Fe-Ti oxide ores in mafic intrusions: evidence from the Panzhihua Intrusion, SW China. *Journal of Petrology.* 49(2): 295-313.

Pang, K.-N., Li, C., Zhou, M.-F., Ripley, E.M. (2009) Mineral compositional constraints on the petrogenesis and oxide ore genesis of the late Permian Panzhihua layered gabbroic intrusion, SW China. *Lithos.* 110: 199-214.

Paton, C., Hellstrom, J., Paul, B., Woodhead, J., Hergt, J. (2011) Iolite: freeware for the visualization of mass spectrometric data. *Journal of Analytical Atomic Spectrometry.* 26(12): 2508-2518.

Pearce, N.J.G. (1990) Zirconium and niobium-bearing ilmenites from the Igaliko dyke swarm, South Greenland. *Mineralogical Magazine.* 54: 585-588.

Philpotts, A.R. (1967) Origin of certain iron-titanium oxide and apatite rocks. *Economic Geology.* 62: 303-315.

Piché, M., Guha, J., Daigneault, R. (1993) Stratigarphic and structural aspects of the volcanic rocks of the Matagmi mining camp, Quebec: implications for the Norita deposit. *Economic Geology*. 88: 1542-1558.

Price, G.D. (1981). Subsolidus phase relations in the titanomagnetite solid solution series. *American Mineralogist.* 66: 751-758.

Raudsepp, M., Turnock, A.C., Hawthorne, F.C. (1991). Amphibole synthesis at low pressure: what grows and what doesn't. *European Journal of Mineralogy.* 3: 983-1004.

Reynolds, I.M. (1985a) Contrasted mineralogy and textural relationships in the uppermost titaniferous magnetite layers of the Bushveld Complex in the Bierkraal area north of Rustenberg. *Economic Geology.* 80: 1027-1048.

Reynolds, I.M. (1985b). The nature and origin of titaniferous magnetite-rich layers in the Upper Zone of the Bushveld Complex: a review and synthesis. *Economic Geology*. 80: 1089-1908.

Roedder, E. (1978) Silicate liquid immiscibility in magma and in the system K_2O-FeO-Al_2O_3-SiO_2: an example of serendipity. *Geochimica et Cosmochimica Acta.* 42: 1597-1617.

Roudaut, S. (2013) Les minéralisations en vanadium du Complexe de la Riviére Bell, Matagami, Québec. Université du Québec à Montreal. Unpublished M.Sc. thesis.

Ross, P.-S., McNicoll, V.J., Debreil, J.-A., Carr, P. (2014) Precise U-Pb geochronology of the Matagami mining camp, Abitibi greenstone belt, Quebec: stratigraphic constraints and implications for volcanogenic massive sulfide exploration. *Economic Geology.* 100: 89-101.

Schumacher, J.C. (2007) Metamorphic amphiboles: composition and coexistence. *Reviews in Mineralogy & Geochemistry.* 67: 359-416.

Scoates, J.S. and Wall, C.J. (2015) Geochronology of layered intrusions. In: Charlier, B., Namur, O., Latypov, R., Tegner, C. (eds.), *Layered Intrusions*. Springer Netherlands, Dordrecht, p. 3-74.

Sharpe, J.I. (1968) Geology and sulfide deposits of the Matagami area, Abitibi-East County. Quebec Department of Natural Resources, Geological Report 137.

Sisson, T.W. and Grove, T.L. (1993) Experimental investigations of the role of H_2O in calc-alkaline differentiation and subduction zone magmatism. *Contributions to Mineralogy and Petrology.* 113: 143-166.

Snyder, D., Carmichael, I.S.E., Wiebe, R.A. (1993) Experimental study of liquid evolution in an Fe-rich, layered mafic intrusion: constraints of Fe-Ti oxide precipitation on the T-fo_2 and T-ρ paths of tholeiitic magmas. *Contributions to Mineralogy and Petrology.* 113: 73-86.

Song, X.-Y., Qi, H.-W., Hu, R.-Z., Chen, L-M., Yu, S.-Y., Zhang, J.-F. (2013). Formation of thick stratiform Fe-Ti oxide layers in layered intrusion and frequent replenishment of fractionated mafic magma: evidence from the Panzhihua intrusion, SW China. *Geochemistry, Geophysics, Geosystems.* 14(3): 712-732.

Spear, F.S. (1981) Amphibole-plagioclase equilibria: an empirical model for the relation albite + tremolite = edenite + 4 quartz. *Contributions to Mineralogy and Petrology.* 77(4): 355-364.

Tan, W., He, H., Wang, C.Y., Dong, H., Liang, X., Zhu, J. (2016) Magnetite exsolution in ilmenite from the Fe-Ti oxide gabbro in the Xinjie intrusion (SW China) and sources of unusually strong remnant magnetization. *American Mineralogist.* 101: 2579-2767.

Taner, M.F., Ercit, T.S., and Gault, R.A. (1998) Vanadium-bearing magnetite from the Matagami and Chibougamau mining districts, Abitibi, Québec, Canada. *Exploration and Mining Geology.* 7(4): 299-311.

Tanner, D., Mavrogenes, J.A., Arculus, R.J., Jenner, F.E. (2014) Trace element stratigraphy of the Bellevue Core, northern Bushveld: multiple magma injections obscured by diffusive processes. *Journal of Petrology.* 55(5): 859-882.

Tegner, C., Cawthorn, R.G., Kruger, F.J. (2006) Cyclicity in the Main and Upper Zones of the Bushveld Complex, South Africa: crystallization in a zoned magma sheet. *Journal of Petrology.* 47(11): 2257-2279.

Tollari, N., Toplis, M.J., and Barnes, S.-J. (2006) Predicting phosphate saturation in silicate magmas: an experimental study of the effects of melt composition and temperature. *Geochimica et Cosmochimica Acta.* 70(6): 1518-1536.

Toplis, M.J. and Carroll, M.R. (1995) An experimental study of the influence of oxygen fugacity on Fe-Ti oxide stability, phase relations, and mineral-melt equilibria in ferro-basaltic systems. *Journal of Petrology.* 36(5): 1137-1170.

Toplis, M.J. and Carroll, M.R. (1996) Differentiation of ferro-basaltic magmas under conditions open and closed to oxygen: implications for the Skaergaard intrusion and other natural systems. *Journal of Petrology.* 37(4): 837-858.

Toplis, M.J. and Corgne, A. (2002) An experimental study of element partitioning between magnetite, clinopyroxene and iron-bearing silicate liquids with particular emphasis on vanadium. *Contributions to Mineralogy and Petrology.* 144: 22-37.

Ulmer, G.C. (1969) Experimental investigations of chromite spinels. *Economic Geology Monograph.* 4: 114-131.

Van Orman, J.A. and Crispin, K.L. (2010) Diffusion in Oxides. *Reviews in Mineralogy and Geochemistry*. 72(1): 757-825.

Vernon, R.H. (2004) *A practical guide to rock microstructure*. Cambridge: Cambridge University Press. 606 p.

Vincent, E.A. and Phillips, R. (1954) Iron titanium minerals in the layered gabbros of the Skaergaard intrusion, East Greenland. *Geochimica et Cosmochimica Acta.* 6: 1-26.

Vincent, E.A., Wright, J.B., Chevallier, R., Mathieu, S. (1957) Heating experiments on some natural titaniferous magnetites. *Mineralogical Magazine.* 31: 624-655.

Von Gruenewaldt, G., Klemm, D.D., Henckel, J., Dehm, R. (1985) Exsolution features in titanomagnetites from massive magnetite layers and their host rocks of the Upper Zone, eastern Bushveld Complex. *Economic Geology.* 80: 1049-1061.

Wager, L.R. and Brown, G.M. (1968). *Layered igneous rocks*. Edinburgh: Oliver & Boyd, 588 p.

Willemse, J. (1969). The vanadiferous magnetite iron ore of the Bushveld Igneous Complex. *Economic Geology Monograph.* 4: 137-208.

Zhou, M.-F., Robinson, P.T., Lesher, M.C., Keays, R.R., Zhang, C.-Z., Malpas, J. (2005) Geochemistry, petrogenesis and metallogenesis of the Panzhihua gabbroic layered intrusion and associated Fe-Ti-V oxide deposits, Sichuan province, SW, China. *Journal of Petrology.* 46(11): 2253-2280.

APPENDIX 1

Full results from EMPA analyses of magnetite and ilmenite

Analysis ID		CaO	Cr_2O_3	Al_2O_3	ZnO	FeO	Fe_2O_3	TiO_2	NiO	MnO	V_2O_3	MgO	SiO_2	Total	Total Fe (%):
14-2a mt 2		0.00	0.09	3.67	0.14	36.81	51.45	6.54	0.03	0.16	1.32	0.63	0.03	100.86	65.74
14-2a mt 3		0.00	0.09	3.44	0.07	37.85	49.89	7.25	0.03	0.16	1.47	0.38	0.05	100.68	65.25
14-2a mt 5		0.00	0.11	3.96	0.00	35.93	52.55	5.45	0.03	0.11	1.47	0.56	0.03	100.19	65.98
14-2a mt 6		0.00	0.10	2.75	0.05	32.66	60.44	2.08	0.02	0.07	1.48	0.51	0.03	100.19	69.82
14-2a mt 7		0.00	0.06	4.66	0.03	38.15	47.63	7.88	0.03	0.17	1.32	0.71	0.04	100.68	63.70
MA12-2A	**Avg.**	**0.00**	**0.09**	**3.70**	**0.06**	**36.28**	**52.39**	**5.84**	**0.03**	**0.13**	**1.41**	**0.56**	**0.04**	**100.52**	**66.10**
Magnetite	*Std.*	*0.00*	*0.02*	*0.70*	*0.05*	*2.21*	*4.86*	*2.29*	*0.00*	*0.04*	*0.08*	*0.12*	*0.01*	*0.31*	*2.26*
14-2d mt 1		0.00	0.10	4.92	0.21	42.57	37.56	12.82	0.02	0.29	1.12	0.57	0.03	100.20	58.97
14-2d mt 2-1		0.00	0.12	4.26	0.00	42.16	37.96	12.60	0.01	0.25	1.10	0.55	0.03	99.03	58.99
14-2d mt 2-2		0.00	0.11	1.59	0.24	40.81	43.59	11.32	0.03	0.23	1.12	0.25	0.02	99.32	62.43
14-2d mt 3		0.01	0.11	4.67	0.13	41.38	39.77	12.09	0.03	0.25	1.11	1.02	0.04	100.61	59.85
14-2d mt 4		0.00	0.12	4.29	0.00	38.83	46.53	8.64	0.03	0.19	1.37	0.68	0.02	100.70	63.33
14-2d mt 6		0.00	0.10	4.18	0.00	39.66	44.77	9.28	0.04	0.18	1.47	0.42	0.04	100.14	62.54
MA14-2D	**Avg.**	**0.00**	**0.11**	**3.99**	**0.10**	**40.90**	**41.70**	**11.13**	**0.03**	**0.23**	**1.22**	**0.58**	**0.03**	**100.00**	**61.02**
Magnetite	*Std.*	*0.00*	*0.01*	*1.21*	*0.11*	*1.44*	*3.77*	*1.77*	*0.01*	*0.04*	*0.16*	*0.26*	*0.01*	*0.68*	*1.96*
14-3a mt 3		0.00	0.14	0.49	0.00	38.57	50.58	8.40	0.03	0.24	1.19	0.03	0.02	99.70	66.29
14-3a mt 4		0.00	0.17	1.31	0.08	31.93	64.23	0.85	0.02	0.03	1.34	0.05	0.03	100.05	72.26
14-3a mt 5		0.00	0.14	1.20	0.00	32.21	63.07	1.28	0.02	0.07	1.43	0.04	0.04	99.50	71.55
14-3a mt 6		0.00	0.15	1.02	0.00	35.58	57.56	4.65	0.01	0.16	1.16	0.12	0.15	100.56	69.63
14-3a mt 7		0.02	0.19	0.54	0.04	39.22	49.04	9.19	0.01	0.29	1.24	0.07	0.02	99.86	65.55
MA14-3A	**Avg.**	**0.00**	**0.16**	**0.91**	**0.02**	**35.50**	**56.90**	**4.87**	**0.02**	**0.16**	**1.27**	**0.06**	**0.05**	**99.93**	**69.06**
Magnetite	*Std.*	*0.01*	*0.02*	*0.38*	*0.04*	*3.42*	*6.96*	*3.88*	*0.01*	*0.11*	*0.11*	*0.04*	*0.06*	*0.40*	*3.03*
14-3b-t mt 1		0.00	0.23	1.41	0.00	32.76	63.25	1.48	0.03	0.08	1.43	0.05	0.02	100.74	72.08
14-3b-t mt 3		0.01	0.17	1.61	0.00	33.14	60.29	2.46	0.03	0.09	1.38	0.13	0.03	99.34	70.04
14-3b-t mt 4		0.00	0.16	1.17	0.03	32.48	63.28	1.42	0.02	0.04	1.34	0.04	0.03	100.01	71.90
14-3b-t mt 5		0.00	0.17	1.35	0.36	32.01	63.49	1.27	0.01	0.06	1.25	0.07	0.02	100.06	71.74
14-3b-t mt 8		0.00	0.15	3.33	0.00	32.34	63.31	0.54	0.03	0.03	1.44	0.12	0.02	101.30	71.83
MA14-3B-T	**Avg.**	**0.00**	**0.18**	**1.77**	**0.08**	**32.55**	**62.72**	**1.43**	**0.02**	**0.06**	**1.37**	**0.08**	**0.02**	**100.29**	**71.52**
Magnetite	*Std.*	*0.00*	*0.03*	*0.79*	*0.14*	*0.38*	*1.22*	*0.61*	*0.01*	*0.02*	*0.07*	*0.04*	*0.00*	*0.67*	*0.75*
14-4 mt 10		0.00	0.04	0.79	0.00	31.65	66.08	0.41	0.00	0.02	1.16	0.01	0.04	100.20	73.50
14-4 mt 5		0.00	0.01	0.61	0.05	31.32	65.62	0.46	0.00	0.05	1.23	0.02	0.03	99.39	72.91
14-4 mt 7		0.00	0.03	0.64	0.00	31.54	66.96	0.24	0.00	0.01	1.03	0.02	0.03	100.50	74.11
14-4 mt 8-1		0.01	0.02	0.34	0.18	31.10	67.14	0.14	0.00	0.01	1.04	0.00	0.03	100.01	73.94
14-4 mt 8-2		0.00	0.04	0.65	0.00	31.94	65.75	0.80	0.02	0.05	1.00	0.01	0.02	100.28	73.45
MA14-3	**Avg.**	**0.00**	**0.03**	**0.61**	**0.05**	**31.51**	**66.31**	**0.41**	**0.00**	**0.03**	**1.09**	**0.01**	**0.03**	**100.08**	**73.58**
Magnetite	*Std.*	*0.00*	*0.01*	*0.15*	*0.07*	*0.29*	*0.63*	*0.23*	*0.01*	*0.02*	*0.09*	*0.01*	*0.01*	*0.38*	*0.42*
14-5a mt 2		0.00	0.06	0.20	0.15	35.20	57.65	4.91	0.03	0.14	1.19	0.03	0.02	99.58	69.43
14-5a mt 3-1		0.00	0.07	2.96	0.43	40.71	42.91	10.96	0.01	0.38	1.03	0.15	0.05	99.66	61.83
14-5a mt 3-2		0.01	0.08	0.23	0.00	34.77	58.12	4.49	0.02	0.15	1.10	0.01	0.01	98.99	69.49
14-5a mt 4		0.00	0.06	0.39	0.00	37.96	52.56	7.65	0.03	0.27	1.15	0.04	0.03	100.15	67.40
14-5a mt 8		0.00	0.08	0.31	0.02	34.11	60.49	3.47	0.03	0.12	1.17	0.01	0.01	99.82	70.88
MA14-5A	**Avg.**	**0.00**	**0.07**	**0.82**	**0.12**	**36.55**	**54.35**	**6.30**	**0.02**	**0.21**	**1.13**	**0.05**	**0.02**	**99.64**	**67.81**
Magnetite	*Std.*	*0.00*	*0.01*	*1.07*	*0.16*	*2.46*	*6.28*	*2.71*	*0.01*	*0.10*	*0.06*	*0.05*	*0.01*	*0.38*	*3.19*
14-5c mt 3-1		0.00	0.11	0.33	0.25	36.02	56.53	5.58	0.02	0.14	1.26	0.00	0.02	100.26	69.13

Analysis ID		CaO	Cr_2O_3	Al_2O_3	ZnO	FeO	Fe_2O_3	TiO_2	NiO	MnO	V_2O_3	MgO	SiO_2	Total	Total Fe (%):
14-5c mt 3-2		0.00	0.09	0.62	0.20	36.36	53.93	6.26	0.03	0.15	1.47	0.01	0.01	99.13	67.35
14-5c mt 4		0.00	0.09	0.04	0.16	32.37	64.04	1.62	0.01	0.04	1.45	0.00	0.03	99.85	72.42
14-5c mt 5		0.00	0.10	0.14	0.14	31.61	66.73	0.47	0.00	0.00	1.40	0.00	0.02	100.61	73.98
14-5c mt 6		0.01	0.07	0.18	0.12	38.64	50.34	8.67	0.01	0.25	1.27	0.01	0.01	99.57	66.15
MA14-5C	**Avg.**	**0.00**	**0.09**	**0.26**	**0.17**	**35.00**	**58.31**	**4.52**	**0.01**	**0.12**	**1.37**	**0.00**	**0.02**	**99.88**	**69.81**
Magnetite	*Std.*	*0.00*	*0.01*	*0.20*	*0.05*	*2.63*	*6.16*	*3.04*	*0.01*	*0.09*	*0.09*	*0.00*	*0.01*	*0.52*	*2.97*
14-6a-t mt 1		0.00	0.12	0.51	0.11	36.59	55.10	6.19	0.00	0.16	1.08	0.03	0.02	99.91	68.42
14-6a-t mt 3-1		0.00	0.12	0.96	0.00	34.86	58.43	4.09	0.01	0.10	1.31	0.06	0.03	99.97	69.80
14-6a-t mt 3-2		0.00	0.11	0.75	0.00	34.71	59.36	3.81	0.01	0.11	1.32	0.01	0.03	100.22	70.42
14-6a-t mt 3-3		0.01	0.12	0.62	0.19	35.25	56.65	5.01	0.03	0.11	1.31	0.08	0.04	99.43	68.69
14-6a-t mt 4		0.00	0.12	1.52	0.00	36.25	56.49	5.18	0.02	0.14	1.18	0.13	0.09	101.12	69.26
MA14-6A-T	**Avg.**	**0.00**	**0.12**	**0.87**	**0.06**	**35.53**	**57.21**	**4.86**	**0.01**	**0.12**	**1.24**	**0.06**	**0.04**	**100.13**	**69.32**
Magnetite	*Std.*	*0.00*	*0.00*	*0.36*	*0.08*	*0.75*	*1.51*	*0.85*	*0.01*	*0.02*	*0.10*	*0.04*	*0.02*	*0.56*	*0.73*
14-6b mt 1		0.00	0.07	0.24	0.12	36.35	55.21	6.17	0.01	0.19	1.03	0.01	0.02	99.42	68.34
14-6b mt 2		0.00	0.07	0.67	0.26	37.83	51.84	7.78	0.01	0.25	1.06	0.02	0.01	99.79	66.75
14-6b mt 3		0.00	0.09	0.74	0.00	39.47	48.51	9.43	0.02	0.29	0.94	0.04	0.02	99.55	65.31
14-6b mt 4		0.00	0.05	0.47	0.09	42.41	42.04	12.89	0.01	0.37	0.94	0.02	0.00	99.28	62.34
14-6b mt 5		0.00	0.06	0.66	0.41	34.53	59.08	4.21	0.01	0.14	1.01	0.05	0.00	100.16	70.07
MA14-6B	**Avg.**	**0.00**	**0.07**	**0.56**	**0.18**	**38.12**	**51.34**	**8.10**	**0.01**	**0.25**	**1.00**	**0.03**	**0.01**	**99.64**	**66.56**
Magnetite	*Std.*	*0.00*	*0.01*	*0.18*	*0.14*	*2.70*	*5.82*	*2.96*	*0.00*	*0.08*	*0.05*	*0.01*	*0.01*	*0.31*	*2.64*
14-7a mt 2		0.00	0.09	0.06	0.00	31.31	67.25	0.29	0.04	0.03	0.98	0.00	0.02	100.07	74.17
14-7a mt 3		0.00	0.09	0.16	0.04	32.18	66.50	0.93	0.02	0.04	1.05	0.00	0.01	101.02	74.20
14-7a mt 4-1		0.00	0.07	0.01	0.00	31.32	67.69	0.18	0.03	0.01	1.02	0.01	0.03	100.37	74.52
14-7a mt 4-2		0.00	0.09	0.05	0.00	31.39	66.91	0.40	0.02	0.02	1.05	0.00	0.01	99.93	73.96
14-7a mt 6		0.00	0.09	0.11	0.05	31.50	66.11	0.72	0.03	0.03	0.93	0.00	0.00	99.57	73.42
MA14-7A	**Avg.**	**0.00**	**0.09**	**0.08**	**0.02**	**31.54**	**66.89**	**0.50**	**0.03**	**0.03**	**1.01**	**0.00**	**0.01**	**100.19**	**74.05**
Magnetite	*Std.*	*0.00*	*0.01*	*0.05*	*0.02*	*0.33*	*0.55*	*0.28*	*0.01*	*0.01*	*0.05*	*0.00*	*0.01*	*0.49*	*0.36*
14-7b mt 1-1		0.00	0.07	0.18	0.06	31.53	66.56	0.55	0.01	0.02	1.04	0.00	0.01	100.03	73.79
14-7b mt 1-2		0.00	0.10	0.13	0.00	33.05	63.20	2.27	0.01	0.06	1.04	0.02	0.00	99.88	72.24
14-7b mt 2		0.00	0.10	0.19	0.00	31.62	67.46	0.33	0.02	0.02	1.07	0.00	0.01	100.82	74.55
14-7b mt 5-1		0.00	0.07	0.01	0.15	31.61	67.23	0.56	0.02	0.02	1.09	0.02	0.00	100.79	74.37
14-7b mt 5-2		0.00	0.09	0.22	0.10	37.00	54.13	6.83	0.01	0.22	1.05	0.01	0.00	99.66	67.95
MA14-7B	**Avg.**	**0.00**	**0.09**	**0.15**	**0.06**	**32.96**	**63.72**	**2.11**	**0.01**	**0.07**	**1.06**	**0.01**	**0.00**	**100.24**	**72.58**
Magnetite	*Std.*	*0.00*	*0.01*	*0.07*	*0.06*	*2.10*	*5.03*	*2.46*	*0.00*	*0.08*	*0.02*	*0.01*	*0.00*	*0.48*	*2.45*
14-8a mt 10		0.01	0.22	0.06	0.00	36.19	57.00	5.56	0.01	0.23	1.23	0.02	0.04	100.57	69.62
14-8a mt 5		0.00	0.17	0.61	0.24	37.33	52.93	7.24	0.04	0.33	1.14	0.03	0.03	100.09	67.25
14-8a mt 6-1		0.01	0.21	1.26	0.48	39.48	47.47	9.80	0.03	0.43	0.93	0.06	0.03	100.20	64.51
14-8a mt 6-2		0.00	0.20	1.30	0.34	36.19	54.10	6.12	0.05	0.28	0.86	0.00	0.02	99.46	67.36
14-8a mt 7		0.00	0.16	0.16	0.00	35.17	58.78	4.56	0.01	0.21	1.10	0.00	0.01	100.16	70.29
14-8a mt 9		0.00	0.15	0.59	0.00	41.64	42.64	12.22	0.02	0.51	1.06	0.02	0.02	98.87	62.27
MA14-8A	**Avg.**	**0.00**	**0.19**	**0.66**	**0.18**	**37.67**	**52.15**	**7.58**	**0.03**	**0.33**	**1.05**	**0.02**	**0.03**	**99.89**	**66.88**
Magnetite	*Std.*	*0.00*	*0.03*	*0.48*	*0.19*	*2.23*	*5.54*	*2.64*	*0.01*	*0.11*	*0.12*	*0.02*	*0.01*	*0.56*	*2.78*
14-8b mt 3-1		0.00	0.18	0.14	0.08	38.25	51.81	8.15	0.03	0.35	1.05	0.00	0.02	100.06	67.02
14-8b mt 3-2		0.00	0.19	0.19	0.00	33.43	62.36	2.62	0.04	0.11	1.18	0.00	0.01	100.14	71.85

Analysis ID		CaO	Cr_2O_3	Al_2O_3	ZnO	FeO	Fe_2O_3	TiO_2	NiO	MnO	V_2O_3	MgO	SiO_2	Total	Total Fe (%):
14-8b mt 4		0.00	0.20	0.35	0.10	34.94	59.21	4.29	0.03	0.21	1.16	0.02	0.02	100.53	70.46
14-8b mt 6		0.00	0.17	0.09	0.10	34.40	59.32	3.96	0.01	0.19	1.48	0.01	0.02	99.75	70.17
14-8b mt 7		0.00	0.22	0.08	0.19	32.69	63.10	2.05	0.02	0.11	1.53	0.00	0.01	100.00	71.91
MA14-8B	**Avg.**	**0.00**	**0.19**	**0.17**	**0.09**	**34.74**	**59.16**	**4.21**	**0.03**	**0.19**	**1.28**	**0.01**	**0.02**	**100.10**	**70.28**
Magnetite	*Std.*	*0.00*	*0.02*	*0.10*	*0.06*	*1.92*	*4.00*	*2.13*	*0.01*	*0.09*	*0.19*	*0.01*	*0.00*	*0.25*	*1.78*
MA15-1_mt1		0.01	0.43	0.30	0.11	42.39	43.05	12.44	0.03	0.31	1.22	0.01	0.05	100.35	63.11
MA15-1_mt2		0.01	0.66	0.09	0.00	36.11	55.84	5.38	0.02	0.12	2.11	0.00	0.03	100.36	68.66
MA15-1_mt3		0.01	0.45	0.51	0.23	42.49	41.92	12.78	0.04	0.30	1.24	0.02	0.03	100.02	62.30
MA15-1_mt4		0.00	0.46	0.35	0.00	35.84	57.34	5.00	0.03	0.12	1.39	0.00	0.03	100.56	69.64
MA15-1_mt5		0.01	0.39	0.52	0.05	36.14	57.04	5.22	0.02	0.13	1.35	0.00	0.04	100.92	69.61
MA15-1_mt6		0.00	0.51	0.12	0.00	35.68	58.26	4.73	0.01	0.12	1.56	0.02	0.02	101.03	70.24
MA15-1	**Avg.**	**0.01**	**0.48**	**0.32**	**0.07**	**38.11**	**52.24**	**7.59**	**0.03**	**0.18**	**1.48**	**0.01**	**0.03**	**100.54**	**67.26**
Magnetite	*Std.*	*0.00*	*0.09*	*0.17*	*0.08*	*3.07*	*6.94*	*3.56*	*0.01*	*0.09*	*0.30*	*0.01*	*0.01*	*0.35*	*3.26*
MA15-2_mt2		0.01	0.03	2.62	0.01	33.44	60.92	2.51	0.04	0.11	1.07	0.48	0.07	101.30	70.74
MA15-2_mt4		0.00	0.01	2.63	0.05	33.76	59.94	3.05	0.04	0.09	0.89	0.53	0.06	101.06	70.20
MA15-2	**Avg.**	**0.01**	**0.02**	**2.63**	**0.03**	**33.60**	**60.43**	**2.78**	**0.04**	**0.10**	**0.98**	**0.51**	**0.07**	**101.18**	**70.47**
Magnetite	*Std.*	*0.01*	*0.01*	*0.00*	*0.02*	*0.16*	*0.49*	*0.27*	*0.00*	*0.01*	*0.09*	*0.03*	*0.01*	*0.12*	*0.27*
MA32-25_mt1		0.03	0.85	0.13	0.05	33.70	60.32	2.79	0.02	0.07	2.34	0.01	0.05	100.36	70.46
MA32-25_mt2		0.00	0.38	0.16	0.00	32.04	65.48	0.80	0.03	0.03	1.74	0.00	0.03	100.69	73.31
MA32-25_mt5		0.01	0.32	0.09	0.00	31.66	66.06	0.35	0.02	0.00	2.25	0.00	0.02	100.78	73.49
MA32-25_mt6		0.00	0.40	0.12	0.00	31.64	66.54	0.19	0.04	0.01	2.25	0.02	0.04	101.26	73.85
MA32-25	**Avg.**	**0.01**	**0.49**	**0.13**	**0.01**	**32.26**	**64.60**	**1.03**	**0.03**	**0.03**	**2.15**	**0.01**	**0.04**	**100.77**	**72.78**
Magnetite	*Std.*	*0.01*	*0.21*	*0.03*	*0.02*	*0.85*	*2.50*	*1.04*	*0.01*	*0.03*	*0.24*	*0.01*	*0.01*	*0.32*	*1.35*
32-1a mt 3-1		0.00	0.09	0.63	0.11	32.35	65.07	1.29	0.03	0.09	0.99	0.05	0.04	100.74	73.20
32-1a mt 3-2		0.00	0.09	0.52	0.20	32.22	66.21	1.03	0.04	0.05	0.92	0.03	0.02	101.33	74.00
32-1a mt 4-1		0.00	0.08	0.43	0.00	31.95	66.56	0.69	0.02	0.05	0.93	0.04	0.05	100.80	74.08
32-1a mt 4-2		0.00	0.08	0.23	0.19	31.49	66.61	0.54	0.01	0.04	1.02	0.01	0.04	100.26	73.80
MA32-1A	**Avg.**	**0.00**	**0.09**	**0.45**	**0.13**	**32.00**	**66.11**	**0.89**	**0.03**	**0.06**	**0.97**	**0.03**	**0.04**	**100.78**	**73.77**
Magnetite	*Std.*	*0.00*	*0.01*	*0.15*	*0.08*	*0.33*	*0.62*	*0.29*	*0.01*	*0.02*	*0.04*	*0.01*	*0.01*	*0.38*	*0.34*
32-1a mt 5		0.00	0.07	0.25	0.06	32.00	66.57	0.79	0.02	0.04	0.99	0.01	0.03	100.83	74.13
32-1c mt 1		0.00	0.04	0.42	0.00	31.69	66.90	0.43	0.04	0.01	1.13	0.01	0.01	100.67	74.17
32-1c mt 2-1		0.00	0.03	0.30	0.27	31.63	67.09	0.51	0.03	0.01	1.10	0.01	0.03	101.01	74.27
32-1c mt 2-2		0.00	0.05	0.32	0.16	31.66	67.34	0.42	0.01	0.02	1.08	0.02	0.02	101.10	74.49
32-1c mt 3		0.00	0.05	0.37	0.08	31.57	67.19	0.36	0.02	0.01	1.02	0.03	0.03	100.73	74.31
32-1c mt 4		0.00	0.05	0.31	0.00	31.93	65.49	0.95	0.04	0.02	1.15	0.03	0.03	100.00	73.24
MA32-1C	**Avg.**	**0.00**	**0.05**	**0.33**	**0.10**	**31.75**	**66.76**	**0.58**	**0.03**	**0.02**	**1.08**	**0.02**	**0.03**	**100.72**	**74.10**
Magnetite	*Std.*	*0.00*	*0.01*	*0.05*	*0.10*	*0.16*	*0.62*	*0.22*	*0.01*	*0.01*	*0.06*	*0.01*	*0.01*	*0.36*	*0.40*
32-2a-t mt 10		0.00	0.08	0.52	0.04	31.54	66.92	0.38	0.02	0.03	0.87	0.02	0.02	100.45	74.08
32-2a-t mt 6		0.01	0.07	0.92	0.00	31.33	65.45	0.49	0.03	0.04	0.85	0.03	0.02	99.24	72.79
32-2a-t mt 7		0.00	0.07	0.80	0.18	32.27	65.04	1.25	0.03	0.08	0.85	0.04	0.04	100.65	73.13
32-2a-t mt 8		0.00	0.10	0.46	0.00	31.85	67.07	0.43	0.02	0.01	0.99	0.01	0.04	100.98	74.41
32-2a-t mt 9		0.00	0.08	0.71	0.00	31.76	66.80	0.45	0.02	0.04	0.98	0.04	0.01	100.89	74.14
MA32-2A-T	**Avg.**	**0.00**	**0.08**	**0.68**	**0.04**	**31.75**	**66.26**	**0.60**	**0.02**	**0.04**	**0.91**	**0.03**	**0.03**	**100.44**	**73.71**
Magnetite	*Std.*	*0.00*	*0.01*	*0.17*	*0.07*	*0.32*	*0.84*	*0.33*	*0.00*	*0.02*	*0.06*	*0.01*	*0.01*	*0.63*	*0.63*

Analysis ID		CaO	Cr_2O_3	Al_2O_3	ZnO	FeO	Fe_2O_3	TiO_2	NiO	MnO	V_2O_3	MgO	SiO_2	Total	Total Fe (%):
32-2a-b mt 6-2		0.00	0.11	2.21	0.00	33.00	61.53	1.99	0.04	0.10	1.03	0.14	0.01	100.16	70.91
32-2a-b mt 10		0.00	0.07	2.09	0.05	34.39	58.30	3.77	0.04	0.15	0.97	0.24	0.03	100.10	69.37
32-2a-b mt 11-1		0.00	0.07	1.87	0.20	33.51	60.14	3.02	0.03	0.13	1.02	0.31	0.03	100.32	70.18
32-2a-b mt 11-2		0.00	0.09	1.64	0.03	33.91	61.10	2.76	0.03	0.11	1.00	0.06	0.02	100.75	71.21
MA32-2A-B-a	**Avg.**	**0.00**	**0.09**	**1.95**	**0.07**	**33.70**	**60.27**	**2.89**	**0.04**	**0.12**	**1.01**	**0.19**	**0.02**	**100.33**	**70.42**
Magnetite	*Std.*	*0.00*	*0.02*	*0.22*	*0.08*	*0.51*	*1.24*	*0.64*	*0.01*	*0.02*	*0.02*	*0.10*	*0.01*	*0.25*	*0.71*
32-2a-b mt 1 *(diss.px)*		0.00	0.09	2.70	0.14	33.64	60.38	2.52	0.03	0.13	0.86	0.10	0.02	100.61	70.46
32-2a-b mt 2 *(diss.px)*		0.00	0.10	1.50	0.09	33.04	62.44	2.18	0.03	0.10	0.70	0.14	0.02	100.34	71.64
32-2a-b mt 3 *(diss.px)*		0.01	0.07	2.00	0.15	33.80	60.35	3.01	0.02	0.12	0.76	0.19	0.02	100.50	70.55
32-2a-b mt 4 *(diss.px)*		0.00	0.11	3.41	0.00	34.49	58.27	3.27	0.02	0.18	0.70	0.15	0.03	100.63	69.42
MA32-2A-B-b	**Avg.**	**0.00**	**0.09**	**2.40**	**0.10**	**33.74**	**60.36**	**2.75**	**0.03**	**0.13**	**0.76**	**0.15**	**0.02**	**100.52**	**70.52**
Magnetite	*Std.*	*0.00*	*0.01*	*0.72*	*0.06*	*0.52*	*1.47*	*0.42*	*0.01*	*0.03*	*0.07*	*0.03*	*0.00*	*0.12*	*0.79*
32-2b mt 1-1		0.00	0.04	2.22	0.36	33.32	59.97	2.89	0.03	0.10	0.91	0.28	0.03	100.15	69.92
32-2b mt 1-2		0.00	0.04	2.35	0.17	33.80	59.30	3.12	0.02	0.12	0.94	0.22	0.03	100.11	69.73
32-2b mt 5		0.00	0.05	3.26	0.00	34.80	56.62	4.09	0.04	0.15	0.90	0.36	0.02	100.29	68.35
32-2b mt 6		0.00	0.06	2.67	0.13	34.33	58.19	3.93	0.04	0.15	0.89	0.57	0.03	100.99	69.24
32-2b mt 7		0.00	0.04	2.59	0.10	34.42	59.44	3.36	0.02	0.13	0.97	0.27	0.02	101.37	70.28
MA32-2B	**Avg.**	**0.00**	**0.05**	**2.62**	**0.15**	**34.13**	**58.70**	**3.48**	**0.03**	**0.13**	**0.92**	**0.34**	**0.03**	**100.58**	**69.50**
Magnetite	*Std.*	*0.00*	*0.01*	*0.36*	*0.12*	*0.52*	*1.19*	*0.46*	*0.01*	*0.02*	*0.03*	*0.12*	*0.00*	*0.51*	*0.67*
32-3 mt 2		0.00	0.07	0.55	0.00	31.72	67.09	0.43	0.03	0.07	0.99	0.03	0.01	100.99	74.33
32-3 mt 4		0.00	0.07	0.29	0.00	31.69	66.73	0.55	0.02	0.02	1.03	0.02	0.01	100.44	74.03
32-3 mt 6		0.00	0.06	0.48	0.03	31.32	67.00	0.21	0.03	0.01	1.05	0.03	0.02	100.24	73.98
32-3 mt 7		0.00	0.07	0.44	0.39	31.20	66.26	0.52	0.00	0.04	0.96	0.01	0.02	99.91	73.33
32-3 mt 8		0.00	0.08	0.59	0.16	31.31	67.08	0.21	0.01	0.02	0.92	0.01	0.02	100.41	74.04
MA32-3	**Avg.**	**0.00**	**0.07**	**0.47**	**0.12**	**31.45**	**66.83**	**0.38**	**0.02**	**0.03**	**0.99**	**0.02**	**0.02**	**100.40**	**73.94**
Magnetite	*Std.*	*0.00*	*0.01*	*0.10*	*0.15*	*0.21*	*0.31*	*0.15*	*0.01*	*0.02*	*0.05*	*0.01*	*0.00*	*0.35*	*0.33*
32-4-b mt 2		0.00	0.04	0.18	0.04	31.76	67.79	0.41	0.02	0.01	0.91	0.01	0.01	101.18	74.91
32-4-b mt 5		0.00	0.05	0.32	0.00	31.90	67.84	0.40	0.03	0.02	0.90	0.01	0.02	101.49	75.04
32-4-b mt 6		0.00	0.04	0.25	0.01	31.91	66.78	0.73	0.02	0.02	0.84	0.01	0.01	100.62	74.23
MA32-4	**Avg.**	**0.00**	**0.04**	**0.25**	**0.02**	**31.86**	**67.47**	**0.51**	**0.02**	**0.02**	**0.88**	**0.01**	**0.01**	**101.10**	**74.72**
Magnetite	*Std.*	*0.00*	*0.00*	*0.06*	*0.02*	*0.07*	*0.49*	*0.15*	*0.00*	*0.00*	*0.03*	*0.00*	*0.00*	*0.36*	*0.36*
MA32-7_mt1		0.00	0.04	0.54	0.09	32.56	62.77	2.05	0.04	0.06	1.04	0.10	0.04	99.33	71.56
MA32-7_mt2		0.00	0.07	3.69	0.61	33.39	57.73	3.64	0.05	0.16	0.91	0.87	0.04	101.15	68.23
MA32-7_mt3		0.00	0.07	0.29	0.00	31.71	65.50	0.87	0.04	0.02	1.03	0.05	0.04	99.62	73.09
MA32-7_mt4		0.01	0.05	1.08	0.10	35.55	54.91	5.66	0.05	0.19	1.07	0.23	0.05	98.95	67.55
MA32-7_mt5		0.01	0.06	3.14	0.37	34.55	54.43	4.94	0.04	0.19	1.04	0.61	0.04	99.42	66.47
MA32-7_mt6		0.00	0.06	2.49	0.15	32.74	61.24	2.40	0.05	0.10	1.08	0.71	0.05	101.08	70.50
MA32-7	**Avg.**	**0.00**	**0.06**	**1.87**	**0.22**	**33.42**	**59.43**	**3.26**	**0.05**	**0.12**	**1.03**	**0.43**	**0.04**	**99.93**	**69.57**
Magnetite	*Std.*	*0.00*	*0.01*	*1.30*	*0.21*	*1.29*	*4.07*	*1.67*	*0.01*	*0.07*	*0.06*	*0.32*	*0.00*	*0.86*	*2.34*
MA32-9_mt1		0.00	0.00	0.84	0.04	32.56	63.87	1.61	0.01	0.04	1.12	0.12	0.04	100.25	72.42
MA32-9_mt2		0.00	0.00	1.96	0.05	32.77	60.71	2.50	0.03	0.08	0.96	0.45	0.03	99.54	70.11
MA32-9_mt3		0.01	0.00	1.37	0.00	32.44	62.69	1.68	0.01	0.05	0.98	0.14	0.04	99.41	71.42
MA32-9_mt4		0.00	0.00	6.51	0.08	31.00	59.81	0.73	0.01	0.05	0.97	1.24	0.03	100.43	68.17
MA32-9_mt5		0.00	0.00	2.02	0.05	33.41	59.11	3.27	0.02	0.09	0.96	0.51	0.05	99.49	69.31

Analysis ID		CaO	Cr_2O_3	Al_2O_3	ZnO	FeO	Fe_2O_3	TiO_2	NiO	MnO	V_2O_3	MgO	SiO_2	Total	Total Fe (%):
MA32-9_mt6		0.00	0.00	5.19	0.16	33.95	54.71	4.11	0.01	0.13	0.93	1.12	0.05	100.36	66.27
MA32-9	**Avg.**	**0.00**	**0.00**	**2.54**	**0.04**	**32.44**	**61.24**	**1.96**	**0.02**	**0.06**	**1.00**	**0.49**	**0.04**	**99.82**	**70.29**
Magnetite	*Std.*	*0.00*	*0.00*	*2.10*	*0.05*	*0.92*	*2.93*	*1.12*	*0.01*	*0.03*	*0.06*	*0.44*	*0.01*	*0.44*	*2.03*
MA32-12_mt2		0.01	0.01	6.59	0.06	37.61	45.82	7.45	0.04	0.22	0.92	0.71	0.04	99.48	61.92
MA32-12_mt4		0.01	0.02	2.46	0.00	37.42	50.55	7.52	0.01	0.18	0.96	0.53	0.04	99.70	65.46
MA32-12_mt5		0.00	0.00	1.71	0.00	38.33	48.62	8.66	0.03	0.22	0.98	0.36	0.04	98.95	64.60
MA32-12	**Avg.**	**0.01**	**0.01**	**3.59**	**0.02**	**37.79**	**48.33**	**7.88**	**0.03**	**0.21**	**0.95**	**0.53**	**0.04**	**99.38**	**63.99**
Magnetite	*Std.*	*0.00*	*0.01*	*2.15*	*0.03*	*0.39*	*1.94*	*0.55*	*0.01*	*0.02*	*0.02*	*0.14*	*0.00*	*0.31*	*1.51*
MA32-15-mt1		0.00	0.00	2.29	0.08	31.05	63.87	0.76	0.04	0.02	1.12	0.68	0.06	99.97	71.36
MA32-15-mt2		0.01	0.00	0.98	0.00	31.80	64.84	1.05	0.03	0.03	1.17	0.30	0.04	100.25	72.64
MA32-15-mt3		0.00	0.01	0.69	0.09	32.06	64.69	1.42	0.05	0.04	1.12	0.31	0.04	100.52	72.71
MA32-15-mt4		0.00	0.01	0.68	0.05	32.30	64.21	1.63	0.03	0.06	1.15	0.29	0.04	100.45	72.50
MA32-15-mt5		0.00	0.01	0.44	0.03	32.28	64.50	1.56	0.04	0.04	1.09	0.25	0.07	100.30	72.71
MA32-15	**Avg.**	**0.00**	**0.01**	**1.02**	**0.05**	**31.90**	**64.42**	**1.28**	**0.04**	**0.04**	**1.13**	**0.37**	**0.05**	**100.30**	**72.38**
Magnetite	*Std.*	*0.00*	*0.00*	*0.66*	*0.03*	*0.46*	*0.35*	*0.33*	*0.01*	*0.01*	*0.03*	*0.16*	*0.01*	*0.19*	*0.52*
MA32-17-mt1		0.01	0.01	3.56	0.08	34.72	53.27	5.58	0.04	0.14	1.15	1.28	0.08	99.92	65.69
MA32-17-mt2		0.00	0.00	2.16	0.08	33.34	59.04	3.56	0.03	0.09	1.29	0.94	0.04	100.57	69.21
MA32-17-mt3		0.00	0.00	1.03	0.03	33.72	59.23	3.68	0.04	0.10	1.26	0.45	0.04	99.58	69.62
MA32-17-mt4		0.01	0.00	2.93	0.12	34.76	54.29	5.36	0.04	0.13	1.22	0.99	0.04	99.89	66.51
MA32-17-mt5		0.00	0.01	1.88	0.14	33.82	58.72	3.75	0.05	0.09	1.23	0.63	0.05	100.36	69.30
MA32-17	**Avg.**	**0.00**	**0.00**	**2.31**	**0.09**	**34.07**	**56.91**	**4.39**	**0.04**	**0.11**	**1.23**	**0.86**	**0.05**	**100.06**	**68.07**
Magnetite	*Std.*	*0.00*	*0.00*	*0.87*	*0.04*	*0.57*	*2.58*	*0.89*	*0.01*	*0.02*	*0.05*	*0.29*	*0.02*	*0.35*	*1.63*
MA32-18_mt1		0.00	0.16	1.54	0.08	31.97	64.05	0.84	0.04	0.01	1.20	0.08	0.07	100.04	72.15
MA32-18_mt2		0.01	0.13	0.95	0.00	31.84	63.71	1.08	0.02	0.02	1.19	0.05	0.03	99.02	71.79
MA32-18_mt3		0.00	0.17	0.69	0.06	32.46	63.12	1.61	0.01	0.04	1.19	0.02	0.07	99.43	71.77
MA32-18_mt5		0.02	0.17	5.29	0.01	32.98	59.07	1.68	0.05	0.07	1.09	0.53	0.06	101.02	68.98
MA32-18-a	**Avg.**	**0.01**	**0.16**	**2.12**	**0.04**	**32.31**	**62.49**	**1.30**	**0.03**	**0.04**	**1.17**	**0.17**	**0.06**	**99.88**	**71.17**
Magnetite	*Std.*	*0.01*	*0.02*	*1.86*	*0.03*	*0.45*	*2.00*	*0.35*	*0.02*	*0.02*	*0.04*	*0.21*	*0.02*	*0.75*	*1.27*
MA32-18_mt7		0.01	0.23	3.14	0.08	34.26	57.86	3.56	0.03	0.09	1.05	0.50	0.04	100.86	68.94
MA32-18_mt8		0.01	0.20	1.22	0.04	33.74	59.84	3.19	0.03	0.08	1.00	0.18	0.05	99.58	70.11
MA32-18_mt9		0.00	0.19	5.95	0.06	36.71	48.71	6.58	0.02	0.18	1.33	1.04	0.06	100.83	63.54
MA32-18-b	**Avg.**	**0.01**	**0.21**	**3.44**	**0.06**	**34.90**	**55.47**	**4.44**	**0.03**	**0.12**	**1.13**	**0.57**	**0.05**	**100.42**	**67.53**
Magnetite	*Std.*	*0.00*	*0.02*	*1.94*	*0.02*	*1.30*	*4.85*	*1.52*	*0.00*	*0.04*	*0.15*	*0.35*	*0.01*	*0.60*	*2.86*
MA32-18_mt12		0.00	0.15	3.15	0.03	34.74	56.20	4.20	0.03	0.12	1.08	0.48	0.05	100.23	67.98
MA32-18_mt13		0.00	0.13	1.30	0.00	33.24	62.50	2.12	0.02	0.04	0.98	0.11	0.05	100.49	71.83
MA32-18-c	**Avg.**	**0.00**	**0.14**	**2.23**	**0.02**	**33.99**	**59.35**	**3.16**	**0.03**	**0.08**	**1.03**	**0.30**	**0.05**	**100.36**	**69.91**
Magnetite	*Std.*	*0.00*	*0.01*	*0.92*	*0.02*	*0.75*	*3.15*	*1.04*	*0.01*	*0.04*	*0.05*	*0.19*	*0.00*	*0.13*	*1.92*
MA32-19_mt1		0.02	0.67	0.86	0.02	39.67	45.95	9.39	0.03	0.21	1.30	0.06	0.40	98.58	63.46
MA32-19_mt2		0.00	0.68	1.29	0.04	35.14	55.35	4.62	0.03	0.08	1.43	0.02	0.08	98.76	67.60
MA32-19_mt4		0.05	0.54	0.73	0.03	34.49	57.27	3.57	0.02	0.07	1.56	0.05	0.44	98.82	68.64
MA32-19_mt5		0.00	0.44	0.81	0.06	32.50	61.19	1.95	0.04	0.04	1.46	0.00	0.05	98.54	70.29
MA32-19_mt6		0.01	0.43	0.71	0.03	35.80	54.46	5.29	0.03	0.12	1.38	0.01	0.26	98.53	67.37
MA32-19	**Avg.**	**0.02**	**0.55**	**0.88**	**0.04**	**35.52**	**54.84**	**4.96**	**0.03**	**0.10**	**1.43**	**0.03**	**0.25**	**98.65**	**67.47**
Magnetite	*Std.*	*0.02*	*0.11*	*0.21*	*0.01*	*2.35*	*5.01*	*2.48*	*0.01*	*0.06*	*0.09*	*0.02*	*0.16*	*0.12*	*2.26*

Analysis ID		CaO	Cr_2O_3	Al_2O_3	ZnO	FeO	Fe_2O_3	TiO_2	NiO	MnO	V_2O_3	MgO	SiO_2	Total	Total Fe (%):
MA11-11_mt1		0.00	0.16	3.38	0.03	35.86	50.75	6.56	0.04	0.23	1.27	0.93	0.05	99.26	64.53
MA11-11_mt2		0.00	0.20	4.32	0.02	36.46	47.93	7.55	0.07	0.23	1.18	1.23	0.05	99.24	62.76
MA11-11_mt3		0.00	0.19	3.31	0.02	36.79	49.13	7.51	0.04	0.27	1.27	0.91	0.04	99.48	63.92
MA11-11_mt4		0.00	0.18	2.70	0.05	36.06	52.09	6.43	0.05	0.20	1.28	0.74	0.03	99.81	65.71
MA11-11_mt5		0.00	0.21	2.87	0.00	37.00	49.17	7.72	0.07	0.22	1.27	0.88	0.05	99.47	64.10
MA11-11	**Avg.**	**0.00**	**0.19**	**3.32**	**0.02**	**36.43**	**49.81**	**7.15**	**0.05**	**0.23**	**1.25**	**0.94**	**0.04**	**99.45**	**64.20**
Magnetite	*Std.*	*0.00*	*0.02*	*0.56*	*0.02*	*0.43*	*1.45*	*0.54*	*0.01*	*0.02*	*0.04*	*0.16*	*0.01*	*0.21*	*0.96*
MA11-8-mt1		0.01	0.03	3.12	0.07	36.59	52.38	5.93	0.04	0.21	0.86	0.36	0.29	99.89	66.31
MA11-8-mt2		0.00	0.01	2.76	0.04	36.25	53.86	5.61	0.03	0.19	0.92	0.45	0.25	100.38	67.22
MA11-8-mt3		0.00	0.04	2.92	0.07	35.67	53.74	5.75	0.04	0.21	0.95	0.76	0.12	100.27	66.72
MA11-8-mt4		0.00	0.03	2.17	0.12	35.10	56.30	4.82	0.06	0.16	1.00	0.43	0.07	100.26	68.31
MA11-8-mt5		0.00	0.03	3.04	0.04	37.01	50.81	7.20	0.03	0.25	0.93	0.72	0.08	100.14	65.38
MA11-8	**Avg.**	**0.00**	**0.03**	**2.80**	**0.07**	**36.12**	**53.42**	**5.86**	**0.04**	**0.20**	**0.93**	**0.54**	**0.16**	**100.19**	**66.79**
Magnetite	*Std.*	*0.00*	*0.01*	*0.34*	*0.03*	*0.67*	*1.82*	*0.77*	*0.01*	*0.03*	*0.05*	*0.16*	*0.09*	*0.17*	*0.97*
MA11-2-mt1		0.00	0.01	3.91	0.02	37.01	51.50	6.58	0.03	0.17	1.12	0.71	0.08	101.14	65.92
MA11-2-mt3		0.00	0.01	4.01	0.08	36.29	52.57	6.04	0.05	0.15	1.05	0.82	0.07	101.14	66.24
MA11-2-mt4		0.00	0.02	4.29	0.04	35.66	53.14	5.37	0.03	0.12	1.14	0.85	0.09	100.75	66.25
MA11-2-mt6		0.00	0.01	3.50	0.05	36.94	50.63	7.14	0.04	0.19	1.06	0.90	0.09	100.55	65.19
MA11-2	**Avg.**	**0.00**	**0.01**	**3.93**	**0.05**	**36.48**	**51.96**	**6.28**	**0.04**	**0.16**	**1.09**	**0.82**	**0.08**	**100.90**	**65.90**
Magnetite	*Std.*	*0.00*	*0.00*	*0.28*	*0.02*	*0.55*	*0.97*	*0.65*	*0.01*	*0.03*	*0.04*	*0.07*	*0.01*	*0.26*	*0.43*
MA11-2-alt_Mt-1		0.01	0.01	3.02	0.26	36.30	51.66	6.09	0.01	0.15	1.12	0.09	0.08	98.73	65.54
MA11-2-alt_Mt-3		0.00	0.00	2.71	0.05	32.44	61.21	1.55	0.03	0.04	1.10	0.12	0.06	99.25	70.27
MA11-2-alt_Mt-4		0.01	0.00	5.03	0.21	37.94	47.08	7.56	0.03	0.19	0.89	0.22	0.10	99.17	63.13
MA11-2-alt_Mt-5		0.03	0.02	4.93	0.16	37.74	47.85	7.28	0.02	0.18	0.89	0.23	0.09	99.33	63.59
MA11-2 (Altered	**Avg.**	**0.01**	**0.01**	**3.92**	**0.17**	**36.11**	**51.95**	**5.62**	**0.02**	**0.14**	**1.00**	**0.17**	**0.08**	**99.12**	**65.63**
Magnetite	*Std.*	*0.01*	*0.01*	*1.06*	*0.08*	*2.21*	*5.62*	*2.41*	*0.01*	*0.06*	*0.11*	*0.06*	*0.02*	*0.23*	*2.82*
MA03-7-mt1		0.00	0.39	0.12	0.00	31.03	66.11	0.25	0.01	0.01	1.26	0.01	0.14	99.18	73.09
MA03-7-mt2		0.00	0.43	0.05	0.00	30.98	65.94	0.32	0.04	0.02	1.17	0.00	0.16	98.95	72.92
MA03-7-mt3		0.00	0.38	0.03	0.02	30.86	66.74	0.07	0.03	0.02	1.20	0.00	0.14	99.35	73.46
MA03-7-mt4		0.00	0.39	0.06	0.06	31.24	66.94	0.26	0.02	0.02	1.12	0.01	0.06	100.12	73.88
MA03-7-mt5		0.00	0.36	0.06	0.00	31.12	66.99	0.14	0.01	0.01	1.11	0.00	0.07	99.80	73.84
MA03-7-mt6		0.01	0.40	0.05	0.02	31.31	66.69	0.39	0.04	0.03	1.01	0.00	0.08	99.95	73.74
MA03-7-mt7		0.00	0.35	0.13	0.02	31.20	67.29	0.17	0.03	0.01	0.91	0.01	0.10	100.12	74.13
MA03-7	**Avg.**	**0.00**	**0.39**	**0.07**	**0.02**	**31.11**	**66.67**	**0.23**	**0.03**	**0.02**	**1.11**	**0.00**	**0.11**	**99.64**	**73.58**
Magnetite	*Std.*	*0.00*	*0.02*	*0.04*	*0.02*	*0.15*	*0.45*	*0.10*	*0.01*	*0.01*	*0.11*	*0.00*	*0.04*	*0.44*	*0.41*
MA03-4-mt1		0.00	0.33	0.34	0.00	31.85	66.36	0.67	0.05	0.02	1.03	0.02	0.06	100.67	73.86
MA03-4-mt2		0.00	0.32	0.24	0.04	38.23	51.67	8.06	0.05	0.22	1.05	0.02	0.04	99.90	66.90
MA03-4-mt3		0.00	0.38	1.34	0.01	31.97	64.07	0.81	0.05	0.01	1.35	0.01	0.05	100.00	72.16
MA03-4-mt4		0.01	0.47	0.28	0.00	31.78	66.15	0.58	0.05	0.02	1.32	0.00	0.05	100.66	73.65
MA03-4-mt5		0.01	0.40	0.85	0.00	33.15	62.55	2.09	0.04	0.05	1.18	0.00	0.03	100.32	71.81
MA03-4-mt6		0.00	0.37	0.92	0.06	34.91	57.18	4.47	0.05	0.11	1.32	0.06	0.03	99.45	68.86
MA03-4	**Avg.**	**0.00**	**0.38**	**0.66**	**0.02**	**33.65**	**61.33**	**2.78**	**0.05**	**0.07**	**1.21**	**0.02**	**0.04**	**100.17**	**71.21**
Magnetite	*Std.*	*0.00*	*0.05*	*0.41*	*0.02*	*2.32*	*5.29*	*2.72*	*0.00*	*0.07*	*0.13*	*0.02*	*0.01*	*0.43*	*2.53*
MA03-1B_mt1		0.00	1.46	4.87	0.04	38.48	43.41	9.04	0.04	0.21	1.24	1.06	0.06	99.91	60.66

Analysis ID		CaO	Cr_2O_3	Al_2O_3	ZnO	FeO	Fe_2O_3	TiO_2	NiO	MnO	V_2O_3	MgO	SiO_2	Total	Total Fe (%):
MA03-1B_mt2		0.00	1.57	4.28	0.07	38.61	42.76	9.34	0.07	0.21	1.18	0.87	0.06	99.02	60.24
MA03-1B_mt3		0.01	1.30	4.74	0.02	39.02	42.05	9.52	0.05	0.26	1.22	0.78	0.07	99.04	59.98
MA03-1B_mt4		0.01	1.35	4.86	0.00	37.92	44.79	8.22	0.06	0.21	1.24	0.97	0.14	99.77	61.34
MA03-1B_mt5		0.00	1.48	5.11	0.04	38.62	41.84	9.35	0.06	0.22	1.23	1.00	0.08	99.03	59.53
MA03-1B	**Avg.**	**0.00**	**1.43**	**4.77**	**0.03**	**38.53**	**42.97**	**9.09**	**0.06**	**0.22**	**1.22**	**0.94**	**0.08**	**99.35**	**60.35**
Magnetite	*Std.*	*0.00*	*0.10*	*0.27*	*0.02*	*0.35*	*1.07*	*0.46*	*0.01*	*0.02*	*0.02*	*0.10*	*0.03*	*0.40*	*0.61*
MA03-1A-mt1		0.00	0.36	1.63	0.00	34.08	56.89	3.89	0.04	0.10	1.31	0.27	0.07	98.64	68.06
MA03-1A-mt2		0.02	0.45	4.77	0.07	32.18	58.40	1.65	0.07	0.06	1.49	0.76	0.09	100.01	67.90
MA03-1A-mt3		0.00	0.41	2.87	0.03	38.92	45.26	9.34	0.05	0.23	1.19	0.50	0.07	98.86	62.40
MA03-1A-mt4		0.00	0.39	2.73	0.03	37.09	49.38	7.32	0.05	0.17	1.24	0.53	0.08	99.01	64.32
MA03-1A-mt5		0.01	0.36	2.52	0.04	31.95	61.61	1.19	0.07	0.05	1.47	0.41	0.14	99.81	70.24
MA03-1A-mt6		0.01	0.48	5.16	0.00	35.24	49.43	5.72	0.06	0.14	1.28	0.99	0.09	98.60	63.07
MA03-1A	**Avg.**	**0.01**	**0.42**	**3.61**	**0.03**	**35.08**	**52.82**	**5.04**	**0.06**	**0.13**	**1.33**	**0.64**	**0.09**	**99.26**	**65.59**
Magnetite	*Std.*	*0.01*	*0.04*	*1.26*	*0.02*	*2.51*	*5.81*	*2.93*	*0.01*	*0.06*	*0.11*	*0.24*	*0.02*	*0.55*	*2.89*
T3-C4-1-mt1		0.00	0.00	3.23	0.13	37.34	49.26	7.50	0.03	0.18	1.08	0.53	0.07	99.36	64.41
T3-C4-1-mt2		0.01	0.00	3.36	0.19	38.31	46.83	8.71	0.01	0.21	1.01	0.60	0.08	99.32	63.19
T3-C4-1-mt3		0.00	0.00	3.51	0.10	39.50	43.95	10.04	0.03	0.25	0.98	0.64	0.10	99.10	61.79
T3-C4-1-mt4		0.00	0.00	4.07	0.04	38.46	46.61	8.65	0.03	0.26	1.08	0.74	0.08	100.02	63.13
T3-C4-1-mt5		0.00	0.00	4.22	0.06	37.83	47.74	7.87	0.04	0.23	0.96	0.66	0.11	99.72	63.57
T3-C4-1	**Avg.**	**0.00**	**0.00**	**3.68**	**0.10**	**38.29**	**46.88**	**8.55**	**0.03**	**0.23**	**1.02**	**0.63**	**0.09**	**99.50**	**63.22**
Magnetite	*Std.*	*0.00*	*0.00*	*0.39*	*0.05*	*0.72*	*1.74*	*0.87*	*0.01*	*0.03*	*0.05*	*0.07*	*0.01*	*0.33*	*0.85*
T3-C4-2-mt1		0.00	0.00	3.84	0.02	37.01	49.62	6.96	0.03	0.22	1.09	0.55	0.08	99.42	64.45
T3-C4-2-mt2		0.00	0.00	3.55	0.11	37.80	48.79	7.84	0.03	0.18	1.02	0.63	0.08	100.03	64.36
T3-C4-2-mt3		0.00	0.02	3.05	0.07	38.49	47.62	8.64	0.02	0.18	1.05	0.61	0.09	99.84	63.93
T3-C4-2-mt4		0.00	0.00	4.42	0.14	39.47	44.66	9.57	0.02	0.26	0.99	0.68	0.08	100.28	62.32
T3-C4-2-mt5		0.00	0.03	3.55	0.03	38.19	47.26	8.46	0.01	0.19	0.94	0.66	0.06	99.37	63.45
T3-C4-2	**Avg.**	**0.00**	**0.01**	**3.68**	**0.07**	**38.19**	**47.59**	**8.29**	**0.02**	**0.21**	**1.02**	**0.63**	**0.08**	**99.79**	**63.70**
Magnetite	*Std.*	*0.00*	*0.01*	*0.45*	*0.05*	*0.81*	*1.69*	*0.87*	*0.01*	*0.03*	*0.05*	*0.04*	*0.01*	*0.35*	*0.78*
TA1-1_mt1		0.00	0.01	3.48	0.00	40.14	42.39	10.88	0.03	0.25	0.92	0.67	0.03	98.80	61.02
TA1-1_mt2		0.00	0.03	4.08	0.06	39.55	42.86	10.43	0.02	0.23	0.85	0.86	0.02	98.99	60.98
TA1-1_mt3		0.00	0.02	3.16	0.00	40.19	42.93	10.83	0.03	0.23	0.91	0.61	0.03	98.94	61.48
TA1-1_mt4		0.00	0.03	3.30	0.06	39.46	44.65	10.00	0.02	0.28	0.89	0.63	0.04	99.35	62.30
TA1-1_mt5		0.01	0.03	3.85	0.03	39.96	42.01	11.09	0.02	0.28	0.87	0.95	0.00	99.10	60.60
TA1-1	**Avg.**	**0.00**	**0.02**	**3.57**	**0.03**	**39.86**	**42.97**	**10.65**	**0.02**	**0.25**	**0.89**	**0.74**	**0.02**	**99.04**	**61.28**
Magnetite	*Std.*	*0.00*	*0.01*	*0.34*	*0.03*	*0.30*	*0.90*	*0.39*	*0.00*	*0.02*	*0.03*	*0.14*	*0.01*	*0.18*	*0.58*
TA1-4_mt1		0.00	0.00	3.52	0.04	39.89	42.27	11.07	0.03	0.32	0.86	0.91	0.03	98.93	60.76
TA1-4_mt2		0.01	0.01	3.63	0.01	40.28	42.64	11.20	0.04	0.27	0.87	0.98	0.02	99.95	61.32
TA1-4_mt3		0.01	0.00	4.18	0.10	40.09	41.34	11.27	0.03	0.25	0.86	1.04	0.04	99.21	60.17
TA1-4_mt4		0.00	0.02	3.86	0.06	39.82	42.15	11.07	0.03	0.26	0.84	1.09	0.04	99.23	60.61
TA1-4_mt5		0.00	0.03	3.50	0.02	40.54	40.80	11.86	0.03	0.25	0.86	1.02	0.03	98.94	60.07
TA1-4	**Avg.**	**0.00**	**0.01**	**3.74**	**0.05**	**40.12**	**41.84**	**11.29**	**0.03**	**0.27**	**0.86**	**1.01**	**0.03**	**99.25**	**60.58**
Magnetite	*Std.*	*0.00*	*0.01*	*0.26*	*0.03*	*0.26*	*0.67*	*0.29*	*0.00*	*0.03*	*0.01*	*0.06*	*0.01*	*0.37*	*0.45*
TA1-5_mt1		0.00	0.03	3.78	0.06	40.21	42.14	10.92	0.02	0.22	0.91	0.73	0.04	99.06	60.88
TA1-5_mt2		0.01	0.04	3.82	0.08	40.23	42.34	10.94	0.03	0.23	0.95	0.81	0.05	99.53	61.05

Analysis ID		CaO	Cr_2O_3	Al_2O_3	ZnO	FeO	Fe_2O_3	TiO_2	NiO	MnO	V_2O_3	MgO	SiO_2	Total	Total Fe (%):
TA1-5_mt3		0.01	0.05	4.26	0.06	40.22	41.95	11.03	0.05	0.26	0.88	0.93	0.04	99.74	60.74
TA1-5_mt4		0.01	0.05	4.43	0.06	40.02	42.00	10.75	0.02	0.24	0.94	0.87	0.03	99.42	60.64
TA1-5_mt5		0.00	0.03	4.24	0.01	39.72	43.84	10.06	0.05	0.24	0.96	0.76	0.04	99.95	61.86
TA1-6	**Avg.**	**0.01**	**0.04**	**4.11**	**0.05**	**40.08**	**42.45**	**10.74**	**0.03**	**0.24**	**0.93**	**0.82**	**0.04**	**99.54**	**61.03**
Magnetite	*Std.*	0.00	0.01	0.26	0.02	0.20	0.71	0.35	0.01	0.01	0.03	0.07	0.01	0.30	0.44
TA1-6-mt1		0.00	0.00	4.62	0.05	40.01	40.83	11.14	0.05	0.28	0.90	1.04	0.06	98.98	59.72
TA1-6-mt2		0.01	0.04	3.83	0.00	38.95	43.58	9.95	0.05	0.25	1.03	0.91	0.07	98.67	61.12
TA1-6-mt3		0.00	0.00	3.84	0.03	39.07	43.83	9.94	0.03	0.24	0.96	0.89	0.08	98.91	61.39
TA1-6-mt4		0.00	0.00	4.95	0.06	41.17	38.25	12.49	0.02	0.32	0.92	1.21	0.05	99.44	58.53
TA1-6-mt5		0.00	0.02	2.23	0.05	42.18	40.26	13.09	0.02	0.33	0.89	0.69	0.06	99.82	60.79
TA1-6	**Avg.**	**0.00**	**0.01**	**3.89**	**0.04**	**40.28**	**41.35**	**11.32**	**0.03**	**0.28**	**0.94**	**0.95**	**0.06**	**99.16**	**60.31**
Magnetite	*Std.*	*0.00*	*0.02*	*0.94*	*0.02*	*1.24*	*2.11*	*1.29*	*0.01*	*0.04*	*0.05*	*0.17*	*0.01*	*0.41*	*1.06*
TA2-1-mt1		0.01	0.00	4.01	0.11	39.36	45.74	9.54	0.03	0.21	1.00	0.87	0.09	100.96	63.08
TA2-1-mt2		0.00	0.01	4.31	0.00	39.43	44.91	9.59	0.04	0.31	0.96	0.77	0.08	100.41	62.49
TA2-1-mt3		0.00	0.00	4.18	0.09	38.18	47.54	8.35	0.04	0.29	1.04	0.87	0.12	100.70	63.66
TA2-1-mt4		0.00	0.04	3.69	0.03	38.69	47.20	8.71	0.03	0.45	1.05	0.69	0.17	100.75	63.75
TA2-1-mt5		0.00	0.00	2.36	0.00	39.56	45.28	9.99	0.03	0.25	1.02	0.50	0.10	99.10	62.86
TA2-1	**Avg.**	**0.00**	**0.01**	**3.71**	**0.05**	**39.04**	**46.13**	**9.24**	**0.03**	**0.30**	**1.01**	**0.74**	**0.11**	**100.38**	**63.17**
Magnetite	*Std.*	*0.00*	*0.02*	*0.71*	*0.05*	*0.53*	*1.05*	*0.61*	*0.00*	*0.08*	*0.03*	*0.14*	*0.03*	*0.67*	*0.48*
TA2-3-mt1		0.00	0.00	3.72	0.04	38.99	46.72	9.12	0.03	0.25	0.95	0.82	0.11	100.75	63.59
TA2-3-mt2		0.02	0.03	3.26	0.01	40.63	43.00	11.06	0.03	0.30	0.86	0.73	0.14	100.08	61.84
TA2-3-mt3		0.01	0.02	3.98	0.02	38.91	46.55	9.03	0.03	0.38	0.94	0.79	0.13	100.79	63.40
TA2-3-mt4		0.00	0.00	3.48	0.03	39.39	44.85	9.91	0.04	0.28	0.86	0.77	0.10	99.71	62.41
TA2-3-mt5		0.00	0.01	3.84	0.01	39.27	45.89	9.49	0.06	0.40	0.90	0.75	0.09	100.71	63.14
TA2-3	**Avg.**	**0.01**	**0.01**	**3.66**	**0.02**	**39.44**	**45.40**	**9.72**	**0.04**	**0.32**	**0.90**	**0.77**	**0.11**	**100.41**	**62.87**
Magnetite	*Std.*	*0.01*	*0.01*	*0.26*	*0.01*	*0.62*	*1.37*	*0.74*	*0.01*	*0.06*	*0.04*	*0.03*	*0.02*	*0.44*	*0.65*
TA2-4-mt1		0.01	0.01	4.13	0.10	39.03	45.41	9.36	0.02	0.47	0.95	0.69	0.09	100.27	62.59
TA2-4-mt2		0.00	0.02	3.92	0.00	38.80	47.15	8.82	0.03	0.40	0.83	0.65	0.06	100.67	63.79
TA2-4-mt3		0.00	0.03	3.87	0.02	38.95	46.29	9.09	0.04	0.34	0.89	0.64	0.06	100.22	63.22
TA2-4-mt4		0.01	0.00	3.31	0.02	41.16	42.81	11.51	0.03	0.29	0.78	0.73	0.06	100.71	62.06
TA2-4-mt5		0.00	0.02	3.80	0.00	39.41	45.81	9.51	0.03	0.33	0.91	0.68	0.06	100.56	63.17
TA2-4	**Avg.**	**0.00**	**0.02**	**3.81**	**0.03**	**39.47**	**45.49**	**9.66**	**0.03**	**0.37**	**0.87**	**0.68**	**0.07**	**100.49**	**62.97**
Magnetite	*Std.*	*0.00*	*0.01*	*0.27*	*0.04*	*0.87*	*1.46*	*0.96*	*0.01*	*0.06*	*0.06*	*0.03*	*0.01*	*0.20*	*0.59*
TA2-6-mt1		0.00	0.00	3.89	0.00	37.17	50.25	7.10	0.05	0.29	0.95	0.68	0.06	100.43	65.06
TA2-6-mt2		0.00	0.00	4.29	0.00	39.04	45.72	9.28	0.05	0.31	0.92	0.84	0.07	100.52	62.84
TA2-6-mt3		0.00	0.01	3.80	0.00	39.56	45.58	9.70	0.03	0.24	0.91	0.78	0.06	100.67	63.10
TA2-6-mt4		0.00	0.01	4.07	0.06	38.69	46.51	9.04	0.03	0.58	0.86	0.69	0.05	100.59	63.21
TA2-6-mt5		0.00	0.00	4.01	0.06	40.14	43.43	10.47	0.02	0.27	0.80	0.68	0.05	99.93	61.83
TA2-6-mt6		0.00	0.00	2.99	0.00	39.62	45.41	9.92	0.04	0.22	0.88	0.57	0.04	99.69	63.01
TA2-6	**Avg.**	**0.00**	**0.00**	**3.84**	**0.02**	**39.04**	**46.15**	**9.25**	**0.04**	**0.32**	**0.89**	**0.71**	**0.06**	**100.31**	**63.17**
Magnetite	*Std.*	*0.00*	*0.00*	*0.41*	*0.03*	*0.95*	*2.06*	*1.07*	*0.01*	*0.12*	*0.05*	*0.09*	*0.01*	*0.36*	*0.96*

Analysis ID		CaO	Cr_2O_3	Al_2O_3	ZnO	FeO	Fe_2O_3	TiO_2	NiO	MnO	V_2O_3	MgO	SiO_2	Total	Total Fe (%):
14-2a ilm 1-1		0.00	0.00	0.09	0.00	46.83		50.76	0.00	0.82	0.02	0.71	0.00	99.23	32.75
14-2a ilm 1-2		0.00	0.00	0.06	0.00	47.38		51.10	0.00	0.80	0.00	0.64	0.00	99.98	33.14
14-2a ilm 3		0.00	0.00	0.02	0.00	47.22		50.66	0.00	0.74	0.01	0.44	0.00	99.09	33.03
14-2a ilm 4		0.01	0.01	0.07	0.03	47.48		51.24	0.00	0.74	0.02	0.54	0.00	100.14	33.21
14-2a ilm 5		0.00	0.02	0.08	0.01	47.17		50.91	0.00	0.80	0.00	0.65	0.00	99.64	32.99
MA14-2A	**Avg.**	**0.00**	**0.01**	**0.06**	**0.01**	**47.22**		**50.93**	**0.00**	**0.78**	**0.01**	**0.60**	**0.00**	**99.62**	**33.02**
Ilmenite	*Std.*	*0.00*	*0.01*	*0.02*	*0.01*	*0.22*		*0.21*	*0.00*	*0.03*	*0.01*	*0.10*	*0.00*	*0.41*	*0.16*
14-2d ilm 1		0.00	0.00	0.01	0.00	46.69		51.66	0.00	0.79	0.00	0.70	0.00	99.85	32.65
14-2d ilm 3		0.01	0.01	0.00	0.00	46.07		51.07	0.01	0.72	0.00	1.00	0.03	98.92	32.22
14-2d ilm 4		0.00	0.01	0.00	0.00	45.25		52.12	0.00	0.79	0.00	1.09	0.00	99.26	31.65
14-2d ilm 5		0.00	0.01	0.14	0.05	46.90		51.10	0.01	0.82	0.00	0.48	0.00	99.51	32.80
14-2d ilm 6		0.00	0.02	0.02	0.00	46.62		51.35	0.00	0.73	0.00	0.39	0.00	99.13	32.61
MA14-2D	**Avg.**	**0.00**	**0.01**	**0.03**	**0.01**	**46.31**		**51.46**	**0.00**	**0.77**	**0.00**	**0.73**	**0.01**	**99.33**	**32.39**
Ilmenite	*Std.*	*0.00*	*0.01*	*0.05*	*0.02*	*0.59*		*0.39*	*0.00*	*0.04*	*0.00*	*0.28*	*0.01*	*0.32*	*0.42*
14-3a ilm 1		0.00	0.00	0.01	0.00	47.19		50.28	0.00	1.47	0.01	0.15	0.00	99.11	33.00
14-3a ilm 1-2		0.00	0.00	0.06	0.01	46.47		51.11	0.00	1.48	0.00	0.17	0.00	99.30	32.50
14-3a ilm 2		0.00	0.01	0.08	0.00	46.98		50.86	0.00	1.52	0.00	0.14	0.01	99.60	32.86
14-3a ilm 6		0.00	0.00	0.04	0.04	47.62		49.79	0.00	1.54	0.00	0.10	0.01	99.14	33.31
14-3a ilm 8		0.00	0.01	0.07	0.00	47.78		49.59	0.00	1.54	0.01	0.04	0.00	99.04	33.42
MA14-3A	**Avg.**	**0.00**	**0.00**	**0.05**	**0.01**	**47.21**		**50.33**	**0.00**	**1.51**	**0.00**	**0.12**	**0.00**	**99.24**	**33.02**
Ilmenite	*Std.*	*0.00*	*0.00*	*0.02*	*0.02*	*0.47*		*0.59*	*0.00*	*0.03*	*0.00*	*0.05*	*0.00*	*0.20*	*0.33*
14-3b-t ilm 2-1		0.00	0.00	0.00	0.00	47.72		51.04	0.00	1.29	0.09	0.02	0.01	100.17	33.38
14-3b-t ilm 2-2		0.00	0.02	0.08	0.18	46.52		50.88	0.00	1.35	0.04	0.05	0.01	99.13	32.54
14-3b-t ilm 3		0.00	0.02	0.03	0.00	46.51		50.89	0.00	1.31	0.00	0.11	0.00	98.87	32.53
14-3b-t ilm 6		0.00	0.00	0.00	0.11	47.12		50.53	0.00	1.31	0.01	0.10	0.00	99.18	32.96
14-3b-t ilm 7		0.00	0.02	0.05	0.00	47.68		50.32	0.00	1.21	0.01	0.14	0.00	99.43	33.35
MA14-3B-T	**Avg.**	**0.00**	**0.01**	**0.03**	**0.06**	**47.11**		**50.73**	**0.00**	**1.29**	**0.03**	**0.08**	**0.00**	**99.36**	**32.95**
Ilmenite	*Std.*	*0.00*	*0.01*	*0.03*	*0.07*	*0.53*		*0.27*	*0.00*	*0.05*	*0.03*	*0.04*	*0.00*	*0.44*	*0.37*
14-3B-B-ilm1		0.01	0.02	0.00	0.02	48.61		50.16	0.00	1.07	0.27	0.05	0.08	100.29	34.00
14-3B-B-ilm2		0.00	0.05	0.01	0.00	48.15		51.39	0.00	1.14	0.14	0.01	0.06	100.96	33.68
14-3B-B-ilm3		0.00	0.04	0.01	0.00	48.14		50.38	0.01	1.07	0.08	0.05	0.05	99.85	33.67
14-3B-B-ilm4		0.00	0.08	0.00	0.04	47.66		51.31	0.00	1.13	0.11	0.04	0.04	100.40	33.33
14-3B-B-ilm5		0.00	0.02	0.00	0.03	48.04		51.33	0.01	1.11	0.05	0.04	0.09	100.72	33.60
MA14-3B-B	**Avg.**	**0.00**	**0.04**	**0.00**	**0.02**	**48.12**		**50.91**	**0.00**	**1.10**	**0.13**	**0.04**	**0.06**	**100.44**	**33.66**
Ilmenite	*Std.*	*0.00*	*0.02*	*0.00*	*0.02*	*0.30*		*0.53*	*0.00*	*0.03*	*0.08*	*0.01*	*0.02*	*0.38*	*0.21*
14-4 ilm 6		0.00	0.00	0.00	0.00	48.80		48.59	0.00	1.11	0.00	0.06	0.00	98.56	34.13
14-4 ilm 9		0.00	0.00	0.00	0.02	46.79		50.80	0.00	1.16	0.00	0.06	0.01	98.84	32.72
14-4 ilm 10		0.00	0.02	0.00	0.04	49.18		48.76	0.00	0.96	0.09	0.03	0.00	99.08	34.40
MA14-4-a	**Avg.**	**0.00**	**0.01**	**0.00**	**0.02**	**48.26**		**49.38**	**0.00**	**1.08**	**0.03**	**0.05**	**0.00**	**98.83**	**33.75**
Ilmenite	*Std.*	*0.00*	*0.01*	*0.00*	*0.02*	*1.05*		*1.00*	*0.00*	*0.08*	*0.04*	*0.01*	*0.00*	*0.21*	*0.73*
14-4 ilm 2 *(Leuco)*		0.00	0.02	0.04	0.00	47.51		49.69	0.00	1.15	0.07	0.03	0.01	98.52	33.23
14-4 ilm 3 *(Leuco)*		0.01	0.00	0.04	0.00	47.75		49.32	0.01	1.10	0.21	0.03	0.00	98.47	33.40
MA14-4-b	**Avg.**	**0.01**	**0.01**	**0.04**	**0.00**	**47.63**		**49.51**	**0.01**	**1.13**	**0.14**	**0.03**	**0.01**	**98.50**	**33.31**
Ilmenite	*Std.*	*0.01*	*0.01*	*0.00*	*0.00*	*0.12*		*0.18*	*0.01*	*0.02*	*0.07*	*0.00*	*0.01*	*0.02*	*0.08*

Analysis ID		CaO	Cr_2O_3	Al_2O_3	ZnO	FeO	Fe_2O_3	TiO_2	NiO	MnO	V_2O_3	MgO	SiO_2	Total	Total Fe (%):
14-5a ilm 1		0.00	0.00	0.06	0.24	50.28		47.90	0.00	1.47	0.07	0.13	0.01	100.16	35.17
14-5a ilm 2		0.00	0.01	0.03	0.09	50.37		47.36	0.01	1.46	0.17	0.11	0.00	99.61	35.23
14-5a ilm 5		0.00	0.01	0.00	0.16	48.70		48.55	0.00	1.50	0.09	0.15	0.00	99.16	34.06
14-5a ilm 6		0.01	0.01	0.04	0.04	48.12		49.82	0.00	1.54	0.10	0.14	0.00	99.82	33.66
14-5a ilm 7		0.00	0.00	0.05	0.07	48.16		49.28	0.00	1.50	0.09	0.18	0.00	99.33	33.68
MA14-5A	**Avg.**	**0.00**	**0.01**	**0.04**	**0.12**	**49.13**		**48.58**	**0.00**	**1.49**	**0.10**	**0.14**	**0.00**	**99.62**	**34.36**
Ilmenite	*Std.*	*0.00*	*0.00*	*0.02*	*0.07*	*1.00*		*0.89*	*0.00*	*0.03*	*0.03*	*0.02*	*0.00*	*0.35*	*0.70*
14-5c ilm 1-1		0.00	0.00	0.00	0.12	51.49		45.46	0.00	1.23	0.15	0.05	0.01	98.51	36.01
14-5c ilm 1-2		0.00	0.01	0.07	0.00	51.04		46.75	0.00	1.20	0.16	0.06	0.00	99.29	35.70
14-5c ilm 2		0.01	0.01	0.09	0.23	49.93		48.34	0.00	1.14	0.17	0.06	0.00	99.98	34.92
14-5c ilm 3		0.00	0.03	0.00	0.00	48.75		48.59	0.01	1.11	0.16	0.05	0.01	98.71	34.10
MA14-5C	**Avg.**	**0.00**	**0.01**	**0.04**	**0.09**	**50.30**		**47.29**	**0.00**	**1.17**	**0.16**	**0.06**	**0.01**	**99.12**	**35.18**
Ilmenite	*Std.*	*0.00*	*0.01*	*0.04*	*0.10*	*1.06*		*1.27*	*0.00*	*0.05*	*0.01*	*0.01*	*0.01*	*0.57*	*0.74*
14-5c ilm 7 *(Leuco*)		0.00	0.03	0.00	0.00	50.09		46.88	0.00	1.34	0.38	0.04	0.01	98.77	35.03
14-5c ilm 8 *(Leuco)*		0.00	0.04	0.00	0.00	49.69		47.36	0.01	1.63	0.25	0.02	0.01	99.01	34.75
MA14-5C (tr)	**Avg.**	**0.00**	**0.04**	**0.00**	**0.00**	**49.89**		**47.12**	**0.01**	**1.49**	**0.32**	**0.03**	**0.01**	**98.89**	**34.89**
Ilmenite	*Std.*	*0.00*	*0.01*	*0.00*	*0.00*	*0.20*		*0.24*	*0.01*	*0.15*	*0.06*	*0.01*	*0.00*	*0.12*	*0.14*
14-6a-t ilm 1-1		0.00	0.01	0.06	0.12	50.19		48.14	0.01	1.00	0.06	0.21	0.02	99.82	35.10
14-6a-t ilm 1-2		0.01	0.01	0.09	0.17	49.94		48.53	0.00	1.01	0.11	0.16	0.00	100.03	34.93
14-6a-t ilm 2		0.00	0.01	0.00	0.00	49.69		48.94	0.01	0.91	0.13	0.25	0.00	99.94	34.75
14-6a-t ilm 5		0.01	0.00	0.05	0.11	49.80		47.98	0.00	1.03	0.10	0.11	0.01	99.20	34.83
MA14-6A-T	**Avg.**	**0.01**	**0.01**	**0.05**	**0.10**	**49.91**		**48.40**	**0.01**	**0.99**	**0.10**	**0.18**	**0.01**	**99.75**	**34.90**
Ilmenite	*Std.*	*0.01*	*0.00*	*0.03*	*0.06*	*0.19*		*0.37*	*0.01*	*0.05*	*0.03*	*0.05*	*0.01*	*0.32*	*0.13*
14-6b ilm 3-1		0.00	0.01	0.11	0.28	48.09		48.95	0.00	1.28	0.12	0.06	0.00	98.90	33.63
14-6b ilm 3-2		0.00	0.00	0.02	0.00	47.96		49.10	0.00	1.38	0.06	0.10	0.01	98.63	33.54
14-6b ilm 5		0.00	0.01	0.00	0.08	49.82		47.65	0.00	1.32	0.07	0.10	0.00	99.05	34.84
14-6b ilm 6		0.00	0.02	0.07	0.14	48.52		48.44	0.01	1.33	0.07	0.07	0.00	98.67	33.93
MA14-6B-a		**0.00**	**0.01**	**0.05**	**0.13**	**48.60**		**48.54**	**0.00**	**1.33**	**0.08**	**0.08**	**0.00**	**98.81**	**33.99**
Ilmenite		*0.00*	*0.01*	*0.04*	*0.10*	*0.74*		*0.57*	*0.00*	*0.04*	*0.02*	*0.02*	*0.00*	*0.17*	*0.51*
14-6b ilm 7 *(diss)*		0.00	0.06	0.03	0.20	48.09		48.85	0.00	1.66	0.48	0.05	0.00	99.42	33.63
14-6b ilm 8 *(diss)*		0.01	0.03	0.10	0.00	47.61		48.89	0.00	1.49	0.37	0.14	0.02	98.66	33.30
14-6b ilm 9 *(diss)*		0.00	0.04	0.02	0.00	46.84		49.67	0.00	1.47	0.39	0.15	0.00	98.58	32.76
MA14-6B-b	**Avg.**	**0.00**	**0.04**	**0.05**	**0.07**	**47.51**		**49.14**	**0.00**	**1.54**	**0.41**	**0.11**	**0.01**	**98.89**	**33.23**
Ilmenite	*Std.*	*0.01*	*0.02*	*0.04*	*0.10*	*0.24*		*0.02*	*0.00*	*0.09*	*0.06*	*0.05*	*0.01*	*0.38*	*0.17*
14-7a ilm 1		0.00	0.00	0.07	0.15	49.42		47.82	0.00	1.44	0.05	0.08	0.01	99.04	34.56
14-7a ilm 2		0.00	0.01	0.03	0.00	49.02		48.17	0.00	1.43	0.09	0.09	0.01	98.85	34.28
14-7a ilm 3		0.00	0.00	0.02	0.11	48.72		48.64	0.01	1.42	0.09	0.09	0.00	99.10	34.07
14-7a ilm 5-1		0.00	0.03	0.00	0.11	49.38		47.82	0.00	1.44	0.12	0.05	0.00	98.95	34.54
MA14-7A	**Avg.**	**0.00**	**0.01**	**0.03**	**0.09**	**49.14**		**48.11**	**0.00**	**1.43**	**0.09**	**0.08**	**0.01**	**98.99**	**34.37**
Ilmenite	*Std.*	*0.00*	*0.01*	*0.03*	*0.06*	*0.29*		*0.34*	*0.00*	*0.01*	*0.02*	*0.02*	*0.01*	*0.09*	*0.20*
14-7a ilm 7 *(diss)*		0.00	0.00	0.04	0.21	49.33		47.58	0.00	1.44	0.09	0.06	0.00	98.75	34.50
14-7a ilm 9 *(diss)*		0.00	0.02	0.00	0.00	49.17		47.67	0.01	1.47	0.28	0.06	0.00	98.68	34.39
14-7a ilm 10 *(diss)*		0.00	0.02	0.08	0.00	49.42		47.33	0.00	1.47	0.17	0.05	0.00	98.54	34.56
MA14-7A (tr)	**Avg.**	**0.00**	**0.01**	**0.04**	**0.07**	**49.31**		**47.53**	**0.00**	**1.46**	**0.18**	**0.06**	**0.00**	**98.66**	**34.49**
Ilmenite	*Std.*	*0.00*	*0.01*	*0.03*	*0.10*	*0.10*		*0.14*	*0.00*	*0.01*	*0.08*	*0.00*	*0.00*	*0.09*	*0.07*

Analysis ID		CaO	Cr_2O_3	Al_2O_3	ZnO	FeO	Fe_2O_3	TiO_2	NiO	MnO	V_2O_3	MgO	SiO_2	Total	Total Fe (%):
14-8a ilm 1 *(diss)*		0.00	0.09	0.12	0.18	46.42		50.29	0.00	2.31	0.84	0.05	0.01	100.31	32.47
14-8a ilm 2 *(diss)*		0.00	0.08	0.00	0.05	45.34		50.92	0.00	2.70	0.78	0.12	0.00	99.99	31.71
14-8a ilm 3 *(diss)*		0.00	0.11	0.02	0.00	46.21		50.53	0.00	2.36	0.39	0.04	0.01	99.67	32.32
14-8a ilm 4 *(diss)*		0.01	0.09	0.00	0.33	45.77		51.17	0.00	2.21	0.50	0.09	0.00	100.17	32.01
MA14-8A (tr)	**Avg.**	**0.00**	**0.09**	**0.04**	**0.14**	**45.94**		**50.73**	**0.00**	**2.40**	**0.63**	**0.08**	**0.01**	**100.04**	**32.13**
Ilmenite	*Std.*	*0.00*	*0.01*	*0.05*	*0.13*	*0.42*		*0.34*	*0.00*	*0.18*	*0.19*	*0.03*	*0.01*	*0.24*	*0.29*
14-8a ilm 6		0.00	0.02	0.00	0.13	48.63		49.01	0.00	1.96	0.00	0.03	0.00	99.78	34.01
14-8a ilm 7-1		0.00	0.03	0.02	0.00	47.66		49.39	0.00	1.88	0.07	0.02	0.00	99.07	33.33
14-8a ilm 7-2		0.00	0.01	0.00	0.00	47.92		50.04	0.00	1.85	0.09	0.03	0.00	99.94	33.52
14-8a ilm 8		0.00	0.01	0.07	0.00	47.82		48.91	0.00	1.91	0.03	0.08	0.00	98.83	33.45
MA14-8A	**Avg.**	**0.00**	**0.02**	**0.02**	**0.03**	**48.01**		**49.34**	**0.00**	**1.90**	**0.05**	**0.04**	**0.00**	**99.41**	**33.58**
Ilmenite	*Std.*	*0.00*	*0.01*	*0.03*	*0.06*	*0.37*		*0.44*	*0.00*	*0.04*	*0.03*	*0.02*	*0.00*	*0.47*	*0.26*
14-8b ilm 1-1		0.00	0.01	0.00	0.00	47.11		50.08	0.01	1.85	0.06	0.07	0.00	99.19	32.95
14-8b ilm 1-2		0.00	0.00	0.00	0.09	47.86		48.72	0.00	1.95	0.05	0.06	0.00	98.73	33.47
14-8b ilm 2		0.00	0.00	0.02	0.00	47.23		49.64	0.00	1.89	0.04	0.08	0.00	98.90	33.03
14-8b ilm 4		0.00	0.02	0.00	0.02	46.85		50.08	0.00	1.98	0.04	0.05	0.00	99.04	32.77
14-8b ilm 5		0.00	0.01	0.04	0.08	47.64		49.46	0.00	1.83	0.06	0.08	0.00	99.20	33.32
MA14-8B	**Avg.**	**0.00**	**0.01**	**0.01**	**0.04**	**47.34**		**49.60**	**0.00**	**1.90**	**0.05**	**0.07**	**0.00**	**99.01**	**33.11**
Ilmenite	*Std.*	*0.00*	*0.01*	*0.02*	*0.04*	*0.36*		*0.50*	*0.00*	*0.06*	*0.01*	*0.01*	*0.00*	*0.18*	*0.26*
MA15-1_ilm1		0.02	0.04	0.00	0.02	42.55	7.38	48.62	0.00	1.05	0.16	0.06	0.03	99.93	35.50
MA15-1_ilm2		0.00	0.06	0.00	0.00	43.51	5.82	49.64	0.01	1.06	0.36	0.04	0.01	100.50	34.95
MA15-1_ilm3		0.00	0.03	0.01	0.06	43.08	7.01	49.27	0.00	1.08	0.22	0.05	0.00	100.81	35.58
MA15-1_ilm4		0.00	0.04	0.01	0.01	43.11	6.74	49.38	0.01	1.18	0.05	0.05	0.00	100.59	35.39
MA15-1_ilm5		0.01	0.06	0.01	0.05	43.00	6.78	49.16	0.01	1.05	0.20	0.05	0.00	100.38	35.34
MA15-1_ilm6		0.01	0.01	0.02	0.07	43.95	4.89	50.19	0.00	0.98	0.19	0.07	0.00	100.38	34.54
MA15-1	**Avg.**	**0.01**	**0.04**	**0.01**	**0.04**	**43.20**	**6.44**	**49.38**	**0.01**	**1.07**	**0.20**	**0.05**	**0.01**	**100.43**	**35.22**
Ilmenite	*Std.*	*0.00*	*0.02*	*0.01*	*0.03*	*0.36*	*0.79*	*0.37*	*0.00*	*0.06*	*0.10*	*0.01*	*0.00*	*0.16*	*0.37*
MA15-2_ilm1		0.00	0.00	0.03	0.03	43.46	2.73	51.54	0.00	1.47	0.00	0.80	0.04	100.10	32.52
MA15-2_ilm2		0.01	0.00	0.04	0.02	43.44	3.40	51.41	0.02	1.47	0.00	0.73	0.03	100.57	33.02
MA15-2_ilm3		0.00	0.00	0.02	0.00	43.89	2.69	51.81	0.00	1.44	0.00	0.73	0.04	100.62	32.79
MA15-2_ilm4		0.01	0.00	0.03	0.00	43.95	2.63	51.91	0.00	1.41	0.00	0.73	0.00	100.66	32.78
MA15-2_ilm5		0.00	0.04	0.04	0.00	44.26	2.70	52.21	0.01	1.42	0.00	0.72	0.03	101.43	33.05
MA15-2	**Avg.**	**0.00**	**0.01**	**0.03**	**0.01**	**43.80**	**2.83**	**51.78**	**0.01**	**1.44**	**0.00**	**0.74**	**0.03**	**100.68**	**32.83**
Ilmenite	*Std.*	*0.00*	*0.02*	*0.01*	*0.01*	*0.31*	*0.29*	*0.28*	*0.01*	*0.02*	*0.00*	*0.03*	*0.01*	*0.43*	*0.19*
MA32-25_ilm1		0.00	0.02	0.02	0.00	45.50	2.31	51.59	0.00	0.86	0.09	0.02	0.00	100.40	33.62
MA32-25_ilm2		0.00	0.00	0.00	0.00	45.60	1.16	51.80	0.00	0.87	0.00	0.06	0.00	99.50	32.79
MA32-25_ilm3		0.01	0.02	0.00	0.04	45.57	2.49	51.78	0.00	0.89	0.09	0.03	0.00	100.92	33.81
MA32-25_ilm4		0.01	0.04	0.00	0.05	45.07	3.37	51.21	0.00	0.88	0.09	0.03	0.01	100.76	34.14
MA32-25	**Avg.**	**0.01**	**0.02**	**0.01**	**0.02**	**45.44**	**2.33**	**51.60**	**0.00**	**0.88**	**0.07**	**0.04**	**0.00**	**100.40**	**33.59**
Ilmenite	*Std.*	*0.01*	*0.01*	*0.01*	*0.02*	*0.21*	*0.79*	*0.24*	*0.00*	*0.01*	*0.04*	*0.02*	*0.00*	*0.55*	*0.50*
32-1a ilm 1		0.00	0.00	0.00	0.04	47.07		50.18	0.00	1.67	0.00	0.19	0.00	99.15	32.92
32-1a ilm 2		0.00	0.00	0.00	0.11	46.61		50.91	0.01	1.62	0.00	0.27	0.00	99.53	32.60
32-1a ilm 5		0.00	0.00	0.06	0.00	46.19		50.91	0.00	1.64	0.00	0.27	0.00	99.07	32.31
32-1a ilm 6		0.00	0.00	0.09	0.01	46.98		50.11	0.00	1.60	0.00	0.24	0.00	99.03	32.86
32-1a ilm 7		0.00	0.00	0.00	0.04	47.02		51.14	0.00	1.76	0.00	0.18	0.00	100.14	32.89

Analysis ID		CaO	Cr_2O_3	Al_2O_3	ZnO	FeO	Fe_2O_3	TiO_2	NiO	MnO	V_2O_3	MgO	SiO_2	Total	Total Fe (%):
MA32-1A	**Avg.**	**0.00**	**0.00**	**0.03**	**0.04**	**46.77**		**50.65**	**0.00**	**1.66**	**0.00**	**0.23**	**0.00**	**99.38**	**32.71**
Ilmenite	*Std.*	*0.00*	*0.00*	*0.04*	*0.04*	*0.33*		*0.42*	*0.00*	*0.06*	*0.00*	*0.04*	*0.00*	*0.42*	*0.23*
32-1c ilm 2		0.00	0.00	0.00	0.00	46.60		50.80	0.00	1.56	0.01	0.28	0.00	99.25	32.59
32-1c ilm 3		0.01	0.00	0.00	0.13	47.10		50.68	0.00	1.50	0.00	0.22	0.01	99.65	32.94
32-1c ilm 5		0.01	0.00	0.14	0.01	46.60		50.37	0.00	1.50	0.00	0.25	0.00	98.88	32.59
32-1c ilm 6		0.01	0.01	0.00	0.00	46.76		50.54	0.00	1.47	0.00	0.27	0.00	99.06	32.70
32-1c ilm 7		0.00	0.01	0.04	0.00	46.88		50.16	0.02	1.52	0.00	0.18	0.01	98.82	32.79
MA32-1c	**Avg.**	**0.01**	**0.00**	**0.04**	**0.03**	**46.79**		**50.51**	**0.00**	**1.51**	**0.00**	**0.24**	**0.00**	**99.13**	**32.72**
Ilmenite	*Std.*	*0.00*	*0.00*	*0.05*	*0.05*	*0.19*		*0.23*	*0.01*	*0.03*	*0.00*	*0.04*	*0.00*	*0.30*	*0.13*
32-2a-t ilm 1		0.00	0.02	0.00	0.00	47.34		49.34	0.01	1.54	0.00	0.09	0.02	98.36	33.11
32-2a-t ilm 2		0.00	0.01	0.02	0.00	47.83		49.25	0.00	1.62	0.05	0.10	0.01	98.89	33.45
32-2a-t ilm 3		0.00	0.00	0.07	0.08	48.35		48.71	0.00	1.70	0.00	0.11	0.01	99.03	33.82
32-2a-t ilm 4		0.02	0.00	0.00	0.11	48.37		48.85	0.00	1.67	0.03	0.09	0.00	99.14	33.83
32-2a-t ilm 5		0.00	0.00	0.00	0.12	47.77		49.63	0.00	1.73	0.00	0.11	0.00	99.36	33.41
MA32-2A-T	**Avg.**	**0.00**	**0.01**	**0.02**	**0.06**	**47.93**		**49.16**	**0.00**	**1.65**	**0.02**	**0.10**	**0.01**	**98.96**	**33.52**
Ilmenite	*Std.*	*0.01*	*0.01*	*0.03*	*0.05*	*0.39*		*0.33*	*0.00*	*0.07*	*0.02*	*0.01*	*0.01*	*0.34*	*0.27*
32-2a-b ilm 1		0.00	0.00	0.06	0.07	47.74		49.22	0.00	1.82	0.00	0.07	0.01	98.99	33.39
32-2a-b ilm 2		0.00	0.00	0.05	0.22	47.40		49.49	0.01	1.83	0.00	0.05	0.00	99.05	33.15
32-2a-b ilm 3		0.01	0.00	0.11	0.00	47.52		49.53	0.01	1.80	0.00	0.04	0.01	99.03	33.24
32-2a-b ilm 5		0.00	0.00	0.10	0.00	47.84		49.21	0.00	1.79	0.00	0.05	0.00	98.99	33.46
MA32-2A-B-a	**Avg.**	**0.00**	**0.00**	**0.08**	**0.07**	**47.63**		**49.36**	**0.01**	**1.81**	**0.00**	**0.05**	**0.01**	**99.02**	**33.31**
AVERAGE:	*Std.*	*0.00*	*0.00*	*0.03*	*0.09*	*0.17*		*0.15*	*0.01*	*0.02*	*0.00*	*0.01*	*0.01*	*0.03*	*0.12*
32-2a-b ilm 7 *(diss)*		0.00	0.02	0.00	0.00	48.76		49.14	0.00	1.70	0.01	0.07	0.00	99.70	34.10
32-2a-b ilm 8 *(diss)*		0.00	0.01	0.07	0.00	47.93		49.82	0.00	1.66	0.00	0.09	0.00	99.58	33.52
32-2a-b ilm 9 *(diss)*		0.00	0.02	0.04	0.09	47.63		50.03	0.01	1.71	0.00	0.07	0.02	99.62	33.31
32-2a-b ilm 11 *(diss)*		0.00	0.00	0.02	0.00	48.13		49.03	0.00	1.66	0.00	0.08	0.00	98.92	33.66
MA32-2A-B-b	**Avg.**	**0.00**	**0.01**	**0.03**	**0.02**	**48.11**		**49.51**	**0.00**	**1.68**	**0.00**	**0.08**	**0.01**	**99.46**	**33.65**
Ilmenite	*Std.*	*0.00*	*0.01*	*0.03*	*0.04*	*0.41*		*0.43*	*0.00*	*0.02*	*0.00*	*0.01*	*0.01*	*0.31*	*0.29*
32-2b ilm 1		0.00	0.00	0.11	0.00	47.33		49.59	0.00	1.55	0.00	0.19	0.00	98.77	33.10
32-2b ilm 2		0.00	0.00	0.00	0.03	46.92		50.75	0.00	1.62	0.00	0.15	0.00	99.47	32.82
32-2b ilm 3		0.00	0.02	0.00	0.01	48.41		49.28	0.01	1.54	0.00	0.19	0.00	99.46	33.86
32-2b ilm 4-1		0.00	0.02	0.00	0.25	47.80		49.81	0.00	1.58	0.00	0.14	0.01	99.61	33.43
32-2b ilm 4-2		0.00	0.01	0.04	0.09	47.18		50.29	0.00	1.60	0.00	0.13	0.00	99.34	33.00
MA32-2B	**Avg.**	**0.00**	**0.01**	**0.03**	**0.08**	**47.53**		**49.94**	**0.00**	**1.58**	**0.00**	**0.16**	**0.00**	**99.33**	**33.24**
Ilmenite	*Std.*	*0.00*	*0.01*	*0.04*	*0.09*	*0.53*		*0.52*	*0.00*	*0.03*	*0.00*	*0.03*	*0.00*	*0.29*	*0.37*
32-3 ilm 1		0.00	0.01	0.05	0.11	46.38		51.14	0.00	1.88	0.00	0.15	0.00	99.72	32.44
32-3 ilm 2		0.00	0.00	0.07	0.20	46.54		51.70	0.00	1.85	0.00	0.15	0.00	100.51	32.55
32-3 ilm 3-1		0.00	0.02	0.00	0.00	50.25		46.92	0.00	1.72	0.05	0.15	0.01	99.12	35.14
32-3 ilm 3-2		0.00	0.02	0.07	0.00	48.37		49.42	0.01	1.70	0.04	0.13	0.00	99.76	33.83
32-3 ilm 5		0.00	0.01	0.00	0.00	49.42		48.41	0.00	1.61	0.01	0.17	0.01	99.64	34.56
MA32-3	**Avg.**	**0.00**	**0.01**	**0.04**	**0.06**	**48.19**		**49.52**	**0.00**	**1.75**	**0.02**	**0.15**	**0.00**	**99.75**	**33.71**
Ilmenite	*Std.*	*0.00*	*0.01*	*0.03*	*0.08*	*1.54*		*1.75*	*0.00*	*0.10*	*0.02*	*0.01*	*0.00*	*0.44*	*1.07*
32-4-b ilm 1		0.01	0.03	0.05	0.18	48.74		48.27	0.01	1.21	0.12	0.12	0.01	98.75	34.09
32-4-b ilm 2		0.00	0.02	0.04	0.00	46.80		50.50	0.00	1.45	0.01	0.12	0.01	98.95	32.73
32-4-b ilm 3-1		0.00	0.03	0.10	0.13	49.27		48.11	0.00	1.29	0.09	0.15	0.01	99.18	34.46

Analysis ID		CaO	Cr_2O_3	Al_2O_3	ZnO	FeO	Fe_2O_3	TiO_2	NiO	MnO	V_2O_3	MgO	SiO_2	Total	Total Fe (%):
32-4-b ilm 3-2		0.01	0.04	0.04	0.00	47.43		50.35	0.00	1.46	0.05	0.17	0.01	99.56	33.17
32-4-b ilm 4		0.00	0.00	0.05	0.02	47.91		49.77	0.00	1.41	0.07	0.16	0.00	99.39	33.51
MA32-4	**Avg.**	**0.00**	**0.02**	**0.06**	**0.07**	**48.03**		**49.40**	**0.00**	**1.36**	**0.07**	**0.14**	**0.01**	**99.17**	**33.59**
Ilmenite	*Std.*	*0.00*	*0.01*	*0.02*	*0.07*	*0.89*		*1.02*	*0.00*	*0.10*	*0.04*	*0.02*	*0.00*	*0.29*	*0.62*
MA32-7_ilm1		0.00	0.00	0.00	0.00	43.51	1.78	51.58	0.01	1.27	0.00	0.90	0.01	99.06	31.81
MA32-7_ilm2		0.00	0.00	0.01	0.00	44.98	0.00	52.52	0.00	1.42	0.00	0.43	0.01	99.37	31.46
MA32-7_ilm3		0.00	0.00	0.01	0.00	44.00	1.13	52.06	0.01	1.17	0.00	0.93	0.02	99.32	31.65
MA32-7_ilm4		0.00	0.00	0.02	0.00	43.31	2.60	51.23	0.01	1.17	0.00	0.89	0.01	99.24	32.31
MA32-7_ilm5		0.00	0.00	0.01	0.00	44.63	0.82	52.11	0.02	1.37	0.00	0.47	0.00	99.42	31.85
MA32-7	**Avg.**	**0.00**	**0.00**	**0.01**	**0.00**	**44.09**	**1.27**	**51.90**	**0.01**	**1.28**	**0.00**	**0.72**	**0.01**	**99.28**	**31.82**
Ilmenite	*Std.*	*0.00*	*0.00*	*0.01*	*0.00*	*0.64*	*0.88*	*0.45*	*0.01*	*0.10*	*0.00*	*0.22*	*0.01*	*0.13*	*0.28*
MA32-9_ilm1		0.00	0.00	0.04	0.00	44.85	2.20	51.31	0.00	1.09	0.00	0.11	0.00	99.60	33.08
MA32-9_ilm2		0.01	0.00	0.03	0.01	41.84	8.36	47.96	0.00	1.08	0.00	0.10	0.00	99.40	35.76
MA32-9_ilm3		0.00	0.00	0.01	0.00	44.31	2.63	50.82	0.01	1.20	0.00	0.10	0.00	99.07	33.03
MA32-9_ilm4		0.00	0.00	0.02	0.00	45.18	1.15	51.72	0.00	1.08	0.00	0.14	0.00	99.29	32.49
MA32-9_ilm5		0.00	0.00	0.01	0.02	45.28	0.51	52.15	0.00	1.13	0.00	0.26	0.00	99.36	32.07
MA32-9_ilm6		0.00	0.01	0.16	0.02	43.85	3.42	50.70	0.01	1.12	0.00	0.33	0.00	99.62	33.33
MA32-9	**Avg.**	**0.00**	**0.00**	**0.05**	**0.01**	**44.22**	**3.05**	**50.78**	**0.00**	**1.12**	**0.00**	**0.17**	**0.00**	**99.39**	**33.29**
Ilmenite	*Std.*	*0.00*	*0.00*	*0.05*	*0.01*	*1.17*	*2.56*	*1.35*	*0.00*	*0.04*	*0.00*	*0.09*	*0.00*	*0.19*	*1.18*
MA32-12_ilm1		0.00	0.00	0.01	0.00	44.50	1.89	51.49	0.00	1.12	0.00	0.38	0.00	99.39	32.59
MA32-12_ilm2		0.00	0.01	0.00	0.00	44.76	1.67	51.71	0.01	1.13	0.00	0.35	0.02	99.66	32.60
MA32-12_ilm3		0.00	0.00	0.02	0.00	44.25	2.05	51.21	0.00	1.14	0.00	0.37	0.00	99.04	32.54
MA32-12_ilm4		0.00	0.00	0.10	0.00	43.94	1.15	52.32	0.01	0.99	0.00	1.19	0.01	99.70	31.63
MA32-12_ilm5		0.00	0.00	0.02	0.01	43.03	1.58	51.68	0.01	0.85	0.00	1.46	0.02	98.66	31.32
MA32-12	**Avg.**	**0.00**	**0.00**	**0.03**	**0.00**	**44.10**	**1.67**	**51.68**	**0.01**	**1.05**	**0.00**	**0.75**	**0.01**	**99.29**	**32.14**
Ilmenite	*Std.*	*0.00*	*0.00*	*0.04*	*0.00*	*0.60*	*0.31*	*0.37*	*0.00*	*0.11*	*0.00*	*0.48*	*0.01*	*0.39*	*0.55*
MA32-15-ilm1		0.01	0.00	0.02	0.00	44.62		51.46	0.02	0.90	0.01	2.40	0.04	99.48	31.21
MA32-15-ilm2		0.00	0.00	0.00	0.03	44.85		51.97	0.00	0.91	0.04	2.04	0.02	99.86	31.37
MA32-15-ilm3		0.01	0.01	0.01	0.00	44.57		52.64	0.01	0.93	0.01	2.33	0.05	100.57	31.17
MA32-15-ilm4		0.00	0.02	0.04	0.00	46.03		51.12	0.01	0.97	0.00	1.84	0.03	100.06	32.19
MA32-15-ilm5		0.01	0.00	0.01	0.01	46.00		50.36	0.01	0.93	0.00	1.92	0.03	99.28	32.17
MA32-15	**Avg.**	**0.01**	**0.01**	**0.02**	**0.01**	**45.21**		**51.51**	**0.01**	**0.93**	**0.01**	**2.11**	**0.03**	**99.85**	**31.62**
Ilmenite	*Std.*	*0.00*	*0.01*	*0.01*	*0.01*	*0.66*		*0.77*	*0.01*	*0.02*	*0.01*	*0.22*	*0.01*	*0.45*	*0.46*
MA32-17-ilm1		0.00	0.00	0.02	0.01	44.82		50.86	0.01	0.86	0.00	1.99	0.04	98.61	31.35
MA32-17-ilm2		0.00	0.00	0.02	0.00	45.30		51.24	0.00	0.91	0.00	1.97	0.03	99.47	31.68
MA32-17-ilm3		0.00	0.02	0.06	0.00	45.24		51.48	0.01	0.93	0.00	2.00	0.02	99.76	31.64
MA32-17-ilm4		0.00	0.00	0.03	0.00	45.20		51.38	0.01	0.97	0.00	1.80	0.03	99.42	31.61
MA32-17-ilm5		0.00	0.00	0.03	0.03	45.32		50.63	0.01	1.02	0.00	1.68	0.03	98.75	31.70
MA32-17	**Avg.**	**0.00**	**0.00**	**0.03**	**0.01**	**45.18**		**51.12**	**0.01**	**0.94**	**0.00**	**1.89**	**0.03**	**99.20**	**31.60**
Ilmenite	*Std.*	*0.00*	*0.01*	*0.01*	*0.01*	*0.18*		*0.32*	*0.00*	*0.05*	*0.00*	*0.13*	*0.01*	*0.44*	*0.13*
MA32-18_ilm1		0.00	0.01	0.00	0.01	43.92	2.88	50.80	0.00	0.66	0.00	0.63	0.02	98.93	32.96
MA32-18_ilm2		0.01	0.00	0.02	0.00	43.90	3.16	50.53	0.01	0.78	0.00	0.42	0.01	98.84	33.16
MA32-18_ilm3		0.00	0.01	0.02	0.02	44.75	3.16	51.34	0.00	0.84	0.00	0.32	0.01	100.47	33.75
MA32-18_ilm4		0.01	0.01	0.04	0.04	43.84	3.71	50.71	0.00	0.69	0.00	0.58	0.01	99.64	33.55
MA32-18_ilm5		0.01	0.00	0.02	0.01	44.66	2.58	51.00	0.00	0.88	0.00	0.18	0.02	99.36	33.24

Analysis ID		CaO	Cr_2O_3	Al_2O_3	ZnO	FeO	Fe_2O_3	TiO_2	NiO	MnO	V_2O_3	MgO	SiO_2	Total	Total Fe (%):
MA32-18-a	**Avg.**	**0.01**	**0.01**	**0.02**	**0.02**	**44.21**	**3.10**	**50.88**	**0.00**	**0.77**	**0.00**	**0.43**	**0.01**	**99.45**	**33.33**
Ilmenite	*Std.*	*0.00*	*0.00*	*0.01*	*0.01*	*0.40*	*0.37*	*0.28*	*0.00*	*0.08*	*0.00*	*0.17*	*0.00*	*0.59*	*0.28*
MA32-18_ilm6		0.00	0.05	0.06	0.00	42.25	3.35	50.99	0.01	0.59	0.00	1.69	0.01	99.01	32.15
MA32-18_ilm7		0.01	0.00	0.03	0.01	42.90	2.75	51.77	0.01	0.58	0.00	1.72	0.02	99.81	32.14
MA32-18_ilm8		0.01	0.01	0.02	0.00	42.20	3.30	50.90	0.00	0.58	0.00	1.70	0.04	98.76	32.08
MA32-18_ilm9		0.00	0.01	0.04	0.00	42.54	3.46	51.32	0.01	0.62	0.00	1.70	0.04	99.74	32.44
MA32-18-b	**Avg.**	**0.01**	**0.02**	**0.04**	**0.00**	**42.47**	**3.22**	**51.25**	**0.01**	**0.59**	**0.00**	**1.70**	**0.03**	**99.33**	**32.20**
Ilmenite	*Std.*	*0.01*	*0.02*	*0.01*	*0.00*	*0.28*	*0.27*	*0.34*	*0.00*	*0.02*	*0.00*	*0.01*	*0.01*	*0.45*	*0.14*
MA32-18_ilm11		0.00	0.00	0.06	0.06	43.64	3.12	50.75	0.00	0.70	0.00	0.70	0.00	99.02	32.95
MA32-18_ilm12		0.00	0.00	0.01	0.00	44.19	2.31	51.64	0.00	0.84	0.00	0.80	0.02	99.81	32.70
MA32-18_ilm13		0.00	0.00	0.02	0.03	43.61	2.84	50.85	0.01	0.73	0.00	0.77	0.02	98.88	32.71
MA32-18-c	**Avg.**	**0.00**	**0.00**	**0.03**	**0.03**	**43.81**	**2.76**	**51.08**	**0.00**	**0.76**	**0.00**	**0.76**	**0.01**	**99.24**	**32.79**
Ilmenite	*Std.*	*0.00*	*0.00*	*0.02*	*0.02*	*0.27*	*0.34*	*0.40*	*0.00*	*0.06*	*0.00*	*0.04*	*0.01*	*0.41*	*0.11*
MA32-19_ilm1		0.00	0.04	0.03	0.02	42.92	6.20	48.77	0.01	0.91	0.05	0.02	0.03	99.00	34.84
MA32-19_ilm2		0.01	0.02	0.01	0.00	43.55	5.21	49.57	0.00	0.92	0.06	0.05	0.00	99.40	34.51
MA32-19_ilm3		0.01	0.05	0.01	0.00	44.14	4.60	50.14	0.01	0.91	0.03	0.02	0.02	99.94	34.45
MA32-19_ilm4		0.00	0.02	0.01	0.00	43.53	5.49	49.36	0.00	0.85	0.10	0.01	0.01	99.38	34.71
MA32-19_ilm5		0.00	0.05	0.04	0.02	43.20	5.46	49.06	0.00	0.89	0.13	0.02	0.02	98.89	34.46
MA32-19	**Avg.**	**0.00**	**0.04**	**0.02**	**0.01**	**43.47**	**5.39**	**49.38**	**0.00**	**0.90**	**0.07**	**0.02**	**0.02**	**99.32**	**34.59**
Ilmenite	*Std.*	*0.00*	*0.01*	*0.01*	*0.01*	*0.41*	*0.52*	*0.47*	*0.00*	*0.02*	*0.04*	*0.01*	*0.01*	*0.37*	*0.16*
MA11-11_ilm1		0.01	0.01	0.04	0.02	42.49	2.85	51.58	0.00	1.11	0.00	1.56	0.03	99.71	31.93
MA11-11_ilm2		0.00	0.00	0.03	0.01	42.62	2.73	51.53	0.00	1.11	0.00	1.46	0.01	99.50	31.93
MA11-11_ilm3		0.00	0.00	0.02	0.00	44.21	2.14	51.94	0.00	1.62	0.00	0.49	0.01	100.43	32.58
MA11-11_ilm4		0.00	0.04	0.03	0.02	43.39	3.17	51.05	0.00	1.57	0.00	0.53	0.02	99.82	32.81
MA11-11_ilm5		0.00	0.02	0.04	0.00	43.22	3.03	51.42	0.00	1.20	0.00	1.03	0.02	99.98	32.58
MA11-11	**Avg.**	**0.00**	**0.01**	**0.03**	**0.01**	**43.19**	**2.78**	**51.50**	**0.00**	**1.32**	**0.00**	**1.01**	**0.02**	**99.89**	**32.37**
Ilmenite	*Std.*	*0.00*	*0.01*	*0.01*	*0.01*	*0.62*	*0.36*	*0.29*	*0.00*	*0.23*	*0.00*	*0.45*	*0.01*	*0.31*	*0.37*
MA11-8-ilm1		0.00	0.00	0.02	0.00	46.46		50.55	0.01	1.33	0.00	0.59	0.14	99.10	32.49
MA11-8-ilm2		0.00	0.00	0.03	0.03	46.94		50.80	0.01	1.50	0.00	0.48	0.17	99.96	32.83
MA11-8-ilm3		0.00	0.01	0.07	0.02	46.42		50.77	0.01	1.34	0.00	1.16	0.05	99.85	32.47
MA11-8-ilm4		0.00	0.00	0.12	0.00	46.28		51.47	0.01	1.31	0.00	1.01	0.07	100.27	32.37
MA11-8-ilm5		0.01	0.02	0.04	0.00	46.50		50.58	0.01	1.30	0.00	0.91	0.06	99.43	32.52
MA11-8	**Avg.**	**0.00**	**0.01**	**0.06**	**0.01**	**46.52**		**50.83**	**0.01**	**1.36**	**0.00**	**0.83**	**0.10**	**99.72**	**32.54**
Ilmenite	*Std.*	*0.00*	*0.01*	*0.04*	*0.01*	*0.22*		*0.33*	*0.00*	*0.07*	*0.00*	*0.26*	*0.05*	*0.41*	*0.16*
MA11-2-ilm1		0.00	0.00	0.05	0.02	46.92		51.15	0.01	0.85	0.00	0.96	0.04	100.00	32.82
MA11-2-ilm2		0.00	0.00	0.02	0.00	46.84		51.75	0.00	0.85	0.00	1.02	0.04	100.52	32.76
MA11-2-ilm3		0.00	0.00	0.02	0.00	46.66		51.59	0.02	0.85	0.01	1.10	0.05	100.30	32.63
MA11-2-ilm4		0.00	0.00	0.02	0.02	46.68		51.84	0.01	1.03	0.00	0.89	0.05	100.54	32.65
MA11-2-ilm5		0.01	0.00	0.05	0.00	46.36		51.32	0.00	0.93	0.00	1.19	0.05	99.91	32.42
MA11-2	**Avg.**	**0.00**	**0.00**	**0.03**	**0.01**	**46.69**		**51.53**	**0.01**	**0.90**	**0.00**	**1.03**	**0.05**	**100.25**	**32.66**
Ilmenite	*Std.*	*0.00*	*0.00*	*0.01*	*0.01*	*0.19*		*0.26*	*0.01*	*0.07*	*0.00*	*0.10*	*0.00*	*0.26*	*0.13*
MA11-2-alt_ilm-1		0.01	0.00	0.00	0.00	47.01		51.09	0.00	1.07	0.00	0.02	0.05	99.25	32.88
MA11-2-alt_ilm-2		0.00	0.01	0.00	0.03	46.73		52.07	0.00	1.10	0.00	0.06	0.04	100.04	32.68
MA11-2-alt_ilm-3		0.01	0.01	0.01	0.00	47.03		51.57	0.00	1.04	0.00	0.06	0.03	99.76	32.89
MA11-2-alt_ilm-4		0.00	0.00	0.00	0.00	47.09		51.62	0.00	1.07	0.00	0.03	0.03	99.83	32.93

Analysis ID		CaO	Cr_2O_3	Al_2O_3	ZnO	FeO	Fe_2O_3	TiO_2	NiO	MnO	V_2O_3	MgO	SiO_2	Total	Total Fe (%):
MA11-2-alt_ilm-5		0.00	0.03	0.00	0.00	46.55		51.98	0.01	1.03	0.01	0.04	0.04	99.69	32.56
MA11-2 (Altered	**Avg.**	**0.00**	**0.01**	**0.00**	**0.01**	**46.88**		**51.67**	**0.00**	**1.06**	**0.00**	**0.04**	**0.04**	**99.72**	**32.79**
Ilmenite	*Std.*	*0.00*	*0.01*	*0.00*	*0.01*	*0.21*		*0.35*	*0.00*	*0.02*	*0.00*	*0.02*	*0.01*	*0.26*	*0.14*
MA03-7-ilm1		0.00	0.07	0.02	0.00	48.32		49.99	0.01	1.69	0.12	0.03	0.12	100.37	33.80
MA03-7-ilm2		0.01	0.07	0.01	0.03	48.47		50.00	0.01	1.69	0.04	0.01	0.06	100.40	33.90
MA03-7-ilm3		0.00	0.02	0.01	0.00	48.47		50.45	0.01	1.73	0.04	0.04	0.03	100.80	33.90
MA03-7-ilm4		0.00	0.00	0.00	0.04	48.34		50.42	0.00	1.65	0.05	0.03	0.03	100.56	33.81
MA03-7-ilm5		0.01	0.01	0.00	0.00	48.34		50.06	0.00	1.68	0.11	0.03	0.04	100.29	33.81
MA03-7	**Avg.**	**0.00**	**0.03**	**0.01**	**0.01**	**48.39**		**50.18**	**0.01**	**1.69**	**0.07**	**0.03**	**0.05**	**100.48**	**33.84**
Ilmenite	*Std.*	*0.00*	*0.03*	*0.01*	*0.02*	*0.07*		*0.21*	*0.00*	*0.03*	*0.04*	*0.01*	*0.03*	*0.18*	*0.05*
MA03-6-ilm1		0.01	0.08	0.01	0.04	48.81		49.51	0.01	1.20	0.33	0.08	0.03	100.11	34.14
MA03-6-ilm2		0.01	0.06	0.01	0.03	47.40		51.33	0.00	1.34	0.22	0.08	0.10	100.58	33.15
MA03-6-ilm3		0.00	0.12	0.02	0.02	49.23		49.49	0.00	1.19	0.23	0.04	0.07	100.43	34.43
MA03-6-ilm4		0.03	0.10	0.01	0.05	48.02		50.24	0.00	1.52	0.29	0.07	0.15	100.48	33.59
MA03-6-ilm5		0.01	0.07	0.01	0.00	47.59		49.69	0.00	1.82	0.49	0.07	0.10	99.85	33.28
MA03-6	**Avg.**	**0.01**	**0.09**	**0.01**	**0.03**	**48.21**		**50.05**	**0.00**	**1.41**	**0.31**	**0.07**	**0.09**	**100.29**	**33.72**
Ilmenite	*Std.*	*0.01*	*0.02*	*0.00*	*0.02*	*0.70*		*0.69*	*0.00*	*0.24*	*0.10*	*0.01*	*0.04*	*0.27*	*0.49*
MA03-4-ilm1		0.01	0.00	0.00	0.01	48.96		50.13	0.01	1.26	0.03	0.04	0.02	100.47	34.24
MA03-4-ilm2		0.01	0.03	0.01	0.00	48.51		51.54	0.01	1.05	0.05	0.07	0.02	101.29	33.93
MA03-4-ilm3		0.00	0.01	0.00	0.02	48.67		50.78	0.01	1.11	0.04	0.07	0.02	100.75	34.04
MA03-4-ilm4		0.00	0.01	0.02	0.07	48.52		50.52	0.00	1.17	0.07	0.04	0.02	100.44	33.93
MA03-4-ilm5		0.00	0.01	0.00	0.01	48.81		50.67	0.00	1.21	0.09	0.02	0.02	100.84	34.14
MA03-4	**Avg.**	**0.00**	**0.01**	**0.01**	**0.02**	**48.69**		**50.73**	**0.01**	**1.16**	**0.06**	**0.05**	**0.02**	**100.76**	**34.06**
	Std.	*0.00*	*0.01*	*0.01*	*0.02*	*0.17*		*0.46*	*0.00*	*0.07*	*0.02*	*0.02*	*0.00*	*0.31*	*0.12*
MA03-2-ilm1		0.00	0.01	0.02	0.05	47.47		49.33	0.00	1.18	0.63	0.05	0.08	98.82	33.20
MA03-2-ilm2		0.00	0.02	0.01	0.07	47.61		50.52	0.00	1.06	0.30	0.01	0.04	99.64	33.30
MA03-2-ilm3		0.01	0.00	0.00	0.04	48.23		49.55	0.00	1.02	0.11	0.02	0.03	99.00	33.73
MA03-2-ilm4		0.00	0.00	0.02	0.03	48.36		49.86	0.01	1.01	0.17	0.01	0.04	99.52	33.82
MA03-2-ilm5		0.01	0.00	0.01	0.03	48.17		49.87	0.00	1.12	0.18	0.00	0.03	99.43	33.69
MA03-2	**Avg.**	**0.00**	**0.01**	**0.01**	**0.04**	**47.97**		**49.83**	**0.00**	**1.08**	**0.28**	**0.02**	**0.04**	**99.28**	**33.55**
Ilmenite	*Std.*	*0.00*	*0.01*	*0.01*	*0.01*	*0.36*		*0.40*	*0.00*	*0.06*	*0.19*	*0.02*	*0.02*	*0.32*	*0.25*
MA03-1B_ilm1		0.00	0.07	0.14	0.02	43.79	1.50	52.35	0.01	0.70	0.00	1.44	0.01	100.03	31.79
MA03-1B_ilm2		0.00	0.06	0.04	0.06	43.80	2.07	52.12	0.01	0.66	0.00	1.34	0.03	100.19	32.24
MA03-1B_ilm3		0.01	0.05	0.04	0.00	43.76	2.09	52.04	0.00	0.73	0.00	1.35	0.09	100.16	32.23
MA03-1B_ilm4		0.00	0.04	0.04	0.00	44.04	1.76	52.06	0.02	0.80	0.00	1.14	0.06	99.96	32.17
MA03-1B_ilm5		0.01	0.02	0.05	0.02	44.41	1.34	52.60	0.00	0.81	0.00	1.17	0.03	100.46	32.10
MA03-1B	**Avg.**	**0.00**	**0.05**	**0.06**	**0.02**	**43.96**	**1.75**	**52.23**	**0.01**	**0.74**	**0.00**	**1.29**	**0.04**	**100.16**	**32.11**
Ilmenite	*Std.*	*0.00*	*0.02*	*0.04*	*0.02*	*0.25*	*0.30*	*0.21*	*0.01*	*0.06*	*0.00*	*0.11*	*0.03*	*0.17*	*0.17*
MA03-1A-ilm1		0.00	0.03	0.04	0.00	46.07		51.56	0.01	0.83	0.00	1.02	0.04	99.60	32.22
MA03-1A-ilm2		0.00	0.01	0.05	0.00	46.25		51.50	0.01	0.95	0.00	1.00	0.08	99.85	32.35
MA03-1A-ilm3		0.00	0.00	0.07	0.01	46.10		52.20	0.01	0.79	0.00	1.20	0.03	100.41	32.24
MA03-1A-ilm4		0.01	0.01	0.05	0.00	46.27		51.55	0.02	0.85	0.00	1.11	0.05	99.92	32.36
MA03-1A-ilm5		0.00	0.00	0.02	0.00	46.13		52.29	0.01	0.76	0.00	1.31	0.04	100.56	32.26
MA03-1A	**Avg.**	**0.00**	**0.01**	**0.05**	**0.00**	**46.16**		**51.82**	**0.01**	**0.84**	**0.00**	**1.13**	**0.05**	**100.07**	**32.29**
Ilmenite	*Std.*	*0.00*	*0.01*	*0.02*	*0.00*	*0.08*		*0.35*	*0.00*	*0.06*	*0.00*	*0.12*	*0.02*	*0.36*	*0.06*

Analysis ID		CaO	Cr_2O_3	Al_2O_3	ZnO	FeO	Fe_2O_3	TiO_2	NiO	MnO	V_2O_3	MgO	SiO_2	Total	Total Fe (%):
T3-C4-1-ilm1		0.01	0.00	0.05	0.00	45.84		52.03	0.00	0.69	0.00	1.31	0.03	99.96	32.06
T3-C4-1-ilm2		0.01	0.00	0.04	0.06	45.80		50.85	0.00	0.68	0.00	1.41	0.05	98.90	32.03
T3-C4-1-ilm3		0.00	0.03	0.04	0.03	45.51		51.46	0.00	0.69	0.00	1.60	0.04	99.40	31.83
T3-C4-1-ilm4		0.00	0.00	0.05	0.00	45.82		51.32	0.00	0.72	0.00	1.35	0.05	99.31	32.05
T3-C4-1-ilm5		0.00	0.00	0.06	0.02	45.83		50.99	0.00	0.68	0.00	1.50	0.04	99.12	32.05
T3-C4-1		**0.00**	**0.01**	**0.05**	**0.02**	**45.76**		**51.33**	**0.00**	**0.69**	**0.00**	**1.43**	**0.04**	**99.34**	**32.00**
Ilmenite		*0.00*	*0.01*	*0.01*	*0.02*	*0.13*		*0.41*	*0.00*	*0.01*	*0.00*	*0.10*	*0.01*	*0.36*	*0.09*
T3-C4-2-ilm1		0.00	0.02	0.04	0.00	45.27		51.50	0.01	0.65	0.00	1.66	0.04	99.19	31.66
T3-C4-2-ilm2		0.00	0.00	0.03	0.00	46.17		51.72	0.02	0.66	0.00	1.59	0.04	100.23	32.29
T3-C4-2-ilm3		0.00	0.00	0.06	0.00	46.20		51.14	0.00	0.67	0.00	1.38	0.04	99.49	32.31
T3-C4-2-ilm4		0.01	0.02	0.04	0.04	45.83		51.41	0.01	0.65	0.00	1.57	0.02	99.60	32.05
T3-C4-2-ilm5		0.00	0.00	0.04	0.00	45.67		51.48	0.01	0.66	0.00	1.60	0.02	99.48	31.94
T3-C4-2	**Avg.**	**0.00**	**0.01**	**0.04**	**0.01**	**45.83**		**51.45**	**0.01**	**0.66**	**0.00**	**1.56**	**0.03**	**99.60**	**32.05**
Ilmenite	*Std.*	*0.00*	*0.01*	*0.01*	*0.02*	*0.34*		*0.19*	*0.01*	*0.01*	*0.00*	*0.09*	*0.01*	*0.34*	*0.24*
TA1-6-ilm1		0.00	0.00	0.03	0.00	43.93		51.70	0.01	0.62	0.00	2.28	0.03	98.60	30.72
TA1-6-ilm2		0.00	0.00	0.01	0.00	44.48		51.38	0.01	0.64	0.00	2.10	0.02	98.64	31.11
TA1-6-ilm4		0.00	0.00	0.03	0.00	44.25		51.60	0.00	0.65	0.00	2.21	0.02	98.76	30.95
TA1-6	**Avg.**	**0.00**	**0.00**	**0.02**	**0.00**	**44.22**		**51.56**	**0.01**	**0.64**	**0.00**	**2.20**	**0.02**	**98.67**	**30.93**
Ilmenite	*Std.*	*0.00*	*0.00*	*0.01*	*0.00*	*0.23*		*0.13*	*0.00*	*0.01*	*0.00*	*0.07*	*0.00*	*0.07*	*0.16*
TA1-5_ilm1		0.00	0.01	0.04	0.02	43.81	1.96	51.89	0.01	0.77	0.00	1.16	0.01	99.68	32.16
TA1-5_ilm2		0.00	0.01	0.04	0.04	44.03	1.07	52.37	0.01	0.74	0.00	1.28	0.00	99.59	31.63
TA1-5_ilm3		0.01	0.00	0.04	0.00	44.18	0.57	53.59	0.01	0.59	0.00	1.91	0.00	100.90	31.34
TA1-5_ilm4		0.00	0.00	0.02	0.00	43.13	1.53	52.40	0.01	0.61	0.00	1.89	0.00	99.59	31.35
TA1-5_ilm5		0.00	0.01	0.03	0.00	44.59	0.94	52.65	0.00	0.74	0.00	1.13	0.00	100.09	31.92
TA1-5	**Avg.**	**0.00**	**0.01**	**0.03**	**0.01**	**43.95**	**1.21**	**52.58**	**0.01**	**0.69**	**0.00**	**1.47**	**0.00**	**99.97**	**31.68**
Ilmenite	*Std.*	*0.00*	*0.00*	*0.01*	*0.02*	*0.48*	*0.48*	*0.56*	*0.00*	*0.07*	*0.00*	*0.35*	*0.00*	*0.50*	*0.32*
TA1-4_ilm1		0.01	0.01	0.03	0.03	43.15	1.18	52.92	0.01	0.65	0.00	2.10	0.00	100.09	31.10
TA1-4_ilm2		0.01	0.01	0.06	0.00	42.52	1.50	52.74	0.00	0.62	0.00	2.41	0.02	99.89	30.90
TA1-4_ilm3		0.01	0.00	0.03	0.00	43.20	0.96	52.93	0.00	0.67	0.00	2.09	0.01	99.91	30.96
TA1-4_ilm4		0.00	0.02	0.03	0.00	42.23	1.90	52.45	0.01	0.61	0.00	2.42	0.00	99.67	31.01
TA1-4_ilm5		0.00	0.00	0.02	0.00	42.82	1.30	53.07	0.00	0.61	0.00	2.41	0.00	100.23	30.96
TA1-4	**Avg.**	**0.01**	**0.01**	**0.03**	**0.01**	**42.78**	**1.37**	**52.82**	**0.00**	**0.63**	**0.00**	**2.29**	**0.01**	**99.96**	**30.99**
Ilmenite	*Std.*	*0.00*	*0.01*	*0.01*	*0.01*	*0.37*	*0.32*	*0.21*	*0.00*	*0.02*	*0.00*	*0.16*	*0.01*	*0.19*	*0.06*
TA1-1_ilm1		0.00	0.00	0.03	0.00	43.52	1.50	52.55	0.00	0.69	0.00	1.71	0.00	100.00	31.60
TA1-1_ilm2		0.00	0.01	0.06	0.00	43.48	1.98	52.11	0.01	0.67	0.00	1.52	0.01	99.86	31.95
TA1-1_ilm3		0.00	0.02	0.04	0.00	44.50	1.59	52.40	0.01	0.82	0.00	1.01	0.01	100.40	32.36
TA1-1_ilm4		0.00	0.00	0.02	0.02	44.05	1.22	52.51	0.01	0.79	0.00	1.32	0.00	99.94	31.76
TA1-1_ilm5		0.01	0.00	0.03	0.02	43.02	1.25	52.43	0.02	0.62	0.00	1.95	0.01	99.36	31.06
TA1-1	**Avg.**	**0.00**	**0.01**	**0.04**	**0.01**	**43.71**	**1.51**	**52.40**	**0.01**	**0.72**	**0.00**	**1.50**	**0.01**	**99.91**	**31.75**
Ilmenite	*Std.*	*0.00*	*0.01*	*0.01*	*0.01*	*0.51*	*0.28*	*0.15*	*0.01*	*0.08*	*0.00*	*0.32*	*0.00*	*0.33*	*0.43*
TA2-1-ilm1		0.00	0.00	0.04	0.00	45.29		52.17	0.01	0.67	0.00	2.01	0.07	100.26	31.68
TA2-1-ilm2		0.00	0.00	0.04	0.02	44.91		52.39	0.00	0.67	0.00	2.02	0.09	100.14	31.41
TA2-1-ilm3		0.00	0.00	0.07	0.04	45.71		52.06	0.00	0.75	0.00	1.58	0.06	100.27	31.97
TA2-1-ilm4		0.00	0.00	0.03	0.00	45.42		52.36	0.00	0.68	0.00	1.86	0.06	100.41	31.77
TA2-1-ilm5		0.00	0.00	0.03	0.00	45.57		52.35	0.02	0.74	0.00	1.61	0.06	100.38	31.87

Analysis ID		CaO	Cr_2O_3	Al_2O_3	ZnO	FeO	Fe_2O_3	TiO_2	NiO	MnO	V_2O_3	MgO	SiO_2	Total	Total Fe (%):
TA2-1	**Avg.**	**0.00**	**0.00**	**0.04**	**0.01**	**45.38**		**52.27**	**0.01**	**0.70**	**0.00**	**1.82**	**0.07**	**100.29**	**31.74**
Ilmenite	*Std.*	*0.00*	*0.00*	*0.01*	*0.02*	*0.27*		*0.13*	*0.01*	*0.04*	*0.00*	*0.19*	*0.01*	*0.10*	*0.19*
TA2-3-ilm1		0.00	0.00	0.03	0.05	45.28		52.57	0.02	0.61	0.00	2.02	0.06	100.64	31.67
TA2-3-ilm2		0.00	0.00	0.02	0.10	45.49		52.67	0.01	0.66	0.00	1.99	0.07	101.01	31.82
TA2-3-ilm3		0.00	0.00	0.02	0.04	44.78		52.78	0.01	0.65	0.00	2.16	0.05	100.49	31.32
TA2-3-ilm4		0.00	0.00	0.04	0.00	45.22		52.56	0.01	0.63	0.00	2.03	0.10	100.59	31.63
TA2-3-ilm5		0.01	0.01	0.03	0.00	44.65		52.49	0.01	0.60	0.00	2.13	0.07	100.00	31.23
TA2-3	**Avg.**	**0.00**	**0.00**	**0.03**	**0.04**	**45.08**		**52.61**	**0.01**	**0.63**	**0.00**	**2.07**	**0.07**	**100.55**	**31.53**
Ilmenite	*Std.*	*0.00*	*0.00*	*0.01*	*0.04*	*0.32*		*0.10*	*0.00*	*0.02*	*0.00*	*0.07*	*0.02*	*0.32*	*0.22*
TA2-4-ilm1		0.00	0.00	0.03	0.00	45.24		52.64	0.00	0.61	0.00	1.90	0.02	100.44	31.64
TA2-4-ilm2		0.00	0.00	0.04	0.00	45.97		52.14	0.01	0.67	0.00	1.74	0.05	100.62	32.15
TA2-4-ilm4		0.00	0.00	0.03	0.00	45.71		52.17	0.01	0.64	0.00	1.94	0.06	100.56	31.97
TA2-4-ilm5		0.00	0.00	0.03	0.00	45.96		51.56	0.00	0.70	0.00	1.62	0.02	99.89	32.14
TA2-4	**Avg.**	**0.00**	**0.00**	**0.03**	**0.00**	**45.72**		**52.13**	**0.01**	**0.66**	**0.00**	**1.80**	**0.04**	**100.38**	**31.98**
Ilmenite	*Std.*	*0.00*	*0.00*	*0.00*	*0.00*	*0.30*		*0.38*	*0.01*	*0.03*	*0.00*	*0.13*	*0.02*	*0.29*	*0.21*
TA2-6-ilm1		0.00	0.00	0.03	0.00	45.39		51.22	0.01	0.62	0.00	1.83	0.01	99.11	31.75
TA2-6-ilm2		0.00	0.00	0.02	0.00	45.66		51.77	0.02	0.67	0.00	1.58	0.02	99.74	31.93
TA2-6-ilm3		0.01	0.00	0.04	0.01	45.95		51.73	0.02	0.68	0.00	1.67	0.01	100.12	32.14
TA2-6-ilm4		0.01	0.02	0.03	0.00	45.25		52.10	0.01	0.61	0.00	1.83	0.01	99.87	31.65
TA2-6-ilm5		0.00	0.00	0.03	0.00	45.65		52.28	0.01	0.69	0.00	1.67	0.02	100.35	31.93
TA2-6	**Avg.**	**0.00**	**0.00**	**0.03**	**0.00**	**45.58**		**51.82**	**0.01**	**0.65**	**0.00**	**1.72**	**0.01**	**99.84**	**31.88**
Ilmenite	*Std.*	*0.00*	*0.01*	*0.01*	*0.00*	*0.24*		*0.36*	*0.00*	*0.03*	*0.00*	*0.10*	*0.00*	*0.42*	*0.17*

APPENDIX 2

Full results from LA-ICP-MS analyses of magnetite and ilmenite

Analysis ID	Notes	Analysis Length (s)	Fe (wt%)	24Mg	27Al	29Si	31P	44Ca	45SC	47Ti	51V	52Cr	55Mn	59Co
14-2A-MT-2.D		53.4	**57.88**	3542.12	14527.3	735.05	5.50	13.20	19.79	98971.1	7402.58	507.59	2494.54	178.26
14-2A-MT-3.D		49.9	**57.88**	2552.41	11459.8	810.29	11.17	25.47	28.36	166109.4	6655.95	540.00	6482.32	146.08
14-2A-MT-5.D		49.9	**57.88**	2392.67	15106.1	297.49	8.10	9.26	6.72	30270.1	8745.34	621.61	829.97	170.62
14-2A-MT-6.D		49.9	**57.88**	5151.13	9260.5	1828.94	1.16	47.46	39.36	175369.9	6135.05	464.18	4109.33	163.97
14-2A-MT-7.D		49.9	**57.88**	2848.75	17102.9	214.15	2.72	-3.47	9.45	40086.2	8317.05	496.94	1067.27	171.78
MA14-2A	**Avg.**		**57.88**	**3297.42**	**13491.3**	**777.18**	**5.73**	**18.38**	**20.74**	**102161.3**	**7451.19**	**526.06**	**2996.68**	**166.14**
Magnetite	*Std.*		***57.88***	*1007.08*	*2783.9*	*575.53*	*3.61*	*17.22*	*12.08*	*60795.9*	*978.93*	*53.56*	*2100.34*	*11.01*
14-2D-MT-3.D		49.9	**59.63**	4430.70	19243.5	369.72	7.16	4.77	29.34	107338.7	6941.24	774.03	2922.00	221.42
14-2D-MT-1.D		49.9	**59.63**	2450.90	22046.2	276.10	5.37	10.73	19.99	74421.5	7805.91	841.42	1805.68	160.95
14-2D-MT-2-1.D		37.4	**59.63**	3524.29	22660.4	228.99	4.17	5.37	20.69	73228.9	7782.06	863.48	1801.50	203.53
14-2D-MT-2-2.D		49.9	**59.63**	2868.33	22308.6	320.23	8.94	4.17	19.92	72692.2	7686.65	848.57	1809.25	222.37
14-2D-MT-4.D		49.9	**59.63**	2975.67	20227.4	264.17	-11.33	20.87	21.53	76747.2	7561.42	798.48	1962.51	212.29
14-2D-MT-6.D		49.9	**59.63**	2880.26	24151.2	351.83	4.00	13.78	10.71	68040.8	8730.22	719.77	1468.16	221.30
MA14-2D	**Avg.**		**59.63**	**3188.36**	**21772.9**	**301.84**	**3.05**	**9.95**	**20.36**	**78744.9**	**7751.25**	**807.62**	**1961.52**	**206.97**
Magnetite	*Std.*		***59.63***	*638.06*	*1612.1*	*49.72*	*6.66*	*6.00*	*5.41*	*13050.7*	*525.78*	*49.78*	*454.42*	*21.64*
14-3A-MT-3.D		35.4	**63.57**	1156.94	9446.2	293.05	5.59	19.07	16.15	82003.0	8174.87	992.30	3394.54	136.61
14-3A-MT-4.D		49.9	**63.57**	519.99	3381.8	1067.95	-0.06	38.14	6.42	64839.5	7558.26	1090.83	2269.38	59.69
14-3A-MT-5.D		49.9	**63.57**	826.39	6738.2	1589.20	9.92	51.49	3.94	54033.0	7672.68	987.85	2116.82	64.59
14-3A-MT-6.D		49.9	**63.57**	673.82	4850.3	743.75	7.37	88.36	5.47	67382.3	7431.12	965.60	2650.79	49.20
14-3A-MT-7.D		49.9	**63.57**	638.86	5250.7	362.34	2.99	6.93	7.95	85181.4	8282.93	1099.09	3528.03	92.62
MA14-3A	**Avg.**		**63.57**	**763.20**	**5933.5**	**811.26**	**5.16**	**40.80**	**7.98**	**70687.8**	**7823.97**	**1027.13**	**2791.91**	**80.54**
Magnetite	*Std.*		***63.57***	*219.83*	*2056.1*	*478.69*	*3.46*	*28.29*	*4.28*	*11494.4*	*341.06*	*56.18*	*575.11*	*31.50*
14-3B-T-MT-1.D		49.9	**65.48**	350.30	12519.2	254.71	0.39	5.76	4.39	37976.7	9107.86	1081.68	1551.81	133.90
14-3B-T-MT-3.D		49.9	**65.48**	610.25	13540.7	227.86	8.38	5.63	4.71	51726.9	8931.07	1047.63	1918.48	160.81
14-3B-T-MT-4.D		45.3	**65.48**	517.27	9088.2	464.89	0.65	16.37	3.34	47143.5	7798.32	1094.12	1885.74	115.50
14-3B-T-MT-5.D		54.6	**65.48**	477.98	8178.1	214.76	2.36	1.57	5.96	89703.6	6914.38	984.12	3391.71	117.27
14-3B-T-MT-8.D		46.4	**65.48**	929.77	17220.5	615.48	3.27	21.61	5.17	47798.2	8557.85	1022.75	1754.78	138.16
MA14-3B-T	**Avg.**		**65.48**	**577.11**	**12109.3**	**355.54**	**3.01**	**10.19**	**4.71**	**54869.8**	**8261.89**	**1046.06**	**2100.50**	**133.13**
Magnetite	*Std.*		***65.48***	*195.10*	*3253.4*	*158.63*	*2.89*	*7.53*	*0.87*	*17990.8*	*810.15*	*39.90*	*658.34*	*16.46*
14-4-MT-10.D		49.9	**68.55**	268.04	5237.5	2200.57	4.11	1515.04	4.57	29957.9	7232.41	332.97	767.80	19.44
14-4-MT-5.D		51.6	**68.55**	295.47	6149.3	1967.49	5.55	1247.68	5.07	43188.8	7835.68	304.10	1172.27	26.80
14-4-MT-7.D		49.9	**68.55**	678.68	9357.6	3331.71	-0.41	87.06	3.35	25364.8	7109.01	317.88	829.50	31.74
14-4-MT-8-1.D		53.5	**68.55**	282.44	12065.4	397.61	5.14	39.76	7.75	62383.8	6224.67	271.75	1782.39	36.88
14-4-MT-8-2.D		49.9	**68.55**	241.99	14122.1	856.92	1.23	59.64	3.85	36607.6	6362.46	307.05	1028.30	33.39
MA14-4	**Avg.**		**68.55**	**353.33**	**9386.4**	**1750.86**	**3.13**	**589.84**	**4.92**	**39500.6**	**6952.85**	**306.75**	**1116.05**	**29.65**
Magnetite	*Std.*		***68.55***	*163.64*	*3385.2*	*1037.17*	*2.32*	*651.95*	*1.53*	*12934.4*	*593.42*	*20.22*	*362.84*	*6.05*
14-5A-MT-2.D		49.9	**64.19**	553.92	3408.3	109.76	2.50	17.33	6.93	74327.3	7766.50	526.90	3010.32	128.76
14-5A-MT-3-1.D		49.9	**64.19**	521.83	3921.8	164.96	1.35	14.70	6.32	80938.5	7484.08	453.47	3408.27	139.99

Analysis ID		60Ni	63Cu	66Zn	69Ga	74Ge	89Y	90Zr	93Nb	95Mo	118Sn	178Hf	181Ta	182W	208Pb
14-2A-MT-2.D		241.93	0.85	635.50	52.09	0.80	0.11	13.89	2.03	0.79	1.20	0.67	0.10	0.12	0.02
14-2A-MT-3.D		228.62	1.06	393.57	45.38	0.74	0.08	24.37	3.76	0.93	0.49	1.20	0.18	0.07	0.03
14-2A-MT-5.D		280.71	0.11	398.20	62.28	1.02	0.01	1.57	0.02	0.74	1.25	0.11	0.00	0.01	0.02
14-2A-MT-6.D		235.56	2.60	596.14	39.82	0.82	0.23	32.41	4.80	0.86	1.04	1.16	0.24	0.10	0.13
14-2A-MT-7.D		289.74	0.08	416.72	56.95	1.01	0.01	2.37	0.04	0.63	1.24	0.19	0.00	0.00	0.00
MA14-2A	**Avg.**	**255.31**	**0.94**	**488.03**	**51.30**	**0.88**	**0.09**	**14.92**	**2.13**	**0.79**	**1.04**	**0.67**	**0.10**	**0.06**	**0.04**
Magnetite	*Std.*	*24.95*	*0.92*	*105.37*	*8.00*	*0.12*	*0.08*	*12.10*	*1.93*	*0.10*	*0.29*	*0.46*	*0.09*	*0.05*	*0.05*
14-2D-MT-3.D		320.23	1.41	577.84	46.99	1.03	0.05	24.87	1.12	0.55	0.72	0.86	0.09	0.01	0.01
14-2D-MT-1.D		264.77	0.51	499.13	51.52	1.14	0.02	14.85	0.34	0.44	0.85	0.52	0.02	0.00	0.27
14-2D-MT-2-1.D		309.49	0.70	492.57	49.73	0.88	0.03	14.52	0.29	0.57	0.83	0.53	0.02	0.00	0.00
14-2D-MT-2-2.D		316.65	0.18	480.04	49.85	0.71	0.04	13.33	0.24	0.55	0.86	0.60	0.02	0.01	-0.01
14-2D-MT-4.D		305.32	1.34	574.26	50.57	0.91	0.08	16.30	0.30	0.52	0.80	0.58	0.03	0.01	0.02
14-2D-MT-6.D		293.99	0.11	601.69	61.24	0.86	0.21	13.95	0.18	0.78	1.09	0.54	0.02	0.00	0.02
MA14-2D	**Avg.**	**301.74**	**0.71**	**537.59**	**51.65**	**0.92**	**0.07**	**16.30**	**0.41**	**0.57**	**0.86**	**0.61**	**0.03**	**0.01**	**0.05**
Magnetite	*Std.*	*18.55*	*0.51*	*48.12*	*4.51*	*0.14*	*0.06*	*3.94*	*0.32*	*0.10*	*0.11*	*0.12*	*0.03*	*0.01*	*0.10*
14-3A-MT-3.D		200.24	0.24	1176.01	47.68	1.19	0.05	17.04	0.43	0.54	0.88	0.55	0.03	0.02	0.02
14-3A-MT-4.D		178.94	0.75	555.59	35.66	0.95	0.18	12.21	0.36	0.51	0.39	0.37	0.01	0.03	0.32
14-3A-MT-5.D		154.60	8.26	1093.37	38.33	1.00	0.31	5.72	0.33	0.50	0.51	0.24	0.02	0.00	0.33
14-3A-MT-6.D		124.85	1.08	686.54	33.06	0.89	0.10	11.19	0.40	0.53	0.54	0.38	0.03	0.02	0.01
14-3A-MT-7.D		187.08	0.43	729.76	42.02	0.96	0.07	14.56	0.51	0.67	0.45	0.38	0.03	0.00	0.03
MA14-3A	**Avg.**	**169.14**	**2.15**	**848.25**	**39.35**	**1.00**	**0.14**	**12.14**	**0.41**	**0.55**	**0.56**	**0.38**	**0.02**	**0.01**	**0.14**
Magnetite	*Std.*	*26.68*	*3.07*	*242.22*	*5.11*	*0.10*	*0.10*	*3.79*	*0.06*	*0.06*	*0.17*	*0.10*	*0.01*	*0.01*	*0.15*
14-3B-T-MT-1.D		210.31	0.12	603.04	54.54	1.05	0.03	3.16	0.18	0.60	0.44	0.11	0.01	0.01	0.00
14-3B-T-MT-3.D		236.50	0.17	1100.01	64.30	1.13	0.04	5.11	0.24	0.72	0.78	0.24	0.01	0.01	0.00
14-3B-T-MT-4.D		228.51	0.60	948.76	55.72	0.94	0.03	6.29	0.34	0.62	0.60	0.20	0.01	0.01	0.02
14-3B-T-MT-5.D		227.21	4.58	749.71	52.32	0.89	0.05	11.46	0.79	0.74	0.43	0.23	0.05	0.06	0.02
14-3B-T-MT-8.D		216.07	0.45	1381.57	63.84	1.11	0.06	5.43	0.20	0.60	0.74	0.26	0.02	0.02	0.11
MA14-3B-T	**Avg.**	**223.72**	**1.18**	**956.62**	**58.14**	**1.02**	**0.04**	**6.29**	**0.35**	**0.65**	**0.60**	**0.21**	**0.02**	**0.02**	**0.03**
Magnetite	*Std.*	*9.35*	*1.71*	*271.67*	*4.96*	*0.09*	*0.01*	*2.78*	*0.23*	*0.06*	*0.15*	*0.05*	*0.02*	*0.02*	*0.04*
14-4-MT-10.D		50.52	1.78	1118.80	79.18	1.40	0.26	1.23	1.17	1.84	0.53	0.15	0.02	0.08	0.09
14-4-MT-5.D		54.43	1.49	2186.86	75.75	1.38	0.36	1.12	1.67	2.32	0.77	0.14	0.02	0.07	0.40
14-4-MT-7.D		63.82	0.25	1741.26	86.38	1.29	0.15	0.75	0.51	2.27	0.68	0.09	0.01	0.02	0.07
14-4-MT-8-1.D		66.29	0.64	1453.34	73.35	1.22	0.12	2.47	1.58	2.14	1.23	0.29	0.02	0.04	0.11
14-4-MT-8-2.D		66.22	2.06	3434.54	76.03	1.26	0.04	0.62	0.90	2.15	0.99	0.07	0.02	0.02	0.23
MA14-4	**Avg.**	**60.26**	**1.24**	**1986.96**	**78.14**	**1.31**	**0.19**	**1.24**	**1.17**	**2.14**	**0.84**	**0.15**	**0.02**	**0.05**	**0.18**
Magnetite	*Std.*	*6.53*	*0.69*	*804.27*	*4.52*	*0.07*	*0.11*	*0.65*	*0.43*	*0.17*	*0.25*	*0.08*	*0.01*	*0.03*	*0.12*
14-5A-MT-2.D		208.73	0.55	1526.98	42.36	0.74	0.09	3.49	0.58	0.69	0.23	0.16	0.02	0.13	0.04
14-5A-MT-3-1.D		203.98	0.52	1810.04	41.79	0.73	0.12	4.26	0.46	0.65	0.24	0.13	0.03	0.16	0.06

Analysis ID	Notes	Analysis Length (s)	Fe (wt%)	24Mg	27Al	29Si	31P	44Ca	45SC	47Ti	51V	52Cr	55Mn	59Co
14-5A-MT-3-2.D		49.9	**64.19**	279.85	3222.1	125.80	-0.13	11.68	2.94	39602.7	7111.80	453.22	1784.37	121.05
14-5A-MT-4.D		48.4	**64.19**	577.67	3279.9	519.91	-2.50	102.06	4.54	63929.2	7683.06	526.90	2708.65	105.33
14-5A-MT-8.D		49.9	**64.19**	557.13	3761.3	146.34	-3.47	5.78	5.72	67010.1	7143.89	486.53	2894.79	142.69
MA14-5A	**Avg.**		64.19	**498.08**	**3518.7**	**213.35**	**-0.45**	**30.31**	**5.29**	**65161.6**	**7437.87**	**489.40**	**2761.28**	**127.56**
Magnetite	*Std.*		***64.19***	*110.57*	*275.1*	*154.40*	*2.25*	*36.08*	*1.41*	*14079.1*	*269.44*	*32.93*	*539.55*	*13.57*
14-5C-MT-3-1.D		49.9	**65.89**	137.32	2747.7	133.76	0.20	13.38	3.04	68197.7	8532.95	772.25	2214.61	60.03
14-5C-MT-3-2.D		37.7	**65.89**	625.97	1825.2	1475.97	3.36	251.05	1.01	40721.0	10160.47	844.07	1331.01	45.20
14-5C-MT-4.D		*16.3*	***65.89***	*88.95*	*2128.3*	*178.57*	*3.95*	*21.88*	*2.01*	*58248.1*	*9290.70*	*809.15*	*1885.16*	*43.49*
14-5C-MT-4.D		*14.4*	***65.89***	*74.00*	*1660.5*	*256.98*	*4.48*	*78.41*	*1.55*	*43422.5*	*9462.02*	*735.35*	*1390.31*	*40.98*
14-5C-MT-6.D		49.9	**65.89**	122.43	2490.7	189.11	5.40	16.47	3.02	64046.6	8981.01	720.19	2105.89	50.80
MA14-5C	**Avg.**		65.89	**241.91**	**2243.2**	**503.54**	**3.29**	**82.32**	**2.21**	**56066.5**	**9261.36**	**777.77**	**1826.20**	**49.59**
Magnetite	*Std.*		***65.89***	*222.66*	*388.0*	*562.21*	*1.93*	*98.37*	*0.86*	*10828.7*	*597.83*	*44.02*	*355.04*	*6.76*
14-6AT-MT-3-1.D		49.9	**66.82**	584.68	5686.5	227.19	0.60	4.01	2.94	48044.4	8720.15	759.09	1547.58	132.51
14-6AT-MT-3-2.D		49.9	**66.82**	532.56	6642.0	302.70	1.34	5.81	2.96	51118.1	8737.52	735.03	1606.38	137.25
14-6AT-MT-3-3.D		*16.8*	***66.82***	*608.07*	*5512.7*	*273.97*	*-1.34*	*-6.68*	*3.08*	*47977.5*	*8927.30*	*795.17*	*1483.43*	*122.62*
14-6AT-MT-3-3.D		*27.8*	***66.82***	*612.75*	*5265.5*	*294.01*	*0.67*	*4.01*	*2.31*	*37486.6*	*8947.34*	*845.95*	*1183.40*	*122.48*
14-6AT-MT-4.D		*19.9*	***66.82***	*605.40*	*3975.9*	*1496.79*	*2.61*	*87.54*	*3.68*	*52387.7*	*7945.03*	*605.67*	*1623.75*	*140.32*
14-6AT-MT-4.D		*16.2*	***66.82***	*511.85*	*5452.6*	*521.20*	*2.94*	*11.36*	*3.81*	*50449.9*	*7891.57*	*607.40*	*1626.43*	*109.59*
MA14-6A-T	**Avg.**		66.82	**572.92**	**5581.3**	**468.89**	**1.15**	**15.79**	**3.06**	**48029.8**	**8579.63**	**731.85**	**1540.11**	**128.44**
Magnetite	*Std.*		***66.82***	*28.75*	*720.3*	*341.97*	*1.05*	*21.80*	*0.42*	*4036.1*	*389.91*	*79.84*	*125.13*	*11.19*
14-6B-MT-1.D		49.9	**64.81**	512.67	4374.9	265.73	-0.78	31.76	7.91	63062.8	6863.67	532.89	2339.74	129.56
14-6B-MT-2.D		49.9	**64.81**	293.60	6734.0	170.46	-1.30	16.85	5.81	69803.4	7336.81	482.79	2637.88	98.26
14-6B-MT-3.D		49.9	**64.81**	486.10	6092.4	725.90	4.28	91.39	5.95	58914.8	6792.38	566.98	2216.60	114.33
14-6B-MT-4.D		49.9	**64.81**	224.90	4711.9	176.94	3.69	8.88	4.43	59562.9	7084.04	512.67	2151.78	102.08
14-6B-MT-5.D		*12.0*	***64.81***	*438.78*	*5496.1*	*220.36*	*3.24*	*69.35*	*6.07*	*61053.6*	*6578.50*	*445.91*	*2300.85*	*144.34*
14-6B-MT-5.D		*33.0*	***64.81***	*285.82*	*3811.0*	*121.85*	*32.41*	*18.02*	*5.37*	*56387.1*	*6565.53*	*504.24*	*2080.49*	*125.35*
14-6B-MT-6.D		49.9	**64.81**	328.60	4433.2	189.25	0.91	9.40	5.48	60275.9	6999.78	641.65	2307.34	120.75
MA14-6B	**Avg.**		64.81	**362.10**	**5101.3**	**279.41**	**5.24**	**31.67**	**5.86**	**61542.4**	**6940.95**	**537.60**	**2298.79**	**115.90**
Magnetite	*Std.*		***64.81***	*103.23*	*955.6*	*203.00*	*8.91*	*28.29*	*1.04*	*4046.7*	*240.50*	*54.36*	*168.57*	*12.42*
14-7A-MT-2.D		45.6	**65.52**	260.13	2483.3	258.82	-0.13	21.62	6.88	47832.0	6093.67	580.54	1959.15	99.73
14-7A-MT-3.D		32.8	**65.52**	72.08	858.4	196.57	-0.85	22.93	6.03	40427.9	6722.69	694.55	1644.63	86.56
14-7A-MT-4-1.D		*9.8*	***65.52***	*454.08*	*23.0*	*230.64*	*-2.62*	*13.10*	*103.33*	*514357.9*	*3649.65*	*131.24*	*19925.63*	*202.01*
14-7A-MT-4-1.D		*20.6*	***65.52***	*108.77*	*976.3*	*453.42*	*3.28*	*224.74*	*1.70*	*14022.0*	*6244.37*	*582.50*	*642.13*	*85.05*
14-7A-MT-4-2.D		46.3	**65.52**	139.56	808.6	310.58	-1.31	63.56	4.13	30271.8	6938.92	533.36	1303.91	86.49
14-7A-MT-6.D		*28.4*	***65.52***	*138.25*	*2083.6*	*210.99*	*0.85*	*37.35*	*3.16*	*25816.2*	*6185.40*	*581.85*	*1159.76*	*86.62*
14-7A-MT-6.D		*9.1*	***65.52***	*119.25*	*1369.4*	*550.40*	*-8.52*	*504.53*	*2.42*	*23457.3*	*6309.89*	*543.84*	*1113.90*	*77.91*
MA14-7A	**Avg.**		65.52	**165.07**	**1346.1**	**288.16**	**-0.47**	**83.03**	**10.89**	**63776.8**	**6275.96**	**563.66**	**2581.38**	**96.00**
Magnetite	*Std.*		***65.52***	*66.83*	*720.7*	*60.87*	*1.03*	*59.53*	*11.84*	*56215.8*	*534.34*	*82.95*	*2152.90*	*14.41*

Analysis ID		60Ni	63Cu	66Zn	69Ga	74Ge	89Y	90Zr	93Nb	95Mo	118Sn	178Hf	181Ta	182W	208Pb
14-5A-MT-3-2.D		213.61	0.49	1816.46	44.29	0.78	0.06	2.05	0.18	0.58	0.20	0.08	0.02	0.07	0.03
14-5A-MT-4.D		209.18	0.42	1463.44	43.97	0.83	0.08	2.95	0.44	0.58	0.19	0.09	0.03	0.13	0.05
14-5A-MT-8.D		210.34	0.47	2073.21	43.26	0.80	0.13	3.11	0.60	0.45	0.30	0.11	0.02	0.14	0.04
MA14-5A	**Avg.**	**209.17**	**0.49**	**1738.03**	**43.13**	**0.78**	**0.10**	**3.17**	**0.45**	**0.59**	**0.23**	**0.12**	**0.02**	**0.13**	**0.04**
Magnetite	*Std.*	*3.10*	*0.04*	*220.74*	*0.94*	*0.04*	*0.02*	*0.72*	*0.15*	*0.08*	*0.04*	*0.03*	*0.00*	*0.03*	*0.01*
14-5C-MT-3-1.D		144.37	0.43	2464.34	31.97	0.80	0.16	2.37	1.04	0.53	0.22	0.12	0.02	0.05	0.05
14-5C-MT-3-2.D		143.12	0.09	292.56	31.76	0.92	0.06	0.84	0.29	0.57	0.07	0.03	0.02	0.05	0.06
14-5C-MT-4.D		*143.18*	*-0.16*	*1607.75*	*28.66*	*0.64*	*0.12*	*1.50*	*0.61*	*0.51*	*0.13*	*0.06*	*0.02*	*0.02*	*0.05*
14-5C-MT-4.D		*148.26*	*0.05*	*1192.64*	*28.66*	*0.65*	*0.07*	*1.36*	*0.48*	*0.48*	*0.10*	*0.06*	*0.02*	*0.04*	*0.06*
14-5C-MT-6.D		123.88	0.21	2101.94	28.93	0.74	0.14	2.12	0.78	0.51	0.15	0.10	0.03	0.07	0.08
MA14-5C	**Avg.**	**139.23**	**0.17**	**1568.02**	**30.33**	**0.77**	**0.11**	**1.69**	**0.66**	**0.53**	**0.14**	**0.08**	**0.02**	**0.05**	**0.06**
Magnetite	*Std.*	*8.91*	*0.18*	*827.53*	*1.54*	*0.10*	*0.04*	*0.60*	*0.28*	*0.03*	*0.05*	*0.03*	*0.00*	*0.02*	*0.01*
14-6AT-MT-3-1.D		179.08	0.32	1075.15	54.53	0.88	0.06	2.02	0.28	0.74	0.13	0.06	0.01	0.59	0.01
14-6AT-MT-3-2.D		179.01	0.50	1162.69	53.92	0.73	0.04	2.24	0.26	0.69	0.13	0.08	0.01	0.47	0.06
14-6AT-MT-3-3.D		*183.82*	*0.21*	*829.92*	*55.86*	*1.00*	*0.05*	*2.30*	*0.38*	*0.84*	*0.11*	*0.12*	*0.01*	*0.53*	*0.03*
14-6AT-MT-3-3.D		*187.10*	*0.37*	*759.76*	*56.26*	*0.84*	*0.03*	*1.92*	*0.32*	*0.51*	*0.10*	*0.07*	*0.01*	*0.41*	*0.02*
14-6AT-MT-4.D		*183.09*	*2.47*	*1490.11*	*44.44*	*0.84*	*0.04*	*1.44*	*0.37*	*0.88*	*0.11*	*0.06*	*0.01*	*0.33*	*0.18*
14-6AT-MT-4.D		*173.07*	*0.55*	*955.54*	*50.38*	*0.65*	*0.02*	*1.78*	*0.34*	*0.76*	*0.17*	*0.10*	*0.01*	*0.43*	*0.08*
MA14-6A-T	**Avg.**	**180.02**	**0.83**	**1093.93**	**51.88**	**0.80**	**0.04**	**1.91**	**0.32**	**0.74**	**0.13**	**0.08**	**0.01**	**0.46**	**0.07**
Magnetite	*Std.*	*4.33*	*0.83*	*234.90*	*4.17*	*0.10*	*0.01*	*0.28*	*0.04*	*0.08*	*0.02*	*0.02*	*0.00*	*0.08*	*0.06*
14-6B-MT-1.D		195.41	0.38	905.43	44.27	0.84	0.10	2.62	0.59	0.46	0.28	0.14	0.02	0.73	0.07
14-6B-MT-2.D		166.96	0.32	1867.90	54.38	0.73	0.07	4.45	0.32	0.51	0.23	0.15	0.02	0.78	0.01
14-6B-MT-3.D		179.92	0.70	1335.14	46.47	0.82	0.08	3.37	0.45	0.51	0.27	0.14	0.02	0.79	0.08
14-6B-MT-4.D		141.49	0.30	1530.88	44.59	0.76	0.08	3.69	0.44	0.60	0.21	0.13	0.02	0.84	0.03
14-6B-MT-5.D		*204.68*	*0.62*	*1218.48*	*44.98*	*0.89*	*0.07*	*3.05*	*0.52*	*0.57*	*0.29*	*0.12*	*0.02*	*0.94*	*0.00*
14-6B-MT-5.D		*192.56*	*0.33*	*841.27*	*43.68*	*0.80*	*0.04*	*2.95*	*0.49*	*0.50*	*0.28*	*0.13*	*0.01*	*0.50*	*0.00*
14-6B-MT-6.D		184.85	0.37	1170.52	43.94	0.81	0.07	2.42	0.59	0.53	0.20	0.08	0.02	0.58	0.05
MA14-6B	**Avg.**	**177.40**	**0.41**	**1292.00**	**46.28**	**0.80**	**0.07**	**3.25**	**0.48**	**0.52**	**0.24**	**0.13**	**0.02**	**0.72**	**0.04**
Magnetite	*Std.*	*18.81*	*0.13*	*335.96*	*3.72*	*0.04*	*0.02*	*0.68*	*0.09*	*0.04*	*0.03*	*0.02*	*0.00*	*0.09*	*0.03*
14-7A-MT-2.D		217.28	0.28	2188.48	27.13	0.75	0.16	1.37	0.34	0.31	0.28	0.09	0.01	0.05	0.07
14-7A-MT-3.D		209.35	0.16	537.29	35.25	0.74	0.09	0.62	0.24	0.21	0.12	0.03	0.01	0.02	0.05
14-7A-MT-4-1.D		*58.84*	*17.69*	*154.63*	*1.23*	*0.19*	*0.47*	*12.91*	*5.24*	*2.27*	*1.68*	*1.07*	*0.11*	*0.10*	*0.03*
14-7A-MT-4-1.D		*236.01*	*0.41*	*602.81*	*36.17*	*1.05*	*0.03*	*0.30*	*0.09*	*0.29*	*0.12*	*0.01*	*0.00*	*0.09*	*0.09*
14-7A-MT-4-2.D		241.58	0.25	446.87	35.05	0.81	0.05	0.77	0.17	0.28	0.21	0.06	0.00	0.02	0.06
14-7A-MT-6.D		*204.30*	*0.92*	*1932.94*	*34.14*	*0.75*	*0.11*	*0.88*	*0.23*	*0.30*	*0.17*	*0.05*	*0.01*	*0.01*	*0.03*
14-7A-MT-6.D		*204.76*	*0.41*	*1199.08*	*32.37*	*0.74*	*0.10*	*0.52*	*0.20*	*0.29*	*0.10*	*0.01*	*0.01*	*0.01*	*0.09*
MA14-7A	**Avg.**	**210.32**	**1.49**	**1077.29**	**31.21**	**0.76**	**0.11**	**1.58**	**0.54**	**0.41**	**0.28**	**0.12**	**0.01**	**0.04**	**0.06**
Magnetite	*Std.*	*20.22*	*2.25*	*743.82*	*4.33*	*0.02*	*0.04*	*1.41*	*0.60*	*0.26*	*0.18*	*0.12*	*0.01*	*0.03*	*0.01*

Analysis ID	Notes	Analysis Length (s)	Fe (wt%)	24Mg	27Al	29Si	31P	44Ca	45SC	47Ti	51V	52Cr	55Mn	59Co
14-7B-MT-1-1.D		49.9	**67.60**	281.88	3156.8	223.74	-0.14	0.81	5.98	48196.3	6462.23	594.17	1933.26	89.84
14-7B-MT-1-2.D		49.9	**67.60**	294.72	2440.2	186.57	7.23	1.22	5.62	45762.8	7131.43	651.63	1845.38	92.61
14-7B-MT-2.D		*5.8*	***67.60***	*229.83*	*6556.9*	*270.39*	*-6.08*	*200.76*	*7.91*	*60701.7*	*6489.26*	*682.05*	*2615.98*	*103.42*
14-7B-MT-2.D		*14.6*	***67.60***	*197.38*	*3048.6*	*290.66*	*-4.06*	*141.95*	*5.34*	*40693.1*	*6759.65*	*735.45*	*1737.23*	*89.97*
14-7B-MT-5-1.D		49.9	**67.60**	267.01	4488.4	150.74	2.84	14.87	4.64	47317.5	7185.51	647.57	1906.22	106.13
14-7B-MT-5-2.D		*15.6*	***67.60***	*210.23*	*3900.3*	*210.23*	*9.46*	*93.28*	*9.04*	*63202.7*	*7381.54*	*598.23*	*2602.47*	*103.22*
14-7B-MT-5-2.D		*13.5*	***67.60***	*189.27*	*4373.5*	*160.20*	*-4.06*	*8.11*	*6.56*	*48669.5*	*7537.01*	*602.96*	*2014.38*	*104.17*
MA14-7B	**Avg.**		**67.60**	**250.15**	**3650.5**	**206.59**	**1.70**	**45.87**	**6.04**	**48825.1**	**6983.10**	**642.81**	**2000.37**	**97.21**
Magnetite	*Std.*		***67.60***	*39.08*	*746.8*	*45.45*	*3.94*	*59.63*	*1.05*	*3905.7*	*359.44*	*45.30*	*170.86*	*6.45*
14-8A-MT-10.D		48.1	**65.21**	284.30	5979.5	192.36	5.48	35.28	4.39	53861.3	8503.05	1415.00	2986.50	93.05
14-8A-MT-5.D		43.1	**65.21**	402.33	6944.6	528.18	3.13	139.54	4.63	58360.6	7968.35	1210.90	3084.31	57.51
14-8A-MT-6-1.D		49.9	**65.21**	460.36	7864.0	198.88	1.89	3.98	8.31	63055.6	6885.90	1475.64	3612.49	122.98
14-8A-MT-6-2.D		*23.7*	***65.21***	*294.74*	*5770.9*	*239.31*	*5.22*	*18.26*	*5.48*	*58034.6*	*5868.67*	*1536.94*	*3090.83*	*94.55*
14-8A-MT-6-2.D		*7.4*	***65.21***	*217.79*	*5731.7*	*189.10*	*2.61*	*7.82*	*3.68*	*36711.8*	*5933.87*	*1483.47*	*2040.99*	*82.88*
14-8A-MT-7.D		49.9	**65.21**	301.91	6233.8	215.18	2.87	19.17	5.89	50796.6	7086.74	1226.55	2784.36	75.12
14-8A-MT-9.D		26.3	**65.21**	521.66	6546.8	599.91	0.65	59.34	7.34	69185.1	8437.84	1167.21	3768.99	93.12
MA14-8A	**Avg.**		**65.21**	**374.49**	**6555.0**	**326.98**	**3.10**	**45.51**	**5.94**	**58034.6**	**7461.02**	**1336.58**	**3179.51**	**88.92**
Magnetite	*Std.*		***65.21***	*93.84*	*698.7*	*169.28*	*1.60*	*45.54*	*1.44*	*6394.3*	*935.82*	*139.80*	*376.92*	*19.92*
14-8B-MT-3-1.D		49.9	**69.10**	214.22	4394.9	331.69	6.08	5.80	5.15	46229.0	7815.40	1358.54	2480.75	60.19
14-8B-MT-3-2.D		41.4	**69.10**	233.56	5065.2	213.52	4.49	7.05	6.25	49200.4	8319.85	1387.56	2612.04	77.26
14-8B-MT-4.D		49.9	**69.10**	122.31	1789.7	158.93	5.18	20.66	1.85	37314.9	7760.12	1454.59	1983.22	48.23
14-8B-MT-6.D		24.4	**69.10**	43.95	1230.0	144.42	5.53	11.75	1.08	6219.2	11249.76	1743.44	415.99	21.91
14-8B-MT-7.D		36.0	**69.10**	170.68	4325.8	228.04	-0.97	42.84	4.03	30543.0	10904.25	1641.17	1769.00	33.10
MA14-8B	**Avg.**		**69.10**	**156.94**	**3361.1**	**215.32**	**4.06**	**17.62**	**3.67**	**33901.3**	**9209.88**	**1517.06**	**1852.20**	**48.14**
Magnetite	*Std.*		***69.10***	*68.27*	*1543.6*	*66.20*	*2.57*	*13.65*	*1.95*	*15331.5*	*1540.81*	*149.97*	*782.20*	*19.53*
MA15-1_mt1.d		54.8	**64.96**	363.14	3501.5	851.01	24.04	123.43	4.05	68015.9	10374.54	3520.98	2397.12	94.20
MA15-1_mt2.d		*5.1*	***64.96***	*155.91*	*461.2*	*610.65*	*42.88*	*18.84*	*1.66*	*57297.1*	*15526.09*	*4865.71*	*1831.95*	*48.79*
MA15-1_mt2.d		*33.2*	***64.96***	*90.36*	*372.2*	*488.52*	*34.43*	*39.63*	*2.07*	*66781.7*	*15389.66*	*5047.60*	*2299.68*	*52.75*
MA15-1_mt4.d		54.8	**64.96**	207.23	5612.8	503.46	26.63	19.49	4.53	78215.1	9523.53	3033.76	2721.94	100.43
MA15-1_mt3.d		*28.2*	***64.96***	*134.47*	*3897.8*	*474.23*	*16.24*	*1.95*	*2.28*	*56647.5*	*9952.29*	*3800.32*	*2013.84*	*83.28*
MA15-1_mt3.d		*13.7*	***64.96***	*146.82*	*4346.0*	*461.24*	*20.14*	*0.00*	*2.57*	*66197.0*	*9653.46*	*3618.42*	*2286.69*	*91.27*
MA15-1_mt5.d		54.8	**64.96**	198.79	5638.8	430.05	24.04	12.99	4.11	69640.0	9841.85	3105.22	2338.66	102.32
MA15-1_mt6.d		54.8	**64.96**	109.79	3137.7	473.58	18.84	11.69	2.12	39562.3	11004.68	3430.03	1383.71	82.44
MA15-1	**Avg.**		**64.96**	**186.08**	**3719.8**	**538.80**	**24.43**	**34.30**	**3.20**	**63453.5**	**11001.19**	**3642.41**	**2197.00**	**86.25**
Magnetite	*Std.*		***64.96***	*89.09*	*1774.1*	*141.83*	*5.89*	*41.28*	*1.05*	*12011.7*	*2027.00*	*662.82*	*409.80*	*16.81*
MA15-2_mt1.d		54.8	**61.91**	3330.70	10728.8	446.98	23.53	2.48	21.61	87229.6	5807.05	241.94	3900.26	191.48
MA15-2_mt2.d		54.8	**61.91**	3256.41	10481.2	514.46	29.72	-3.71	21.48	79676.7	6580.91	261.01	3392.61	191.79
MA15-2_mt3.d		54.8	**61.91**	3231.64	10481.2	496.51	30.95	-4.95	17.64	54913.2	7057.61	247.64	2470.16	196.62

Analysis ID		60Ni	63Cu	66Zn	69Ga	74Ge	89Y	90Zr	93Nb	95Mo	118Sn	178Hf	181Ta	182W	208Pb
14-7B-MT-1-1.D		203.40	0.12	2649.78	39.95	0.76	0.05	2.26	0.36	0.36	0.20	0.08	0.01	0.04	0.04
14-7B-MT-1-2.D		207.32	0.47	1987.34	36.30	0.72	0.07	1.83	0.32	0.27	0.22	0.08	0.01	0.06	0.02
14-7B-MT-2.D		*191.30*	*19.74*	*4461.37*	*33.26*	*0.89*	*0.09*	*1.72*	*0.43*	*0.28*	*0.28*	*0.12*	*0.01*	*0.01*	*0.07*
14-7B-MT-2.D		*208.20*	*6.69*	*2737.66*	*36.91*	*1.05*	*0.07*	*1.77*	*0.32*	*0.24*	*0.13*	*0.05*	*0.01*	*0.09*	*0.05*
14-7B-MT-5-1.D		201.23	0.32	2676.82	50.97	0.86	0.04	1.78	0.18	0.33	0.16	0.06	0.01	0.02	0.04
14-7B-MT-5-2.D		*195.69*	*0.41*	*1987.34*	*42.86*	*0.81*	*0.11*	*2.32*	*0.26*	*0.30*	*0.11*	*0.11*	*0.00*	*0.03*	*0.09*
14-7B-MT-5-2.D		*206.17*	*0.20*	*2893.13*	*38.39*	*0.80*	*0.05*	*2.18*	*0.22*	*0.39*	*0.16*	*0.07*	*0.00*	*0.00*	*0.06*
MA14-7B	**Avg.**	**203.18**	**2.33**	**2589.97**	**40.77**	**0.83**	**0.06**	**1.98**	**0.29**	**0.31**	**0.18**	**0.08**	**0.01**	**0.04**	**0.05**
Magnetite	*Std.*	*2.36*	*4.04*	*403.75*	*5.45*	*0.10*	*0.02*	*0.23*	*0.07*	*0.04*	*0.03*	*0.01*	*0.00*	*0.02*	*0.02*
14-8A-MT-10.D		256.00	0.21	2666.98	41.41	1.07	0.18	4.90	0.37	0.49	0.25	0.18	0.02	0.03	0.12
14-8A-MT-5.D		292.39	0.30	2999.54	41.08	0.90	0.25	6.65	0.28	0.50	0.23	0.25	0.02	0.02	-0.12
14-8A-MT-6-1.D		319.45	0.55	2151.84	40.04	0.95	0.13	5.54	0.39	0.46	0.27	0.21	0.02	0.01	0.07
14-8A-MT-6-2.D		*284.30*	*0.52*	*2549.61*	*37.49*	*1.03*	*0.11*	*4.74*	*0.68*	*0.39*	*0.34*	*0.21*	*0.02*	*0.03*	*0.08*
14-8A-MT-6-2.D		*301.91*	*0.29*	*1858.41*	*35.73*	*1.04*	*0.06*	*4.56*	*0.30*	*0.28*	*0.26*	*0.22*	*0.01*	*0.01*	*0.01*
14-8A-MT-7.D		277.13	0.30	2562.65	46.17	1.04	0.19	4.23	0.42	0.50	0.28	0.17	0.02	0.02	0.07
14-8A-MT-9.D		307.13	0.59	2758.27	44.73	1.03	0.40	5.26	0.29	0.48	0.22	0.17	0.03	0.01	0.06
MA14-8A	**Avg.**	**290.10**	**0.40**	**2587.34**	**41.75**	**1.00**	**0.21**	**5.21**	**0.39**	**0.46**	**0.26**	**0.20**	**0.02**	**0.02**	**0.04**
Magnetite	*Std.*	*20.37*	*0.14*	*269.81*	*2.99*	*0.06*	*0.10*	*0.76*	*0.10*	*0.05*	*0.03*	*0.03*	*0.00*	*0.01*	*0.07*
14-8B-MT-3-1.D		341.50	-0.01	3068.12	42.15	1.02	0.13	3.39	0.20	1.29	0.30	0.10	0.01	0.15	0.01
14-8B-MT-3-2.D		315.10	0.17	3337.61	42.91	1.14	0.12	3.82	0.23	1.31	0.29	0.14	0.02	0.17	0.03
14-8B-MT-4.D		284.77	0.08	1181.64	40.08	1.01	0.09	2.40	0.20	1.33	0.26	0.11	0.01	0.13	0.07
14-8B-MT-6.D		229.83	0.29	628.83	40.63	1.11	0.01	0.33	0.03	0.85	0.17	0.02	0.00	0.03	0.04
14-8B-MT-7.D		270.19	0.36	2957.55	54.94	1.36	0.06	2.24	0.15	0.82	0.20	0.08	0.00	0.14	0.03
MA14-8B	**Avg.**	**288.28**	**0.18**	**2234.75**	**44.14**	**1.13**	**0.08**	**2.44**	**0.16**	**1.12**	**0.24**	**0.09**	**0.01**	**0.12**	**0.04**
Magnetite	*Std.*	*38.23*	*0.13*	*1106.46*	*5.49*	*0.13*	*0.04*	*1.21*	*0.07*	*0.23*	*0.05*	*0.04*	*0.01*	*0.05*	*0.02*
MA15-1_mt1.d		211.13	0.70	1948.88	48.27	0.75	0.11	3.09	0.52	0.88	2.61	0.10	0.02	0.09	0.08
MA15-1_mt2.d		*198.79*	*0.29*	*17.41*	*38.98*	*0.61*	*0.01*	*0.92*	*0.33*	*0.90*	*2.92*	*0.01*	*0.03*	*0.11*	*0.05*
MA15-1_mt2.d		*207.88*	*0.47*	*32.48*	*38.46*	*0.67*	*0.03*	*1.32*	*0.50*	*0.98*	*3.61*	*0.05*	*0.02*	*0.12*	*0.09*
MA15-1_mt4.d		250.63	0.66	2299.68	59.44	0.67	0.05	4.39	0.51	0.69	2.64	0.12	0.02	0.11	0.04
MA15-1_mt3.d		*214.38*	*0.51*	*3222.15*	*45.80*	*0.57*	*0.04*	*2.79*	*0.53*	*1.00*	*3.42*	*0.08*	*0.02*	*0.13*	*0.04*
MA15-1_mt3.d		*209.83*	*0.66*	*3650.90*	*45.99*	*0.68*	*0.03*	*2.90*	*0.58*	*0.95*	*3.74*	*0.06*	*0.02*	*0.12*	*0.05*
MA15-1_mt5.d		248.16	0.39	2208.73	66.26	0.69	0.05	4.06	0.40	0.64	2.79	0.11	0.02	0.11	0.04
MA15-1_mt6.d		228.02	0.38	1942.38	48.46	0.64	0.03	1.70	0.24	0.72	3.68	0.05	0.01	0.09	0.03
MA15-1	**Avg.**	**226.25**	**0.52**	**1965.37**	**51.14**	**0.67**	**0.05**	**2.89**	**0.45**	**0.81**	**3.13**	**0.08**	**0.02**	**0.11**	**0.05**
Magnetite	*Std.*	*17.64*	*0.13*	*988.80*	*9.13*	*0.05*	*0.03*	*1.14*	*0.10*	*0.14*	*0.45*	*0.03*	*0.01*	*0.02*	*0.02*
MA15-2_mt1.d		210.74	0.63	426.55	42.47	1.03	0.03	11.91	0.50	0.25	2.32	0.39	0.04	0.01	0.10
MA15-2_mt2.d		217.86	0.33	425.31	42.90	1.05	0.05	12.09	0.44	0.28	2.69	0.41	0.03	0.01	0.08
MA15-2_mt3.d		237.73	0.49	451.93	43.15	1.06	0.05	10.05	0.21	0.25	2.09	0.27	0.01	0.00	0.03

Analysis ID	Notes	Analysis Length (s)	Fe (wt%)	24Mg	27Al	29Si	31P	44Ca	45SC	47Ti	51V	52Cr	55Mn	59Co
MA15-2_mt4.d		54.8	**61.91**	3429.75	9942.6	554.70	24.76	0.00	28.11	88405.8	5961.82	245.22	3634.05	211.73
MA15-2_mt5.d		54.8	**61.91**	3745.49	9917.8	499.60	19.81	1.24	39.31	107102.3	5930.87	244.97	4110.75	202.57
MA15-2	**Avg.**		**61.91**	**3398.80**	**10310.3**	**502.45**	**25.75**	**-0.99**	**25.63**	**83465.5**	**6267.65**	**248.16**	**3501.56**	**198.84**
Magnetite	*Std.*		***61.91***	*186.55*	*323.4*	*34.63*	*4.10*	*2.87*	*7.62*	*16893.0*	*477.76*	*6.68*	*569.78*	*7.60*
MA32_25_mt6.d		*18.8*	***70.46***	*34.39*	*1134.4*	*528.47*	*-1.41*	*26.07*	*0.30*	*9653.4*	*17051.96*	*3206.05*	*283.96*	*50.31*
MA32_25_mt6.d		*13.2*	***70.46***	*90.19*	*2233.7*	*676.44*	*12.68*	*21.84*	*0.48*	*30298.9*	*16558.72*	*3410.39*	*859.64*	*53.90*
MA32-25_mt1.d		6.1	**70.46**	18.11	500.3	746.90	88.78	-4.93	0.06	1014.7	19800.00	7750.89	92.31	43.19
MA32-25_mt2.d		*18.2*	***70.46***	*267.76*	*894.9*	*1141.49*	*11.27*	*197.30*	*0.61*	*18884.0*	*14444.84*	*3537.22*	*563.70*	*42.21*
MA32-25_mt2.d		*18.3*	***70.46***	*514.38*	*2008.2*	*1613.59*	*29.59*	*352.31*	*1.51*	*57779.4*	*12753.74*	*3480.85*	*1521.99*	*56.93*
MA32-25_mt4.d		38.2	**70.46**	68.35	1303.6	662.35	38.75	43.69	0.68	35442.7	15149.47	3847.26	1014.66	57.00
MA32-25_mt5.d		*11.7*	***70.46***	*465.05*	*4227.8*	*1846.12*	*2.82*	*260.71*	*0.23*	*11908.2*	*16911.03*	*3043.99*	*363.59*	*57.43*
MA32-25_mt5.d		*36.9*	***70.46***	*276.92*	*2409.8*	*937.15*	*7.75*	*14.09*	*0.69*	*32271.9*	*16135.94*	*2952.38*	*965.34*	*61.09*
MA32-25	**Avg.**		**70.46**	**171.49**	**1538.3**	**906.53**	**31.79**	**82.30**	**0.55**	**24078.5**	**16343.40**	**4274.36**	**698.67**	**52.36**
Magnetite	*Std.*		**70.46**	*153.79*	*755.6*	*306.66*	*31.02*	*99.69*	*0.33*	*13503.8*	*2057.84*	*1761.41*	*355.90*	*5.92*
32-1A-MT-3-1.D		*14.9*	***61.54***	*960.04*	*2984.7*	*176.62*	*1.23*	*36.92*	*15.51*	*117543.7*	*5335.62*	*482.48*	*5255.62*	*99.88*
32-1A-MT-3-1.D		*31.2*	***61.54***	*898.50*	*3150.9*	*129.24*	*0.12*	*17.85*	*15.51*	*110158.8*	*5624.87*	*478.18*	*4874.06*	*95.88*
32-1A-MT-3-2.D		52.2	**61.54**	572.33	1334.2	224.63	14.15	32.00	12.31	74464.9	5027.92	444.33	3409.38	82.71
32-1A-MT-4-1.D		49.9	**61.54**	736.65	1753.9	227.70	2.65	30.16	18.22	96619.7	5144.84	505.25	4400.20	81.73
32-1A-MT-4-2.D		49.9	**61.54**	720.03	925.6	163.70	0.68	22.77	15.32	95450.4	5864.88	467.71	4381.73	83.88
32-1A-MT-5.D		49.9	**61.54**	673.26	1717.0	178.47	-3.02	7.38	15.69	91696.4	5298.70	689.88	4160.19	83.82
MA32-1A	**Avg.**		**61.54**	**724.14**	**1765.6**	**187.81**	**2.99**	**23.27**	**15.41**	**94156.1**	**5373.51**	**517.35**	**4269.81**	**85.86**
Magnetite	*Std.*		***61.54***	*112.74*	*730.4*	*33.12*	*5.87*	*8.68*	*1.88*	*12164.3*	*297.87*	*88.47*	*512.16*	*5.71*
32-1C-MT-1.D		*7.1*	***62.43***	*817.87*	*4001.9*	*124.86*	*0.00*	*-0.62*	*30.53*	*105947.9*	*5874.90*	*284.07*	*4538.84*	*66.55*
32-1C-MT-1.D		*44.7*	***62.43***	*678.02*	*3852.1*	*153.58*	*0.00*	*-0.50*	*18.92*	*66802.7*	*6274.46*	*293.18*	*3027.97*	*65.68*
32-1C-MT-2-1.D		49.9	**62.43**	488.22	1670.7	145.47	0.06	-0.94	14.05	52505.7	6424.30	277.14	2185.14	54.69
32-1C-MT-2-2.D		50.7	**62.43**	930.24	2079.0	226.63	4.12	21.54	30.40	106759.5	5606.44	282.32	4520.11	67.99
32-1C-MT-3.D		49.9	**62.43**	849.08	2228.8	561.89	-5.18	35.59	25.53	97207.4	5279.91	291.75	4083.08	68.36
32-1C-MT-4.D		52.8	**62.43**	724.22	1423.5	146.09	3.56	2.12	39.96	110505.5	5924.84	287.19	4682.44	65.12
MA32-1C	**Avg.**		**62.43**	**737.81**	**2254.9**	**245.94**	**0.51**	**11.56**	**26.09**	**87833.5**	**5890.99**	**286.06**	**3741.33**	**64.39**
Magnetite	*Std.*		***62.43***	*150.69*	*858.1*	*160.96*	*3.32*	*14.61*	*8.80*	*22148.9*	*411.79*	*5.69*	*925.87*	*5.01*
32-2A-T-MT-10.D		49.9	**66.11**	346.41	6478.7	383.43	-0.26	1.72	2.48	7549.6	5727.01	516.38	585.06	99.16
32-2A-T-MT-6.D		49.8	**66.11**	529.53	8131.4	561.93	-1.19	19.17	3.26	22873.7	5711.81	465.54	1216.40	103.99
32-2A-T-MT-7.D		52.8	**66.11**	1269.29	6161.3	2485.69	0.07	284.27	6.94	89247.0	4792.90	603.57	4098.75	82.90
32-2A-T-MT-8.D		49.9	**66.11**	1070.96	7853.7	1011.47	1.85	93.87	14.08	122962.5	5639.09	597.62	5572.98	113.18
32-2A-T-MT-9.D		49.9	**66.11**	771.49	8752.8	177.17	2.51	36.36	9.78	50903.9	6271.09	595.31	2551.80	110.34
MA32-2A-T	**Avg.**		**66.11**	**797.54**	**7475.6**	**923.94**	**0.59**	**87.08**	**7.31**	**58707.3**	**5628.38**	**555.68**	**2805.00**	**101.91**
Magnetite	*Std.*		***66.11***	*338.62*	*992.5*	*827.96*	*1.38*	*103.34*	*4.29*	*42481.7*	*474.96*	*55.31*	*1835.83*	*10.69*
32-2A-B-MT-6-1.D		49.9	**64.11**	1528.91	13224.9	149.37	5.26	6.67	10.37	59682.1	6232.33	480.53	2846.28	133.28

Analysis ID		60Ni	63Cu	66Zn	69Ga	74Ge	89Y	90Zr	93Nb	95Mo	118Sn	178Hf	181Ta	182W	208Pb
MA15-2_mt4.d		234.33	0.73	427.17	39.44	0.93	0.10	13.34	0.43	0.19	4.27	0.45	0.03	0.01	0.03
MA15-2_mt5.d		233.83	0.32	399.93	38.57	0.92	0.13	18.76	0.58	0.17	3.03	0.60	0.04	0.01	0.02
MA15-2	**Avg.**	**226.90**	**0.50**	**426.18**	**41.31**	**1.00**	**0.07**	**13.23**	**0.43**	**0.23**	**2.88**	**0.42**	**0.03**	**0.01**	**0.05**
Magnetite	*Std.*	*10.62*	*0.16*	*16.46*	*1.91*	*0.06*	*0.04*	*2.96*	*0.12*	*0.04*	*0.77*	*0.11*	*0.01*	*0.00*	*0.03*
MA32_25_mt6.d		*289.60*	*0.11*	*605.98*	*70.18*	*1.14*	*0.00*	*0.78*	*0.05*	*0.35*	*2.61*	*0.01*	*0.00*	*0.08*	*0.10*
MA32_25_mt6.d		*293.12*	*0.25*	*1803.84*	*68.00*	*1.30*	*0.00*	*2.37*	*0.07*	*0.47*	*2.61*	*0.02*	*0.00*	*0.20*	*0.11*
MA32-25_mt1.d		247.32	-0.06	96.53	53.27	1.48	0.00	0.17	0.00	0.73	1.97	0.00	0.00	0.03	0.06
MA32-25_mt2.d		*233.94*	*0.04*	*52.85*	*49.61*	*0.94*	*0.01*	*0.66*	*0.12*	*0.30*	*2.27*	*0.03*	*0.00*	*0.08*	*0.05*
MA32-25_mt2.d		*249.44*	*0.37*	*1183.77*	*50.03*	*1.06*	*0.03*	*2.25*	*0.43*	*0.25*	*3.23*	*0.09*	*0.01*	*0.23*	*0.18*
MA32-25_mt4.d		251.55	0.23	761.00	50.31	1.09	0.02	1.56	0.29	0.27	2.18	0.08	0.01	0.17	0.07
MA32-25_mt5.d		*255.07*	*0.11*	*2888.97*	*59.33*	*1.04*	*0.01*	*1.35*	*0.02*	*0.32*	*2.47*	*0.01*	*0.00*	*0.06*	*0.02*
MA32-25_mt5.d		*246.62*	*0.47*	*1881.35*	*60.67*	*0.89*	*0.02*	*1.71*	*0.08*	*0.32*	*2.80*	*0.05*	*0.00*	*0.15*	*0.35*
MA32-25	**Avg.**	**256.06**	**0.19**	**940.21**	**56.60**	**1.14**	**0.01**	**1.25**	**0.14**	**0.40**	**2.44**	**0.04**	**0.00**	**0.12**	**0.12**
Magnetite	*Std.*	*17.79*	*0.14*	*674.12*	*7.37*	*0.19*	*0.01*	*0.54*	*0.12*	*0.17*	*0.31*	*0.03*	*0.00*	*0.05*	*0.08*
32-1A-MT-3-1.D		*219.70*	*0.68*	*1963.16*	*23.88*	*1.19*	*0.20*	*17.17*	*0.89*	*0.51*	*0.59*	*0.38*	*0.03*	*0.15*	*0.04*
32-1A-MT-3-1.D		*212.50*	*0.86*	*2135.48*	*25.48*	*1.10*	*0.24*	*8.86*	*0.85*	*0.55*	*0.61*	*0.36*	*0.06*	*0.06*	*0.03*
32-1A-MT-3-2.D		212.62	0.54	643.72	18.40	1.13	0.12	7.14	0.51	0.52	0.54	0.23	0.02	0.04	0.03
32-1A-MT-4-1.D		184.25	0.97	982.81	17.42	0.92	0.34	10.95	0.97	0.52	0.57	0.38	0.06	0.27	0.07
32-1A-MT-4-2.D		163.08	1.91	288.01	15.42	1.00	0.25	5.91	0.62	0.48	0.51	0.30	0.05	0.13	0.17
32-1A-MT-5.D		180.75	0.23	921.89	20.31	1.05	0.32	12.62	0.97	0.57	0.46	0.39	0.05	0.27	0.04
MA32-1A	**Avg.**	**191.11**	**0.89**	**983.23**	**19.30**	**1.04**	**0.25**	**9.63**	**0.79**	**0.52**	**0.54**	**0.33**	**0.05**	**0.16**	**0.07**
Magnetite	*Std.*	*19.83*	*0.57*	*600.77*	*3.24*	*0.08*	*0.08*	*2.62*	*0.19*	*0.03*	*0.05*	*0.06*	*0.01*	*0.09*	*0.05*
32-1C-MT-1.D		*249.11*	*0.19*	*2722.06*	*41.21*	*0.58*	*0.11*	*18.04*	*0.67*	*0.57*	*0.77*	*0.68*	*0.03*	*0.04*	*0.03*
32-1C-MT-1.D		*250.17*	*0.41*	*2640.89*	*36.09*	*0.95*	*0.08*	*11.67*	*0.37*	*0.32*	*0.59*	*0.46*	*0.03*	*0.02*	*0.02*
32-1C-MT-2-1.D		189.86	0.32	889.04	28.16	0.93	0.14	5.44	0.48	0.39	0.47	0.31	0.02	0.04	0.03
32-1C-MT-2-2.D		184.55	1.16	1435.95	29.66	0.91	0.22	10.49	0.89	0.61	0.67	0.62	0.04	0.25	0.20
32-1C-MT-3.D		190.73	0.70	1417.22	27.78	0.91	0.30	23.72	0.64	0.52	0.64	0.77	0.03	0.09	0.25
32-1C-MT-4.D		209.77	0.48	824.11	24.97	0.89	0.22	16.54	0.92	0.53	0.68	0.71	0.05	0.07	0.04
MA32-1C	**Avg.**	**204.99**	**0.61**	**1443.67**	**29.47**	**0.91**	**0.19**	**13.75**	**0.67**	**0.48**	**0.62**	**0.58**	**0.03**	**0.09**	**0.11**
Magnetite	*Std.*	*24.09*	*0.30*	*656.12*	*3.96*	*0.01*	*0.08*	*6.14*	*0.20*	*0.09*	*0.07*	*0.17*	*0.01*	*0.08*	*0.10*
32-2A-T-MT-10.D		223.25	0.45	610.19	48.92	1.30	0.02	0.52	0.00	0.21	0.31	0.02	0.00	0.00	0.21
32-2A-T-MT-6.D		229.86	0.19	1110.63	40.52	1.20	0.04	2.31	0.05	0.32	0.34	0.06	0.00	0.03	0.24
32-2A-T-MT-7.D		193.70	5.09	1461.01	32.20	1.14	0.12	6.08	0.43	0.42	0.31	0.17	0.02	0.05	1.42
32-2A-T-MT-8.D		191.05	1.27	1130.46	35.30	1.08	0.08	13.35	0.55	0.54	0.31	0.31	0.02	0.08	0.20
32-2A-T-MT-9.D		229.60	0.19	646.55	40.52	1.06	0.06	5.86	0.26	0.36	0.33	0.15	0.02	0.03	0.04
MA32-2A-T	**Avg.**	**213.49**	**1.44**	**991.77**	**39.49**	**1.16**	**0.06**	**5.63**	**0.26**	**0.37**	**0.32**	**0.14**	**0.01**	**0.04**	**0.42**
Magnetite	*Std.*	*17.42*	*1.87*	*321.97*	*5.69*	*0.09*	*0.03*	*4.40*	*0.21*	*0.11*	*0.01*	*0.10*	*0.01*	*0.03*	*0.50*
32-2A-B-MT-6-1.D		265.97	0.27	472.46	42.31	0.81	0.03	5.63	0.20	0.35	0.41	0.18	0.01	0.02	0.03

Analysis ID	Notes	Analysis Length (s)	Fe (wt%)	24Mg	27Al	29Si	31P	44Ca	45SC	47Ti	51V	52Cr	55Mn	59Co
32-2A-B-MT-6-2.D		45.0	**64.11**	889.78	12571.1	371.81	1.47	32.05	11.28	68336.4	6231.04	487.91	3173.22	130.01
32-2A-B-MT-10.D		49.9	**64.11**	2609.09	13846.8	112.83	0.58	5.13	10.71	56669.2	6269.51	506.69	2634.73	133.28
32-2A-B-MT-11-1.D		53.4	**64.11**	2012.91	12032.6	175.01	-0.26	6.41	12.18	77567.5	5987.44	650.03	3378.35	132.25
32-2A-B-MT-11-2.D		*42.1*	***64.11***	*641.70*	*12590.3*	*615.41*	*0.32*	*21.80*	*7.87*	*61989.9*	*6224.63*	*587.21*	*2923.21*	*145.52*
32-2A-B-MT-11-2.D		*9.1*	***64.11***	*608.36*	*11282.6*	*628.23*	*-4.49*	*16.03*	*7.88*	*56925.6*	*6115.66*	*600.03*	*2673.20*	*122.44*
MA32-2A-B_1	**Avg.**		**64.11**	**1535.29**	**12806.5**	**285.34**	**1.30**	**14.21**	**10.48**	**64668.6**	**6185.11**	**542.93**	**2982.25**	**134.04**
Magnetite	*Std.*		***64.11***	*722.09*	*650.1*	*188.87*	*2.10*	*10.60*	*1.44*	*7503.5*	*100.93*	*66.14*	*262.05*	*3.87*
32-2A-B-MT-1.D		49.9	**67.65**	689.40	12861.2	460.05	-1.62	16.85	3.48	22887.6	5899.49	690.08	1355.12	138.22
32-2A-B-MT-2.D		53.1	**67.65**	1522.23	14410.5	500.64	-0.07	277.38	7.71	64272.0	4627.58	511.47	3233.90	145.19
32-2A-B-MT-3.D		49.9	**67.65**	1223.87	10824.8	669.78	-0.68	11.03	6.81	24409.8	4971.27	533.80	1420.75	113.39
32-2A-B-MT-4.D		31.0	**67.65**	548.00	9742.3	608.89	0.00	399.16	4.60	41269.4	4877.91	648.13	2131.12	112.10
MA32-2A-B_2	**Avg.**		**67.65**	**995.88**	**11959.7**	**559.84**	**-0.59**	**176.11**	**5.65**	**38209.7**	**5094.06**	**595.87**	**2035.22**	**127.22**
Magnetite	*Std.*		***67.65***	*394.83*	*1804.4*	*83.60*	*0.65*	*167.80*	*1.69*	*16686.9*	*481.70*	*75.14*	*756.00*	*14.69*
32-2B-MT-1-1.D		49.9	**62.89**	1390.44	12137.3	276.70	3.14	39.62	16.41	89300.1	5521.51	381.73	3666.33	150.74
32-2B-MT-1-2.D		*19.9*	***62.89***	*1200.52*	*12690.7*	*234.57*	*7.55*	*14.46*	*13.08*	*71062.8*	*5835.95*	*413.80*	*3094.06*	*154.83*
32-2B-MT-1-2.D		*27.0*	***62.89***	*1299.25*	*12407.7*	*226.39*	*-0.06*	*7.11*	*12.14*	*66912.2*	*5829.66*	*408.77*	*2873.95*	*156.78*
32-2B-MT-5.D		49.9	**62.89**	1460.25	11678.2	197.47	-0.57	9.31	13.90	77603.0	5672.44	393.68	3307.88	166.46
32-2B-MT-6.D		49.9	**62.89**	2509.21	12728.4	147.79	-1.64	5.35	12.83	66660.6	5722.75	388.58	2748.18	162.94
32-2B-MT-7.D		49.9	**62.89**	1255.23	12363.7	172.94	-2.14	9.12	10.63	56032.7	6137.81	380.47	2452.61	166.09
MA32-2B	**Avg.**		**62.89**	**1574.50**	**12287.0**	**204.95**	**0.39**	**14.72**	**13.26**	**71653.6**	**5777.37**	**391.07**	**3028.45**	**160.44**
Magnetite	*Std.*		***62.89***	*473.94*	*361.0*	*44.98*	*2.31*	*12.56*	*1.90*	*11177.0*	*206.10*	*11.01*	*424.00*	*6.14*
32-3-MT-2.D		52.8	**62.88**	245.86	2420.9	299.31	0.94	57.22	2.40	13959.3	6005.00	523.79	830.01	81.24
32-3-MT-4.D		50.6	**62.88**	477.88	2710.1	396.14	-1.95	39.61	9.81	113812.1	5250.45	389.85	5344.77	80.67
32-3-MT-6.D		51.2	**62.88**	242.72	2042.3	322.57	-0.25	32.07	4.34	35778.5	6797.28	537.62	1691.46	63.95
32-3-MT-7.D		49.9	**62.88**	490.46	2700.0	202.47	2.96	17.61	5.41	62879.6	5451.66	516.24	2892.46	101.74
32-3-MT-8.D		49.9	**62.88**	1465.09	3760.2	210.02	-3.08	42.13	23.20	189896.4	4414.15	441.41	8614.50	130.48
MA32-3	**Avg.**		**62.88**	**584.40**	**2726.7**	**286.10**	**-0.28**	**37.73**	**9.03**	**83265.2**	**5583.71**	**481.78**	**3874.64**	**91.62**
Magnetite	*Std.*		***62.88***	*453.24*	*571.1*	*72.66*	*2.13*	*12.96*	*7.49*	*62892.3*	*793.30*	*56.83*	*2815.25*	*22.83*
32-4B-MT-2.D		49.9	**64.65**	424.12	2540.9	248.91	2.33	31.03	7.82	71764.9	5469.65	295.98	2728.36	112.43
32-4B-MT-5.D		40.5	**64.65**	516.58	3245.6	263.14	0.58	21.85	9.31	86635.1	5424.39	249.04	3310.24	137.97
32-4B-MT-6.D		*18.0*	***64.65***	*479.73*	*2624.9*	*329.73*	*-1.94*	*47.84*	*12.35*	*121547.8*	*4868.38*	*226.35*	*4512.79*	*125.75*
32-4B-MT-6.D		*23.8*	***64.65***	*264.43*	*3452.5*	*102.15*	*1.03*	*413.78*	*5.56*	*66592.7*	*5236.90*	*261.20*	*2605.52*	*111.66*
32-4B-MT-7-1.D		49.9	**64.65**	297.40	2515.0	297.40	3.10	290.94	5.24	51075.9	5560.17	235.79	2114.16	134.03
32-4B-MT-7-2.D		49.9	**64.65**	486.19	2392.2	394.38	6.66	45.90	7.69	74351.0	5333.88	240.19	2999.90	142.04
MA32-4B	**Avg.**		**64.65**	**416.28**	**2758.0**	**280.79**	**2.49**	**129.19**	**7.71**	**74815.8**	**5373.27**	**253.44**	**2915.86**	**128.84**
Magnetite	*Std.*		***64.65***	*80.80*	*344.1*	*64.83*	*2.40*	*118.66*	*1.36*	*13791.9*	*164.58*	*21.77*	*469.34*	*11.64*
MA32-7_mt1.d		54.8	**65.73**	1004.33	2964.4	429.21	15.58	11.17	8.53	25502.6	7801.96	477.85	1590.63	216.90
MA32-7_mt2.d		54.8	**65.73**	2543.69	4916.5	467.99	27.61	9.86	19.72	65728.4	7098.67	443.01	2694.86	235.04

Analysis ID		60Ni	63Cu	66Zn	69Ga	74Ge	89Y	90Zr	93Nb	95Mo	118Sn	178Hf	181Ta	182W	208Pb
32-2A-B-MT-6-2.D		260.59	0.44	871.83	39.36	1.11	0.03	7.32	0.21	0.39	0.39	0.22	0.01	0.02	0.04
32-2A-B-MT-10.D		258.47	0.17	496.18	42.31	1.15	0.02	6.15	0.20	0.53	0.46	0.17	0.01	0.12	0.01
32-2A-B-MT-11-1.D		256.81	0.46	679.52	39.87	1.04	0.04	7.13	0.47	0.51	0.47	0.25	0.02	0.00	0.03
32-2A-B-MT-11-2.D		*249.37*	*8.46*	*961.58*	*40.58*	*1.01*	*0.03*	*7.10*	*0.30*	*0.51*	*0.47*	*0.23*	*0.01*	*0.04*	*0.21*
32-2A-B-MT-11-2.D		*244.24*	*0.62*	*603.23*	*38.91*	*1.01*	*0.03*	*6.71*	*0.32*	*0.40*	*0.28*	*0.27*	*0.00*	*0.00*	*0.02*
MA32-2A-B_1	**Avg.**	**258.06**	**1.68**	**683.55**	**40.83**	**1.02**	**0.03**	**6.65**	**0.28**	**0.45**	**0.43**	**0.21**	**0.01**	**0.04**	**0.06**
Magnetite	*Std.*	*5.71*	*2.69*	*179.46*	*1.25*	*0.12*	*0.01*	*0.65*	*0.11*	*0.07*	*0.03*	*0.03*	*0.01*	*0.04*	*0.06*
32-2A-B-MT-1.D		199.51	0.20	576.42	42.49	1.01	0.01	0.77	0.01	0.35	0.26	0.05	0.00	0.01	0.02
32-2A-B-MT-2.D		201.61	2.30	544.62	37.55	1.00	0.04	2.40	0.43	0.32	0.32	0.08	0.02	0.02	0.04
32-2A-B-MT-3.D		229.35	0.07	487.11	40.66	1.06	0.04	1.20	0.00	0.32	0.38	0.06	0.00	-0.01	0.00
32-2A-B-MT-4.D		161.02	1.22	960.70	38.70	1.09	0.17	4.46	0.22	0.29	0.25	0.12	0.01	0.01	0.09
MA32-2A-B_2	**Avg.**	**197.87**	**0.95**	**642.21**	**39.85**	**1.04**	**0.06**	**2.21**	**0.17**	**0.32**	**0.30**	**0.08**	**0.01**	**0.01**	**0.04**
Magnetite	*Std.*	*24.32*	*0.90*	*186.64*	*1.89*	*0.04*	*0.06*	*1.43*	*0.17*	*0.02*	*0.05*	*0.03*	*0.01*	*0.01*	*0.03*
32-2B-MT-1-1.D		211.93	1.07	740.81	36.47	1.01	0.11	13.52	0.50	0.37	0.55	0.35	0.02	0.02	0.05
32-2B-MT-1-2.D		*222.62*	*0.22*	*527.63*	*38.42*	*0.86*	*0.09*	*8.18*	*0.33*	*0.31*	*0.52*	*0.23*	*0.01*	*0.01*	*0.04*
32-2B-MT-1-2.D		*229.04*	*0.08*	*564.10*	*39.68*	*0.89*	*0.05*	*8.46*	*0.28*	*0.40*	*0.48*	*0.30*	*0.01*	*0.02*	*0.03*
32-2B-MT-5.D		225.14	0.47	554.04	38.74	1.06	0.05	8.87	0.27	0.28	0.45	0.28	0.02	0.02	0.04
32-2B-MT-6.D		223.88	0.37	436.44	37.86	0.97	0.04	7.61	0.39	0.25	0.46	0.25	0.02	0.00	0.02
32-2B-MT-7.D		230.73	0.82	514.42	40.00	1.01	0.04	7.30	0.25	0.38	0.46	0.18	0.01	0.02	0.05
MA32-2B	**Avg.**	**223.60**	**0.57**	**558.87**	**38.44**	**0.99**	**0.06**	**9.13**	**0.34**	**0.33**	**0.48**	**0.26**	**0.02**	**0.01**	**0.04**
Magnetite	*Std.*	*6.28*	*0.33*	*100.20*	*1.20*	*0.06*	*0.03*	*2.26*	*0.09*	*0.05*	*0.04*	*0.06*	*0.00*	*0.01*	*0.01*
32-3-MT-2.D		167.20	0.25	464.05	39.49	0.88	0.01	0.49	0.06	0.28	0.07	0.02	0.00	0.02	0.04
32-3-MT-4.D		107.40	0.53	1094.10	32.95	0.86	0.10	4.78	0.52	0.69	0.22	0.13	0.02	0.10	0.36
32-3-MT-6.D		163.30	0.63	459.02	35.97	0.70	0.04	2.06	0.10	0.36	0.08	0.03	0.01	0.04	0.26
32-3-MT-7.D		177.89	0.83	386.71	37.35	0.68	0.03	4.59	0.35	0.45	0.15	0.11	0.02	0.05	0.16
32-3-MT-8.D		137.71	0.51	543.91	29.93	0.61	0.08	13.46	1.12	0.77	0.48	0.53	0.04	0.17	0.11
MA32-3	**Avg.**	**150.70**	**0.55**	**589.56**	**35.14**	**0.75**	**0.05**	**5.07**	**0.43**	**0.51**	**0.20**	**0.16**	**0.02**	**0.08**	**0.19**
Magnetite	*Std.*	*25.35*	*0.19*	*257.13*	*3.36*	*0.11*	*0.03*	*4.49*	*0.38*	*0.19*	*0.15*	*0.19*	*0.01*	*0.06*	*0.11*
32-4B-MT-2.D		188.59	0.33	1066.78	34.14	0.63	0.05	4.33	0.53	0.66	0.20	0.12	0.02	0.12	0.02
32-4B-MT-5.D		195.51	0.48	1150.82	38.86	0.68	0.04	5.55	0.74	0.65	0.27	0.22	0.02	0.08	0.28
32-4B-MT-6.D		*198.10*	*0.62*	*1124.96*	*34.98*	*0.80*	*0.09*	*8.60*	*0.65*	*0.59*	*0.30*	*0.19*	*0.04*	*0.13*	*0.05*
32-4B-MT-6.D		*204.30*	*0.80*	*1668.05*	*38.99*	*0.72*	*0.07*	*3.88*	*0.35*	*0.67*	*0.19*	*0.10*	*0.02*	*0.11*	*0.03*
32-4B-MT-7-1.D		208.70	0.27	943.93	39.18	0.83	0.07	3.16	0.27	0.76	0.20	0.09	0.01	0.11	0.02
32-4B-MT-7-2.D		202.49	0.17	693.08	35.49	0.69	0.04	4.07	0.39	0.69	0.23	0.10	0.02	0.13	0.04
MA32-4B	**Avg.**	**199.39**	**0.39**	**1057.77**	**36.99**	**0.72**	**0.06**	**4.60**	**0.48**	**0.68**	**0.23**	**0.13**	**0.02**	**0.11**	**0.08**
Magnetite	*Std.*	*6.83*	*0.19*	*243.49*	*1.94*	*0.07*	*0.02*	*1.01*	*0.16*	*0.04*	*0.03*	*0.05*	*0.01*	*0.02*	*0.10*
MA32-7_mt1.d		300.38	0.25	1121.98	48.64	1.14	0.02	2.03	0.01	0.67	2.81	0.10	0.00	0.01	0.02
MA32-7_mt2.d		288.55	0.55	827.52	45.75	1.05	0.05	6.38	0.15	0.51	3.32	0.27	0.01	0.08	0.12

Analysis ID	Notes	Analysis Length (s)	Fe (wt%)	24Mg	27Al	29Si	31P	44Ca	45SC	47Ti	51V	52Cr	55Mn	59Co
MA32-7_mt3.d		54.8	**65.73**	1192.31	4219.8	441.69	24.98	10.52	12.09	33061.4	7769.10	560.01	1531.47	211.78
MA32-7_mt4.d		54.8	**65.73**	2142.75	6119.3	487.05	20.38	1.97	15.25	48113.2	8058.30	542.26	1800.96	237.61
MA32-7_mt5.d		54.8	**65.73**	1925.84	5199.1	534.37	28.92	-1.97	20.18	59812.8	7769.10	501.51	2431.95	236.49
MA32-7_mt6.d		54.8	**65.73**	3279.85	6645.1	455.50	22.35	6.57	18.67	62836.4	7177.54	524.51	2096.74	222.23
MA32-7	**Avg.**		**65.73**	**2014.79**	**5010.7**	**469.30**	**23.30**	**6.35**	**15.74**	**49175.8**	**7612.44**	**508.19**	**2024.43**	**226.68**
Magnetite	*Std.*		***65.73***	*848.75*	*1323.5*	*37.71*	*4.94*	*5.32*	*4.68*	*16703.1*	*383.90*	*43.19*	*469.45*	*11.16*
MA32-9_mt1.d		54.8	**63.06**	1954.87	8456.4	586.46	22.07	6.31	8.29	64132.2	7201.48	84.12	2345.84	98.18
MA32-9_mt2.d		54.8	**63.06**	4029.55	13747.1	504.48	24.59	6.31	12.86	73717.4	6135.76	73.47	2724.20	166.61
MA32-9_mt3.d		52.8	**63.06**	2358.45	12271.5	495.02	30.27	-2.52	9.80	63753.9	6356.47	79.58	2093.60	153.30
MA32-9_mt4.d		54.8	**63.06**	3480.92	12353.5	457.82	27.75	7.57	12.35	78762.2	6142.06	77.75	2698.98	157.78
MA32-9_mt5.d		54.8	**63.06**	3998.02	13993.1	558.71	26.49	19.55	13.81	65267.3	6703.30	74.98	2270.17	157.15
MA32-9_mt6.d		*23.4*	***63.06***	*2257.56*	*10442.8*	*536.01*	*21.44*	*11.98*	*13.12*	*58898.2*	*6457.37*	*73.15*	*1891.81*	*113.26*
MA32-9_mt6.d		*25.3*	***63.06***	*2005.31*	*12044.5*	*448.36*	*16.40*	*12.61*	*16.02*	*75735.3*	*6205.13*	*72.65*	*2383.68*	*109.16*
MA32-9	**Avg.**		**63.06**	**2991.35**	**12016.3**	**515.48**	**25.00**	**8.25**	**11.96**	**68882.1**	**6477.53**	**77.13**	**2380.09**	**140.69**
Magnetite	*Std.*		***63.06***	*871.21*	*1839.5*	*43.59*	*3.75*	*6.69*	*2.22*	*5544.0*	*374.61*	*3.90*	*248.13*	*26.06*
MA32-12_mt1.d		54.8	**61.72**	2876.20	19837.1	451.80	21.60	4.94	16.63	65115.7	7030.03	109.49	2111.48	151.59
MA32-12_mt2.d		54.8	**61.72**	2462.67	17985.5	423.41	22.22	11.73	16.00	60610.1	6789.32	106.35	2131.84	151.53
MA32-12_mt3.d		54.8	**61.72**	2684.87	18979.2	467.23	15.43	12.34	17.95	64683.7	6789.32	105.98	2197.89	130.79
MA32-12_mt4.d		54.8	**61.72**	4351.33	18948.4	525.86	24.69	24.69	20.43	71349.5	6758.45	111.72	2326.88	175.35
MA32-12_mt5.d		54.8	**61.72**	3092.22	20096.4	606.10	17.90	25.92	18.91	67954.9	6795.49	110.17	2214.55	143.69
MA32-12	**Avg.**		**61.72**	**3093.46**	**19169.3**	**494.88**	**20.37**	**15.92**	**17.99**	**65942.8**	**6832.52**	**108.74**	**2196.53**	**150.59**
Magnetite	*Std.*		***61.72***	*662.46*	*747.2*	*64.90*	*3.29*	*8.10*	*1.59*	*3577.4*	*99.60*	*2.23*	*75.81*	*14.52*
MA3215-mt1.d		53.8	**61.84**	7729.64	16696.0	2046.81	14.84	50.71	35.87	128621.3	6288.84	136.66	3091.86	150.82
MA3215-mt2.d		53.8	**61.84**	8657.20	14469.9	2968.18	30.30	33.39	24.12	76678.1	6851.56	142.84	2411.65	131.16
MA3215-mt3.d		53.8	**61.84**	8100.67	12120.1	1273.85	19.17	47.61	24.73	74822.9	6523.82	133.57	2077.73	166.34
MA3215-mt4.d		53.8	**61.84**	5812.69	9337.4	1719.07	35.25	30.30	21.15	69257.6	6431.06	152.74	2226.14	106.30
MA3215-mt5.d		53.8	**61.84**	5936.37	9893.9	1978.79	28.45	21.64	25.97	78533.2	6696.96	155.83	2411.65	96.84
MA32-15	**Avg.**		**61.84**	**7247.31**	**12503.5**	**1997.34**	**25.60**	**36.73**	**26.37**	**85582.6**	**6558.45**	**144.33**	**2443.80**	**130.29**
Magnetite	*Std.*		***61.84***	*1296.66*	*3099.4*	*621.73*	*8.37*	*12.19*	*5.60*	*24308.4*	*220.92*	*9.74*	*388.40*	*29.23*
MA3217-mt1.d		53.8	**63.13**	6527.80	13118.7	611.74	27.15	-29.67	23.11	70707.3	7929.32	270.83	2190.66	165.09
MA3217-mt2.d		53.8	**63.13**	6849.77	12380.1	639.52	40.40	-18.31	22.73	73232.6	7594.72	266.42	2209.60	161.74
MA3217-mt3.d		53.8	**63.13**	5631.33	12411.7	659.09	34.72	8.84	14.08	46906.7	8352.30	255.68	1622.48	191.29
MA3217-mt4.d		53.8	**63.13**	6691.94	12493.7	589.02	20.83	-1.26	23.80	74495.2	7998.76	256.95	2222.23	175.63
MA3217-mt5.d		53.8	**63.13**	5214.66	13251.3	573.23	34.72	-6.94	18.31	55555.7	8080.83	251.26	1824.50	196.65
MA32-17	**Avg.**		**63.13**	**6183.10**	**12731.1**	**614.52**	**31.57**	**-9.47**	**20.40**	**64179.5**	**7991.19**	**260.23**	**2013.90**	**178.08**
Magnetite	*Std.*		**63.13**	*718.42*	*419.1*	*35.27*	*7.63*	*14.96*	*4.14*	*12285.2*	*273.64*	*8.10*	*274.79*	*15.50*
MA32-18_mt1.d		23.2	**65.90**	1535.37	19900.5	698.49	29.65	51.40	4.42	44347.8	8507.13	1653.98	1172.94	148.92
MA32-18_mt2.d		54.8	**65.90**	1891.21	23393.0	1021.38	23.72	28.34	3.56	42634.5	8428.05	1597.31	1188.10	141.61

Analysis ID		60Ni	63Cu	66Zn	69Ga	74Ge	89Y	90Zr	93Nb	95Mo	118Sn	178Hf	181Ta	182W	208Pb
MA32-7_mt3.d		314.18	0.24	1148.93	49.76	1.06	0.03	2.65	0.03	0.61	3.56	0.11	0.00	0.02	0.04
MA32-7_mt4.d		323.19	0.27	932.69	49.03	0.99	0.04	4.40	0.08	0.42	4.40	0.21	0.00	0.02	0.04
MA32-7_mt5.d		307.61	0.44	1022.73	48.44	0.98	0.02	6.44	0.18	0.48	4.75	0.30	0.01	0.07	0.02
MA32-7_mt6.d		301.04	0.85	563.29	45.68	0.93	0.09	7.16	0.15	0.29	4.48	0.29	0.01	0.04	0.01
MA32-7	**Avg.**	**305.82**	**0.43**	**936.19**	**47.88**	**1.03**	**0.04**	**4.84**	**0.10**	**0.50**	**3.88**	**0.21**	**0.00**	**0.04**	**0.04**
Magnetite	*Std.*	*12.05*	*0.24*	*218.24*	*1.74*	*0.07*	*0.03*	*2.15*	*0.07*	*0.14*	*0.77*	*0.09*	*0.00*	*0.03*	*0.04*
MA32-9_mt1.d		133.69	0.92	382.78	49.94	1.12	0.02	4.86	0.17	0.33	2.46	0.13	0.01	0.05	0.08
MA32-9_mt2.d		181.42	0.70	525.29	46.79	0.97	0.02	7.57	0.15	0.32	4.42	0.22	0.01	0.01	0.06
MA32-9_mt3.d		179.41	0.70	452.14	45.34	0.89	0.02	6.81	0.14	0.30	3.68	0.18	0.01	0.02	0.09
MA32-9_mt4.d		171.71	0.59	408.63	44.27	0.84	0.01	6.65	0.20	0.28	4.31	0.24	0.01	0.01	0.05
MA32-9_mt5.d		189.81	0.28	530.97	47.17	0.97	0.03	7.68	0.17	0.34	4.36	0.22	0.01	0.01	0.07
MA32-9_mt6.d		*174.05*	*0.50*	*459.71*	*44.84*	*0.96*	*0.04*	*6.34*	*0.14*	*0.37*	*3.56*	*0.18*	*0.00*	*0.03*	*0.20*
MA32-9_mt6.d		*172.47*	*0.50*	*505.11*	*42.63*	*0.95*	*0.05*	*7.18*	*0.22*	*0.31*	*3.88*	*0.27*	*0.01*	*0.01*	*0.17*
MA32-9	**Avg.**	**171.54**	**0.61**	**463.86**	**46.20**	**0.96**	**0.02**	**6.72**	**0.17**	**0.32**	**3.83**	**0.20**	**0.01**	**0.02**	**0.09**
Magnetite	*Std.*	*17.93*	*0.20*	*55.41*	*2.09*	*0.09*	*0.01*	*0.92*	*0.02*	*0.02*	*0.68*	*0.04*	*0.00*	*0.01*	*0.04*
MA32-12_mt1.d		205.28	0.46	416.00	44.19	0.88	0.02	4.26	0.04	0.16	2.89	0.25	0.00	0.00	0.06
MA32-12_mt2.d		198.74	0.88	357.98	43.64	0.81	0.02	3.79	0.05	0.17	2.53	0.17	0.01	0.01	0.03
MA32-12_mt3.d		203.86	0.49	356.13	43.33	0.84	0.07	4.25	0.04	0.15	2.57	0.24	0.01	0.01	0.08
MA32-12_mt4.d		214.17	0.69	366.01	44.19	0.78	0.00	5.01	0.10	0.14	3.10	0.27	0.01	0.00	0.03
MA32-12_mt5.d		188.31	0.44	362.92	43.82	0.84	0.00	4.60	0.06	0.16	4.58	0.20	0.01	0.01	0.02
MA32-12	**Avg.**	**202.07**	**0.59**	**371.81**	**43.83**	**0.83**	**0.02**	**4.38**	**0.06**	**0.16**	**3.13**	**0.22**	**0.01**	**0.01**	**0.05**
Magnetite	*Std.*	*8.49*	*0.17*	*22.37*	*0.33*	*0.03*	*0.02*	*0.41*	*0.02*	*0.01*	*0.75*	*0.04*	*0.00*	*0.01*	*0.02*
MA3215-mt1.d		239.93	1.19	240.55	39.95	0.87	0.05	11.13	0.25	0.14	7.36	0.39	0.03	0.02	0.07
MA3215-mt2.d		246.73	0.95	262.81	41.00	1.07	0.08	8.60	0.28	0.14	6.21	0.36	0.01	0.01	0.08
MA3215-mt3.d		261.57	0.62	228.80	38.09	0.91	0.06	8.10	0.14	0.12	5.94	0.24	0.01	0.01	0.09
MA3215-mt4.d		217.05	1.20	151.50	37.35	0.98	0.05	7.17	0.20	0.18	5.21	0.33	0.01	0.02	0.10
MA3215-mt5.d		217.67	0.83	81.56	36.42	0.96	0.06	9.52	0.19	0.16	5.87	0.41	0.02	0.05	0.07
MA32-15	**Avg.**	**236.59**	**0.96**	**193.04**	**38.56**	**0.96**	**0.06**	**8.90**	**0.21**	**0.15**	**6.12**	**0.35**	**0.02**	**0.02**	**0.08**
Magnetite	*Std.*	*19.22*	*0.25*	*75.09*	*1.88*	*0.08*	*0.01*	*1.51*	*0.06*	*0.02*	*0.79*	*0.07*	*0.01*	*0.02*	*0.01*
MA3217-mt1.d		224.12	0.43	304.29	45.52	0.90	0.04	7.89	0.20	0.15	6.12	0.33	0.01	0.00	0.03
MA3217-mt2.d		233.59	0.65	258.21	42.93	0.93	0.06	9.09	0.26	0.14	5.71	0.35	0.02	0.00	0.05
MA3217-mt3.d		270.20	0.64	321.97	44.63	0.86	0.05	5.39	0.11	0.17	5.93	0.20	0.01	0.00	0.06
MA3217-mt4.d		234.22	0.66	250.00	44.44	0.78	0.04	6.82	0.21	0.14	4.84	0.27	0.02	0.00	0.05
MA3217-mt5.d		241.79	0.51	285.35	45.39	0.93	0.03	4.86	0.13	0.18	6.30	0.21	0.01	0.00	0.24
MA32-17	**Avg.**	**240.78**	**0.58**	**283.97**	**44.58**	**0.88**	**0.05**	**6.81**	**0.18**	**0.15**	**5.78**	**0.27**	**0.01**	**0.00**	**0.09**
Magnetite	*Std.*	*17.60*	*0.10*	*30.32*	*1.03*	*0.06*	*0.01*	*1.75*	*0.06*	*0.02*	*0.57*	*0.07*	*0.00*	*0.00*	*0.09*
MA32-18_mt1.d		220.09	4.42	654.34	60.89	1.07	0.00	3.68	0.03	0.32	4.09	0.13	0.00	0.01	0.07
MA32-18_mt2.d		217.59	3.89	705.08	61.61	0.98	0.01	2.77	0.01	0.28	3.70	0.14	0.00	0.01	0.08

Analysis ID	Notes	Analysis Length (s)	Fe (wt%)	24Mg	27Al	29Si	31P	44Ca	45SC	47Ti	51V	52Cr	55Mn	59Co
MA32-18_mt3.d		2.5	**65.90**	950.87	15946.7	1798.95	9.23	75.12	5.23	52650.6	8414.87	1377.22	1284.97	55.02
MA32-18_mt4.d		5.9	**65.90**	1495.83	21877.4	843.46	-1.32	52.06	4.42	38021.8	9620.76	1667.16	1039.83	56.80
MA32-18_mt5.d		54.8	**65.90**	1317.91	20888.9	1825.31	18.45	92.25	7.72	68465.6	7881.12	1354.81	1930.74	198.35
MA32-18-a	**Avg.**		**65.90**	**1438.24**	**20401.3**	**1237.52**	**15.95**	**59.83**	**5.07**	**49224.0**	**8570.39**	**1530.10**	**1323.32**	**120.14**
Magnetite	*Std.*		***65.90***	*306.57*	*2508.4*	*480.26*	*10.93*	*21.95*	*1.42*	*10720.7*	*570.41*	*136.20*	*313.59*	*55.96*
MA32-18_mt6.d		54.8	**62.52**	4714.10	21319.7	569.57	34.39	-2.50	17.19	84403.6	7427.52	1577.41	2650.90	196.19
MA32-18_mt7.d		*11.3*	***62.52***	*3976.35*	*20444.4*	*900.31*	*36.89*	*11.25*	*7.41*	*43889.9*	*8096.50*	*1713.08*	*1556.78*	*152.74*
MA32-18_mt7.d		*12.5*	***62.52***	*3651.24*	*19006.4*	*543.93*	*38.76*	*6.88*	*14.82*	*73149.8*	*7890.18*	*1630.55*	*2307.03*	*151.93*
MA32-18_mt8.d		46.2	**62.52**	3801.29	21319.7	530.18	20.01	3.13	7.99	43827.4	8177.77	1569.28	1625.55	156.80
MA32-18_mt9.d		48.9	**62.52**	4407.75	19319.1	605.83	21.26	8.13	13.88	75025.4	7558.81	1461.12	2382.06	192.32
MA32-18_mt10.d		*15.1*	***62.52***	*4088.89*	*19694.2*	*531.43*	*7.50*	*-1.88*	*7.80*	*42827.0*	*8071.49*	*1519.27*	*1606.80*	*175.06*
MA32-18_mt10.d		*30.5*	***62.52***	*4363.98*	*18631.3*	*606.46*	*27.51*	*6.88*	*14.94*	*82528.0*	*7502.54*	*1493.01*	*2675.91*	*164.87*
MA32-18-b	**Avg.**		**62.52**	**4200.22**	**20125.8**	**599.96**	**26.88**	**4.34**	**12.59**	**66386.1**	**7768.60**	**1555.83**	**2186.42**	**173.17**
Magnetite	*Std.*		***62.52***	*354.30*	*999.9*	*61.41*	*7.64*	*4.10*	*3.02*	*13909.0*	*276.35*	*71.40*	*358.30*	*18.02*
MA32-18_mt12.d		54.8	**66.24**	2391.30	23826.9	554.44	23.18	9.27	4.76	50011.9	7584.59	1392.38	1531.49	180.11
MA32-18_mt13.d		54.8	**66.24**	2821.86	24111.7	854.51	16.56	3.97	4.07	44513.9	7909.17	1412.92	1442.06	205.68
MA32-18_mt11.d		*8.5*	***66.24***	*602.79*	*20269.7*	*635.91*	*11.92*	*104.00*	*4.01*	*46699.8*	*8001.90*	*1400.33*	*1330.12*	*80.15*
MA32-18_mt11.d		*19.0*	***66.24***	*881.00*	*21462.1*	*682.28*	*19.21*	*80.81*	*4.35*	*47627.2*	*8101.26*	*1463.26*	*1323.49*	*103.53*
MA32-18-c	**Avg.**		**66.24**	**2002.71**	**23010.6**	**692.30**	**18.90**	**33.74**	**4.36**	**47288.7**	**7854.76**	**1416.37**	**1433.03**	**160.70**
Magnetite	*Std.*		***66.24***	*871.90*	*1360.7*	*123.71*	*3.03*	*38.41*	*0.29*	*2244.8*	*202.08*	*21.13*	*84.32*	*46.71*
MA32-19_mt1.d		47.3	**65.10**	287.07	4608.7	2942.31	26.04	126.28	2.94	57869.7	10324.11	5337.81	1751.06	47.98
MA32-19_mt2.d		*7.1*	***65.10***	*729.07*	*12107.7*	*8071.81*	*7.81*	*73.56*	*2.42*	*46282.7*	*10936.00*	*5767.44*	*1353.98*	*56.18*
MA32-19_mt2.d		*18.9*	***65.10***	*364.53*	*8722.8*	*3339.39*	*26.04*	*32.55*	*3.19*	*58585.7*	*10877.42*	*5617.72*	*1549.27*	*59.24*
MA32-19_mt3.d		52.0	**65.10**	527.92	7765.9	4979.79	21.48	139.95	3.88	51295.1	9966.08	5038.37	1406.06	65.62
MA32-19_mt4.d		52.2	**65.10**	471.29	5734.9	4413.46	14.32	911.33	1.93	53898.9	11547.90	4999.32	1555.78	32.48
MA32-19_mt5.d		38.0	**65.10**	119.12	6008.3	1210.77	11.07	90.48	1.75	30529.7	9809.86	3352.41	937.37	56.76
MA32-19_mt6.d		39.7	**65.10**	130.19	7512.0	1809.65	26.04	260.38	3.12	45176.1	10623.55	3664.86	1327.94	49.67
MA32-19	**Avg.**		**65.10**	**333.32**	**6879.8**	**3331.78**	**20.00**	**262.03**	**2.77**	**48997.9**	**10527.49**	**4675.24**	**1412.34**	**51.82**
Magnetite	*Std.*		***65.10***	*165.00*	*1637.2*	*1446.31*	*5.60*	*297.77*	*0.73*	*9150.4*	*585.37*	*857.69*	*250.01*	*10.42*
MA11-11_mt1.d		54.8	**62.99**	5719.17	17944.8	465.47	-25.19	3.15	19.97	70544.8	9271.60	1426.01	2935.17	214.15
MA11-11_mt2.d		*9.0*	***62.99***	*5051.51*	*16250.5*	*535.38*	*4.41*	*28.97*	*12.98*	*43145.7*	*9731.41*	*1486.48*	*1637.65*	*187.70*
MA11-11_mt2.d		*30.1*	***62.99***	*5038.92*	*16811.1*	*629.86*	*30.23*	*44.72*	*13.25*	*43334.7*	*9303.10*	*1384.44*	*1669.14*	*192.49*
MA11-11_mt3.d		54.8	**62.99**	4912.94	17699.2	553.65	26.45	-1.89	14.54	45350.2	9624.33	1390.11	1973.37	197.97
MA11-11_mt4.d		53.1	**62.99**	4736.58	15916.7	616.64	25.82	19.53	17.76	59837.1	9202.32	1412.79	2658.03	202.69
MA11-11_mt5.d		54.8	**62.99**	4635.80	16754.4	472.40	44.72	14.49	12.97	46106.1	9592.84	1588.52	1645.21	188.39
MA11-11	**Avg.**		**62.99**	**5009.26**	**16999.3**	**543.24**	**19.21**	**15.27**	**15.68**	**53025.9**	**9418.62**	**1445.09**	**2174.73**	**198.92**
Magnetite	*Std.*		***62.99***	*381.61*	*737.1*	*64.44*	*23.43*	*15.01*	*2.74*	*10534.4*	*168.13*	*72.63*	*528.36*	*9.11*
MA11-8_mt1.d		48.8	**63.00**	1732.4	11301.7	741.5	24.1	6.3	8.7	55248.7	6318.6	938.0	2519.9	161.9

Analysis ID		60Ni	63Cu	66Zn	69Ga	74Ge	89Y	90Zr	93Nb	95Mo	118Sn	178Hf	181Ta	182W	208Pb
MA32-18_mt3.d		158.81	6.46	308.39	60.03	0.72	0.02	10.28	0.16	0.33	2.11	0.36	0.00	0.01	0.06
MA32-18_mt4.d		164.74	14.69	400.65	66.16	1.12	0.00	6.46	0.01	0.30	3.47	0.11	0.00	0.01	0.04
MA32-18_mt5.d		247.77	19.04	577.25	57.86	0.94	0.02	9.16	0.15	0.24	2.96	0.27	0.01	0.01	0.07
MA32-18-a	**Avg.**	**201.80**	**9.70**	**529.14**	**61.31**	**0.96**	**0.01**	**6.47**	**0.07**	**0.29**	**3.26**	**0.20**	**0.00**	**0.01**	**0.06**
Magnetite	*Std.*	*34.41*	*6.07*	*151.12*	*2.73*	*0.14*	*0.01*	*2.94*	*0.07*	*0.03*	*0.68*	*0.10*	*0.01*	*0.00*	*0.01*
MA32-18_mt6.d		250.08	24.38	499.54	49.33	0.86	0.00	13.44	0.17	0.22	2.74	0.44	0.01	0.00	0.03
MA32-18_mt7.d		*185.69*	*8.38*	*368.25*	*52.21*	*0.91*	*0.01*	*3.07*	*0.01*	*0.22*	*3.58*	*0.16*	*0.00*	*0.00*	*0.00*
MA32-18_mt7.d		*174.43*	*45.64*	*329.49*	*51.33*	*0.91*	*0.00*	*9.94*	*0.11*	*0.19*	*3.78*	*0.38*	*0.00*	*0.01*	*0.04*
MA32-18_mt8.d		196.32	2.75	476.41	52.71	0.91	0.00	3.27	0.01	0.21	2.67	0.17	0.00	0.00	0.02
MA32-18_mt9.d		242.58	0.91	414.52	50.02	0.86	0.00	9.38	0.10	0.20	5.01	0.29	0.01	0.00	0.03
MA32-18_mt10.d		*201.94*	*0.51*	*460.78*	*52.02*	*0.90*	*0.00*	*3.39*	*0.01*	*0.21*	*4.54*	*0.16*	*0.00*	*0.00*	*0.01*
MA32-18_mt10.d		*196.32*	*175.06*	*421.39*	*48.45*	*0.86*	*0.00*	*10.94*	*0.13*	*0.20*	*4.85*	*0.36*	*0.01*	*0.00*	*0.03*
MA32-18-b	**Avg.**	**213.39**	**34.65**	**434.55**	**50.69**	**0.88**	**0.00**	**8.24**	**0.09**	**0.21**	**3.77**	**0.29**	**0.01**	**0.00**	**0.02**
Magnetite	*Std.*	*27.76*	*42.72*	*52.72*	*1.31*	*0.02*	*0.00*	*3.33*	*0.05*	*0.01*	*0.98*	*0.09*	*0.00*	*0.00*	*0.01*
MA32-18_mt12.d		280.20	0.46	524.63	55.71	0.90	0.01	2.92	0.03	0.31	3.28	0.14	0.00	0.00	0.04
MA32-18_mt13.d		267.61	45.04	565.04	60.21	0.87	0.00	2.46	0.00	0.38	2.97	0.14	0.00	0.01	0.05
MA32-18_mt11.d		*218.46*	*39.74*	*914.12*	*59.15*	*1.01*	*0.04*	*2.71*	*0.00*	*0.36*	*3.04*	*0.14*	*0.00*	*0.00*	*0.09*
MA32-18_mt11.d		*239.79*	*7.22*	*595.51*	*59.88*	*0.96*	*0.02*	*2.25*	*0.01*	*0.33*	*2.79*	*0.15*	*0.00*	*0.01*	*0.05*
MA32-18-c	**Avg.**	**260.34**	**20.93**	**594.57**	**58.53**	**0.92**	**0.01**	**2.59**	**0.01**	**0.34**	**3.04**	**0.15**	**0.00**	**0.01**	**0.05**
Magnetite	*Std.*	*19.87*	*18.38*	*72.24*	*2.01*	*0.04*	*0.01*	*0.24*	*0.01*	*0.03*	*0.17*	*0.00*	*0.00*	*0.00*	*0.01*
MA32-19_mt1.d		249.97	2.28	663.97	47.58	0.95	0.00	1.65	0.25	0.31	3.65	0.07	0.01	0.02	0.13
MA32-19_mt2.d		*259.08*	*0.53*	*397.08*	*58.98*	*1.18*	*0.01*	*0.93*	*0.19*	*0.13*	*3.38*	*0.06*	*0.01*	*0.11*	*0.01*
MA32-19_mt2.d		*263.64*	*0.51*	*390.57*	*57.35*	*1.07*	*0.01*	*1.63*	*0.29*	*0.25*	*3.62*	*0.09*	*0.01*	*0.00*	*0.07*
MA32-19_mt3.d		318.32	11.72	703.03	49.08	1.03	0.01	1.71	0.20	0.25	3.33	0.09	0.00	0.00	0.12
MA32-19_mt4.d		202.84	0.68	611.90	56.11	1.12	0.07	3.57	0.19	0.29	3.48	0.14	0.01	0.01	0.17
MA32-19_mt5.d		225.88	0.35	863.16	54.88	0.98	0.00	1.50	0.07	0.27	2.36	0.08	0.00	0.01	0.03
MA32-19_mt6.d		310.50	0.81	605.39	55.14	1.06	0.00	1.77	0.16	0.26	2.51	0.08	0.00	0.02	0.06
MA32-19	**Avg.**	**261.65**	**2.72**	**639.97**	**53.43**	**1.04**	**0.02**	**1.94**	**0.19**	**0.27**	**3.15**	**0.09**	**0.00**	**0.02**	**0.10**
Magnetite	*Std.*	*41.78*	*4.07*	*140.04*	*3.75*	*0.06*	*0.02*	*0.74*	*0.06*	*0.03*	*0.51*	*0.02*	*0.00*	*0.01*	*0.05*
MA11-11_mt1.d		459.17	0.40	306.74	49.26	0.85	0.00	8.38	0.24	0.55	3.48	0.33	0.01	0.26	0.07
MA11-11_mt2.d		*477.44*	*11.21*	*266.43*	*48.63*	*0.89*	*0.00*	*3.56*	*0.01*	*0.21*	*3.87*	*0.14*	*0.00*	*0.02*	*0.07*
MA11-11_mt2.d		*469.88*	*0.39*	*239.35*	*48.18*	*0.91*	*0.00*	*2.97*	*0.01*	*0.17*	*4.11*	*0.14*	*0.00*	*0.07*	*0.05*
MA11-11_mt3.d		467.99	0.25	272.10	50.14	0.93	0.00	3.15	0.02	0.15	4.55	0.15	0.00	0.02	0.03
MA11-11_mt4.d		464.84	0.55	345.17	46.61	0.91	0.01	7.24	0.14	0.19	2.46	0.29	0.01	0.03	0.15
MA11-11_mt5.d		478.07	0.37	288.48	47.62	0.93	0.00	3.17	0.03	0.12	2.65	0.16	0.00	0.00	0.08
MA11-11	**Avg.**	**468.34**	**0.89**	**291.62**	**48.38**	**0.91**	**0.00**	**5.01**	**0.09**	**0.24**	**3.44**	**0.22**	**0.00**	**0.07**	**0.08**
Magnetite	*Std.*	*6.35*	*1.00*	*33.48*	*1.23*	*0.03*	*0.00*	*2.31*	*0.09*	*0.16*	*0.80*	*0.08*	*0.01*	*0.10*	*0.04*
MA11-8_mt1.d		283.5	3.1	422.1	40.8	1.0	0.2	5.0	0.1	0.2	5.1	0.2	0.0	0.1	0.0

Analysis ID	Notes		Analysis Length (s)	Fe (wt%)	24Mg	27Al	29Si	31P	44Ca	45SC	47Ti	51V	52Cr	55Mn	59Co
MA11-8_mt2.d			48.8	**63.00**	2236.4	12290.8	471.2	32.8	0.6	8.6	55941.7	6545.4	883.2	2450.6	169.1
MA11-8_mt5.d			48.8	**63.00**	3653.9	12731.8	561.9	32.8	-3.1	16.2	72888.0	6747.0	997.9	3131.0	206.8
MA11-8_mt4.d			48.8	**63.00**	4264.9	12492.4	519.7	34.0	-0.6	15.5	75722.9	6803.7	1002.3	3231.8	193.1
MA11-8_mt3.d			48.8	**63.00**	4542.1	12479.8	567.0	32.8	3.8	14.7	76226.9	6671.4	945.0	3231.8	201.8
MA11-8		**Avg.**		**63.00**	**2971.90**	**12204.2**	**573.59**	**30.90**	**0.79**	**12.28**	**64950.3**	**6603.70**	**955.36**	**2833.31**	**182.72**
Magnetite		*Std.*		**63.00**	*1185.22*	*628.0*	*117.90*	*4.60*	*4.00*	*4.16*	*10867.9*	*220.00*	*56.31*	*405.00*	*20.84*
MA11-2_mt1.d			48.8	**63.76**	3851.1	18005.9	63.8	-45.9	-31.9	9.8	55662.6	7919.0	310.5	1944.7	202.8
MA11-2_mt2.d			48.8	**63.76**	4482.3	17189.7	-163.9	-59.5	-49.7	10.8	53239.7	7549.2	325.2	1721.5	198.6
MA11-2_mt3.d			48.8	**63.76**	4456.8	17202.5	-130.1	-64.1	-55.5	13.3	64971.6	7166.6	299.0	2276.2	207.0
MA11-2_mt4.d			48.8	**63.76**	4131.7	17680.7	644.0	24.4	17.9	10.9	55280.0	7963.6	316.3	1734.3	209.6
MA11-2_mt5.d			48.8	**63.76**	4833.0	18949.5	-471.8	-57.4	-49.7	11.1	50243.0	7734.1	303.3	1734.3	217.2
MA11-2_mt6.d			48.8	**63.76**	4915.9	18107.9	197.7	-27.4	-12.8	11.5	51199.4	7734.1	307.3	1900.1	199.5
MA11-2		**Avg.**		**63.76**	**4445.14**	**17856.0**	**23.27**	**-38.31**	**-30.29**	**11.23**	**55099.4**	**7677.78**	**310.27**	**1885.17**	**205.81**
Magnetite		*Std.*		**63.76**	*406.14*	*660.8*	*379.73*	*33.43*	*28.35*	*1.18*	*5292.7*	*291.22*	*9.40*	*214.02*	*7.03*
MA11-2_alt-mt-1.d	**30 um**		11.5	**64.31**	893.92	16592.2	1228.34	14.15	15.43	3.35	36078.4	8321.82	383.94	1144.09	67.98
MA11-2_alt-mt-2.d	**30 um**		14.7	**64.31**	746.01	15884.8	1183.32	25.72	10.93	10.61	69455.7	7910.23	325.41	2122.26	72.99
MA11-2_alt-mt-3.d	**30 um**		11.1	**64.31**	1607.77	15820.5	2057.95	-5.14	-13.51	4.30	35306.6	8000.27	342.78	1202.61	100.32
MA11-2_alt-mt-5.d	**30 um**		39.6	**64.31**	881.06	12026.1	1331.23	35.37	585.23	8.63	43474.1	7035.61	299.69	1399.40	63.80
MA11-2_alt-mt-6.d	**30 um**		39.7	**64.31**	775.59	17878.4	707.42	-12.86	34.73	5.28	39615.5	8218.92	320.91	1250.20	96.08
MA11-2 (Altered)		**Avg.**		**64.31**	**980.87**	**15640.4**	**1301.65**	**11.45**	**126.56**	**6.43**	**44786.1**	**7897.37**	**334.54**	**1423.71**	**80.23**
Magnetite		*Std.*		***64.31***	*318.69*	*1952.9*	*434.82*	*18.16*	*229.85*	*2.74*	*12670.7*	*455.40*	*28.25*	*359.37*	*15.02*
MA03-7-MT1.d			53.8	**68.78**	70.09	344.6	619.02	23.39	35.08	0.86	46289.1	9065.24	7827.20	2482.97	28.54
MA03-7-MT2.d			53.8	**68.78**	62.73	313.0	584.63	34.39	-8.94	0.82	40855.5	8308.66	7758.42	2173.46	29.64
MA03-7-MT3.d			53.8	**68.78**	65.48	217.3	547.49	33.70	0.69	0.84	41749.6	9422.90	7139.39	2180.34	33.98
MA03-7-MT4.d			53.8	**68.78**	129.31	381.7	1059.22	32.33	481.46	0.58	30332.1	7971.64	7091.25	1671.36	26.07
MA03-7-MT5.d			53.8	**68.78**	112.80	264.8	526.86	19.95	71.53	0.97	56399.8	9216.56	7909.73	2957.55	35.70
MA03-7-MT6.d			35.3	**68.78**	93.54	254.5	529.61	27.51	1.38	0.39	23522.9	7153.15	8260.51	1251.80	39.07
MA03-7-MT-7.d			53.8	**68.78**	364.54	1162.4	499.34	51.59	-7.57	0.51	23522.9	6706.08	6307.15	1203.66	69.26
MA03-7		**Avg.**		**68.78**	**128.35**	**419.8**	**623.74**	**31.84**	**81.95**	**0.71**	**37524.6**	**8263.46**	**7470.52**	**1988.73**	**37.47**
Magnetite		*Std.*		**68.78**	*113.96*	*362.1*	*214.80*	*10.47*	*194.28*	*0.22*	*12776.9*	*1085.45*	*705.07*	*667.66*	*15.53*
MA03-4_mt1.d			48.8	**67.45**	1005.0	11331.6	688.0	-17.5	-4.7	2.8	54971.8	7298.1	6650.6	2394.5	321.7
MA03-4_mt2.d			48.8	**67.45**	600.3	11129.3	1416.5	24.0	43.8	1.5	31027.1	8417.8	8114.2	1362.5	211.1
MA03-4_mt3.d			33.8	**67.45**	363.6	12491.8	542.3	8.0	22.9	1.7	45933.5	9753.3	7318.3	1768.5	174.0
MA03-4_mt4.d			48.8	**67.45**	327.8	10839.2	413.5	-1.6	10.1	3.1	39256.0	9577.9	7493.7	1469.1	209.1
MA03-4_mt5.d			48.8	**67.45**	398.0	11709.3	843.1	9.2	37.1	1.2	37299.9	8916.9	7756.8	1454.2	222.6
MA03-4_mt6.d			48.8	**67.45**	541.6	13894.7	692.7	23.0	16.9	4.4	65763.9	9955.6	6191.9	2401.2	174.6
MA03-4		**Avg.**		**67.45**	**539.38**	**11899.3**	**766.01**	**7.52**	**21.02**	**2.46**	**45708.7**	**8986.60**	**7254.26**	**1808.34**	**218.86**
Magnetite		*Std.*			251.5	1132.1	350.7	15.7	17.8	1.2	12774.7	1005.6	713.7	476.6	54.3

Analysis ID		60Ni	63Cu	66Zn	69Ga	74Ge	89Y	90Zr	93Nb	95Mo	118Sn	178Hf	181Ta	182W	208Pb
MA11-8_mt2.d		288.5	0.3	398.1	40.8	1.0	0.0	5.6	0.1	0.2	5.4	0.1	0.0	0.1	0.0
MA11-8_mt5.d		303.0	0.3	447.9	43.5	0.9	0.0	8.3	0.2	0.2	5.8	0.3	0.0	0.1	0.0
MA11-8_mt4.d		299.9	0.4	432.2	43.7	0.9	0.0	8.5	0.2	0.2	5.3	0.3	0.0	0.1	0.0
MA11-8_mt3.d		302.3	0.3	434.7	42.6	0.9	0.0	7.2	0.2	0.1	9.3	0.3	0.0	0.0	0.0
MA11-8	**Avg.**	**293.73**	**1.03**	**425.08**	**42.18**	**0.92**	**0.05**	**6.86**	**0.17**	**0.17**	**5.38**	**0.21**	**0.01**	**0.08**	**0.03**
Magnetite	*Std.*	*9.24*	*1.41*	*20.86*	*1.60*	*0.06*	*0.08*	*1.83*	*0.05*	*0.01*	*0.27*	*0.07*	*0.00*	*0.02*	*0.01*
MA11-2_mt1.d		275.4	0.3	304.1	48.3	1.0	0.0	4.2	0.1	0.2	3.6	0.2	0.0	0.0	0.1
MA11-2_mt2.d		284.2	0.2	276.7	43.9	0.8	0.0	4.7	0.1	0.2	3.8	0.2	0.0	0.0	0.1
MA11-2_mt3.d		285.9	0.4	329.0	42.1	0.7	0.0	6.2	0.1	0.2	3.2	0.2	0.0	0.0	0.1
MA11-2_mt4.d		307.3	0.3	382.6	48.1	0.9	0.0	4.4	0.1	0.2	4.1	0.2	0.0	0.0	0.1
MA11-2_mt5.d		308.8	0.2	327.7	46.4	0.8	0.0	4.4	0.1	0.2	4.4	0.2	0.0	0.0	0.0
MA11-2_mt6.d		315.0	0.3	364.1	45.4	0.9	0.0	4.4	0.1	0.2	3.3	0.2	0.0	0.0	0.1
MA11-2	**Avg.**	**296.10**	**0.29**	**330.70**	**45.72**	**0.85**	**0.00**	**4.72**	**0.08**	**0.19**	**3.73**	**0.18**	**0.00**	**0.01**	**0.08**
Magnetite	*Std.*	*16.22*	*0.07*	*38.56*	*2.41*	*0.09*	*0.00*	*0.74*	*0.02*	*0.03*	*0.44*	*0.03*	*0.00*	*0.01*	*0.04*
MA11-2_alt-mt-1.d		100.32	1.75	1652.79	51.19	1.16	0.94	3.04	0.01	0.12	4.18	0.08	0.00	0.00	0.17
MA11-2_alt-mt-2.d		120.26	2.44	1620.63	51.26	0.92	0.77	5.98	0.19	0.23	5.02	0.17	0.01	0.01	0.21
MA11-2_alt-mt-3.d		179.43	1.40	1119.01	54.15	0.84	0.34	2.80	0.00	0.18	4.69	0.07	0.00	0.00	0.17
MA11-2_alt-mt-5.d		154.99	1.13	900.35	45.34	0.86	0.57	3.13	0.01	0.15	4.50	0.08	0.01	0.05	0.33
MA11-2_alt-mt-6.d		145.34	5.40	1574.33	54.99	0.85	0.48	3.19	0.01	0.17	3.42	0.07	0.00	0.01	0.38
MA11-2 (Altered)	**Avg.**	**140.07**	**2.42**	**1373.42**	**51.38**	**0.92**	**0.62**	**3.63**	**0.04**	**0.17**	**4.36**	**0.09**	**0.00**	**0.01**	**0.25**
Magnetite	*Std.*	*27.46*	*1.55*	*305.96*	*3.38*	*0.12*	*0.21*	*1.18*	*0.07*	*0.03*	*0.54*	*0.04*	*0.00*	*0.02*	*0.09*
MA03-7-MT1.d		190.59	0.32	30.06	31.78	0.65	0.02	0.66	0.30	0.26	5.84	0.02	0.01	0.04	0.05
MA03-7-MT2.d		206.34	0.37	24.62	28.34	0.59	0.02	0.61	0.34	0.31	5.60	0.03	0.01	0.03	0.04
MA03-7-MT3.d		207.03	0.33	20.22	32.26	0.71	0.02	0.55	0.27	0.30	6.14	0.03	0.01	0.03	0.03
MA03-7-MT4.d		187.08	0.31	20.50	27.26	0.68	0.04	0.37	0.20	0.32	7.66	0.03	0.00	0.05	0.63
MA03-7-MT5.d		237.29	0.52	36.66	30.68	0.63	0.01	0.77	0.38	0.44	2.96	0.04	0.01	0.03	0.24
MA03-7-MT6.d		233.17	0.27	25.59	27.17	0.63	0.00	0.20	0.21	0.33	2.90	0.02	0.01	0.01	0.15
MA03-7-MT-7.d		258.61	0.20	334.27	23.10	0.63	0.00	0.39	0.14	0.32	3.16	0.01	0.00	0.01	0.04
MA03-7	**Avg.**	**217.16**	**0.33**	**70.27**	**28.65**	**0.65**	**0.02**	**0.50**	**0.26**	**0.33**	**4.89**	**0.03**	**0.01**	**0.03**	**0.17**
Magnetite	*Std.*	*26.03*	*0.11*	*126.19*	*3.18*	*0.04*	*0.01*	*0.20*	*0.09*	*0.05*	*2.01*	*0.01*	*0.00*	*0.02*	*0.23*
MA03-4_mt1.d		484.3	2.1	725.1	52.4	0.6	0.0	3.0	0.4	0.3	4.1	0.1	0.0	0.2	0.0
MA03-4_mt2.d		392.6	1.6	1015.1	51.5	0.6	0.1	2.2	0.2	0.2	5.9	0.0	0.0	0.1	0.1
MA03-4_mt3.d		443.1	0.4	642.1	59.3	0.6	0.0	1.6	0.3	0.2	7.0	0.0	0.0	0.1	0.1
MA03-4_mt4.d		416.2	0.6	879.5	62.7	0.6	0.0	2.5	0.3	0.3	4.2	0.1	0.0	0.1	0.1
MA03-4_mt5.d		418.9	0.6	1021.9	77.3	0.6	0.0	1.6	0.3	0.2	3.2	0.0	0.0	0.2	0.1
MA03-4_mt6.d		383.1	0.5	491.7	61.2	0.5	0.1	3.1	0.3	0.2	3.5	0.1	0.0	0.2	0.2
MA03-4	**Avg.**	**423.02**	**0.97**	**795.91**	**60.73**	**0.59**	**0.04**	**2.33**	**0.31**	**0.24**	**4.66**	**0.05**	**0.01**	**0.15**	**0.09**
Magnetite	*Std.*	36.7	0.7	213.2	9.3	0.0	0.0	0.7	0.1	0.0	1.5	0.0	0.0	0.0	0.1

Analysis ID	Notes	Analysis Length (s)	Fe (wt%)	24Mg	27Al	29Si	31P	44Ca	45SC	47Ti	51V	52Cr	55Mn	59Co
MA03-1B_mt1.d		48.8	**60.17**	5655.8	24849.5	622.1	36.7	4.2	11.8	57039.6	9139.6	11119.1	1801.4	241.3
MA03-1B_mt2.d		48.8	**60.17**	5487.4	23489.7	610.1	39.1	13.2	11.4	57099.8	9320.1	11913.3	1707.6	227.6
MA03-1B_mt3.d		48.8	**60.17**	4548.7	24909.7	727.4	41.5	7.8	10.4	57280.3	8923.0	10517.4	1940.4	236.9
MA03-1B_mt4.d		48.8	**60.17**	4885.7	23026.4	623.3	30.7	4.8	10.8	54211.7	9452.4	10710.0	1778.6	232.9
MA03-1b_mt5.d		48.8	**60.17**	4151.6	21480.1	592.1	27.7	-1.8	11.0	55114.2	9049.3	10788.2	1788.2	229.7
MA03-1B	**Avg.**		**60.17**	**4945.84**	**23551.1**	**635.02**	**35.14**	**5.66**	**11.08**	**56149.1**	**9176.88**	**11009.61**	**1803.25**	**233.69**
Magnetite	*Std.*			630.4	1423.0	53.2	5.8	5.5	0.5	1396.5	211.3	549.9	84.9	5.5
MA03-1A_mt1.d		48.8	**61.82**	4315.0	22359.9	578.6	41.4	5.6	11.1	52855.2	8939.0	9241.9	1777.3	205.8
MA03-1A_mt2.d		35.4	**61.82**	4630.2	21574.8	692.4	40.8	8.0	9.2	51680.6	9211.0	11183.0	1712.4	211.4
MA03-1A_mt3.d		48.8	**61.82**	4797.1	22285.7	772.7	48.8	32.1	11.1	52917.0	9130.7	9625.2	1693.8	212.8
MA03-1A_mt4.d		48.8	**61.82**	4828.1	22706.1	659.6	47.6	3.1	11.1	53226.1	9130.7	9260.5	1726.6	214.4
MA03-1A_mt5.d		48.8	**61.82**	4976.4	20214.8	581.1	40.8	-6.2	16.1	81848.2	8691.7	10088.8	2664.4	214.7
MA03-1A_mt6.d		48.8	**61.82**	5186.6	22811.2	803.6	47.0	9.9	16.8	79128.2	8883.4	10503.0	2509.8	196.7
MA03-1A	**Avg.**		**61.82**	**4788.90**	**21992.1**	**681.35**	**44.41**	**8.76**	**12.57**	**61942.5**	**8997.74**	**9983.75**	**2014.06**	**209.31**
Magnetite	*Std.*		**61.82**	*298.24*	*973.2*	*94.34*	*3.78*	*12.76*	*3.12*	*14400.8*	*195.44*	*764.33*	*447.43*	*6.97*
T3C4-1-MT1.d		53.8	**61.39**	3290.46	16538.2	725.62	52.79	-2.46	15.78	68387.5	6998.37	129.78	2234.57	150.71
T3C4-1-MT2.d		53.8	**61.39**	3566.71	16642.6	639.68	48.50	-1.23	16.58	69615.3	6973.81	130.51	2363.48	154.95
T3C4-1-MT3.d		53.8	**61.39**	3216.79	16931.1	720.71	31.31	5.53	15.22	64028.9	7231.64	140.40	1989.01	122.96
T3C4-1-MT4.d		51.6	**61.39**	3609.68	16673.3	686.94	41.13	17.80	14.18	61880.3	7121.14	133.03	2228.43	167.59
T3C4-1-MT5.d		53.8	**61.39**	3235.21	15476.2	593.02	52.18	-11.05	13.51	67466.7	6630.03	136.53	2406.46	157.34
T3-C4-1	**Avg.**		**61.39**	**3383.77**	**16452.3**	**673.19**	**45.18**	**1.72**	**15.05**	**66275.8**	**6991.00**	**134.05**	**2244.39**	**150.71**
Magnetite	*Std.*		**61.39**	*189.18*	*564.5*	*56.45*	*9.04*	*10.75*	*1.23*	*3217.1*	*226.66*	*4.42*	*162.80*	*16.71*
T3C4-2-MT1.d		53.8	**62.47**	3317.37	15499.8	687.84	32.49	-27.49	12.12	56788.9	7309.46	114.08	1842.98	166.12
T3C4-2-MT2.d		53.8	**62.47**	3361.10	16655.6	633.49	19.99	-5.00	17.74	67534.4	7215.75	106.64	2130.36	169.62
T3C4-2-MT3.d		39.6	**62.47**	3579.76	17049.2	696.59	36.86	-16.24	12.12	57726.0	7740.53	124.45	2076.64	200.73
T3C4-2-MT4.d		53.8	**62.47**	3542.28	15974.6	677.84	28.74	-3.12	11.98	52228.3	7403.17	121.45	1892.96	166.87
T3C4-2-MT5.d		53.8	**62.47**	3979.59	15749.7	662.22	19.37	5.62	15.37	64473.2	7265.73	118.08	2249.06	195.54
T3-C4-2	**Avg.**		**62.47**	**3556.02**	**16185.8**	**671.60**	**27.49**	**-9.25**	**13.87**	**59750.1**	**7386.93**	**116.94**	**2038.40**	**179.78**
Magnetite	*Std.*		**62.47**	*262.26*	*646.4*	*24.84*	*7.69*	*12.83*	*2.60*	*6171.4*	*209.34*	*6.93*	*168.55*	*16.91*
TA1-1_mt1.d		54.8	**60.76**	4016.01	21058.2	453.24	29.16	11.54	20.68	65131.1	7114.60	303.05	2563.93	167.63
TA1-1_mt2.d		54.8	**60.76**	4781.55	20110.4	503.67	33.42	26.13	23.53	72604.2	6944.48	292.24	1941.17	156.81
TA1-1_mt3.d		54.8	**60.76**	3785.14	18227.0	455.67	15.80	9.11	19.92	65617.1	7078.15	288.59	2145.32	149.22
TA1-1_mt4.d		54.8	**60.76**	4125.37	19016.8	474.51	15.80	13.37	20.34	66710.8	6920.18	280.94	1874.95	136.28
TA1-1_mt5.d		54.8	**60.76**	5243.30	20475.0	452.64	10.33	14.58	21.85	69870.1	7120.68	291.63	2295.99	189.14
TA1-1	**Avg.**		**60.76**	**4390.27**	**19777.5**	**467.95**	**20.90**	**14.95**	**21.26**	**67986.7**	**7035.62**	**291.29**	**2164.27**	**159.81**
Magnetite	*Std.*		***60.76***	*539.85*	*1021.8*	*19.60*	*8.82*	*5.89*	*1.30*	*2837.8*	*85.92*	*7.13*	*249.37*	*17.87*
TA1-4_mt1.d		54.8	**60.35**	5280.34	18544.5	441.74	27.16	0.60	23.13	70726.3	6680.38	223.22	2289.55	177.78
TA1-4_mt2.d		54.8	**60.35**	5437.24	18478.2	522.60	34.40	22.93	22.44	69217.7	6782.97	228.23	2153.77	191.12

Analysis ID		60Ni	63Cu	66Zn	69Ga	74Ge	89Y	90Zr	93Nb	95Mo	118Sn	178Hf	181Ta	182W	208Pb
MA03-1B_mt1.d		512.6	0.3	533.1	50.8	0.9	0.0	4.7	0.1	0.2	7.4	0.2	0.0	0.0	0.0
MA03-1B_mt2.d		514.4	0.3	444.0	50.8	0.8	0.0	4.6	0.1	0.2	8.3	0.2	0.0	0.0	0.0
MA03-1B_mt3.d		506.6	0.3	534.3	51.5	0.8	0.0	4.4	0.1	0.2	9.7	0.2	0.0	0.0	0.0
MA03-1B_mt4.d		507.8	0.3	479.5	51.2	0.9	0.0	4.3	0.1	0.2	9.0	0.2	0.0	0.0	0.0
MA03-1b_mt5.d		505.4	0.5	350.8	49.1	0.9	0.0	4.0	0.0	0.2	7.0	0.2	0.0	0.0	0.1
MA03-1B	**Avg.**	**509.39**	**0.37**	**468.35**	**50.69**	**0.85**	**0.00**	**4.40**	**0.06**	**0.18**	**8.29**	**0.21**	**0.00**	**0.00**	**0.03**
Magnetite	*Std.*	3.9	0.1	76.0	0.9	0.0	0.0	0.3	0.0	0.0	1.1	0.0	0.0	0.0	0.0
MA03-1A_mt1.d		430.3	0.3	377.1	49.9	0.7	0.0	4.2	0.1	0.2	5.2	0.2	0.0	0.0	0.0
MA03-1A_mt2.d		455.0	40.8	479.1	52.3	0.9	0.0	3.2	0.1	0.2	4.0	0.2	0.0	0.0	0.1
MA03-1A_mt3.d		460.6	0.4	438.9	50.1	0.9	0.0	4.2	0.0	0.2	5.8	0.2	0.0	0.0	0.1
MA03-1A_mt4.d		463.0	0.4	432.1	51.1	2.3	0.1	4.2	0.1	0.2	8.0	0.2	0.0	0.0	0.0
MA03-1A_mt5.d		416.0	0.7	312.2	50.0	0.8	0.0	10.0	0.3	0.2	4.4	0.4	0.0	0.0	0.0
MA03-1A_mt6.d		418.5	64.3	517.4	48.8	0.9	0.0	12.4	0.3	0.2	5.4	0.4	0.0	0.0	0.0
MA03-1A	**Avg.**	**440.56**	**17.81**	**426.14**	**50.36**	**1.08**	**0.02**	**6.37**	**0.14**	**0.19**	**5.49**	**0.25**	**0.01**	**0.01**	**0.05**
Magnetite	*Std.*	*21.47*	*27.92*	*73.11*	*1.19*	*0.62*	*0.03*	*3.85*	*0.14*	*0.01*	*1.41*	*0.11*	*0.01*	*0.00*	*0.02*
T3C4-1-MT1.d		188.16	0.54	446.91	44.94	0.91	0.02	5.73	0.21	0.15	6.97	0.22	0.01	0.01	0.03
T3C4-1-MT2.d		190.12	0.79	456.74	45.61	0.96	0.03	6.16	0.22	0.19	7.30	0.27	0.01	0.00	0.04
T3C4-1-MT3.d		173.36	0.51	491.73	47.21	1.04	0.04	5.00	0.18	0.22	7.18	0.27	0.01	0.00	0.07
T3C4-1-MT4.d		195.22	10.13	483.13	47.09	1.04	0.02	5.04	0.13	0.14	6.82	0.23	0.00	0.00	0.04
T3C4-1-MT5.d		175.57	0.75	455.51	45.31	0.99	0.03	5.34	0.21	0.20	4.80	0.23	0.01	0.02	0.08
T3-C4-1	**Avg.**	**184.49**	**2.54**	**466.80**	**46.03**	**0.99**	**0.03**	**5.46**	**0.19**	**0.18**	**6.62**	**0.24**	**0.01**	**0.01**	**0.05**
Magnetite	*Std.*	*9.53*	*4.24*	*19.44*	*1.05*	*0.05*	*0.01*	*0.49*	*0.04*	*0.03*	*1.03*	*0.02*	*0.00*	*0.01*	*0.02*
T3C4-2-MT1.d		209.29	0.77	413.58	47.61	1.06	0.03	4.77	0.09	0.19	7.78	0.15	0.00	0.00	0.04
T3C4-2-MT2.d		210.97	0.67	435.44	47.67	1.03	0.03	6.23	0.17	0.20	6.60	0.25	0.01	0.01	0.05
T3C4-2-MT3.d		221.78	0.56	454.19	47.61	0.97	0.02	3.62	0.10	0.18	8.22	0.20	0.00	0.01	0.12
T3C4-2-MT4.d		218.66	0.74	436.69	48.48	1.00	0.03	3.50	0.09	0.19	6.07	0.20	0.00	0.00	0.11
T3C4-2-MT5.d		255.52	1.02	468.56	47.17	0.99	0.02	5.37	0.14	0.14	5.97	0.23	0.01	0.00	0.05
T3-C4-2	**Avg.**	**223.24**	**0.75**	**441.69**	**47.71**	**1.01**	**0.03**	**4.70**	**0.12**	**0.18**	**6.93**	**0.21**	**0.00**	**0.00**	**0.07**
Magnetite	*Std.*	*18.78*	*0.17*	*20.81*	*0.48*	*0.04*	*0.00*	*1.16*	*0.04*	*0.02*	*1.02*	*0.04*	*0.00*	*0.00*	*0.04*
TA1-1_mt1.d		260.04	0.48	305.61	47.69	0.89	0.00	4.82	0.06	0.19	4.61	0.23	0.00	0.00	0.03
TA1-1_mt2.d		255.18	0.40	306.21	45.63	0.87	0.00	6.54	0.08	0.16	3.74	0.28	0.01	0.00	0.02
TA1-1_mt3.d		249.71	0.67	249.71	45.63	0.89	0.00	5.07	0.07	0.16	4.61	0.22	0.00	0.00	0.06
TA1-1_mt4.d		233.61	0.32	297.10	43.20	0.82	0.01	5.29	0.07	0.15	3.62	0.22	0.00	0.00	0.03
TA1-1_mt5.d		265.51	0.38	326.87	45.26	0.92	0.00	6.08	0.08	0.18	3.70	0.31	0.00	0.00	0.02
TA1-1	**Avg.**	**252.81**	**0.45**	**297.10**	**45.48**	**0.88**	**0.00**	**5.56**	**0.07**	**0.17**	**4.05**	**0.25**	**0.00**	**0.00**	**0.03**
Magnetite	*Std.*	*10.93*	*0.12*	*25.64*	*1.43*	*0.03*	*0.00*	*0.65*	*0.01*	*0.01*	*0.45*	*0.04*	*0.00*	*0.00*	*0.01*
TA1-4_mt1.d		268.60	0.39	276.39	43.69	0.80	0.00	5.93	0.09	0.15	3.17	0.28	0.01	0.00	0.03
TA1-4_mt2.d		277.72	0.56	280.01	43.69	0.82	0.00	5.99	0.10	0.15	4.94	0.24	0.01	0.00	0.01

Analysis ID	Notes	Analysis Length (s)	Fe (wt%)	24Mg	27Al	29Si	31P	44Ca	45SC	47Ti	51V	52Cr	55Mn	59Co
TA1-4_mt3.d		54.8	**60.35**	5606.21	18798.0	510.53	27.76	15.09	22.79	68553.8	6704.52	233.30	2088.60	185.81
TA1-4_mt4.d		54.8	**60.35**	5805.35	19196.3	505.10	25.35	10.26	24.32	70967.7	6680.38	231.13	2221.97	200.71
TA1-4_mt5.d		54.8	**60.35**	5557.93	18454.0	518.98	24.14	4.22	23.86	69157.3	6855.38	245.25	2007.13	175.97
TA1-4	**Avg.**		**60.35**	**5537.41**	**18694.2**	**499.79**	**27.76**	**10.62**	**23.31**	**69724.6**	**6740.73**	**232.23**	**2152.20**	**186.28**
Magnetite	*Std.*		***60.35***	*174.97*	*279.1*	*29.67*	*3.56*	*7.91*	*0.69*	*948.5*	*68.59*	*7.33*	*98.82*	*9.06*
TA1-5_mt1.d		*8.3*	***60.83***	*4324.92*	*20256.0*	*450.13*	*4.26*	*26.16*	*17.46*	*66242.5*	*7396.77*	*376.53*	*1776.20*	*162.60*
TA1-5_mt1.d		*34.6*	***60.83***	*4008.61*	*19471.3*	*559.62*	*4.26*	*15.82*	*19.36*	*67337.4*	*7080.46*	*340.64*	*1817.56*	*168.86*
TA1-5_mt2.d		54.8	**60.83**	4397.92	19428.7	574.22	15.21	13.38	19.33	67641.5	7147.38	373.49	1857.71	166.73
TA1-5_mt3.d		53.8	**60.83**	4762.89	20444.5	546.85	17.64	34.67	20.83	66485.8	7086.55	326.59	1995.18	182.67
TA1-5_mt4.d		54.8	**60.83**	4105.94	19440.9	576.66	18.25	26.76	20.46	64965.1	7050.05	318.20	1837.03	175.61
TA1-5_mt5.d		54.8	**60.83**	3996.45	20073.5	506.10	21.90	-3.04	19.04	64113.5	7141.29	315.09	2187.40	184.68
TA1-5	**Avg.**		**60.83**	**4266.56**	**19802.0**	**548.47**	**15.45**	**17.92**	**19.73**	**66066.4**	**7113.34**	**336.19**	**1937.38**	**175.47**
Magnetite	*Std.*		***60.83***	*283.25*	*397.1*	*25.90*	*5.99*	*12.80*	*0.76*	*1327.2*	*38.61*	*21.82*	*140.43*	*7.40*
TA1-6_mt1.d		*10.7*	***60.31***	*4354.41*	*17670.9*	*566.92*	*42.22*	*13.27*	*19.90*	*60008.8*	*7424.21*	*277.43*	*2074.68*	*163.44*
TA1-6_mt1.d		*29.7*	***60.31***	*4384.57*	*17683.0*	*681.51*	*48.25*	*17.49*	*19.28*	*61818.1*	*7303.59*	*283.46*	*2000.50*	*157.11*
TA1-6_mt2.d		49.8	**60.31**	4704.21	19359.6	626.62	39.80	-2.41	17.80	59466.0	7593.08	288.89	2249.58	174.66
TA1-6_mt3.d		49.8	**60.31**	5283.19	18937.5	601.29	49.45	-3.62	18.74	59405.7	7840.35	290.70	2394.32	197.82
TA1-6_mt4.d		49.8	**60.31**	4842.92	19781.8	677.29	45.84	8.44	20.81	62602.2	7375.96	276.82	2412.42	188.77
TA1-6_mt5.d		49.8	**60.31**	4848.96	17912.2	584.41	44.63	-2.41	20.83	58923.3	7490.55	282.25	2448.60	196.01
TA1-6	**Avg.**		**60.31**	**4811.17**	**18734.2**	**628.15**	**45.28**	**3.27**	**19.52**	**60347.2**	**7527.10**	**284.10**	**2305.01**	**183.21**
Magnetite	*Std.*		**60.31**	326.17	910.7	37.35	3.54	8.81	1.31	1562.0	202.08	5.65	176.32	16.41
TA2-1_mt1.d		49.8	**63.17**	4124.83	17851.1	481.34	24.64	8.84	14.89	52934.2	7864.33	286.78	2135.06	192.60
TA2-1_mt2.d		49.8	**63.17**	4055.34	17446.8	569.77	19.58	0.63	15.13	54071.2	7763.27	308.26	2090.84	191.21
TA2-1_mt3.d		49.8	**63.17**	4649.12	19670.3	603.25	24.64	6.32	16.46	54260.7	8382.30	319.63	2514.06	205.93
TA2-1_mt4.d		49.8	**63.17**	4402.76	17497.4	795.91	46.74	5.05	16.70	52428.9	8255.97	325.94	2406.68	182.62
TA2-1_mt5.d		49.8	**63.17**	4573.31	18760.7	540.71	32.85	8.21	16.78	52744.7	8489.69	323.42	2444.58	209.72
TA2-1	**Avg.**		**63.17**	**4361.07**	**18245.3**	**598.19**	**29.69**	**5.81**	**16.00**	**53288.0**	**8151.11**	**312.80**	**2318.24**	**196.41**
Magnetite	*Std.*		**63.17**	*264.12*	*955.1*	*119.25*	*10.65*	*3.26*	*0.91*	*824.3*	*320.84*	*16.04*	*191.96*	*11.17*
TA2-3_mt1.d		49.8	**62.87**	4507.78	19420.5	598.52	35.21	-2.51	19.27	56017.2	7110.60	503.59	2116.20	197.79
TA2-3_mt2.d		49.8	**62.87**	4231.15	19238.2	584.69	31.44	6.29	20.41	54193.9	7060.30	470.58	2509.14	219.42
TA2-3_mt3.d		49.8	**62.87**	4683.82	19998.9	589.72	34.58	6.29	19.43	55954.3	6984.86	472.22	1953.37	189.30
TA2-3_mt4.d		49.8	**62.87**	4275.16	18942.7	550.11	31.44	5.03	21.34	51804.9	7003.72	440.09	3168.65	201.44
TA2-3_mt5.d		49.8	**62.87**	4218.58	18062.6	526.85	14.46	16.35	19.80	51804.9	6909.41	445.75	2309.22	192.19
TA2-3	**Avg.**		**62.87**	**4383.30**	**19132.6**	**569.98**	**29.42**	**6.29**	**20.05**	**53955.0**	**7013.78**	**466.45**	**2411.32**	**200.03**
Magnetite	*Std.*		**62.87**	*204.81*	*711.6*	*30.31*	*8.54*	*6.71*	*0.85*	*2094.8*	*76.43*	*25.26*	*471.79*	*11.83*
TA2-4_mt1.d		49.8	**62.97**	3859.93	20326.0	640.38	42.82	-3.78	16.61	50248.3	6813.12	362.06	2489.75	208.68
TA2-4_mt2.d		49.8	**62.97**	4011.05	20590.5	594.42	27.08	-6.93	18.32	51318.8	6680.88	353.25	2506.12	209.18
TA2-4_mt3.d		49.8	**62.97**	3948.08	21346.1	592.53	19.52	12.59	19.22	51066.9	7058.69	367.10	2537.60	210.31

Analysis ID		60Ni	63Cu	66Zn	69Ga	74Ge	89Y	90Zr	93Nb	95Mo	118Sn	178Hf	181Ta	182W	208Pb
TA1-4_mt3.d		272.77	0.41	306.56	45.50	0.86	0.00	6.19	0.08	0.16	4.41	0.27	0.01	0.00	0.03
TA1-4_mt4.d		278.38	0.33	303.54	44.60	0.82	0.00	6.50	0.08	0.17	4.70	0.32	0.01	0.00	0.02
TA1-4_mt5.d		263.11	0.33	273.97	44.66	0.90	0.00	6.34	0.07	0.15	3.27	0.30	0.00	0.00	0.02
TA1-4	**Avg.**	**272.12**	**0.40**	**288.10**	**44.43**	**0.84**	**0.00**	**6.19**	**0.08**	**0.16**	**4.10**	**0.28**	**0.01**	**0.00**	**0.02**
Magnetite	*Std.*	*5.73*	*0.08*	*14.01*	*0.68*	*0.03*	*0.00*	*0.21*	*0.01*	*0.01*	*0.74*	*0.03*	*0.00*	*0.00*	*0.01*
TA1-5_mt1.d		*248.79*	*8.52*	*444.66*	*45.20*	*0.86*	*0.03*	*4.62*	*0.07*	*0.22*	*4.34*	*0.25*	*0.00*	*0.00*	*0.09*
TA1-5_mt1.d		*256.94*	*0.30*	*291.37*	*45.01*	*0.86*	*0.01*	*5.13*	*0.07*	*0.16*	*4.52*	*0.22*	*0.00*	*0.00*	*0.08*
TA1-5_mt2.d		268.13	0.50	352.20	46.29	1.16	0.00	5.29	0.09	0.16	4.19	0.26	0.00	0.00	0.04
TA1-5_mt3.d		266.55	0.50	395.39	46.78	0.91	0.02	5.15	0.07	0.17	3.95	0.25	0.01	0.01	0.06
TA1-5_mt4.d		270.44	0.29	291.37	45.07	0.85	0.00	5.61	0.07	0.18	3.50	0.26	0.01	0.00	0.06
TA1-5_mt5.d		285.29	0.68	313.27	45.99	0.89	0.00	4.82	0.06	0.18	4.34	0.22	0.01	0.01	0.14
TA1-5	**Avg.**	**269.16**	**0.77**	**334.63**	**45.84**	**0.94**	**0.01**	**5.18**	**0.07**	**0.17**	**4.09**	**0.24**	**0.00**	**0.00**	**0.08**
Magnetite	*Std.*	*9.59*	*0.57*	*36.10*	*0.68*	*0.11*	*0.01*	*0.26*	*0.01*	*0.01*	*0.34*	*0.02*	*0.00*	*0.00*	*0.03*
TA1-6_mt1.d		*261.14*	*0.49*	*241.24*	*43.30*	*0.73*	*0.00*	*5.37*	*0.06*	*0.12*	*4.35*	*0.25*	*0.01*	*0.00*	*0.07*
TA1-6_mt1.d		*251.49*	*5.79*	*237.62*	*43.06*	*1.27*	*0.00*	*5.66*	*0.17*	*0.18*	*3.98*	*0.22*	*0.01*	*0.03*	*0.07*
TA1-6_mt2.d		269.59	0.57	290.09	45.11	0.83	0.00	4.81	0.08	0.20	3.87	0.22	0.01	0.00	0.04
TA1-6_mt3.d		297.33	1.16	319.04	46.50	0.88	0.00	4.92	0.07	0.18	4.01	0.22	0.01	0.00	0.03
TA1-6_mt4.d		295.52	27.14	346.78	44.87	0.87	0.01	5.52	0.07	0.13	4.02	0.26	0.01	0.00	0.04
TA1-6_mt5.d		281.65	0.50	281.65	43.42	0.84	0.00	5.58	0.07	0.17	3.92	0.26	0.01	0.00	0.06
TA1-6	**Avg.**	**279.63**	**6.75**	**295.23**	**44.61**	**0.91**	**0.00**	**5.28**	**0.09**	**0.17**	**3.98**	**0.24**	**0.01**	**0.00**	**0.05**
Magnetite	*Std.*	18.20	11.51	40.76	1.37	0.12	0.00	0.39	0.03	0.03	0.08	0.02	0.00	0.01	0.02
TA2-1_mt1.d		300.68	0.55	210.35	46.11	0.84	0.00	3.88	0.04	0.18	3.87	0.18	0.00	0.00	0.01
TA2-1_mt2.d		291.83	0.38	219.51	44.22	0.89	0.00	4.32	0.05	0.18	3.99	0.22	0.00	0.01	0.05
TA2-1_mt3.d		300.04	0.36	305.73	47.06	0.91	0.01	4.33	0.05	0.20	4.79	0.23	0.00	0.00	0.05
TA2-1_mt4.d		292.46	0.51	257.72	45.73	0.94	0.02	4.14	0.05	0.13	4.35	0.20	0.00	0.01	0.06
TA2-1_mt5.d		312.68	0.59	275.41	49.97	0.93	0.01	4.25	0.05	0.15	4.45	0.21	0.00	0.01	0.07
TA2-1	**Avg.**	**299.54**	**0.48**	**253.74**	**46.62**	**0.90**	**0.01**	**4.18**	**0.05**	**0.17**	**4.29**	**0.21**	**0.00**	**0.01**	**0.05**
Magnetite	*Std.*	*8.42*	*0.10*	*39.51*	*2.13*	*0.04*	*0.01*	*0.19*	*0.00*	*0.03*	*0.37*	*0.02*	*0.00*	*0.00*	*0.03*
TA2-3_mt1.d		279.52	0.29	277.26	46.84	0.85	0.00	5.09	0.04	0.17	4.82	0.22	0.00	0.00	0.03
TA2-3_mt2.d		292.47	0.28	254.62	46.90	0.96	0.00	4.72	0.04	0.15	4.82	0.24	0.00	0.00	0.03
TA2-3_mt3.d		271.98	0.24	289.20	46.21	0.88	0.00	5.14	0.04	0.14	4.65	0.23	0.00	0.00	0.13
TA2-3_mt4.d		277.51	0.24	247.08	45.64	0.87	0.00	4.95	0.04	0.14	5.22	0.24	0.00	0.00	0.07
TA2-3_mt5.d		286.44	0.22	217.78	46.02	0.94	0.00	4.82	0.04	0.14	4.66	0.24	0.00	0.00	0.83
TA2-3	**Avg.**	**281.58**	**0.25**	**257.19**	**46.32**	**0.90**	**0.00**	**4.94**	**0.04**	**0.15**	**4.83**	**0.23**	**0.00**	**0.00**	**0.22**
Magnetite	*Std.*	*7.99*	*0.03*	*27.79*	*0.54*	*0.05*	*0.00*	*0.18*	*0.00*	*0.01*	*0.23*	*0.01*	*0.00*	*0.00*	*0.35*
TA2-4_mt1.d		278.32	0.24	292.80	48.04	0.90	0.00	4.63	0.04	0.19	8.26	0.20	0.00	0.01	0.02
TA2-4_mt2.d		263.84	0.17	259.43	46.41	0.87	0.00	4.82	0.04	0.17	7.18	0.23	0.00	0.00	0.01
TA2-4_mt3.d		282.10	0.37	294.69	48.36	0.90	0.00	4.82	0.05	0.14	6.59	0.22	0.00	0.01	0.02

Analysis ID	Notes		Analysis Length (s)	Fe (wt%)	24Mg	27Al	29Si	31P	44Ca	45SC	47Ti	51V	52Cr	55Mn	59Co
TA2-4_mt4.d			49.8	**62.97**	4143.28	20004.9	573.64	32.11	-8.82	19.68	51381.7	6724.96	336.25	3154.69	195.45
TA2-4_mt5.d			49.8	**62.97**	3740.29	18323.6	533.34	29.59	0.63	19.45	49555.7	6964.24	390.40	3091.72	198.35
TA2-4		**Avg.**		**62.97**	**3940.53**	**20118.2**	**586.86**	**30.22**	**-1.26**	**18.65**	**50714.3**	**6848.38**	**361.81**	**2755.97**	**204.39**
Magnetite		*Std.*		**62.97**	*152.26*	*1118.8*	*38.71*	*8.47*	*8.53*	*1.25*	*789.7*	*159.83*	*19.83*	*336.41*	*6.94*
TA2-6_mt1.d			48.8	**62.89**	4452.6	21068.2	520.7	45.9	1.3	19.5	58110.5	6603.5	299.0	1851.5	165.3
TA2-6_mt2.d			48.8	**62.89**	4377.2	20250.6	624.5	45.9	14.5	18.0	57984.7	6842.4	290.6	2715.6	185.5
TA2-6_mt3.d			48.8	**62.89**	3792.3	20200.3	532.7	66.7	0.6	16.4	57041.3	6943.1	290.2	2367.8	190.0
TA2-6_mt4.d			48.8	**62.89**	4075.3	20571.4	533.9	29.6	17.6	19.6	58299.1	6729.2	282.6	2654.0	205.2
TA2-6_mt5.d			48.8	**62.89**	4440.0	21319.7	615.1	57.2	1.9	15.4	59116.7	6911.6	301.8	1915.6	178.7
TA2-6_mt6.d			48.8	**62.89**	3584.7	21822.9	558.5	52.8	8.2	14.4	56035.1	7068.8	298.9	2710.6	207.6
TA2-6		**Avg.**		**62.89**	**4120.35**	**20872.2**	**564.23**	**49.68**	**7.34**	**17.22**	**57764.6**	**6849.78**	**293.85**	**2369.18**	**188.71**
Magnetite		*Std.*		**62.89**	*367.45*	*643.6*	*44.84*	*12.56*	*7.33*	*2.15*	*1076.7*	*164.79*	*7.30*	*397.83*	*16.07*

Analysis ID		60Ni	63Cu	66Zn	69Ga	74Ge	89Y	90Zr	93Nb	95Mo	118Sn	178Hf	181Ta	182W	208Pb
TA2-4_mt4.d		273.28	0.37	292.80	45.53	0.89	0.00	4.76	0.03	0.15	7.76	0.22	0.00	0.00	0.04
TA2-4_mt5.d		301.62	0.46	254.39	48.67	0.91	0.00	4.18	0.03	0.14	4.61	0.23	0.00	0.00	0.05
TA2-4	**Avg.**	**279.83**	**0.32**	**278.82**	**47.40**	**0.89**	**0.00**	**4.64**	**0.04**	**0.16**	**6.88**	**0.22**	**0.00**	**0.00**	**0.03**
Magnetite	*Std.*	*13.97*	*0.11*	*20.10*	*1.37*	*0.01*	*0.00*	*0.27*	*0.01*	*0.02*	*1.41*	*0.01*	*0.00*	*0.00*	*0.02*
TA2-6_mt1.d		244.3	0.2	322.6	46.1	0.8	0.0	4.9	0.0	0.2	6.2	0.2	0.0	0.0	0.0
TA2-6_mt2.d		283.0	0.5	484.3	48.2	0.9	0.0	4.2	0.0	0.2	5.9	0.2	0.0	0.0	0.1
TA2-6_mt3.d		286.8	0.4	259.1	47.0	0.9	0.0	4.5	0.0	0.2	5.4	0.2	0.0	0.0	0.1
TA2-6_mt4.d		279.7	0.2	281.4	47.0	0.9	0.0	4.7	0.0	0.1	5.5	0.2	0.0	0.0	0.2
TA2-6_mt5.d		263.9	0.4	373.6	46.9	1.0	0.0	4.1	0.0	0.1	5.3	0.2	0.0	0.0	0.1
TA2-6_mt6.d		281.7	0.4	430.2	48.2	0.9	0.0	3.8	0.0	0.2	4.8	0.2	0.0	0.0	0.1
TA2-6	**Avg.**	**273.25**	**0.35**	**358.52**	**47.23**	**0.91**	**0.00**	**4.37**	**0.04**	**0.16**	**5.52**	**0.20**	**0.00**	**0.00**	**0.10**
Magnetite	*Std.*	*16.25*	*0.12*	*87.51*	*0.81*	*0.06*	*0.00*	*0.43*	*0.01*	*0.02*	*0.50*	*0.02*	*0.00*	*0.00*	*0.05*

Source file	Notes	Analysis Length (s)	Fe (wt%)	24Mg	27Al	29Si	31P	44Ca	45SC	47Ti	51V	52Cr	55Mn	59Co
14-2A-ILM-1-1.D		49.9	**33.02**	4093.49	197.79	74.63	0.63	6.27	66.57	279316	546.81	20.27	5511.0	94.01
14-2A-ILM-1-2.D		49.9	**33.02**	4375.15	212.98	729.74	1.42	6.93	64.85	281363	528.65	16.68	5550.7	93.74
14-2A-ILM-3.D		49.9	**33.02**	2329.56	180.62	53.49	1.32	6.93	48.04	276047	573.56	23.61	5841.2	90.05
14-2A-ILM-5.D		49.9	**33.02**	3543.05	172.36	72.31	3.63	79.25	56.99	274991	556.06	18.43	5316.2	102.03
14-2A-ILM-4.D		49.9	**33.02**	3203.27	154.20	104.01	5.88	10.57	51.48	282057	559.69	21.50	5006.8	103.42
MA-14-2A	**Avg.**		**33.02**	**3508.90**	**183.59**	**206.84**	**2.58**	**21.99**	**57.59**	**278755**	**552.95**	**20.10**	**5445.2**	**96.65**
Ilmenite	*Std.*		***33.02***	*717.99*	*20.32*	*261.95*	*1.94*	*28.67*	*7.24*	*2812*	*14.89*	*2.40*	*276.1*	*5.17*
14-2D-ILM-1.D		49.9	**32.39**	3951.58	265.60	174.91	-3.56	1.94	71.39	272724	376.05	26.88	5726.6	61.83
14-2D-ILM-4.D		49.9	**32.39**	4456.86	524.72	119.20	10.04	5.18	73.07	271104	482.61	50.53	5146.8	91.53
14-2D-ILM-5.D		49.9	**32.39**	2409.82	136.14	101.38	-8.75	5.51	77.64	269809	370.22	20.86	5318.4	83.18
MA-14-2D	**Avg.**		**32.39**	**3606.09**	**308.82**	**131.83**	**-0.76**	**4.21**	**74.03**	**271212**	**409.63**	**32.76**	**5397.3**	**78.85**
Ilmenite	*Std.*		***32.39***	*870.68*	*161.56*	*31.32*	*7.92*	*1.61*	*2.64*	*1193*	*51.66*	*12.80*	*243.2*	*12.51*
14-3A-ILM-1-1.D		49.9	**33.02**	822.86	52.24	72.97	0.99	-0.03	49.83	270863	650.82	55.24	10057.9	60.62
14-3A-ILM-1-2.D		49.9	**33.02**	1099.90	28.13	85.85	3.37	3.47	47.22	273141	480.11	35.33	10183.4	65.51
14-3A-ILM-2.D		49.9	**33.02**	1001.50	145.62	144.63	5.61	7.26	40.58	272349	554.08	52.77	10437.6	66.01
14-3A-ILM-6.D		49.9	**33.02**	739.98	106.32	136.37	-4.19	168.40	44.91	271722	654.46	56.99	9922.5	46.59
14-3A-ILM-8.D		49.9	**33.02**	416.05	69.57	93.78	5.42	8.98	26.12	277599	709.27	55.84	11012.2	34.24
MA-14-3A	**Avg.**		**33.02**	**816.06**	**80.38**	**106.72**	**2.24**	**37.62**	**41.73**	**273135**	**609.75**	**51.23**	**10322.7**	**54.60**
Ilmenite	*Std.*		***33.02***	*236.98*	*41.39*	*28.49*	*3.62*	*65.47*	*8.38*	*2354*	*81.85*	*8.07*	*384.3*	*12.36*
14-3B-T-ILM-2-1.D		49.9	**32.95**	228.21	38.55	82.70	3.30	6.10	22.08	276121	730.17	70.74	9285.3	37.33
14-3B-T-ILM-2-2.D		49.9	**32.95**	331.81	197.04	58.32	1.58	5.07	22.87	279087	880.09	82.38	9608.2	54.83
14-3B-T-ILM-3.D		49.9	**32.95**	707.11	117.63	95.23	7.91	3.62	15.65	276352	528.85	41.39	8840.5	78.55
14-3B-T-ILM-6.D		49.9	**32.95**	658.01	263.60	90.61	-0.33	5.93	20.00	259976	678.77	52.95	8590.1	66.49
14-3B-T-ILM-7.D		49.9	**32.95**	709.41	79.08	131.14	2.31	3.95	21.88	255824	683.05	51.11	8102.4	55.88
MA-14-3B-T	**Avg.**		**32.95**	**526.91**	**139.18**	**91.60**	**2.95**	**4.94**	**20.49**	**269472**	**700.19**	**59.71**	**8885.3**	**58.62**
Ilmenite	*Std.*		***32.95***	*205.06*	*81.28*	*23.51*	*2.75*	*1.00*	*2.60*	*9596*	*112.58*	*14.77*	*526.3*	*13.67*
MA14-3Bb_ilm1.d		36.0	**33.66**	331.17	33.32	461.08	17.50	54.86	5.10	257798	1975.56	636.08	7757.5	25.88
MA14-3Bb_ilm2.d		49.8	**33.66**	281.36	12.22	484.63	23.22	-2.02	6.90	246019	1797.18	520.98	8006.6	24.74
MA14-3Bb_ilm3.d		49.8	**33.66**	318.71	11.38	441.22	19.18	31.64	6.35	235249	1050.04	222.46	8279.2	25.01
MA14-3Bb_ilm4.d		49.8	**33.66**	367.51	20.73	484.63	27.93	-3.37	10.02	259144	1383.23	642.14	7865.2	35.47
MA14-3Bb_ilm5.d		49.8	**33.66**	380.98	16.89	450.98	23.22	117.79	5.21	252750	771.38	409.58	8339.7	33.89
MA14-3B-B	**Avg.**		**33.66**	**335.95**	**18.91**	**464.51**	**22.21**	**39.78**	**6.72**	**250192**	**1395.48**	**486.25**	**8049.6**	**29.00**
Ilmenite	*Std.*		*33.66*	*39.76*	*8.90*	*19.67*	*4.07*	*49.97*	*2.00*	*9814*	*501.71*	*175.66*	*254.0*	*5.24*
14-4-ILM-5.D		49.9	**33.75**	319.28	260.21	168.75	1.35	9.18	30.44	263959	683.44	18.12	7182.0	12.71
14-4-ILM-6.D		49.9	**33.75**	368.21	229.50	87.41	2.36	4.93	33.45	262103	637.20	17.18	7161.8	19.02
14-4-ILM-9.D		49.9	**33.75**	297.68	121.50	89.78	4.42	6.38	29.43	269156	575.10	18.29	7425.0	15.57
14-4-ILM-10.D		49.9	**33.75**	176.11	249.75	172.13	2.40	155.25	33.89	261968	776.25	23.39	6645.4	12.52
MA-14-4a	**Avg.**		**33.75**	**290.32**	**215.24**	**129.52**	**2.63**	**43.93**	**31.80**	**264296**	**668.00**	**19.25**	**7103.5**	**14.95**
Ilmenite	*Std.*		***33.75***	*70.72*	*55.24*	*40.95*	*1.12*	*64.29*	*1.91*	*2914*	*73.37*	*2.43*	*284.1*	*2.64*
14-4-ILM-1.D		49.9	**33.31**	284.13	25.88	82.94	5.00	6.16	16.16	252490	1878.68	54.26	6895.2	20.00

Source file		60Ni	63Cu	66Zn	69Ga	74Ge	89Y	90Zr	93Nb	95Mo	118Sn	178Hf	181Ta	182W	208Pb
14-2A-ILM-1-1.D		41.08	0.98	25.26	0.73	0.05	0.15	71.95	32.76	0.52	0.44	3.03	2.46	0.28	0.01
14-2A-ILM-1-2.D		34.57	0.46	21.10	0.45	0.09	0.21	80.14	36.45	0.51	0.43	4.03	2.67	0.15	0.01
14-2A-ILM-3.D		41.90	1.30	41.64	0.59	0.07	0.09	61.91	31.53	0.53	0.33	3.11	2.45	0.30	0.01
14-2A-ILM-5.D		43.92	1.14	29.39	0.54	0.07	0.19	75.02	35.76	0.45	0.43	3.56	2.68	0.15	0.00
14-2A-ILM-4.D		38.01	0.60	29.09	0.38	0.06	0.16	69.61	34.84	0.53	0.37	3.78	2.67	0.23	0.01
MA-14-2A	**Avg.**	**39.89**	**0.90**	**29.30**	**0.54**	**0.07**	**0.16**	**71.73**	**34.27**	**0.51**	**0.40**	**3.50**	**2.59**	**0.22**	**0.01**
Ilmenite	*Std.*	*3.27*	*0.32*	*6.87*	*0.12*	*0.01*	*0.04*	*6.04*	*1.85*	*0.03*	*0.04*	*0.38*	*0.11*	*0.06*	*0.00*
14-2D-ILM-1.D		34.01	1.36	18.04	0.63	0.04	0.15	136.04	21.70	0.48	0.20	3.72	1.59	0.05	0.01
14-2D-ILM-4.D		40.88	1.43	21.05	1.23	0.10	0.18	135.71	21.96	0.46	0.26	3.64	1.61	0.07	0.01
14-2D-ILM-5.D		31.39	0.97	7.94	0.33	0.08	0.15	138.56	23.26	0.41	0.22	3.88	1.84	0.06	0.00
MA-14-2D	**Avg.**	**35.42**	**1.25**	**15.68**	**0.73**	**0.07**	**0.16**	**136.77**	**22.31**	**0.45**	**0.22**	**3.75**	**1.68**	**0.06**	**0.01**
Ilmenite	*Std.*	*4.00*	*0.20*	*5.61*	*0.38*	*0.03*	*0.01*	*1.27*	*0.68*	*0.03*	*0.02*	*0.10*	*0.11*	*0.01*	*0.01*
14-3A-ILM-1-1.D		25.33	0.58	37.21	1.11	0.02	0.23	80.24	20.49	0.65	0.37	2.51	1.39	0.05	0.03
14-3A-ILM-1-2.D		17.24	0.88	31.93	0.78	0.07	0.21	77.76	26.45	0.79	0.28	2.71	1.97	0.12	0.01
14-3A-ILM-2.D		31.27	0.54	32.10	1.17	0.10	0.22	75.45	22.85	0.79	0.32	2.77	1.60	0.04	0.01
14-3A-ILM-6.D		21.63	0.75	26.94	0.93	0.05	0.22	74.30	17.83	0.74	0.35	2.09	1.17	0.06	0.03
14-3A-ILM-8.D		13.77	0.68	45.60	1.12	0.07	0.38	69.94	11.69	0.75	0.36	1.97	0.56	0.03	0.01
MA-14-3A	**Avg.**	**21.85**	**0.69**	**34.76**	**1.02**	**0.06**	**0.25**	**75.54**	**19.86**	**0.74**	**0.34**	**2.41**	**1.34**	**0.06**	**0.02**
Ilmenite	*Std.*	*6.12*	*0.12*	*6.32*	*0.15*	*0.02*	*0.06*	*3.46*	*4.97*	*0.05*	*0.03*	*0.32*	*0.47*	*0.03*	*0.01*
14-3B-T-ILM-2-1.D		21.19	1.01	23.69	1.13	0.05	0.13	31.27	17.86	0.81	0.21	1.02	1.30	0.18	0.00
14-3B-T-ILM-2-2.D		21.35	2.36	32.95	1.37	0.01	0.16	37.27	16.48	0.84	0.28	1.64	0.99	0.14	0.00
14-3B-T-ILM-3.D		24.71	1.23	33.77	1.33	0.04	0.11	43.72	27.15	0.78	0.32	2.58	1.86	0.11	0.00
14-3B-T-ILM-6.D		26.82	0.58	34.73	1.42	0.01	0.09	36.15	17.04	0.69	0.32	1.63	1.10	0.05	0.00
14-3B-T-ILM-7.D		20.46	0.45	33.54	1.75	0.01	0.38	23.07	19.41	0.67	0.38	1.37	1.41	0.13	0.01
MA-14-3B-T	**Avg.**	**22.91**	**1.13**	**31.74**	**1.40**	**0.02**	**0.17**	**34.29**	**19.58**	**0.76**	**0.30**	**1.65**	**1.33**	**0.12**	**0.00**
Ilmenite	*Std.*	*2.45*	*0.68*	*4.06*	*0.20*	*0.02*	*0.11*	*6.88*	*3.91*	*0.07*	*0.05*	*0.52*	*0.30*	*0.04*	*0.00*
MA14-3Bb_ilm1.d		4.51	2.79	37.39	0.37	0.06	0.01	8.82	31.03	0.38	2.19	0.54	1.94	0.38	0.04
MA14-3Bb_ilm2.d		5.69	3.49	49.07	0.19	0.11	0.01	6.60	40.99	0.36	2.74	0.46	2.55	0.22	0.01
MA14-3Bb_ilm3.d		8.75	4.58	58.56	0.24	0.07	0.01	6.73	48.03	0.39	2.34	0.42	2.88	0.29	0.04
MA14-3Bb_ilm4.d		12.49	2.40	55.97	0.15	0.08	0.00	5.55	48.53	0.71	2.62	0.30	2.71	0.51	0.03
MA14-3Bb_ilm5.d		12.55	3.30	60.14	0.13	0.09	0.01	4.75	25.81	0.64	2.15	0.24	1.46	0.69	0.05
MA14-3B-B	**Avg.**	**8.80**	**3.31**	**52.23**	**0.22**	**0.08**	**0.01**	**6.49**	**38.88**	**0.50**	**2.41**	**0.39**	**2.31**	**0.42**	**0.04**
Ilmenite	*Std.*	*3.73*	*0.83*	*9.31*	*0.09*	*0.02*	*0.00*	*1.53*	*10.17*	*0.17*	*0.26*	*0.12*	*0.59*	*0.19*	*0.02*
14-4-ILM-5.D		4.69	0.53	37.97	2.79	0.11	0.10	12.25	62.64	1.11	0.72	1.18	4.59	0.20	0.04
14-4-ILM-6.D		5.91	0.89	42.80	2.66	0.13	0.12	11.75	55.22	1.15	0.81	1.36	3.40	0.16	0.01
14-4-ILM-9.D		4.55	0.76	43.23	2.78	0.05	0.09	16.54	63.05	0.99	0.76	1.74	4.31	0.19	0.02
14-4-ILM-10.D		4.09	0.49	30.31	2.73	0.03	0.19	15.66	48.36	0.97	0.77	1.00	3.69	0.39	0.03
MA-14-4a	**Avg.**	**4.81**	**0.67**	**38.58**	**2.74**	**0.08**	**0.13**	**14.05**	**57.32**	**1.06**	**0.76**	**1.32**	**4.00**	**0.24**	**0.03**
Ilmenite	*Std.*	*0.67*	*0.16*	*5.20*	*0.05*	*0.04*	*0.04*	*2.08*	*6.04*	*0.08*	*0.03*	*0.28*	*0.47*	*0.09*	*0.01*
14-4-ILM-1.D		4.03	0.56	33.84	1.26	0.12	0.08	7.89	51.20	1.19	0.44	0.56	2.93	0.79	0.02

Source file	Notes	Analysis Length (s)	Fe (wt%)	24Mg	27Al	29Si	31P	44Ca	45SC	47Ti	51V	52Cr	55Mn	59Co
14-4-ILM-2.D		49.9	**33.31**	259.48	93.93	89.27	7.99	16.32	13.66	253456	1562.24	66.52	6998.4	13.60
14-4-ILM-3.D		49.9	**33.31**	224.51	47.97	85.94	5.66	21.32	10.90	254488	1598.88	89.94	6881.8	18.42
14-4-ILM-4.D		49.9	**33.31**	177.88	46.97	179.87	2.33	153.23	11.31	248259	1189.83	59.89	6821.9	8.32
MA-14-4b	**Avg.**		**33.31**	**236.50**	**53.69**	**109.51**	**5.25**	**49.26**	**13.00**	**252173**	**1557.41**	**67.65**	**6899.3**	**15.09**
Ilmenite	*Std.*		***33.31***	*39.93*	*24.85*	*40.69*	*2.02*	*60.27*	*2.10*	*2368*	*244.99*	*13.58*	*63.5*	*4.56*
14-5A-ILM-1.D		49.9	**34.36**	766.89	41.85	126.44	5.50	7.22	22.26	251678	1196.03	34.46	9778.5	85.28
14-5A-ILM-2.D		48.1	**34.36**	704.01	42.67	68.37	0.69	8.93	23.88	252846	1242.41	37.97	9823.2	99.16
14-5A-ILM-5.D		49.9	**34.36**	811.90	83.84	73.18	2.37	18.55	28.93	255869	1098.45	32.85	10080.8	90.74
14-5A-ILM-6.D		49.9	**34.36**	725.66	63.84	80.06	3.78	5.15	25.22	248792	1105.66	25.94	9819.7	99.26
14-5A-ILM-7.D		49.9	**34.36**	956.89	48.03	47.76	-3.40	-0.34	22.33	253086	967.54	30.58	9696.0	78.85
MA-14-5A	**Avg.**		**34.36**	**793.07**	**56.05**	**79.16**	**1.79**	**7.90**	**24.53**	**252454**	**1122.02**	**32.36**	**9839.7**	**90.66**
Ilmenite	*Std.*		***34.36***	*89.84*	*15.98*	*25.98*	*3.04*	*6.17*	*2.46*	*2291*	*94.51*	*4.01*	*129.0*	*7.93*
14-5C-ILM-2.D		49.9	**35.18**	700.11	439.77	700.11	4.57	56.29	22.66	255840	1390.38	60.93	7616.8	36.03
14-5C-ILM-3.D		49.9	**35.18**	439.42	29.97	66.14	0.95	9.11	12.60	266465	1223.97	64.28	8320.4	58.72
14-5C-ILM-4.D		43.7	**35.18**	394.74	100.62	394.03	5.73	429.22	18.12	263967	1634.18	63.29	7662.5	55.16
MA-14-5C-a	**Avg.**		**35.18**	**511.42**	**190.12**	**386.76**	**3.75**	**164.87**	**17.79**	**262091**	**1416.18**	**62.83**	**7866.6**	**49.97**
Ilmenite	*Std.*		***35.18***	*134.67*	*178.87*	*258.87*	*2.04*	*187.91*	*4.11*	*4536*	*168.46*	*1.40*	*321.5*	*9.97*
14-5C-ILM-8.D		35.6	**34.89**	345.44	170.98	251.23	3.49	97.70	6.44	264734	2065.67	247.39	11424.0	45.64
MA-14-5C-b	**Avg.**		**34.89**	**345.44**	**170.98**	**251.23**	**3.49**	**97.70**	**6.44**	**264734**	**2065.67**	**247.39**	**11424.0**	**45.64**
Ilmenite	*Std.*			*0.00*	*0.00*	*0.00*	*0.00*	*0.00*	*0.00*	*0*	*0.00*	*0.00*	*0.0*	*0.00*
14-6AT-ILM-2.D		42.6	**34.90**	1543.78	98.43	91.80	4.19	4.89	13.72	271619	994.05	65.30	6764.3	76.51
14-6AT-ILM-4.D		49.9	**34.90**	662.12	534.02	114.83	4.12	39.44	23.63	271410	1093.18	58.88	7250.2	69.28
14-6AT-ILM-5.D		49.9	**34.90**	716.92	255.49	84.47	2.16	21.64	20.03	270328	1049.90	57.49	7130.8	64.29
MA-14-6A-T	**Avg.**		**34.90**	**974.27**	**295.98**	**97.03**	**3.49**	**21.99**	**19.13**	**271119**	**1045.71**	**60.56**	**7048.4**	**70.03**
Ilmenite	*Std.*		***34.90***	*403.33*	*180.12*	*12.94*	*0.94*	*14.11*	*4.10*	*566*	*40.58*	*3.40*	*206.7*	*5.01*
14-6B-ILM-1-2.D		49.9	**33.99**	486.04	19.17	80.21	2.04	16.31	32.05	279390	1033.27	77.67	12827.5	62.85
14-6B-ILM-3-1.D		49.9	**33.99**	536.69	190.00	62.88	5.54	5.10	28.41	260696	911.25	37.90	8922.1	68.42
14-6B-ILM-3-2.D		49.9	**33.99**	726.69	142.07	61.18	2.38	108.77	29.33	268956	758.64	32.77	9095.5	78.24
14-6B-ILM-4.D		49.9	**33.99**	528.53	42.11	86.67	2.86	-0.68	22.60	264129	828.65	42.69	8752.2	76.14
14-6B-ILM-5.D		49.9	**33.99**	459.87	83.31	68.32	0.37	7.48	23.55	267494	929.60	43.78	9245.0	72.36
MA-14-6B-a	**Avg.**		**33.99**	**547.56**	**95.33**	**71.85**	**2.64**	**27.40**	**27.19**	**268133**	**892.28**	**46.96**	**9768.5**	**71.60**
Ilmenite	*Std.*		***33.99***	*93.85*	*63.13*	*9.96*	*1.67*	*41.05*	*3.58*	*6311*	*93.32*	*15.84*	*1538.4*	*5.51*
14-68-ILM-7.D		44.8	**33.23**	551.63	229.29	299.08	-0.07	12.96	9.23	279338	3798.28	339.29	11664.0	25.29
14-6B-ILM-8.D		*8.3*	***33.23***	*805.18*	*70.12*	*432.00*	*5.32*	*535.02*	*11.46*	*291335*	*2302.90*	*175.79*	*10185.2*	*44.10*
14-6B-ILM-8.D		*21.2*	***33.23***	*1365.79*	*505.11*	*687.88*	*6.65*	*146.22*	*11.90*	*286250*	*2675.08*	*210.02*	*10268.3*	*43.60*
14-6B-ILM-9.D		49.9	**33.23**	991.61	64.80	139.57	3.69	46.52	13.81	285320	2495.63	171.01	10191.9	37.38
14-6B-ILM-10		49.9	**33.23**	942.09	18.61	80.75	1.00	14.29	13.99	290504	2758.16	222.98	10577.4	53.80
MA-14-6B-b	**Avg.**		**33.23**	**923.34**	**173.85**	**283.82**	**2.72**	**82.35**	**12.20**	**285711**	**2905.61**	**233.41**	**10669.6**	**40.05**
Ilmenite	*Std.*		***33.23***	*236.76*	*143.77*	*207.69*	*2.46*	*100.94*	*1.92*	*4111*	*524.19*	*63.84*	*592.9*	*10.34*
14-7A-ILM-7.D		49.9	**34.37**	443.31	17.73	95.19	0.34	65.29	8.16	258665	1105.18	84.61	9680.6	70.07

Source file		60Ni	63Cu	66Zn	69Ga	74Ge	89Y	90Zr	93Nb	95Mo	118Sn	178Hf	181Ta	182W	208Pb
14-4-ILM-2.D		5.40	0.64	38.51	1.35	0.07	0.07	8.96	52.46	1.34	0.39	0.78	3.31	0.31	0.02
14-4-ILM-3.D		3.16	0.65	32.51	0.73	0.05	0.07	6.16	52.10	1.01	0.42	0.61	3.36	0.27	0.01
14-4-ILM-4.D		4.86	0.60	39.11	1.01	0.07	0.12	8.93	53.63	1.14	0.35	0.78	3.67	1.08	0.01
MA-14-4b	**Avg.**	**4.36**	**0.61**	**35.99**	**1.09**	**0.08**	**0.08**	**7.99**	**52.35**	**1.17**	**0.40**	**0.68**	**3.32**	**0.61**	**0.01**
Ilmenite	*Std.*	*0.85*	*0.04*	*2.86*	*0.24*	*0.03*	*0.02*	*1.14*	*0.87*	*0.12*	*0.04*	*0.10*	*0.26*	*0.34*	*0.00*
14-5A-ILM-1.D		34.91	0.70	42.06	3.37	0.14	0.09	9.83	11.17	0.82	0.32	0.48	0.86	0.22	0.01
14-5A-ILM-2.D		38.79	0.87	50.68	3.58	0.03	0.09	9.96	13.21	0.79	0.32	0.50	1.14	0.09	0.01
14-5A-ILM-5.D		33.22	1.64	48.14	2.96	0.09	0.08	9.93	15.15	0.77	0.24	0.42	1.17	0.08	0.01
14-5A-ILM-6.D		43.19	1.05	73.53	3.30	0.10	0.08	12.82	15.44	0.92	0.30	0.59	1.30	0.15	0.00
14-5A-ILM-7.D		25.18	0.96	59.06	3.34	0.02	0.06	10.99	15.60	0.69	0.40	0.47	1.38	0.18	0.01
MA-14-5A	**Avg.**	**35.06**	**1.05**	**54.69**	**3.31**	**0.07**	**0.08**	**10.71**	**14.11**	**0.80**	**0.32**	**0.49**	**1.17**	**0.15**	**0.01**
Ilmenite	*Std.*	*6.02*	*0.32*	*10.89*	*0.20*	*0.04*	*0.01*	*1.14*	*1.71*	*0.07*	*0.05*	*0.06*	*0.18*	*0.05*	*0.01*
14-5C-ILM-2.D		15.94	0.95	51.29	1.69	0.17	0.10	10.55	17.70	0.63	0.25	0.35	1.59	0.13	0.02
14-5C-ILM-3.D		23.43	1.85	89.85	2.09	0.06	0.06	3.10	22.48	0.65	0.21	0.27	1.91	0.06	0.01
14-5C-ILM-4.D		19.88	0.84	75.99	1.06	0.07	0.06	6.05	25.22	0.58	0.22	0.42	2.62	0.09	0.02
MA-14-5C-a	**Avg.**	**19.75**	**1.21**	**72.38**	**1.61**	**0.10**	**0.08**	**6.57**	**21.80**	**0.62**	**0.23**	**0.35**	**2.04**	**0.09**	**0.02**
Ilmenite	*Std.*	*3.06*	*0.45*	*15.95*	*0.42*	*0.05*	*0.02*	*3.07*	*3.11*	*0.03*	*0.02*	*0.06*	*0.43*	*0.03*	*0.00*
14-5C-ILM-8.D		12.28	0.69	65.60	0.38	0.03	0.06	1.62	46.09	1.33	0.22	0.16	4.17	0.32	0.07
MA-14-5C-b	**Avg.**	**12.28**	**0.69**	**65.60**	**0.38**	**0.03**	**0.06**	**1.62**	**46.09**	**1.33**	**0.22**	**0.16**	**4.17**	**0.32**	**0.07**
Ilmenite	*Std.*	*0.00*	*0.00*	*0.00*	*0.00*	*0.00*	*0.00*	*0.00*	*0.00*	*0.00*	*0.00*	*0.00*	*0.00*	*0.00*	*0.00*
14-6AT-ILM-2.D		22.65	1.64	51.34	2.92	0.11	0.09	9.56	24.12	0.57	0.16	0.45	1.91	0.30	0.01
14-6AT-ILM-4.D		27.15	0.61	41.95	2.09	0.02	0.09	15.92	6.86	0.71	0.22	0.57	0.49	2.30	0.01
14-6AT-ILM-5.D		22.86	1.31	44.19	2.29	0.17	0.08	11.97	16.21	0.49	0.17	0.49	1.02	0.15	0.00
MA-14-6A-T	**Avg.**	**24.22**	**1.19**	**45.83**	**2.44**	**0.10**	**0.09**	**12.48**	**15.73**	**0.59**	**0.18**	**0.50**	**1.14**	**0.92**	**0.01**
Ilmenite	*Std.*	*2.07*	*0.43*	*4.00*	*0.35*	*0.06*	*0.00*	*2.62*	*7.05*	*0.09*	*0.03*	*0.05*	*0.59*	*0.98*	*0.00*
14-6B-ILM-1-2.D		43.57	0.51	78.55	1.29	0.08	0.09	22.09	11.25	1.05	0.24	1.06	1.01	0.21	0.12
14-6B-ILM-3-1.D		20.05	1.40	36.67	2.60	0.06	0.16	16.08	10.67	0.65	0.29	0.60	0.71	1.12	0.01
14-6B-ILM-3-2.D		17.71	0.32	24.13	2.20	0.04	0.13	13.87	16.04	0.63	0.22	0.71	1.15	0.18	0.00
14-6B-ILM-4.D		19.24	0.82	27.33	2.32	0.07	0.13	12.37	14.60	0.59	0.23	0.53	0.90	0.21	0.01
14-6B-ILM-5.D		23.55	1.20	47.89	2.73	0.10	0.15	13.90	8.72	0.69	0.32	0.58	0.44	1.54	0.01
Ilmenite	**Avg.**	**24.83**	**0.85**	**42.91**	**2.23**	**0.07**	**0.13**	**15.66**	**12.26**	**0.72**	**0.26**	**0.69**	**0.84**	**0.65**	**0.03**
Ilmenite	*Std.*	*9.57*	*0.40*	*19.64*	*0.51*	*0.02*	*0.03*	*3.43*	*2.68*	*0.17*	*0.04*	*0.19*	*0.25*	*0.57*	*0.05*
14-68-ILM-7.D		11.50	0.62	48.82	0.25	0.10	0.07	2.91	31.00	0.87	0.10	0.24	2.54	0.43	0.02
14-6B-ILM-8.D		*9.37*	*1.56*	*39.41*	*0.08*	*-0.01*	*0.12*	*4.79*	*20.77*	*0.67*	*0.10*	*0.12*	*1.70*	*0.51*	*0.00*
14-6B-ILM-8.D		*16.68*	*0.70*	*41.27*	*0.48*	*-0.02*	*0.09*	*10.90*	*22.00*	*0.79*	*0.11*	*0.22*	*1.81*	*0.41*	*0.08*
14-6B-ILM-9.D		14.26	0.57	43.50	0.23	0.03	0.09	21.60	11.59	0.73	0.08	0.44	0.76	0.74	0.03
14-6B-ILM-10		17.84	0.78	57.02	0.18	0.02	0.07	7.03	17.21	0.70	0.07	0.21	1.81	1.05	0.04
MA-14-6B-b	**Avg.**	**14.56**	**0.73**	**47.52**	**0.26**	**0.03**	**0.08**	**10.18**	**20.37**	**0.77**	**0.09**	**0.27**	**1.72**	**0.66**	**0.04**
Ilmenite	*Std.*	*2.25*	*0.14*	*6.21*	*0.07*	*0.04*	*0.01*	*6.97*	*7.10*	*0.06*	*0.01*	*0.10*	*0.63*	*0.26*	*0.01*
14-7A-ILM-7.D		10.76	1.58	80.41	0.27	-0.07	0.07	3.01	11.66	0.84	0.22	0.23	1.19	0.13	0.02

Source file	Notes	Analysis Length (s)	Fe (wt%)	24Mg	27Al	29Si	31P	44Ca	45SC	47Ti	51V	52Cr	55Mn	59Co
14-7A-ILM-8.D		49.9	**34.37**	389.01	23.02	96.57	-5.81	10.65	12.63	254748	1019.95	39.86	9828.4	70.59
MA14-7A-a	**Avg.**		**34.37**	**416.16**	**20.38**	**95.88**	**-2.73**	**37.97**	**10.39**	**256707**	**1062.57**	**62.24**	**9754.5**	**70.33**
Ilmenite	*Std.*		***34.37***	*27.15*	*2.65*	*0.69*	*3.08*	*27.32*	*2.23*	*1959*	*42.61*	*22.37*	*73.9*	*0.26*
14-7A-ILM-1.D		49.9	**34.49**	589.69	11.97	114.49	2.76	5.86	46.90	263052	980.41	35.73	9731.7	116.18
14-7A-ILM-2.D		49.9	**34.49**	647.29	60.69	244.84	1.03	144.84	54.42	267604	1133.52	38.45	9562.7	114.04
14-7A-ILM-3.D		49.9	**34.49**	696.60	203.46	275.88	-2.76	52.07	53.83	266915	976.27	36.24	9907.6	116.46
14-7A-ILM-5-1.D		46.0	**34.49**	412.10	12.69	106.90	3.79	87.59	27.31	262742	1178.01	37.83	9800.7	88.87
14-7A-ILM-5-2.D		32.4	**34.49**	410.72	32.07	131.04	3.45	25.86	37.11	255879	1170.42	37.42	9604.1	96.66
MA-14-7A-b	**Avg.**		**34.49**	**551.28**	**64.18**	**174.63**	**1.66**	**63.25**	**43.91**	**263238**	**1087.73**	**37.13**	**9721.3**	**106.44**
Ilmenite	*Std.*		***34.49***	*119.11*	*71.86*	*71.11*	*2.40*	*49.12*	*10.39*	*4172*	*90.58*	*1.01*	*126.5*	*11.47*
14-7B-ILM-1-1.D		49.9	**33.82**	436.65	44.65	402.49	-1.35	2.71	36.06	256886	998.12	46.91	9845.9	95.85
14-7B-ILM-1-2.D		49.9	**33.82**	454.24	54.46	145.44	3.72	24.69	31.42	261283	1070.84	44.71	9785.0	98.15
14-7B-ILM-2.D		49.9	**33.82**	421.10	34.09	100.79	2.91	0.68	31.52	259016	1014.69	48.10	9805.3	104.41
14-7B-ILM-3.D		49.9	**33.82**	449.85	18.26	80.84	-0.71	10.49	19.26	262669	1354.61	67.95	9808.7	75.19
14-7B-ILM-4.D		49.9	**33.82**	396.41	15.96	68.32	7.10	5.21	23.81	260200	1170.28	58.01	9544.8	69.00
MA-14-7B-a	**Avg.**		**33.82**	**431.65**	**33.48**	**159.58**	**2.33**	**8.75**	**28.41**	**260011**	**1121.71**	**53.14**	**9757.9**	**88.52**
Ilmenite	*Std.*		***33.82***	*21.07*	*14.85*	*124.25*	*3.09*	*8.62*	*6.03*	*1974*	*131.09*	*8.70*	*108.3*	*13.84*
14-7B-ILM-6.D		49.9	**34.73**	642.59	468.92	767.63	-0.35	35.78	20.15	267248	2869.07	91.56	10264.1	73.32
14-7B-ILM-7.D		49.9	**34.73**	649.54	270.93	420.29	2.08	79.89	11.68	264330	2650.25	103.61	9902.8	58.70
14-7B-ILM-8.D		*19.8*	***34.73***	*788.47*	*448.08*	*687.74*	*5.56*	*250.09*	*13.03*	*267803*	*2282.06*	*109.62*	*10086.9*	*59.74*
14-7B-ILM-8.D		*15.0*	***34.73***	*541.16*	*114.62*	*197.99*	*5.21*	*114.97*	*12.08*	*267803*	*2337.63*	*117.75*	*10514.1*	*57.45*
MA-14-7B-b	**Avg.**		**34.73**	**657.95**	**347.99**	**554.75**	**2.38**	**102.48**	**14.81**	**266460**	**2608.46**	**102.77**	**10146.1**	**63.59**
Ilmenite	*Std.*		***34.73***	*17.04*	*86.57*	*152.26*	*2.36*	*65.65*	*3.79*	*1523*	*231.74*	*8.83*	*172.0*	*6.88*
14-8A-ILM-1.D		49.9	**32.13**	439.82	19.60	60.08	-1.93	35.66	5.88	266750	5651.13	526.88	14804.1	55.61
14-8A-ILM-2.D		49.9	**32.13**	922.04	103.13	452.99	5.14	87.71	14.26	285287	5397.33	542.95	19019.1	52.78
14-8A-ILM-3.D		49.9	**32.13**	472.27	111.16	469.05	2.51	263.44	5.20	282075	2448.07	600.45	16741.3	51.98
14-8A-ILM-4.D		49.9	**32.13**	596.60	46.91	289.14	-3.15	228.10	11.53	264501	4809.40	618.44	14710.9	70.17
MA-14-8A-a	**Avg.**		**32.13**	**607.68**	**70.20**	**317.82**	**0.64**	**153.73**	**9.22**	**274653**	**4576.48**	**572.18**	**16318.9**	**57.64**
Ilmenite	*Std.*		***32.13***	*190.70*	*38.29*	*164.62*	*3.34*	*94.69*	*3.81*	*9134*	*1266.20*	*38.23*	*1757.1*	*7.36*
14-8A-ILM-6.D		49.9	**33.58**	317.30	28.57	85.96	5.37	3.69	29.25	261023	650.38	67.72	13239.2	81.79
14-8A-ILM-7-1.D		48.4	**33.58**	889.78	742.04	1007.29	1.01	107.44	43.35	259244	849.82	74.81	12376.3	68.06
14-8A-ILM-7-2.D		49.9	**33.58**	295.47	144.38	184.67	-0.67	9.07	29.14	259042	862.91	94.58	12728.8	55.64
14-8A-ILM-8.D		*32.0*	***33.58***	*524.46*	*11.79*	*94.35*	*6.72*	*21.82*	*39.69*	*268612*	*833.03*	*71.42*	*13162.0*	*63.02*
14-8A-ILM-8.D		*10.8*	***33.58***	*520.43*	*8.63*	*90.66*	*1.01*	*19.14*	*39.12*	*266597*	*787.03*	*67.02*	*13497.7*	*61.91*
MA-14-8A-b	**Avg.**		**33.58**	**506.50**	**231.49**	**342.83**	**2.75**	**35.34**	**35.32**	**261853**	**796.13**	**76.86**	**12897.8**	**67.06**
Ilmenite	*Std.*		***33.58***	*238.49*	*299.18*	*385.59*	*2.64*	*42.11*	*6.27*	*3690*	*85.48*	*10.55*	*367.1*	*9.58*
14-8B-ILM-1-1.D		49.9	**33.11**	468.48	15.36	82.11	2.68	18.87	33.64	269269	956.16	71.18	11746.8	70.19
14-8B-ILM-2.D		46.5	**33.11**	517.48	56.62	70.52	3.97	20.86	31.12	266852	885.64	59.20	12074.6	73.86
14-8B-ILM-4.D		49.9	**33.11**	343.00	20.99	74.49	4.30	15.89	23.24	264601	855.18	74.79	12468.5	48.50
14-8B-ILM-5.D		49.9	**33.11**	473.45	15.66	64.23	2.32	13.91	29.53	263872	978.68	67.11	11412.4	65.82

Source file		60Ni	63Cu	66Zn	69Ga	74Ge	89Y	90Zr	93Nb	95Mo	118Sn	178Hf	181Ta	182W	208Pb
14-7A-ILM-8.D		9.55	1.64	95.19	0.23	0.02	0.08	1.38	14.41	0.87	0.23	0.13	1.35	0.14	0.02
MA14-7A-a	**Avg.**	**10.15**	**1.61**	**87.80**	**0.25**	**-0.02**	**0.08**	**2.19**	**13.04**	**0.85**	**0.22**	**0.18**	**1.27**	**0.13**	**0.02**
Ilmenite	*Std.*	*0.60*	*0.03*	*7.39*	*0.02*	*0.05*	*0.00*	*0.82*	*1.37*	*0.02*	*0.01*	*0.05*	*0.08*	*0.00*	*0.00*
14-7A-ILM-1.D		38.31	1.80	84.04	0.83	-0.01	0.11	8.97	11.97	0.71	0.37	0.59	0.96	0.03	0.09
14-7A-ILM-2.D		34.49	0.65	88.97	0.64	0.16	0.08	5.55	8.78	0.82	0.45	0.43	0.63	0.06	0.03
14-7A-ILM-3.D		38.38	1.04	80.56	1.30	0.06	0.13	9.76	11.53	0.79	0.28	0.53	0.78	0.02	0.04
14-7A-ILM-5-1.D		27.38	1.10	81.97	0.50	0.04	0.07	7.79	13.63	0.76	0.32	0.36	1.17	0.10	0.02
14-7A-ILM-5-2.D		32.35	1.87	88.80	0.74	0.04	0.08	2.03	12.59	0.93	0.40	0.28	1.03	0.13	0.02
MA-14-7A-b	**Avg.**	**34.18**	**1.29**	**84.87**	**0.80**	**0.06**	**0.09**	**6.82**	**11.70**	**0.80**	**0.36**	**0.44**	**0.91**	**0.07**	**0.04**
Ilmenite	*Std.*	*4.11*	*0.47*	*3.46*	*0.27*	*0.05*	*0.02*	*2.78*	*1.62*	*0.07*	*0.06*	*0.11*	*0.19*	*0.04*	*0.03*
14-7B-ILM-1-1.D		39.64	0.90	84.90	1.47	0.09	0.78	1251.45	8.83	0.82	0.32	27.73	0.76	0.07	0.05
14-7B-ILM-1-2.D		36.39	0.53	74.38	1.02	0.10	0.14	64.26	11.35	0.79	0.30	2.00	1.14	0.04	0.02
14-7B-ILM-2.D		46.41	0.44	72.89	2.29	0.08	0.09	8.39	10.41	0.72	0.24	0.47	0.90	0.01	1.25
14-7B-ILM-3.D		32.74	0.67	80.87	0.77	0.07	0.06	6.05	10.82	0.71	0.27	0.34	0.89	0.04	0.01
14-7B-ILM-4.D		35.68	0.56	77.45	0.52	0.11	0.07	4.06	12.84	0.75	0.22	0.30	1.19	0.04	0.01
MA-14-7B-a	**Avg.**	**38.17**	**0.62**	**78.10**	**1.21**	**0.09**	**0.23**	**266.84**	**10.85**	**0.76**	**0.27**	**6.17**	**0.98**	**0.04**	**0.27**
Ilmenite	*Std.*	*4.66*	*0.16*	*4.37*	*0.62*	*0.02*	*0.28*	*492.82*	*1.30*	*0.04*	*0.04*	*10.80*	*0.16*	*0.02*	*0.49*
14-7B-ILM-6.D		29.35	0.95	81.56	0.52	0.02	0.08	0.87	7.63	0.91	0.17	0.13	0.68	0.19	0.04
14-7B-ILM-7.D		23.27	1.05	89.23	0.29	0.13	0.08	3.20	12.28	0.80	0.17	0.18	1.15	0.08	0.03
14-7B-ILM-8.D		*25.29*	*1.29*	*91.66*	*0.37*	*0.00*	*0.07*	*1.34*	*12.71*	*0.84*	*0.13*	*0.19*	*1.25*	*0.22*	*0.06*
14-7B-ILM-8.D		*22.06*	*1.49*	*138.94*	*0.19*	*0.06*	*0.07*	*0.84*	*12.85*	*0.98*	*0.13*	*0.10*	*1.07*	*0.28*	*0.09*
MA-14-7B-b	**Avg.**	**25.51**	**1.13**	**94.29**	**0.37**	**0.06**	**0.08**	**1.73**	**10.89**	**0.87**	**0.15**	**0.16**	**1.00**	**0.17**	**0.05**
Ilmenite	*Std.*	*2.73*	*0.18*	*12.96*	*0.11*	*0.05*	*0.00*	*1.04*	*2.32*	*0.05*	*0.02*	*0.02*	*0.23*	*0.07*	*0.02*
14-8A-ILM-1.D		16.96	0.67	79.51	0.04	0.11	0.07	2.25	5.80	1.16	0.04	0.09	0.28	0.17	0.07
14-8A-ILM-2.D		49.57	0.98	78.55	0.13	0.11	0.08	2.07	7.26	1.53	0.06	0.11	0.72	0.17	0.11
14-8A-ILM-3.D		10.89	0.75	60.40	0.06	0.07	0.08	1.30	9.61	1.30	0.04	0.08	0.97	0.17	0.15
14-8A-ILM-4.D		25.03	1.05	63.96	0.12	0.05	0.07	3.66	7.26	1.01	0.07	0.22	0.45	0.25	0.09
MA-14-8A-a	**Avg.**	**25.61**	**0.86**	**70.61**	**0.09**	**0.09**	**0.08**	**2.32**	**7.48**	**1.25**	**0.05**	**0.13**	**0.61**	**0.19**	**0.11**
Ilmenite	*Std.*	*14.71*	*0.16*	*8.53*	*0.04*	*0.02*	*0.01*	*0.85*	*1.36*	*0.19*	*0.02*	*0.06*	*0.26*	*0.04*	*0.03*
14-8A-ILM-6.D		39.65	1.21	66.21	1.31	0.16	0.07	33.07	11.75	1.02	0.21	1.11	0.83	0.08	0.01
14-8A-ILM-7-1.D		39.96	1.55	69.94	0.81	0.05	0.12	11.82	16.12	1.11	0.29	0.59	1.30	0.21	0.02
14-8A-ILM-7-2.D		41.40	0.83	61.34	1.16	0.08	0.17	67.15	9.10	1.06	0.29	1.68	0.60	0.07	0.03
14-8A-ILM-8.D		*29.45*	*0.60*	*66.48*	*0.23*	*0.23*	*0.07*	*10.38*	*19.44*	*0.94*	*0.21*	*0.54*	*1.88*	*0.20*	*-0.04*
14-8A-ILM-8.D		*32.00*	*0.66*	*61.11*	*0.26*	*0.07*	*0.09*	*10.68*	*20.62*	*0.81*	*0.23*	*0.73*	*2.02*	*0.22*	*-0.07*
MA-14-8A-b	**Avg.**	**37.78**	**1.05**	**65.66**	**0.88**	**0.12**	**0.11**	**30.62**	**14.18**	**1.02**	**0.25**	**0.99**	**1.16**	**0.14**	**0.00**
Ilmenite	*Std.*	*4.48*	*0.36*	*3.06*	*0.41*	*0.06*	*0.04*	*22.92*	*4.07*	*0.08*	*0.03*	*0.45*	*0.50*	*0.07*	*0.03*
14-8B-ILM-1-1.D		44.83	0.71	81.71	1.67	0.10	0.08	22.68	12.90	1.00	0.21	1.02	1.19	0.13	0.02
14-8B-ILM-2.D		53.97	0.56	72.01	1.40	0.07	0.10	28.31	11.57	1.00	0.34	1.07	1.07	0.24	0.02
14-8B-ILM-4.D		45.49	1.06	77.37	1.66	0.05	0.11	25.26	7.85	1.28	0.30	0.95	0.86	0.64	0.02
14-8B-ILM-5.D		41.19	1.14	87.57	1.57	0.04	0.09	25.46	11.66	0.97	0.25	0.90	1.09	0.32	0.01

Source file	Notes	Analysis Length (s)	Fe (wt%)	24Mg	27Al	29Si	31P	44Ca	45SC	47Ti	51V	52Cr	55Mn	59Co
MA-14-8B	**Avg.**		**33.11**	**450.60**	**27.16**	**72.84**	**3.32**	**17.38**	**29.38**	**266149**	**918.92**	**68.07**	**11925.6**	**64.59**
Ilmenite	*Std.*		***33.11***	*64.99*	*17.15*	*6.48*	*0.84*	*2.67*	*3.84*	*2110*	*50.32*	*5.80*	*391.3*	*9.72*
MA15-1_ilm1.d		54.8	35.22	480.72	28.67	528.26	7.40	107.06	21.13	259904	1563.65	259.55	7994.3	77.83
MA15-1_ilm2.d		54.8	35.22	358.16	37.33	338.09	20.78	8.45	9.51	246521	2250.39	345.48	8008.4	61.17
MA15-1_ilm3.d		54.8	35.22	371.89	58.81	309.91	19.02	14.79	11.20	240886	2060.21	301.46	8240.8	75.01
MA15-1_ilm4.d		54.8	35.22	327.87	78.89	390.91	25.71	-4.58	6.16	222221	1257.26	176.79	8240.8	74.77
MA15-1_ilm5.d		54.8	35.22	351.82	38.32	309.91	13.73	-3.17	10.78	251452	1891.17	285.61	8054.2	67.55
MA15-1_ilm6.d		54.8	35.22	494.10	44.73	341.61	20.07	10.21	10.67	249338	1243.17	183.13	8064.8	90.65
MA15-1	**Avg.**		**35.22**	**397.43**	**47.79**	**369.78**	**17.78**	**22.13**	**11.57**	**245054**	**1710.97**	**258.67**	**8100.6**	**74.50**
Ilmenite	*Std.*		*35.22*	*65.06*	*16.65*	*75.86*	*5.81*	*38.62*	*4.59*	*11695*	*385.53*	*61.24*	*102.1*	*9.11*
MA15-2_ilm1.d		54.3	32.83	4728.02	149.06	367.73	22.66	5.58	60.18	270548	418.30	8.60	10769.4	114.59
MA15-2_ilm2.d		54.8	32.83	4442.37	126.08	380.87	20.36	8.87	49.71	254131	408.45	5.00	11984.2	77.82
MA15-2_ilm3.d		54.3	32.83	4143.59	137.90	298.78	7.88	9.19	76.57	274488	383.17	8.21	10674.2	130.68
MA15-2_ilm4.d		54.3	32.83	4531.02	155.96	439.97	8.54	1.31	87.60	288278	436.69	11.13	10572.4	140.20
MA15-2_ilm5.d		52.8	32.83	4169.85	131.99	288.93	9.52	2.63	76.60	274160	418.96	8.96	10542.8	128.38
MA15-2	**Avg.**		**32.83**	**4402.97**	**140.20**	**355.26**	**13.79**	**5.52**	**70.13**	**272321**	**413.11**	**8.38**	**10908.6**	**118.33**
Ilmenite	*Std.*		*32.83*	*221.46*	*10.94*	*55.81*	*6.36*	*3.19*	*13.45*	*10924*	*17.52*	*1.97*	*543.7*	*21.85*
MA32-25_ilm1.d		54.8	33.59	243.53	22.17	262.34	14.11	-2.69	6.31	243194	1101.76	158.88	7121.1	59.22
MA32-25_ilm2.d		54.8	33.59	361.43	18.04	277.12	24.19	24.52	6.94	231101	645.61	89.69	6247.8	57.57
MA32-25_ilm3.d		54.8	33.59	227.07	14.98	241.18	18.47	3.69	4.63	228750	1034.58	140.07	6818.8	54.42
MA32-25_ilm4.d		54.3	33.59	196.17	10.18	261.33	15.45	1.68	4.83	219345	1266.35	189.45	6986.8	60.80
MA32-25	**Avg.**		**33.59**	**257.05**	**16.34**	**260.49**	**18.05**	**6.80**	**5.68**	**230597**	**1012.08**	**144.52**	**6793.6**	**58.00**
Ilmenite	*Std.*		*33.59*	*62.62*	*4.38*	*12.78*	*3.88*	*10.49*	*0.98*	*8499*	*227.77*	*36.23*	*332.8*	*2.36*
32-1A-ILM-1.D		49.9	**32.71**	1302.99	8.18	23.88	-3.43	1.05	60.98	276104	312.74	10.30	11067.1	75.05
32-1A-ILM-2.D		49.9	**32.71**	1321.63	11.68	117.77	1.80	8.51	41.61	280553	369.01	13.87	11973.2	81.88
32-1A-ILM-5.D		49.9	**32.71**	1448.24	20.51	34.02	-3.73	8.18	43.61	277543	330.08	14.23	11829.3	81.62
32-1A-ILM-6.D		49.9	**32.71**	1407.67	7.36	67.72	-0.95	6.87	49.20	270543	248.62	4.71	10697.4	63.40
32-1A-ILM-7.D		49.9	**32.71**	980.10	12.40	60.85	3.34	66.74	57.18	289189	441.96	18.91	13759.4	72.43
MA-32-1A	**Avg.**		**32.71**	**1292.13**	**12.03**	**60.85**	**-0.60**	**18.27**	**50.52**	**278786**	**340.48**	**12.41**	**11865.3**	**74.88**
Ilmenite	*Std.*		***32.71***	*164.97*	*4.67*	*32.78*	*2.80*	*24.38*	*7.52*	*6133*	*63.92*	*4.72*	*1058.5*	*6.82*
32-1C-ILM-2.D		49.9	**32.72**	1583.82	21.34	68.06	1.67	3.60	85.08	275663	379.59	11.09	10497.7	63.97
32-1C-ILM-3.D		49.9	**32.72**	1079.88	10.01	78.54	-0.98	4.25	95.55	276448	497.72	18.46	11011.5	52.10
32-1C-ILM-5.D		49.9	**32.72**	1256.58	15.64	67.08	-0.43	-1.64	74.45	276187	479.73	13.71	10713.7	51.44
32-1C-ILM-6.D		49.9	**32.72**	1330.54	12.11	63.16	3.27	12.11	84.39	266926	389.08	14.79	9876.0	57.10
32-1C-ILM-7.D		*31.3*	***32.72***	*1312.21*	*26.90*	*605.39*	*-0.65*	*15.05*	*78.54*	*275958*	*308.26*	*8.28*	*10896.9*	*55.04*
32-1C-ILM-7.D		*16.2*	***32.72***	*1336.43*	*20.45*	*52.68*	*0.00*	*3.93*	*86.39*	*275467*	*347.52*	*9.56*	*10327.5*	*57.99*
MA-32-1C	**Avg.**		**32.72**	**1314.26**	**16.76**	**138.79**	**0.62**	**5.92**	**84.14**	**274203**	**413.55**	**13.35**	**10560.4**	**56.13**
Ilmenite	*Std.*		***32.72***	*162.00*	*5.52*	*139.24*	*1.61*	*5.14*	*6.84*	*3649*	*65.83*	*3.31*	*379.4*	*4.49*
32-2A-T-ILM-1.D		49.9	**33.52**	614.49	13.04	50.29	0.34	2.68	42.14	274156	583.65	27.02	11039.3	60.41
32-2A-T-ILM-2.D		49.9	**33.52**	538.39	55.98	141.13	1.74	35.87	34.76	273888	640.97	34.46	11565.7	55.95

Source file		60Ni	63Cu	66Zn	69Ga	74Ge	89Y	90Zr	93Nb	95Mo	118Sn	178Hf	181Ta	182W	208Pb
MA-14-8B	**Avg.**	**46.37**	**0.87**	**79.67**	**1.57**	**0.06**	**0.09**	**25.43**	**11.00**	**1.06**	**0.27**	**0.99**	**1.05**	**0.33**	**0.02**
Ilmenite	*Std.*	*4.68*	*0.24*	*5.71*	*0.11*	*0.02*	*0.01*	*1.99*	*1.89*	*0.13*	*0.05*	*0.06*	*0.12*	*0.19*	*0.00*
MA15-1_ilm1.d		34.23	2.62	48.39	1.90	0.10	0.09	9.37	10.00	0.31	1.83	0.33	0.66	0.21	0.03
MA15-1_ilm2.d		40.11	2.73	46.03	2.79	0.07	0.01	7.64	8.33	0.24	2.46	0.26	0.50	0.16	0.01
MA15-1_ilm3.d		43.11	2.98	58.11	3.09	0.02	0.01	5.67	10.57	0.17	2.05	0.21	0.74	0.11	0.05
MA15-1_ilm4.d		40.15	4.19	63.04	2.56	0.04	0.01	6.44	12.15	0.13	3.39	0.27	0.89	0.08	0.02
MA15-1_ilm5.d		32.01	2.81	53.00	1.50	0.05	0.01	8.14	14.69	0.15	2.37	0.30	1.18	0.10	0.02
MA15-1_ilm6.d		38.67	4.30	69.77	2.36	0.06	0.01	4.47	13.63	0.05	2.77	0.17	0.94	0.04	0.01
MA15-1	**Avg.**	**38.05**	**3.27**	**56.39**	**2.37**	**0.06**	**0.02**	**6.96**	**11.56**	**0.17**	**2.48**	**0.26**	**0.82**	**0.12**	**0.02**
Ilmenite	*Std.*	*3.78*	*0.70*	*8.26*	*0.53*	*0.02*	*0.03*	*1.62*	*2.17*	*0.08*	*0.51*	*0.06*	*0.22*	*0.06*	*0.01*
MA15-2_ilm1.d		30.67	3.02	35.03	0.82	0.02	0.07	49.09	10.90	0.05	1.53	1.17	0.75	0.05	0.08
MA15-2_ilm2.d		20.09	4.96	44.65	0.65	0.06	0.06	44.69	11.06	0.05	1.60	1.38	0.81	0.03	0.07
MA15-2_ilm3.d		37.43	2.87	39.66	0.70	0.07	0.09	55.36	10.64	0.06	1.72	1.35	0.75	0.05	0.01
MA15-2_ilm4.d		39.73	2.67	29.65	0.68	0.06	0.10	63.04	12.28	0.05	2.02	1.64	0.88	0.05	0.02
MA15-2_ilm5.d		38.38	2.25	26.46	0.52	0.07	0.10	57.89	11.69	0.06	1.57	1.57	0.81	0.05	0.03
MA15-2	**Avg.**	**33.26**	**3.15**	**35.09**	**0.67**	**0.06**	**0.09**	**54.01**	**11.31**	**0.06**	**1.69**	**1.42**	**0.80**	**0.05**	**0.04**
Ilmenite	*Std.*	*7.29*	*0.94*	*6.58*	*0.10*	*0.02*	*0.02*	*6.47*	*0.59*	*0.00*	*0.18*	*0.17*	*0.05*	*0.01*	*0.03*
MA32-25_ilm1.d		30.60	4.37	51.06	0.94	0.06	0.01	16.19	8.57	0.09	1.84	0.44	0.54	1.43	0.05
MA32-25_ilm2.d		26.74	2.91	42.16	1.11	0.04	0.01	19.35	10.58	0.10	2.92	0.74	0.72	0.65	0.03
MA32-25_ilm3.d		32.78	4.87	46.86	1.00	0.05	0.01	11.59	4.81	0.05	1.81	0.32	0.25	1.76	0.03
MA32-25_ilm4.d		32.78	4.80	44.34	0.94	0.08	0.00	14.11	6.68	0.05	1.83	0.54	0.41	1.25	0.03
MA32-25	**Avg.**	**30.73**	**4.24**	**46.10**	**1.00**	**0.06**	**0.01**	**15.31**	**7.66**	**0.07**	**2.10**	**0.51**	**0.48**	**1.27**	**0.04**
Ilmenite	*Std.*	*2.47*	*0.79*	*3.31*	*0.07*	*0.01*	*0.00*	*2.84*	*2.15*	*0.02*	*0.47*	*0.15*	*0.17*	*0.40*	*0.01*
32-1A-ILM-1.D		15.08	1.20	44.36	0.25	0.17	0.20	42.53	14.52	0.86	0.26	1.58	1.30	0.36	0.02
32-1A-ILM-2.D		24.37	0.90	42.72	0.63	0.05	0.43	44.49	13.44	0.87	0.20	1.53	1.30	0.55	0.03
32-1A-ILM-5.D		19.24	1.50	49.33	0.51	0.06	0.37	42.20	13.29	0.79	0.21	1.32	1.14	0.15	0.82
32-1A-ILM-6.D		12.89	2.12	39.45	0.23	0.00	0.16	44.03	13.58	0.73	0.20	1.63	1.24	0.09	0.03
32-1A-ILM-7.D		19.99	0.82	29.48	0.35	0.03	0.49	44.82	11.22	1.02	0.33	1.26	1.02	1.54	0.06
MA-32-1A	**Avg.**	**18.31**	**1.31**	**41.07**	**0.39**	**0.06**	**0.33**	**43.61**	**13.21**	**0.85**	**0.24**	**1.46**	**1.20**	**0.54**	**0.19**
Ilmenite	*Std.*	*4.01*	*0.47*	*6.62*	*0.16*	*0.06*	*0.13*	*1.06*	*1.08*	*0.10*	*0.05*	*0.15*	*0.10*	*0.53*	*0.31*
32-1C-ILM-2.D		19.14	0.44	78.21	0.50	0.13	0.19	49.74	15.01	0.72	0.21	2.20	1.22	0.09	0.01
32-1C-ILM-3.D		18.75	0.62	25.62	0.75	0.02	0.30	68.39	10.14	0.84	0.28	2.10	0.84	0.36	0.02
32-1C-ILM-5.D		19.70	0.66	40.28	0.78	0.01	0.30	56.28	11.00	0.79	0.28	2.12	0.81	0.30	0.07
32-1C-ILM-6.D		16.72	1.19	48.33	0.76	0.05	0.35	65.12	11.75	0.77	0.23	2.11	1.05	0.37	0.03
32-1C-ILM-7.D		*14.99*	*0.91*	*98.17*	*0.77*	*0.10*	*0.59*	*59.88*	*13.47*	*0.80*	*0.19*	*2.01*	*1.15*	*2.13*	*0.05*
32-1C-ILM-7.D		*16.17*	*0.98*	*37.04*	*0.64*	*0.02*	*0.38*	*52.36*	*13.19*	*0.77*	*0.23*	*1.80*	*1.18*	*0.16*	*0.01*
MA-32-1C	**Avg.**	**17.94**	**0.77**	**53.96**	**0.70**	**0.06**	**0.33**	**59.37**	**12.25**	**0.78**	**0.24**	**2.10**	**1.02**	**0.52**	**0.03**
Ilmenite	*Std.*	*1.62*	*0.27*	*20.77*	*0.10*	*0.04*	*0.11*	*6.65*	*1.74*	*0.04*	*0.04*	*0.08*	*0.16*	*0.48*	*0.02*
32-2A-T-ILM-1.D		16.83	1.28	37.28	0.98	0.14	0.14	39.62	9.77	0.79	0.28	1.21	0.96	0.08	0.03
32-2A-T-ILM-2.D		15.29	0.58	35.37	1.32	0.09	0.17	40.23	6.28	0.95	0.29	1.18	0.46	0.10	0.02

Source file	Notes	Analysis Length (s)	Fe (wt%)	24Mg	27Al	29Si	31P	44Ca	45SC	47Ti	51V	52Cr	55Mn	59Co
32-2A-T-ILM-3.D		49.9	**33.52**	681.87	30.77	105.60	6.20	55.98	44.55	273821	528.00	26.82	11307.5	68.22
32-2A-T-ILM-4.D		49.9	**33.52**	614.15	274.89	261.48	1.51	43.92	37.41	267552	452.57	21.05	11458.4	67.65
32-2A-T-ILM-5.D		43.8	**33.52**	590.35	81.80	30.84	1.98	3.35	30.07	262155	395.24	9.86	11320.9	60.74
MA-32-2A-T	**Avg.**		**33.52**	**607.85**	**91.30**	**117.87**	**2.35**	**28.36**	**37.79**	**270315**	**520.09**	**23.84**	**11338.4**	**62.60**
Ilmenite	*Std.*		***33.52***	*46.25*	*94.69*	*81.80*	*2.01*	*21.66*	*5.17*	*4776*	*88.16*	*8.19*	*177.1*	*4.68*
32-2A-B-ILM-1.D		49.9	**33.31**	436.36	76.95	43.64	-3.30	7.36	32.18	280404	502.65	25.62	12594.5	55.06
32-2A-B-ILM-2.D		49.9	**33.31**	411.38	166.55	61.29	1.93	11.63	23.65	274741	397.72	19.29	12494.6	53.60
32-2A-B-ILM-3.D		49.9	**33.31**	463.01	81.61	349.76	1.27	109.92	23.52	274974	492.99	33.94	12234.8	46.57
32-2A-B-ILM-5.D		49.9	**33.31**	372.07	36.77	78.94	-0.70	31.31	26.58	268745	416.38	13.79	11758.4	50.73
MA32-2A-B-a	**Avg.**		**33.31**	**420.71**	**90.47**	**133.41**	**-0.20**	**40.06**	**26.48**	**274716**	**452.43**	**23.16**	**12270.6**	**51.49**
Ilmenite	*Std.*		***33.31***	*33.49*	*47.26*	*125.53*	*2.03*	*41.34*	*3.51*	*4125*	*45.99*	*7.50*	*323.5*	*3.24*
32-2A-B-ILM-7.D		49.9	**33.65**	391.35	96.58	62.59	-2.02	42.74	29.51	263580	520.90	15.95	11494.8	61.61
32-2A-B-ILM-8.D		49.9	**33.65**	612.43	255.40	195.17	0.34	205.26	49.70	277410	453.60	16.89	11834.7	67.57
32-2A-B-ILM-9.D		49.9	**33.65**	427.02	75.04	46.44	0.00	121.14	30.32	272766	508.45	22.61	11663.0	59.73
32-2A-B-ILM-11.D		49.9	**33.65**	334.14	256.41	56.87	1.08	5.05	37.82	277612	563.30	20.22	11676.5	57.84
MA32-2A-B-b	**Avg.**		**33.65**	**441.23**	**170.86**	**90.27**	**-0.15**	**93.55**	**36.84**	**272842**	**511.56**	**18.92**	**11667.3**	**61.69**
Ilmenite	*Std.*		***33.65***	*104.24*	*85.39*	*60.84*	*1.15*	*76.90*	*8.10*	*5688*	*39.16*	*2.66*	*120.3*	*3.65*
32-2B-ILM-1.D		49.9	**33.24**	1112.91	186.15	81.77	2.49	67.81	46.87	276233	464.38	13.20	10879.8	72.93
32-2B-ILM-2.D		*28.6*	***33.24***	*1356.24*	*210.42*	*83.77*	*-0.33*	*329.09*	*48.57*	*275369*	*493.96*	*12.93*	*10673.7*	*77.12*
32-2B-ILM-2.D		*13.7*	***33.24***	*1193.35*	*112.02*	*18.95*	*-0.66*	*196.12*	*46.07*	*272577*	*486.32*	*11.40*	*10467.6*	*73.99*
32-2B-ILM-3.D		49.9	**33.24**	1098.95	127.65	49.20	0.33	18.62	48.20	277231	497.95	14.99	10816.6	75.03
32-2B-ILM-4-1.D		49.9	**33.24**	747.26	38.89	169.53	0.23	93.08	40.06	280721	429.47	11.20	11285.3	78.18
32-2B-ILM-4-2.D		49.9	**33.24**	942.72	94.74	59.50	1.80	41.22	46.04	274738	518.89	13.73	11052.7	77.45
MA32-2B	**Avg.**		**33.24**	**1041.07**	**125.20**	**84.56**	**0.88**	**101.36**	**45.78**	**276678**	**480.44**	**13.11**	**10928.3**	**75.94**
Ilmenite	*Std.*		***33.24***	*186.22*	*54.68*	*43.77*	*1.09*	*95.68*	*2.96*	*2259*	*30.86*	*1.27*	*228.5*	*1.86*
32-3-ILM-1.D		49.9	**33.71**	791.74	46.45	55.95	-5.60	5.12	33.71	248409	874.99	34.65	11058.8	84.74
32-3-ILM-2.D		52.5	**33.71**	690.96	44.15	51.91	-0.74	185.38	34.62	246623	752.64	23.90	11038.5	78.60
32-3-ILM-3-1.D		49.9	**33.71**	704.44	26.05	47.86	0.67	3.24	29.09	252791	823.09	37.41	11365.5	90.57
32-3-ILM-3-2.D		49.9	**33.71**	798.48	28.55	67.41	-0.67	16.18	25.18	243623	915.78	42.47	11106.0	92.62
32-3-ILM-5.D		49.9	**33.71**	956.22	85.95	23.93	1.38	6.07	31.72	254308	706.13	38.59	10856.5	94.14
MA32-3	**Avg.**		**33.71**	**788.37**	**46.23**	**49.41**	**-0.99**	**43.20**	**30.86**	**249151**	**814.53**	**35.40**	**11085.1**	**88.13**
Ilmenite	*Std.*		***33.71***	*94.68*	*21.46*	*14.32*	*2.44*	*71.23*	*3.42*	*3933*	*76.89*	*6.28*	*163.8*	*5.74*
32-4B-ILM-1.D		49.9	**33.59**	1330.25	480.37	671.84	-0.67	44.01	32.52	253621	839.80	16.43	8928.8	93.96
32-4B-ILM-2.D		49.9	**33.59**	833.09	50.72	70.54	4.13	87.34	24.82	266386	794.12	12.63	9651.0	105.98
32-4B-ILM-3-1.D		49.9	**33.59**	977.20	27.92	78.61	0.00	15.79	29.46	265546	793.78	13.60	9819.0	105.58
32-4B-ILM-3-2.D		49.9	**33.59**	954.69	12.50	67.86	-3.36	1.31	35.44	266487	837.79	14.71	9647.7	107.26
32-4B-ILM-4.D		49.9	**33.59**	888.85	33.86	107.49	2.79	16.80	36.35	259197	909.00	17.20	9469.6	97.62
MA32-4	**Avg.**		**33.59**	**996.81**	**121.07**	**199.27**	**0.58**	**33.05**	**31.72**	**262247**	**834.90**	**14.91**	**9503.2**	**102.08**
Ilmenite	*Std.*		***33.59***	*174.24*	*180.06*	*236.71*	*2.64*	*30.45*	*4.21*	*5093*	*42.14*	*1.70*	*307.7*	*5.30*
MA32-7_ilm1.d		54.8	31.82	4995.40	37.90	274.91	9.55	5.73	44.58	229725	420.00	23.70	9768.1	171.82

Source file		60Ni	63Cu	66Zn	69Ga	74Ge	89Y	90Zr	93Nb	95Mo	118Sn	178Hf	181Ta	182W	208Pb
32-2A-T-ILM-3.D		20.55	0.91	32.42	1.43	0.08	0.30	54.31	10.96	0.92	0.26	1.36	1.11	0.07	0.01
32-2A-T-ILM-4.D		16.12	0.67	54.64	1.24	0.07	0.16	46.93	10.14	0.87	0.20	1.17	0.99	0.04	0.03
32-2A-T-ILM-5.D		13.41	1.55	48.81	1.33	-0.04	0.13	44.25	12.74	0.84	0.24	1.33	1.22	0.08	0.01
MA-32-2A-T	**Avg.**	**16.44**	**1.00**	**41.70**	**1.26**	**0.07**	**0.18**	**45.07**	**9.98**	**0.88**	**0.25**	**1.25**	**0.95**	**0.08**	**0.02**
Ilmenite	*Std.*	*2.35*	*0.36*	*8.53*	*0.15*	*0.06*	*0.06*	*5.34*	*2.12*	*0.06*	*0.03*	*0.08*	*0.26*	*0.02*	*0.01*
32-2A-B-ILM-1.D		14.59	0.37	43.97	1.35	0.05	0.21	45.63	8.76	0.86	0.20	1.05	0.74	0.10	0.00
32-2A-B-ILM-2.D		17.45	0.38	89.94	1.15	0.07	0.25	38.64	6.79	0.87	0.23	0.48	0.58	0.35	0.05
32-2A-B-ILM-3.D		15.02	0.41	21.52	1.06	0.01	0.30	70.28	6.77	0.99	0.33	1.32	0.55	0.08	0.00
32-2A-B-ILM-5.D		12.12	0.57	25.08	1.41	0.05	0.27	38.97	11.02	0.90	0.17	0.98	1.01	0.11	0.03
MA32-2A-B-a	**Avg.**	**14.80**	**0.43**	**45.13**	**1.24**	**0.04**	**0.26**	**48.38**	**8.33**	**0.91**	**0.23**	**0.96**	**0.72**	**0.16**	**0.02**
Ilmenite	*Std.*	*1.89*	*0.08*	*27.24*	*0.14*	*0.02*	*0.03*	*12.95*	*1.75*	*0.05*	*0.06*	*0.30*	*0.18*	*0.11*	*0.02*
32-2A-B-ILM-7.D		13.43	0.99	54.51	1.53	0.10	0.19	51.48	10.58	0.86	0.27	1.86	0.98	0.11	0.09
32-2A-B-ILM-8.D		14.67	0.43	61.81	1.41	0.01	0.16	50.14	12.21	0.82	0.19	1.61	1.09	0.02	0.02
32-2A-B-ILM-9.D		15.31	0.87	49.80	1.36	-0.01	0.16	51.15	6.69	0.80	0.33	1.44	0.49	0.04	0.01
32-2A-B-ILM-11.D		14.07	0.50	97.58	1.23	0.05	0.18	58.21	5.94	0.84	0.28	1.58	0.42	0.05	0.01
MA32-2A-B-b	**Avg.**	**14.37**	**0.70**	**65.93**	**1.38**	**0.04**	**0.17**	**52.75**	**8.85**	**0.83**	**0.27**	**1.62**	**0.74**	**0.06**	**0.03**
Ilmenite	*Std.*	*0.70*	*0.24*	*18.77*	*0.11*	*0.04*	*0.01*	*3.20*	*2.62*	*0.02*	*0.05*	*0.15*	*0.29*	*0.03*	*0.03*
32-2B-ILM-1.D		15.76	1.13	55.35	1.31	0.04	0.40	48.20	10.68	0.81	0.22	1.68	0.94	0.02	0.01
32-2B-ILM-2.D		*23.80*	*1.23*	*64.16*	*1.38*	*0.03*	*0.46*	*55.51*	*8.95*	*0.72*	*0.31*	*1.41*	*0.75*	*0.04*	*0.03*
32-2B-ILM-2.D		*21.31*	*0.44*	*45.87*	*1.27*	*0.12*	*0.58*	*67.48*	*7.69*	*0.55*	*0.38*	*1.80*	*0.72*	*0.04*	*0.01*
32-2B-ILM-3.D		18.81	0.95	48.96	1.50	0.10	0.59	45.87	9.63	0.89	0.25	1.38	0.76	0.03	0.33
32-2B-ILM-4-1.D		17.58	0.57	23.40	1.22	0.06	0.82	60.83	9.44	0.77	0.29	1.69	0.99	0.05	0.02
32-2B-ILM-4-2.D		19.08	1.05	53.52	1.41	0.01	0.70	55.51	9.95	0.80	0.34	1.58	0.95	0.02	0.00
MA32-2B	**Avg.**	**18.85**	**0.94**	**47.89**	**1.36**	**0.05**	**0.60**	**53.96**	**9.65**	**0.79**	**0.29**	**1.57**	**0.88**	**0.03**	**0.08**
Ilmenite	*Std.*	*2.38*	*0.19*	*12.61*	*0.09*	*0.03*	*0.15*	*5.96*	*0.70*	*0.07*	*0.05*	*0.11*	*0.10*	*0.01*	*0.13*
32-3-ILM-1.D		24.50	0.38	47.96	2.71	0.09	0.15	15.40	16.11	0.87	0.19	0.64	1.57	0.10	0.03
32-3-ILM-2.D		19.92	0.79	38.69	2.53	0.07	0.12	10.31	14.97	0.84	0.21	0.40	1.47	0.36	0.05
32-3-ILM-3-1.D		30.03	0.59	33.50	2.33	0.16	0.16	10.08	9.41	0.92	0.18	0.49	0.82	0.26	0.05
32-3-ILM-3-2.D		26.56	0.57	41.73	2.74	0.18	0.21	28.31	10.11	0.84	0.26	0.86	0.71	0.11	0.05
32-3-ILM-5.D		26.22	0.83	63.94	1.70	0.00	0.10	24.94	15.94	0.95	0.20	0.94	1.33	0.07	0.03
MA32-3	**Avg.**	**25.45**	**0.63**	**45.17**	**2.40**	**0.10**	**0.15**	**17.81**	**13.31**	**0.88**	**0.21**	**0.67**	**1.18**	**0.18**	**0.04**
Ilmenite	*Std.*	*3.30*	*0.16*	*10.49*	*0.38*	*0.06*	*0.04*	*7.52*	*2.93*	*0.04*	*0.03*	*0.21*	*0.35*	*0.11*	*0.01*
32-4B-ILM-1.D		20.42	0.81	35.47	2.79	0.03	0.12	16.16	8.73	0.79	0.28	0.55	0.87	0.42	0.04
32-4B-ILM-2.D		24.99	1.32	40.11	2.38	0.13	0.10	30.23	7.19	0.84	0.30	0.70	0.61	0.48	0.01
32-4B-ILM-3-1.D		24.25	0.66	43.17	1.96	0.13	0.15	29.90	9.64	0.82	0.27	0.85	0.93	0.42	0.02
32-4B-ILM-3-2.D		23.45	0.35	32.42	1.60	0.02	0.13	24.52	10.85	0.83	0.24	0.83	1.03	0.30	0.02
32-4B-ILM-4.D		19.92	1.21	39.91	1.94	0.05	0.12	24.76	11.42	0.78	0.23	0.82	0.95	0.12	0.02
MA32-4	**Avg.**	**22.61**	**0.87**	**38.21**	**2.13**	**0.07**	**0.12**	**25.11**	**9.57**	**0.81**	**0.26**	**0.75**	**0.88**	**0.35**	**0.02**
Ilmenite	*Std.*	*2.05*	*0.35*	*3.80*	*0.41*	*0.05*	*0.01*	*5.09*	*1.51*	*0.02*	*0.03*	*0.11*	*0.15*	*0.13*	*0.01*
MA32-7_ilm1.d		57.59	4.87	119.00	0.36	0.10	0.07	29.91	11.07	0.06	1.71	1.12	0.72	0.01	0.02

Source file	Notes	Analysis Length (s)	Fe (wt%)	24Mg	27Al	29Si	31P	44Ca	45SC	47Ti	51V	52Cr	55Mn	59Co
MA32-7_ilm2.d		51.0	31.82	3207.24	12.47	242.77	10.82	0.95	65.86	223997	461.36	21.80	10054.4	124.73
MA32-7_ilm3.d		53.9	31.82	4810.85	48.71	300.04	15.59	7.00	65.48	256133	434.31	24.25	7808.1	150.18
MA32-7_ilm4.d		54.1	31.82	4607.22	91.00	285.09	15.27	1.91	67.68	250724	472.49	29.78	8333.1	138.09
MA32-7_ilm5.d		53.5	31.82	1788.16	19.73	435.90	16.86	3.50	51.54	219225	359.54	17.02	11613.5	84.64
MA32-7	**Avg.**		**31.82**	**3881.77**	**41.96**	**307.74**	**13.62**	**3.82**	**59.03**	**235961**	**429.54**	**23.31**	**9515.4**	**133.89**
Ilmenite	*Std.*		*31.82*	*1366.37*	*30.95*	*74.66*	*3.22*	*2.54*	*10.34*	*16485*	*44.36*	*4.60*	*1505.8*	*32.52*
MA32-9_ilm1.d		54.8	33.29	602.61	117.52	316.29	14.32	13.98	21.97	226061	449.46	5.16	8323.3	37.69
MA32-9_ilm2.d		54.8	33.29	539.35	63.59	266.35	11.65	2.33	21.31	227059	429.48	3.17	8156.8	32.76
MA32-9_ilm3.d		54.8	33.29	599.28	34.72	281.66	13.98	11.99	21.21	239711	478.42	4.41	8290.0	42.72
MA32-9_ilm4.d		54.8	33.29	822.34	111.20	279.33	12.98	0.00	23.41	249033	469.43	4.93	7990.4	50.31
MA32-9_ilm5.d		54.3	33.29	1368.35	329.60	268.34	12.98	-2.33	39.29	259354	421.49	3.90	7584.2	74.98
MA32-9_ilm6.d		54.8	33.29	1734.57	165.80	299.64	11.65	35.62	51.04	269009	393.53	2.35	8066.9	63.69
MA32-9	**Avg.**		**33.29**	**944.42**	**137.07**	**285.27**	**12.93**	**10.27**	**29.70**	**245038**	**440.30**	**3.99**	**8068.6**	**50.36**
Ilmenite	*Std.*		*33.29*	*450.74*	*95.59*	*17.61*	*1.02*	*12.82*	*11.47*	*15850*	*29.00*	*0.98*	*245.8*	*14.79*
MA32-12_ilm1.d		53.5	32.14	2182.12	421.00	254.85	16.07	-2.57	43.39	239101	411.04	6.72	7574.8	64.92
MA32-12_ilm2.d		54.8	32.14	1963.59	353.51	279.92	23.14	1.29	50.65	240708	390.47	4.66	7841.5	61.35
MA32-12_ilm3.d		54.8	32.14	2082.50	867.71	279.92	15.43	5.78	45.86	232674	384.36	4.92	8195.0	63.82
MA32-12_ilm4.d		54.8	32.14	6964.15	343.87	301.13	20.57	-6.75	51.58	267061	362.83	5.98	6935.2	73.72
MA32-12_ilm5.d		42.2	32.14	7970.05	655.60	327.80	12.21	-5.78	49.91	261919	354.15	5.62	6331.0	83.88
MA32-12	**Avg.**		**32.14**	**4232.48**	**528.34**	**288.72**	**17.48**	**-1.61**	**48.28**	**248293**	**380.57**	**5.58**	**7375.5**	**69.54**
Ilmenite	*Std.*		*32.14*	*2975.13*	*227.75*	*27.31*	*4.35*	*5.19*	*3.50*	*15198*	*22.66*	*0.83*	*743.8*	*9.28*
MA3215-ilm1.d		53.8	**31.62**	12838.80	125.23	395.28	11.38	-4.74	72.42	253614	597.67	7.43	6482.6	73.36
MA3215-ilm2.d		53.8	**31.62**	11953.37	129.65	347.85	14.55	13.28	61.03	252981	503.75	6.36	6564.9	102.77
MA3215-ilm3.d		50.6	**31.62**	12490.96	163.81	354.17	16.76	2.85	65.14	253614	603.99	7.62	6409.9	71.82
MA3215-ilm4.d		53.8	**31.62**	10087.63	171.39	398.45	20.24	5.69	61.98	239700	597.35	7.65	6960.2	68.43
MA3215-ilm5.d		53.8	**31.62**	10909.82	87.91	404.77	20.24	0.95	57.24	249503	512.29	7.12	6798.9	84.43
MA32-15	**Avg.**		**31.62**	**11656.12**	**135.60**	**380.10**	**16.63**	**3.60**	**63.56**	**249882**	**563.01**	**7.24**	**6643.3**	**80.16**
Ilmenite	*Std.*		*31.62*	*1140.30*	*33.52*	*26.87*	*3.81*	*6.62*	*5.70*	*5943*	*50.36*	*0.53*	*229.7*	*13.99*
MA3217-ilm1.d		53.8	**31.60**	11090.23	163.67	336.81	27.49	10.43	65.72	279941	559.25	12.20	6300.3	121.96
MA3217-ilm2.d		53.8	**31.60**	11058.63	164.30	410.75	18.96	104.27	67.33	267303	516.91	14.79	6793.2	96.78
MA3217-ilm3.d		53.8	**31.60**	11090.23	179.78	382.31	33.49	7.27	63.70	260984	577.26	11.06	6455.1	122.91
MA3217-ilm4.d		53.8	**31.60**	9510.42	138.39	407.59	30.33	13.27	63.51	256876	537.13	12.76	6761.6	107.74
MA3217-ilm5.d		50.9	**31.60**	9510.42	134.28	492.90	12.64	18.64	79.31	266671	523.55	10.93	7166.0	105.21
MA32-17	**Avg.**		**31.60**	**10451.99**	**156.08**	**406.07**	**24.58**	**30.77**	**67.91**	**266355**	**542.82**	**12.35**	**6695.2**	**110.92**
Ilmenite	*Std.*		*31.60*	*859.62*	*19.20*	*56.84*	*8.59*	*41.30*	*6.56*	*8722*	*25.16*	*1.57*	*335.1*	*11.27*
MA32-18_ilm1.d		54.8	33.33	3249.81	193.99	391.31	19.33	-0.67	28.23	278983	477.30	61.10	5233.0	79.23
MA32-18_ilm2.d		*30.6*	*33.33*	*2096.54*	*586.63*	*903.28*	*9.67*	*35.66*	*23.30*	*275984*	*453.64*	*48.50*	*5896.3*	*52.93*
MA32-18_ilm2.d		*18.7*	*33.33*	*2486.52*	*194.99*	*393.31*	*-3.33*	*-4.00*	*24.03*	*277317*	*443.97*	*42.46*	*5593.0*	*58.30*
MA32-18_ilm3.d		24.4	33.33	1436.58	201.32	409.98	17.00	13.00	29.76	276983	464.64	47.33	6133.0	18.73

Source file		60Ni	63Cu	66Zn	69Ga	74Ge	89Y	90Zr	93Nb	95Mo	118Sn	178Hf	181Ta	182W	208Pb
MA32-7_ilm2.d		24.50	4.58	54.09	0.38	0.07	0.06	42.13	7.83	0.06	2.08	1.23	0.50	0.53	0.03
MA32-7_ilm3.d		45.21	2.85	65.19	0.37	0.07	0.10	39.45	12.73	0.07	2.76	1.33	0.93	0.02	0.02
MA32-7_ilm4.d		43.65	3.49	74.14	0.82	0.06	0.09	45.21	4.30	0.04	2.76	1.24	0.28	0.11	0.01
MA32-7_ilm5.d		18.52	5.63	44.23	0.20	0.09	0.04	31.56	4.87	0.10	2.20	1.29	0.44	0.90	0.07
MA32-7	**Avg.**	**37.90**	**4.28**	**71.33**	**0.43**	**0.08**	**0.07**	**37.65**	**8.16**	**0.07**	**2.30**	**1.24**	**0.57**	**0.32**	**0.03**
Ilmenite	*Std.*	*16.04*	*1.11*	*28.94*	*0.23*	*0.02*	*0.02*	*6.66*	*3.71*	*0.02*	*0.46*	*0.08*	*0.25*	*0.39*	*0.02*
MA32-9_ilm1.d		8.22	4.79	72.25	1.26	0.07	0.22	20.51	5.93	0.07	1.75	0.63	0.38	0.20	0.04
MA32-9_ilm2.d		6.92	4.10	53.27	1.36	0.07	0.23	27.63	8.82	0.10	3.05	0.98	0.67	0.16	0.04
MA32-9_ilm3.d		8.86	3.14	43.95	1.23	0.05	0.41	22.01	7.19	0.09	1.68	0.62	0.50	0.15	0.06
MA32-9_ilm4.d		11.75	3.46	63.92	1.23	0.05	0.12	21.97	6.83	0.10	1.89	0.79	0.49	0.09	0.05
MA32-9_ilm5.d		17.95	2.15	70.25	1.50	0.08	0.12	34.92	9.09	0.11	2.25	1.28	0.72	0.15	0.03
MA32-9_ilm6.d		19.94	2.48	53.54	0.97	0.04	0.20	34.96	7.52	0.13	1.90	1.03	0.52	0.09	0.05
MA32-9	**Avg.**	**12.27**	**3.35**	**59.53**	**1.26**	**0.06**	**0.22**	**27.00**	**7.56**	**0.10**	**2.09**	**0.89**	**0.55**	**0.14**	**0.05**
Ilmenite	*Std.*	*4.97*	*0.90*	*10.11*	*0.16*	*0.01*	*0.10*	*6.04*	*1.10*	*0.02*	*0.47*	*0.23*	*0.12*	*0.04*	*0.01*
MA32-12_ilm1.d		26.32	4.69	32.14	0.99	0.09	0.03	32.39	9.16	0.04	1.53	1.17	0.62	0.01	0.10
MA32-12_ilm2.d		28.73	3.99	29.05	0.79	0.08	0.03	37.02	8.90	0.07	1.93	1.28	0.65	0.01	0.02
MA32-12_ilm3.d		24.36	4.66	50.13	1.27	0.09	0.02	31.56	9.00	0.05	1.83	1.12	0.60	0.01	0.05
MA32-12_ilm4.d		27.19	3.13	23.36	0.79	0.07	0.03	36.35	9.51	0.05	1.90	1.35	0.68	0.01	0.05
MA32-12_ilm5.d		33.00	2.82	39.21	0.77	0.06	0.04	34.23	9.67	0.05	2.14	1.27	0.70	0.01	0.07
MA32-12	**Avg.**	**27.92**	**3.86**	**34.78**	**0.92**	**0.08**	**0.03**	**34.31**	**9.25**	**0.05**	**1.87**	**1.23**	**0.65**	**0.01**	**0.06**
Ilmenite	*Std.*	*3.25*	*0.86*	*10.31*	*0.22*	*0.01*	*0.01*	*2.38*	*0.33*	*0.01*	*0.22*	*0.09*	*0.04*	*0.00*	*0.03*
MA3215-ilm1.d		24.76	3.02	56.29	1.12	0.12	0.05	32.22	9.96	0.08	3.81	1.04	0.73	0.01	0.03
MA3215-ilm2.d		44.81	2.26	61.54	1.06	0.14	0.17	30.01	11.07	0.04	2.71	1.09	0.86	0.02	0.05
MA3215-ilm3.d		33.90	2.75	62.68	1.15	0.09	0.08	40.73	11.19	0.03	3.13	1.52	0.90	0.01	0.00
MA3215-ilm4.d		13.31	3.15	74.95	1.68	0.12	0.08	34.25	10.06	0.03	5.25	1.11	0.69	0.02	0.07
MA3215-ilm5.d		29.25	3.92	58.19	1.08	0.17	0.10	28.93	11.23	0.04	3.92	1.24	0.81	0.02	0.13
MA32-15	**Avg.**	**29.21**	**3.02**	**62.73**	**1.22**	**0.13**	**0.09**	**33.23**	**10.70**	**0.04**	**3.76**	**1.20**	**0.80**	**0.01**	**0.06**
Ilmenite	*Std.*	*11.60*	*0.61*	*7.29*	*0.26*	*0.03*	*0.04*	*4.67*	*0.64*	*0.02*	*0.97*	*0.20*	*0.09*	*0.01*	*0.05*
MA3217-ilm1.d		42.97	2.00	28.47	0.94	0.17	0.13	48.03	11.34	0.07	3.03	1.62	0.87	0.01	0.03
MA3217-ilm2.d		36.40	1.91	52.54	1.26	0.09	0.18	38.74	9.35	0.03	2.95	1.36	0.67	0.01	0.03
MA3217-ilm3.d		42.72	2.24	21.30	0.97	0.09	0.19	47.01	12.54	0.05	2.94	1.75	0.90	0.02	0.06
MA3217-ilm4.d		31.15	3.22	52.77	1.09	0.10	0.28	33.78	10.65	0.03	4.55	1.20	0.69	0.01	0.12
MA3217-ilm5.d		28.56	2.16	58.45	1.29	0.14	0.37	42.97	9.95	0.03	4.23	1.36	0.71	0.02	0.11
MA32-17	**Avg.**	**36.36**	**2.31**	**42.71**	**1.11**	**0.12**	**0.23**	**42.10**	**10.77**	**0.04**	**3.54**	**1.46**	**0.77**	**0.01**	**0.07**
Ilmenite	*Std.*	*6.56*	*0.53*	*16.64*	*0.16*	*0.03*	*0.10*	*5.93*	*1.24*	*0.01*	*0.79*	*0.22*	*0.11*	*0.01*	*0.04*
MA32-18_ilm1.d		29.13	2.01	41.50	0.73	0.07	0.00	77.93	8.40	0.05	1.84	1.82	0.45	0.05	0.01
MA32-18_ilm2.d		*27.10*	*3.97*	*45.00*	*0.88*	*0.07*	*0.00*	*58.00*	*12.20*	*0.03*	*2.17*	*1.46*	*0.92*	*0.09*	*0.10*
MA32-18_ilm2.d		*27.60*	*1.99*	*43.83*	*0.74*	*0.13*	*0.00*	*60.40*	*13.90*	*0.06*	*1.74*	*1.51*	*1.06*	*0.08*	*0.07*
MA32-18_ilm3.d		9.47	2.57	52.20	0.87	0.02	0.01	64.33	10.17	0.03	1.90	1.55	0.53	0.05	0.04

Source file	Notes	Analysis Length (s)	Fe (wt%)	24Mg	27Al	29Si	31P	44Ca	45SC	47Ti	51V	52Cr	55Mn	59Co
MA32-18_ilm4.d		54.8	33.33	3229.81	170.32	326.65	22.67	0.00	28.33	284650	523.64	47.13	5086.4	41.93
MA32-18_ilm5.d		54.8	33.33	1263.26	177.99	416.64	0.00	-5.67	19.03	282650	477.64	54.93	6546.3	20.40
MA32-18-a	**Avg.**		**33.33**	**2284.79**	**236.33**	**450.87**	**12.75**	**5.46**	**25.79**	**279951**	**478.64**	**51.34**	**5756.0**	**43.05**
Ilmenite	*Std.*		*33.33*	*947.22*	*113.43*	*149.05*	*9.83*	*10.93*	*4.44*	*3574*	*27.59*	*6.48*	*610.2*	*25.28*
MA32-18_ilm6.d		54.8	32.20	8823.97	155.55	389.67	24.48	-7.08	30.37	224464	479.84	70.85	4073.8	113.36
MA32-18_ilm7.d		54.8	32.20	9661.29	602.22	363.91	20.93	12.24	31.37	258278	611.88	111.10	4251.0	117.55
MA32-18_ilm8.d		54.8	32.20	9113.81	150.72	296.28	18.36	-8.70	34.04	228650	573.24	60.87	4573.0	115.29
MA32-18_ilm9.d		54.8	32.20	8437.52	151.36	444.42	19.97	10.95	40.96	246363	462.45	72.88	4846.7	84.05
MA32-18-b			**32.20**	**9009.15**	**264.96**	**373.57**	**20.93**	**1.85**	**34.18**	**239439**	**531.85**	**78.92**	**4436.1**	**107.56**
Ilmenite			*32.20*	*446.45*	*194.73*	*53.26*	*2.24*	*9.77*	*4.14*	*13634*	*62.53*	*19.13*	*297.0*	*13.65*
MA32-18_ilm11.d		54.8	32.79	4058.88	204.26	275.40	20.33	2.30	23.41	262614	430.81	44.56	4721.2	91.24
MA32-18_ilm12.d		54.8	32.79	5042.46	511.46	636.04	18.69	7.21	21.90	271466	381.30	56.65	6363.7	93.44
MA32-18_ilm13.d		54.8	32.79	3672.01	186.55	377.04	15.74	14.10	22.23	252451	470.15	65.34	5737.5	87.54
MA32-18-c	**Avg.**		**32.79**	**4257.78**	**300.76**	**429.49**	**18.25**	**7.87**	**22.51**	**262177**	**427.42**	**55.52**	**5607.5**	**90.74**
Ilmenite	*Std.*		*32.79*	*706.54*	*182.69*	*185.96*	*2.33*	*5.93*	*0.79*	*9515*	*44.52*	*10.44*	*829.0*	*2.98*
MA32-19_ilm1.d		54.8	34.59	643.42	1833.41	1937.19	12.80	6.92	15.91	273628	1179.61	199.25	6081.4	67.77
MA32-19_ilm2.d		54.8	34.59	264.63	140.10	318.25	16.60	-4.50	14.56	258062	1110.43	268.09	6437.7	72.06
MA32-19_ilm3.d		54.8	34.59	245.26	103.78	387.44	20.06	8.30	16.40	256678	1062.00	205.48	6372.0	71.33
MA32-19_ilm4.d		54.8	34.59	240.77	224.85	319.64	22.49	-3.46	15.46	262905	1120.80	232.81	6707.5	74.51
MA32-19_ilm5.d		54.8	34.59	222.78	134.91	359.76	16.60	8.99	13.04	226928	1279.93	260.14	7541.2	60.19
MA32-19	**Avg.**		**34.59**	**323.37**	**487.41**	**664.46**	**17.71**	**3.25**	**15.08**	**255640**	**1150.55**	**233.15**	**6628.0**	**69.17**
Ilmenite	*Std.*		*34.59*	*179.53*	*753.78*	*712.07*	*3.70*	*6.65*	*1.32*	*17376*	*83.55*	*31.08*	*557.0*	*5.57*
MA11-11_ilm1.d		54.5	32.37	8253.91	203.27	307.50	15.21	-1.29	63.96	268333	579.72	56.97	8347.8	93.12
MA11-11_ilm2.d		54.8	32.37	8409.28	205.21	234.35	-37.87	2.59	60.40	268981	528.90	51.95	8241.0	101.38
MA11-11_ilm3.d		54.8	32.37	3796.80	126.24	377.09	25.89	4.86	62.41	273188	525.98	44.73	10856.3	67.84
MA11-11_ilm4.d		54.8	32.37	3893.91	178.03	427.26	22.33	5.50	56.16	257004	575.51	53.80	10778.6	66.91
MA11-11_ilm5.d		54.8	32.37	5755.08	210.39	290.67	24.60	16.51	54.28	246970	589.43	58.00	8545.2	98.40
MA11-11	**Avg.**		**32.37**	**6021.80**	**184.63**	**327.37**	**10.03**	**5.63**	**59.44**	**262895**	**559.91**	**53.09**	**9353.8**	**85.53**
Ilmenite	*Std.*		*32.37*	*2011.57*	*31.27*	*67.60*	*24.24*	*5.94*	*3.67*	*9601*	*26.91*	*4.71*	*1199.3*	*15.06*
MA11-8_ilm1.d		48.8	**32.54**	3904.33	240.77	299.33	19.20	-6.83	29.58	273954	491.29	39.04	9923.5	120.71
MA11-8_ilm2.d		48.8	**32.54**	2479.25	170.49	331.22	25.70	-2.93	43.14	275581	362.45	24.24	10665.3	90.03
MA11-8_ilm3.d		48.8	**32.54**	6650.38	175.37	368.63	26.35	2.93	51.28	273303	452.25	39.66	9796.6	123.96
MA11-8_ilm4.d		48.8	**32.54**	5062.62	129.17	358.87	24.73	-5.86	47.76	260939	428.83	34.39	9682.7	102.81
MA11-8_ilm5.d		48.8	**32.54**	5088.64	141.53	340.65	15.29	-10.09	40.93	257035	384.58	28.34	9468.0	109.00
MA11-8	**Avg.**		**32.54**	**4637.04**	**171.47**	**339.74**	**22.25**	**-4.56**	**42.54**	**268162**	**423.88**	**33.13**	**9907.2**	**109.30**
Ilmenite	*Std.*		*32.54*	*1551.73*	*43.31*	*26.96*	*4.81*	*4.90*	*8.29*	*8529*	*51.70*	*6.73*	*455.7*	*13.77*
MA11-2_ilm1.d		48.8	**32.66**	5734.5	180.6	16.3	-87.5	-24.2	34.5	245576	503.6	12.7	5969.6	87.5
MA11-2_ilm2.d		48.8	**32.66**	5884.7	160.0	13.1	-36.9	-29.1	41.7	255046	465.4	13.1	6462.7	98.3
MA11-2_ilm3.d		48.8	**32.66**	5744.3	309.9	147.0	-19.6	-20.2	34.8	259618	542.4	18.2	6273.3	105.8
MA11-2_ilm4.d		48.8	**32.66**	5584.2	148.6	-450.7	-55.5	-37.6	47.1	249821	454.3	11.1	7396.7	82.4

Source file		60Ni	63Cu	66Zn	69Ga	74Ge	89Y	90Zr	93Nb	95Mo	118Sn	178Hf	181Ta	182W	208Pb
MA32-18_ilm4.d		27.77	2.57	27.80	0.42	0.06	0.00	62.76	19.93	0.08	1.98	1.94	1.44	0.14	0.02
MA32-18_ilm5.d		19.57	2.74	52.96	1.02	0.08	0.00	67.43	12.47	0.04	1.54	1.53	0.94	0.10	0.04
MA32-18-a	**Avg.**	**22.64**	**2.62**	**43.80**	**0.77**	**0.07**	**0.00**	**66.27**	**12.76**	**0.05**	**1.85**	**1.66**	**0.87**	**0.09**	**0.04**
Ilmenite	*Std.*	*8.26*	*0.43*	*10.20*	*0.22*	*0.03*	*0.00*	*7.20*	*4.39*	*0.02*	*0.19*	*0.20*	*0.40*	*0.04*	*0.03*
MA32-18_ilm6.d		53.14	4.86	48.56	0.27	0.07	0.00	40.77	12.69	0.08	1.69	1.31	0.81	0.06	0.02
MA32-18_ilm7.d		55.65	3.64	72.78	1.45	0.10	0.00	52.85	16.62	0.08	2.33	1.64	1.24	0.06	0.02
MA32-18_ilm8.d		54.75	5.22	32.53	0.29	0.07	0.00	50.11	11.01	0.07	1.63	1.32	0.69	0.03	0.01
MA32-18_ilm9.d		42.99	4.99	23.99	0.25	0.04	0.01	49.66	3.42	0.03	2.82	1.11	0.16	0.01	0.01
MA32-18-b		**51.63**	**4.68**	**44.47**	**0.56**	**0.07**	**0.00**	**48.35**	**10.93**	**0.07**	**2.12**	**1.34**	**0.72**	**0.04**	**0.01**
Ilmenite		*5.07*	*0.61*	*18.58*	*0.51*	*0.02*	*0.00*	*4.54*	*4.79*	*0.02*	*0.49*	*0.19*	*0.38*	*0.02*	*0.01*
MA32-18_ilm11.d		35.51	2.57	34.20	0.24	0.06	0.00	59.41	18.29	0.06	1.63	1.34	1.31	0.14	0.01
MA32-18_ilm12.d		46.56	3.77	33.15	0.49	0.04	0.01	48.39	11.70	0.07	2.60	1.12	0.65	0.04	0.01
MA32-18_ilm13.d		40.98	4.29	46.13	0.56	0.04	0.00	53.21	9.70	0.06	1.76	1.10	0.70	0.06	0.03
MA32-18-c	**Avg.**	**41.02**	**3.54**	**37.82**	**0.43**	**0.05**	**0.00**	**53.67**	**13.23**	**0.06**	**1.99**	**1.19**	**0.89**	**0.08**	**0.02**
Ilmenite	*Std.*	*5.52*	*0.88*	*7.21*	*0.17*	*0.01*	*0.00*	*5.52*	*4.49*	*0.00*	*0.53*	*0.14*	*0.37*	*0.05*	*0.01*
MA32-19_ilm1.d		41.86	1.96	36.39	1.90	0.10	0.00	10.24	11.31	0.09	2.09	0.55	0.91	0.03	0.01
MA32-19_ilm2.d		47.50	3.03	50.54	2.44	0.06	0.01	11.69	9.13	0.07	1.97	0.53	0.56	0.03	0.01
MA32-19_ilm3.d		39.54	2.92	41.20	1.87	0.11	0.01	10.24	12.73	0.11	2.83	0.57	0.90	0.05	0.02
MA32-19_ilm4.d		40.44	3.00	46.01	2.05	0.08	0.01	11.42	12.63	0.11	2.48	0.53	0.88	0.05	0.03
MA32-19_ilm5.d		47.39	3.39	49.81	2.77	0.12	0.06	10.86	9.72	0.13	2.16	0.48	0.63	0.14	0.02
MA32-19	**Avg.**	**43.34**	**2.86**	**44.79**	**2.21**	**0.09**	**0.02**	**10.89**	**11.10**	**0.10**	**2.31**	**0.53**	**0.78**	**0.06**	**0.02**
Ilmenite	*Std.*	*3.83*	*0.53*	*5.98*	*0.39*	*0.03*	*0.02*	*0.66*	*1.64*	*0.02*	*0.35*	*0.03*	*0.16*	*0.05*	*0.00*
MA11-11_ilm1.d		53.15	3.93	53.08	0.81	0.03	0.01	47.58	15.05	0.05	1.77	1.62	1.06	0.02	0.05
MA11-11_ilm2.d		60.66	2.95	41.33	0.96	0.05	0.01	40.07	15.34	0.04	1.69	1.43	1.07	0.01	0.03
MA11-11_ilm3.d		39.36	2.39	48.78	0.38	0.05	0.01	44.34	16.54	0.04	2.84	1.59	1.31	0.01	0.04
MA11-11_ilm4.d		48.49	4.50	57.19	0.99	0.03	0.03	45.96	11.33	0.05	2.97	1.35	0.64	0.03	0.04
MA11-11_ilm5.d		64.48	4.24	44.25	0.90	0.08	0.01	50.24	16.44	0.07	1.83	1.72	1.23	0.01	0.05
MA11-11	**Avg.**	**53.23**	**3.60**	**48.93**	**0.81**	**0.05**	**0.01**	**45.64**	**14.94**	**0.05**	**2.22**	**1.54**	**1.06**	**0.02**	**0.04**
Ilmenite	*Std.*	*8.91*	*0.80*	*5.75*	*0.22*	*0.02*	*0.01*	*3.40*	*1.90*	*0.01*	*0.56*	*0.13*	*0.23*	*0.01*	*0.01*
MA11-8_ilm1.d		61.49	3.22	28.31	0.63	0.09	0.02	46.20	14.32	0.07	3.45	1.65	0.97	0.03	0.14
MA11-8_ilm2.d		42.75	0.85	22.68	0.76	0.05	0.20	48.97	9.25	0.05	3.81	1.15	0.61	0.07	0.02
MA11-8_ilm3.d		52.32	1.59	20.01	0.53	0.05	0.02	47.18	11.29	0.05	5.86	1.65	0.82	0.02	0.05
MA11-8_ilm4.d		44.57	2.33	31.01	0.99	0.06	0.08	47.31	8.65	0.04	6.12	1.26	0.56	0.20	0.05
MA11-8_ilm5.d		34.88	2.37	31.07	0.98	0.03	0.05	43.34	8.72	0.03	5.00	1.13	0.55	0.12	0.05
MA11-8	**Avg.**	**47.20**	**2.07**	**26.61**	**0.78**	**0.06**	**0.07**	**46.60**	**10.44**	**0.05**	**4.85**	**1.37**	**0.70**	**0.09**	**0.06**
Ilmenite	*Std.*	*10.11*	*0.89*	*5.03*	*0.21*	*0.02*	*0.08*	*2.08*	*2.41*	*0.01*	*1.19*	*0.27*	*0.18*	*0.07*	*0.04*
MA11-2_ilm1.d		15.9	2.2	29.2	0.4	0.1	0.0	43.6	11.5	0.1	4.0	1.5	0.8	0.0	0.1
MA11-2_ilm2.d		34.5	2.1	35.9	0.4	0.0	0.0	44.0	10.5	0.0	5.2	1.5	0.7	0.0	0.1
MA11-2_ilm3.d		41.9	2.0	37.8	0.6	0.0	0.0	42.2	11.2	0.1	5.0	1.6	0.9	0.0	0.1
MA11-2_ilm4.d		10.0	1.6	49.7	0.4	0.0	0.1	46.6	10.6	0.0	3.0	1.5	0.8	0.0	0.0

Source file	Notes		Analysis Length (s)	Fe (wt%)	24Mg	27Al	29Si	31P	44Ca	45SC	47Ti	51V	52Cr	55Mn	59Co
MA11-2_ilm5.d			48.8	**32.66**	6315.7	167.9	-610.7	-93.4	-16.0	46.9	251781	443.8	11.9	6821.9	91.4
MA11-2		**Avg.**		**32.66**	**5852.68**	**193.39**	**-177.00**	**-58.59**	**-25.41**	**40.99**	**252369**	**481.88**	**13.40**	**6584.8**	**93.08**
Ilmenite		*Std.*		*32.66*	*279.84*	*66.17*	*332.19*	*31.82*	*8.33*	*6.20*	*5308*	*40.69*	*2.80*	*549.0*	*9.19*
MA11-2_alt-ilm_3.d	**30 um**		54.8	32.79	461.02	113.78	354.12	32.13	-3.93	29.44	255101	406.59	13.31	7357.9	28.49
MA11-2_alt-ilm-1.d	**30 um**		25.8	32.79	570.53	281.99	773.83	3.28	2.30	74.83	266577	636.11	11.64	7738.3	27.31
MA11-2_alt-ilm-2.d	**30 um**		54.8	32.79	488.89	58.36	416.42	44.92	18.03	45.54	260019	421.01	12.92	7459.6	29.41
MA11-2_alt-ilm4.d	**30 um**		54.8	32.79	436.10	157.39	682.02	25.90	-8.20	61.45	263298	941.05	20.46	7630.1	24.20
MA11-2_alt-ilm-5.d	**30 um**		22.7	32.79	426.26	101.65	590.21	23.28	-5.57	94.11	273135	803.34	11.18	7672.7	25.87
MA11-2 (Altered)		**Avg.**		**32.79**	**476.56**	**142.63**	**563.32**	**25.90**	**0.52**	**61.07**	**263626**	**641.62**	**13.90**	**7571.7**	**27.06**
Ilmenite		*Std.*		*32.79*	*51.75*	*76.49*	*157.78*	*13.56*	*9.41*	*22.46*	*6082*	*209.64*	*3.37*	*141.2*	*1.86*
MA03-7-ILM2.d			53.8	**33.84**	281.57	14.38	439.95	16.92	-1.69	9.31	272094	1062.66	340.46	12048.0	47.89
MA03-7-ILM3.d			53.8	**33.84**	297.48	28.43	724.23	16.58	521.18	5.99	254835	700.54	367.53	12149.5	38.34
MA03-7-ILM4.d			53.8	**33.84**	292.06	11.40	358.73	24.37	6.09	6.29	239267	1049.12	464.32	12555.6	43.28
MA03-7-ILM5.d			53.8	**33.84**	268.71	11.07	298.49	17.94	-4.74	5.21	215239	873.14	283.94	12555.6	38.75
MA03-7		**Avg.**		**33.84**	**284.95**	**16.32**	**455.35**	**18.95**	**130.21**	**6.70**	**245359**	**921.36**	**364.06**	**12327.2**	**42.07**
Ilmenite		*Std.*		*33.84*	*12.68*	*8.21*	*188.39*	*3.66*	*260.68*	*1.80*	*24145*	*170.66*	*75.37*	*267.0*	*4.48*
MA03-6_ilm1.d	**30 um**		49.8	**33.72**	560.39	27.18	499.03	36.08	-19.22	5.23	266373	3078.46	1490.34	8392.4	36.18
MA03-6_ilm2.d	**30 um**		49.1	**33.72**	503.75	106.21	586.69	32.03	-2.02	3.91	282895	2656.98	1898.33	9822.1	52.74
MA03-6_ilm3.d	**30 um**		49.8	**33.72**	340.22	32.50	495.66	24.28	-0.34	14.33	250862	2495.14	1433.02	8159.8	24.78
MA03-6_ilm4.d	**30 um**		49.8	**33.72**	455.53	65.41	546.23	18.54	32.71	7.21	261652	2633.38	2070.29	11127.0	56.28
MA03-6_ilm5.d	**30 um**		49.8	**33.72**	544.55	45.52	674.36	29.33	16.86	8.08	274128	3537.03	1527.43	14094.2	43.66
MA03-6		**Avg.**		**33.72**	**480.89**	**55.37**	**560.39**	**28.05**	**5.60**	**7.75**	**267182**	**2880.20**	**1683.88**	**10319.1**	**42.73**
Ilmenite		*Std.*		*33.72*	*88.50*	*32.02*	*73.89*	*6.83*	*19.82*	*4.03*	*12173*	*427.13*	*282.92*	*2425.2*	*12.74*
MA03-4_ilm1.d			48.8	**34.06**	517.7	456.4	1072.8	31.3	136.2	11.2	247932	1014.9	317.4	9280.4	102.0
MA03-4_ilm2.d			48.8	**34.06**	551.7	117.5	228.2	-8.5	119.2	13.4	214216	1117.1	281.0	7799.0	107.3
MA03-4_ilm3.d			48.8	**34.06**	423.0	43.6	396.8	11.8	9.5	14.4	249975	893.3	344.0	8119.1	113.9
MA03-4_ilm4.d			48.8	**34.06**	418.2	197.5	316.0	0.1	-2.7	14.1	245889	1014.9	271.4	8565.2	116.8
MA03-4_ilm5.d			48.8	**34.06**	366.8	180.5	1260.1	36.4	177.1	6.6	233628	851.4	285.4	8616.3	95.0
MA03-4		**Avg.**		**34.06**	**455.47**	**199.09**	**654.77**	**14.23**	**87.87**	**11.94**	**238328**	**978.31**	**299.83**	**8476.0**	**107.01**
Ilmenite		*Std.*		*34.06*	*76.55*	*156.02*	*475.51*	*19.43*	*80.04*	*3.21*	*14904*	*106.37*	*30.12*	*561.4*	*8.84*
MA03-3_ilm5.d	**30 um**		49.8	**33.21**	348.07	18.70	528.09	47.83	28.90	7.45	263048	1717.12	558.64	9286.4	33.55
MA03-3_ilm1.d	**30 um**		49.8	**33.21**	488.56	22.88	584.55	38.86	28.90	8.47	268030	2158.85	588.54	10199.7	39.36
MA03-3_ilm2.d	**30 um**		49.8	**33.21**	506.50	19.23	564.62	32.22	23.25	4.53	276333	1737.05	1119.28	10820.8	39.32
MA03-3_ilm3.d	**30 um**		49.8	**33.21**	418.82	28.73	667.58	39.19	-0.33	3.06	267698	2590.62	886.79	10482.1	41.25
MA03-3_ilm4.d	**30 um**		49.8	**33.21**	279.65	21.62	488.23	33.88	15.28	8.81	263048	1756.97	747.29	9342.8	37.10
MA03-3		**Avg.**		**33.21**	**408.32**	**22.23**	**566.62**	**38.39**	**19.20**	**6.47**	**267631**	**1992.12**	**780.11**	**10026.4**	**38.12**
Ilmenite		*Std.*		*33.21*	*95.36*	*4.02*	*67.36*	*6.09*	*12.26*	*2.54*	*5429*	*381.44*	*230.89*	*686.2*	*2.95*
MA03-2_ilm1.d			49.8	**33.55**	379.44	19.93	348.24	-105.34	-17.11	2.67	238532	3878.24	413.32	7984.6	29.12
MA03-2_ilm2.d			49.8	**33.55**	253.29	14.93	845.43	235.18	23.48	5.67	253294	1670.73	169.76	6877.5	22.91
MA03-2_ilm3.d			49.8	**33.55**	213.37	20.57	502.23	16.10	-7.72	8.59	245577	1190.98	102.63	7048.6	22.85

Source file		60Ni	63Cu	66Zn	69Ga	74Ge	89Y	90Zr	93Nb	95Mo	118Sn	178Hf	181Ta	182W	208Pb
MA11-2_ilm5.d		23.2	2.2	28.1	0.3	0.0	0.0	42.7	10.5	0.0	2.9	1.3	0.7	0.0	0.1
MA11-2	**Avg.**	**25.08**	**2.04**	**36.14**	**0.39**	**0.03**	**0.03**	**43.84**	**10.85**	**0.05**	**4.02**	**1.50**	**0.78**	**0.02**	**0.09**
Ilmenite	*Std.*	*13.10*	*0.23*	*8.63*	*0.10*	*0.02*	*0.03*	*1.68*	*0.44*	*0.01*	*1.08*	*0.11*	*0.05*	*0.00*	*0.04*
MA11-2_alt-ilm_3.d		6.85	2.16	42.69	0.76	0.06	0.11	27.44	3.44	0.02	4.62	0.48	0.19	0.17	0.61
MA11-2_alt-ilm-1.d		17.38	8.20	18.92	0.76	0.00	0.11	31.08	2.16	0.04	4.66	0.72	0.18	0.17	0.37
MA11-2_alt-ilm-2.d		10.03	1.86	28.69	0.58	0.03	0.12	30.79	2.56	0.01	4.56	0.59	0.18	0.19	0.26
MA11-2_alt-ilm4.d		4.98	1.89	23.08	0.41	0.10	0.08	29.87	1.70	0.03	5.05	0.65	0.14	0.18	0.37
MA11-2_alt-ilm-5.d		8.10	2.30	20.30	0.17	-0.03	0.15	31.51	1.95	0.03	4.43	0.62	0.19	0.22	0.31
MA11-2 (Altered)	**Avg.**	**9.47**	**3.28**	**26.74**	**0.54**	**0.03**	**0.11**	**30.14**	**2.36**	**0.03**	**4.66**	**0.61**	**0.18**	**0.19**	**0.39**
Ilmenite	*Std.*	*4.28*	*2.46*	*8.65*	*0.23*	*0.04*	*0.02*	*1.45*	*0.61*	*0.01*	*0.21*	*0.08*	*0.02*	*0.02*	*0.12*
MA03-7-ILM2.d		24.60	1.78	63.83	0.35	0.08	0.01	8.33	13.67	0.09	5.60	0.35	1.05	0.17	0.04
MA03-7-ILM3.d		19.46	1.83	62.57	0.21	0.10	0.02	6.60	13.16	0.15	3.77	0.18	0.98	0.18	0.10
MA03-7-ILM4.d		23.83	2.41	63.29	0.32	0.05	0.01	6.33	10.56	0.12	3.33	0.29	0.72	0.18	0.17
MA03-7-ILM5.d		27.28	3.25	68.02	0.34	0.05	0.01	6.13	10.83	0.09	2.78	0.18	0.66	0.09	0.26
MA03-7	**Avg.**	**23.79**	**2.32**	**64.43**	**0.30**	**0.07**	**0.01**	**6.84**	**12.06**	**0.11**	**3.87**	**0.25**	**0.85**	**0.16**	**0.14**
Ilmenite	*Std.*	*3.24*	*0.68*	*2.45*	*0.07*	*0.02*	*0.01*	*1.01*	*1.59*	*0.03*	*1.22*	*0.08*	*0.19*	*0.05*	*0.10*
MA03-6_ilm1.d		5.16	1.62	38.40	0.44	0.09	0.00	2.88	19.32	0.51	2.73	0.07	1.58	0.41	0.02
MA03-6_ilm2.d		21.07	1.62	91.04	0.89	0.09	0.00	6.68	14.13	0.68	3.37	0.08	1.25	1.00	0.04
MA03-6_ilm3.d		11.60	1.73	29.71	1.36	0.11	0.04	4.75	16.96	0.64	2.87	0.16	0.98	0.79	0.01
MA03-6_ilm4.d		19.35	1.98	70.81	0.72	0.10	0.01	3.06	12.88	0.52	3.14	0.10	0.59	0.97	0.03
MA03-6_ilm5.d		13.79	1.83	51.08	0.66	0.09	0.00	6.64	9.37	0.47	4.32	0.14	0.50	0.86	0.05
MA03-6	**Avg.**	**14.20**	**1.75**	**56.21**	**0.82**	**0.10**	**0.01**	**4.80**	**14.53**	**0.56**	**3.28**	**0.11**	**0.98**	**0.81**	**0.03**
Ilmenite	*Std.*	*6.37*	*0.15*	*24.86*	*0.34*	*0.01*	*0.01*	*1.84*	*3.82*	*0.09*	*0.63*	*0.04*	*0.45*	*0.24*	*0.02*
MA03-4_ilm1.d		51.8	1.3	35.1	1.1	0.2	0.1	15.5	8.2	0.1	5.4	0.4	0.6	0.6	0.0
MA03-4_ilm2.d		51.1	2.9	28.2	1.0	0.1	0.1	14.4	10.9	0.1	2.9	0.4	0.9	0.5	0.1
MA03-4_ilm3.d		56.4	1.2	22.3	1.0	0.1	0.1	14.0	9.9	0.1	6.3	0.5	0.7	0.6	0.0
MA03-4_ilm4.d		52.3	1.6	36.6	1.2	0.1	0.0	15.7	8.9	0.1	3.5	0.4	0.6	0.2	0.0
MA03-4_ilm5.d		64.3	1.7	27.4	1.1	0.1	0.1	9.0	9.1	0.1	5.1	0.2	0.8	0.5	0.0
MA03-4	**Avg.**	**55.19**	**1.73**	**29.95**	**1.09**	**0.08**	**0.07**	**13.73**	**9.41**	**0.08**	**4.63**	**0.37**	**0.72**	**0.47**	**0.04**
Ilmenite	*Std.*	*5.50*	*0.66*	*5.89*	*0.10*	*0.05*	*0.02*	*2.72*	*1.06*	*0.01*	*1.40*	*0.12*	*0.13*	*0.14*	*0.03*
MA03-3_ilm5.d		16.37	1.00	39.26	0.32	0.08	0.00	3.14	13.58	0.22	3.45	0.16	0.66	0.46	0.01
MA03-3_ilm1.d		13.95	1.15	45.54	0.27	0.07	0.01	4.28	22.72	0.15	7.07	0.26	1.14	0.30	0.41
MA03-3_ilm2.d		13.38	1.24	52.11	0.19	0.08	0.00	2.69	53.51	0.38	5.28	0.16	4.91	0.75	0.01
MA03-3_ilm3.d		14.98	1.31	46.40	0.23	0.01	0.00	4.12	10.03	0.31	6.91	0.26	0.39	0.42	0.15
MA03-3_ilm4.d		28.90	1.25	40.72	0.35	0.05	0.00	4.12	12.62	0.15	2.99	0.24	0.69	0.38	0.00
MA03-3	**Avg.**	**17.52**	**1.19**	**44.80**	**0.27**	**0.06**	**0.00**	**3.67**	**22.49**	**0.24**	**5.14**	**0.21**	**1.56**	**0.46**	**0.12**
Ilmenite	*Std.*	*6.46*	*0.12*	*5.10*	*0.07*	*0.03*	*0.00*	*0.71*	*17.99*	*0.10*	*1.89*	*0.05*	*1.89*	*0.17*	*0.17*
MA03-2_ilm1.d		-3.19	3.03	49.55	0.28	0.07	0.00	1.59	31.33	0.54	3.09	0.13	1.83	1.61	0.08
MA03-2_ilm2.d		30.63	1.83	43.18	1.02	0.22	0.02	3.24	19.59	0.34	3.36	0.19	0.97	2.08	0.03
MA03-2_ilm3.d		15.13	2.46	47.67	1.52	0.06	0.01	3.18	42.24	0.19	4.50	0.33	2.39	1.59	0.03

Source file	Notes	Analysis Length (s)	Fe (wt%)	24Mg	27Al	29Si	31P	44Ca	45SC	47Ti	51V	52Cr	55Mn	59Co
MA03-2_ilm4.d		49.3	**33.55**	244.24	57.70	523.70	29.19	-0.67	8.55	247255	1180.92	81.86	7179.4	22.85
MA03-2_ilm5.d		49.8	**33.55**	190.89	19.26	493.17	27.17	-6.04	8.60	253965	1352.02	108.36	7169.4	21.10
MA03-2	**Avg.**		**33.55**	**256.25**	**26.48**	**542.55**	**40.46**	**-1.61**	**6.82**	**247724**	**1854.58**	**175.19**	**7251.9**	**23.77**
Ilmenite	*Std.*		*33.55*	*73.21*	*17.60*	*182.97*	*122.55*	*15.23*	*2.64*	*6310*	*1148.45*	*137.09*	*427.3*	*3.09*
MA03-1B-ilm1.d		48.8	**31.73**	8598.6	335.4	431.5	23.2	9.5	40.8	252563	558.4	380.7	4689.5	95.8
MA03-1B_ilm2.d		48.8	**31.73**	7595.9	358.5	379.8	20.3	-1.9	41.9	251611	476.9	241.8	4721.3	110.4
MA03-1B_ilm3.d		48.8	**31.73**	7389.7	154.8	368.4	18.7	7.6	49.4	260812	491.8	211.9	4956.1	100.7
MA03-1B_ilm4.d		48.8	**31.73**	6466.4	146.3	447.4	25.7	8.6	46.1	254466	461.7	226.9	5809.6	100.7
MA03-1B_ilm5.d		48.8	**31.73**	6577.4	152.9	372.8	19.4	2.2	51.3	260812	440.1	235.7	5673.1	98.9
MA03-1B	**Avg.**		**31.73**	**7325.59**	**229.59**	**399.98**	**21.45**	**5.20**	**45.91**	**256053**	**485.77**	**259.42**	**5169.9**	**101.30**
Ilmenite	*Std.*		*31.73*	*865.40*	*107.50*	*36.69*	*2.92*	*4.88*	*4.56*	*4465*	*44.90*	*68.75*	*533.9*	*5.47*
MA03-1A_ilm1.d		48.8	**32.29**	5369.3	159.5	365.8	29.7	11.6	42.6	251839	454.0	237.3	6002.2	96.2
MA03-1A_ilm2.d		48.8	**32.29**	5505.0	153.0	419.7	38.4	-0.6	51.1	262494	437.8	239.9	6903.0	93.6
MA03-1A_ilm3.d		48.8	**32.29**	6589.8	151.7	371.3	31.3	7.4	48.2	258297	483.3	225.7	5708.4	99.8
MA03-1A_ilm4.d		*22.1*	***32.29***	*6137.8*	*163.7*	*348.7*	*30.3*	*-10.3*	*52.3*	*262494*	*450.7*	*237.6*	*6202.4*	*92.0*
MA03-1A_ilm4.d		*22.8*	***32.29***	*6205.6*	*169.8*	*361.6*	*28.4*	*7.4*	*52.0*	*263463*	*458.5*	*229.9*	*6073.2*	*93.3*
MA03-1A_ilm5.d		48.8	**32.29**	6715.7	144.3	386.8	34.9	8.4	44.5	254422	486.6	223.4	5685.8	65.6
MA03-1A	**Avg.**		**32.29**	**6070.40**	**155.08**	**379.78**	**32.74**	**5.10**	**47.72**	**258008**	**463.27**	**232.00**	**6087.2**	**89.56**
Ilmenite	*Std.*		*32.29*	*613.96*	*8.49*	*25.07*	*3.85*	*5.77*	*4.14*	*4896*	*20.94*	*7.19*	*494.9*	*13.69*
T3C4-1-ILM1.d		53.8	**32.00**	8106.75	560.08	350.77	28.48	-5.12	39.53	261797	461.83	5.15	4829.5	77.29
T3C4-1-ILM2.d		53.8	**32.00**	8289.18	560.08	361.01	24.64	25.92	44.13	258917	448.06	4.50	4899.9	93.81
T3C4-1-ILM3.d		53.8	**32.00**	8321.18	168.34	390.46	21.44	-2.88	46.50	261477	407.10	3.22	4807.1	85.68
T3C4-1-ILM4.d		53.8	**32.00**	8161.16	320.05	368.05	27.84	-16.00	45.67	265958	428.54	4.10	4867.9	77.13
T3C4-1-ILM5.d		53.8	**32.00**	7361.05	150.74	342.45	32.96	-20.48	41.51	241634	393.02	3.19	5476.0	80.01
T3-C4-1	**Avg.**		**32.00**	**8047.86**	**351.86**	**362.55**	**27.08**	**-3.71**	**43.47**	**257957**	**427.71**	**4.03**	**4976.1**	**82.78**
Ilmenite	*Std.*		*32.00*	*394.00*	*201.15*	*18.40*	*4.33*	*18.12*	*2.91*	*9467*	*28.32*	*0.84*	*281.7*	*7.06*
T3C4-2-ILM1.d		53.8	**32.05**	8525.86	461.55	307.70	14.42	-1.92	52.76	264430	471.17	4.74	4647.6	93.27
T3C4-2-ILM2.d		53.8	**32.05**	8589.96	589.76	323.73	21.15	-6.73	48.72	267315	586.55	7.15	4666.8	94.55
T3C4-2-ILM3.d		53.8	**32.05**	8141.23	419.88	410.27	26.60	-9.62	51.03	250006	450.33	4.87	4609.1	90.71
T3C4-2-ILM4.d		53.8	**32.05**	8557.91	320.52	391.04	21.15	6.09	61.80	260584	443.60	5.26	4727.7	92.95
T3C4-2-ILM5.d		53.8	**32.05**	8750.22	155.45	375.01	22.76	31.09	59.07	251930	398.73	3.46	4705.2	95.19
T3-C4-2	**Avg.**		**32.05**	**8513.04**	**389.43**	**361.55**	**21.22**	**3.78**	**54.67**	**258853**	**470.08**	**5.10**	**4671.3**	**93.34**
Ilmenite	*Std.*		*32.05*	*225.05*	*162.60*	*44.03*	*4.40*	*16.38*	*5.53*	*7614*	*70.27*	*1.33*	*46.9*	*1.73*
TA1-1_ilm1.d		54.8	31.75	10160.00	363.54	293.05	11.43	9.53	54.51	265748	419.42	17.15	4826.0	76.20
TA1-1_ilm2.d		42.5	31.75	6064.25	406.40	279.40	14.29	-0.95	57.21	247968	443.23	14.99	5403.9	61.79
TA1-1_ilm3.d		54.8	31.75	5883.28	167.01	320.68	6.35	10.48	65.06	253683	352.43	9.27	5737.2	59.18
TA1-1_ilm4.d		54.8	31.75	7994.65	396.88	260.67	19.69	8.89	65.37	278448	414.34	12.60	5540.4	72.42
TA1-1_ilm5.d		50.7	31.75	10953.75	342.90	260.35	18.42	-0.32	61.63	264795	422.28	11.84	4883.2	86.36
TA1-1	**Avg.**		**31.75**	**8211.19**	**335.34**	**282.83**	**14.03**	**5.52**	**60.76**	**262128**	**410.34**	**13.17**	**5278.1**	**71.19**
Ilmenite	*Std.*		*31.75*	*2068.57*	*87.21*	*22.56*	*4.84*	*5.06*	*4.29*	*10568*	*30.58*	*2.70*	*362.2*	*9.89*

Source file		60Ni	63Cu	66Zn	69Ga	74Ge	89Y	90Zr	93Nb	95Mo	118Sn	178Hf	181Ta	182W	208Pb
MA03-2_ilm4.d		14.33	2.78	52.40	1.95	0.05	0.01	5.43	32.11	0.16	4.70	0.41	1.65	1.32	0.02
MA03-2_ilm5.d		14.56	2.43	47.64	0.71	0.03	0.01	4.70	29.99	0.21	4.07	0.31	2.51	2.18	0.01
MA03-2	**Avg.**	**14.29**	**2.50**	**48.09**	**1.10**	**0.09**	**0.01**	**3.63**	**31.05**	**0.29**	**3.94**	**0.27**	**1.87**	**1.75**	**0.03**
Ilmenite	*Std.*	*11.97*	*0.45*	*3.36*	*0.66*	*0.08*	*0.01*	*1.49*	*8.04*	*0.16*	*0.70*	*0.11*	*0.62*	*0.36*	*0.03*
MA03-1B-ilm1.d		80.0	1.7	19.4	0.9	0.0	0.0	64.4	19.9	0.1	4.7	2.1	1.4	0.0	0.0
MA03-1B_ilm2.d		84.1	2.3	25.4	0.5	0.1	0.0	53.1	16.4	0.0	6.0	1.7	1.2	0.0	0.0
MA03-1B_ilm3.d		70.9	2.0	12.9	0.4	0.1	0.0	58.9	14.8	0.0	5.4	1.6	1.0	0.0	0.0
MA03-1B_ilm4.d		71.7	2.2	13.9	0.5	0.0	0.0	54.3	11.0	0.0	7.2	1.4	0.6	0.0	0.1
MA03-1B_ilm5.d		65.1	1.5	12.4	0.5	0.0	0.0	58.0	9.9	0.0	5.7	1.6	0.7	0.0	0.0
MA03-1B	**Avg.**	**74.35**	**1.94**	**16.78**	**0.53**	**0.04**	**0.01**	**57.75**	**14.40**	**0.04**	**5.79**	**1.65**	**0.99**	**0.02**	**0.04**
Ilmenite	*Std.*	*7.58*	*0.33*	*5.55*	*0.19*	*0.02*	*0.00*	*4.45*	*4.05*	*0.01*	*0.92*	*0.25*	*0.35*	*0.01*	*0.03*
MA03-1A_ilm1.d		53.2	2.7	16.1	0.4	0.0	0.0	41.0	14.7	0.0	2.6	1.3	1.0	0.1	0.1
MA03-1A_ilm2.d		55.7	2.0	12.6	0.7	0.1	0.0	57.1	10.7	0.0	3.5	1.7	0.6	0.0	0.0
MA03-1A_ilm3.d		70.4	2.5	14.6	0.5	0.0	0.0	55.1	14.0	0.0	3.1	1.6	0.9	0.1	0.0
MA03-1A_ilm4.d		*62.2*	*1.8*	*11.9*	*0.5*	*0.1*	*0.0*	*53.8*	*12.6*	*0.0*	*4.1*	*1.7*	*0.8*	*0.1*	*0.0*
MA03-1A_ilm4.d		*60.6*	*1.8*	*11.9*	*0.4*	*0.1*	*0.0*	*51.9*	*13.3*	*0.0*	*3.7*	*1.8*	*0.9*	*0.1*	*0.0*
MA03-1A_ilm5.d		51.4	2.1	14.6	0.3	0.0	0.0	58.6	17.0	0.1	3.2	1.9	1.3	0.1	0.0
MA03-1A	**Avg.**	**58.42**	**2.19**	**13.97**	**0.46**	**0.04**	**0.01**	**52.95**	**13.85**	**0.04**	**3.27**	**1.65**	**0.94**	**0.05**	**0.04**
Ilmenite	*Std.*	*7.68*	*0.36*	*1.71*	*0.12*	*0.02*	*0.01*	*7.00*	*2.32*	*0.01*	*0.47*	*0.22*	*0.24*	*0.02*	*0.02*
T3C4-1-ILM1.d		30.82	1.53	69.77	1.47	0.04	0.10	35.49	9.06	0.07	2.65	1.46	0.68	0.00	0.03
T3C4-1-ILM2.d		36.20	2.11	86.09	1.15	0.13	0.09	39.30	9.28	0.08	3.51	1.50	0.71	0.01	0.05
T3C4-1-ILM3.d		32.26	2.32	32.23	0.25	0.06	0.06	44.65	8.64	0.03	3.96	1.48	0.67	0.02	0.07
T3C4-1-ILM4.d		29.32	3.23	52.49	0.61	0.11	0.09	38.63	9.28	0.04	4.13	1.29	0.70	0.01	0.06
T3C4-1-ILM5.d		29.41	3.17	26.85	0.31	0.09	0.05	39.75	7.55	0.05	4.43	1.16	0.57	0.03	0.11
T3-C4-1	**Avg.**	**31.60**	**2.47**	**53.49**	**0.76**	**0.09**	**0.08**	**39.56**	**8.76**	**0.05**	**3.73**	**1.38**	**0.67**	**0.02**	**0.07**
Ilmenite	*Std.*	*2.84*	*0.72*	*24.95*	*0.53*	*0.04*	*0.02*	*3.29*	*0.73*	*0.02*	*0.69*	*0.15*	*0.05*	*0.01*	*0.03*
T3C4-2-ILM1.d		38.46	1.88	57.69	1.24	0.06	0.12	41.32	9.74	0.06	3.27	1.62	0.71	0.01	0.06
T3C4-2-ILM2.d		41.35	2.21	77.57	1.48	0.09	0.11	36.15	9.62	0.04	3.11	1.29	0.68	0.01	0.11
T3C4-2-ILM3.d		35.83	2.08	66.03	1.15	0.17	0.14	36.06	9.10	0.07	4.78	1.38	0.69	0.00	0.15
T3C4-2-ILM4.d		38.01	2.70	52.57	0.41	0.08	0.12	44.90	8.56	0.03	4.65	1.35	0.63	0.26	0.13
T3C4-2-ILM5.d		33.43	2.11	33.11	0.31	0.00	0.12	41.89	7.40	0.02	4.94	1.43	0.48	0.00	0.18
T3-C4-2	**Avg.**	**37.42**	**2.19**	**57.39**	**0.92**	**0.08**	**0.12**	**40.07**	**8.88**	**0.04**	**4.15**	**1.41**	**0.64**	**0.06**	**0.13**
Ilmenite	*Std.*	*2.97*	*0.30*	*16.54*	*0.53*	*0.06*	*0.01*	*3.86*	*0.95*	*0.02*	*0.88*	*0.13*	*0.10*	*0.11*	*0.05*
TA1-1_ilm1.d		39.66	3.46	30.32	0.95	0.06	0.02	39.56	9.62	0.06	2.05	1.47	0.70	0.01	0.03
TA1-1_ilm2.d		33.05	2.84	29.34	1.15	0.11	0.03	46.61	10.48	0.07	2.45	1.57	0.86	0.01	0.02
TA1-1_ilm3.d		33.31	3.24	22.70	0.29	0.04	0.04	43.43	8.29	0.04	2.34	1.37	0.57	0.02	0.05
TA1-1_ilm4.d		36.83	2.92	29.85	0.86	0.07	0.04	49.18	10.48	0.05	2.23	1.67	0.78	0.02	0.02
TA1-1_ilm5.d		46.67	2.83	28.58	1.00	0.05	0.04	50.48	11.02	0.05	2.11	1.69	0.87	0.02	0.02
TA1-1	**Avg.**	**37.90**	**3.06**	**28.16**	**0.85**	**0.06**	**0.03**	**45.85**	**9.98**	**0.05**	**2.24**	**1.55**	**0.76**	**0.02**	**0.03**
Ilmenite	*Std.*	*5.02*	*0.25*	*2.79*	*0.29*	*0.02*	*0.01*	*3.96*	*0.96*	*0.01*	*0.14*	*0.12*	*0.11*	*0.01*	*0.01*

Source file	Notes	Analysis Length (s)	Fe (wt%)	24Mg	27Al	29Si	31P	44Ca	45SC	47Ti	51V	52Cr	55Mn	59Co
TA1-4_ilm1.d		54.8	30.99	8770.17	165.18	266.51	15.80	3.10	59.00	239243	330.97	7.56	5125.7	76.55
TA1-4_ilm2.d		54.8	30.99	12984.81	210.11	288.21	18.59	3.72	46.61	218789	365.68	7.62	4555.5	99.48
TA1-4_ilm3.d		54.8	30.99	10102.74	254.12	313.00	24.17	-2.17	64.71	265894	343.99	9.27	5060.7	89.25
TA1-4_ilm4.d		54.8	30.99	12860.85	328.49	325.40	16.11	3.72	60.52	272092	381.18	9.39	4567.9	105.99
TA1-4_ilm5.d		54.8	30.99	12922.83	427.66	316.10	16.11	5.27	60.31	265274	467.95	12.18	4279.7	95.45
TA1-4	**Avg.**		**30.99**	**11528.28**	**277.11**	**301.84**	**18.16**	**2.73**	**58.23**	**252259**	**377.95**	**9.20**	**4717.9**	**93.34**
Ilmenite	*Std.*		*30.99*	*1759.62*	*92.58*	*21.52*	*3.17*	*2.55*	*6.12*	*20191*	*48.21*	*1.68*	*323.9*	*10.01*
TA1-5_ilm1.d		54.5	31.68	7223.04	212.26	327.57	21.86	6.97	65.64	278150	388.71	14.16	5192.4	68.71
TA1-5_ilm2.d		54.8	31.68	7571.52	199.58	367.49	15.84	1.58	66.84	270230	366.54	10.33	5594.7	83.32
TA1-5_ilm3.d		54.8	31.68	10581.12	231.26	334.22	23.13	5.07	60.67	277517	377.63	9.73	4523.9	80.66
TA1-5_ilm5.d		26.9	31.68	6557.76	516.38	275.62	14.26	6.02	55.82	254390	408.99	15.90	5103.6	76.03
TA1-5-ilm4.d		54.8	31.68	10391.04	411.84	328.52	12.04	3.48	55.15	260726	430.53	16.98	4299.0	100.74
TA1-5	**Avg.**		**31.68**	**8464.90**	**314.27**	**326.68**	**17.42**	**4.63**	**60.83**	**268203**	**394.48**	**13.42**	**4942.7**	**81.89**
Ilmenite	*Std.*		*31.68*	*1683.21*	*127.14*	*29.44*	*4.33*	*1.91*	*4.83*	*9343*	*22.84*	*2.92*	*469.7*	*10.65*
TA1-6_ilm1.d		49.8	**30.95**	11266.76	266.19	356.57	29.10	12.07	50.30	221311	428.38	13.62	4441.7	99.05
TA1-6_ilm2.d		49.8	**30.95**	10957.24	451.91	350.38	24.45	7.74	47.61	221930	516.60	19.50	4104.3	91.62
TA1-6_ilm3.d		49.8	**30.95**	9719.13	132.48	318.81	22.60	7.43	65.59	228740	374.84	11.67	4930.8	87.60
TA1-6_ilm4.d		49.8	**30.95**	11762.01	219.76	328.10	20.74	4.95	44.32	207692	436.43	12.69	4305.5	98.12
TA1-6_ilm5.d		49.8	**30.95**	12164.39	433.34	362.15	26.31	1.24	52.37	240502	547.86	17.09	4389.1	98.12
TA1-6	**Avg.**		**30.95**	**11173.91**	**300.74**	**343.20**	**24.64**	**6.69**	**52.04**	**224035**	**460.82**	**14.91**	**4434.3**	**94.90**
Ilmenite	*Std.*		*30.95*	*935.26*	*138.29*	*18.79*	*3.24*	*3.98*	*8.15*	*11961*	*70.23*	*3.27*	*305.8*	*5.05*
TA2-1_ilm1.d		49.8	**31.74**	10791.18	199.95	371.34	26.66	-1.90	52.85	244706	457.99	14.16	4849.7	111.40
TA2-1_ilm2.d		49.8	**31.74**	10854.66	235.18	317.39	17.77	10.47	54.40	252958	455.45	13.65	4833.8	110.77
TA2-1_ilm3.d		49.8	**31.74**	8252.08	151.08	374.52	17.77	4.13	55.42	228837	441.49	9.20	5297.2	77.76
TA2-1_ilm4.d		49.8	**31.74**	10251.62	133.30	342.78	16.82	-6.67	67.10	231058	435.14	8.51	5097.2	100.61
TA2-1_ilm5.d		49.8	**31.74**	9204.24	121.88	330.08	15.55	4.13	58.34	218680	442.76	10.19	4792.6	81.57
TA2-1	**Avg.**		**31.74**	**9870.76**	**168.28**	**347.22**	**18.92**	**2.03**	**57.62**	**235248**	**446.56**	**11.14**	**4974.1**	**96.42**
Ilmenite	*Std.*		*31.74*	*1120.79*	*47.83*	*25.15*	*4.42*	*6.54*	*5.66*	*13567*	*9.75*	*2.60*	*216.6*	*15.94*
TA2-3_ilm1.d		49.8	**31.53**	10657.73	523.43	327.93	13.87	-13.56	58.02	245317	531.94	48.56	4203.2	103.77
TA2-3_ilm2.d		49.8	**31.53**	10689.26	356.31	285.36	21.76	-6.31	49.06	213785	436.08	35.32	4269.4	94.60
TA2-3_ilm3.d		49.8	**31.53**	11729.81	239.64	343.07	29.64	8.20	60.45	237119	408.65	23.65	4534.3	99.58
TA2-3_ilm4.d		49.8	**31.53**	10973.05	485.59	343.70	29.32	-5.99	53.67	235857	524.69	35.63	4490.1	105.00
TA2-3_ilm5.d		49.8	**31.53**	10752.33	422.53	378.38	27.75	3.78	58.08	235542	491.90	33.74	4310.4	102.16
TA2-3	**Avg.**		**31.53**	**10960.44**	**405.50**	**335.69**	**24.47**	**-2.77**	**55.86**	**233524**	**478.65**	**35.38**	**4361.5**	**101.02**
Ilmenite	*Std.*		*31.53*	*447.37*	*112.41*	*33.67*	*6.72*	*8.70*	*4.52*	*11738*	*54.42*	*8.86*	*143.7*	*4.13*
TA2-4_ilm1.d		49.8	**31.98**	10027.85	649.12	394.27	26.22	2.56	57.46	247179	377.64	14.77	4483.1	94.94
TA2-4_ilm2.d		49.8	**31.98**	10264.48	623.54	316.57	12.47	4.16	47.17	232470	485.40	22.22	4518.3	87.94
TA2-4_ilm3.d		49.8	**31.98**	9912.74	332.56	353.98	20.47	-6.40	66.99	235028	383.40	15.92	4614.2	95.26
TA2-4_ilm4.d		49.8	**31.98**	10904.01	153.17	358.14	15.67	4.48	71.12	231830	409.62	10.04	4447.9	106.16
TA2-4_ilm5.d		49.8	**31.98**	8122.05	127.27	321.68	24.62	-0.96	70.86	213603	382.12	13.56	4946.8	84.10

Source file		60Ni	63Cu	66Zn	69Ga	74Ge	89Y	90Zr	93Nb	95Mo	118Sn	178Hf	181Ta	182W	208Pb
TA1-4_ilm1.d		36.72	3.33	23.09	0.40	0.08	0.03	40.07	7.62	0.05	1.71	1.27	0.46	0.01	0.02
TA1-4_ilm2.d		48.96	5.42	36.26	0.78	0.05	0.02	37.22	9.24	0.07	1.94	1.29	0.66	0.00	0.01
TA1-4_ilm3.d		42.52	2.87	23.09	0.52	0.05	0.03	44.63	7.87	0.04	2.70	1.40	0.46	0.01	0.01
TA1-4_ilm4.d		48.38	2.57	26.31	0.79	0.09	0.04	45.37	10.47	0.06	2.09	1.49	0.78	0.01	0.01
TA1-4_ilm5.d		48.69	2.40	33.84	1.09	0.08	0.07	49.12	11.47	0.06	2.01	1.65	0.93	0.01	0.02
TA1-4	**Avg.**	**45.05**	**3.32**	**28.52**	**0.72**	**0.07**	**0.04**	**43.28**	**9.33**	**0.06**	**2.09**	**1.42**	**0.66**	**0.01**	**0.01**
Ilmenite	*Std.*	*4.80*	*1.10*	*5.52*	*0.24*	*0.02*	*0.02*	*4.18*	*1.48*	*0.01*	*0.33*	*0.14*	*0.18*	*0.00*	*0.00*
TA1-5_ilm1.d		37.26	2.70	19.61	0.36	0.08	0.03	44.10	9.08	0.05	2.72	1.37	0.58	0.01	0.05
TA1-5_ilm2.d		37.51	2.65	19.32	0.47	0.04	0.06	47.90	10.30	0.04	2.18	1.44	0.73	0.01	0.06
TA1-5_ilm3.d		42.64	2.96	30.13	0.73	0.06	0.04	47.68	13.12	0.08	1.98	1.67	1.06	0.02	0.02
TA1-5_ilm5.d		48.25	5.32	35.16	1.12	0.08	0.02	44.38	10.52	0.06	1.78	1.49	0.76	0.01	0.06
TA1-5-ilm4.d		50.34	2.66	38.05	1.09	0.06	0.03	43.37	11.63	0.06	1.89	1.57	0.88	0.02	0.04
TA1-5	**Avg.**	**43.20**	**3.26**	**28.45**	**0.75**	**0.07**	**0.04**	**45.49**	**10.93**	**0.06**	**2.11**	**1.51**	**0.80**	**0.02**	**0.05**
Ilmenite	*Std.*	*5.38*	*1.04*	*7.76*	*0.31*	*0.01*	*0.01*	*1.91*	*1.36*	*0.01*	*0.33*	*0.10*	*0.16*	*0.00*	*0.01*
TA1-6_ilm1.d		46.61	3.32	33.37	0.73	0.05	0.02	44.08	9.94	0.05	2.93	1.44	0.65	0.01	0.03
TA1-6_ilm2.d		46.71	3.00	41.79	1.23	0.04	0.03	46.24	11.76	0.07	2.65	1.56	0.91	0.02	0.06
TA1-6_ilm3.d		41.69	3.14	20.71	0.22	0.03	0.03	48.94	7.74	0.03	2.79	1.43	0.46	0.01	0.04
TA1-6_ilm4.d		49.83	4.64	36.83	0.73	0.11	0.04	37.61	9.53	0.05	2.90	1.23	0.63	0.02	0.04
TA1-6_ilm5.d		53.86	3.06	44.88	1.15	0.08	0.05	49.46	12.66	0.08	4.62	1.61	1.03	0.01	0.02
TA1-6	**Avg.**	**47.74**	**3.43**	**35.52**	**0.81**	**0.06**	**0.04**	**45.27**	**10.33**	**0.06**	**3.18**	**1.45**	**0.74**	**0.02**	**0.04**
Ilmenite	*Std.*	*4.49*	*0.69*	*9.39*	*0.40*	*0.03*	*0.01*	*4.80*	*1.94*	*0.02*	*0.81*	*0.15*	*0.23*	*0.00*	*0.01*
TA2-1_ilm1.d		53.64	16.82	31.80	0.49	0.09	0.06	43.70	9.97	0.08	4.44	1.47	0.66	0.03	0.08
TA2-1_ilm2.d		51.67	3.15	32.91	0.71	0.07	0.09	45.01	10.44	0.06	3.06	1.68	0.71	0.01	0.05
TA2-1_ilm3.d		42.47	4.06	30.15	0.45	0.08	0.06	41.36	10.70	0.09	6.16	1.42	0.81	0.02	0.05
TA2-1_ilm4.d		48.56	3.36	23.14	0.28	0.06	0.09	44.88	9.97	0.07	3.28	1.47	0.78	0.02	0.05
TA2-1_ilm5.d		44.91	3.81	24.76	0.28	0.06	0.07	42.24	8.00	0.06	2.78	1.41	0.48	0.00	0.03
TA2-1	**Avg.**	**48.25**	**6.24**	**28.55**	**0.44**	**0.07**	**0.07**	**43.44**	**9.81**	**0.07**	**3.95**	**1.49**	**0.69**	**0.02**	**0.05**
Ilmenite	*Std.*	*4.62*	*5.93*	*4.36*	*0.18*	*0.01*	*0.01*	*1.61*	*1.06*	*0.01*	*1.39*	*0.11*	*0.13*	*0.01*	*0.02*
TA2-3_ilm1.d		55.21	1.74	38.78	1.44	0.09	0.02	43.26	10.09	0.05	3.02	1.59	0.83	0.01	0.05
TA2-3_ilm2.d		47.96	3.69	38.78	0.96	0.07	0.06	31.00	8.14	0.03	2.72	1.15	0.56	0.00	0.06
TA2-3_ilm3.d		48.46	2.48	31.50	0.77	0.06	0.05	44.49	9.89	0.08	3.00	1.70	0.67	0.02	0.08
TA2-3_ilm4.d		54.61	3.23	49.19	1.37	0.09	0.06	43.80	11.67	0.05	2.97	1.61	0.86	0.01	0.10
TA2-3_ilm5.d		50.73	2.84	40.68	1.26	0.06	0.06	44.52	10.94	0.05	3.08	1.69	0.84	0.01	0.25
TA2-3	**Avg.**	**51.40**	**2.80**	**39.79**	**1.16**	**0.07**	**0.05**	**41.41**	**10.15**	**0.05**	**2.96**	**1.55**	**0.75**	**0.01**	**0.11**
Ilmenite	*Std.*	*3.38*	*0.74*	*6.32*	*0.29*	*0.01*	*0.02*	*5.85*	*1.33*	*0.02*	*0.14*	*0.23*	*0.13*	*0.00*	*0.08*
TA2-4_ilm1.d		44.64	1.75	44.13	0.77	0.06	0.03	50.78	10.39	0.04	6.29	1.72	0.82	0.01	0.01
TA2-4_ilm2.d		44.35	2.29	43.81	1.47	0.08	0.02	42.37	11.61	0.07	3.64	1.64	1.02	0.01	0.02
TA2-4_ilm3.d		44.42	2.75	31.02	0.64	0.05	0.05	47.52	9.85	0.07	4.39	1.72	0.74	0.01	0.01
TA2-4_ilm4.d		48.28	2.69	20.37	0.33	0.05	0.04	59.16	12.82	0.05	3.78	1.88	1.07	0.01	0.06
TA2-4_ilm5.d		38.82	3.45	24.08	0.24	0.03	0.04	47.52	7.71	0.05	3.28	1.39	0.52	0.01	0.06

Source file	Notes	Analysis Length (s)	Fe (wt%)	24Mg	27Al	29Si	31P	44Ca	45SC	47Ti	51V	52Cr	55Mn	59Co
TA2-4	**Avg.**		**31.98**	**9846.22**	**377.13**	**348.93**	**19.89**	**0.77**	**62.72**	**232022**	**407.64**	**15.30**	**4602.1**	**93.68**
Ilmenite	*Std.*		*31.98*	*1037.31*	*249.64*	*31.45*	*5.82*	*4.55*	*10.30*	*12023*	*45.25*	*4.45*	*202.4*	*8.44*
TA2-6_ilm1.d		48.8	**31.88**	8352.2	156.8	314.6	25.8	1.3	76.2	268737	404.9	12.1	4746.7	84.8
TA2-6_ilm2.d		48.8	**31.88**	10105.5	506.9	304.8	31.9	-1.6	62.1	270969	387.6	16.6	4494.9	100.2
TA2-6_ilm3.d		48.8	**31.88**	8384.1	154.9	344.3	23.3	4.8	82.0	267462	384.8	12.0	5084.6	76.8
TA2-6_ilm4.d		44.1	**31.88**	10520.0	157.8	414.4	43.4	5.1	74.5	274156	399.8	7.9	4453.4	104.0
TA2-6_ilm5.d		48.8	**31.88**	9850.5	653.5	356.7	31.9	8.3	55.8	265549	504.3	24.3	4510.8	98.6
TA2-6	**Avg.**		**31.88**	**9442.46**	**325.99**	**346.97**	**31.24**	**3.57**	**70.11**	**269375**	**416.27**	**14.60**	**4658.1**	**92.87**
Ilmenite	*Std.*		*31.88*	*1009.45*	*237.78*	*43.24*	*7.75*	*3.81*	*10.81*	*3321*	*49.92*	*6.24*	*264.6*	*11.53*

Source file		60Ni	63Cu	66Zn	69Ga	74Ge	89Y	90Zr	93Nb	95Mo	118Sn	178Hf	181Ta	182W	208Pb
TA2-4	**Avg.**	**44.10**	**2.59**	**32.68**	**0.69**	**0.05**	**0.04**	**49.47**	**10.47**	**0.05**	**4.27**	**1.67**	**0.83**	**0.01**	**0.03**
Ilmenite	*Std.*	*3.39*	*0.63*	*10.99*	*0.49*	*0.02*	*0.01*	*6.20*	*1.93*	*0.01*	*1.19*	*0.18*	*0.22*	*0.00*	*0.03*
TA2-6_ilm1.d		39.0	1.5	18.1	0.2	0.1	0.1	54.2	9.6	0.0	3.9	1.6	0.7	0.0	0.6
TA2-6_ilm2.d		46.1	0.9	33.5	0.8	0.1	0.1	46.8	10.1	0.0	3.6	1.8	0.8	0.0	0.2
TA2-6_ilm3.d		40.5	1.8	15.8	0.2	0.0	0.1	56.4	8.6	0.0	4.1	1.7	0.6	0.0	0.1
TA2-6_ilm4.d		46.7	2.1	22.7	0.4	0.1	0.1	58.1	12.1	0.0	6.3	1.8	0.9	0.0	0.1
TA2-6_ilm5.d		52.3	1.8	44.3	1.6	0.1	0.1	46.4	11.1	0.1	5.4	1.7	0.9	0.0	0.2
TA2-6	**Avg.**	**44.92**	**1.62**	**26.88**	**0.66**	**0.06**	**0.08**	**52.37**	**10.31**	**0.04**	**4.68**	**1.73**	**0.78**	**0.01**	**0.25**
Ilmenite	*Std.*	*5.32*	*0.44*	*11.88*	*0.59*	*0.03*	*0.03*	*5.44*	*1.35*	*0.02*	*1.14*	*0.08*	*0.13*	*0.00*	*0.19*

APPENDIX 3

Full results from EMPA analyses of silicate minerals

PLAGIOCLASE		Oxide Wt %												End Member Calculations (%)		
Analysis ID		**K2O**	**CaO**	**Al2O3**	**FeO**	**MnO**	**TiO2**	**SiO2**	**MgO**	**Na2O**	**Cr2O3**	**BaO**	**TOTAL**	**Ab**	**An**	**Or**
14-2D-plag-1		0.08	12.72	30.78	0.14	0.02	0.02	52.09	0.01	4.40	0.00	0.00	100.25	38.32	61.23	0.45
14-2D-plag-2		0.05	14.29	32.01	0.09	0.00	0.00	50.05	0.00	3.61	0.00	0.00	100.10	31.32	68.40	0.27
14-2D-plag-3		0.05	12.88	30.59	0.06	0.02	0.00	51.73	0.00	4.26	0.00	0.01	99.60	37.34	62.38	0.28
14-2D-plag-4		0.06	13.00	30.82	0.13	0.00	0.02	51.86	0.00	4.18	0.00	0.00	100.06	36.65	63.00	0.35
MA14-2D	**Avg.**	**0.06**	**13.22**	**31.05**	**0.10**	**0.01**	**0.01**	**51.43**	**0.00**	**4.11**	**0.00**	**0.00**	**100.01**	**35.91**	**63.75**	**0.34**
Plagioclase	*Std.*	*0.01*	*0.62*	*0.56*	*0.03*	*0.01*	*0.01*	*0.81*	*0.00*	*0.30*	*0.00*	*0.00*	*0.24*	*2.71*	*2.76*	*0.07*
148A-plag-6		0.04	13.03	30.74	0.08	0.00	0.00	51.77	0.00	4.21	0.00	0.02	99.88	36.81	62.99	0.21
148A-plag-7		0.04	13.24	30.92	0.11	0.02	0.00	51.63	0.00	4.14	0.00	0.00	100.09	36.08	63.71	0.21
148A-plag-9		0.04	13.24	30.94	0.13	0.00	0.02	51.19	0.00	4.03	0.00	0.04	99.63	35.44	64.32	0.25
MA14-8A	**Avg.**	**0.04**	**13.17**	**30.87**	**0.10**	**0.01**	**0.01**	**51.53**	**0.00**	**4.13**	**0.00**	**0.02**	**99.87**	**36.11**	**63.67**	**0.22**
Plagioclase	*Std.*	*0.00*	*0.10*	*0.09*	*0.02*	*0.01*	*0.01*	*0.25*	*0.00*	*0.07*	*0.00*	*0.02*	*0.19*	*0.56*	*0.54*	*0.02*
MA11-2_plag-1		0.04	11.37	29.27	0.09	0.00	0.00	53.80	0.00	5.15	0.00	0.00	99.71	44.96	54.80	0.23
MA11-2_plag-2		0.03	12.83	30.51	0.09	0.00	0.00	52.00	0.00	4.24	0.00	0.00	99.70	37.35	62.47	0.18
MA11-2_plag-3		0.03	12.71	30.59	0.13	0.00	0.00	52.01	0.00	4.30	0.01	0.00	99.79	37.92	61.90	0.18
MA11-2	**Avg.**	**0.03**	**12.30**	**30.12**	**0.10**	**0.00**	**0.00**	**52.60**	**0.00**	**4.57**	**0.01**	**0.00**	**99.73**	**40.08**	**59.72**	**0.20**
Plagioclase	*Std.*	*0.00*	*0.66*	*0.61*	*0.02*	*0.00*	*0.00*	*0.84*	*0.00*	*0.42*	*0.01*	*0.00*	*0.04*	*3.46*	*3.49*	*0.03*
M03-6_plag-1		0.03	13.34	31.19	0.12	0.02	0.00	51.17	0.00	3.99	0.00	0.00	99.87	35.07	64.78	0.15
M03-6_plag-2		0.02	13.82	31.50	0.05	0.00	0.00	50.77	0.00	3.75	0.01	0.00	99.93	32.92	66.96	0.12
M03-6_plag-3		0.02	13.46	31.42	0.20	0.00	0.11	50.78	0.00	3.97	0.00	0.00	99.95	34.76	65.16	0.09
M03-6_plag-4		0.03	13.64	31.30	0.06	0.00	0.00	50.94	0.00	3.87	0.00	0.00	99.85	33.85	65.95	0.19
MA03-6	**Avg.**	**0.02**	**13.64**	**31.41**	**0.10**	**0.00**	**0.04**	**50.83**	**0.00**	**3.86**	**0.01**	**0.00**	**99.91**	**33.84**	**66.02**	**0.13**
Plagioclase	*Std.*	*0.01*	*0.15*	*0.08*	*0.06*	*0.00*	*0.05*	*0.08*	*0.00*	*0.09*	*0.01*	*0.00*	*0.04*	*0.75*	*0.74*	*0.04*
M03-3_plag-1		0.04	12.27	30.17	0.04	0.01	0.00	52.67	0.00	4.65	0.00	0.00	99.86	40.58	59.18	0.24
M03-3_plag-2		0.02	12.93	30.71	0.03	0.00	0.00	51.46	0.00	4.10	0.00	0.00	99.27	36.42	63.44	0.14
M03-3_plag-3		0.03	12.85	30.77	0.07	0.02	0.00	51.89	0.00	4.25	0.01	0.00	99.89	37.41	62.43	0.16
M03-3_plag-4		0.01	13.87	31.59	0.05	0.00	0.00	50.47	0.00	3.69	0.00	0.00	99.68	32.50	67.43	0.07
MA03-3	**Avg.**	**0.03**	**13.22**	**31.02**	**0.05**	**0.01**	**0.00**	**51.27**	**0.00**	**4.02**	**0.00**	**0.00**	**99.61**	**35.44**	**64.43**	**0.12**
Plagioclase	*Std.*	*0.01*	*0.46*	*0.40*	*0.02*	*0.01*	*0.00*	*0.60*	*0.00*	*0.24*	*0.00*	*0.00*	*0.26*	*2.12*	*2.16*	*0.04*
M03-2_plag-1		0.05	12.40	30.26	0.09	0.03	0.01	52.27	0.01	4.49	0.01	0.00	99.62	39.48	60.21	0.31
M03-2_plag-2		0.03	12.67	30.44	0.04	0.01	0.00	52.34	0.00	4.41	0.00	0.00	99.94	38.60	61.21	0.19
M03-2_plag-3		0.03	12.54	30.41	0.04	0.00	0.00	52.27	0.00	4.41	0.01	0.00	99.72	38.80	61.03	0.17
M03-2_plag-4		0.03	13.68	31.45	0.01	0.00	0.00	50.64	0.00	3.81	0.00	0.00	99.62	33.45	66.38	0.17
MA03-2	**Avg.**	**0.04**	**12.96**	**30.77**	**0.03**	**0.00**	**0.00**	**51.75**	**0.00**	**4.21**	**0.00**	**0.00**	**99.76**	**36.95**	**62.87**	**0.18**
Plagioclase	*Std.*	*0.01*	*0.51*	*0.48*	*0.01*	*0.00*	*0.00*	*0.79*	*0.00*	*0.28*	*0.01*	*0.00*	*0.13*	*2.48*	*2.48*	*0.01*
MA03-1B_plag-1		0.03	13.25	30.87	0.28	0.00	0.00	51.16	0.09	3.94	0.00	0.00	99.60	34.91	64.94	0.15
MA03-1B_plag-2		0.03	13.41	31.09	0.19	0.02	0.00	51.20	0.01	3.89	0.02	0.00	99.85	34.34	65.47	0.20
MA03-1B_plag-3		0.01	13.85	31.33	0.20	0.00	0.00	50.75	0.01	3.71	0.01	0.00	99.88	32.63	67.33	0.04
MA03-1B	**Avg.**	**0.02**	**13.50**	**31.10**	**0.22**	**0.01**	**0.00**	**51.04**	**0.04**	**3.84**	**0.01**	**0.00**	**99.78**	**33.96**	**65.91**	**0.13**
Plagioclase	*Std.*	*0.01*	*0.26*	*0.19*	*0.04*	*0.01*	*0.00*	*0.20*	*0.04*	*0.10*	*0.01*	*0.00*	*0.13*	*0.97*	*1.02*	*0.07*
MA03-1A_plag-1		0.01	14.46	31.74	0.18	0.00	0.00	49.81	0.01	3.34	0.01	0.00	99.57	29.44	70.49	0.07
MA03-1A_plag-2		0.02	13.66	31.27	0.20	0.00	0.01	50.95	0.03	3.85	0.01	0.00	99.99	33.73	66.17	0.11
MA03-1A_plag-3		0.03	12.52	30.22	0.17	0.00	0.00	52.34	0.00	4.39	0.00	0.00	99.67	38.76	61.07	0.17
MA03-1A	**Avg.**	**0.02**	**13.55**	**31.08**	**0.18**	**0.00**	**0.01**	**51.03**	**0.02**	**3.86**	**0.01**	**0.00**	**99.75**	**33.97**	**65.91**	**0.11**
Plagioclase	*Std.*	*0.01*	*0.80*	*0.64*	*0.01*	*0.00*	*0.00*	*1.04*	*0.01*	*0.43*	*0.00*	*0.00*	*0.18*	*3.81*	*3.85*	*0.04*

OLIVINE		Oxide Wt %														End Member Calculation (%)	
Analysis ID		**K_2O**	**CaO**	**Al_2O_3**	**FeO**	**MnO**	**TiO_2**	**SiO_2**	**MgO**	**Na_2O**	**Cr_2O_3**	**NiO**	**ZnO**	**V_2O_3**	**TOTAL**	**Fo**	**Fa**
142D-olv-3		0.02	0.02	0.00	43.55	0.57	0.01	34.96	21.26	0.00	0.01	0.03	0.02	0.00	100.45	46.52	53.48
142D-olv-4		0.01	0.04	0.00	43.56	0.58	0.00	34.79	21.08	0.02	0.00	0.02	0.00	0.00	100.10	46.31	53.69
142D-olv-5		0.01	0.03	0.00	43.28	0.55	0.00	34.89	21.57	0.01	0.00	0.02	0.02	0.00	100.38	47.04	52.96
142D-olv-1		0.02	0.03	0.01	42.08	0.53	0.00	35.33	22.45	0.00	0.00	0.06	0.00	0.00	100.51	48.74	51.26
142D-olv-2		0.01	0.02	0.01	42.66	0.60	0.02	35.03	21.95	0.00	0.00	0.04	0.00	0.00	100.34	47.84	52.16
MA14-2D	**Avg.**	**0.01**	**0.03**	**0.00**	**43.03**	**0.56**	**0.01**	**35.00**	**21.66**	**0.01**	**0.00**	**0.03**	**0.01**	**0.00**	**100.36**	**47.29**	**52.71**
Olivine	*Std.*	*0.01*	*0.01*	*0.00*	*0.57*	*0.02*	*0.01*	*0.18*	*0.49*	*0.01*	*0.00*	*0.02*	*0.01*	*0.00*	*0.14*	*0.90*	*0.90*
MA11-8_olv-1		0.00	0.06	0.00	39.55	0.67	0.00	35.10	24.95	0.00	0.00	0.02	0.00	0.00	100.36	52.93	47.07
MA11-8_olv-2		0.00	0.01	0.00	38.26	0.76	0.00	34.93	25.08	0.00	0.00	0.03	0.00	0.00	99.07	53.88	46.12
MA11-8_olv-3		0.00	0.04	0.00	38.25	0.76	0.00	34.87	25.12	0.00	0.02	0.02	0.00	0.00	99.09	53.93	46.07
MA11-8_olv-4		0.00	0.04	0.01	38.26	0.74	0.00	34.97	25.05	0.00	0.02	0.05	0.00	0.00	99.14	53.85	46.15
MA11-8	**Avg.**	**0.00**	**0.04**	**0.00**	**38.58**	**0.73**	**0.00**	**34.97**	**25.05**	**0.00**	**0.01**	**0.03**	**0.00**	**0.00**	**99.41**	**53.65**	**46.35**
	Std.	*0.00*	*0.02*	*0.01*	*0.56*	*0.04*	*0.00*	*0.08*	*0.06*	*0.00*	*0.01*	*0.01*	*0.00*	*0.00*	*0.55*	*0.42*	*0.42*
MA11-2_olv-1		0.00	0.01	0.00	38.07	0.63	0.00	35.35	26.07	0.00	0.01	0.03	0.00	0.00	100.19	54.97	45.03
MA11-2_olv-2		0.00	0.02	0.01	37.09	0.59	0.00	35.35	25.96	0.00	0.00	0.02	0.00	0.00	99.04	55.51	44.49
MA11-2_olv-3		0.00	0.03	0.01	37.09	0.62	0.00	35.46	26.19	0.02	0.01	0.02	0.00	0.00	99.46	55.72	44.28
MA11-2_olv-4		0.00	0.02	0.01	37.95	0.56	0.00	35.34	25.72	0.00	0.01	0.02	0.00	0.00	99.64	54.71	45.29
MA11-2	**Avg.**	**0.00**	**0.02**	**0.01**	**37.55**	**0.60**	**0.00**	**35.37**	**25.98**	**0.00**	**0.01**	**0.02**	**0.00**	**0.00**	**99.58**	**55.23**	**44.77**
St.Dev	*Std.*	*0.00*	*0.01*	*0.00*	*0.46*	*0.03*	*0.00*	*0.05*	*0.17*	*0.01*	*0.01*	*0.01*	*0.00*	*0.00*	*0.41*	*0.41*	*0.41*
MA03-1B_olv-3		0.00	0.03	0.00	39.29	0.51	0.00	35.08	25.32	0.01	0.01	0.02	0.00	0.00	100.27	53.47	46.53
MA03-1B_olv-2		0.00	0.05	0.00	39.07	0.53	0.00	35.01	25.65	0.01	0.00	0.02	0.00	0.00	100.34	53.92	46.08
MA03-1B_olv-3		0.00	0.03	0.01	38.11	0.53	0.00	35.29	25.44	0.00	0.01	0.02	0.00	0.00	99.45	54.34	45.66
MA03-1B	**Avg.**	**0.00**	**0.04**	**0.00**	**38.82**	**0.53**	**0.00**	**35.13**	**25.47**	**0.01**	**0.00**	**0.02**	**0.00**	**0.00**	**100.02**	**53.91**	**46.09**
St.Dev	*Std.*	*0.00*	*0.01*	*0.00*	*0.51*	*0.01*	*0.00*	*0.12*	*0.14*	*0.01*	*0.00*	*0.00*	*0.00*	*0.00*	*0.41*	*0.35*	*0.35*
MA03-1A_olv-3		0.00	0.05	0.01	36.88	0.46	0.00	35.20	26.28	0.01	0.01	0.00	0.00	0.00	98.90	55.95	44.05
MA03-1A_olv-2		0.01	0.07	0.00	37.10	0.54	0.00	35.07	26.12	0.00	0.01	0.06	0.00	0.00	98.99	55.65	44.35
MA03-1A_olv-1		0.00	0.05	0.00	37.25	0.49	0.00	35.08	26.00	0.00	0.01	0.04	0.00	0.00	98.92	55.45	44.55
MA03-1A_olv-4		0.00	0.05	0.00	39.14	0.58	0.00	34.86	25.31	0.00	0.01	0.04	0.00	0.00	99.98	53.54	46.46
MA03-1A_olv-5		0.00	0.01	0.00	41.42	0.56	0.00	34.83	24.35	0.02	0.01	0.02	0.00	0.00	101.22	51.17	48.83
MA03-1A	**Avg.**	**0.00**	**0.04**	**0.00**	**38.36**	**0.52**	**0.00**	**35.01**	**25.61**	**0.00**	**0.01**	**0.03**	**0.00**	**0.00**	**99.60**	**54.35**	**45.65**
St.Dev	*Std.*	*0.01*	*0.02*	*0.00*	*1.73*	*0.04*	*0.00*	*0.14*	*0.72*	*0.01*	*0.00*	*0.02*	*0.00*	*0.00*	*0.90*	*1.80*	*1.80*

CLINOPYROXENE		Wt.% Oxide													
Analysis ID		**K_2O**	**CaO**	**Al_2O_3**	**ZnO**	**FeO**	**MnO**	**TiO_2**	**SiO_2**	**MgO**	**V_2O_3**	**Na_2O**	**Cr_2O_3**	**TOTAL**	**Mg#**
14-2D-cpx-2		0.02	21.51	1.78	0.01	10.00	0.25	0.38	51.19	13.08	0.08	0.26	0.02	98.58	69.98
14-2D-cpx-3		0.01	21.92	1.63	0.00	9.55	0.25	0.36	51.56	13.34	0.05	0.22	0.00	98.89	71.34
14-2D-cpx-4		0.02	21.61	1.76	0.00	10.03	0.26	0.37	51.40	12.95	0.03	0.27	0.03	98.73	69.71
MA14-2D	**Avg.**	**0.02**	**21.68**	**1.72**	**0.01**	**9.86**	**0.25**	**0.37**	**51.38**	**13.12**	**0.05**	**0.25**	**0.02**	**98.73**	**70.34**
Clinopyroxene	*Std.*	*0.00*	*0.17*	*0.06*	*0.01*	*0.22*	*0.00*	*0.01*	*0.15*	*0.16*	*0.02*	*0.02*	*0.01*	*0.13*	*0.71*
14-5A-cpx-5		0.01	22.64	1.59	0.06	9.31	0.30	0.17	51.57	12.61	0.09	0.23	0.02	98.60	70.70
MA14-5A	**Avg.**	**0.01**	**22.64**	**1.59**	**0.06**	**9.31**	**0.30**	**0.17**	**51.57**	**12.61**	**0.09**	**0.23**	**0.02**	**98.60**	**70.70**
148A-cpx-3		0.01	21.17	1.86	0.01	10.47	0.30	0.38	50.98	13.09	0.03	0.22	0.01	98.53	69.02
148A-cpx-4		0.02	22.29	1.78	0.00	8.75	0.36	0.30	51.64	13.26	0.06	0.20	0.01	98.67	72.99
148A-cpx-1		0.01	21.62	1.94	0.00	9.90	0.31	0.36	51.25	13.07	0.03	0.22	0.00	98.72	70.18
148A-cpx-2		0.02	21.57	1.66	0.03	9.79	0.33	0.28	51.57	13.32	0.05	0.19	0.03	98.84	70.82
MA14-8A	**Avg.**	**0.02**	**21.66**	**1.81**	**0.01**	**9.73**	**0.33**	**0.33**	**51.36**	**13.19**	**0.04**	**0.21**	**0.01**	**98.69**	**70.75**
Clinopyroxene	*Std.*	*0.00*	*0.40*	*0.10*	*0.01*	*0.62*	*0.02*	*0.04*	*0.26*	*0.11*	*0.01*	*0.01*	*0.01*	*0.11*	*1.44*
32-3-cpx-3		0.01	21.93	1.61	0.00	8.94	0.33	0.32	51.75	13.23	0.06	0.40	0.01	98.59	72.51
32-3-cpx-4		0.02	22.75	1.90	0.04	8.29	0.32	0.36	51.51	12.85	0.04	0.43	0.02	98.53	73.41
MA32-3	**Avg.**	**0.01**	**22.34**	**1.76**	**0.02**	**8.62**	**0.32**	**0.34**	**51.63**	**13.04**	**0.05**	**0.41**	**0.02**	**98.56**	**72.96**
Clinopyroxene	*Std.*	*0.01*	*0.41*	*0.14*	*0.02*	*0.33*	*0.00*	*0.02*	*0.12*	*0.19*	*0.01*	*0.02*	*0.01*	*0.03*	*0.45*
MA32-15_cpx-1-1		0.00	22.35	1.85	0.00	8.06	0.18	0.41	51.94	14.47	0.02	0.28	0.00	99.57	76.19
MA32-15_cpx-1-2		0.00	22.27	1.93	0.00	7.97	0.24	0.46	51.57	14.04	0.03	0.27	0.00	98.77	75.85
MA32-15_cpx-2-1		0.00	25.27	1.19	0.00	3.67	0.07	0.17	52.91	15.85	0.00	0.00	0.00	99.14	88.49
MA32-15_cpx-2-2		0.00	25.33	0.89	0.00	3.46	0.03	0.17	53.42	16.11	0.01	0.01	0.00	99.42	89.26
MA32-15	**Avg.**	**0.00**	**23.80**	**1.47**	**0.00**	**5.79**	**0.13**	**0.30**	**52.46**	**15.12**	**0.02**	**0.14**	**0.00**	**99.23**	**82.45**
Clinopyroxene	*Std.*	*0.00*	*1.49*	*0.44*	*0.00*	*2.23*	*0.09*	*0.13*	*0.74*	*0.88*	*0.01*	*0.13*	*0.00*	*0.31*	*6.43*
MA32-17_cpx-2		0.00	24.86	0.55	0.00	4.03	0.07	0.08	53.42	15.72	0.01	0.02	0.02	98.78	87.41
MA32-17_cpx-3		0.01	22.02	1.64	0.06	8.56	0.24	0.29	51.68	14.08	0.04	0.23	0.01	98.85	74.56
MA32-17_cpx-4		0.00	22.43	1.97	0.00	8.35	0.23	0.45	51.15	13.96	0.05	0.23	0.00	98.80	74.88
MA32-17	**Avg.**	**0.00**	**23.10**	**1.39**	**0.02**	**6.98**	**0.18**	**0.27**	**52.08**	**14.59**	**0.03**	**0.16**	**0.01**	**98.81**	**78.95**
Clinopyroxene	*Std.*	*0.00*	*1.25*	*0.60*	*0.03*	*2.09*	*0.08*	*0.15*	*0.97*	*0.80*	*0.02*	*0.10*	*0.01*	*0.03*	*5.98*
MA11-2_cpx-1		0.00	21.90	2.19	0.05	8.77	0.21	0.44	51.53	14.03	0.02	0.23	0.00	99.36	74.04
MA11-2_cpx-2		0.00	22.13	2.03	0.00	8.43	0.24	0.38	51.74	14.23	0.00	0.22	0.01	99.42	75.05
MA11-2	**Avg.**	**0.00**	**22.01**	**2.11**	**0.02**	**8.60**	**0.23**	**0.41**	**51.63**	**14.13**	**0.01**	**0.22**	**0.00**	**99.39**	**74.54**
Clinopyroxene	*Std.*	*0.00*	*0.12*	*0.08*	*0.02*	*0.17*	*0.02*	*0.03*	*0.10*	*0.10*	*0.01*	*0.00*	*0.00*	*0.03*	*0.51*
MA03-1B_cpx-1		0.00	21.29	2.45	0.04	9.63	0.25	0.49	50.88	13.46	0.06	0.34	0.03	98.92	71.36
MA03-1B_cpx-2		0.00	21.46	2.34	0.02	9.22	0.23	0.53	51.00	13.54	0.07	0.28	0.04	98.73	72.36
MA03-1B_cpx-3		0.01	21.57	2.23	0.03	9.10	0.25	0.46	51.10	13.46	0.07	0.33	0.01	98.63	72.50
MA03-1B	**Avg.**	**0.00**	**21.44**	**2.34**	**0.03**	**9.32**	**0.24**	**0.50**	**50.99**	**13.49**	**0.07**	**0.32**	**0.03**	**98.76**	**72.08**
Clinopyroxene	*Std.*	*0.00*	*0.12*	*0.09*	*0.01*	*0.23*	*0.01*	*0.03*	*0.09*	*0.04*	*0.01*	*0.03*	*0.01*	*0.12*	*0.51*
MA03-1A_cpx-1		0.00	21.59	1.83	0.00	8.87	0.22	0.35	51.49	14.26	0.06	0.26	0.03	98.98	74.13
MA03-1A_cpx-2		0.00	22.00	2.20	0.00	8.85	0.18	0.42	50.92	13.86	0.08	0.32	0.04	98.89	73.63
MA03-1A_cpx-3		0.00	21.50	2.46	0.00	9.27	0.24	0.49	51.01	13.71	0.12	0.31	0.03	99.15	72.49
MA03-1A_cpx-4		0.00	21.61	2.30	0.00	9.16	0.21	0.47	50.92	13.80	0.07	0.30	0.02	98.87	72.87
MA03-1A_cpx-5		0.00	21.49	2.14	0.00	9.45	0.28	0.45	50.90	13.81	0.06	0.32	0.02	98.91	72.26
MA03-1A	**Avg.**	**0.00**	**21.64**	**2.18**	**0.00**	**9.12**	**0.23**	**0.44**	**51.05**	**13.89**	**0.08**	**0.30**	**0.03**	**98.96**	**73.08**
Clinopyroxene	*Std.*	*0.00*	*0.19*	*0.21*	*0.00*	*0.23*	*0.03*	*0.05*	*0.22*	*0.19*	*0.02*	*0.02*	*0.01*	*0.10*	*0.70*